

**A Biomimetic Synthesis of the Octalin Core of
Integramycin, Isolation of Alkaloids From Amazonian
Plants, and Polyols From Renewable Resources.**

A DISSERTATION
SUBMITTED TO THE FACULTY OF THE GRADUATE SCHOOL
OF THE UNIVERSITY OF MINNESOTA
BY

Susanna J. Emond

IN PARTIAL FULFILLMENT OF THE REQUIREMENTS
FOR THE DEGREE OF
DOCTOR OF PHILOSOPHY

Thomas R. Hoye, Adviser

July 2012

© Susanna J. Emond 2012

Acknowledgements

First and foremost, I would like to thank my adviser, Professor Thomas R. Hoye. He is a superior scientist and teacher. Under his guidance, I gained more technical knowledge than I ever expected. I finally have the confidence to call myself a chemist. Beyond the scientific skills I acquired, Tom has inspired me to take risks (for example, dismantling an entire vacuum pump), see every life experience as a learning opportunity, and pay attention to the details. Tom has a special gift, and I am so grateful to spend these years working with him. He has remarkable patience and a great sense of humor as well.

I would also like to acknowledge the chemists I have worked with over the years. I appreciate the scholarly and fun environment they created from my first day. I was lucky enough to work alongside Drs. Dorian Nelson, Elena Sizova, Amanda Schmit, and Greg Hanson. My current lab environment also fosters academic and personal advancement; I am fortunate to call Dr. Beeru Baire, Brian Woods, and Andrew Mullins my colleagues and friends. Additional group members who have guided me are Patrick Willoughby, Josh Marell, Susan Brown, Adam Wohl, and Andrew Michel.

Beyond my co-workers, I received support from my committee members: Profs. Wayland Noland, Daniel Harki, and Steven Kass. I would like to thank Profs. Marc Hillmyer and Dennis McKenna and Dr. Senthil Gurusamy-Thangavelu for the opportunity to perform interdisciplinary work and expand my knowledge.

I also owe a thank you to all the teachers in my life. Of course, my high school teachers began by inspiring me to pursue the sciences, and the faculty of the Chemistry Department at Marquette University instilled my initial chemical knowledge. My undergraduate advisor, Prof. Rajendra Rathore, gave me the confidence to pursue graduate studies in organic chemistry.

Finally, I would like to thank my family and friends for their continued support. My parents, Tom and Kathy, sisters Stacy and Terri, brother TJ, and grandparents Thomas and Marilyn are amazing. My fellow graduate student friends are some of the brightest and enjoyable people I have ever met. Beyond, the U, I re-entered the community at Totino-Grace High School and I am grateful to be involved in their athletic department as a mentor and coach.

Abstract

This document is a presentation and discussion on three projects in three parts.

Part One is a detailed summary of organic chemistry efforts in the synthesis of a model of the natural product integramycin. This concludes six years of work on various synthetic routes and analysis of spontaneous Diels-Alder chemistry. The goal was to probe part of our group's larger biosynthetic hypothesis concerning spontaneity in the biosynthesis of polyketides.

Part Two summarizes the natural products chemistry that I performed while being supported by a UMN Graduate School Interdisciplinary Doctoral Fellowship. This was a year-long effort (academic year 2010-2011) in identifying the main chemical components of various plant samples from the Amazon. The goal was to isolate new natural products, elucidate their novel structures, and study the biological activity of these constituents.

Part Three is a summary of the advances I made as a polymer chemist through the support of the UMN Center for Sustainable Polymers. This work began in the summer of 2010 and includes the investigation of both soybean oil and natural terpenoids as precursors to polyols for use in polyurethanes. The goal was to prepare sustainable polyurethanes for flexible foam applications.

Table of Contents

Acknowledgement	i
Abstract	ii
Table of Contents	iii
List of Tables	vi
List of Figures	vii
List of Schemes	ix
List of Pictures	xiv
Chart	xv
List of Abbreviations	xvi
PART ONE – Integramycin	
Chapter I. Introduction and Background	1
A. Isolation and Biology	1
B. Previous Work on Integramycin	5
1. Floreancig's Synthesis of the Spirocycle	5
2. Roush's Synthesis of the Spirocycle and Octalin	6
C. Mechanistic and Biosynthetic Considerations	10
1. The Diels-Alder Reaction – Key Predictions and Details	10
2. Self-Assembly in Natural Product Synthesis	13
3. Hoye Group Biosynthetic Hypothesis	16
Chapter II. Synthetic Strategies and Progress Toward a Model Compound	21
A. Retrosynthetic Analysis I	21
1. Route to Aldehyde 30 .	22
2. Routes to Heterocycles 32 and 33 and Various Coupling Reactions	32
3. Route to Heterocycle 32 by Lacey-Dieckmann	38
4. Short Study on 3-acyl Tetramic Acids 76 and 77 .	46
5. Summary of Retrosynthetic Analysis I	51
B. Retrosynthetic Analysis II	52
1. Route to Ene-Aldehyde 97	53
2. The Heterocycle	55
3. Attempts to Synthesize and Attach Selected Model Heterocycles to 97	63
4. Summary of Retrosynthetic Analysis II	70
C. Retrosynthetic Analysis III	70
1. Build 1,3-dioxenone from Aldehyde 30 .	70
2. Build Dicarbonyl First, Then React at α -site	72
3. Amide Bond As Last Step Before Dieckmann	73
4. Summary of Retrosynthetic Analysis III.	79
D. Conclusions for Chapter II	79

Chapter III. Intramolecular Diels Alder	81
A. Observed Reactions	81
1. IMDA of Ene-Aldehyde	97
2. Other Trienes IMDA	85
3. Summary of Findings	89
B. Characterization Studies	89
1. NMR Strategies	91
2. Substrate Modifications	94
3. Epimerizations to <i>7epi-endo-I</i> and <i>7epi-endo-II</i> .	96
4. The D2 Strategy	102
C. Post IMDA: Additional Reactions Toward Model 26	106
D. Comparison to Natural Product, Conclusions, and State of the Project	108
References for Part One	111
Part One Experimental	122
PART TWO – Isolation of Natural Products	
Chapter IV. Alkaloids from Amazonian Plants	179
A. Introduction and Background	179
1. Ethnopharmacology and Schizophrenia	179
2. The Approach (Scheme II-1)	180
3. Final Consideration/Motivation	181
B. Previous Work	182
1. McKenna and Roth	182
2. Ziyad and Laura	184
C. My Contributions to This Project	185
1. Reverse-Phase Medium Pressure Liquid Chromatography (RPLC).	186
2. Application of RPLC to Collected Amazonian Plants	193
3. Alkaloids Prepared	202
D. Concluding remarks and Future Directions	204
1. Biological Activity of Alkaloids in <i>Tabernaemontana</i> Series	204
2. Future directions	205
E. Selected Experimentals and ¹H NMR data	206
References for Part Two	210
Selected Inserted PDFs	217
PART THREE – Polyols From Renewable Resources	
General Introduction and background	225
Chapter V. Polyols from Soybean Oil	227
A. Introduction and Previous Work	227
B. My Studies on Soybean Oil (SBO)	228
1. General Characteristics and Handling of Soybean Oil	228
2. Studies on Olefin Functionalization	239
C. Studies on Epoxidized Soybean Oil	258
1. General Studies With Methyl Epoxy Soyates	258

2. Thiolate Opening of Methyl Epoxy Soyates	259
D. Summary and Outlook	267
Chapter VI. Polyols from Terpenoids	268
A. Background and Previous Work	268
B. Methone and Carvomenthone	269
1. The Baeyer-Villiger (BV) Reaction	269
2. Ring-Opening of Menthide and Carvomenthide	271
3. Triol Carbamate Linkage Reactions	277
C. NMR Studies and Comparison to Computational Studies	279
1. Motivation	279
2. Collection of Experimental Data on Menthones and Carvomenthone	280
3. Collection of Experimental Data on Menthides and Carvomenthides	286
D. Concluding Remarks	292
References for Part Three	293
Part Three Experimental	300
Cumulative Bibliography	359

List of Tables

Table I-1. Oxidation Conditions of Model 42 .	30
Table I-2. Summary of C3 Alkylation and Acylation Reactions.	58
Table I-3. IMDA of Ene-aldehyde 97 .	83
Table I-4: ^{13}C and ^1H NMR Data for <i>endo</i> -I (CDCl_3 , 125 and 500 MHz).	174
Table I-5: ^{13}C and ^1H NMR Data for <i>endo</i> -II (CDCl_3 , 125 and 500 MHz).	175
Table I-6: ^{13}C and ^1H NMR Data for 7- <i>epi-endo</i> -I (CDCl_3 , 125 and 500 MHz).	176
Table I-7: ^{13}C and ^1H NMR Data for 7- <i>epi-endo</i> -II (CDCl_3 , 125 and 500 MHz)	177
Table I-8: ^{13}C and ^1H NMR Data for <i>endo</i> -I (C_6D_6 , 125 and 500 MHz)	178
Table II-1: Extraction Details for Plant Samples	198
Table III-1: ^{13}C and ^1H NMR Data for Menthone (<i>trans</i> - 400)	349
Table III-2: ^{13}C and ^1H NMR Data for Isomenthone (<i>cis</i> - 400)	350
Table III-3: ^{13}C and ^1H NMR for <i>Trans</i> Carvomenthone (<i>trans</i> - 404)	351
Table III-4: ^{13}C and ^1H NMR for <i>Cis</i> Carvomenthone (<i>cis</i> - 404)	352
Table III-5: ^{13}C and ^1H NMR Data for Menthide (<i>trans</i> - 401)	353
Table III-6: ^{13}C and ^1H NMR Data for Isomenthide (<i>cis</i> - 401)	354
Table III-7: ^{13}C and ^1H NMR for <i>Trans</i> Carvomenthide (<i>trans</i> - 405)	355
Table III-8: ^{13}C and ^1H NMR for <i>Cis</i> Carvomenthide (<i>cis</i> - 405)	356
Table III-9: ^{13}C and ^1H NMR for Abnormal <i>Trans</i> Carvomenthide (<i>trans</i> - 406)	357
Table III-10: ^{13}C and ^1H NMR for Abnormal <i>Cis</i> Carvomenthide (<i>cis</i> - 406)	358

List of Figures

Figure I-1. The HIV Life-cycle	1
Figure I-2. Early HIV-Integrase Inhibitors.	2
Figure I-3. Structures of Integramycin and Methanol Adduct (1a and 1b)	3
Figure I-4. Singh's Chem 3D Model of Integramycin (1a) and Key NMR Data.	4
Figure I-5. Integramycin 1a and Antipode 2 .	9
Figure I-6. Houk's Transition State Analysis of Terminally Substituted Dienophiles.	11
Figure I-7. FMO Analysis on Activated Dienophiles.	11
Figure I-8. Octalinoyl-Containing Tetramic Acids.	17
Figure I-9. Exo vs. <i>endo</i> IMDA of 1,7,9-Decatrienes.	18
Figure I-10. Potential Stereoisomers From Johnson-Claisen.	26
Figure I-11. Mechanism of Crimmons' Aldol Reaction (Hexanal Substrate).	29
Figure I-12. Equilibrium Between the Acid and Conjugate Base of Tetramate	32,44
Figure I-13. Model Tetramates.	46
Figure I-14. Royles' Illustration of Tautomeric Forms of 3-acetyl- 2,4-Pyrrolidinedione.	47
Figure I-15. Dimers of Tetramic and Tetronic Acids.	50
Figure I-16. Anionic, Dianionic, and Trianionic Forms of Tetramate	76.
Figure I-17. Substrates for C3Anion Chemistry.	55
Figure I-18. Various Heterocycles Under Study.	64
Figure I-19. Target IMDA Precursor.	81
Figure I-20. Two Main Stereoisomers From IMDA of 97 .	82
Figure I-21. General Key Features of all IMDA of 97 .	90
Figure I-22. Benzene Titrations of major IMDA isomer <i>endo</i> -I in CDCl ₃ .	92
Figure I-23. Benzene Titrations of Minor IMDA isomer <i>endo</i> -II in CDCl ₃ .	93
Figure I-24. Stacked ¹ H NMR of <i>endo</i> -I (bottom) and <i>7epi-endo</i> -I (top) in CDCl ₃ .	99
Figure I-25. Stacked ¹ H NMR of <i>endo</i> -II (bottom) and <i>7epi-endo</i> -II (top) in CDCl ₃ .	101
Figure I-26. Summary of Structural Assignments IMDA Products of 97 .	102
Figure I-27. Stacked ¹ H NMR of <i>endo</i> -I (bottom) and <i>endo</i> -II-d ₂ (top) in Benzene.	104
Figure I-28. Stacked ¹ H NMR of <i>endo</i> -II (bottom) and <i>endo</i> -II-d ₂ (top) in CDCl ₃ .	105
Figure II-1. Compounds Isolated in Previous Studies.	185
Figure II-2. Model Alkaloids for RPLC Development.	187
Figure II-3. Selected Alkaloids from <i>T. heterophylla</i> .	194
Figure II-4. Alkaloids from <i>T. heterophylla</i> Representing a More Diverse Family.	195
Figure II-5. Selected Alkaloids from <i>T. siphilitica</i> .	196
Figure II-6. Selected Alkaloids from <i>T. sananho</i> .	197
Figure II-7. Alkaloids found from <i>T. heterophylla</i>	199
Figure II-8. Alkaloids found from <i>T. siphilitica</i>	200

Figure II-9. Alkaloids found from <i>T. sananho</i>	201
Figure III-1. A Soyoil Triglyceride.	227
Figure III-2. NMR spectrum of Cleavage with Octyl Amine at Low Conversion.	231
Figure III-3. Cleavage Products of MSBO.	233
Figure III-4. Potential Products of Cyclohexene Oligomerization.	236
Figure III-5. Potential Products of Oxidative Oligomerization of Cyclohexene.	237
Figure III-6. Epoxidized Soy Triglyceride with 6 Epoxides.	258
Figure III-7. Terpenes and Terpenoids.	268
Figure III-8. Model Compounds Derived from Menthide and 407 .	274
Figure III-9. Model Compounds Derived From <i>trans</i> and <i>cis</i> Carvomenthide (405).	275
Figure III-10. Different Ways to Attach Three Monomers to 407 .	275
Figure III-11. Higher Order Oligomers from Thermal Ring-opening of Carvomenthides.	276
Figure III-12. Renewable Ketones From Previous Studies.	280
Figure III-13. Major Conformation of Menthone (400).	282
Figure III-14. Major Conformers of Isomenthone (<i>cis</i> - 400).	283
Figure III-15. Conformational Preference of <i>trans</i> Carvomenthone (<i>trans</i> - 404).	285
Figure III-16. Major Conformer of <i>cis</i> Carvomenthone (<i>cis</i> - 404).	286
Figure III-17. Conformational Preference of <i>trans</i> - 401 .	287
Figure III-18. Conformational Preference of <i>cis</i> - 401 .	288
Figure III-19. Conformational Preference of <i>trans</i> - 405 .	289
Figure III-20. Conformational Preference of <i>cis</i> - 405 .	289
Figure III-21. Conformational Preference of Abnormal <i>trans</i> -carvomethide (<i>trans</i> - 406).	290
Figure III-22. Conformational Preference of Abnormal <i>cis</i> carvomenthide (<i>cis</i> - 406).	291

List of Schemes

Scheme I-1. Floreancig Retrosynthetic Analysis.	5
Scheme I-2. Floreancig Route to Spirocycle.	6
Scheme I-3. Roush Retrosynthetic Analysis.	6
Scheme I-4. Roush Route to Spirocycle 5 .	7
Scheme I-5. A. IMDA Examples From the Roush Work.	8
Scheme I-6. Lewis Acid Catalysis of Allylic Alcohol.	8
Scheme I-7. Completion of the Roush Synthesis of Core of Integramycin.	9
Scheme I-8. Gras' Experimental Observations.	12
Scheme I-9. Roush's IMDA Analysis for 1,7,9-decatrien-3-ones.	13
Scheme I-10. The Self-Assembly of Squalene.	13
Scheme I-11. Examples of Diels-Alderases and Substrates.	15
Scheme I-12. Observed IMDA Cyclization During the Synthesis of UCS1025A and its <i>Tetra-epimer</i> .	16
Scheme I-13. Required IMDA Chemistry to Generate Relative Stereochemistry of 2 .	18
Scheme I-14. Change in IMDA Stereochemical Outcome Upon Bond Rotation.	19
Scheme I-15. Plan for Model of 2	20
Scheme I-16. Ultimate Unveiling and IMDA of a General Reactive Triene.	21
Scheme I-17. Retrosynthetic Analysis I.	22
Scheme I-18. Preparation of <i>E,E</i> -diene.	23
Scheme I-19. Regioselectivity of Claisen Rearrangement of 35 .	24
Scheme I-20. Stereoselectivity of Claisen Rearrangement of 35 .	25
Scheme I-21. Johnson-Claisen studies.	26
Scheme I-22. Preparation of Aldol Reagent Imide.	27
Scheme I-23. Crimmons' Aldol Reaction With Hexanal.	27
Scheme I-24. Further Chemistry on Hexanal Aldol Product.	30
Scheme I-25. Crimmins' Aldol on Aldehyde 36 and Generation of Aldehyde 30 .	31
Scheme I-26. Weinreb Amide Route to Aldehyde 30 .	32
Scheme I-27. General Ways to Heterocycles 32 and 33 .	33
Scheme I-28. Oxidation and Reduction of Maleimide (50a).	33
Scheme I-29. Attempted Reductive Amination of Imide 50a .	34
Scheme I-30. Attempted Mitsunobu with 50a .	34
Scheme I-31. Transformation of Maleic Anhydride to Maleimide 50d .	35
Scheme I-32. Attempted Reductive Amination of DMBNH ₂ .	35
Scheme I-33. Azide Route to Aryl Amines.	36
Scheme I-34. Transformation of Maleic Anyhydride to Maleimide 50b .	36
Scheme I-35. Attempted Oxidation of 50b .	36
Scheme I-36. Completion of Heterocycle 59 From 50d .	38
Scheme I-37. The Key C3 Reaction to Build Functionality From 59 and 60a/b .	38
Scheme I-38. Lacey-Dieckman Methodology for HWE Coupling Partner 32 .	39
Scheme I-39. Preparation of 62 .	40
Scheme I-40. Attempted acetoacetylation of amine 62 starting from diketene.	40
Scheme I-41. Preparation of Diketene and Two Step Process to Dicarboxyl.	41

Scheme I-42. Attempted Use of 63 for Acetylation of 62 .	41
Scheme I-43. Preparation of Bromo-Thioesters 70 From Meldrum's Acid.	42
Scheme I-44. Amide 49 From Bromo-Thioesters 70 .	43
Scheme I-45. Use of 1,3-Dioxenone (64) in the Preparation of Phosphorane 74 .	44
Scheme I-46. Attempted Olefination Reactions of Aldehyde 30 .	45
Scheme I-47. Preparation of 76 and 77	48
Scheme I-48. Attempted Functionalization of 3-Carbomethoxy- 2,4-pyrrolidinedione 77 .	49
Scheme I-49. Outcome of Alkylation of 77 .	49
Scheme I-50. Potential Further Functionalization of Tetramate 76 .	50
Scheme I-51. Deuterium Exchange of 76 .	51
Scheme I-52. Retrosynthetic Analysis II.	52
Scheme I-53. Methods for C3-Anion Chemistry.	53
Scheme I-54. Homologation of CyCHO and attempted homologation of aldehyde 97 .	54
Scheme I-55. 3-Step Homologation of Aldehyde 30 .	54
Scheme I-56. Optimization of Homologation Sequence.	55
Scheme I-57. Regiochemistry of Alkylation of 59 and Respective Organometallics.	56
Scheme I-58. Substitution at C5 With a Bulkier Group.	56
Scheme I-59. General Scheme for Metal-Halogen Exchange and Subsequent Reaction.	56
Scheme I-60. Deuterium Substitution at C3 of Iodide 60a .	57
Scheme I-61. Deuterium Substitution at C5 of 59 .	57
Scheme I-62. General Anion Chemistry of Diols 105 .	59
Scheme I-63. Preparation of Diol 105a and Subsequent Substitution Attempt.	59
Scheme I-64. Preparation of Alcohol 111 and C3-Substitution Reaction.	61
Scheme I-65. Attempted C3 Substitution with Aldehyde 36 and Benzaldehyde.	62
Scheme I-66. Reduction of Diol 118 at C5 and Attempted C3-Alkylation.	63
Scheme I-67. Attempted Union of 111 and Ene-Aldehyde 97 .	63
Scheme I-68. Attempt to Synthesize 83b from 1,3-Dioxenone (64).	65
Scheme I-69. Attempt to Synthesize 83b from Decarboxylation.	65
Scheme I-70. Attempt to Synthesize 83b by Dieckmann Reaction.	65
Scheme I-71. Attempt to Synthesize Heterocycle 122 by Ring-opening/ Ring-closing Sequence.	66
Scheme I-72. Attempted DCC Coupling with Ene-acid 129 and Meldrum's acid.	67
Scheme I-73. Direct Aldol on NMP and γ -butyrolactone with 31 .	67
Scheme I-74. Attempted Preparation of Mukaiyama Regent 135 .	68
Scheme I-75. Mukaiyama Aldol Reaction of γ -butyrolactone and Aldehyde 138 .	68
Scheme I-76. Mukaiyama Aldol of γ -Butyrolactone and 138 Under $\text{BF}_3 \cdot \text{OEt}_2$ Promotion.	69
Scheme I-77. Mukaiyama Aldol Reaction of γ -Butyrolactone and Aldehyde 97 .	69
Scheme I-78. Retrosynthetic Analysis III.	70
Scheme I-79. Plan for Building β -keto Amide From Ring-Opening of 145 .	71
Scheme I-80. Attempted Transformation of 30 into β -Keto Donor.	71

Scheme I-81. Attempted Installation of Dicarboxyl by Mukaiyama Chemistry.	72
Scheme I-82. Stepwise Synthesis of Dicarboxyl 151 .	73
Scheme I-83. Further Reaction of 151 to Tricarboxyl 155 .	73
Scheme I-84. Attempted Amide Bond from Acid 151 and Glycine Derivative 62 .	74
Scheme I-85. Attempted HWE with Phosphonate 49 and aldehyde 30 .	75
Scheme I-86. Modified Retrosynthetic Analysis III.	75
Scheme I-87. Use of Phosphonate-thioester 65 in HWE with 30 .	76
Scheme I-88. Thioester-amine Coupling of 159 and 62 .	76
Scheme I-89. Dieckmann Reaction of 157a .	77
Scheme I-90. Coupling with a 1° Amine and Failed Dieckman.	77
Scheme I-91. Additional Attempts at Dieckmann of 157b .	78
Scheme I-92. First Warning of IMDA Lability of 75a .	78
Scheme I-93. Attempted Deprotection Towards IMDA Precursor.	79
Scheme I-94. General Triene Cycloaddition.	81
Scheme I-95. First IMDA Observed.	82
Scheme I-96. <i>E</i> to <i>Z</i> Isomerization and Result of [4+2].	85
Scheme I-97. IMDA of Ester 95 and Methyl Ketone 148 .	86
Scheme I-98. Attempted IMDA of Nitrile 164 and Weinreb Amide 154 .	86
Scheme I-99. Attempted IMDA of β-keto Ester 151 and Alcohol 165 .	87
Scheme I-100. IMDA of Amides 157 .	87
Scheme I-101. IMDA of Tricarboxyl Triene 155 .	88
Scheme I-102. IMDA of Heterocycle Triene 75a .	89
Scheme I-103. IMDA of aldehyde 97 leading to major and minor product and proposed TSs.	90
Scheme I-104. Derivative of IMDA adduct <i>endo</i> -I or <i>endo</i> -II.	94
Scheme I-105. Reduction of <i>endo</i> -I to Alcohol 169 and Attempted Bromoetherification.	95
Scheme I-106. Saponification to Acid 172 and Attempted Iodolactonization.	96
Scheme I-107. D-exchange to For Peak Shape Analysis and <i>J</i> values.	97
Scheme I-108. Observed Epimerization Upon H-D Exchange on <i>endo</i> -I.	97
Scheme I-109. Epimerization of Major IMDA Isomer <i>endo</i> -I.	98
Scheme I-110. Epimerization of Minor IMDA Isomer <i>endo</i> -II.	100
Scheme I-111. D ₂ Incorporation of Octalins <i>endo</i> -I and <i>endo</i> -II from 31 .	103
Scheme I-112. TBS Removal from Octalin 162a .	106
Scheme I-113. Attempted PMB Removal of Octalin 162a .	106
Scheme I-114. Removal of PGs.	107
Scheme I-115. Attempted Dieckmann of 161b .	108
Scheme I-116. Attempted Silylation of 162a .	108
Scheme I-117. Assumption of Identical Stereochemistry of 26 .	109
Scheme II-1. Steps in McKenna's Ethnopharmacological Approach	183
Scheme II-2. Remaining Steps in McKenna's Ethnopharmacological Approach	184
Scheme II-3. Decarboxylation of 201 and 202 .	202

Scheme II-4. Attempted Oxidation of 206.	203
Scheme II-5. Acetylation of 206.	204
Scheme III-1. General Reaction to a Carbamate.	225
Scheme III-2. General Reaction to a Polyurethane.	225
Scheme III-3. Construction of a Cross-linked PU.	225
Scheme III-4. Chromatography of Soyoil.	228
Scheme III-5. Cleavage of Soyoil Into Component Fatty Acid Esters/Amides.	229
Scheme III-6. Partial Cleavage of Soyoil.	231
Scheme III-7. Metathesis of Soybean Oil.	232
Scheme III-8. MPLC of Crude MSBO.	233
Scheme III-9. Observed Oligomerization of 301 and 302.	235
Scheme III-10. Alkene Isomerization of 301 and 302 Under $\text{BF}_3 \cdot \text{OEt}_2$.	235
Scheme III-11. Observed Autoxidation of Linoleic Acid (303).	238
Scheme III-12. Observed Autoxidation of 302.	239
Scheme III-13. Mandy's Thiol-ene on Methyl Oleate (310) and 301.	239
Scheme III-14. Mandy's Bis Thiol-ene on 310 and 301 with 1,3-propanedithiol (311).	241
Scheme III-15. Scale-up of Thiol-ene of 310 and Reduction to Diol.	242
Scheme III-16. Thiol-ene Reaction on Soyoil.	242
Scheme III-17. Transformations of LA.	243
Scheme III-18. Observed Oligomerization of 318 and Route to Potential Recovery.	244
Scheme III-19. Bis Thiol-ene of LA Dithiol (319) With Cyclohexene.	244
Scheme III-20. Attempted Cross-linking of 310 With Dithiols 316, 317, and 319.	245
Scheme III-21. Attempted Reduction of Mono-ene Products 327-329.	245
Scheme III-22. Attempted Cross-linking of Soyoil by 311.	247
Scheme III-23. Radical Chemistry of Thiols.	247
Scheme III-24. General Disulfide Addition Across an Alkene.	248
Scheme III-25. Disulfide Reaction under I_2 conditions: DMDS and 310.	249
Scheme III-26. Disulfide Reaction Under I_2 Conditions on 301.	249
Scheme III-27. Disulfide Reaction Under I_2 Conditions on 302.	250
Scheme III-28. Disulfide Reaction of Dibenzyl disulfide under I_2 conditions on 310.	251
Scheme III-29. Disulfide Reaction of 334 and 310 under I_2 conditions.	251
Scheme III-30. Observed Transesterification of 310 promoted by I_2.	252
Scheme III-31. Attempted disulfide reaction of 349 with 310 under I_2 conditions.	252
Scheme III-32. Disulfide Reaction of 310 Under $\text{BF}_3 \cdot \text{OEt}_2$ Conditions.	253
Scheme III-33. Disulfide Reaction of 301 and 302 under $\text{BF}_3 \cdot \text{OEt}_2$ Conditions.	253
Scheme III-34. Disulfide reaction of 334 and 310 Under $\text{BF}_3 \cdot \text{OEt}_2$ Conditions.	254
Scheme III-35. Disulfide Exchange Reaction of DMDS and 334.	255
Scheme III-36. Mixed Disulfide Reaction of DMDS and 334 on Cyclohexene.	256
Scheme III-37. Mixed Disulfide Reaction of DMDS and 334 on 310.	256

Scheme III-38. Disulfide Exchange reaction of 318 and DMDS or 334 .	257
Scheme III-39. General Strategy for Simultaneous Cross-linking/ Functionalization of Alkenes.	257
Scheme III-40. Attempted Cross-linking / Functionalization of Cyclohexene.	257
Scheme III-41. MPLC Separation of Methyl Epoxy Soyates.	259
Scheme III-42. 365 opening by 332 .	260
Scheme III-43. Reaction of 368 with Isocyanate 371 .	260
Scheme III-44. Epoxy Methyl Linoleate (366) Opening by 332 .	261
Scheme III-45. Byproduct of 332 Opening of 366 .	261
Scheme III-46. 366 Opening by Butanethiol (331).	263
Scheme III-47. Opening of 366 by Mono-protected Mercaptoethanol (378).	263
Scheme III-48. Opening of 367 by 331 .	264
Scheme III-49. Opening of 367 opening by 332 .	265
Scheme III-50. Stability of Hexaol 381 Under Various Conditions.	266
Scheme III-51. Attempted Opening of Epoxide with 368 .	266
Scheme III-52. General Strategy for Converting Terpenes to Polyols	268
Scheme III-53. Polymerization of Cyclohexanone.	269
Scheme III-54. The Baeyer-Villiger Reaction of Menthone.	270
Scheme III-55. Synthesis of <i>trans</i> and <i>cis</i> Carvomenthide (405).	271
Scheme III-57. General ROP of Lactones <i>trans</i> - 401 and 405 With Initiator 407 .	271
Scheme III-58. Ring Opening to Methyl Esters 408 and 409 .	272
Scheme III-59. Ring-opening of Menthide Under Different Monomer Loadings.	273
Scheme III-60. Ring-opening Polymerization Study.	277
Scheme III-61. Carbamate Reaction Diagnostic NMR Resonances.	278
Scheme III-62. Competition Experiment for Carbamate Formation.	278
Scheme III-63. Epimerization of Menthone (400).	281
Scheme III-64. Deuterium Incorporation of 400 .	282
Scheme III-65. Epimerization of Carvomenthone (404).	284
Scheme III-66. Deuterium Incorporation of 404 .	286

List of Pictures

Picture II-1. Normal Phase Chromatogram of <i>T. heterophylla</i> (CMA mobile phase)	188
Picture II-2. Hydroquinidine 4-Cl-benzoate (Alone)	190
Picture II-3. Mixture of 3 Test Alkaloids (Quinine, Hydroquinidine 4-Cl-benzoate, and the Cinchonidine alkaloid)	190
Picture II-4. Quinine, Cinchonidine, and Hydroquinidine Alkaloids (New Conditions).	191
Picture II-5. Uracil Behavior (and Replications).	191
Picture II-6. Improved Separation of a Mixture of Test Alkaloids (Uracil, Quinine, Hydroquinidine 4-chlorobenzoate).	192
Picture II-7. <i>Tabernaemontana heterophylla</i> .	194
Picture II-8. <i>Tabernaemontana siphilitica</i> .	195
Picture II-9. <i>Tabernaemontana sananho</i> .	197
Picture II-10. RPLC of Crude <i>T. siphilitica</i> Extracts	200
Picture II-11. RPLC to Separate 201 and 202 .	200
Picture II-12. RPLC of Crude <i>T. sananho</i> Extracts.	201

Chart

Chart II-1. Phytochemical Distribution of McKenna's Collection

183

List of Abbreviations

Ac	Acetyl
AcCl	Acetyl Chloride
Ar	Aryl
ATA	Acyltetramic Acid
Bn	Benzyl (C ₆ H ₅ CH ₂ -)
BV	Baeyer-Villiger
°C	Degrees Celsius
Calcd	Calculated
COSY	Correlated Spectroscopy
CYP	Cytochrome P450
DBU	1,8-Diazabicyclo[5.4.0]undec-7-ene
DCM	Dichloromethane
DEPT	Distortionless Enhancement Polarization Transfer
DIBALH	Diisobutylaluminum Hydride
DIPEA	Hünig's Base, Diisopropylethylamine
DMAP	4-dimethylaminopyridine
DMB	2,4-Dimethoxybenzyl
DMF	Dimethylformamide
DMP	Dess-Martin Periodinate
DMSO	Dimethylsulfoxide
Dppf	1,1'-Bis(diphenylphosphino)ferrocene
dr	Diastereomeric Ratio
E	Electrophile
<i>ee</i>	Enantiomeric excess
EDG	Electron Donating Group
equiv	Equivalent
Et ₂ O	Diethyl Ether
Et ₃ N or TEA	Triethylamine
EtOAc	Ethyl Acetate
EWG	Electron Withdrawing Group
GCMS or GC/MS	Capillary Gas Chromatography-Mass Spectrometry
HMBC	Hetero-Nuclear Multiple Bond Correlation
HMPA	Hexamethylphosphoramide
HMQC	Heteronuclear Multiple Quantum Correlation
HRMS	High Resolution Mass Spectrometry
HSQC	Heteronuclear Spin Quantum Correlation
IC ₅₀	50% of the concentration for complete inhibition of cellular viability
IMDA	Intra-Molecular Diels-Alder

IR	Infrared
<i>J</i>	Coupling constant (NMR)
LA	Lipoic Acid
LCMS or LC/MS	Liquid Chromatography-Mass Spectrometry
LRMS	Low-Resolution Mass Spectrum
Me	Methyl
MeI	Methyl Iodide
MeOH	Methanol
MIC	Minimum Inhibitory Concentration
mp	Melting Point
MPLC	Medium Pressure Liquid Chromatography
4Å	4-Angstrom
MS	Molecular Sieves
NaHMDS	Sodium Hexamethyldisilazide
NBS	<i>N</i> -Bromosuccinimide
NMP	<i>N</i> -methyl pyrrolidinone
NMR	Nuclear Magnetic Resonance
nOe	Nuclear Overhauser Effect
OTA	Octalinoyl Containing Tetramic Acid
PCC	Pyridinium Chlorochromate
PMB	<i>p</i> -Methoxybenzyl
PPh ₃	Triphenylphosphine
PPTS	Pyridinium <i>p</i> -Toluenesulfonate
py	pyridine
<i>i</i> -Pr or ⁱ Pr	Isopropyl
R _f	Ratio to Front
RT or rt	Room Temperature
SKA	Silyl Ketene Acetal
<i>t</i> _{1/2}	Half-Life Time
TBA	Tetrabutyl Ammonium
TBAF	Tetrabutyl Ammonium Fluoride
TBDPS	tertiary-Butyldiphenylsilyl
TBSCl	tertiary-Butyldimethylsilyl Chloride
TBSOTf	tertiary-Butyldimethylsilyl Triflate
TES	Triethylsilyl
TFA	Trifluoroacetic Acid
TIPS	Triisopropylsilyl
THF	Tetrahydrofuran
TLC	Thin Layer Chromatography
TMS	Trimethylsilyl
t _r	Retention Time

PART ONE – Integramycin

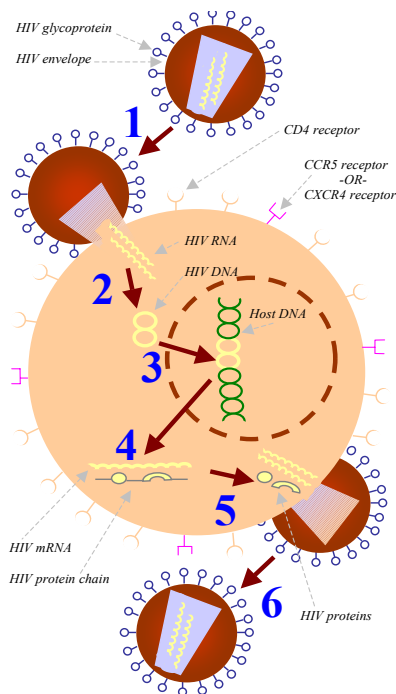
Chapter I. Introduction and Background

I.A. Isolation and Biology

Natural products have long been used as the source of inspiration for or the actual treatment of disease.^{1,2} This is because many are found to have remarkable biological activity for use in modern medicine.³ Those of polyketide origin are among the most potent of natural products and the literature continues to be filled with reports of novel polyketides with outstanding and diverse biological profiles.⁴ There is great promise for developing a natural product or similar small molecule into a drug when the biological target of the small molecules is known. Entire research programs are devoted to this science. One such program was established at Merck for molecules active against HIV-integrase.⁵

The HIV life cycle (Figure I-1⁶) is a well-understood biochemical process.⁷⁻⁹ The virus must enter the host cell, convert its RNA into DNA, integrate that DNA into the host genome, and transcribe that DNA into viral proteins and enzymes.

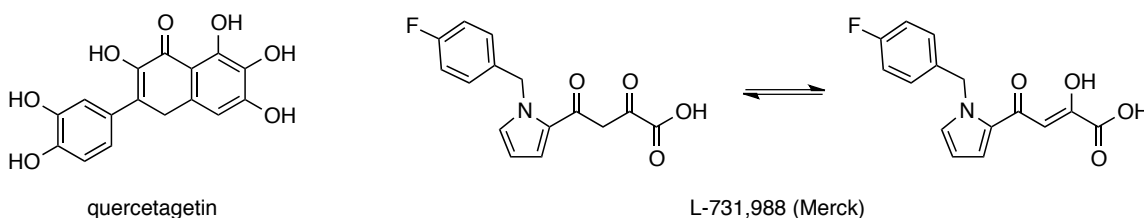
Figure I-1. The HIV life cycle



These proteins are then packaged and expelled from the cell for maturation and infection of additional healthy cells. A series of enzymes play a role in this life cycle, including fusion (step 1), nucleoside (or non-nucleoside) reverse transcriptase (step 2), integrase (step 3), and protease (step 5) enzymes. Integration of viral DNA (step 3) into the host genome is a stepwise process catalyzed by HIV-integrase.

Integrase inhibition alone is sufficient to shut down the entire viral propagation process.⁸ The earliest inhibitors of this type were hydroxylated aromatic inhibitors (Figure I-2). These catechols, however, had too diverse biological profiles and were not developed as lead compounds. A far more successful class of integrase inhibitors were the diketo acids (DKAs). Unfortunately, these inhibitors were too toxic to be developed further.⁷ To date, only one integrase inhibitor, Raltegravin,^{7,10} is FDA-approved for use in treatment of HIV.

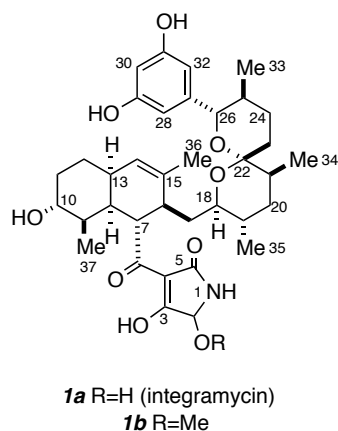
Figure I-2. Early HIV-Integrase Inhibitors.



Despite these limitations, research into the catechols and DKAs resulted in an understanding of the probable catalytic core domain as well as other features of the enzyme. One of the most valuable pieces of information was a possible mode of action for inhibition of HIV-integrase. It likely requires a divalent metal for activity (both catechols and DKAs are effective chelating agents). This makes natural products like polyketides a promising avenue to discovery of active compounds in the suppression or inhibition of the enzyme. This background prompted the research group at Merck to embark on a discovery project aimed at finding natural products for alternative lead structures in the inhibition of HIV-integrase.⁵

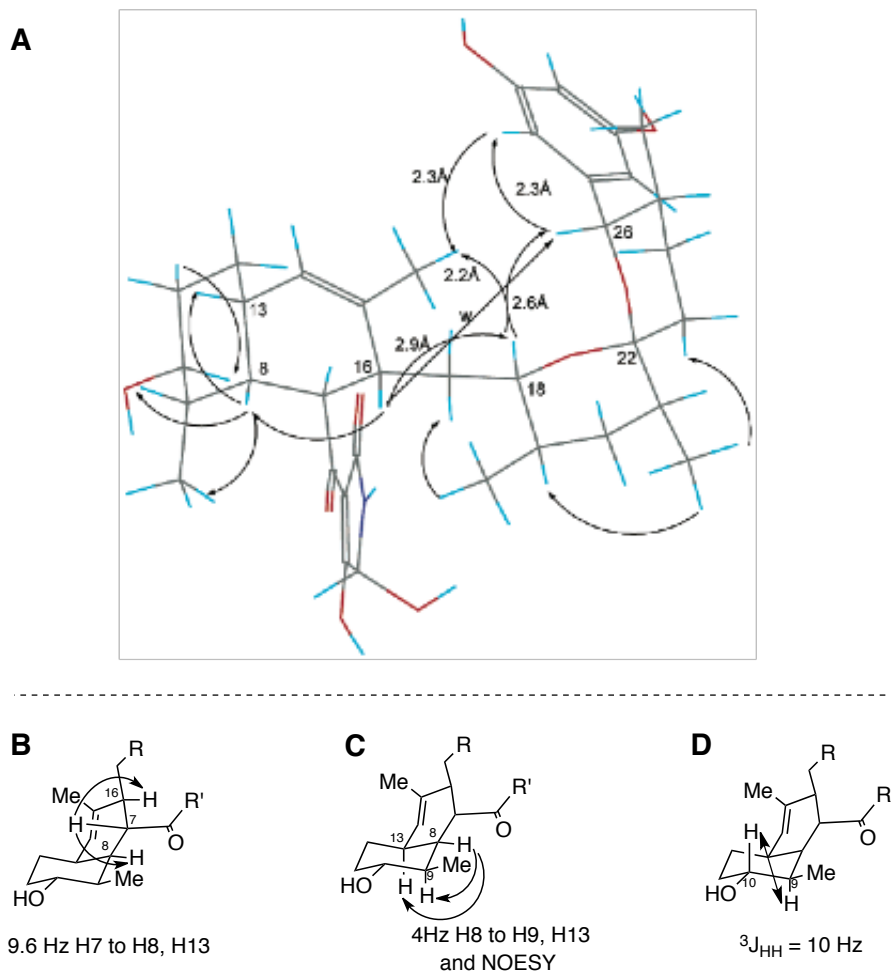
The Merck program began with screening crude fermentation extracts of bacteria cultures for activity against HIV-integrase. Several natural products were identified from initial screening of crude extracts: equisetin,^{11,12} interic acid, and complestatin. From *Actinoplanes* sp. extracts they discovered yet another novel compound, found to inhibit recombinant HIV-I integrase (specifically, the strand transfer reaction). The potent nature of this molecule (IC_{50} 4 μ m) sparked interest in identification and full structural elucidation, and also validated additional research in its stereochemistry, conformation, and biological activity.¹³

Figure I-3. Structures of Integramycin and Methanol Adduct (**1a** and **1b**)



Integramycin (**1a**, Figure I-3) was isolated by size exclusion chromatography and reverse-phase HPLC as a colorless powder. The molecular formula was suggested by high-resolution ESI-MS; its carbon skeleton was elucidated by ^{13}C NMR spectroscopy. The preliminary deduction was further refined with the help of vicinal couplings, NOESY correlations, ChemDraw 3-D modeling, and Dreiding models. Further experimentation (2D TOCSY and HMBC) led to the deduction of the relative stereochemistry shown in Figure I-3. Due to its complex NMR pattern, it was proposed to exist in several tautomeric forms, and this required spectral data to be collected in several solvents. Aminoal **1b** (from reaction with methanol) and the acetate analogue of **1a** (from reaction with acetic anhydride and pyridine, not shown) helped support the assignment. Figure I-4A is the authors' three-dimensional molecular model with the observed NOESY correlations. The most significant of these are independently shown and discussed (Figure I-4B-D).

Figure I-4. A. Singh's Chem 3D Model of Integramycin (**1a**).¹³ **B-D.** Key NMR Data.



H7 experiences a NOESY interaction with both H8 and H16, and the coupling constant (9.6 Hz) indicated a diaxial relationship between all of these protons (arrows in Figure I-4A). H8 couples with both H9 and H13 (arrows in Figure I-4B) where the $^3J_{HH}$ of 4Hz suggests that the latter two are axial with H8 becoming equatorial with respect to them. NOESY correlations were also observed between H8 and H13 and H9 (arrows in Figure I-4B). Coupling constant analysis was enabled by the assumption that the cyclohexene adopts a half chair conformation with the *cis*-fused cyclohexyl unit sitting perpendicular and adopting the expected chair conformation. The observed 10Hz coupling between H10 and both H9 (arrows in Figure I-4C) indicated both of the protons were axial. Compilation of these data gave the relative stereochemistry (7*S*, 8*R*, 9*R*, 13*R*, 16*S*, 18*R*, 19*S*, 21*S*, 23*R*, 25*S*, 26*S*), shown in for **1a** in Figure I-3.

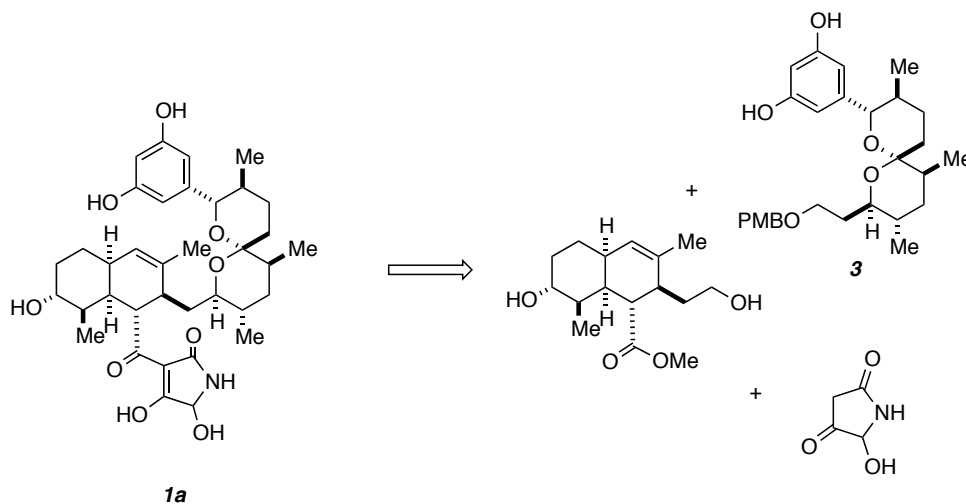
I.B. Previous Work on Integramycin

Because of its unique structure and potential for development into a novel therapy for HIV, integrumycin attracted attention from the synthetic community. It has been the subject of particular study by two groups. The Floreancig¹⁴ and Roush¹⁵ groups both succeeded in a stereoselective synthesis of the spiroketal moiety. The Floreancig report is briefly presented, but a more detailed presentation of Dineen and Roush's studies of the octalin of **1a**¹⁶ are contained in the next section.

I.B.1. Floreancig's Synthesis of the Spirocycle

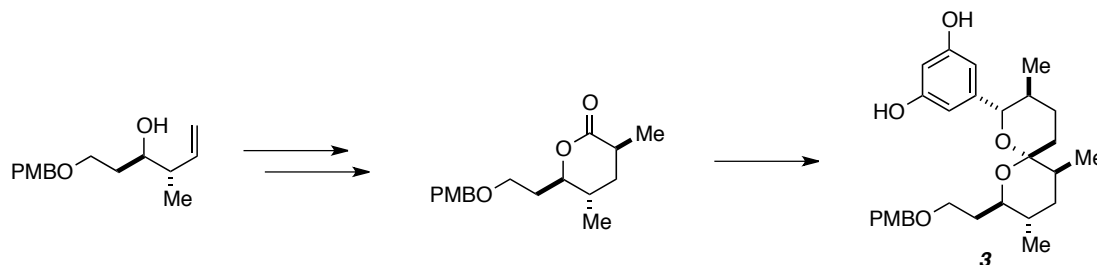
The first synthetic efforts reported for **1a** were those by Wang and Floreancig (Scheme I-1).¹⁴ The authors envisioned the entire molecule being constructed from three smaller segments; these would have the task of supplying the tetramic acid, octalin, and spirocycle **3**.

Scheme I-1. Floreancig Retrosynthetic Analysis.



They saw the spirocycle **3** arise from a C,O-dianion reaction with a lactone (shown in Scheme I-2). This sequence required use of several rather exotic reagents for proper stereocontrol but had the advantage of providing the spirocycle that was poised for further functionalization. The lactone was available in several steps from a homoallylic alcohol; the key reaction of this sequence was the regioselective addition of formic acid across the olefin present in the molecule. $\text{Ru}_3(\text{CO})_{12}$ was utilized as an inexpensive source of the transition metal catalyst.

Scheme I-2. Floreancig Route to Spirocycle.



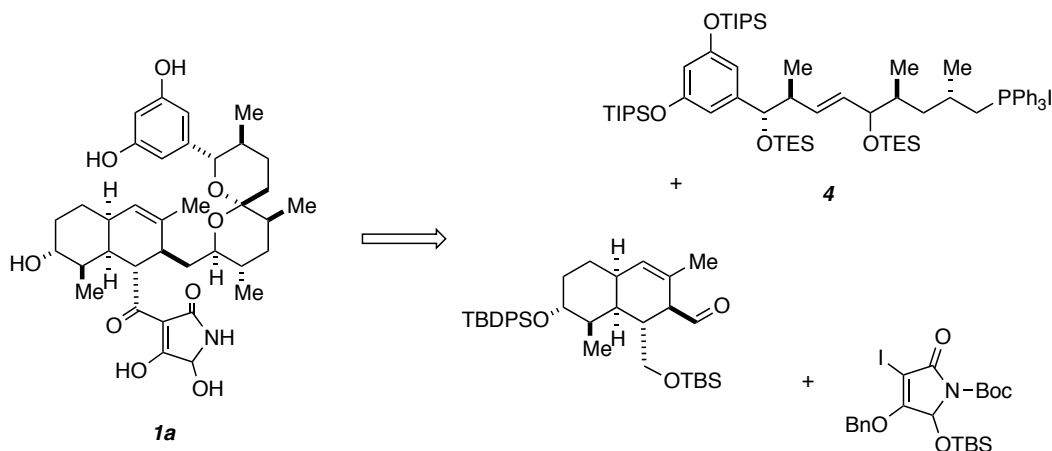
Additional studies in this group were directed at the tetramic acid unit. These are not discussed here, but are reported in thesis documents of interest.¹⁷

I.B.2. Roush's Synthesis of the Spirocycle and Octalin

Two relevant research efforts focused on integrAMYCIN emerged from the Roush group. The first was a synthesis of the octalin unit utilizing their depth of understanding of intramolecular Diels-Alder chemistry.¹⁶ The more recent publication involves a synthesis of the spiroketal.¹⁵

Although their spirocycle studies fall chronologically after their octalin studies, they are discussed first (Scheme I-3). The authors envisioned a construction of the natural product that involved the already formed octalin, a properly functionalized tetramic acid (currently in the form of an alkyl halide), and a linear segment **4** which was proposed to assemble into the spirocycle.

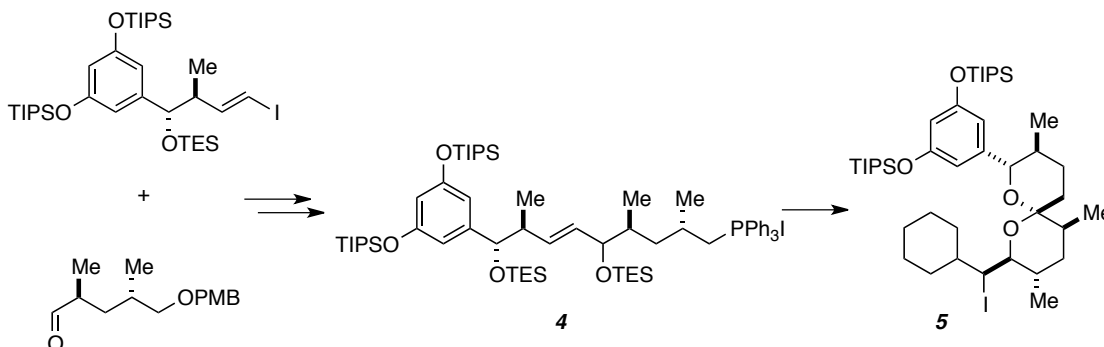
Scheme I-3. Roush Retrosynthetic Analysis.



The successful construction of the spirocycle **5** involved both a Nozaki-Hiyama-Kishi reaction (between an vinyl iodide and aldehyde, leading to **4**) and a Horner-Wadsworth-

Emmons (HWE, not shown) to install the olefin and cyclohexane (Scheme I-4). To complete the closure, the authors chose N-Iodosuccinimide as a promoter. Unfortunately, several more steps were required, and although this route gave modest quantities of valuable synthetic intermediates like spirocycle **5**, no further studies toward a total synthesis of **1a** were revealed.

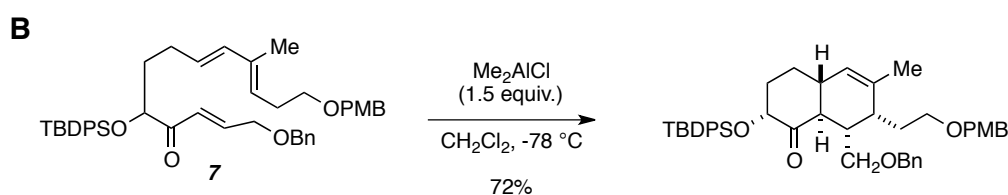
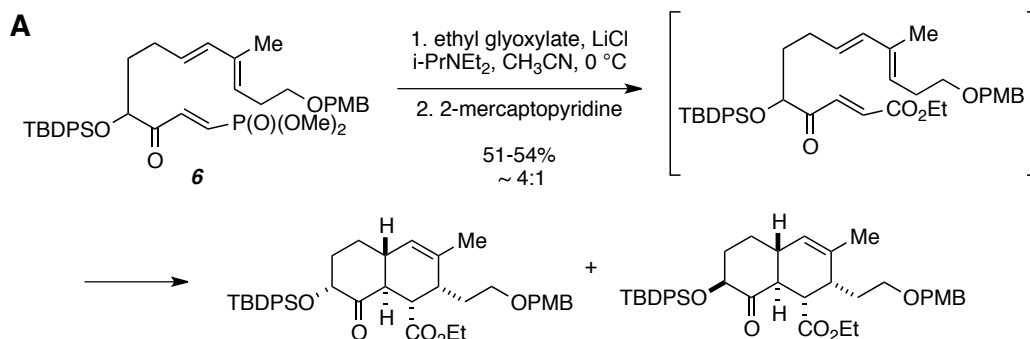
Scheme I-4. Roush Route to Spirocycle **5**.



Prior to this spirocycle synthesis, Dineen and Roush successfully completed a stereoselective synthesis of the octalin core of **1a**.¹⁶ Based on their own previous work,¹⁸ they envisioned the Diels-Alder reaction to proceed in one of two ways, either would give rise to the *cis*-fused bicycle (see Scheme I-9, Transition State (TS) analysis and surrounding discussion).

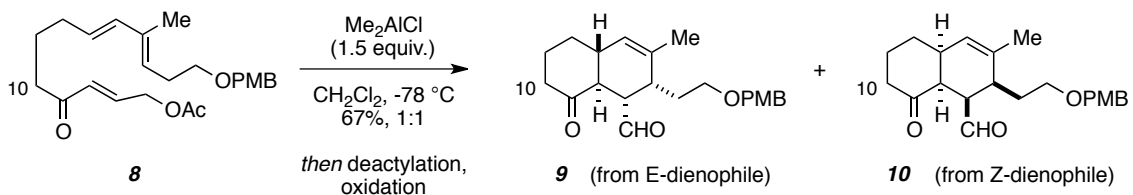
In their initial synthetic work, Dineen and Roush were unsuccessful in observing any *cis*-fused octalins (Scheme I-5A). Their precursor triene (from Horner-Emmons reaction of **6** with ethyl glyoxylate) reacted in situ to give two main stereoisomers in a ratio of 4 to 1. Because they were not expecting any *trans*-fused bicycles, they reasoned that perhaps the terminal carboethoxy group was interfering with their expected Diels-Alder reaction. Thus, they prepared the substrate **7** (Scheme I-5B), but found that it, like **6**, reacted to a *trans*-octalin. All of their adducts were assigned by NOE and coupling constant analysis.

Scheme I-5. A. IMDA Examples From the Roush Work.



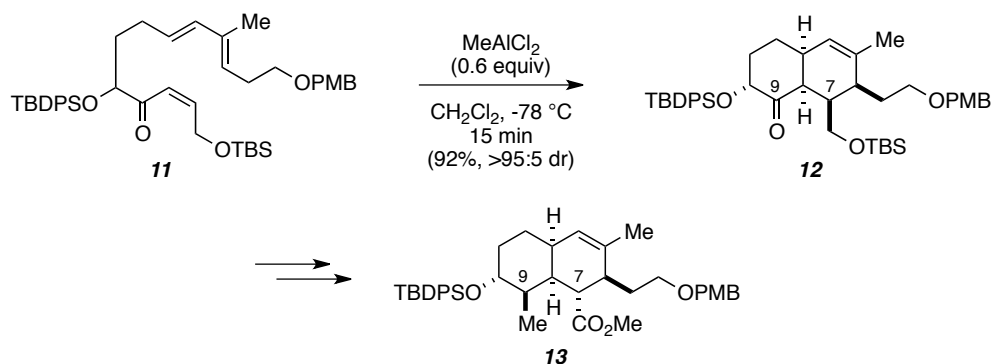
Since these substrates seemed to prefer reaction to give *trans*-fused bicycles, the authors considered altering the tether substituent, and synthesized the C10(H) precursor (**8**, Scheme I-6). Here, they finally observed a competitive IMDA where the *trans*- and *cis*-fused bicycles (**9** and **10**, respectively) were generated in equal molar ratios.

Scheme I-6. Lewis Acid Catalysis of Allylic Alcohol.



Octalin **10**, with the stereochemistry as desired, was surmised to arise from the *Z*-dienophile, so Roush and coworkers' new strategy was to utilize an alkene of this kind. When they completed the required chemistry toward *Z,E,E*-triene **11** (Scheme I-7), they found it cyclized under their same mild conditions, and provided **12** in a straightforward fashion. The *cis* ring fusion procured, they went about accessing the remainder of the stereocenters at C7 and C9 (to **13**, matching the stereochemistry of **1a**) through a series of manipulations. There was also work in this group on a synthesis of the tetramic acid,¹⁹ but those efforts are not summarized here.

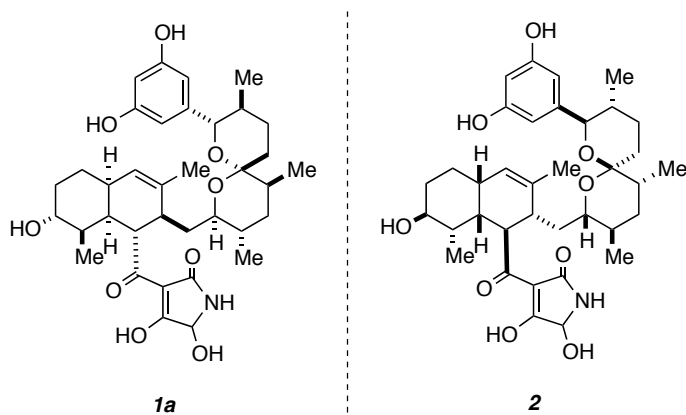
Scheme I-7. Completion of the Roush Synthesis of Core of Integramycin.



In the end, the Roush group prepared *cis*-fused octalin **13** that had the stereochemistry as reported for **1a** and made some key observations that were relevant to our studies. For example, they discovered a reversal in selectivity for IMDA of (otherwise identical) *E*- and *Z*-dienophiles. Interestingly, none of their *E,E,E*-trienes cyclized to give *cis*-fused bicycles. They prefer to think these events occur via boatlike transition states,²⁰ regardless of starting alkene geometry or activation of the dienophile. Their analysis and rationale will enter into our appraisal of integramycin.

We appreciate the Roush work for the successful completion of the octalin portion of the natural product **1a** and their contribution to the body of work on IMDA reactions. However, our interest in integramycin (**1a**) has always been its biosynthesis. The Roush work, although elegant, was not biomimetic and did not address the relative stereochemistry of an IMDA as a biosynthetic event. The absolute configuration of the natural product has not been determined.⁷ For our analysis and the remainder of this document, consideration will be given to the antipode (**2**, Figure I-5).

Figure I-5. Integramycin **1a** and Antipode **2**.



I.C. Mechanistic and Biosynthetic Considerations

We propose a spontaneous (= non-enzymatic) intramolecular Diels-Alder reaction as the key biosynthetic event that accounts for the octalin portion of the natural product integramycin (**1a**). Before more discussion and how we came to think this way, there was a wealth of background information and thought that went into this hypothesis. A detailed understanding of IMDA reactions, polyketide synthesis (including enzymatic involvement), and the outcomes of previous research all figured into our proposal.

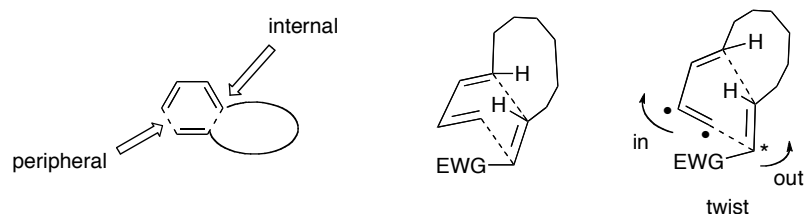
I.C.1. The Diels-Alder Reaction – Key Predictions and Details

I.C.1.a. Asynchronous Reactions and Frontier Molecular Orbital (FMO) analysis

Because this project is fundamentally about our biosynthetic hypothesis and the likelihood of non-enzymatic IMDA based on observed stereochemistry (especially a *cis* ring fusion), we first surveyed the literature for a full understanding of IMDA transition states. In the early days of theory, Dewar suggested that most multi-bond reactions must occur asynchronously. Houk's computations on simple *intermolecular* Diels-Alder reactions did not support this claim.²¹ For IMDA reactions of unsubstituted trienes, *ab initio* studies and molecular mechanics using Monte Carlo conformational searching have found low or no *trans/cis* selectivity. The same report contained experimental work that found no selectivity for the same type of system.

Houk used the concept of asynchronicity (Figure I-6) to explain his observations of a slight preference for one stereochemical result in intramolecular cycloadditions.²¹ The concept is that the “internal” bond is expected to be longer, simply because the unsubstituted termini can approach one another and interact (i.e. for the “peripheral bond”) to a greater extent in the transition state. In the case of other substitution, specifically an electron withdrawing group (EWG) on the dienophile terminus, Houk coined the term “twist-asynchronous” to describe the asynchronous, albeit concerted, nature of the reaction.

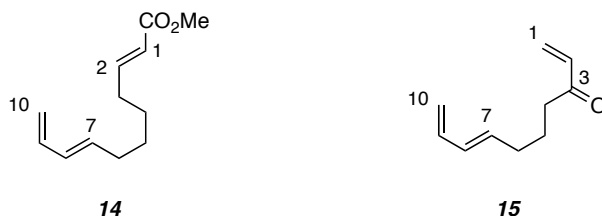
Figure I-6. Houk's IMDA Transition State Analysis of Terminally Substituted Dienophiles.



With an EWG on the terminus of the dienophile, more strain is introduced in the alkyl tether region. Relief of this strain comes from movement of the carbon marked “*” (twisting out), and those marked “•” (swinging inward). Houk claimed there is no additional strain if the tether is four carbons long because it can adopt a chair-like conformation. The outcome of Figure I-6 is a *trans*-fused bicycle.

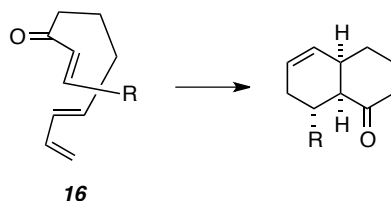
Roush complemented the analysis of IMDA transition states with a Frontier Molecular Orbital (FMO) analysis.²⁰ *Trans* selectivity should increase for the substrate **14** (Figure I-7) since the coefficients on C2 and C7 increase relative to C1 and C10. There is a greater extent of internal bonding in the transition state, so a greater amount of “twist asynchronicity” is expected. Experiments with EWGs at the terminus of the dienophile such as CONR₂, COMe, and CHO support this explanation. Conversely, a high degree of *cis*-selectivity is predicted with an internally activated dienophile (c.f. **15**). Now, the termini C1 and C10 have larger coefficients relative to C2 and C7 and experience greater bonding in the TS.

Figure I-7. FMO Analysis on Activated Dienophiles.



Indeed, strong *cis*-selectivity was experimentally observed²² for internally activated dienophiles (**16**, Scheme 1-8) that supports this FMO analysis.

Scheme I-8. Gras' Experimental Observations.



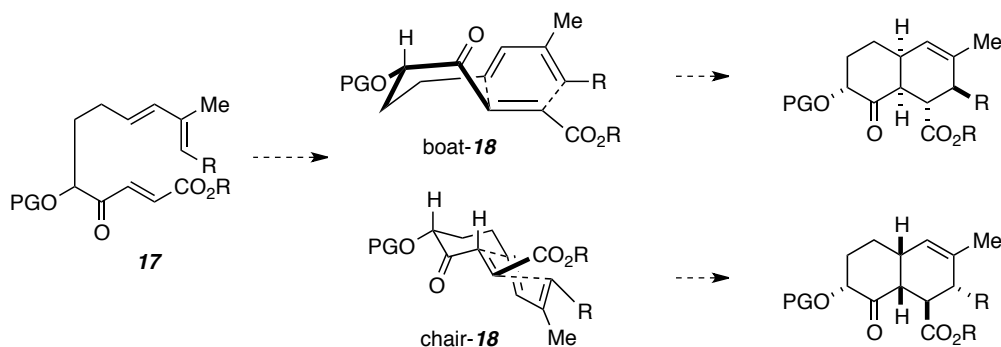
As suggested from Gras' figure, the tether between the diene and dienophile does not have to adopt a chair-like conformation. Houk explored the possibility of half-chair and twist boat transition structures, but these studies were unable to predict experimental outcomes. Further experiments and computations (especially optimized computational parameters) need to be performed to discern the likelihood of these other transition state conformations.

I.C.1.b. Invoking a Boat-like Transition State

In the event where the tether is substituted, Roush and Coe completed a thorough experimental and computational analysis.²⁰ One of the main conclusions was that *cis*-selectivity of certain substrates results from direct involvement of boat-like transition states. They concluded that IMDA of 1,7,9-trienes containing 3-oxo functionality will cyclize through a transition state where the alkyl tether adopts a boat-like conformation, an idea originally introduced and utilized by Taber.²³ A twist boat has also been suggested. When cyclohexanes contain three trigonal centers (as in these systems), the twist boat becomes comparable to a chair. Again, there is not yet sufficient computational support for many of these predictions.

Nevertheless, Roush took these predictions and elected to experimentally study the hypothesis that twist-boat or boat-like conformations of the tether in the transition state are not only tolerated but actually favored in the case of 1,7,9-decatrien-3-ones (e.g **17**, Scheme I-9). The severity of non-bonded interactions in the chair transition state (chair-**18**) forces the tether to adopt a boat-like conformation (boat-**18**). Note that a *cis*-fused bicyclic system is produced from either TS (again, known for this type of activation, see Scheme I-8), but it is possible, with the proper tether, to tailor the reaction to proceed through whichever of **18** produces the desired *cis*-decalin.

Scheme I-9. Roush's IMDA Analysis for 1,7,9-decatrien-3-ones.



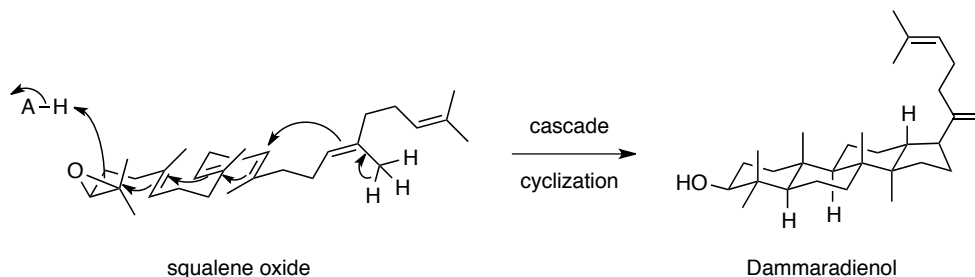
As illustrated in above section, the boat-like transition state may prevail (especially where chair-like is precluded), in some cases, and this will enter into our analysis of **1a** as well.

I.C.2. Self Assembly in Natural Product Synthesis

I.C.2.a. The Squalene Example.

The question of Diels-Alder chemistry in natural product biosynthesis is rooted in a larger question of molecular self-assembly. Molecular self-assembly has been described as the construction of higher-ordered entities by spontaneous union of two or more components through either covalent or non-covalent bonding.²⁴ The prototypical example is that of squalene oxide (Scheme I-10). The process begins with an acyclic chain and is assembled into only one enantiomer of the product dammaradienol under the direction of an enzyme that ensures this stereospecificity.

Scheme I-10. The Self-Assembly of Squalene.



There are numerous examples of natural products that are presumably biosynthesized with elements of self-assembly. Many of the biosynthetic transformations might include a Diels-Alder reaction. However, despite a wealth of study, there are few established Diels-

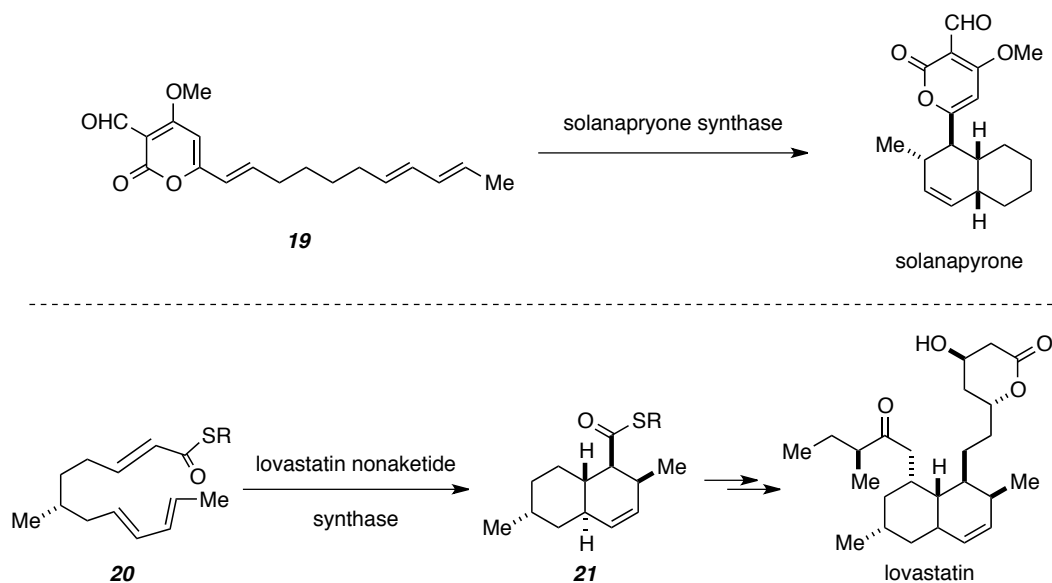
Alderases, or enzymes that catalyze the formation of the Diels-Alder adduct.^{25,26} It is with this background that we began to analyze natural products and investigate potential Diels-Alder chemistry in their biosynthesis.

I.C.2.b. The IMDA Reaction: Enzymatic or Non-enzymatic Catalysis

This section will attempt to incorporate elements of the Diels-Alder discussion with the known facts of biosynthesis and the idea of molecular assembly. As discussed above, the Diels-Alder reaction minimally requires a conjugated 4π electron system (the diene) and a 2π electron moiety (the dienophile). When these elements are located in the same molecule the subsequent IMDA reaction has the ability to generate highly exotic molecular frameworks. IMDA reactions have recently been invoked as key steps in the synthesis of natural products, and there is considerable interest in the possibility of these reactions occurring in nature.

IMDA reactions may be an explanation for chemists who question how living organisms construct such complex molecules, such as **1a**. These intramolecular reactions are possible biological routes for the way molecules are synthesized. We admit that there are established enzymes for IMDA catalysis. For example, the enzymes solanapyrone synthase^{27,28} and lovastatin nonaketide synthase²⁹ (Scheme I-11 top and bottom, respectively) are known Diels-Alderases and their substrates solanapyrone and lovastatin were isolated in optically pure form from precursors (**19** and **20**), as compared to the nonselective laboratory syntheses.

Scheme I-11. Examples of Diels-Alderases and Substrates.



It is relatively easy to propose a Diels-Alder reaction. According to Oikawa, a Diels-Alder reaction is indicated when the precursor and adduct have both been isolated. If these adducts are found alongside their regio- and diastereomers, and if the reaction feasibly occurred without the intervention of an enzyme, it is sometimes labeled a *biological* Diels-Alder cycloaddition.²⁵

It is far more difficult to propose an *enzymatic* Diels-Alder reaction. This is especially the case if no precursor is isolated alongside the natural product (as in the case of **1a**). Natural products that are isolated as racemic mixtures point to non-enzymatic biological pathways. Conversely, those chiral IMDA adducts that appear to arise from achiral precursors suggest the presence of an external chiral influence, i.e. an enzyme. If these chiral molecules arise from chiral precursors, no additional conclusions about the biosynthesis, specifically, the involvement of an enzyme, can be made. Therein lies the difficulty of a biosynthetic hypothesis on spontaneous IMDA reactions.

For our expedition into the world of biosynthetic IMDA, we also took guidance from the known phenomenon of Diels-Alder chemistry in aqueous media.^{30,31} Rate accelerations and increasing amounts of *endo*-derived (*trans*-fused, more discussion to follow) adducts have been reported. Whatever the explanation (hydrophobic effect or hydrogen-bonding that increases the reactivity of the substrate), this supports our hypothesis that a biosynthetic intermediate on the way to integramycin can undergo

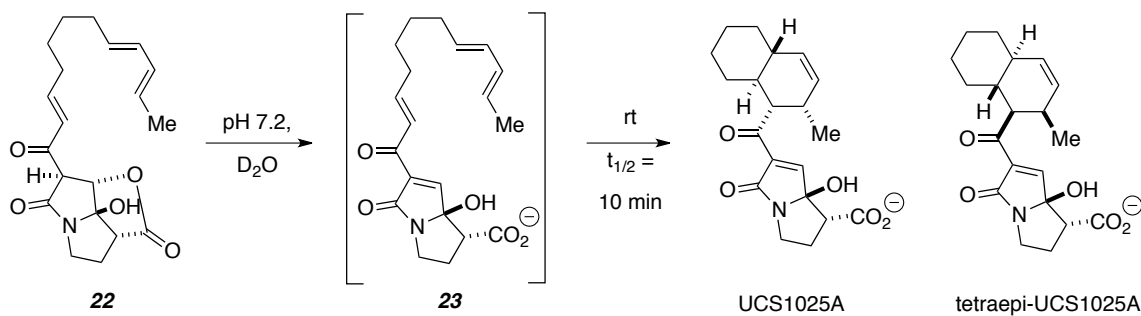
spontaneous Diels-Alder reaction to generate the natural product rapidly and selectively, as mentioned at the outset of this section.

I.C.3. Hoye Group Biosynthetic Hypothesis

I.C.3.a. Biomimetic Total Synthesis of UCS1025A^{32,33}

It had already been established by our group that certain features and reactivity of molecules point to their non-enzymatic biosynthesis. In pioneering work, Hoye and Dovornikovs found that the closed lactone precursor **22** (Scheme I-12), equipped with a tetramic acid-like moiety, underwent lactone opening to **23**. Carboxylate **23** rapidly cyclized at room temperature in D₂O, pH 7.2 (biological conditions) to give the open form of the natural product UCS1025A and its *tetra*-epimer. The lack of diastereoselectivity (they observed a 1:1 mixture of UCS1025A and the *tetra*-epimer) did not support the notion that the substrate-controlled IMDA reaction occurs non-enzymatically, but the observed half-life gives credence to the hypothesis of biosynthetic IMDA.

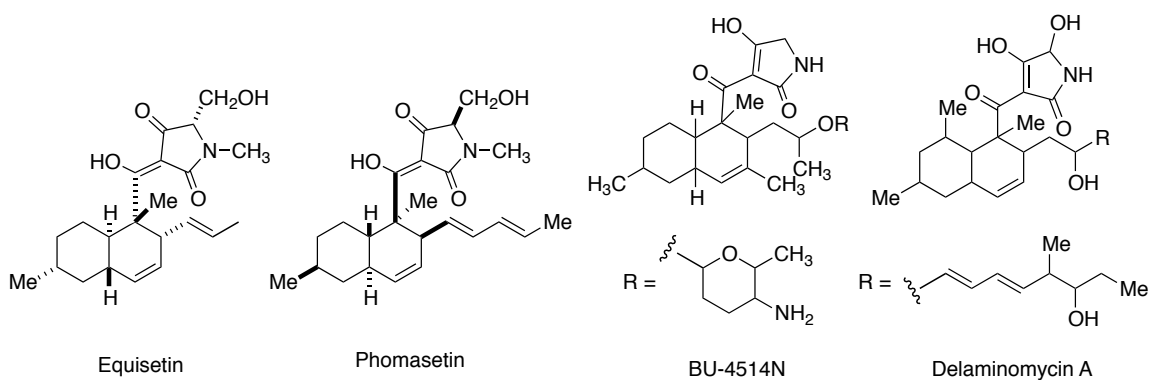
Scheme I-12. Observed IMDA Cyclization During the Synthesis of UCS1025A and its *Tetra*-epimer.



We also noticed in the literature that there were several natural products (e.g. equisetin¹² and phomasetin,¹¹ Figure I-8) that contain octahydronaphthalene units as well as tetramic acid moieties.³⁴ The stereochemistry of these (as *trans*-fused systems) have been unambiguously established by both the isolation group and subsequent syntheses. Two syntheses of equisetin were reported utilizing IMDA reactions that occurred under mild conditions without external asymmetric induction. Importantly, these reactions were found to be highly *endo*-selective, as was that of UCS1025A. The theme of *endo*-

selectivity is prevalent in the natural products that are thought to arise from IMDA reactions. Unfortunately, the synthesis and characterization of tetramic acid-containing natural products is made complicated by complex spectral data. Not only does the tetramic acid exist in several tautomeric forms, there are overlapping signals from the decalin-type fused ring system. Simple coupling constant analysis is often not sufficient for determination of these structures. Indeed, the stereochemistry of BU-4514N³⁵ has not been established. For delaminomycin only the *trans*-fusion of the decalin system can be extracted from its complex ¹H NMR data (Figure I-8).³⁶

Figure I-8. Other Octalinoyl-Containing Tetramic Acids.

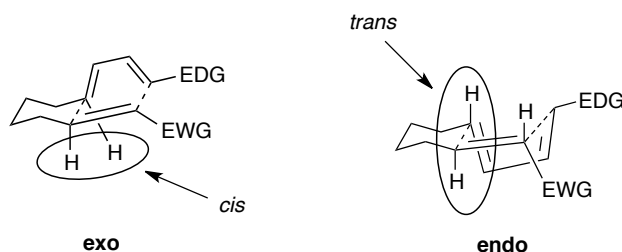


I.C.3.b. The Problem With Integramycin

Before our analysis of the natural product, it is critical to remind the reader that the absolute configuration of the natural product has not been established.⁷ Thus, *for the remainder of this document*, consideration will be given to the antipode of **1a**, i.e. structure **2** (c.f. Figure I-5).

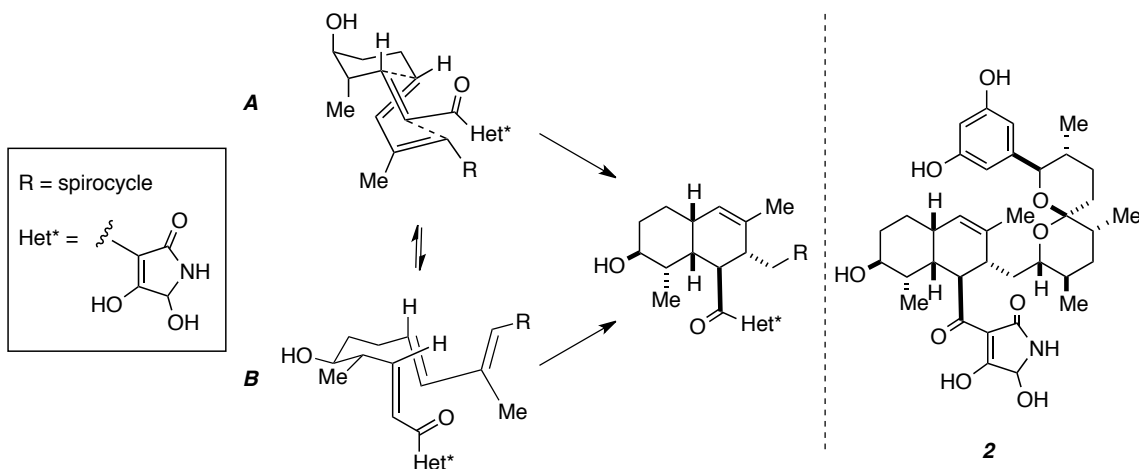
We are now charged with incorporating the background detailing theoretical IMDA (section I.C.1.) with Nature (section I.C.2.) For IMDA reactions to be viable biosynthetic events, the cyclization precursor must contain a highly activated dienophile tethered to a diene fragment. We also learned that there are two modes of cycloaddition, *exo* and *endo*, furnishing *cis*- or *trans*-fused octalins, respectively (Figure I-9). The preferred mode for shown activation (EDG for the diene, EWG for the dienophile) is *endo*.

Figure I-9. Exo vs. *endo* IMDA of 1,7,9-Decatrienes.



The stereochemistry of integramycin (**2**), however, is not consistent with an *endo* mode of cyclization.³⁴ Rather, the stereochemistry as assigned must arise from the *exo* TS **A** of the linear precursor (Scheme I-13). This conformation is unlikely due to the high energetic cost of a number of non-bonding steric interactions, especially those experienced by the two axial substituents (OH and methyl), as well as the eclipsing of the spiroketal substituent (R) and the tetramic acid moiety (“Het*”).

Scheme I-13. Required IMDA Chemistry to Generate Relative Stereochemistry of **2**.

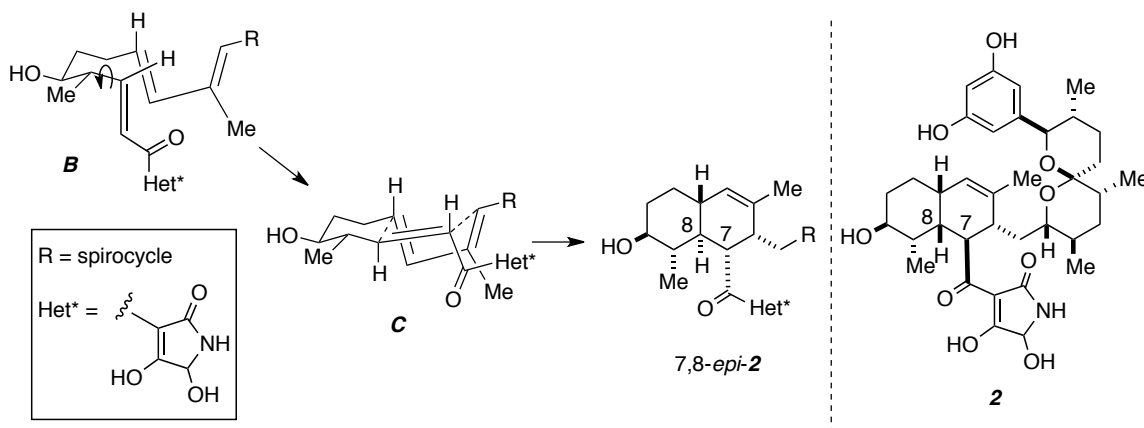


If the tether is allowed to adopt the other chair conformation (**B**, Scheme I-13), the substrate is unable to undergo a concerted [4+2] cycloaddition. Taken together, it seems unlikely that this linear polyketide precursor would be able to proceed through the required transition state that results in the reported stereochemistry of the natural product.

Rather than invoke a Diels-Alderase²⁵ that enables such a high energy preorganization for the cycloaddition leading to integramycin, we note that a simple bond rotation about C8-C9 of transition state **B** (Scheme I-14), results in **C**. Transition state **C** appears to have relieved all the unfavorable energetics of **A**. Moreover, it has now adopted an *endo* organization and is capable of Diels-Alder reaction (removing the

difficulties of **B**). The stereochemical implications, however, of intramolecular reaction of **C** are in contrast to the reported structure of integramycin (**2**). The ring fusion is now *trans*, and the stereochemistry at C7 and C8 is inverted. Nevertheless, of all the transition states considered for the same linear precursor, **C** is probably the lowest in energy, and it being *endo*, is kinetically favored.

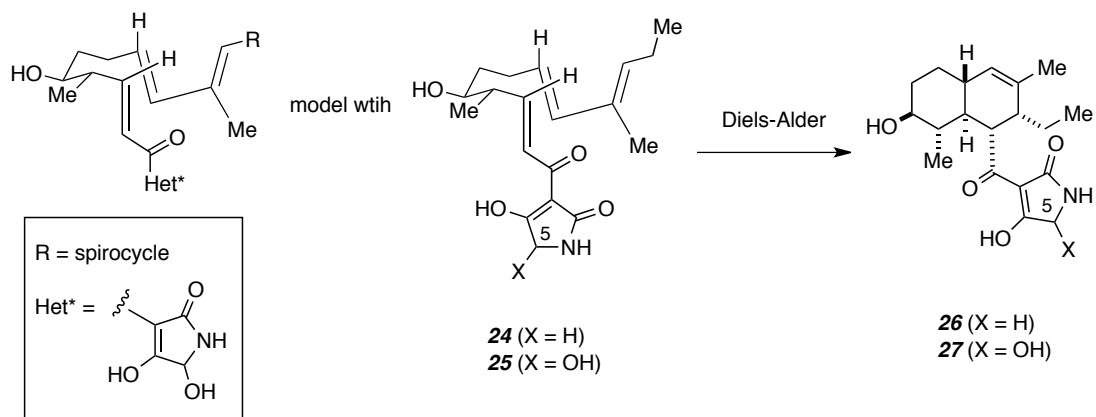
Scheme I-14. Change in IMDA Stereochemical Outcome Upon Bond Rotation.



It is this analysis, alongside our own interpretation of the data provided in the isolation report,¹³ that we hypothesize that the structure **2** is incorrect, and that instead, the natural product exists with the stereochemistry about the octalin as shown in *7,8-epi-2* (Scheme I-14).³⁴

We plan to probe a possible biosynthetic Diels-Alder event and our stereochemical hypothesis through an entirely synthetic effort. We can prepare a linear precursor **24**, which we proposed will cyclize to **26**; octalin **26** performs as a model for **2** (Scheme I-15). An ethyl group is a surrogate for the spirocycle, and a 2,4-pyrrolidinone now takes the places of the more functionalized tetramic acid of **2** (in some cases I will try to incorporate the C5 functionality, linear **25** and cyclized **27**). We plan to perform exhaustive analysis on the IMDA adduct to confidently determine its relative configuration. Once in hand, that information will be used to compare to the data reported for integramycin. We expect that our data for **26** (or **27**) data will match very well to **2**, thus calling the reported structure of integramycin into question.

Scheme I-15. Plan for Model of 2

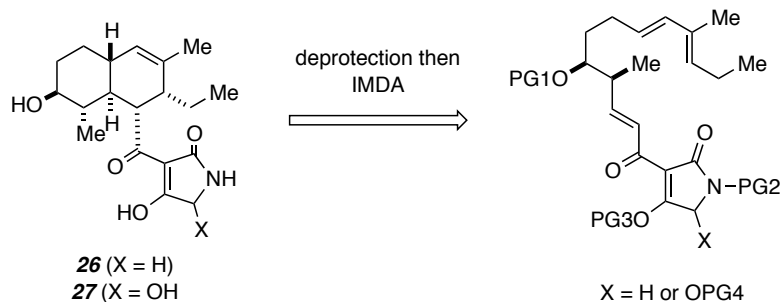


This is the plan we set out with and hoped to answer these big questions:³⁴ Will the Diels-Alder reaction occur on **24**? If so, what is the stereochemistry of the product(s)? Can we further probe the reaction to determine if it is spontaneous in nature? Is the reported structure of integrumycin correct?

Chapter II. Synthetic Strategies and Progress Toward a Model Compound

All synthetic strategies presented in this chapter attempt to construct a Diels-Alder precursor (such as **24** or **25**) in protected form (retrosynthetic arrow, Scheme 1-16) until unveiling and Diels-Alder chemistry occurs. Targeted octalins are **26** and **27**.

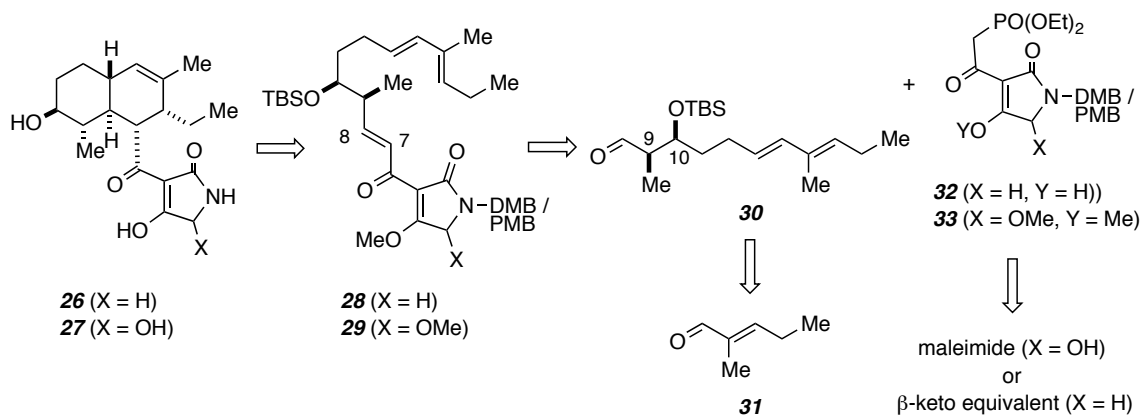
Scheme I-16. Ultimate Unveiling and IMDA of a General Reactive Triene.



II.A. Retrosynthetic Analysis I

This section encompasses all those synthetic routes (Scheme I-17) toward protected precursor **28** (or **29**) that bring in the heterocycle *intact* and where the final carbon-carbon bond (C7-C8) is formed via Horner Wadsworth Emmons (HWE) olefination of aldehyde **30** and phosphonate **32** (or **33**). Aldehyde **30** is available from a C₆ aldehyde **31**. We plan to set both the relative and absolute configuration at what will become C9 and C10 by Crimmins aldol chemistry.³⁷ Routes toward the phosphonate include both a construction from maleimide (for **33**) and the more common Lacey-Dieckmann³⁸ construction (for **32**) using various β -keto amide equivalents.

Scheme I-17. Retrosynthetic Analysis I.



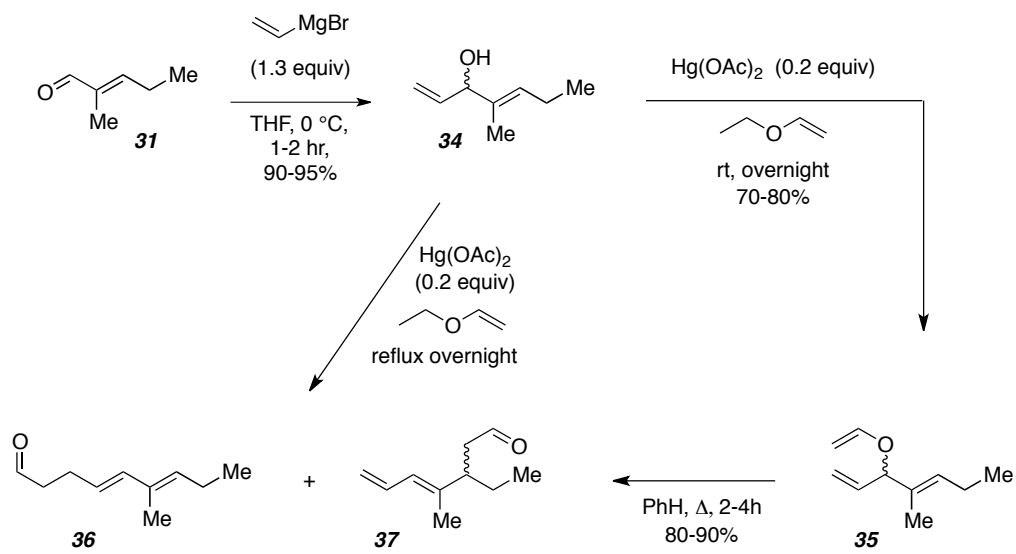
The advantage of this plan is that the heterocycle can be installed at the very end and all that remains is a global deprotection to reveal the reactive substrate. This method relied on a few assumptions; one is that the fully protected **28** (or **29**) is reasonably stable. We also preferred to think that deprotection will occur smoothly to give the IMDA precursor (**24** or **25** from Scheme I-15). The protecting groups were to be deliberately chosen so that the deprotection reaction and the anticipated cyclization event can be easily monitored.

II.A.1. Route to Aldehyde **30**.

II.A.1.a. Work on the *E,E*-diene

In the forward direction, the synthesis of HWE aldehyde **30** began with the vinyl magnesium bromide addition to 2-methyl-2-pentalen (**31**, Scheme I-18). This reaction occurred rapidly at 0 °C and was sufficiently clean that the bis-allylic alcohol **34** could be used without purification.

Scheme I-18. Preparation of *E,E*-diene.



Although 1,4-addition is possible with starting material **31**, only the desired 1,2-addition was observed. This reaction is a reliable >90% yield and the product is easily characterized.

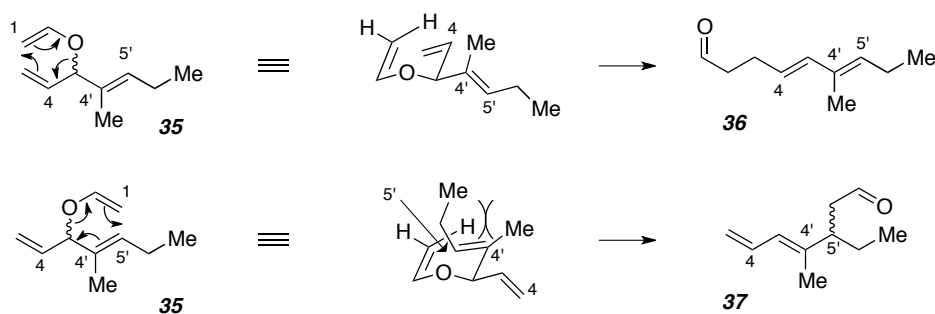
$\text{Hg}(\text{OAc})_2$ -mediated ether formation³⁹ resulted in the allyl-vinyl-ether **35**. Once isolated, **35** underwent reaction upon heating in benzene or toluene and afforded a mixture (2.5:1) of Claisen rearrangement products **36** and **37**. Alternatively, when this reaction was conducted under reflux conditions with catalytic $\text{Hg}(\text{OAc})_2$, full conversion of **34** to the same approximate ratio (by NMR) of **36** and **37** was observed. The transformation usually occurred with good mass recovery. Aldehydes **36** and **37** were somewhat separable in my hands by medium pressure liquid chromatography (MPLC) and **36** was carried forward in ca. 80% purity.

There were two main observations relevant to the Claisen rearrangement of **35**. First, the sigmatropic rearrangement is *regioselective*. The bis-allylic system has two alkenes poised to react, but the terminal alkene engages preferentially over the trisubstituted one. The regioselective rearrangement of bis-allylic-vinyl ether **35** can be rationalized by the effect of the C4' methyl group (Scheme 1-19; 1,4-diene numbering). There are both steric and electronic effects.^{40,41} The C4' methyl group is electron donating, which increases the enthalpic activation parameter (ΔH) for the rearrangement of that olefin. Substitution at C5', theoretically proposed to retard the Claisen rearrangement of that same olefin, has

also been reported to accelerate that regiochemistry (**35**→**36**).⁴² Thus, the substitution at C4' and C5' has opposing effects, and the end result is that a portion of the reaction occurs with undesired regiochemistry, leading to **37**.

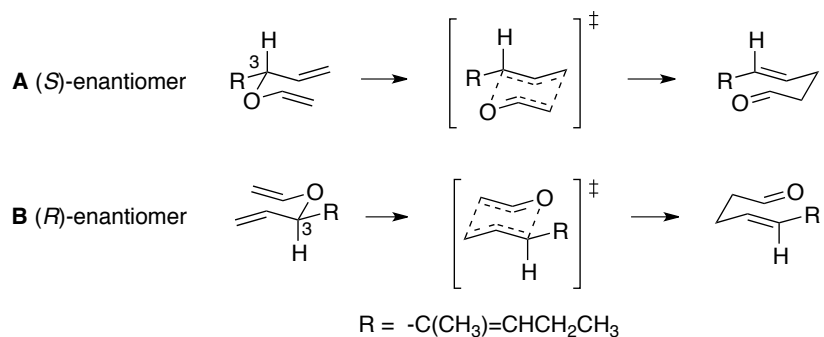
As for sterics, the chair-like TS for the rearrangement with the terminal olefin (**TS(36)**) contains fewer non-bonded steric interactions; the other conformation (**TS(37)**) is more sterically congested, leading to the observed regioselective outcomes. One last consideration is that **36**, being trisubstituted, is the more stable of the two products. The alternative Claisen rearrangement gives a less substituted olefin (**37**).

Scheme I-19. Regioselectivity of Claisen Rearrangement of **35**.



Second, the reaction is *E*-selective. At times, conditions seem to generate very minor amounts of *Z* isomers (by NMR analysis), but overwhelmingly the *trans* alkene is favored. Scheme I-20 illustrates the intermediacy of a chair-like transition state, where for either enantiomer, the alkyl R group is positioned equatorial. In the chair flipped version of these TSs, the R group would occupy an axial position, and these chair conformations would not figure greatly into the product-generating step. The chair-like transition states shown produce only the *E*-alkene. The newly formed *trans*-olefin, conjugated to the existing olefin, results in the requisite *E,E*-diene (contained in **36**) for the IMDA.

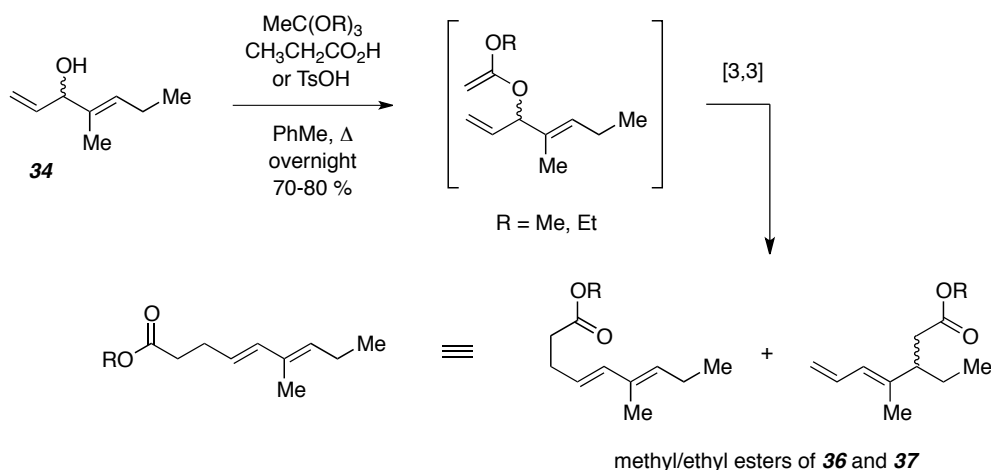
Scheme I-20. Stereoselectivity of Claisen Rearrangement of **35**.



When the intermediate allyl-vinyl-ether **35** could be isolated as the major product (as in the rightmost arrow in Scheme I-18), there was an opportunity to investigate the catalytic effect of Hg(II) on the Claisen rearrangement.⁴³⁻⁴⁵ Several Hg(II) salts were chosen as additives to the reaction of allyl-vinyl ether **35**. This study confirmed catalysis by Hg(II) salts (mild conditions and increased conversion of **35**), but sadly, there was no discernable change in product ratio **36:37**.

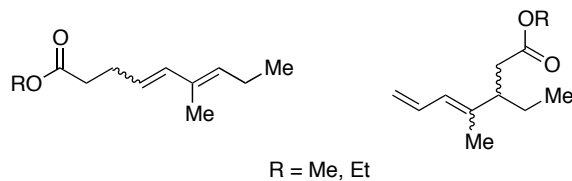
Before moving onto preparation for the aldol reaction (Section II.A.1.b), a short study was conducted on the Johnson-Claisen rearrangement (Scheme I-21). This would also furnish the desired *E,E*-diene, but with a pendent ester instead of aldehyde. A few steps are required for conversion to the necessary aldehyde **36**, but if the regioselectivity were improved, the extra steps would be justified. In the preparation, a solution of bisallylic alcohol **34**, the orthoacetate (trimethyl or triethyl), and an acid catalyst (TsOH or propionic) in toluene was heated to reflux overnight, where the product esters (methyl and ethyl esters of **36** and **37**) were observed and analyzed.

Scheme I-21. Johnson-Claisen studies.



The main conclusions from this study are that (i) the starting material generally underwent 100% conversion to the ketene acetal (brackets of Scheme I-21), (ii) in contrast to the standard Claisen conditions, this intermediate seemed to undergo slower [3,3] sigmatropic rearrangement, (iii) the mixture of constitutional esters from poor regioselectivity was generated with the same make-up (i.e. 2.5:1) (iv) the product esters were as difficult to separate as the corresponding aldehydes **36** and **37** and (v) both TsOH and propionic acid worked well in catalytic amounts, although the latter led to greater conversion of the intermediate ketene acetal. Lastly, there appeared to be a greater contribution from the undesired *Z,E*-alkene (shown in both regioisomers, Figure I-10). Since neither the regioselectivity nor separability of the products improved, this reaction was not useful for constructing the diene. Aldehyde **36** from the Claisen route (Scheme I-18) was carried forward.

Figure I-10. Potential Stereoisomers From Johnson-Claisen.

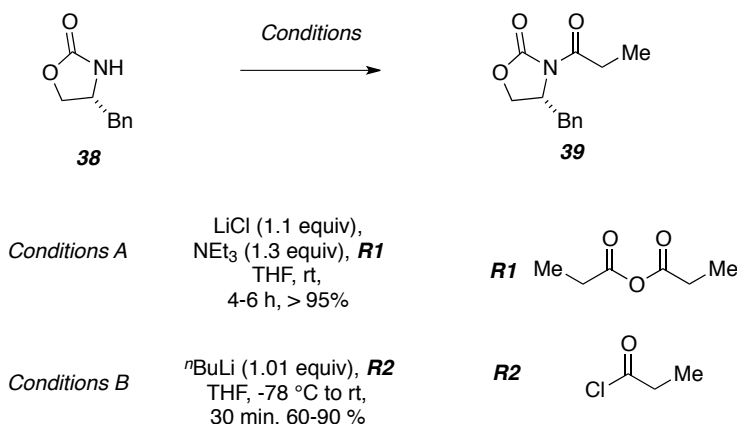


II.A.1.b. Crimmins Aldol Model Studies³⁷ and Application to Aldehyde **36**

For the anticipated aldol reaction for the 1,2-stereochemistry at C9 and C10, propionylated auxiliary **39** must first be prepared. It was usually synthesized from **38** by one of two methods. Although conditions **A**^{46,47} (propionic anhydride as the acylating

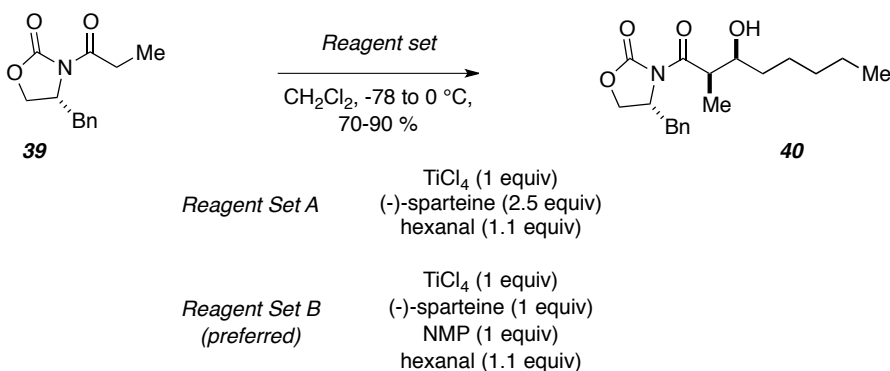
agent in the presence of an amine base and LiCl) were easier, this reaction took longer for less conversion and was not as useful on a big scale. Instead, the established preparation using *n*BuLi and propionyl chloride (conditions **B**) were used.⁴⁸ The crystalline chiral auxiliary **39** was carried forward for use in the aldol reaction.

Scheme I-22. Preparation of Aldol Reagent Imide.



Before using the real substrate (i.e., aldehyde **36**), it was instructive to work out the conditions on a model system (hexanal). Scheme I-23 illustrates the key synthetic step for establishing the required asymmetry. There are well-documented procedures using boron triflate-derived enolates to mediate transformations like **39** (and hexanal) to **40**.⁴⁹ However, the difficulty of making and storing these reagents prompted me to explore titanium catalysis. Crimmins and coworkers concluded years of study in an excellent report³⁷ of the various conditions under which Evans *syn* and *anti*, as well as the “non-Evans *syn*” aldol adducts can be synthesized. The conditions were chosen according to the literature prescription for the desired stereochemical outcome (9*R*, 10*S*).

Scheme I-23. Crimmins’ Aldol Reaction With Hexanal.

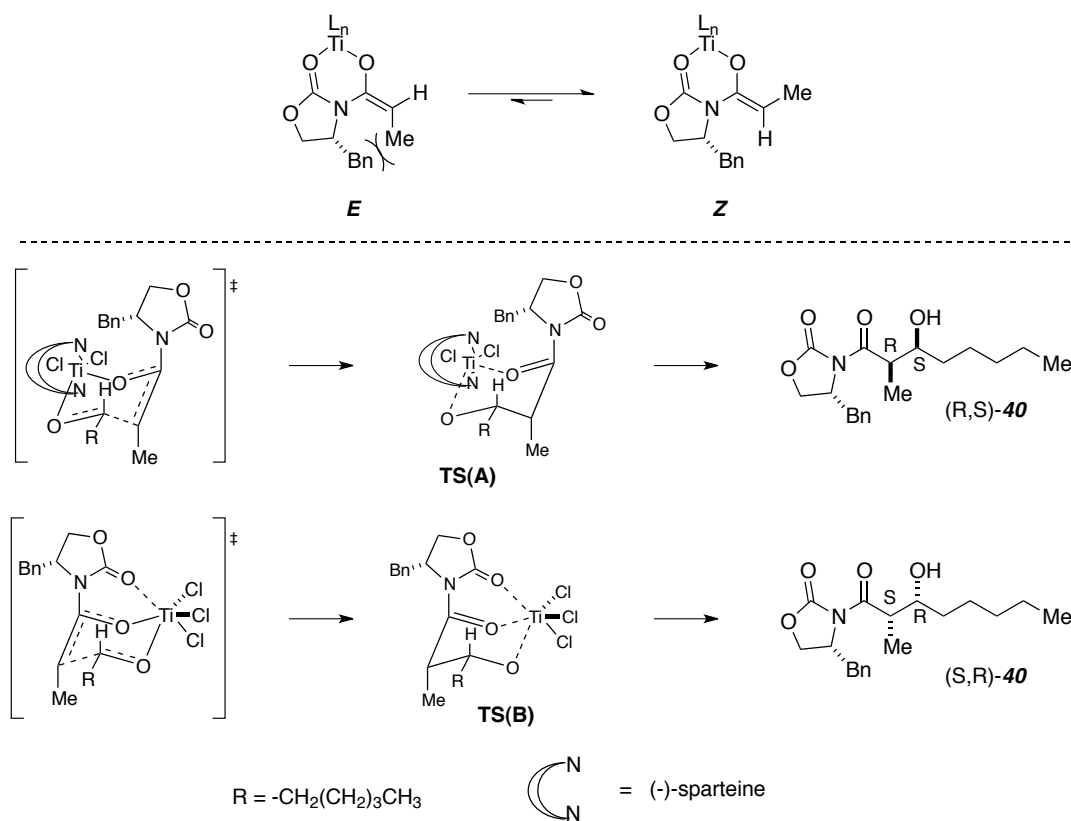


In a series of experiments designed to gain experience with this reaction, the Evans *syn* aldol adduct was obtained from propionaldehyde and hexanal. It was found that although the reaction required both temperature changes and careful order of addition, the workup was simple and good yields were reproducible. In the course of these model studies, I found that the use of the cheaper N-methyl pyrrolidone (NMP, Reagent Set B, Scheme I-23) in the place of one equivalent of (-)-sparteine gave the same results. This verified that (-)-sparteine does not provide asymmetric induction; its role in this reaction is simply as a ligand. Although the NMP is more difficult to remove after the completion of the reaction, it helps to reduce the costs of the reaction system that might otherwise only use (-)-sparteine as a ligand (Reagent Set A).

The reaction is known to give excellent diastereoselectivities. The mechanism of this reaction accounts for the different stereochemical outcomes.³⁷ Key features are the stereoselective generation of the enolate and the interaction of amine ligands with the titanium coordination to the enolate oxygen. As shown in Figure I-11, the *Z*-enolate is formed selectively due to 1,3-allylic strain of the corresponding *E*-enolate.

In the presence of at least two equivalents of amine (e.g. two equivalents of a bidentate ligand such as (-)-sparteine or tetramethylethylenediamine, or one equivalent of a bidentate ligand and one equivalent of a monodentate ligand such as NMP), the addition reaction is expected to proceed through a transition state like **TS(A)**. The excess amine displaces chlorides on the titanium core and organizes the enolate and aldehyde in the chair-like TS geometry. Opposite facial selectivity is observed where an excess of TiCl₄ is used. Here the reaction presumably occurs through the transition state geometry **TS(B)** where chloride comes back to ligate to titanium. Under our conditions, we expect the reaction to go through **TS(A)**, which gives the Evans *syn* product (*R,S*-**40**).

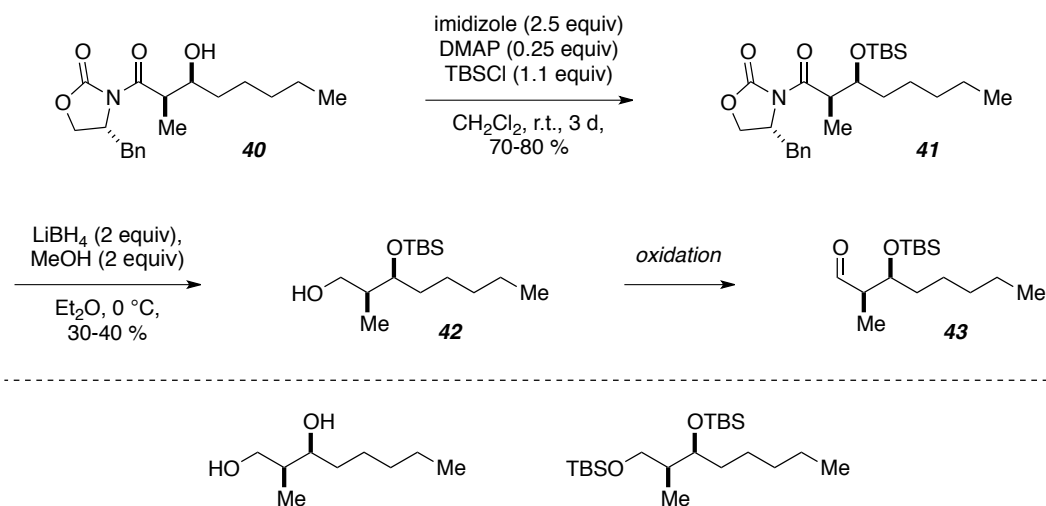
Figure I-11. Mechanism of Crimmons Aldol Reaction (Hexanal Substrate).



While scaling-up the desired aldehyde **30** for use in the aldol reaction, we tried the sequence: aldol reaction, TBS-protection, reductive cleavage of chiral auxiliary, and oxidation to a final aldehyde on a model system (Scheme I-24). Protection of the secondary alcohol **40** to **41** proceeded sluggishly. After a three-day reaction, full conversion of the starting alcohol was reached, but the yield was relatively low for this type of transformation. Optimization entailed running this reaction in DMF (versus CH_2Cl_2) and under extremely high concentration.

The reductive cleavage of **41** was best performed using LiBH_4 . Although somewhat low yielding (36% isolated yield) to alcohol **42**, the reaction was rapid and the auxiliary could be recovered when the reduction was performed on a large scale. The lower yield could be attributed to silyl migration between molecules (bottom of Scheme I-24), but there was never any GCMS evidence for this process (from **42** or **45**, see Scheme I-25). In fact, no major byproduct was observed for this reaction; the low yields could be due to poor mass recovery after the workup.

Scheme I-24. Further Chemistry on Hexanal Aldol Product.



A variety of oxidation conditions were surveyed to determine the optimal oxidation procedure for a primary alcohol like **42**. Many conditions are available for this reaction, and the results ranged from marginally successful to very successful.

Table I-1. Oxidation Conditions of Model **42**.

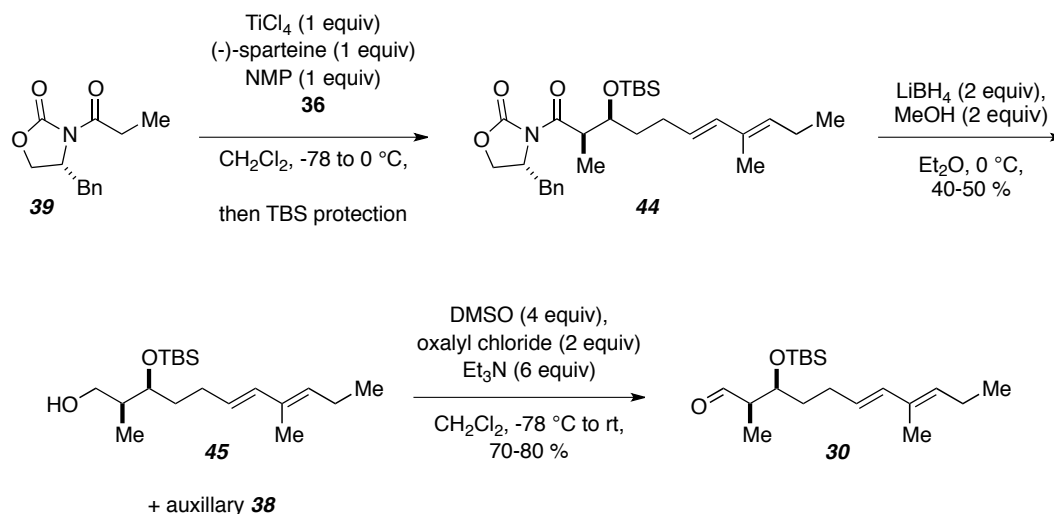
Entry	Scale (mg ROH)	Conditions	Yield	Comments
1	10	IBX (1.5 equiv), DMSO, rt, 4h	80%	clean
2	10	DMP (1.1 equiv), CH ₂ Cl ₂ , rt, 4 h	70%	clean
3	10	(COCl) ₂ (2 equiv), DMSO (4 equiv), Et ₃ N (6 equiv), -50 °C	70%	clean
4	10	^t Pr ₂ EtN (3.2 equiv), DMSO (1 equiv), SO ₃ -py (3.0 equiv), CH ₂ Cl ₂ , rt	60%	H ₂ O workup unsuccessful, loss of mass and purity after CuSO ₄ workup

As illustrated in Table I-1, most conditions lead to complete and clean conversion to the oxidized product **43** (>90% pure by ¹H NMR analysis). After purification, yields typically dropped to 70-80%. The hypervalent iodine reagents, IBX (entry 1) and Dess-Martin periodinane (DMP, entry 2) worked very well and gave **43** in good yields. Swern oxidation also gave the desired product in good yield. Finally, the Parikh-Doering conditions (entry 4) for the oxidation gave the desired product, but it required standard CuSO₄ workup. Although a more tedious process, the aldehyde appeared in 60% yield.

IIA.1.c. Completion of Aldehyde 30.

After completing the oxidation, I tried the sequence on my actual substrate (Scheme I-25). In the aldol reaction with **36**, evidence for the aldol adduct appeared in the ^1H NMR spectrum. This product was purified by MPLC and entered into the protection (to **44**), reduction (to **45**), and oxidation (to **30**) sequence worked out on the hexanal model.

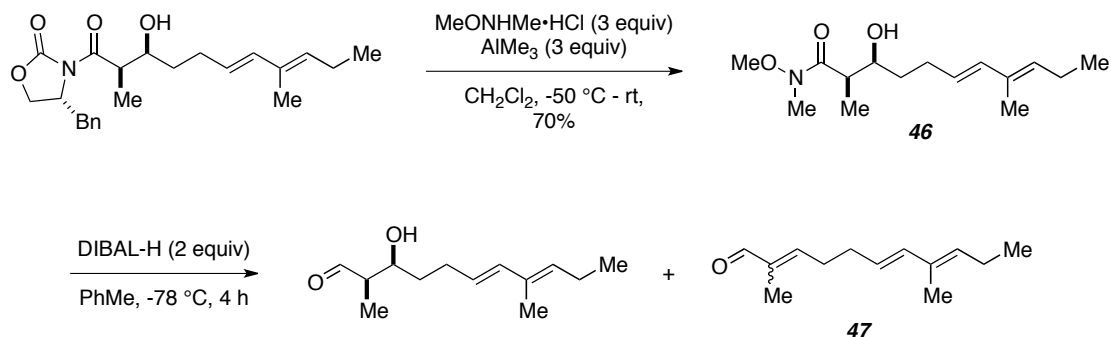
Scheme I-25. Crimmins' Aldol on Aldehyde **36** and Generation of Aldehyde **30**.



Notably, over the course of scale up studies, a number of these steps could be shortened and purification steps combined to achieve higher and faster throughput. For example, chromatography was usually reserved for after the silylation and oxidation steps. The byproducts and remaining reagents after the aldol did not interfere with the TBS protection leading to **44**. Likewise, the cleaved auxiliary **38** did not offend the Swern oxidation of **45**. The sequence has currently been scaled to generate 4-5 grams of purified aldehyde **30**.

Before proceeding, I tried one alternative on the aldol product (corresponding to the un-silylated **44**, Scheme I-25). Trans-amidation to the Weinreb amide⁵⁰ and DIBAL-H reduction would result in nearly the same product (β -hydroxy aldehyde, not numbered, compare to **30**) To this end, the aldol adduct was involved in trans-amidation to **46** using the HCl salt of *N,O*-dimethyl hydroxylamine mediated by AlMe_3 (Scheme I-26). This afforded the amide material for the DIBAL-H reduction, which gave the β -hydroxy aldehyde. ^1H NMR spectrum showed evidence of some compound that could be the elimination product **47**.

Scheme I-26. Weinreb Amide Route to Aldehyde **30**.

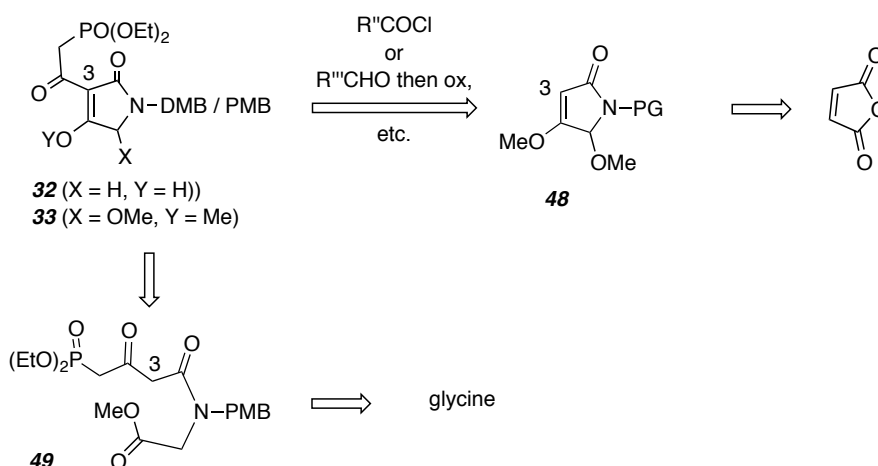


Because the free hydroxyl group would still need protection (resulting in **30**) prior to aldol reaction, the Weinreb amide route was the same number of steps and judged to be unnecessary. Instead, the bulk of the aldol material was protected to **44** and the reductive cleavage-oxidation chemistry was used in scale up reactions (Scheme I-25). This material was ready for the HWE reaction (see Retrosynthetic Analysis I, Scheme I-19) and was stable to storage over months in the refrigerator.

II.A.2. Routes to Heterocycles **32** and **33** and Various Coupling Reactions

The preparation of the HWE coupling partner **32** (or **33**) was far less certain (Scheme I-27, additional retrosynthetic details). We were attracted to the known chemistry to a substrate like **48**,⁵¹ but a bond-forming reaction at C3 on such a heterocycle was going to be a challenge. At this stage, the proper reaction for building functionality off C3 (right arrow in Scheme) was not explicitly worked out, but there were some literature procedures for similar reactions. General compounds **48** would ultimately be built from maleic anhydride.

Scheme I-27. General Ways to Heterocycles **32** and **33**.

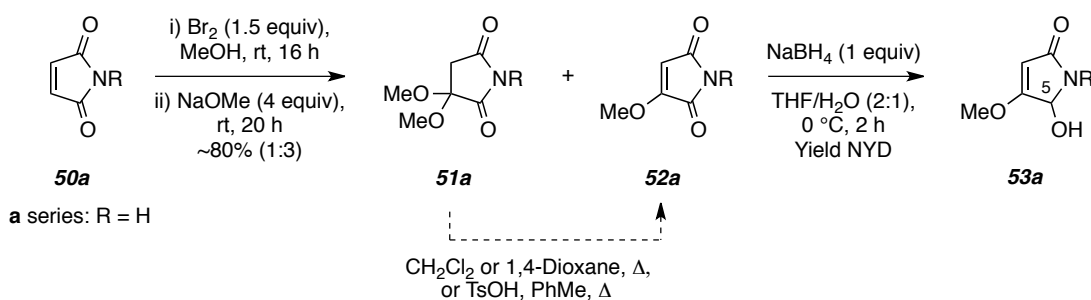


There are several ways to access the heterocycle **32** (downward arrow in Scheme) but the primary and most reliable is a Lacey-Dieckmann³⁸ strategy (from **49**, ultimately from glycine).

II.A.2.a. From Maleimide to Alkyl Halides **60a** and **60b**

Maleimide can be elaborated to a more functional compound such as intermediate **48** (Scheme I-27, retrosynthetic analysis).⁵¹ To test the route starting from maleimide, I attempted the first few steps on the imide itself (Scheme I-28).

Scheme I-28. Oxidation and Reduction of Maleimide (**50a**).^a



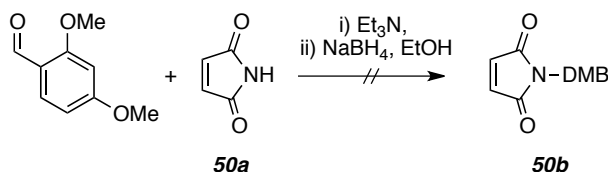
^a The related series **b-d** denote where the R in Scheme I-28 is DMB (**b**), PMB (**c**), or Bn (**d**).

The bromination and elimination steps to **52a** occurred in high yield and essentially oxidized the molecule to the tricarbonyl species. In this case, the ketal **51a** was formed to varying extents. Should it become the main product, it is easily converted to **52a** under acidic conditions. Thermal elimination of MeOH was not attempted. NaBH₄ reduction provided the carbinolamide **53a** with complete regioselectivity, as expected.⁵¹

I knew that the 5-hydroxyl group needed to be transformed into a methyl ether and the nitrogen must be protected before any reaction of **53a**. I then sought to prepare the same animal **53a**, except to protect the imide nitrogen first. 2,4-dimethoxybenzyl (DMB) was chosen as the protecting group. This could be easily removed under mild (oxidation) conditions that the rest of the molecule could tolerate.⁵²

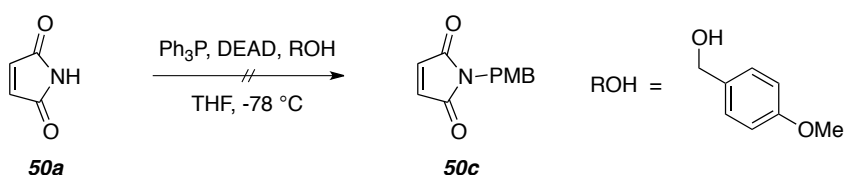
First I tried reductive amination on maleimide (Scheme I-29). I saw no conversion and did not attempt this reaction again. In hindsight, it is very difficult to perform reductive amination on imides like malaimide. The imide nitrogen is not very nucleophilic under standard conditions. This is suggested by the scarcity of examples in the literature that involve direct alkylation.⁵³

Scheme I-29. Attempted Reductive Amination of Imide **50a**.



Maleimide, however, does have proper nucleophilicity under Mitsunobu conditions (Scheme I-30). With the proper primary benzyl alcohol, the protecting group on the imide nitrogen can be installed. Conditions have been designed to ensure that the reactivity of maleimide as a Michael-acceptor does not interfere with the Mitsunobu reaction. Unfortunately, I did not see the desired outcome (**50c**) when I tried to react maleimide with *p*-methoxybenzylalcohol.

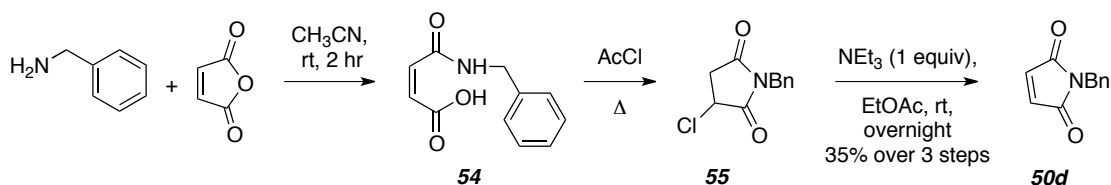
Scheme I-30. Attempted Mitsunobu with **50a**.



Alternatively, the protecting group can be installed by using a ring opening-ring closing sequence on maleic anhydride (Scheme I-31). The first experiments were completed using benzyl amine as a model, with the intention of moving to the DMBNH₂ series after the chemistry was optimized. In the event, benzyl amine quickly opens the anhydride to the amic acid **54**, which then reclosed upon treatment with acetyl chloride.

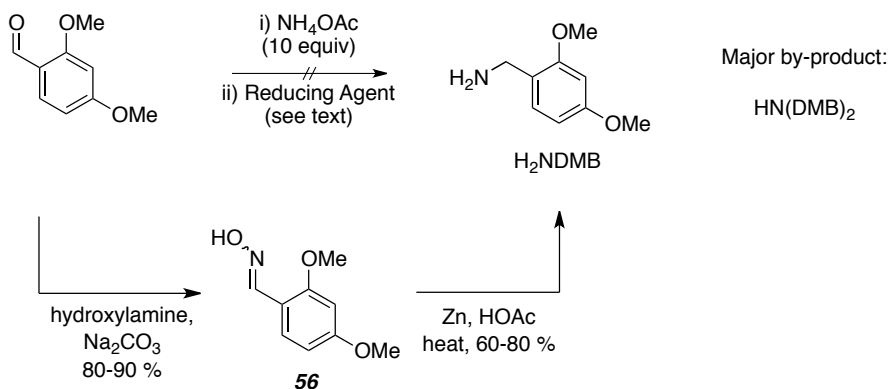
Presumably, the mixed anhydride is reactive enough that the imide (i.e. **50d**) is reformed, although now protected. Depending on how long the reaction required, HCl would sometimes add across the maleimide alkene (byproduct **55**). Elimination with triethylamine cleanly regenerated the maleimide **50d**, which was generally recrystallized for storage.

Scheme I-31. Transformation of Maleic Anhydride to Maleimide **50d**.



Although a straightforward sequence for benzyl amine, synthesis of the DMB variant **50b** (product, Scheme I-29) was hampered at the outset. DMBNH₂ is commercially available, but costly. I attempted to prepare it first by reductive amination of the corresponding aldehyde (Scheme I-32). With NH₄OAc followed by a variety of reducing agents, the desired DMBNH₂ could not be obtained. Only the double alkylation product (DMB)₂NH was isolated along with recovery of varying amounts of the reduced aldehyde.

Scheme I-32. Attempted Reductive Amination of DMBNH₂.

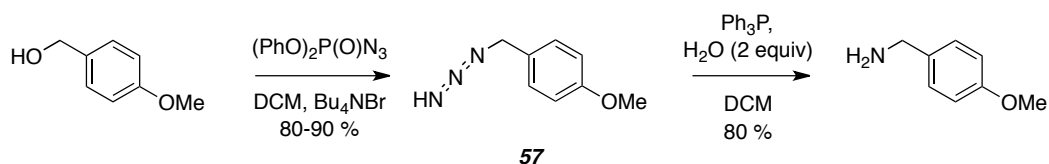


This type of difficulty in reductive amination for the formation of a primary amine has been reported in the literature.⁵⁴ I abandoned that route in favor of a two-step sequence involving the intermediacy of oxime **56**. This material was easily prepared by heating the aldehyde in a basic solution of hydroxylamine. The best conditions for the

reduction were Zn/AcOH, and these afforded the primary amine as desired in sufficient purity for the next step.

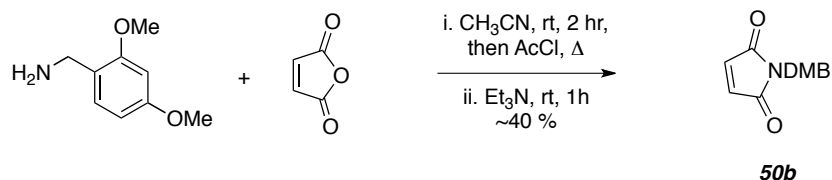
Alternatively, benzyl amines can be prepared in good yield via the corresponding azide, followed by Staudinger reduction. I tested this route on the *p*-methoxybenzyl alcohol (Scheme I-33). Although high yielding and effective, this route was inferior due to the large quantities of triphenylphosphineoxide (TPPO) that are produced in the Staudinger reduction step.

Scheme I-33. Azide Route to Aryl Amines.



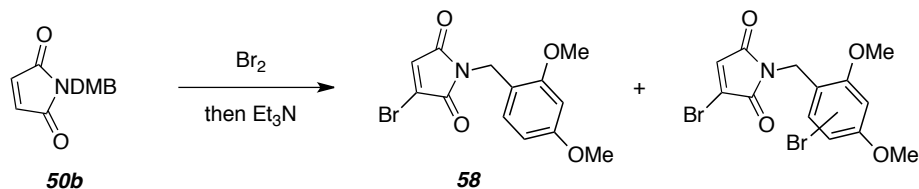
With the DMBNH₂ in hand (see Scheme I-32), the protected maleimide **50b** was realized using the same protocol developed for BnNH₂ (Scheme I-34). The yields were comparable, but the scalability was poor. Because of the added time required to prepare the starting amine, I was never able to generate sufficient quantities (i.e. >one gram) of N-DMB maleimide (**50b**).

Scheme I-34. Transformation of Maleic Anhydride to Maleimide **50b**.



Additionally, I recalled that this sequence calls for bromination of the maleimide **50b** (see Scheme I-28). Under the conditions prescribed, the DMB group was prone to bromination. I tried the reaction anyways, and I saw the mass and characteristic NMR resonances for desired product **58**, but I also found evidence of products having additional bromine incorporation by GCMS.

Scheme I-35. Attempted Oxidation of **50b**.

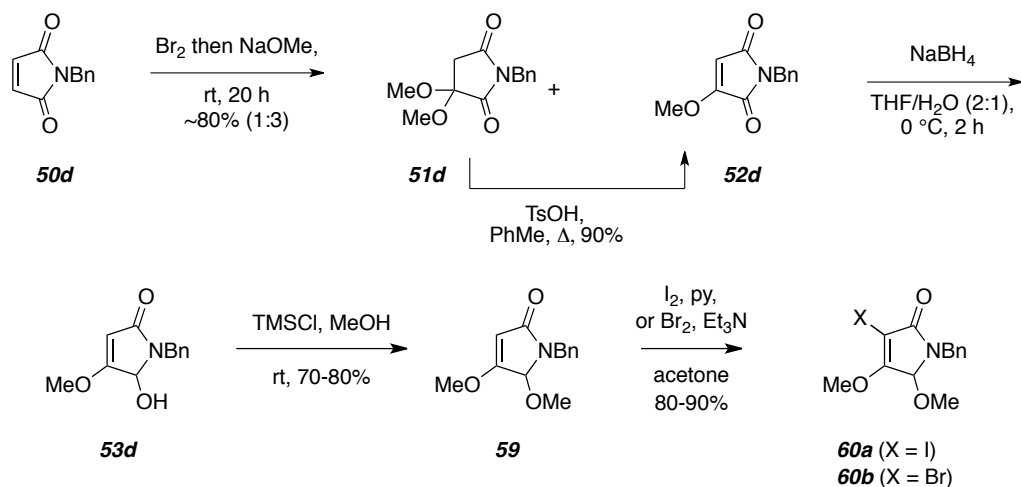


Thus, it was decided that the DMB would be replaced by a different protecting group, and I settled on the PMB variant. It would also be easily removable under mild conditions once the rest of the chemistry on the heterocycle was completed. I already knew I could access larger quantities of the PMBNH₂, and the aromatic moiety is not nearly as electron rich as in the DMB, so it would hopefully remain untouched after maleimide **50c** was treated with electrophilic bromine.

While the sufficient quantities of **50c** were being scaled up in preparation for aldol reaction (shown generally in Scheme I-27), the remaining chemistries were performed on the NBn series (**50-53d**) for practice (Scheme I-36). In order to utilize the regioselective reduction methodology reported by the Coster lab,⁵¹ the maleimide had to be oxidized first. Accordingly, maleimide **50d** was treated with Br₂ and NaOMe. This typically resulted in varying amounts (generally 1:3) of the methoxy maleimide **52d** and the ketal **51d** in a combined yield of 80%. These two solids were easily separated by flash column chromatography. Fractional crystallization may provide an alternate purification method. The conversion of **51d** to **52d** is straightforward under acidic conditions.

Enol ether **52d** was regioselectively reduced (Scheme I-36) to **53d** via treatment with NaBH₄ in THF/H₂O at 0 °C. The crude carbinolamide was treated with TMSCl in MeOH, where the methyl ether was formed in good yield and purified by column chromatography. This heterocycle **59** was typically stored for subsequent reactions, but a portion of it was converted^{55,56} to the iodide **60a** or bromide **60b**. These are all candidates for the aldol reaction (c.f. Scheme I-27); **59** can be deprotonated, whereas **60a** and **60b** can undergo metal-halogen exchange and become reactive in aldol-type reactions (to be discussed later).

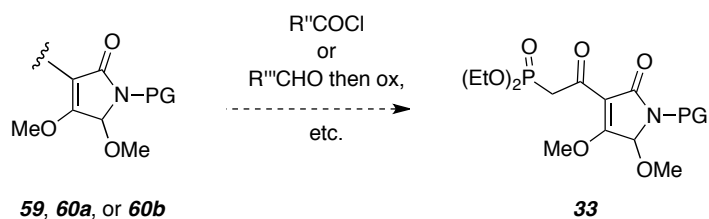
Scheme I-36. Completion of Heterocycle **59** From **50d**.



II.A.2.b. Future Work for the Completion of **33**

At this point in the project, I was not successful in producing sufficient quantities of the necessary heterocycles to be exploited in a later synthetic route toward my desired IMDA precursor. I was not ready to attempt C3-acylation chemistry to build up the phosphonate (general reaction shown in Scheme I-37).

Scheme I-37. The Key C3 Reaction to Build Functionality From **59** and **60a/b**.



In fact, this whole route was disfavored because I was working on the Lacey-Dieckman methodology toward **32** at the time. With this background, it is appropriate to delay all discussion on reactivity and properties of **59**, **60a**, and **60b** to the next section, where they re-enter the synthetic route in a slightly different way (**II.B**).

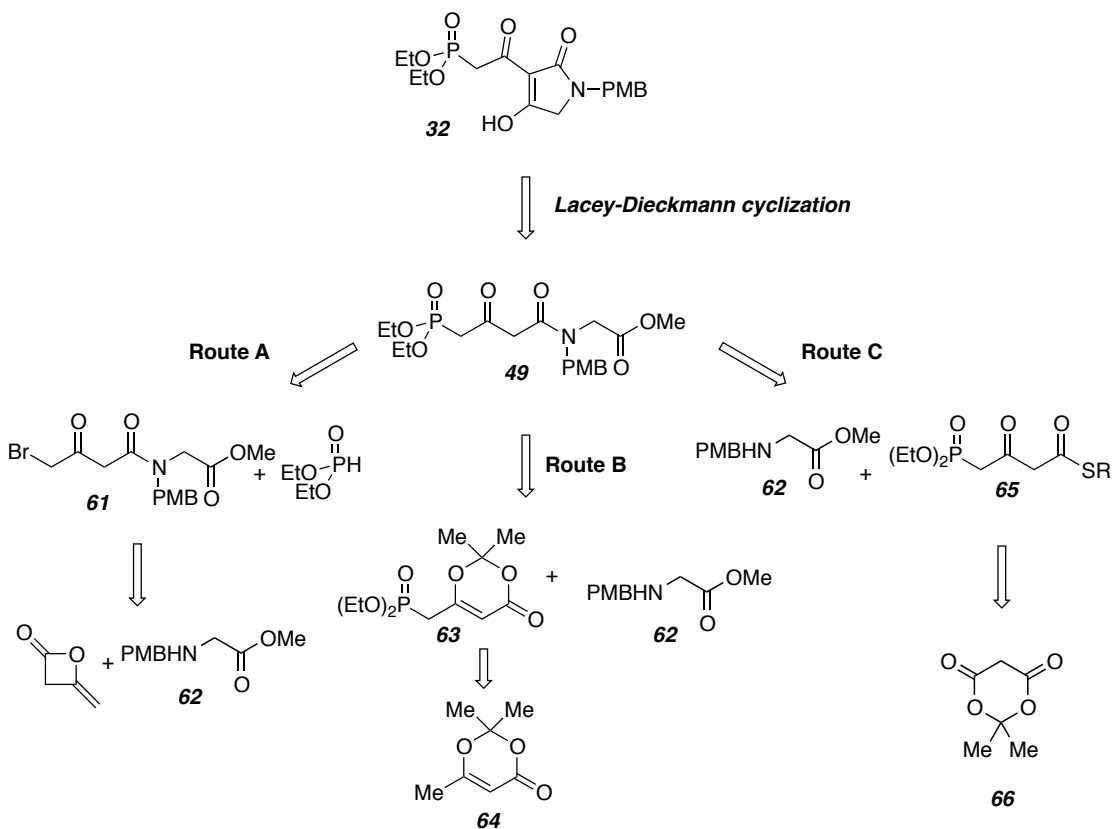
II.A.3. Route to Heterocycle **32** by Lacey-Dieckmann

It was becoming clear by the studies described in the previous section that the C5-OH functionality of **33** required creativity and the use of nearly unprecedented reactions. A quick way into Diels-Alder chemistry was sought in order to learn more about the *E,E*

diene (e.g., in **30**) and its behavior in IMDA reactions (with a proper dienophile placed on the molecule). There is a reported route via Lacey-Dieckmann cyclization (**49** to **32**), shown to be very successful for the synthesis of phosphonate esters of tetramic acids.⁵⁷

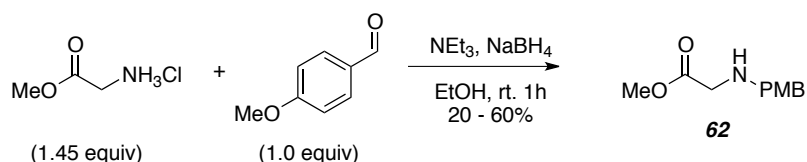
The common acyclic intermediate **49** can be arrived at by one of three routes (Scheme I-38). They mainly differ by the β -keto equivalent employed for transformation into the tricarbonyl **49**. The Schlessinger method (Route A) involves the later-stage installation of the phosphonate ester via bromide displacement of **61** by the sodium salt of diethylphosphite. Bromide **61** comes from reaction of the amine **62** with the product of Br₂-induced ring opening of diketene. Route B requires reaction of appended 1,3-diox-5-en-4-one **63** (available in three steps from **64**) and the amine **62**. Lastly, Route C relies on a thioester/amine coupling reaction to form the amide bond present in **49**. Phosphonate thioester **65** is ultimately built from Meldrum's acid (**66**). In an attempt to quickly access a coupling partner for our aldehyde **30**, work on these routes commenced.

Scheme I-38. Lacey-Dieckman Methodology for HWE Coupling Partner **32**.



All routes required glycine derivative **62**. Reductive amination of the methyl ester of glycine with *p*-OMe benzaldehyde proceeded with satisfactory yields, but enough of **62** was isolated for subsequent syntheses (Scheme I-39). Upon scaling up, the reaction appeared to give higher yields, but there was still a significant amount of one major by-product.

Scheme I-39. Preparation of **62**.

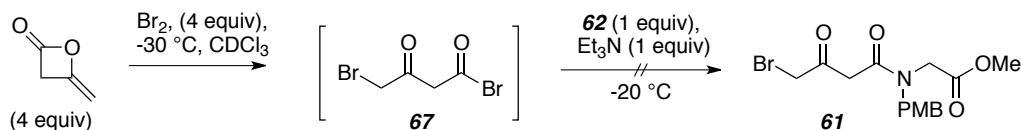


II.A.3.a. Lacey-Dieckmann Starting From Diketene

Route A (Scheme I-38) was attractive because it was fewer steps and the acetylation step using diketene was well-documented in the literature.⁵⁷ It also avoided the use of a very polar phosphonate until later in the sequence, so I hoped that chromatography would be straightforward.

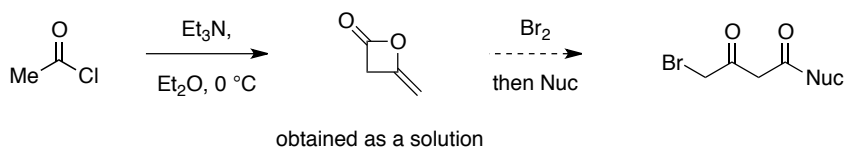
With amine **62** in hand (from Scheme I-39), reaction with diketene was studied (Scheme I-40). Careful vacuum distillation provided the pure diketene, which exists as the β -lactone with an exocyclic methylene. Treatment with Br₂ led to what appeared in the ¹H NMR spectrum to be intermediate **67**, although there were other components present in the reaction mixture. Nevertheless, the glycine derivative **62** was added to this mixture, but remained unreacted (¹H NMR analysis). In the future, more care or screening of reaction conditions (e.g. temperature) is needed to ensure that the presumed intermediate **67** is actually present and that **62** is sufficiently reactive for production of **61**.

Scheme I-40. Attempted acetoacetylation of amine **62** starting from diketene.



While I was working out these factors (including preparation of diketene instead of purifying it from stored samples, see Scheme I-41), I commenced work on the alternative Route B (Scheme I-38).

Scheme I-41. Preparation of Diketene and Two Step Process to Dicarboxyl.

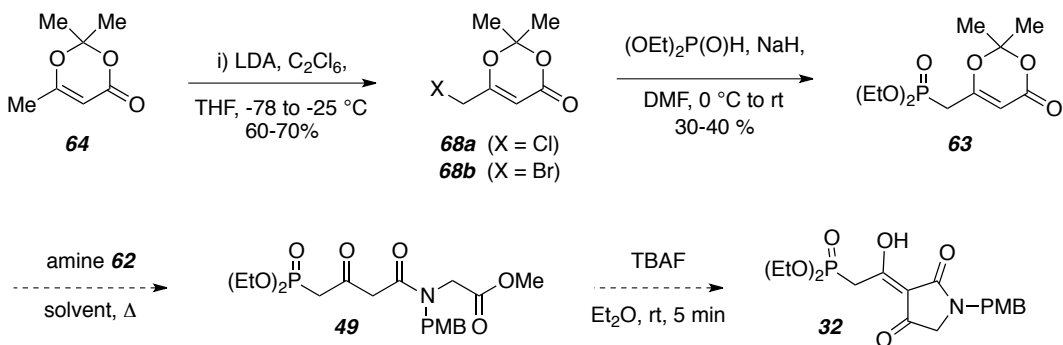


II.A.3.b. Lacey-Dieckmann Starting From 1,3-dioxenone

I then focused on the synthesis of the phosphonate **63** (Scheme I-42). This series of reactions is well-documented^{58,59} and known to give the products reliably. The enolate of **64** is generated by LDA, and subsequent reaction with hexachloroethane gave the δ -Cl product **68a** (the bromide analogue **68b** was prepared a different way in a later study, but included here for numbering). Yields were good but improved upon scale up and the desired chloride **68a** was suitable for use following purification. In my hands, chloride displacement by sodium or potassium diethyl phosphite to give **63** resulted in very little conversion unless a large excess of the phosphite anion was used. Purification was difficult. Phosphonate **63** could be chromatographed, but because it required highly polar mobile phases, excess starting material travelled alongside it. Water workup to remove the excess phosphite was not attempted on scale because of the presumed hydrolytic lability of the 1,3-dioxenone. Distillation required special care due to the thermal lability of **63** above 40 °C. My work on this route ended due to these and other concerns.

Despite the fact that **63** is thermally labile above 40 °C and sensitive to water, this route to **49** deserves more attention. Once the phosphonate **63** is in hand, the reaction with **62** is known to occur quickly and the resulting tricarbonyl **49** is ready for the Lacey-Dieckmann cyclization and subsequent HWE experiments (dotted arrows, Scheme I-42).

Scheme I-42. Attempted Use of **63** for Acetylation of **62**.

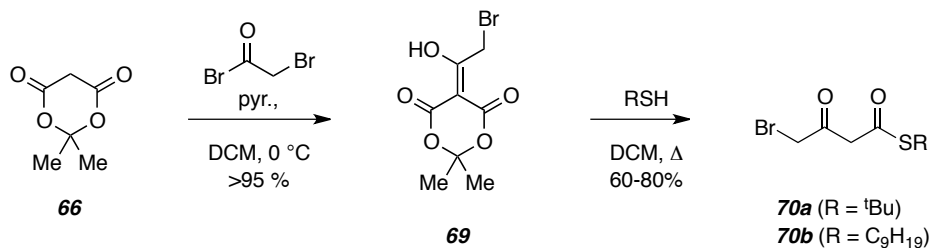


II.A.3.c. Lacey-Dieckmann Starting From Meldrum's acid

There was yet another route toward the phosphonate (Route C, Scheme I-38). This would still require the late-stage Dieckmann reaction, but the Dieckmann substrate **49** would be accessed through a silver-mediated amide bond forming reaction. This route required yet another acetylation source, Meldrum's acid (**66**).^{60,61}

In the forward direction, **66** is cleanly acetylated⁶² with Br-acetyl bromide at 0 °C in the presence of pyridine to the tricarbonyl compound **69** (Scheme I-43). This reaction is easily scaled and the product often crystallized upon storage. Ring-opening occurred by heating with a appropriate thiol [RSH, in Scheme, typically ^tBu and nonyl (mixture of isomers) mercaptan were used and worked equally well] and gave the thioesters **70a**^{63,64} and **70b** in good to excellent yields. This reaction was only complicated by the difficulty in working with volatile mercaptans. Optimization included performing this reaction with (at most) 2 equivalents of thiol and minimal solvent (DCM worked and no significant improvement was noted with any others).

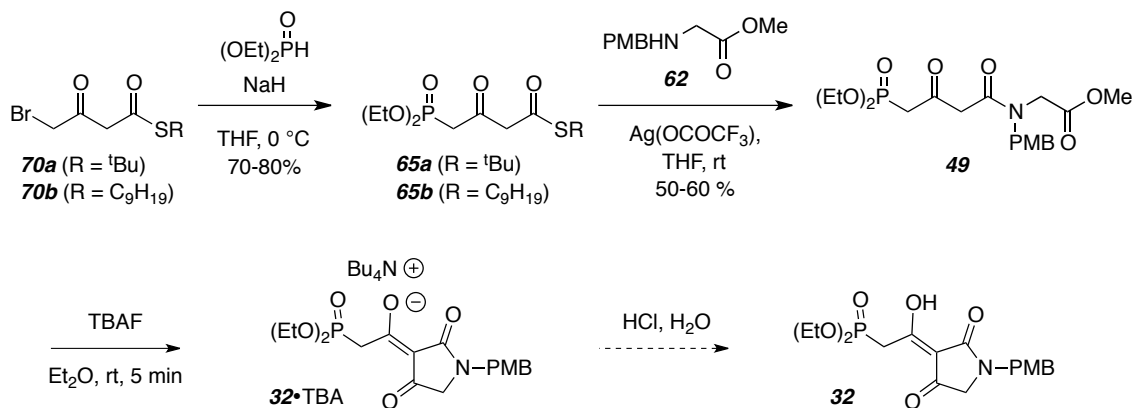
Scheme I-43. Preparation of Bromo-Thioesters **70** From Meldrum's Acid.



The bromide displacement to the phosphonate thioester (Scheme I-44) required some experimentation. Much like the substitution reaction of **68a**, this displacement was only efficient if a large excess of the phosphite anion was used, and the chromatography of the product **65a** and **65b** was tedious because of the leftover phosphite. Later I realized I could take advantage of the water solubility of the phosphite; iterative water washes were able to greatly diminish the proportion of phosphite that remained. This made chromatography of the desired product more manageable. The silver mediated coupling reaction^{61,65,66} with **62** worked quickly to give, majorly, the desired amide **49**. Modest yields accompanied this reaction every time despite full conversion of the thioesters **65**. It could be that once the thioester is activated by treatment with silver, it is prone to

decomposition on its own or by a nucleophile other than the amine **62** that might be present in the reaction. Fortunately, I found appropriate conditions to purify the highly polar **49** by MPLC before attempting the Dieckmann reaction.

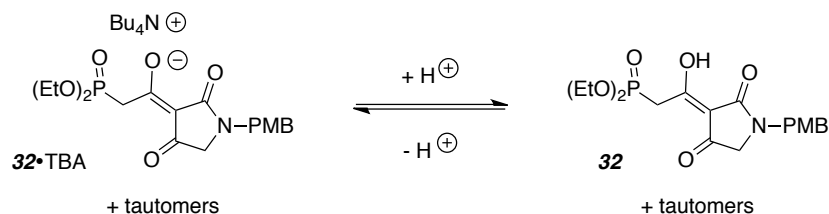
Scheme I-44. Amide 49 From Bromo-Thioesters 70.



The Dieckmann reaction on **49**⁵⁹ was only attempted a few times. The product of the ring closure was clearly observed by LCMS within minutes after treatment with TBAF in Et₂O. The starting material **49** was poorly soluble in ether, so the reaction mixture was commonly heterogeneous. Even so, I observed an increase in heterogeneity after the TBAF was administered. The product heterocycle **32**⁵⁷ was even less soluble in ether, and was observed to precipitate if the reaction was conducted at higher concentration or larger scale. I hypothesized the precipitate was the ammonium salt of the tetramate, **32**•TBA. This precipitate could be collected by filtration, or, surprisingly, extracted into organic solvents such as ethyl acetate or dichloromethane.

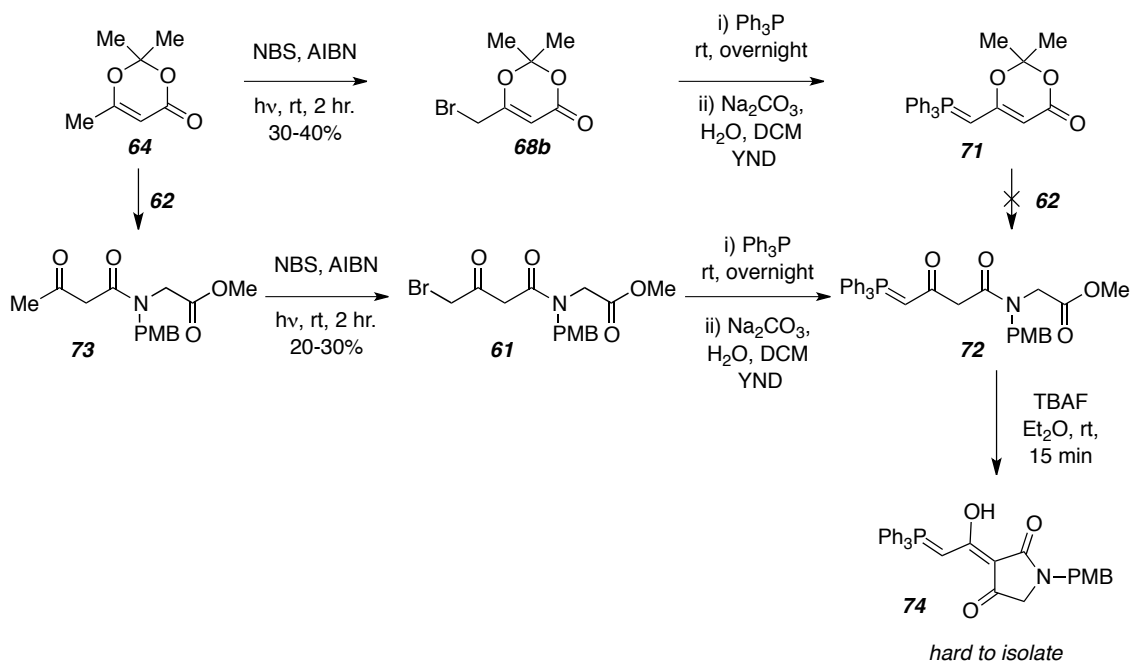
Unfortunately, tetramate **32**•TBA was difficult to purify under normal phase chromatography conditions, and although the cyclized product was obtained and characterized, I had very little material to try the Horner-Wadsworth-Emmons chemistry. In future studies, I took the care to acidify the reaction mixture after the Dieckmann (last step, Scheme I-44) to ensure the neutral tetramic acid **32** was in hand. In summary (Figure I-12), the various anionic forms⁶⁷ and ammonium salts as well as the corresponding neutral tautomeric forms of this species are of interest and could be the result of additional studies.

Figure I-12. Equilibrium Between the Acid and Conjugate Base of Tetramate **32**.



A similar approach can be used to prepare the corresponding phosphorane starting from dioxinone **64**. This is a slight modification from Retrosynthetic Analysis I in Scheme I-17. Phosphorane **72**, instead of **49**, was sought as a Dieckmann substrate. Instead of nucleophilic substitution, the methyl group was brominated under radical conditions (Scheme I-45). Although known for this substrate, the bromination did not proceed efficiently in my hands, and only gave modest yields of the **68b**. Phosphine displacement works well, but the subsequent deprotonation does not. Phosphorane **71**,⁶⁸ although nicely behaved on the LCMS, was difficult to isolate. Opening with **62** and acetone expulsion was even more of a challenge and gave a product that was hard to analyze. There are likely too many functional groups that were labile under the vast array of reaction conditions, so this route to **72** was abandoned in favor of another.

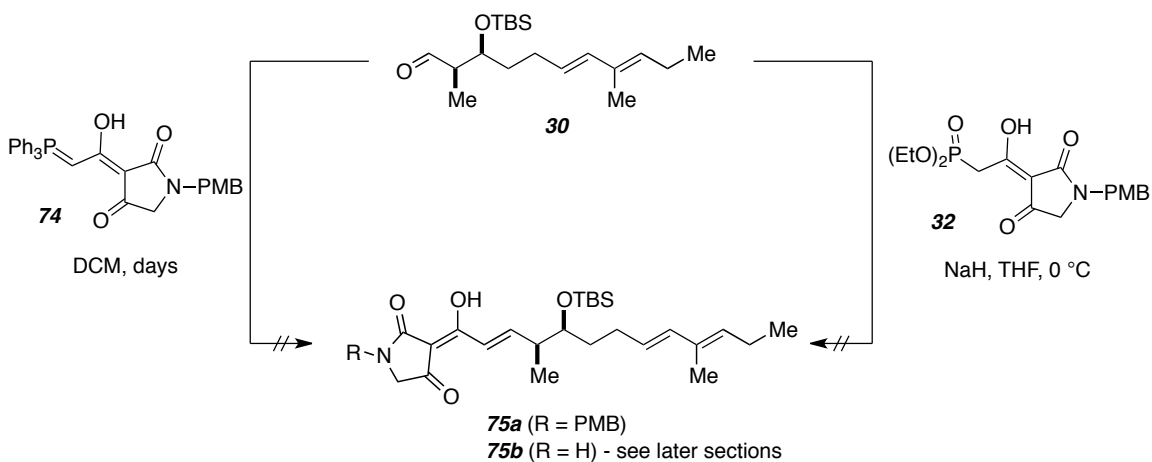
Scheme I-45. Use of 1,3-Dioxenone (**64**) in the Preparation of Phosphorane **74**.



In the second route towards the phosphorane **74**⁶⁸ (downward arrow from **64**, Scheme I-45), the necessary reactions were performed in a different order. The hope was that bromination would be cleaner on a methyl ketone like that in **73**. Additionally, installing the phosphorane near the end would ease the handling of these substrates. First, the amine **62** opened **66** and the bromination of the methyl ketone was attempted. The yields were still poor for this radical reaction, and it appeared that conversion, regiochemistry, and overbromination were the main contributors to this result. Phosphine displacement and deprotonation gave the desired ylide **72**, but this compound was difficult to work with. It was not amenable to chromatography and I was unable to recrystallize it. Still, I attempted TBAF treatment for the ring closure to heterocycle **74**. This gave what might have been the Dieckmann product (monitoring by LCMS), but the product could not be purified. Despite these difficulties, there is still a lot of promise for this route. The ylide is the direct Wittig coupling partner for **30**, and if the sequence could be performed on scale, purification by recrystallization would likely be successful.

Although neither reagent (phosphonate **32** and phosphorane **74**) was in the preferred pure form, I still attempted to use them in the highly-anticipated Horner Wadsworth Emmons⁶¹ and Wittig reactions, respectively (Scheme I-46). Unfortunately, I did not observe any of the coupled product in either case. I saw no reaction in the case of phosphonate **32**. Likewise, I did not see any conversion of aldehyde **30** in the presence of phosphorane **74**.

Scheme I-46. Attempted Olefination Reactions of Aldehyde **30**.

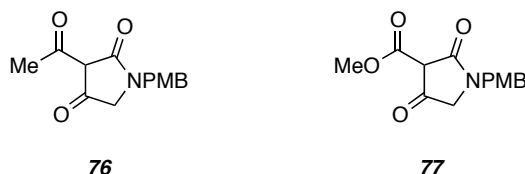


I would still advise further studies here. These types of reagents are known, and more practice in their preparation and use would improve these results. I also think the major obstacle to success is the scale up of the heterocycle. If it could be prepared in larger quantities, purification and reactions on model substrates provide additional insight and increase the likelihood of successful union with aldehyde **30**.

II.A.4. Short Study on 3-Acyl Tetramic Acids **76** and **77**.

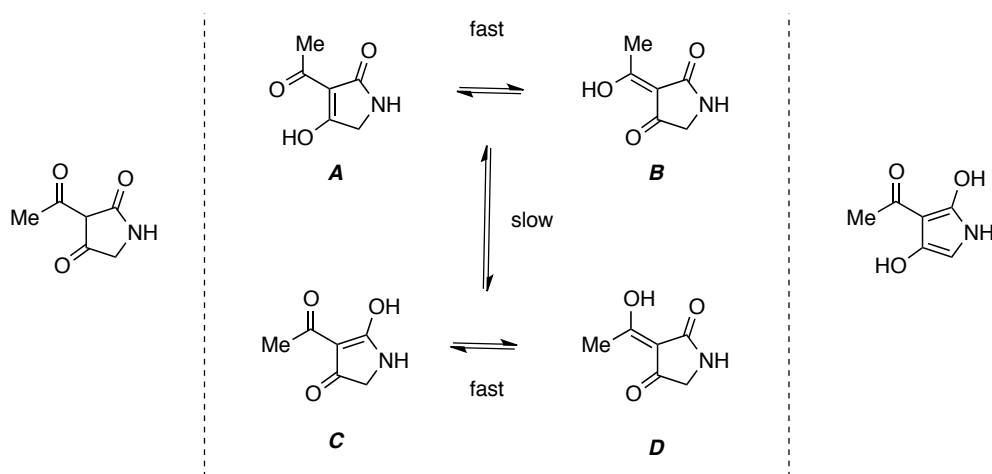
At this stage, the unanswered questions surrounding the behavior of the tetramic acid unit were many (see Figure I-12) and I needed to learn more about these systems. I did not generate sufficient quantities of phosphonate **32** or phosphorane **74** to conduct additional studies. Besides, these compounds contained a lot of interfering functionality; I was more interested in the heterocycle itself. I chose 2,4-pyrrolidinedione **76** and **77** as model systems to perform preliminary studies with the goal of determining the characteristics of tetramic acids.

Figure I-13. Model Tetramates.



B.J.L. Royles previously summarized tetramic and tetronic acids in a comprehensive review.⁶⁹ Contained in this was a discussion on both the acidity and tautomeric preferences. This unit is rarely drawn in the tricarbonyl or doubly enolized (to pyrrole) form (left and right panels of Figure I-14, respectively). Instead, it is known to take one of various mono-enolized tautomeric forms (central panel). With this specific substitution at C3 and with the NH variant, four major forms are predicted. The interconversion between **A** and **B** is internal and rapid, a process too fast to see discrete **A** or **B** on the NMR timescale. Likewise, **C** and **D** are internal tautomeric forms and rapidly interconvert. The pairs **AB** and **CD** can be considered in slow equilibrium with one another. Here, conversion requires an external way to move the proton between species. NMR data and computations suggest a ratio of 15:5:0:80 for **A:B:C:D**.⁶⁹

Figure I-14. Royles' Illustration of Tautomeric Forms of 3-Acetyl-2,4-Pyrrolidinedione.



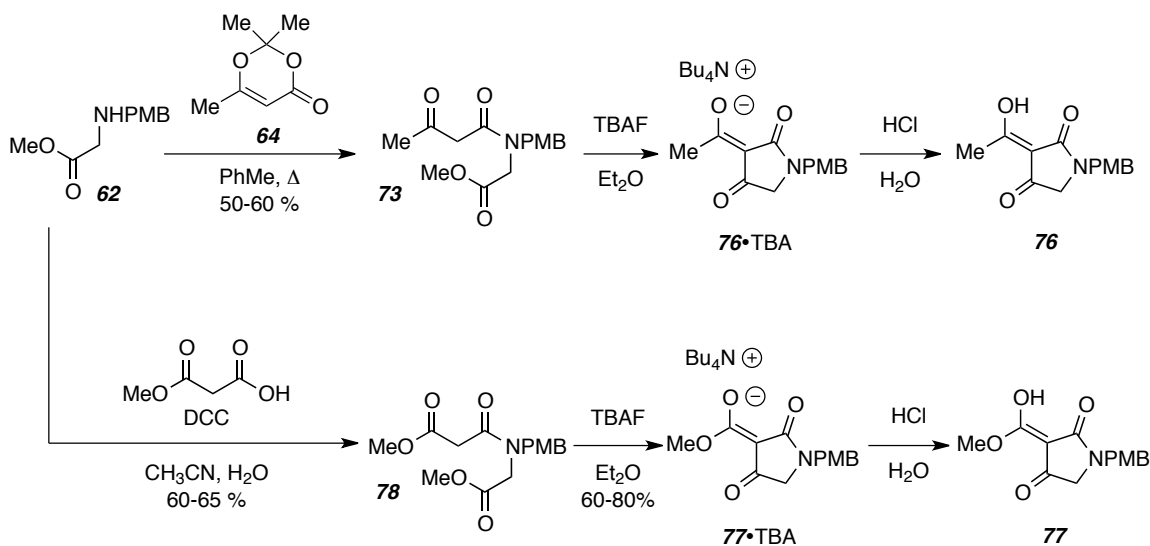
It is with this background that I began my studies on the tetramic acids **76** and **77**.

II.A.4.a. Preparation and Properties of **76** and **77**.

Compound **76** is known in the literature and can be accessed easily by the same ring opening of 1,3-dioxenone **64** (Scheme I-47). It is easily purified by MPLC or column chromatography. The Dieckmann reaction proceeded exceedingly well in Et₂O with two equivalents of TBAF,⁶¹ generating a precipitate that was typically collected by vacuum filtration (it can also be collected by extracting the crude reaction slurry with ethyl acetate, drying, and concentrating). The solid was likely the ammonium salt of the tetramate (**76**•TBA). It was then dissolved in neutral water and treated with acid (HCl or TFA) dropwise until a pH of <2 was achieved. Over the course of this acidification the neutral tetramic acid **76** precipitated and could be obtained in a similar fashion as the salt TBA. Vacuum filtration was the preferred method for reactions performed on scale.

The 3-carbomethoxyl system **77** was also studied (Scheme I-47, lower set of arrows). It was prepared in a different way. Amide **78** was generated under standard peptide bond conditions. The Dieckmann reaction occurred without event to generate the deprotonated heterocycle, **77**•TBA, which underwent acidification under the same conditions as the corresponding ketone **76**. This ester showed similar trends between the salt **77**•TBA and the neutral **77** as observed in the ketone case (reaction times, conditions, solubility).

Scheme I-47. Preparation of **76** and **77**



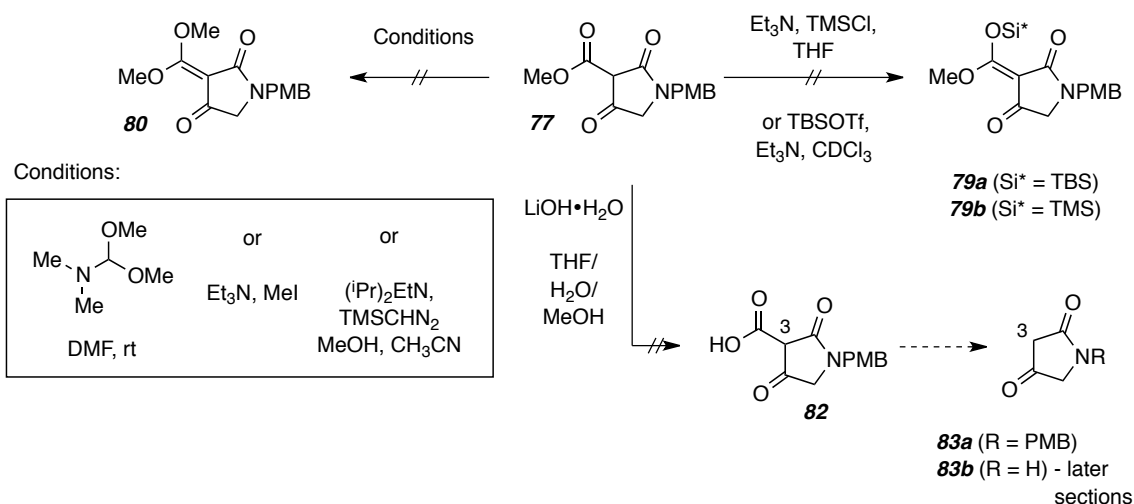
Besides the shift in NMR resonances that accompany this acidification, the salts **76**•TBA and **77**•TBA and the neutral forms **76** and **77**, respectively, display remarkably similar properties. They have similar solubility in most organic solvents and streak on the TLC plate. Despite this last feature, the anionic and neutral form both appeared to be somewhat amenable to column chromatography. There is mainly one tautomer in the ^1H NMR spectrum, making up 90-95% of all possible forms (c.f. Figure I-14). Based on the known preference of **A-D** in Figure I-14,⁶⁹ **76** and **77** are displayed as the exocyclic *Z*-isomer.

II.A.4.b. Alkylation and Further Functionalization Studies of **76** and **77**

I wanted to learn a little more about the tautomeric forms of these tetramic acids. I had more of the ester **77** on hand, so a series of experiments were conducted to trap the various enol forms by O-alkylation or silylation (Scheme I-48). Very few were successful. I attempted to silylate this substrate (right arrow from **77**) with TMSCl in the presence of an amine base and I did not observe any reaction to **79a**. Monitoring the reaction by NMR spectroscopy, I could not see incorporation of TMS. Even with a large excess, I was not convinced that any of the three carbonyls enolized to the silyl ketene acetal, or that any C-Si bond was formed. The same observation was made in the case of TBSCl. For TBS, the silyl enol ether **79b** is presumably more robust. Even so, there was not sufficient NMR evidence for formation of the desired product.

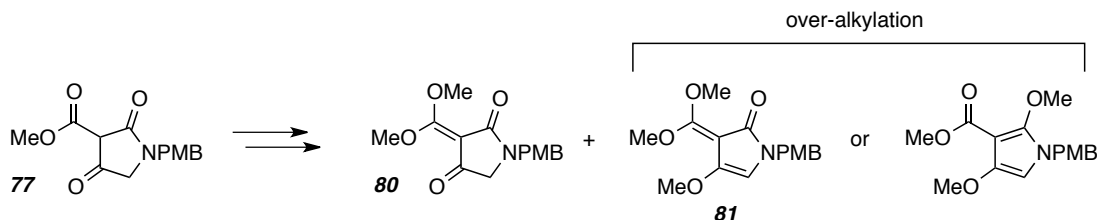
The methylation (Scheme I-48, left arrow from **76**) of these substrates is challenging. The first issue is whether the electrophile is reactive enough, and then, there is the additional concern to where it will react. I tried a variety of conditions and methylating agents, even those more commonly used in the alkylation of carboxylic acids (DMF-dimethyl acetal) or carbanions (methyl iodide). The only conditions that gave the alkylated product **80** were the diazomethane equivalent TMSCHN₂, and there was a small amount of dialkylated product by LCMS (location of the second alkyl group unknown).

Scheme I-48. Attempted Functionalization of 3-Carbomethoxy-2,4-pyrrolidinedione **77**.



There are several ways that additional alkylation might have been occurring (Scheme I-49). My own NMR data suggested that **81** was the likely constitution.

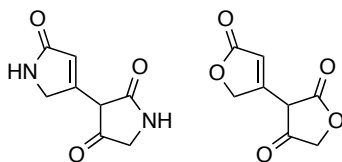
Scheme I-49. Outcome of Alkylation of **77**.



Methyl ester **77** also provided an opportunity to investigate decarboxylation (downward arrow, Scheme I-48) of the corresponding acid **82**. This might have been a way to access 2,4-pyrrolidinedione **83a** (**83b** was sought in a later study and is included here for numbering) with the hope that anion chemistry is possible at C3. Unfortunately, a number of saponification conditions (alkali hydroxides, alkoxide bases, etc) did not effect the transformation to acid **82**. Neither the acid nor the decarboxylated product **83a**

was observed by LCMS. A literature search revealed that heterocycle **83a** was likely unstable anyways; **83b** it is known to partake in decompositions pathways such as dimerization (Figure I-15). The process is known for tetronic acids as well.

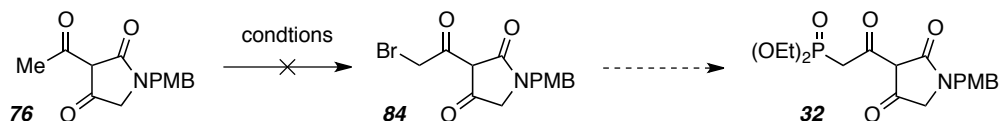
Figure I-15. Dimers of Tetramatic and Tetronic Acids.



The above studies pointed to the difficulty in working with these compounds. They are highly acidic (pH ~ 2-3) and are capable of existing in many tautomeric forms, which I was unable to effectively trap with silylating or methylating agents. In the case where the enol was trapped, it appeared that the exocyclic isomer (**80**, Scheme I-48) was present.

The focus of this set of studies was not necessarily another route to the HWE partner, but I realized that functionality might be built off the 3-acyl tetramate **76**. The goal was to install a reactive group on the methyl ketone. Various bromination conditions were attempted (Scheme I-50). This would be another avenue into the desired phosphonate moiety of **32**.⁵⁹ Although I failed at the time, this line of study is still valuable. Taking the time to optimize the bromination to **84** and displacement to arrive at **32** is justified since **76** is generated in good yield and purity. The route remains attractive.

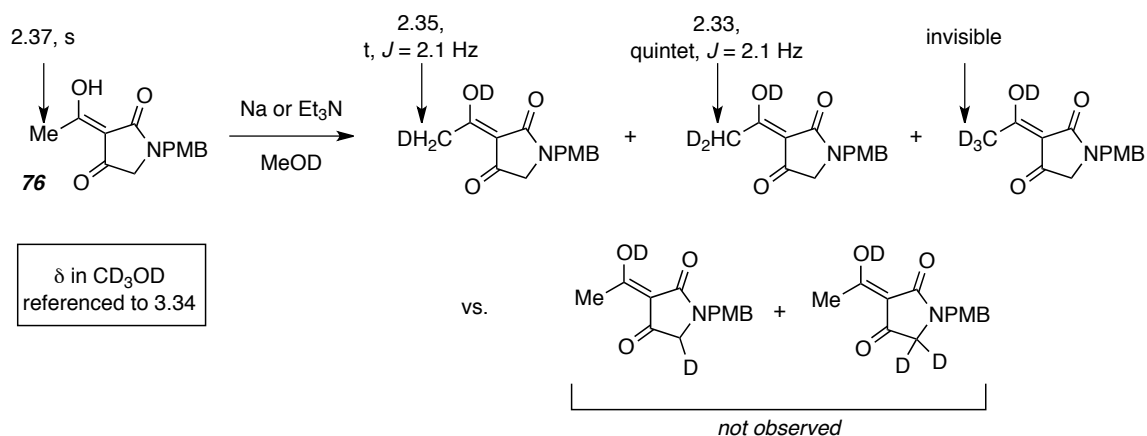
Scheme I-50. Potential Further Functionalization of Tetramate **76**.



II.A.4.c. Deuterium Exchange of Tetramic Acid **76**.

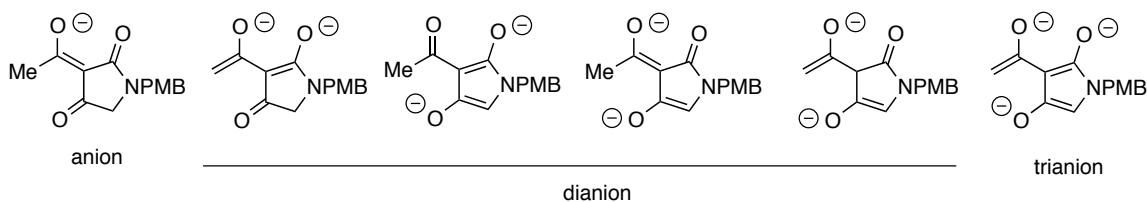
The acidity and reactivity of the resulting anion of the 3-acyl tetramates was investigated in one final way, deuterium incorporation (Scheme I-51). When ketone **76** was treated with a base (NaOMe or TEA) and MeOD, deuterium incorporation occurred at only one site in the molecule. Although only at the methyl ketone, there was an array of products containing 1, 2, or (presumably) 3 deuterium atoms.

Scheme I-51. Deuterium Exchange of 76



These deuterium studies clearly show that the methyl group is more exchangeable than the methylene at C5. The result was the same for 1 equivalent of base versus 2 or 3. A collection of the various anions and polyanions are contained in Figure I-16. The first deprotonation certainly occurs at C3, followed by formation of the dienoyl dianion (second structure), instead of the pyrrole-type anion (third structure). If the latter was in play, D-incorporation would have occurred at C5. Instead, only exchange at the methyl group was noted. Trianion formation under these conditions depends on the on pKa3 for tricarboxyl 76.

Figure I-16. Anionic, Dianionic, and Trianionic Forms of Tetramate 76.



II.A.5. Summary of Retrosynthetic Analysis I

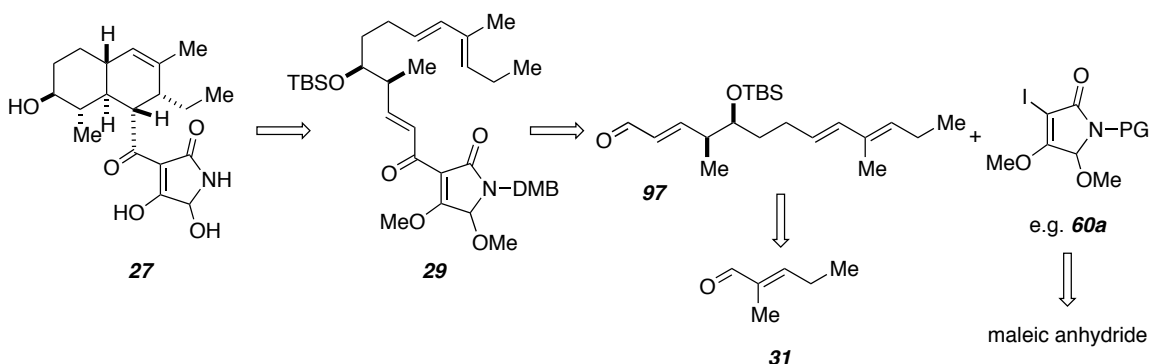
In conclusion, although the aldehyde **30** and phosphonate **32** were successfully prepared, this route was severely hindered by scalability and purification of the latter. Although a late stage HWE has been used successfully for these types of synthetic endeavors,^{57,59} it was not operative for my substrates. Thus, an alternative route was imagined with a different bond-forming event for the preparation of protected intermediate **28** or **29** (General introduction, Scheme I-17). This route (and further along,

Retrosynthetic Analysis III) should make use of some of the best and most robust chemistry from this section for advancing to my goal of a highly reactive IMDA substrate.

II.B. Retrosynthetic Analysis II

This section encompasses all those synthetic routes that bring in the heterocycle intact and where the final carbon-carbon bond is formed via *aldol reaction* of the halo-heterocycle (now with the C5 alcohol, e.g. **60a**) and the ene-aldehyde **97** (Scheme I-52). Routes toward aldehyde **97** follow that presented in **II.A** (i.e., from **31**) but with additional homologation steps. Routes toward the heterocycles **59**, **60a**, and **60b** were featured in **II.A** (i.e., from maleic anhydride), but these halo-heterocycles are now used in an entirely different fashion. Other heterocycles were constructed and are reported in this section so that any various compounds used in a union with ene-aldehyde **97** might be reported together.

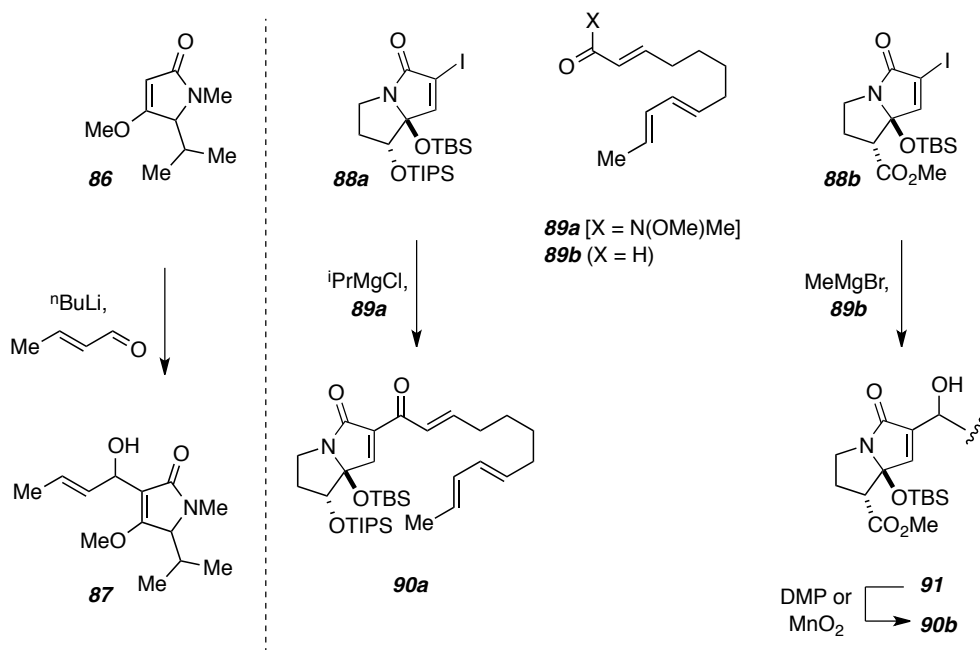
Scheme I-52. Retrosynthetic Analysis II.



This route takes one particular idea from **II.A**. That is, it relies on a way to acetylate or alkylate C3 of the heterocycle **59** (see Scheme I-27, reaction of **48**). The precedent was not explicitly drawn in **II.A** but now is shown in Scheme I-53. Jones and co-workers reported anion chemistry of these types of systems (left panel) and previous members of our group^{27,28} successfully performed substitution reactions (right panel). Jones' method^{70,71} was direct deprotonation of the tetramic acid **86** followed by treatment with an aldehyde electrophile (shown with pentenal) to give alcohol **87** in good yield. Our group's methodology was metal-halogen exchange of **88a** or **88b** (they differ in

protecting groups) followed by treatment with the appropriate electrophile.^{32,33} Weinreb amides, acid chlorides (not shown) and aldehydes were all found to engage in this reaction, giving 3-acyl compounds like **90a** or in the reaction with aldehyde **89b**, alcohol **91**. Oxidation afforded the corresponding ketone **90b** in just one additional step.

Scheme I-53. Methods for C3-Anion Chemistry.



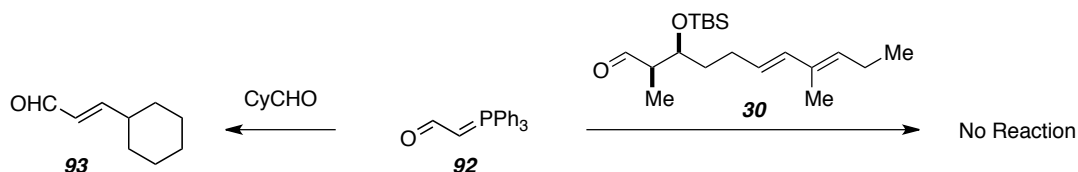
The precedent illustrated above encouraged me to attempt a similar union with my substrate. I had previously prepared the required heterocycles **59**, **60a**, and **60b** (Scheme I-36), so construction of aldehyde **97** was undertaken.

II.B.1. Route to Ene-Aldehyde **97**

Aldehyde **97** is theoretically available in one step from aldehyde **30**, already prepared in Retrosynthetic Analysis I. The two-carbon homologation reaction only requires phosphorane **92**. The model reaction with cyclohexyl carboxaldehyde (Scheme I-54) worked fairly well (left arrow, to **93**). Although full conversion was not realized, and there were few byproducts, the product was identifiable by several methods. Even though this was a modest result, I still tried the reaction on my substrate **30**. Unfortunately, even with excess reagent and days under high concentration, no event occurred to give any

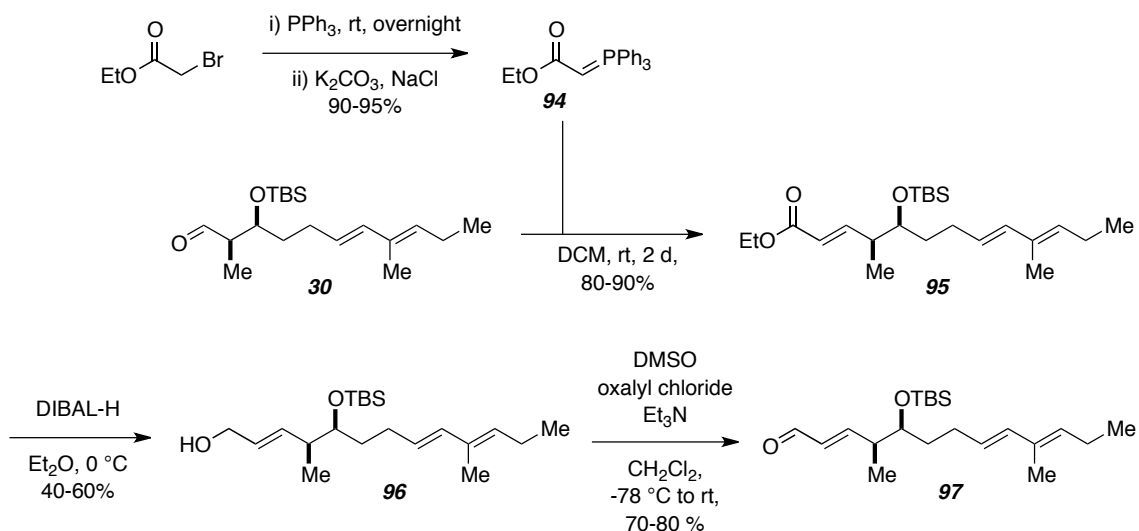
desired product. This result, coupled with the expense of the homologation reagent **92**, prompted me to abandon this method after only one try.

Scheme I-54. Homologation of CyCHO and attempted homologation of aldehyde **97**.



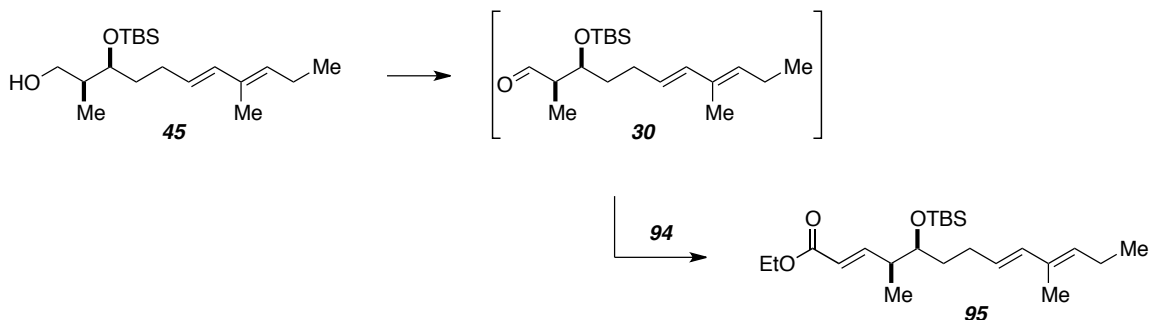
Alternatively, the two-carbon homologation can be effected by a Wittig-reduction-oxidation sequence (Scheme I-55). Although 3 steps in comparison to Scheme I-54, the chemistry is basic and popular, and all the intermediates are amenable to MPLC or column chromatography. The Wittig reagent **94** was easily prepared in two steps from ethyl- α -bromoacetate as shown in Scheme I-55. Bromide displacement by triphenylphosphine and deprotonation afforded phosphorane **94**, which was recrystallized. The aldehyde **30** was reacted with **94**. This key reaction must be conducted under very high concentration, and even then, it is sluggish and I occasionally saw incomplete conversion of the ester **95**. Nevertheless, it was used repeatedly, and could be scaled to >2 grams. The subsequent DIBAL reduction to allylic alcohol **96** and Swern oxidation occurred without event to provide the desired ene-aldehyde **97**.

Scheme I-55. 3-Step Homologation of Aldehyde **30**.



Upon scale up, it was more common to add the phosphorane **94** directly to the pot where Swern oxidation⁷² had been used to produce aldehyde **30** (Scheme I-56). In this way, one work-up and one purification step were avoided.

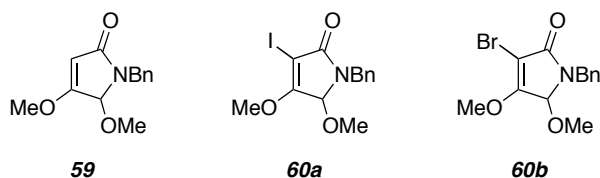
Scheme I-56. Optimization of Homologation Sequence.



II.B.2. The Heterocycle

At the same time, I had the desired heterocycles in hand (Figure I-17, from II.A.) for the coupling reaction. Direct deprotonation of C3,⁷⁰ or metal halide exchange of the iodide **60a** or bromide **60b** generates the organometallic species required for reaction (see Scheme I-53).³³

Figure I-17. Substrates for C3Anion Chemistry.

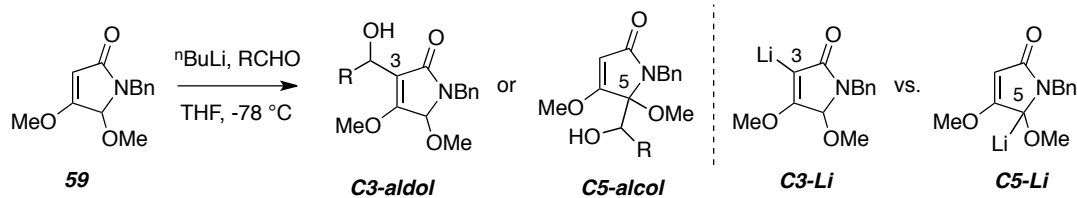


II.B.2.a. From Maleimide Route - Deuterium studies and Reactions of **59**, **60a**, and **60b**

In the case of carbon acid **59**, deprotonation is reported to occur at C3, and reaction with an appropriate aldehyde (shown generally as RCHO, Scheme I-57) would give the aldol product (represented generally as allylic alcohol **C3-aldol**). This is the result if the organometallic **C3-Li** is in play. Alternatively, it has been suggested that if the substitution at C5 is not sufficiently bulky, deprotonation can occur there.⁷⁰ The result of this reaction (with the same aldehyde) delivers a different aldol product, the homoallylic

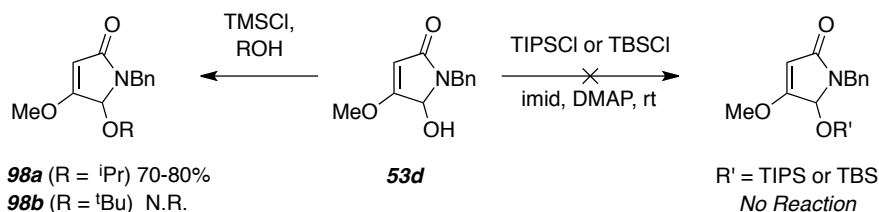
alcohol **C5-aldol**. This requires organometallic **C5-Li** (shown as this isomer, though anionic character certainly exists on the oxygen of the amide) to be operative.

Scheme I-57. Regiochemistry of Alkylation of **59** and Respective Organometallics.



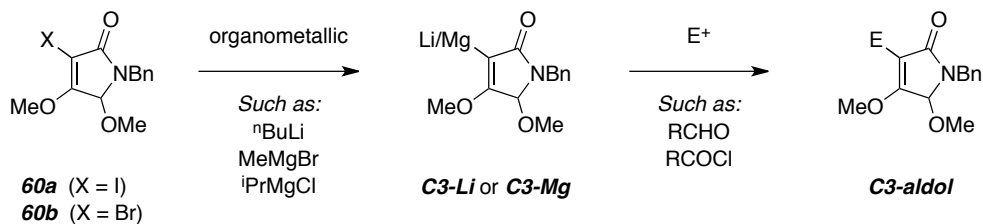
Over the course of my studies, I became convinced that heterocycle **59** was not selective for the desired C3 anion. I attempted to prepare the heterocycle with a larger C5 alkoxy group (Scheme I-58). I was successful in the incorporation of isopropanol into **53d**⁵¹ to furnish aminal **98a**, but I saw no reaction with tBuOH (for **98b**). Similarly, I did not observe any silylation upon treatment of the carbinolamide with TIPSCl or TBSCl. Nevertheless, I could test the isopropoxy-substituted heterocycle **98a** for deprotonation.

Scheme I-58. Substitution at C5 With a Bulkier Group.



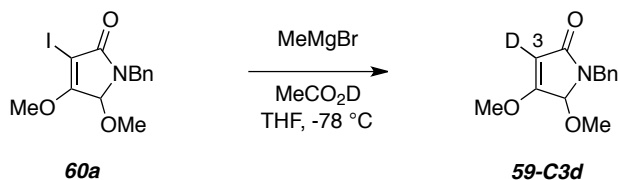
The alkyl halides **60a** and **60b**, as opposed to **59**, are only capable of a C3 anionic species (**C3-Li** or **C3-Mg**, Scheme I-59), and these will provide the C3 alkylated or acylated products of the type **C3-aldol**. The hope was that both aldehydes and acid chlorides were appropriate electrophiles for this reaction.^{32,33} The C3-acyl compound could be generated directly, or simple oxidation of the aldol product would provide the desired functionality.

Scheme I-59. General Scheme for Metal-Halogen Exchange and Subsequent Reaction.



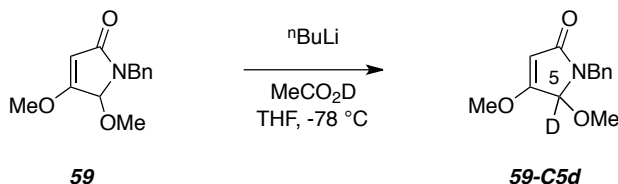
From NMR monitoring of the reaction, it was surprisingly not straightforward to assign the site of alkylation. For this reason, I performed a deuterium study on the alkyl halide first (Scheme I-60), to characterize the species **59-C3d** first, and it would serve as the basis for assignment of regiochemistry for the same experiment on **59**. In the event, metal-halogen exchange with MeMgBr and quenching with acetic acid-d cleanly gave **59-C3d** with full exchange at C3.

Scheme I-60. Deuterium Substitution at C3 of Iodide **60a**.



The deprotonation of **59** and quenching with the same acid afforded a different product (Scheme I-61). From NMR analysis, it was clear that H5 (observed and assigned by **59-C3d**) had exchanged to deuterium. In this case, there was only about 50% exchange, but the result was clear. At C3, there was still a proton. Thus, the anion chemistry on **59** would not be useful unless the site of reaction could be altered by bulk of an electrophile. If the electrophile could not get close enough to C5, reaction at C3 from a species like **C5-Li** (Scheme I-57) is possible. If C5 is sufficiently hindered, even though deuterium incorporation occurred there, an aldehyde might not react there.

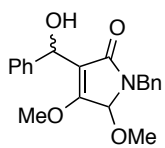
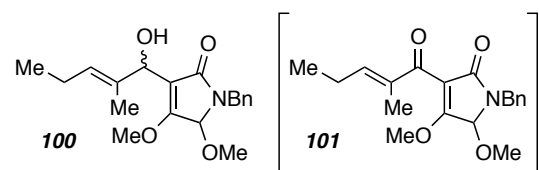
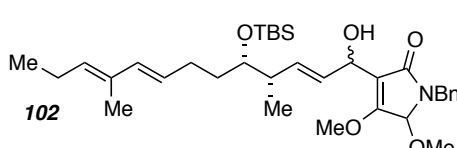
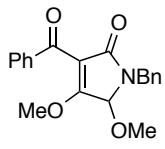
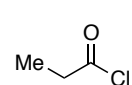
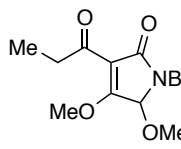
Scheme I-61. Deuterium Substitution at C5 of **59**.



With evidence that more reliable and useful chemistry was available with the halides **60a** and **60b**, a short study was conducted on the various bases and electrophiles that could contribute to and participate in the reaction of these heterocycles. Table I-2 presents a summary of the chemistry used. A detailed discussion is not provided here; it is only noted that two bases (ⁿBuLi, MeMgBr) were found to enable and two types of electrophiles (aldehydes, acid chlorides) were found to participate in the reaction. Even highly functionalized ene-aldehyde **97** was used. The mass of product **102** was confirmed

by LCMS and enough material was obtained for ^1H NMR characterization, but no further studies (e.g. IMDA) could be conducted. Benzylic **99** and allylic alcohol **100** were produced as a mixture of diastereomers (see experimental). The synthesis of the C3-benzoyl- (**103**) and propionyl- (**104**) heterocycles was achieved as well.

Table I-2. Summary of C3-Alkylation and Acylation Reactions.

entry	heterocycle	base	electrophile	product
1a	60a	MeMgBr	PhCHO	 99
1b	60b	$n\text{BuLi}$		
2	60a	MeMgBr	31	 100 and 101
3	60a	MeMgBr	97	 102
4	60b	$n\text{BuLi}$	PhCOCl	 103
5	60a	$n\text{BuLi}$		 104

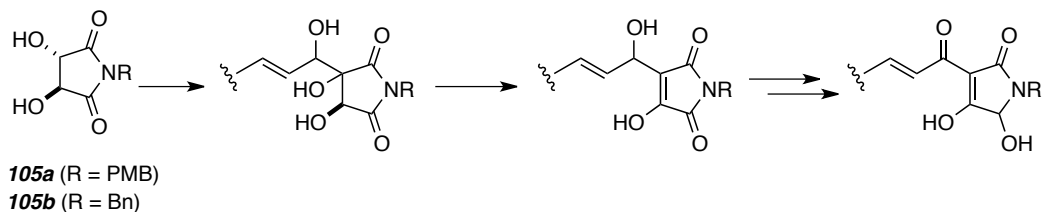
Sadly, although anion chemistry at C3 was promising (Table I-2), experiments were generally unsuccessful. Most often, unreacted starting material was returned or MeMgBr addition to aldehydes was observed. Compounds **99-104** were never generated in good yield. Moreover, scale up of the reagents (both **60a** and **97** for my real system) was tedious and time consuming. They could never be produced on a large enough scale for the reaction to be useful. Additionally, initial experiments for the deprotection of **59** indicated very harsh conditions would be necessary for hydrolysis of the C4 enol ether.

Other routes toward a suitable heterocycle were sought with the hope that aldol chemistry of these was more successful.

II.B.2.b. Attempted Synthesis From Tartaric Acid

There were promising reports for the construction of and subsequent anion chemistry of heterocycles from tartaric acid.⁷³ I hoped to access a structure like **105** (Scheme I-62).

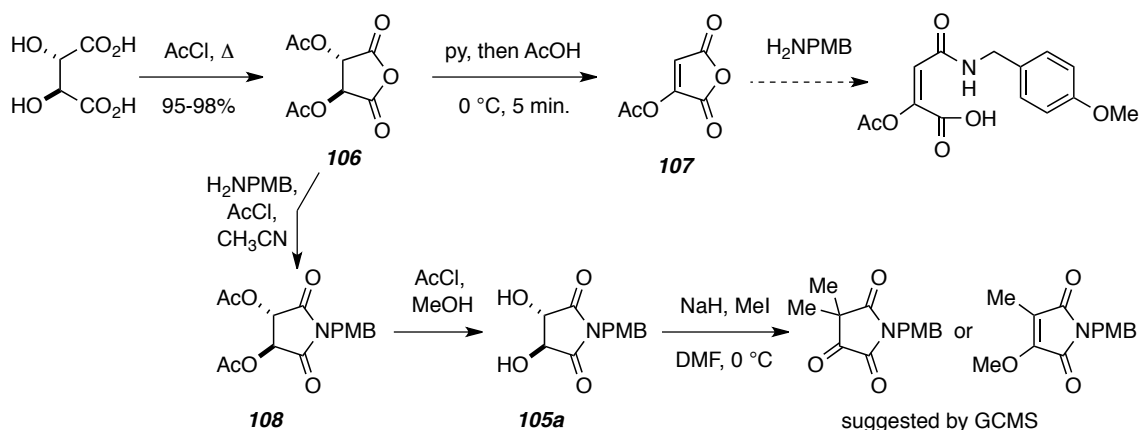
Scheme I-62. General Anion Chemistry of Diols **105**.



Here, deprotonation would be available at C3 or C4 (tetramate numbering). Either way, after alkylation (to the triol shown), loss of water would likely give a bisallylic alcohol (third general structure). Further transformations (oxidation to the ketone, reduction at C5) might be available to afford the desired C3-acylated tetramate.

In order to access the diol for these studies, I used the known route starting from tartaric acid (Scheme I-63, top arrow). The acid was easily converted to the anhydride **106** upon heating in acetyl chloride.⁷³ The product **106** was crystalline and easily handled. Elimination of acetic acid was effected by treatment with pyridine,⁷⁴ and the product enol was re-acetylated to provide **107**. At this stage, I tried to effect ring opening with benzyl amine, but I did not observe any of the desired amic acid.

Scheme I-63. Preparation of Diol **105a** and Subsequent Substitution Attempt.



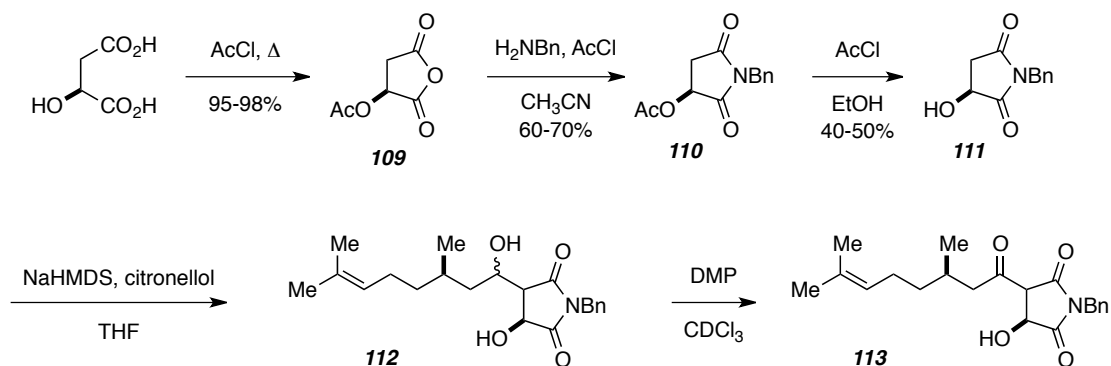
I was, however, able to transform the anhydride **106** into the imide **108** (downward arrow). This process was performed in the same fashion as previously (for series **50a-d**), but the yields were modest. Perhaps alternative protecting groups could be used. Even so, I isolated the imide and then removed the acetyl groups (AcCl, MeOH) in anticipation of anionic chemistry on diol **105a**. At this point, I had come to the end of my available material, but I was still able to run a model anion experiment.⁷⁵ I choose methyl iodide; I wanted to use a sufficiently reactive electrophile. The constitution remains unknown but by GCMS, the mass of two methyl groups were added to the heterocycle. Unfortunately, even if this was more successful, the reaction would not be a very good predictor of the chemistry that I desired for my real substrate (alkyl halide versus ene-aldehydes like **97**).

The chemistry from tartaric acid was not very promising. In favor of other, more reliable chemistries, I moved to the malic acid series. I had more success with this substrate, and even though a number of functional group interconversions remained for the heterocycle to mimic that of **2**, it was a worthwhile study.

II.B.2.c. Attempted Synthesis From Malic Acid⁷⁶

Malic acid was easily dehydrated to the anhydride **109** under the same conditions as the related tartaric acid (Scheme I-64). Anhydride **109** was then converted to imide **110** using the standard conditions (here simple benzyl amine was used in for initial study). Removal of the acetyl group was achieved in modest yield. The free alcohol is typically used for subsequent transformations on the imides like **111**. One such transformation is an aldol reaction.⁷⁷ I chose citronellal as a model; although not α -branched, it is a longer chain aldehyde like the one I would use. In the event, alcohol **111** was treated with two equivalents of commercial NaHMDS at low temperature and subsequent addition of citronellal afforded diol **112**. The relative configuration of the aldol product was not determined, since the two stereogenic centers would be destroyed in the subsequent oxidation reaction. Dess-Martin oxidation converted **112** to its keto-analog **113**. This tricarbonyl substrate likely exists as a collection of tautomeric forms, so the stereochemistry of the C3 substituent was not determined. All of these reactions were monitored by TLC and LCMS.

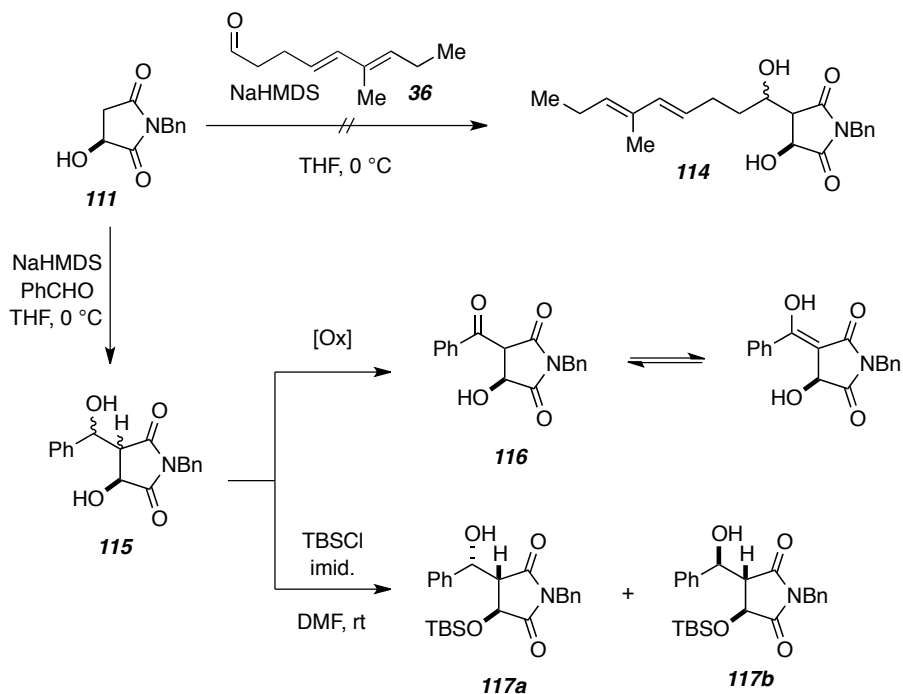
Scheme I-64. Preparation of Alcohol **111** and C3-Substitution Reaction.



The model system (Scheme I-64) was successful, but I continued to practice to ensure the reaction on my system (ene-aldehyde **97**) would succeed. I tried with one of my earlier aldehydes (**36**, Scheme I-65), but unfortunately saw poor yield of the desired aldol product. Frustrated by this result after having success with citronellal, I stepped back to a simpler system, benzaldehyde. Generation of the dianion followed by treatment with the PhCHO gave a mixture of diastereomers **115**, visible by differences in NMR characteristics. A portion of this mixture of diols was monosilylated and separation of diastereomers was performed, giving pure samples of **117a** and **117b**. Based on the literature,⁷⁷ the stereochemistry of the major aldol products (there are two of them) are as shown in Scheme I-65.

Alternatively, treatment of diols **115** with Dess-Martin afforded the 3-acetyl tetramic acid derivatives (middle arrow, Scheme I-65). All the stereochemical information from the aldol reaction is likely be destroyed by keto-enol tautomerization as shown.

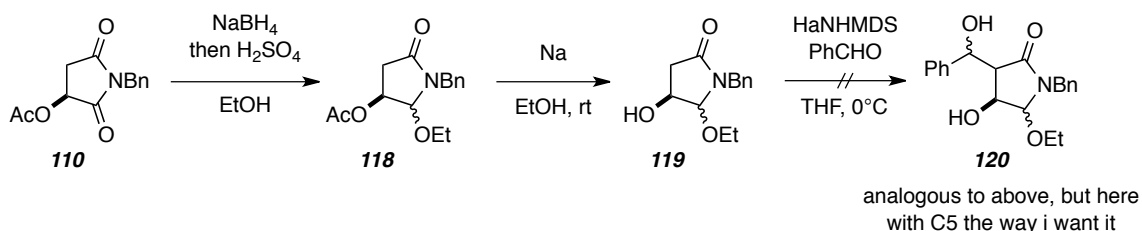
Scheme I-65. Attempted C3 Substitution with Aldehyde **36** and Benzaldehyde.



The reaction conditions now worked out for another model compound, I planned on experimenting on my real system. However, as one last set of experiments, I wanted to ensure that the imide derived from malic acid (e.g. **110**, Scheme I-64) could undergo functional group manipulations. In particular, I wanted to be confident that reduction could occur at C5 so that the carbinolamide was a viable intermediate (see Scheme I-62, last set of reactions).

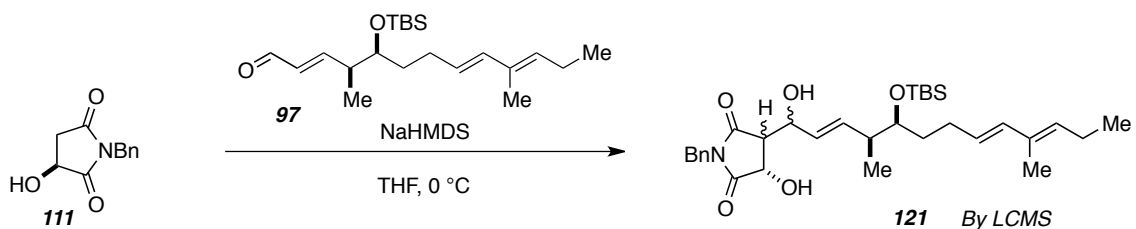
To my delight, reduction by NaBH₄ in ethanol followed by sulfuric acid treatment provided the alkylated carbinol amide **118** (Scheme I-66).⁷⁸ Surprisingly, the acetyl protecting group remained intact, but it was subsequently removed by treatment with NaOEt to afford alcohol **119**. Unfortunately, this reduced compound was not effective in the aldol reaction. No trace of desired product **120** was observed by LCMS when the reaction was attempted with NaHMDS and benzaldehyde. Thus, while the route from malic acid might allow for aldol reaction (successes of Scheme I-64 and I-65), only certain oxidation states are accessible for the heterocycle.

Scheme I-66. Reduction of Diol **118** at C5 and Attempted C3-Alkylation.



Lastly, I did return to the best conditions for the aldol reaction of **111** and finally attempted the experiment on my real substrate, aldehyde **97**. I was very happy to observe the mass of the coupled product **121** by LCMS, but I was unsuccessful in acquiring enough material for full characterization.

Scheme I-67. Attempted Union of **111** and Ene-Aldehyde **97**.



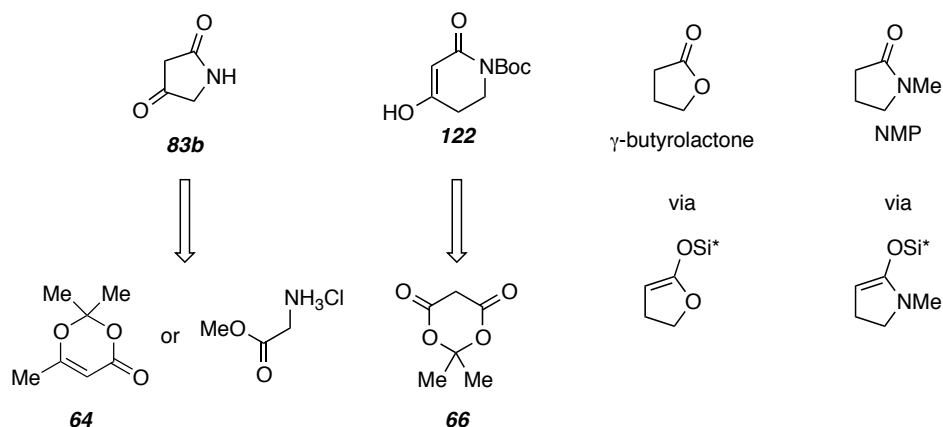
The work on various heterocycles available from malic acid⁷⁶ was promising. Sadly, a lot of these studies went unutilized since I could not prepare the adduct **121** in sufficient quantities to perform additional experimentation (either oxidation state manipulation of the tetramate or IMDA chemistry).

II.B.3. Attempts to Synthesize and Attach Selected Model Heterocycles to 97

It was over the course of these studies that I considered a detour from the heterocycles I was working on. It is clear that integramycin (**2**) contains a tricky tetramic acid. As important as that unit is for the Diels-Alder reaction as described in the introduction, as a brief reprieve, it was worthwhile to attach my triene to any heterocycle. As long as this was straightforward chemistry, I could characterize the IMDA precursor and the product and start to construct a library of IMDA adducts. This would mostly serve as a list of the various half lives and stereochemical outcome of the IMDA reaction. The heterocycles I began targeting are shown in Figure I-18. These all have been reported

to engage in aldol reactions, and I hoped to be successful in that chemistry and begin to study some [4+2] chemistry.

Figure I-18. Various Heterocycles Under Study.



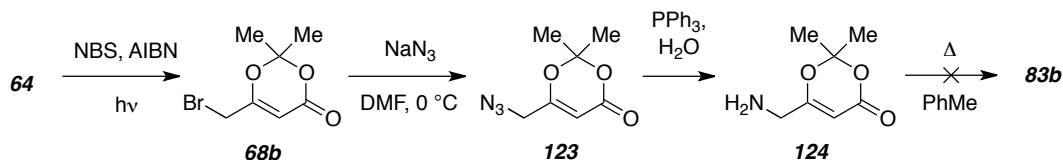
I planned on preparing the tetramic acid **83b** (Figure I-18) by the methodology that afforded the 3-acyl derivatives **77** I studied in **II.A**. For the 6-membered ring **122**, I planned to start with Meldrum's acid (**66**). After what I had discovered with tetramic acids, I hoped this ring would be easier to handle and analyze. Heterocycle **122**⁷⁹ would be useful as a model because it would still result in a tricarbonyl unit to activate the dienophile. Lastly, appending γ -butyrolactone⁸⁰ or NMP⁸¹ looked to be straightforward and would contribute to the conclusions I planned to draw on activation of my triene (e.g. in **97**). With these substrates either direct deprotonation or formation of the silyl enol ethers for use in Mukaiyama aldol chemistry was envisioned.

II.B.3.a. 2,4-Pyrrolidinedione 83b (Tetramic Acid)

I knew that the preparation and handling of 2,4-pyrrolidinedione was going to be tricky. There are numerous reports of this compound being prone to polymerization. Even so, there was enough in the literature to provoke study. 1,3-Dioxenone **64** had already been used as a β -keto equivalent and looked like it would perform the same way with an intramolecular trap. Bromination of the methyl group proceeded as previously described (Section **II.A**). Bromide displacement by NaN₃ occurred nearly quantitatively to afford azide **123**. Standard Staudinger reduction conditions resulted in full conversion of the starting material, but the amine **124** was difficult to purify. A number of attempts were

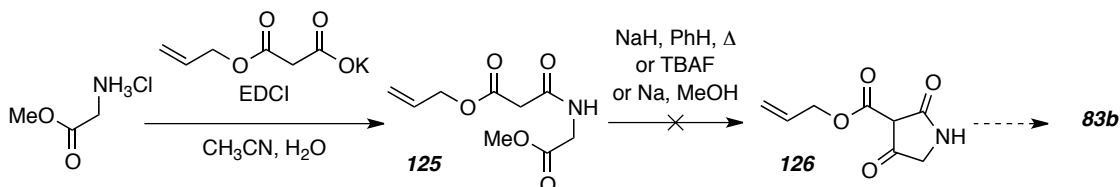
made to either chromatograph or “salt out” the amine, but these were unsuccessful. I did take a portion of the crude material and heated in toluene to try to achieve **83b**, but LCMS did not indicate any desired product.

Scheme I-68. Attempt to Synthesize **83b** from 1,3-Dioxenone (**64**).



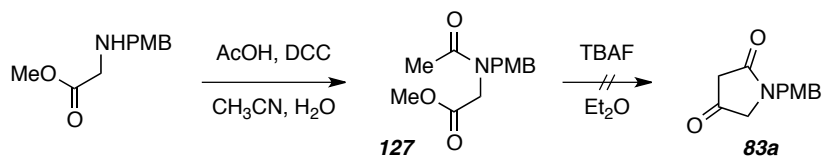
Despite these less encouraging results, a few more experiments were performed in an effort to realize the desired dione **83b**. The Dieckmann reaction had previously proven to be efficient, so ring closure under those conditions and a way to remove any temporary C3 substituent was devised (see Scheme I-69). A pendant allyl ester was sought at the C3 site; I planned to perform subsequent deallylation and decarboxylation. Though the Dieckman precursor amide **125** was easily prepared by standard peptide bond conditions, the Dieckmann reaction failed under a variety of conditions. Cyclized product **126** could not be obtained for further study.

Scheme I-69. Attempt to Synthesize **83b** from Decarboxylation.



I also tried direct ring closure from methyl ketone **127** (Scheme I-70). The precursor was cleanly formed under peptide bond conditions, but it could not be converted to the heterocycle **83a**. This struggle, with this particular Dieckmann substrate, was known in the literature,⁶¹ so this route was not examined any further.

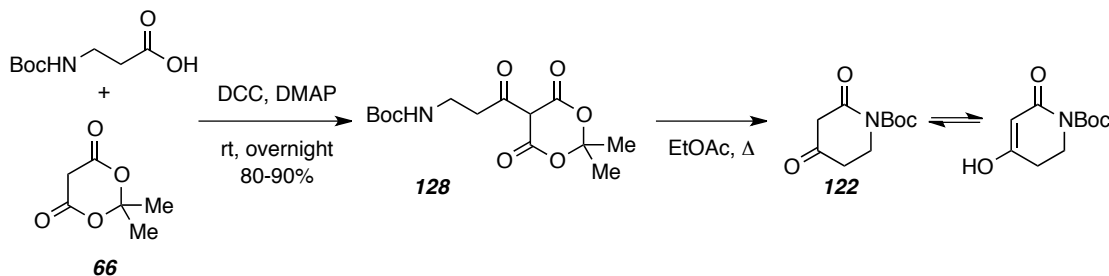
Scheme I-70. Attempt to Synthesize **83b** by Dieckmann Reaction.



II.B.3.b. The 6-membered Ring

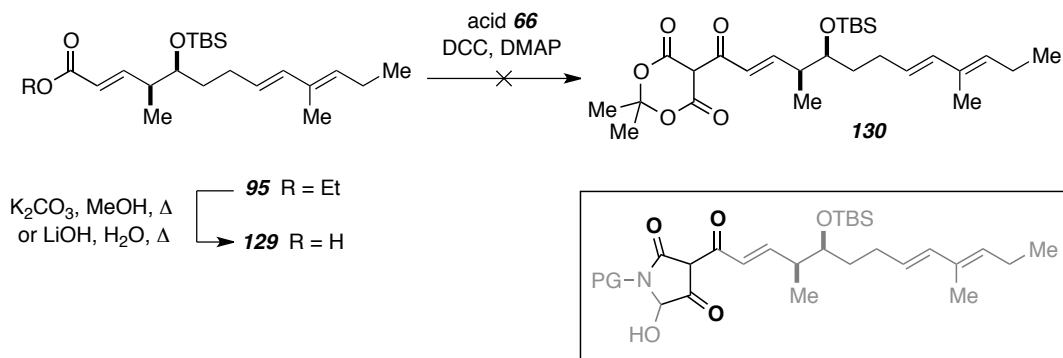
With the very limited success and lessons learned from the previous study, I moved on to what I hoped to be a more manageable heterocycle. Six-membered ring **122** (Scheme I-71) is known⁷⁹ and was likely not subject to the problems of the five-membered ring. It also looked relatively straightforward to synthesize. The reaction began with coupling of N-Boc- β -alanine with Meldrum's acid in the presence of DCC and DMAP. The crude tricarbonyl **128** was sufficiently pure for further reaction. Upon heating in ethyl acetate, the desired ring closure/ring opening was observed in one hour (LCMS), and conversion was modest, but fairly clean to the desired heterocycle **122**. Sadly, heating longer to effect further conversion only led to complications, and I still could not achieve the level of conversion that I desired. Although the LCMS indicated the desired reaction had occurred, I could not confirm this by NMR analysis and I was unable to isolate the desired compound.

Scheme I-71. Attempt to Synthesize Heterocycle **122** by Ring-opening/Ring-closing Sequence.



Although not very encouraging for access to the targeted 6-membered heterocycle, the route above did promote DCC coupling as an effective way to prepare tricarbonyl species much like my desired one (see box, Scheme I-72, bolded). Although the ester **95** could be converted to the corresponding acid **129**, the coupling with Meldrum's acid to **130** was unsuccessful. There are number of factors that might have led to this failure (the acid **129** was used crude, among others) so this reaction is worth attempting again. The tricarbonyl moiety is hypothesized to have a great effect on the chemistry of the attached alkene.

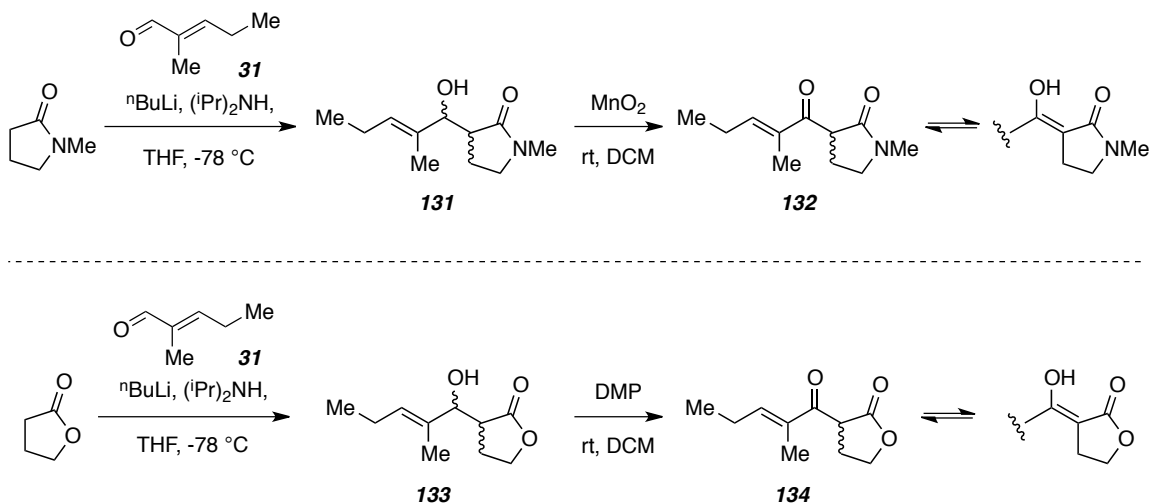
Scheme I-72. Attempted DCC Coupling with Ene-acid **129** and Meldrum's acid.



II.B.3.c. γ -Butyrolactone and NMP

In an effort to attach any heterocycle to aldehyde **97**, the chemistry of γ -butyrolactone and NMP was researched. Test reactions were performed with these heterocycles and model aldehydes. Direct aldol reaction was attempted with NMP⁸¹ and 2-methyl-2-pentenal **31** (Scheme I-73, top). Using LDA as the base, the reaction proceeded in poor yield to give the aldol adduct **131**. Enough desired product was isolated for characterization before oxidation to ketone **132** was carried out with MnO_2 . The desired product was observed by LCMS.

Scheme I-73. Direct Aldol on NMP and γ -butyrolactone with **31**.

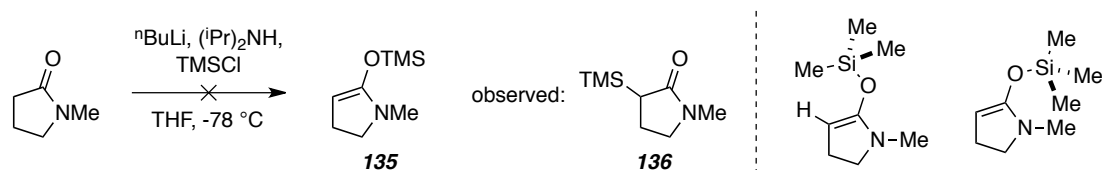


Similarly, the reaction γ -butyrolactone⁸⁰ gave a low yield of adduct **133** (Scheme I-73, bottom). Alcohol **133** was oxidized (this time under Dess-Martin conditions) to

generate the net-acylation product **134**. Low yields were discouraging and prevented me from considering this reaction for the real system (*i.e.* ene-aldehyde **97**).

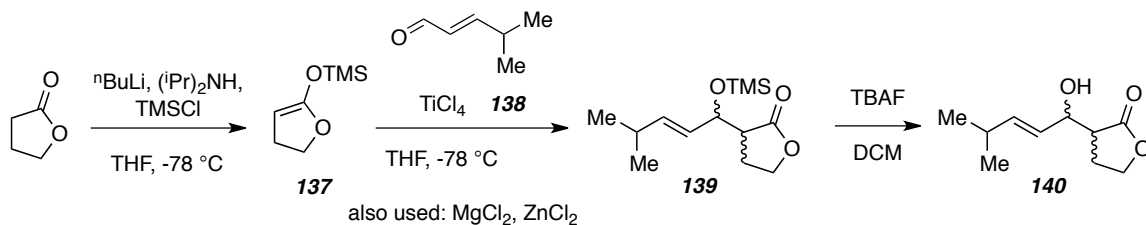
Figuring that the deprotonation was the problem, I considered the corresponding Mukaiyama aldol methodology for this coupling reaction. The silyl enol **135** either could not be prepared from NMP; I saw only C-silylation (**136**, Scheme I-74, left). The expected product is not formed, maybe due to the strain associated with the bulky TMS interfering with either the vinyl proton or the N-methyl group in either rotamer (Scheme I-74, right panel).

Scheme I-74. Attempted Preparation of Mukaiyama Regent **135**.



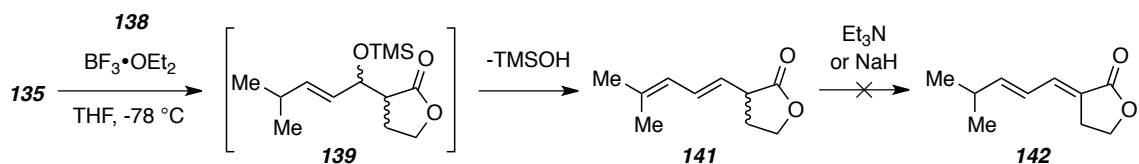
The silyl enol ether derived from butyrolactone (**137**) was realized, however, using LDA as a base and trapping the enolate with TMSCl (Scheme I-75). The Mukaiyama aldol reaction of **137**⁸² with model aldehyde **138** (TiCl₄ as the Lewis Acid) was moderately successful. The aldol adduct was observed by LCMS, but the product had incorporated a TMS group (**139**). The silyl group was easily removed by treatment with TBAF.

Scheme I-75. Mukaiyama Aldol Reaction of γ -butyrolactone and Aldehyde **138**.



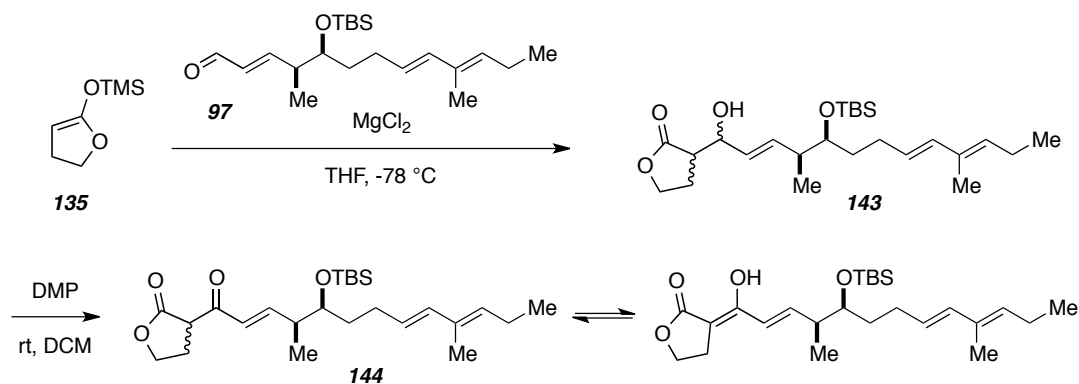
This reaction was attempted with several different Lewis Acids. Under certain conditions (BF₃•OEt₂), the dehydrated product **141** was observed (Scheme I-76). Interestingly, it appeared that the β,γ -unsaturated enone was formed. This requires 1,4 elimination of water (or TMSOH) from what would be considered the less reactive end of system **139**. The diene could not be coerced into conjugation (as in **142**) by treatment with a base.

Scheme I-76. Mukaiyama Aldol of γ -Butyrolactone and **138** Under $\text{BF}_3 \cdot \text{OEt}_2$ Promotion.



With the experience on that model series (Scheme I-76), I moved to my real substrate. The Mukaiyama aldol appeared to be working well, so those conditions were applied. There were additional considerations. The real substrate **97** was very sensitive to acids (Lewis and Bronstead promote IMDA) so a very mild Lewis acid was chosen for the reaction. In practice, the silyl ketene acetal **137** was added to a cooled, stirred solution of aldehyde **97** and MgCl_2 in THF. This reaction was monitored by LCMS, which indicated that a successful union occurred. Aldol adduct **143** was recovered in modest yield, which enabled characterization by ^1H NMR spectroscopy. The oxidation reaction to the corresponding ketone **144** was performed on a very small scale, but its success was confirmed by LCMS.

Scheme I-77. Mukaiyama Aldol Reaction of γ -Butyrolactone and Aldehyde **97**.



Various conclusions were drawn from this study. The aldol reaction with any of these simpler heterocycles worked modestly; it was not robust at the scale it was performed, and it was difficult to justify the time and energy in optimizing these conditions. These substrates would only serve as models to see if any heterocycle imparts reactivity to the triene arm in a Diels-Alder sense. I returned to the real system with candor.

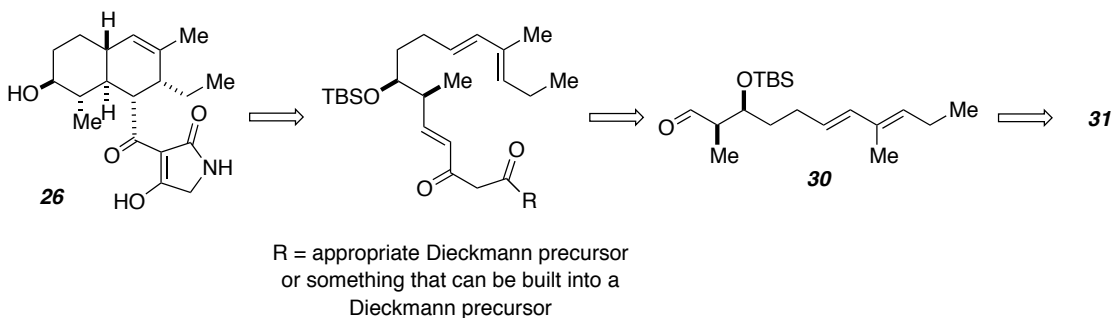
II.B.4. Summary of Retrosynthetic Analysis II

The experiments in Retrosynthetic Analysis II (Section II.B) as a whole were instructive in building functionality into a heterocycle and learning the details of various aldol reactions of these heterocycles. The deuterium studies indicated that there are several acidic sites on some of these five-membered rings. The tartaric and malic acid routes to an appropriate substrate were moderately successful but could not be performed on scale. Moreover, the aldol chemistry was simply not robust enough for application of large quantities of ene-aldehyde **97**. Lastly, although informative in other ways, experimentation with heterocycles **83b**, **122**, γ -butyrolactone, and NMP did not lead to discoveries in IMDA chemistry as I hoped they would.

II.C. Retrosynthetic Analysis III

This section encompasses all those synthetic routes that *build the final heterocycle* from intramolecular Claisen condensation (Dieckmann reaction) of a fully linear precursor. This is markedly different than the previous two sections, where two fragments (one a heterocycle and one the diene or triene chain) were joined as one of the very last reactions. The last reaction in this sequence will be the Dieckmann. This synthesis plan relies on the aldehyde as used in Retrosynthetic Analysis I (**30**, Section II.A.) to build into a long chain that will cyclize first to the heterocycle and then ultimately to the octalin (Scheme I-78).

Scheme I-78. Retrosynthetic Analysis III.

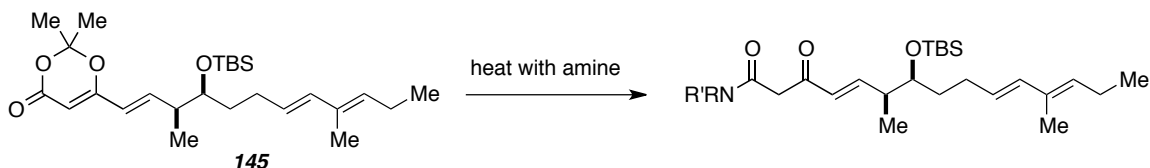


II.C.1. Build 1,3-Dioxenone from Aldehyde 30.

Phosphorane **71** (Scheme I-80) had previously been prepared and used as a β -keto equivalent, a substrate for ring-opening with an amine (II.A.) The idea, if triene **145**

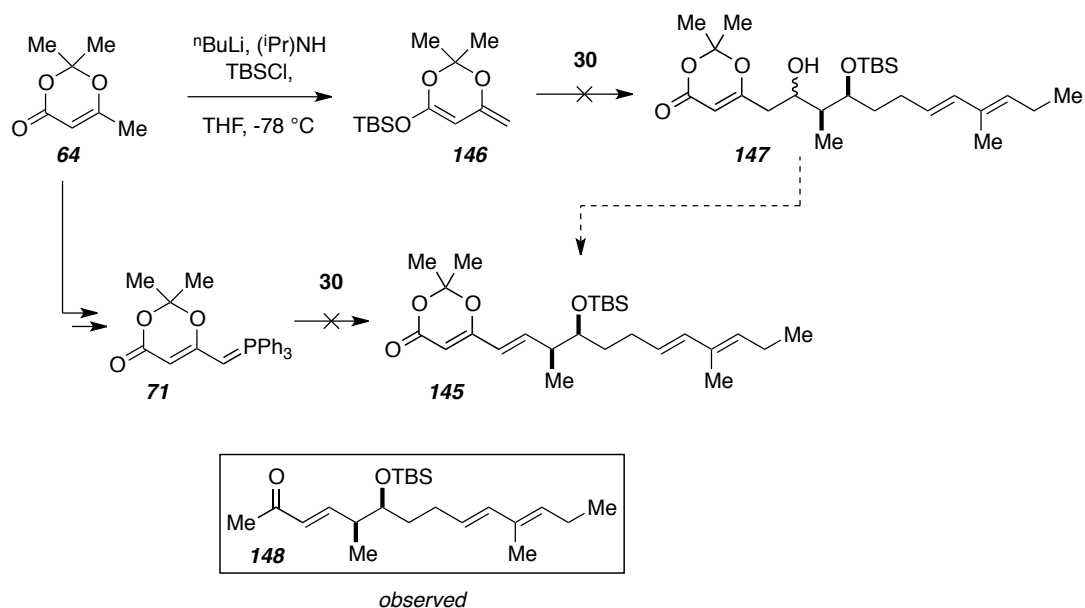
could be obtained, was ring opening by an amine under mild conditions that the rest of the molecule could tolerate (Scheme I-79). This would transform my aldehyde **30** into another β -keto equivalent.

Scheme I-79. Plan for Building β -keto Amide From Ring-Opening of **145**.



Phosphorane **71**⁶⁸ is known to participate in Wittig chemistry on a variety of aldehydes, so I attempted the reaction with aldehyde **30** (Scheme I-80, downward arrow from **64**). Unfortunately, I was unable to effect a successful olefination. The reaction was sluggish and required extremely high concentration and extended times. Although the desired product **145** could be detected by NMR analysis, there was difficulty in purification. The dioxenone, stable to chromatography in its other forms, underwent ring opening and subsequent decarboxylation to the methyl ketone **148**. This was the only triene isolated after column chromatography.

Scheme I-80. Attempted Transformation of **30** into β -Keto Donor.



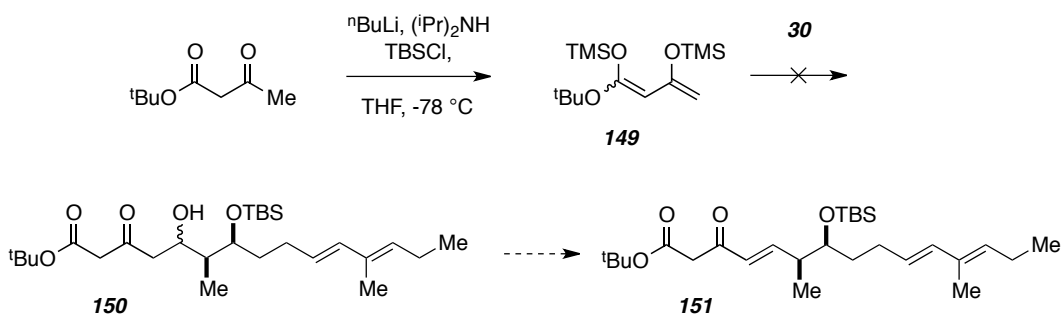
A different way of forming (what would become) the C7-C8 alkene was Mukaiyama aldol followed by dehydration (Scheme I-78, right arrow from **64**). The required reagent **146** was prepared from parent 1,3-dioxenone, but the aldol reaction with aldehyde **30**

failed; no evidence for **147** was observed. With these failures, I set out to study other reactions to append the required functionality to my aldehyde.

II.C.2. Build Dicarbonyl First, Then React at α -Site

Another way to build the additional carbonyl functionality is through aldol/dehydration chemistry (like the attempted reaction with **146**, Scheme I-80). At the start of Scheme I-81, the bis-silylated species **149** was made in preparation for a Mukaiyama reaction. After distillation, the bis-silyl enol ether **149** was used under standard Mukaiyama aldol conditions and reacted with aldehyde **30**. Sadly, the desired product was not present by LCMS. Indeed, no reaction was observed, and the subsequent reaction to eliminate H₂O to complete the olefination to **151** was not needed.

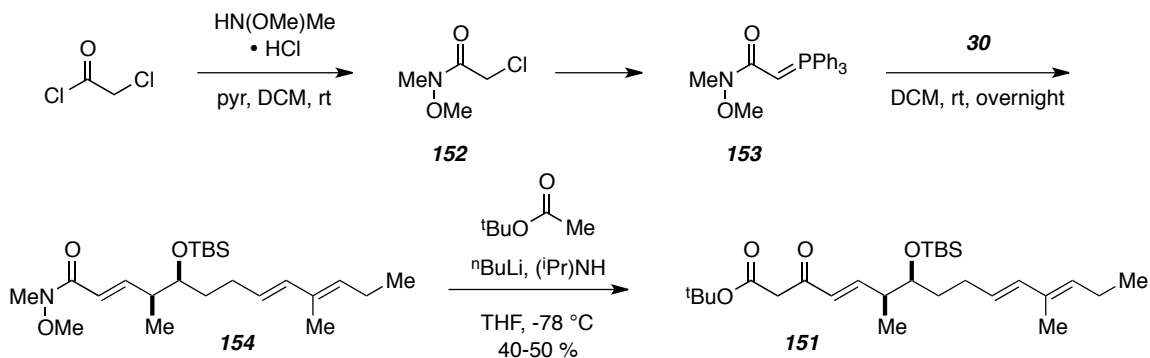
Scheme I-81. Attempted Installation of Dicarbonyl by Mukaiyama Chemistry.



Instead of continuing to work with the aldehyde **30** as an electrophile for aldol-type reactions, I returned to Wittig olefination chemistry. The carbonyl functional groups can be added one at a time. Reaction with phosphorane **153** would furnish the C7-C8 alkene and add one carbonyl (Scheme I-82). The required reagent was prepared in two steps from Cl-acetylchloride. First, amidation by reaction of hydroxyl amine provided the amide **152** in excellent yield, then chloride displacement and deprotonation were straightforward to produce Wittig reagent **153**.⁸³ Olefination gave rise to the α,β -unsaturated Weinreb amide **154**, which carried the rest of the triene chain. After a short chromatography exercise, the substitution reaction was carried out. In the event, the lithium ketene acetal of t-butyl acetate was generated at -78 °C and allowed to react with the amide **154**. This produced β -keto ester **151** in satisfactory yield. Ester **151** was easily

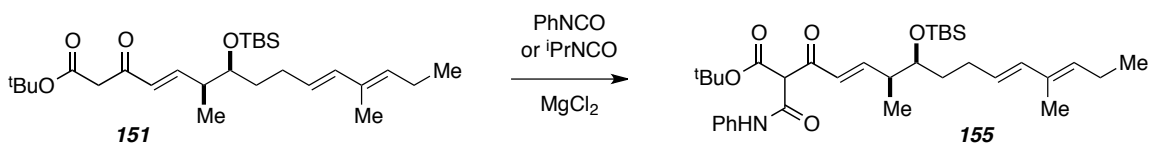
purified by column chromatography and remarkably stable to storage for months in the refrigerator.

Scheme I-82. Stepwise Synthesis of Dicarbonyl **151**.



Ester **151** is reactive and can undergo substitution at the methylene center (Scheme I-83).⁸⁴ Addition of an isocyanate to **151** in the presence of a Lewis acid (MgCl_2) resulted in the acylation to give the tricarbonyl compound **155**. This reaction was only moderately successful with alkyl isocyanates like $i\text{PrNCO}$, but worked well with PhNCO . The carbamate was purified by chromatography and its IMDA behavior was studied (see Chapter III). No additional experiments were performed on ester **151** or anything structurally similar. If this route were to be viable to the desired heterocycle, the proper elements must be present for ring closure to the tetramic acid. Currently, that was not possible on tricarbonyl **155**.

Scheme I-83. Further Reaction of **151** to Tricarbonyl **155**.



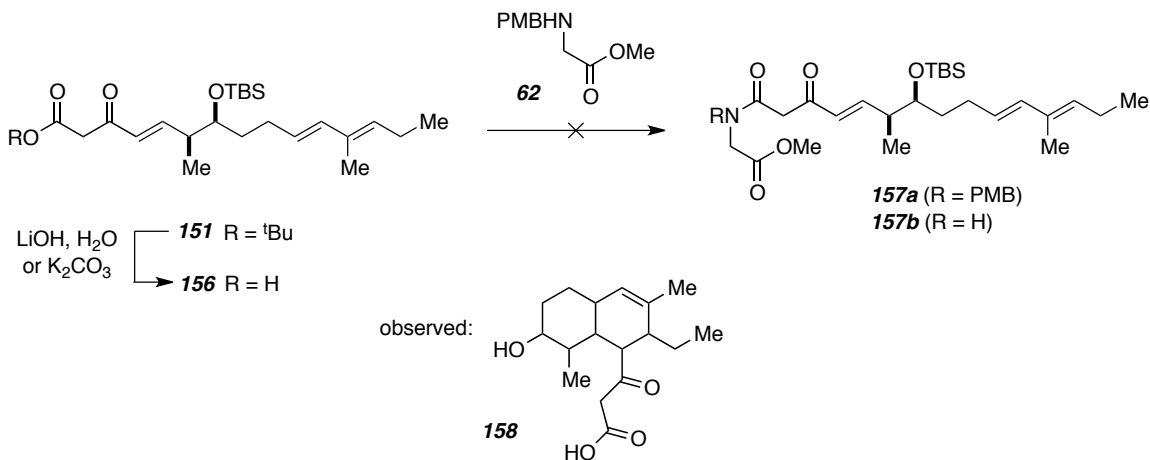
In this section, it was shown that functionality can be built off the aldehyde **30** in a stepwise fashion, but further development into a Dieckmann precursor was not established.

II.C.3. Amide Bond As Last Step Before Dieckmann

II.C.3.a. Peptide Bond from Acid **156** and Amine **62**

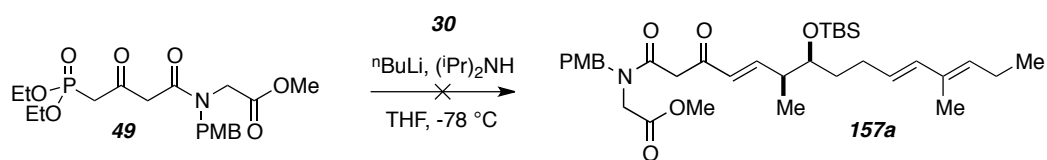
One way to continue to build the proper functionality for the Dieckmann reaction was to transform ester **151** into amide **157a** (Scheme I-84, **157b** is used later and included here for numbering). The ester **151** underwent saponification under basic aqueous conditions⁸⁵ to acid **156**. This substrate was submitted to the coupling conditions with amine **62**. The amide bond was not realized, but the IMDA activity of the substrate (either as the ester **151** or the acid **156**, should it be formed prior to [4+2]) was surprising and very interesting (more discussion is provided in Chapter III).

Scheme I-84. Attempted Amide Bond from Acid **151** and Glycine Derivative **62**.



Studies in this section started to indicate that once the third alkene is installed, the trienes were typically Diels-Alder reactive. Depending on which functionality was present, they underwent IMDA reaction at room temperature or under many of the reaction conditions. Thus, it was wise to build both the alkene and proper carbonyl units at the same time to reduce the number of steps and the opportunities for premature Diels-Alder chemistry. With this strategy in mind, I returned to phosphonate **49**, which I had previously prepared (Scheme I-85, see section II.A. for preparation of **49**). Unfortunately, I was unable to effect any HWE reaction. I saw no reaction to **157a** but recovered both the aldehyde **30** and phosphonate **149**. Likely the dianion was not formed; future studies taught that similar substrates required at least 60 minutes for the double deprotonation event.⁶¹

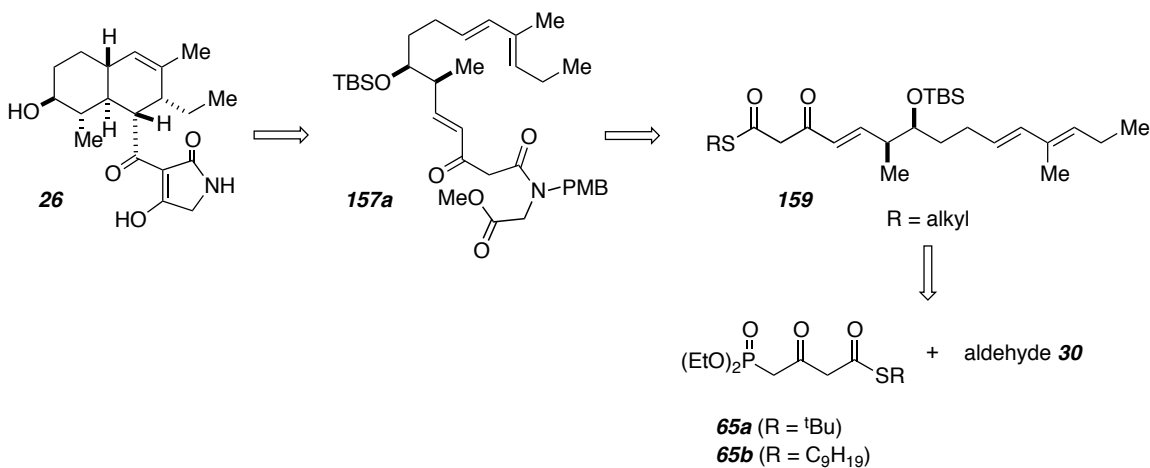
Scheme I-85. Attempted HWE with Phosphonate **49** and aldehyde **30**.



II.C.3.b. Through Thioester **159** and Amine **62**

The last and ultimately most successful sequence that I attempted relied on aldehyde **30** and a Horner-Wadsworth-Emmons olefination that simultaneously installed two of the three required carbonyls (Scheme I-86). It made use of the phosphonates **65** I had previously prepared (section II.A.)

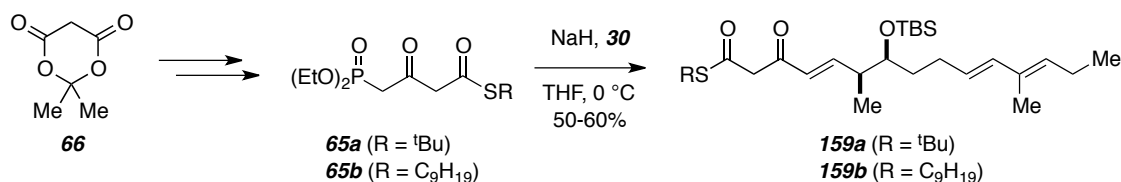
Scheme I-86. Modified Retrosynthetic Analysis III.



Instead of reacting the thioesters **65** as in that sequence (to produce amide **49**), I worked off the other end of the molecule, the thioester would stay intact for triene **159**. After that, thioester/amine coupling as performed before would leave **157a** for deprotection and IMDA chemistry.

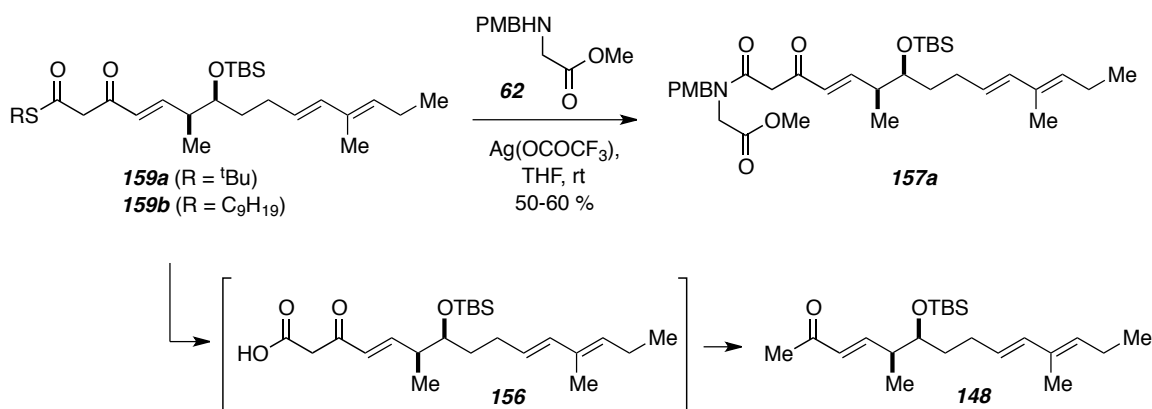
The HWE reaction of **65a/b** and aldehyde **30**⁶¹ (Scheme I-87) required optimization. Eventually, I resorted to using a large excess of the dianion (6 equivalents in most cases) for the best conversion and rate. The unreacted phosphonate **65** could be recovered by MPLC or flash chromatography. The desired trienes **159** were stable to storage over months in the refrigerator.

Scheme I-87. Use of Phosphonate-thioester **65** in HWE with **30**.



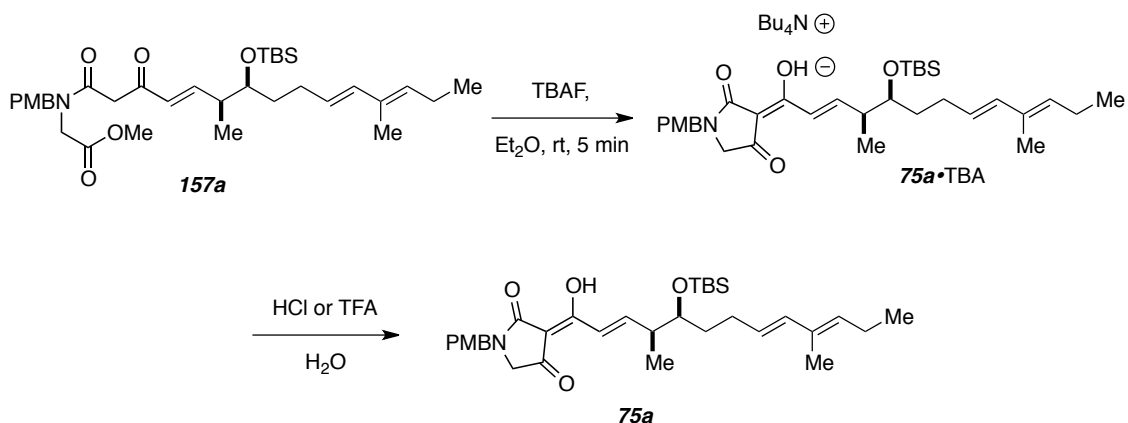
The subsequent thioester-amine reaction⁶⁵ proceeded quickly to give desired amide product **157a** in modest yield (Scheme I-88). The thioester was somewhat labile to Ag(OCOCF₃). At times, what appeared to be the methyl ketone **148** was observed eluting from the MPLC. This might be the result of thioester conversion to the acid **156** followed by decarboxylation under the reaction conditions. Fortunately, the amide product **157a** could easily be separated from the byproducts and was advanced in pure form for the Dieckmann reaction.

Scheme I-88. Thioester-amine Coupling of **159** and **62**.



The Dieckmann conditions were applied as previously and the desired intramolecular Claisen reaction on **157a** occurred to furnish the heterocycle **75a** (Scheme I-89). As before (see discussion in II.A), what is actually produced under the reaction conditions is the Bu₄N⁺ salt. This could be protonated upon treatment with acid (HCl or TFA) and carefully stored for a short time in the refrigerator.

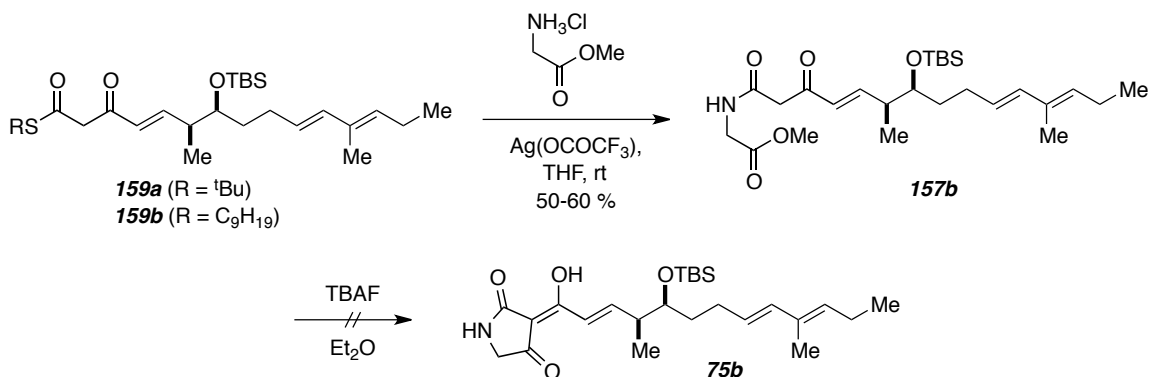
Scheme I-89. Dieckmann Reaction of **157a**.



This almost completed the synthesis of IMDA precursor **24**. The remaining reactions were only the removal of the PMB and TBS groups (gives **24**) and intramolecular Diels-Alder to generate the model of integramycin, octalin **26**.

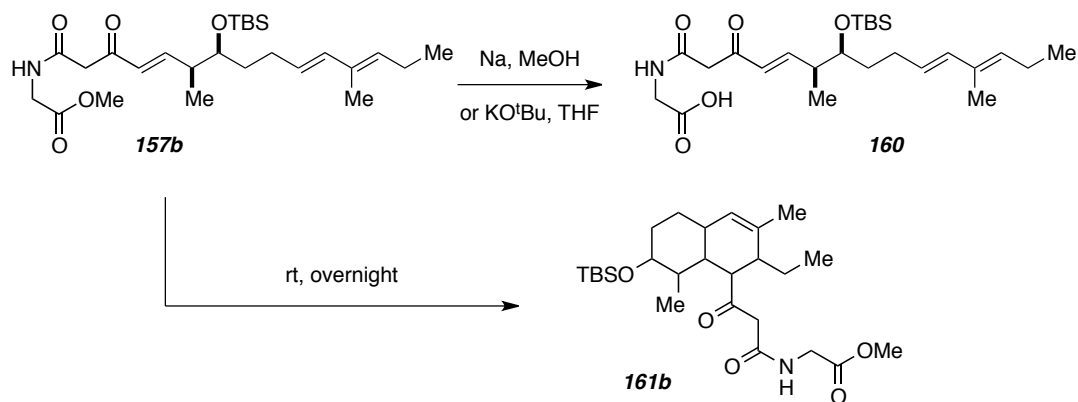
Before attempting the deprotection on **75a**, an analogous sequence was planned for the methyl ester of glycine, a primary amine. Since the PMB group was only used to protect any N-H from anionic chemistry, once that threat was removed, I was free to work with the primary amine in acquiring the amide **157b** (Scheme I-90). Though the thioester amine coupling worked in comparable yield and rate to the N-PMB case, the Dieckmann reaction to **75b** was wholly unsuccessful under TBAF conditions.⁶¹

Scheme I-90. Coupling with a 1° Amine and Failed Dieckman.



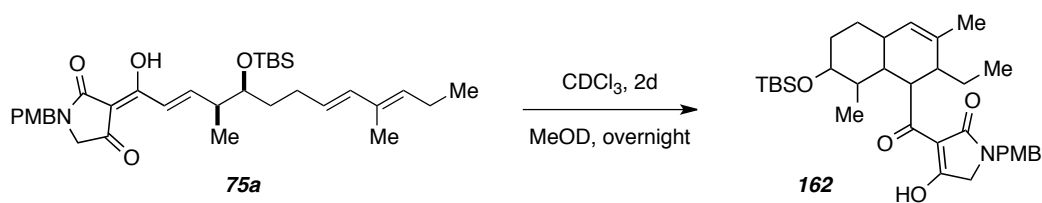
The desired heterocycle could not be realized under other basic conditions (Scheme I-91). I saw conversion to the acid **160** (LCMS), or IMDA reaction with no heterocycle formed. This latter cyclization also occurred overnight upon storage at room temperature (again, the IMDA of these reactive intermediates is discussed in Chapter III).

Scheme I-91. Additional Attempts at Dieckmann of **157b**.



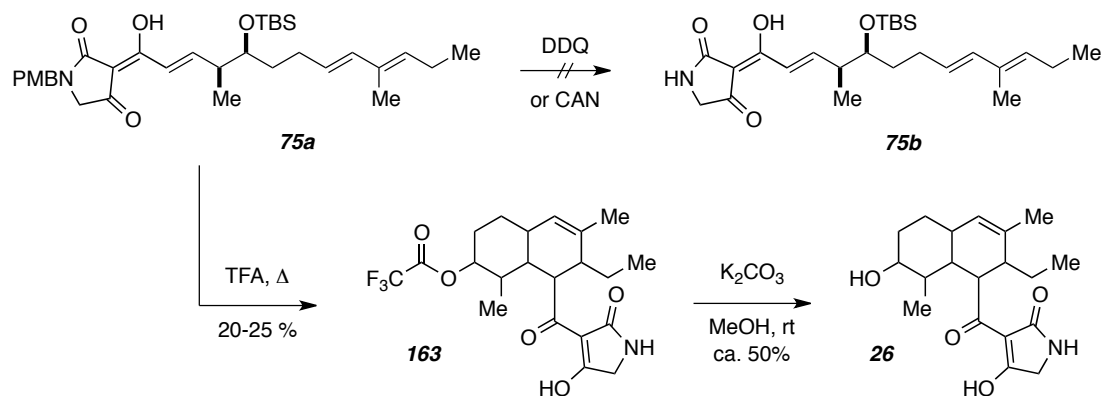
I returned to the more robust PMB-amide **75a**. There are certainly plenty of examples in the literature for protecting group removal, but I was seeking conditions that were mild enough for my triene to remain intact. I already knew that this substrate was prone to Diels-Alder chemistry (Scheme I-92). NMR samples were found to react in either CDCl₃ over a couple days or in MeOD overnight. Octalins **162** (stereochemistry unidentified) appeared in about the same ratio in either case.

Scheme I-92. First Warning of IMDA Lability of **75a**.



For PMB removal, CAN and DDQ were the most appropriate,⁵² but I found neither effected the desired change to NH amide **75b** (Scheme I-93). Although harsh, TFA was used next. The TBS group was particularly labile under these conditions, but the PMB was robust unless the reaction was heated. Unfortunately, as the two protecting groups fell off (or before), the substrate underwent Diels-Alder reaction. A fourth reaction also occurred; the cyclohexanol transesterified to the TFA ester **163**. The remainder of the chemistry on this molecule included basic methanolic removal of the ester and a start to the characterization of the octalinoyl containing tetramic acid (**26**).

Scheme I-93. Attempted Deprotection Towards IMDA Precursor.



II.C.4. Summary of Retrosynthetic Analysis III.

Retrosynthetic plan III was by far the most successful in my efforts to synthesize **26**. Although early efforts to build the appropriate Dieckmann precursor were unsuccessful, ultimately amide **157a** was produced and Dieckmann reaction furnished protected IMDA substrate **75a**. In the end, I succeeded in my goal of building **26** as a model for integramycin (**2**), but my formal study of IMDA of **75a/b** (or the deprotected version **24**) was hindered by premature cycloaddition.

II.D. Conclusions for Chapter II

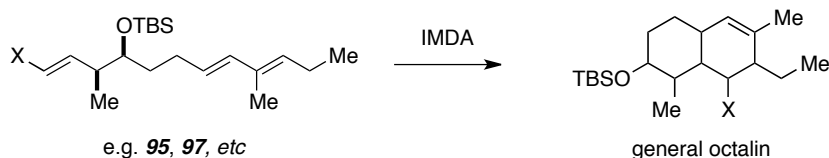
Three retrosynthetic plans were attempted with the ultimate goal of synthesizing IMDA precursor **24** (or **25**). Although none was successful, various key intermediates along the way were used to piece together the protected version **75a**. In section II.A. I discussed the preparation of aldehyde **30**, a key player in all synthetic plans. Although HWE of **30** with an already intact heterocycle failed, key reactions were optimized and parts of this strategy were used in future efforts. The strategy in II.B. attempted to use ene-aldehyde **97** for various coupling reactions. Aldol reactions on this substrate never reached efficiency, and the heterocycles that were far too laborious to prepare. Finally, the studies presented in II.C. or Retrosynthetic Analysis III, did result in the construction of **75a** (protected version of **24**), but simultaneous Diels-Alder chemistry became an added complication before the protecting groups could be removed. Ultimately, **26** was produced by the route, but details are discussed in the next Chapter. This spontaneous

Diels-Alder chemistry leading to **26** set the stage for characterization studies. Both the chemistry and structure elucidation are summarized in Chapter III.

Chapter III. Intramolecular Diels-Alder

A triene can undergo cycloaddition when it is sufficiently activated. I built several trienes over the course of my study (Chapter II) with the general structure shown in Scheme I-94 and many were reactive toward Intramolecular Diels-Alder (IMDA) cycloaddition.

Scheme I-94. General Triene Cycloaddition.



Before discussion of these Diels-Alder reactions, an explanation of the numbering is needed. Any linear triene was numbered as it was previously in Chapters I or II. Octalins were named (not numbered) based on their stereochemical outcomes (e.g. *endo*-I). Cycloadducts of any triene other than **97** were not labelled unless they had already been assigned a number in the previous Chapter(s).

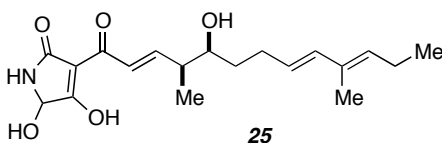
III.A. Observed Reactions

There are two components to the study of the IMDA reactions of various substrates. First, how reactive are these precursors (how fast and selective is the reaction)? Following this is a more fundamental question of the stereochemistry of the Diels-Alder adduct. In this Chapter, reactions of ene-aldehyde **97** are discussed. Following this overview, the IMDA of other trienes is presented for comparison and additional thought. Finally, these studies are summarized before **III.B.** (characterization studies).

III.A.1. IMDA of Ene-Aldehyde **97**

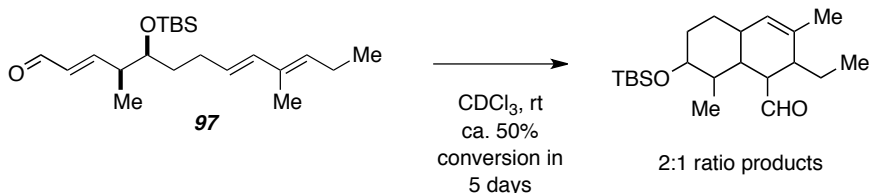
Over the course of my studies toward reactive Diels-Alder precursor **25** (Figure I-19, c.f. Scheme 1-15, Chapter I), I worked through and adjusted several synthetic plans (Chapter II).

Figure I-19. Target IMDA Precursor.



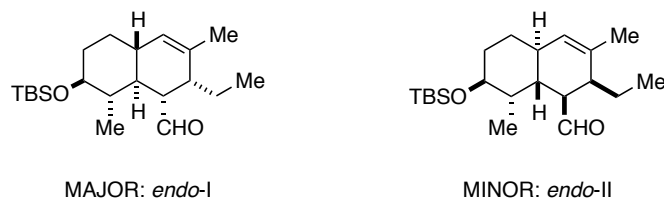
Even though my efforts were focused on construction of reactive substrates, I did not observe any Diels-Alder chemistry until I prepared the enal **97**. It was first indicated from an NMR sample which I had stored for some time before returning to it (Scheme I-95, reaction).

Scheme I-95. First IMDA Observed.



My initial observations were that the reaction proceeded to about 50% completion in 5-6 days, and there were several (but two main) diastereomers that were produced under these conditions. Based on the literature^{32,86} and intuition, these two main isomers are *endo*-I and *endo*-II (Figure I-20). The full discussion and assignment of the two major stereoisomers is deferred to Section III.B, but these are the structures that I used as a platform for all my experiments.

Figure I-20. Two Main Stereoisomers From IMDA reaction of **97**.

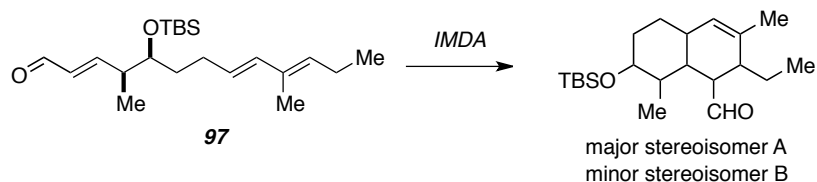


Before embarking on a more routine study to understand the chemistry of this aldehyde, I established methods to analyze both the rate and stereoselectivity of the reaction. Although TLC, GCMS, and LCMS were useful techniques, the best method for monitoring the reaction was ^1H NMR spectroscopy. The starting material was converted under the conditions of any GC method, and generally the substrates were too non-polar for LCMS to be useful. ^1H NMR analysis was the most informative for conversions, isomer ratios, and judging the efficiency of the reaction under various conditions. The aldehyde **97** was the first and became the most studied of all of the trienes prepared.

After the initial result, and methods for analyzing features of the IMDA chemistry, the synthesis of aldehyde **97** was scaled up and subjected to a number of conditions (Table I-3). These were chosen based on intuition for the IMDA and known

catalysis for this type of cyclization. In every case, two main stereoisomers arose from the reaction mixture. Conversion and other noteworthy features of each condition were recorded in this study.

Table I-3. IMDA of Ene-aldehyde **97**.



Entry	Conditions ^a	Time	A:B	Conversion	Notes
1	CDCl ₃ , rt	2 wk	4:1	>95%	5% other isomers
2	CDCl ₃ , Δ	2 hr	3:1	100%	
3	Benzene, Δ	1 hr	1.5:1 to 4:1	100%	5-10% other isomers
4	Toluene, Δ	1 hr	4:1	100%	
5	Xylenes, Δ	< 1hr	2:1	100%	
6	TsOH, CDCl ₃	20 min	1:1	100%	
7	BF ₃ -OEt ₂ , CDCl ₃ , -20 °C	< 30 min	2:1	100%	
8	BF ₃ -OEt ₂ , CD ₂ Cl ₂ , -78 °C	10 min	2:1	100%	
9	Me ₂ AlCl, CDCl ₃ , -78 °C	1 hr	1.5:1	80%	
10	Et ₃ N, CDCl ₃ , rt		bg ^b		
11	Ph ₃ P, CDCl ₃ , rt		bg ^b		
12	I ₂ , CDCl ₃ , rt	< 1hr	1:6	100%	maj. pdt not identified

^a Δ is heating to reflux in these cases, so temperature is the boiling point of the respective solvent

^b background reaction, corresponding to entry 1. If these samples were monitored for the two weeks allowed in entry 1, the same ratio A:B and conversion would likely be observed

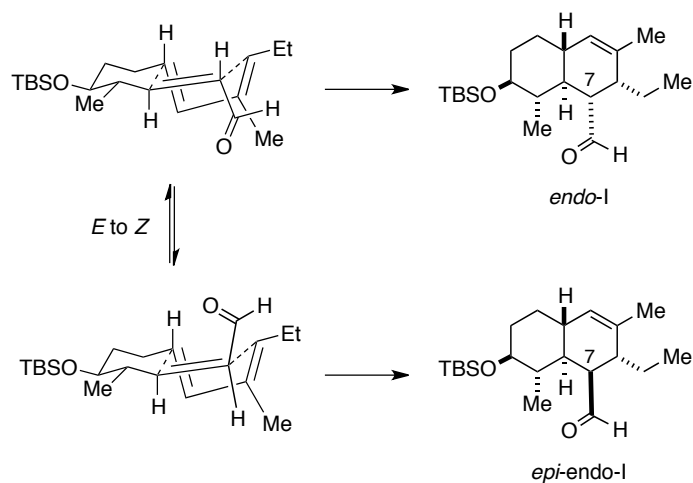
From the initial serendipitous reaction (Scheme I-95), I found that the Diels-Alder reaction of enal **97** followed the general characteristics of Diels-Alder reactions.⁸⁶ For example, the reaction was more rapid but less selective at higher temperatures (entries 1 vs. 2). If the reaction was conducted in higher boiling solvents (benzene, toluene, xylenes, entries 3-5) the outcome was a faster and even less selective cycloaddition. However, there seemed to be a plateau where even as the reaction was conducted at higher and higher temperatures, the selectivity did not continue to diminish. It seems under thermal conditions, the Diels-Alder reaction of **97** proceeded with at least 2:1 diastereoselectivity up to almost 5:1. I also noted that under higher heating and shorter reaction times, there is a larger contribution from isomers other *endo*-I and *endo*-II. No doubt that at higher temperatures, some of the previously unattainable transition states

leading to higher energy isomers can be reached. To add to these considerations, *cis/trans* isomerization could be occurring under very harsh thermal conditions (e.g. entry 5, xylenes boiling point ca. 140 °C).

Besides thermal Diels-Alder chemistry, the aldehyde **97** was found to cyclize under both Bronstead and Lewis acidic conditions (entries 6-9).³³ This type of catalysis has been thoroughly studied by both experimental and theoretical means. In general, reactions become faster and more selective. Interestingly, I observed roughly the same selectivity (A:B) under these Lewis Acidic conditions. Of course, the stereochemistry of A and B has already been predicted to be *endo* in both cases, so little can be learned about *endo* vs. *exo* selectivity. An additional complication for these LA conditions was how rapid the reaction was. In Entry 7, for example, by the time the NMR analysis was performed, all of the starting material was converted to the cycloadducts A and B. The reaction was complete in at most 30 minutes, but likely much more quickly. Thus, for extremely facile IMDAs, there was a limitation with the method of analysis. To add to these factors, many of the reactions were performed on small scale, so catalyst loadings were difficult to judge. Again, a detailed discussion of the identity of molecules A and B is provided in the next section.

Lastly, I tried a few conditions for this Diels-Alder reaction when the geometry of the dienophile may be reversed (isomerization of the starting material from *E* to *Z*). For example, Et₃N, triphenylphosphine, and elemental iodine⁸⁷ are known to cause *cis/trans* isomerization of alkenes. Scheme I-96 shows an example for *endo*-I. I knew that **97** reacted to *endo*-I (top arrow) but if the *Z*-alkene were accessed under the reaction conditions, it might undergo Diels-Alder reaction to give *epi-endo*-I.

Scheme I-96. *E* to *Z* Isomerization and Result of [4+2].



Sadly, in my experiments, I saw no interesting or different IMDA outcomes (entries 10 and 11, just a background reaction). Lastly, observations made entry 12 are probably due to HI catalysis. The stereoisomers were the same as those already observed, so it is likely that no alkene isomerization occurred there.

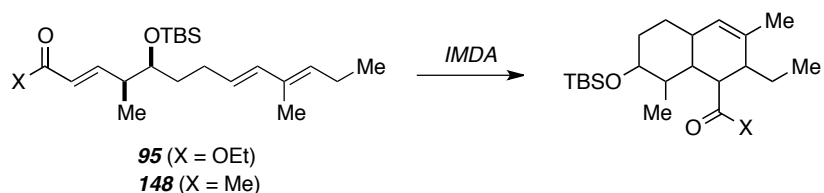
It should be pointed out that study of these other alkenes (like *Z-97*) and the stereochemical outcomes (i.e. *epi-endo-I*, see **III.B.**) are important. Geometrical isomers of the dienophile are especially worthy of study because rates and selectivity of Diels-Alder reactions are closely tied to the nature of the dienophile.²⁰ Very interesting outcomes (other than the epimer of the parent) have been observed.¹⁶ At times, this one change in structure opens a whole new pathway for reactivity by bringing in more accessible transition states, including the likelihood of not only chair, but boat-like, and other details of cycloaddition (see Chapter I). Further study for substrate **97** should include outright construction of the *Z*-alkene to experimentally probe its mode of IMDA.

III.A.2. Other Trienes IMDA

The discovery of the Diels-Alder chemistry engaged by aldehyde **97** was not immediately followed by additional successful attempts at cycloaddition of other substrates. Heating methyl ketone **148** in CDCl₃, for example, affected no change (Scheme I-97). Very rigorous conditions (heating benzene beyond its boiling point for extended reaction times) were required for conversion of ethyl ester **95** into a set of

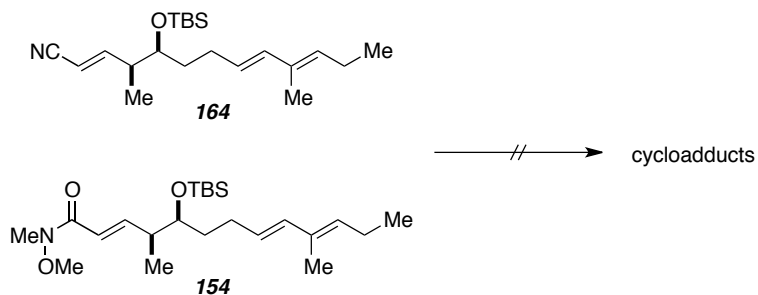
cycloadducts. There were, as expected, two major stereoisomers (approximately 4:1) and several other vinyl resonances indicated a few minor isomers. Unfortunately, these were not as easy to separate as the corresponding aldehydes, so full structural assignment was not attempted. However, comparison to the aldehydes indicated that these isomers possessed the same stereochemistry (full discussion on the stereochemistry is contained in the next section). Efforts to engage ethyl ester **95** in Diels-Alder activity by Lewis acid catalysis were met with failure. When triene **95** was treated with $\text{BF}_3 \cdot \text{Et}_2\text{O}$ or TiCl_4 in CDCl_3 , only decomposition was observed.

Scheme I-97. IMDA of Ester **95** and Methyl Ketone **148**.



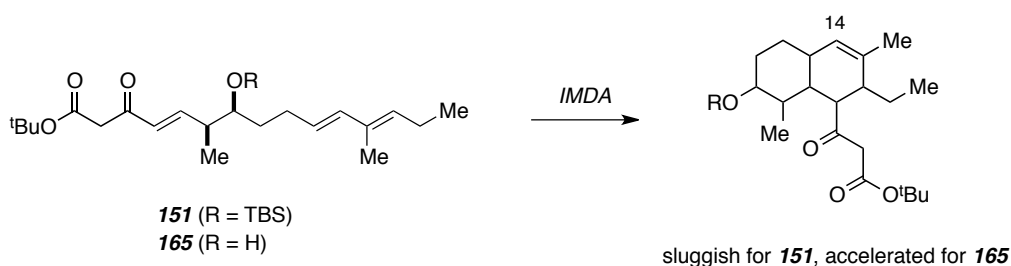
Over the course of my synthetic studies, nitrile **164** and Weinreb amide **154** were also prepared (Scheme I-98). These substrates are also capable of Diels-Alder chemistry, but resisted it. Even after heating **164** overnight in CDCl_3 , NMR did not confer any cyclized product, although broadened peaks and loss of peak integrity were noted. For amide **154**, there was no hint of reaction at room temperature, and the substrate required refluxing CDCl_3 overnight for conversion into a variety of products. Crude NMR analysis betrayed that there were greater than 2 cycloadducts formed in the process, but further purification and analysis was not performed. From these studies and those mentioned above, it seemed only the most electron deficient of the carbonyls, like the aldehyde **97**, are sufficiently to promote facile Diels-Alder cycloaddition on this type of precursor.

Scheme I-98. Attempted IMDA of Nitrile **164** and Weinreb Amide **154**.



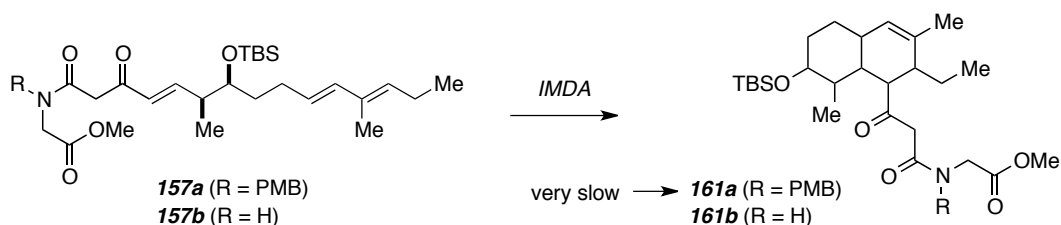
In much the same way, ^tBu acetoacetate derivative **151** (Scheme I-99) was reluctant to undergo cycloaddition. An NMR sample was monitored for 8 days at room temperature, and finally a reaction appeared to take place. Although the adducts were not isolated, crude NMR confirmed that starting material alkenes were being consumed and new, broadened singlets appeared in the expected region for H14. The other resonances that were typically diagnostic (carbinol, α -protons) did not appear in the expected region. Surprisingly, the reaction of the OH analogue of ester **151** (i.e. **165**) was just slightly more reactive. These reactions in particular were hampered by low concentration of triene **165** and insufficient material to attempt a more thorough study.

Scheme I-99. Attempted IMDA of β -keto Ester **151** and Alcohol **165**.



Surprisingly, the pre-Dieckmann substrate **157a** (Scheme I-100) was also not very reactive at room temperature. This substrate has an additional carbonyl that might impart activation, but did not engage in cycloaddition. Heating was not attempted. On the other hand, the free N-H variant **157b** was highly reactive in Diels-Alder chemistry; the formation of IMDA adducts was detected after storage overnight at ambient conditions. The rate or half-life was difficult to gauge but the selectivity was generally between 2:1 and 3:1 in all cases (room temperature, neat or in solution).

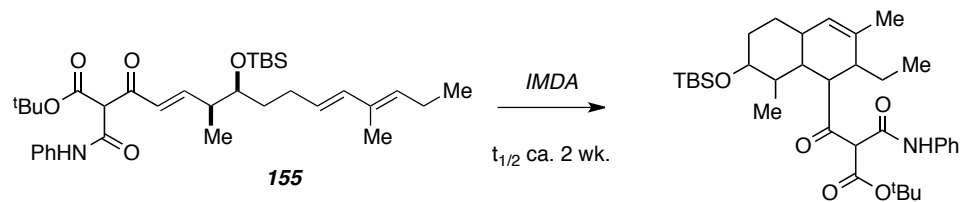
Scheme I-100. IMDA of Amides **157**.



At the time of this study of Diels-Alder reactions, one of the most relevant models prepared was the tricarbonyl **155**. Gratifyingly, this substrate did cyclize under NMR study, although at room temperature the reaction was sluggish and required about two

weeks for ca. 50% conversion. The cycloadducts formed in about 3:1 ratio, which was similar to much of the chemistry already observed for other substrates.

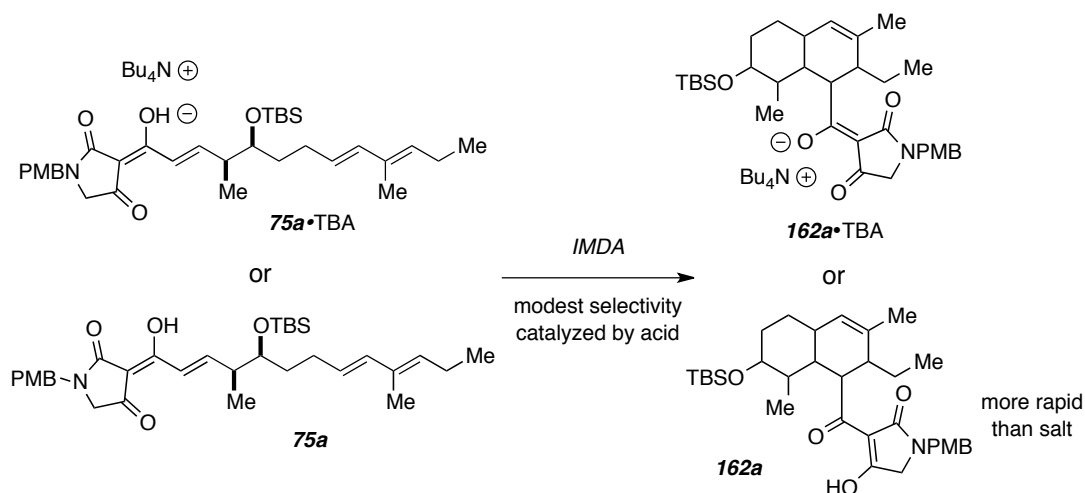
Scheme I-101. IMDA of Tricarbonyl Triene **155**.



In total, a spectrum of Diels-Alder chemistry was observed with these reactive intermediates. Although a broad range of reactivity, the stereochemistry of the resulting octalins was always somewhere in the area of 1:1 to 4:1 in favor of what might be assumed to be the major isomer (from comparison of each to the octalin *endo*-I).

As introduced in the last Chapter, Diels-Alder chemistry of **75a** was observed immediately (c.f. Scheme I-92). As soon as the Dieckmann reaction had taken place, the substrate **75a** (either as the ammonium salt or in neutral form) had to be handled with care. For example, the anionic species (**75a**•TBA) was found to cyclize slowly in polar media (typically methanol) whereas the Diels-Alder reaction of the neutral was even more rapid. The product began to appear by NMR within 5 minutes of neutralizing the anion. The reaction in organic solvents is facile, and seems to be more selective compared to polar solvents. The selectivity, however, was poor, ranging from 2:1 to 1:1 in some of the acidification experiments. Several NMR studies were conducted, and although formal studies are yet to be completed, the half-life of **75a** in IMDA reactions is less than one hour in methanol. For this substrate, acid was found to accelerate the reaction (this had been the case for other trienes).

Scheme I-102. IMDA of Heterocycle Triene **75a**.



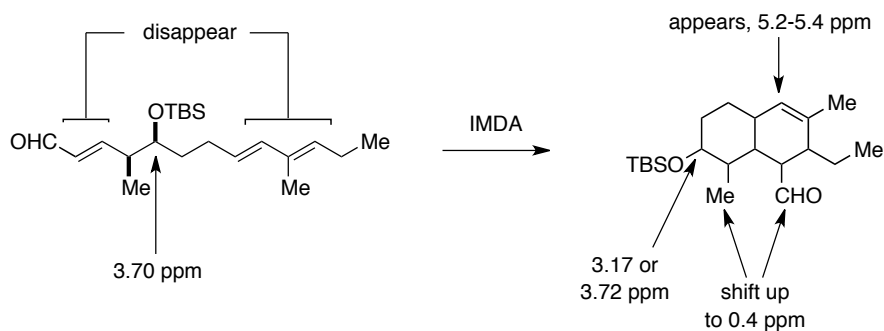
III.A.3. Summary of Findings

In summary, several trienes were found to exhibit Diels-Alder reactivity in either organic or partially aqueous media, or were found to undergo cycloaddition upon storage on the benchtop. There are some general conclusions about this chemistry: i) heating increases the rate but decreases selectivity ii) protecting groups retard the reaction iii) the addition of a carbonyl (and even a second one) does not necessarily activate the dienophile iv) the Dieckmann product **75a** is very reactive and v) acids and polar solvents accelerate the reaction. The following section will describe the characterization studies that were required to draw conclusions about the particular mode of this interesting chemistry.

III.B. Characterization Studies

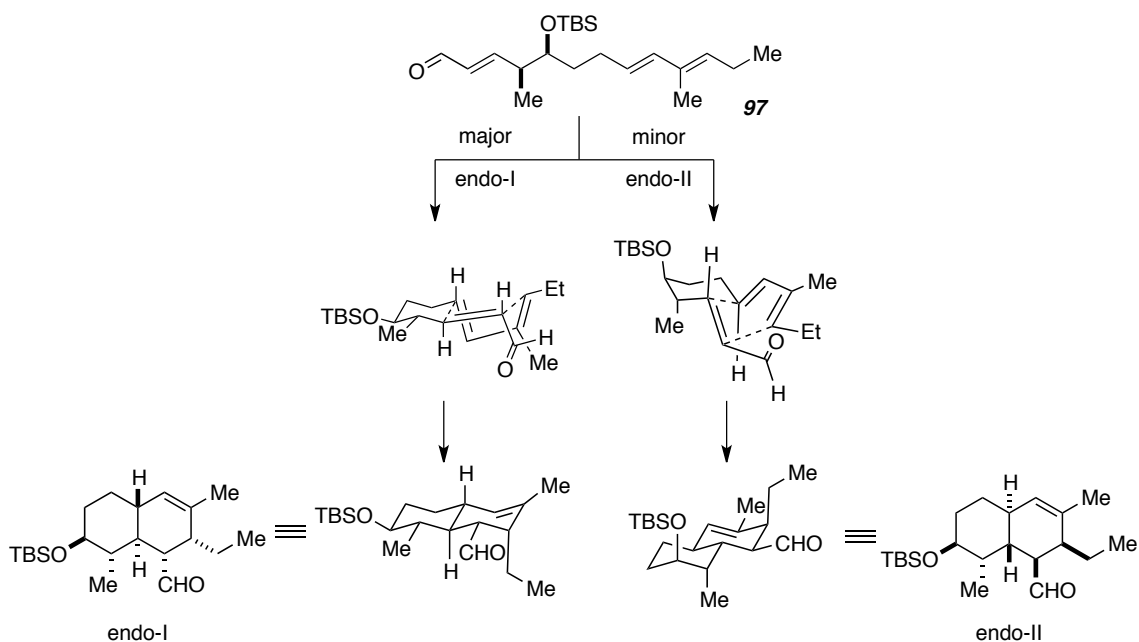
It was clear from initial screening of the ^1H NMR that a Diels-Alder reaction had occurred in many cases (Figure I-21, example of **97**). Consumption of vinyl protons and appearance of a broad singlet corresponding to the lone vinyl proton (i.e. H14) in the octalin product were most illustrative. The mobility of the carbinol also indicated that change was occurring. Moreover, the appearance of a few well-defined resonances and downfield movement of resonances suggested that rigid ring systems were formed.

Figure I-21. General Key Features of all IMDA of **97**.



The NMR was often used to monitor these reactions and it also served as the tool of choice for structural assignment. Beside a few attempts to prepare crystalline derivatives of any of my Diels-Alder adducts, I returned again and again to the power of NMR. Many sophisticated experiments were available and they were utilized to support my assignments from **III.A**. There are 12 protons that must be distinguished for a confident stereochemical assignment to be made. Even after careful purification of each of the two major diastereomers of **97**, the required resolution was not reached. Despite these few unanswered questions, the tentative assignments were made (Scheme I-95) and are expanded upon in Scheme I-103.

Scheme I-103. IMDA of aldehyde **97** leading to major and minor product and proposed TSs.



Both isomers (*endo*-I and *endo*-II) were assigned a *trans* ring-fusion, indicative of an *endo*-type IMDA. The presumed transition states are shown the middle of Scheme I-103. Both lead to the octalin structures as drawn. It is easy to see from the transition states and structures of the products why the left side is favored over the right. In the major case (leftmost arrows), all but one of the substituents occupies an equatorial position on the bicyclic ring system, a feature that is also indicated by the TS toward *endo*-I. In the minor isomer (rightmost arrows), all but one are situated with an axial-like orientation, and this feature appears in the TS for *endo*-II. Both isomers are portrayed in standard decalin fashion (bottom row, with a flat representation alongside it). That is, although one ring is formally a cyclohexene (and probably looks more like a half boat), it is still shown in chair form for simplicity. For the remainder of this chapter, these are the structures upon which I based my experiments and NMR analysis. These will be used to interpret the data that was produced over the course of this chapters' studies. Tables are provided at the end of the experimental for Part One for *endo*-I (Table I-4), *endo*-II (Table I-5), *7epi-endo*-I (Table I-6), and *7epi-endo*-II (Table I-7). There is an additional table for the *endo*-I data in benzene (Table I-8). These contain all ^1H and (most) ^{13}C NMR data.

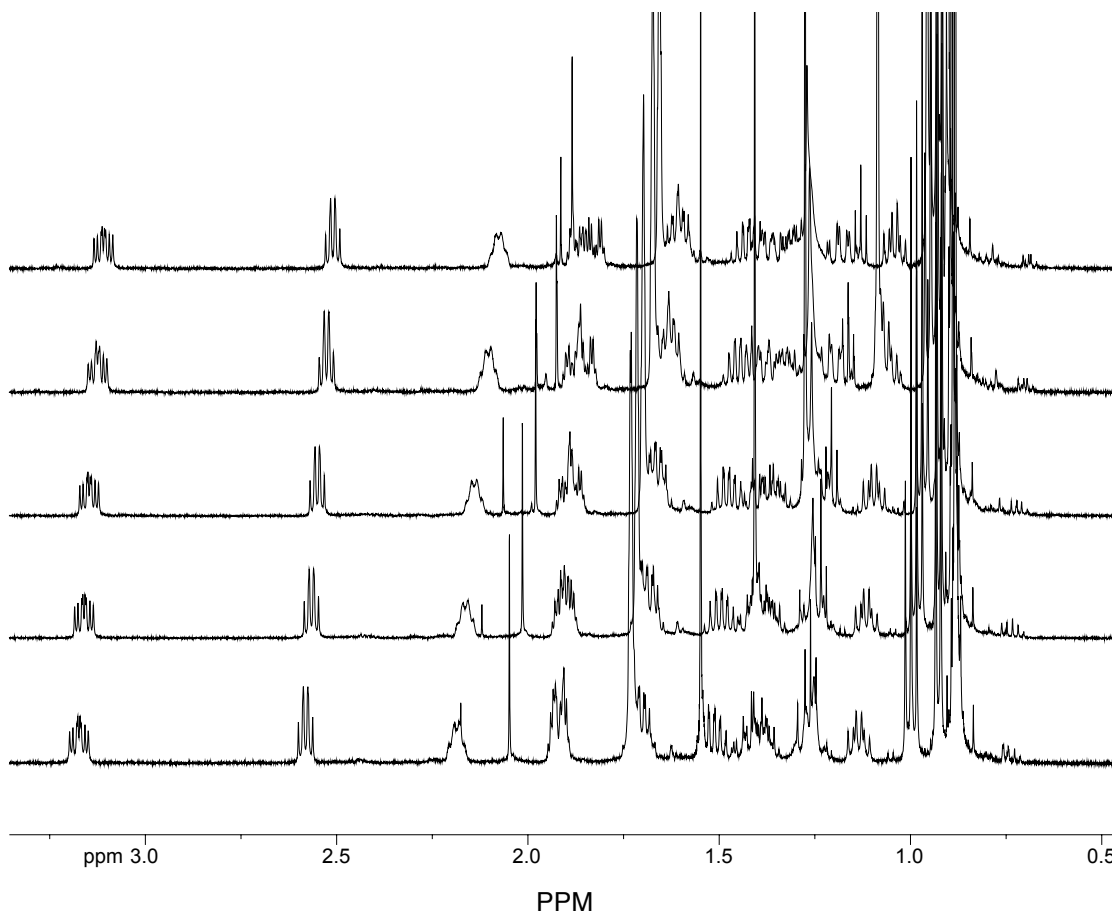
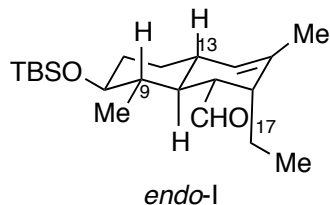
III.B.1. NMR Strategies

The first strategy in combatting the overlapping resonances was a set of NMR methods. Of course, experiments such as ^1H - ^1H COSY, ^1H - ^{13}C HMQC, ^1H - ^{13}C HMBC, and NOE will give relationships and simplify spectra, but I was seeking a way to move the resonances around along the ppm scale. To this end, spectra were taken in a variety of different solvents and solvent pairs. I found that for certain regions of the spectra, benzene titrations were especially advantageous in the separation of two overlapping multiplets. The region most affected by these studies was that inside 1.5-2.5 ppm, and as benzene content of the sample increased, most peaks shifted. The changes were easily tracked. Resonances moved in different increments, so peak resolution was successful in some cases. Brief analysis of the titration studies for each isomer is provided below.

The assignment of a few protons in *endo*-I (Figure I-22 graphic) was straightforward in CDCl_3 . However, benzene titrations (Figure I-22, increasing benzene content as the spectra are overlaid above the original CDCl_3 spectrum) enabled deduction of coupling

constants associated with H17b and H9 (ddq, $J=11, 9.3, 7$ Hz), which were previously overlapped ca. δ 1.85 ppm.

Figure I-22. Benzene Titrations of Major IMDA Isomer *endo*-I in CDCl_3 .

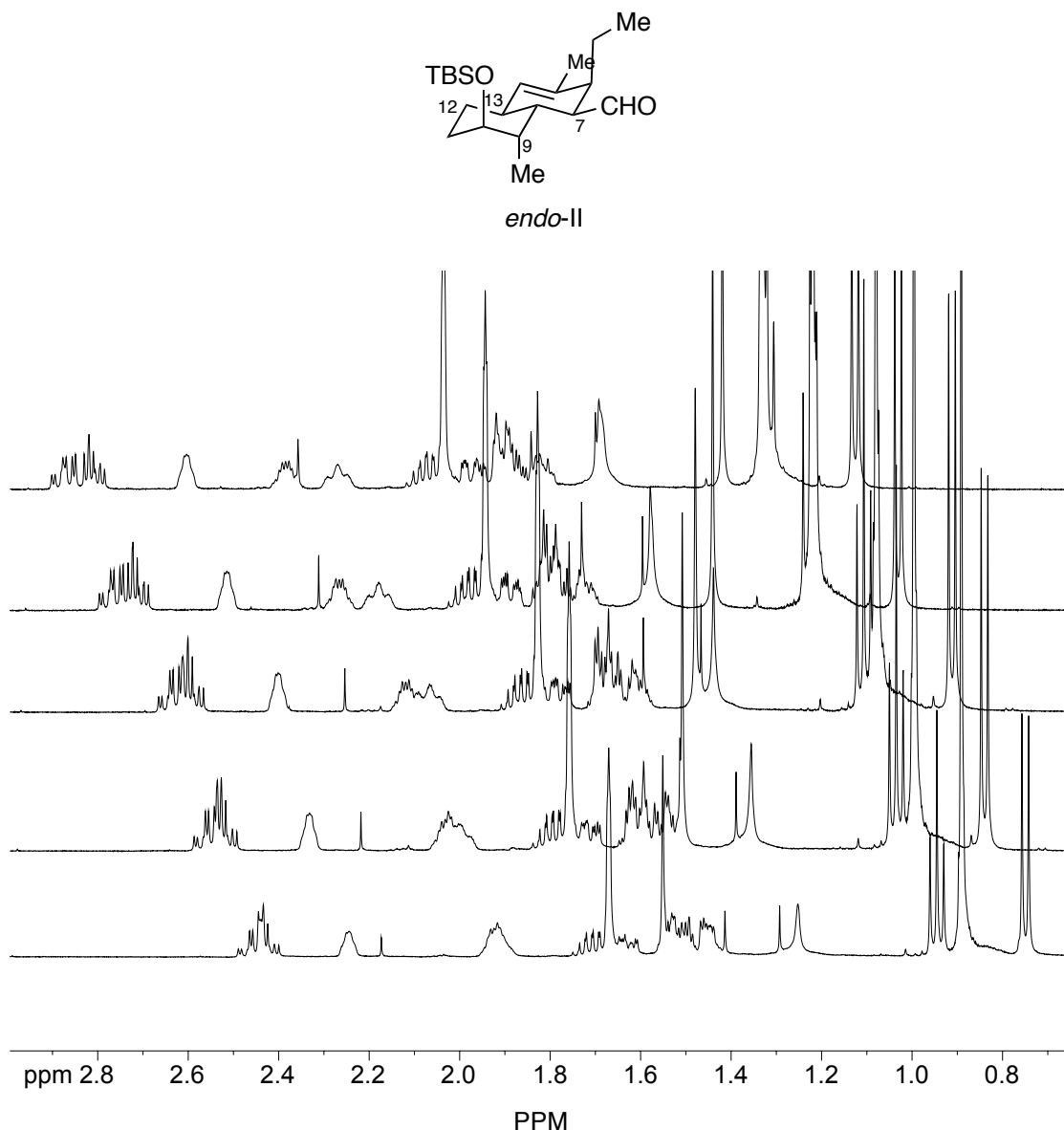


Not all peaks could be pulled apart. Notably, the peak shape of H13 could not be resolved and this was critical to structure assignment. Even through the process of benzene titration, H13 remained underneath the singlet associated with methyl 37 (numbering as in **2**) and the multiplet of H17a.

In the case of the minor isomer, the benzene titration was successful in separating two pairs of overlapping multiplets (Figure I-23, NMR referenced to CDCl_3). H7 and H12ax

(furthest downfield in the figure) were well understood, but certainly H9 and H13 (the second furthest set of overlapping resonances) not accessible by any other means until this titration afforded excellent resolution of the two (δ H9 1.9 ppm to 2.35 ppm δ H13 1.9 ppm to 2.2 ppm). In this stacked plot, each spectrum is referenced to CDCl_3 , so resonance shifts are opposite that of Figure I-22.

Figure I-23. Benzene Titrations of Minor IMDA isomer *endo*-II in CDCl_3 .



Interestingly the H12_{ax} proton resonates at 2.45 ppm, far downfield of its H12_{eq} partner and either of the H11 protons. Presumably, the deshielding from the axial OTBS is responsible for such a phenomenon (see Figure I-23 graphic). This isomer, in general,

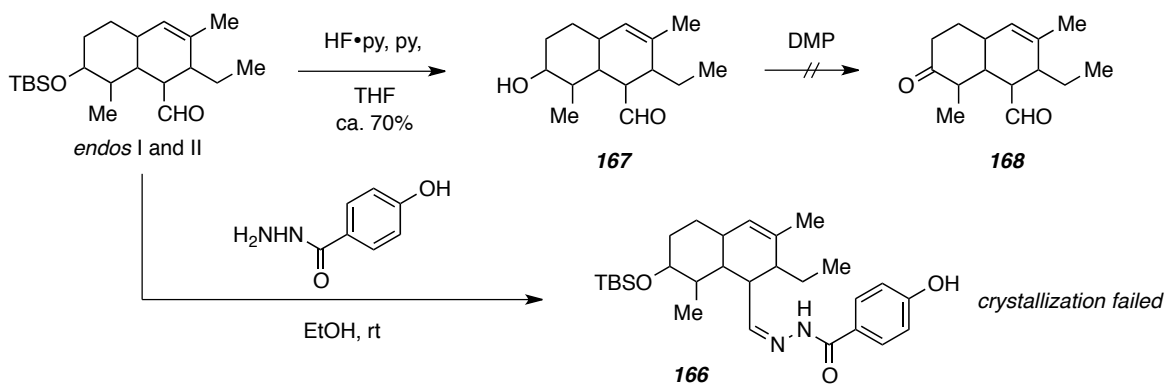
had fewer complications in its spectral data. The peaks were more spread out and it was clear from 1H-1H COSY data that H9, H10, and H16 were all equatorial. H7, H8, and H13 were all understood to be axial. This completed the assignment of relative stereochemistry of the octalin. Despite this confidence, unfortunately, the benzene titrations were not wholly successful in resolving each of the remaining peaks, and alternative means were sought to understand these NMR data.

III.B.2. Substrate Modifications

The complexity in the NMR could not be eased by methods and solvent pairs that I tried (III.B.1.) I turned to minor chemical modifications of the analyte in an attempt to effect small changes in some of the overlapping regions. For example, the aldehydes *endo*-I and *endo*-II can be reduced or oxidized, the TBS group can be removed, or the substrate can undergo bromoetherification or iodolactonization. Each or any of these could result in a substrate with more clarity in its NMR spectra. In all the experiments summarized below, I assumed I was working with stereoisomers as drawn in Scheme I-103.

I tried to prepare a crystalline derivative of the aldehyde according to known procedure (Scheme I-104, bottom arrow). Though the reaction worked to build a solid hydrazine, I could not obtain suitable crystalline sample of **166**.

Scheme I-104. Derivative of IMDA adduct *endo*-I or *endo*-II.

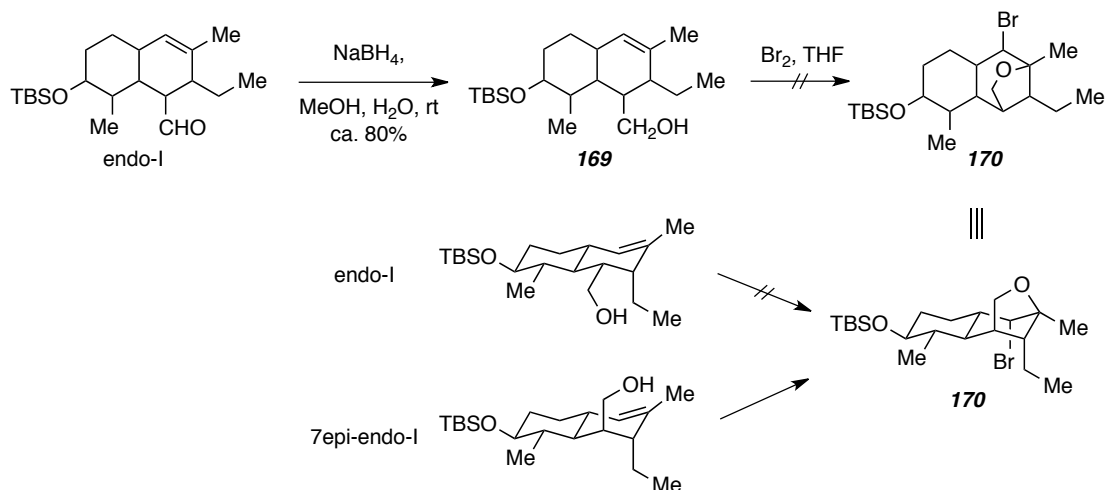


The next easiest modifications were simple protecting and functional group interconversions using the aldehyde and hydroxyl groups as handles. The TBS group was removed with HF•py in a solution of buffered THF (Scheme 104, top arrows). The free

alcohol **167** was readily purified by pipette column, but to my disappointment, the change in octalin substitution did not impart major changes in the NMR. Because H10 had already been assigned and was always resolved, I attempted a destructive method - oxidation of alcohol **167** to cyclohexanone **168**. Sadly, this reaction was not successful, but if it did work, **168** could be valuable in the future. Oxidation would certainly disrupt the octalin and could have a clarifying effect on the resulting NMR spectrum.

Bromoetherification (Scheme I-105)⁸⁸ would indicate if the aldehyde in isomer *endo*-I was equatorial (as in *endo*-I) or axial (as in *7epi-endo*-I). This study began with reduction of *endo*-I by NaBH₄. The primary alcohol **169**, if axial, was situated in a position that made it capable of trapping one of the bromonium ions formed from action on the alkene with Br₂. Although this reaction failed [bromide **170** was not suggested by any analysis, or the regioisomer where OH attacked C14 (not shown)], this experiment should be repeated before attempting to draw stereochemical conclusions about *endo*-I from the lack of reaction. That is, a result of no reaction could indicate that the alcohol is equatorial or that the reaction conditions need to be modified).

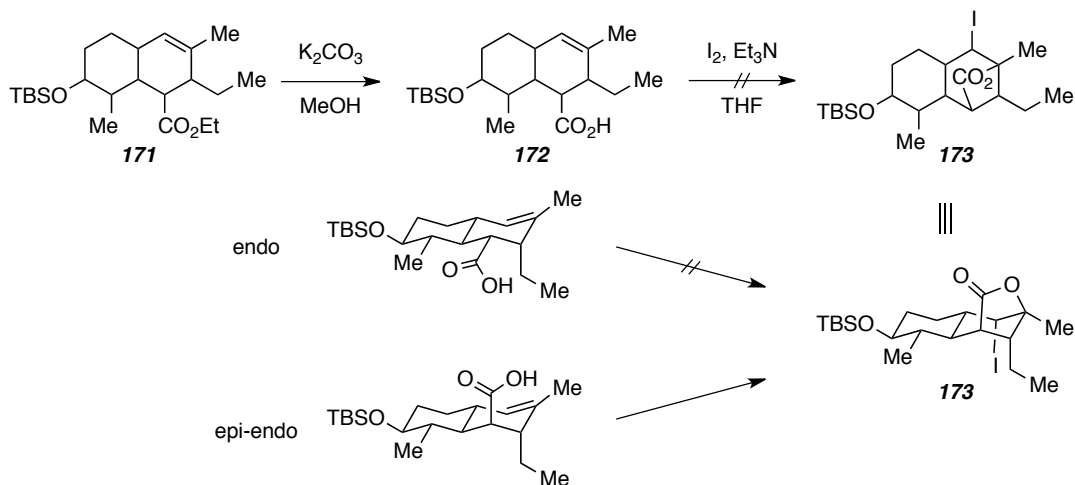
Scheme I-105. Reduction of *endo*-I to Alcohol **169** and Attempted Bromoetherification.



Iodolactonization (Scheme I-106) would provide the same information as bromoetherification (c.f. Scheme I-105). This modification began with saponification of ester **171** (from IMDA of **95**, section III.A.3.) The acid **172** was produced after basic methanolic treatment and subjected to standard iodolactonization conditions. Sadly, no intramolecular closure to lactone **173** was observed. Again, this reaction was only

possible with an axial acid group in *7epi-endo-I*, but before inferring that **172** has an equatorial acid, the experiment should be attempted again to confirm that no reaction meant no *possible* reaction.

Scheme I-106. Saponification to Acid **172** and Attempted Iodolactonization.

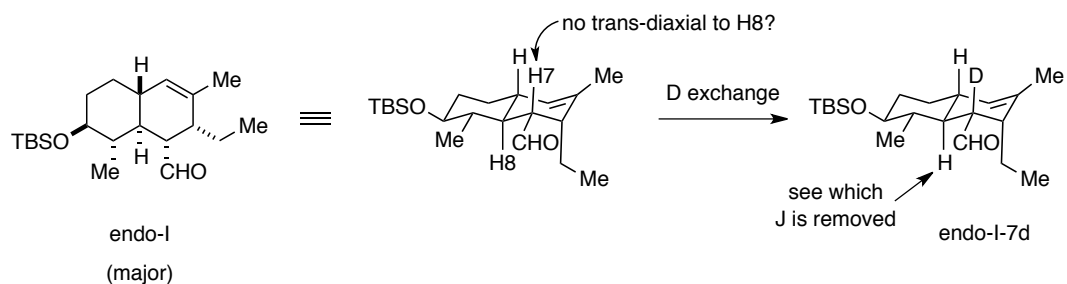


Additional chemical modifications were also available so the substrate was more amenable to NMR study. The most successful were epimerizations (discussed in the next section).

III.B.3. Epimerizations to *7epi-endo-I* and *7epi-endo-II*.

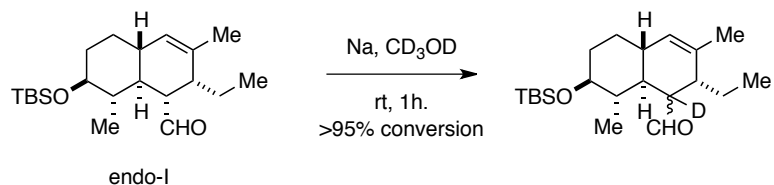
The tentative assignments in Scheme I-103 were not just based on the assumption that the two *endo* modes of cycloaddition were operative. They were also rooted in some of the key features of the NMR. For example, although overlapping multiplets hinder the interpretation of many resonances between 2.2 and 1.1 ppm, the carbinol H10 and α -proton H7 were always visible. One of my biggest concerns with *endo-I* was that since H7 experienced no large $^3J_{\text{HH}}$ (ddd, $J = 6.7, 6.7, 5.4$ Hz), it might be equatorial (Scheme I-107, inconsistent with *endo* mode of addition).

Scheme I-107. D-exchange to For Peak Shape Analysis and *J* values.



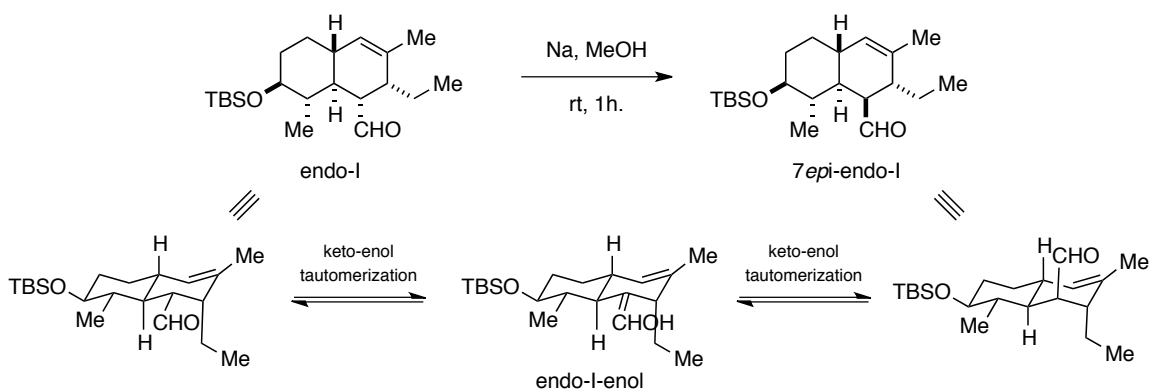
H8 was usually available for interpretation ($\delta = 1.1$ ppm). If H7 were exchanged for D, the peak for H8 would become a dd. From the disappearance of one *J*, I could determine the Hz value of H7-H8 relationship. The first experiment in deuterium exchange (Scheme I-108) indicated that, actually, epimerization⁸⁹ was occurring with Na in MeOH-*d*₄. These conditions successfully installed the deuterium at the most acidic site, but I saw other changes occur in the spectrum besides loss of complexity and the disappearance of one entire resonance. GCMS confirmed that the newly formed octalin was fundamentally different.

Scheme I-108. Observed Epimerization Upon H-D Exchange on *endo*-I.



Reasoning that the most likely reaction was epimerization, I performed the reaction with methanol to confirm that structural changes were occurring under these harshly basic reaction conditions (Scheme I-109, I show *endo*-I as the starting material).⁸⁹ The results were the same. The product octalin had a different retention time on the GCMS ($\Delta = 0.3$ min) and the NMR showed a number of differences (Figure I-24, to be discussed).

Scheme I-109. Epimerization of Major IMDA Isomer *endo*-I.

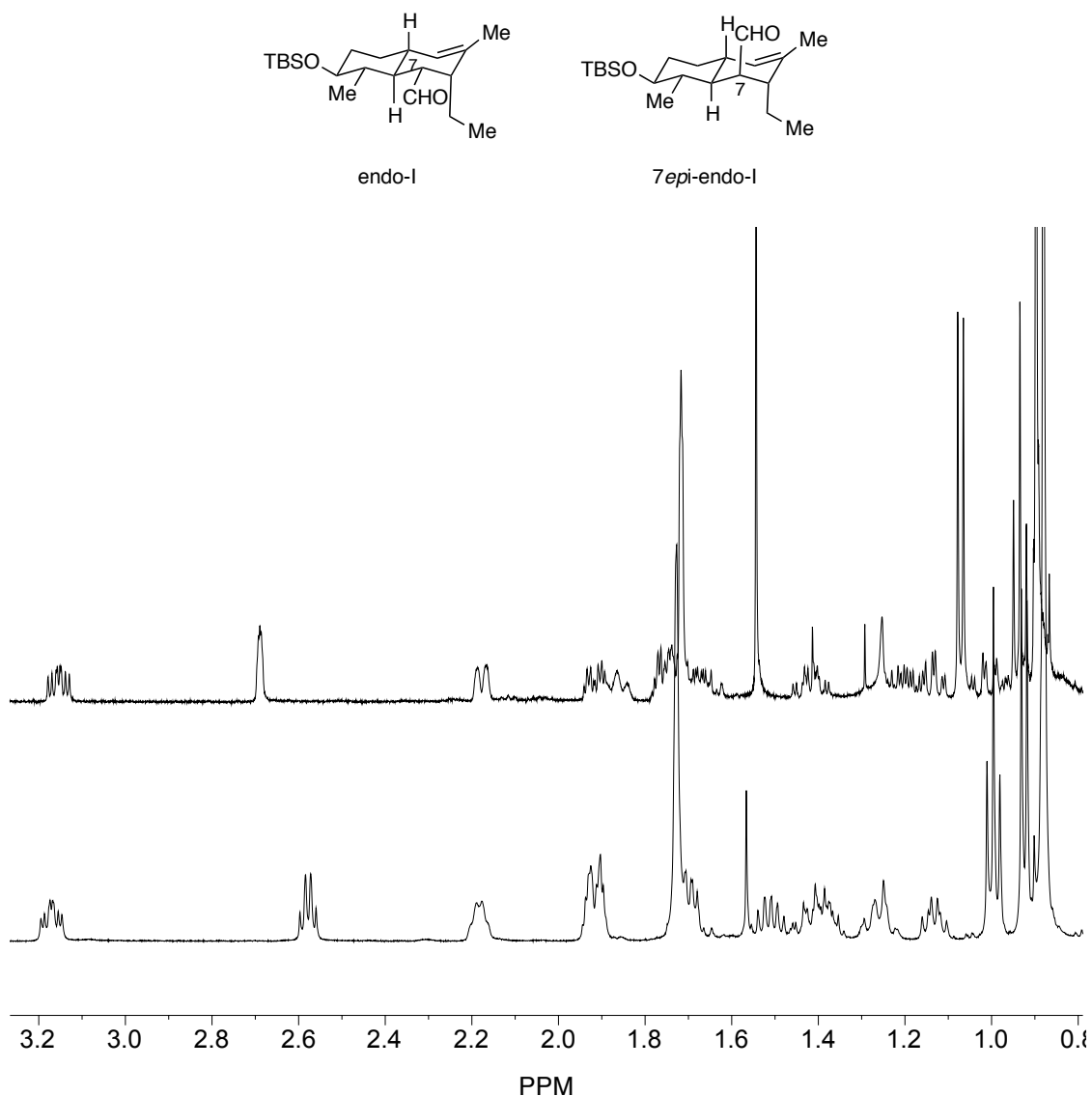


The extent of this epimerization is surprising. As assigned, and required by *endo*-IMDA, the aldehyde substituent is situated equatorial in the starting material (see 3D representation, Scheme I-109), but the conversion to the axial position is facile and nearly quantitative. Intuitively, this does not seem very likely, but it is possible that this epimerization results in the more stable stereoisomer with H7 equatorial. Presumably, the epimerization required the intermediacy of *endo*-I-enol, which then undergoes subsequent keto-enol tautomerization that places H7 equatorial (protonation from the underside of the ring as drawn).

The epimerization helped support the stereochemical assignment (*endo*-I) previously made. The stacked NMRs (Figure I-24 bottom is the starting material, top is the epimerization product) show the shifted resonances, and it makes sense that certain protons are affected electronically by epimerization. Only the main features of this study are mentioned.

Figure I-24 is an expanded region, but the other notable resonances, the aldehyde CH and H14 moved after epimerization. The aldehyde moved from δ 9.46 to 9.74 ppm and H14 moved from δ 5.42 to 5.19 ppm.

Figure I-24. Stacked ^1H NMR of *endo*-I (bottom) and *7epi-endo*-I (top) in CDCl_3 .

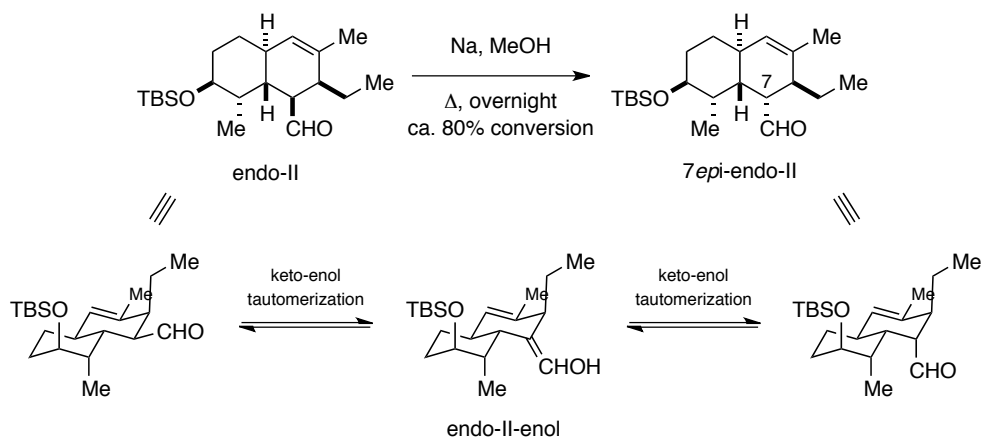


This epimerization supported the tentative assignment of the major isomer in a few ways. First of all, peaks H7 and H9 were now easily identified. The peak shape of H7 changed dramatically; now the biggest coupling constant was not 7, but 2 Hz. This indicated that H7 became equatorial in the epimerization process. The chemical shift was also now 2.69, and that is consistent with equatorial protons being deshielded and moving downfield. The conversion to an axial aldehyde also led to peak shifting. For example, H13, presumed to be axial (but overlapping with others) it moved from ca. 1.7 to 1.83 (!) It must experience heavy through-space deshielding, an action only possible if the CHO

group was axial. A minor shift was even observed for the methyl triplet (located near CHO on the octalin), which moved *upfield* without the equatorial aldehyde to deshield it.

In the case of the thermally minor Diels-Alder isomer, *endo*-II, the same conditions were not sufficient to induce epimerization of the aldehyde (Scheme I-110). There was very little conversion at room temperature, and the substrate required heating for any change. Even after heating overnight, full conversion was not reached (ca. 80 % epimerization).

Scheme I-110. Epimerization of Minor IMDA Isomer *endo*-II.

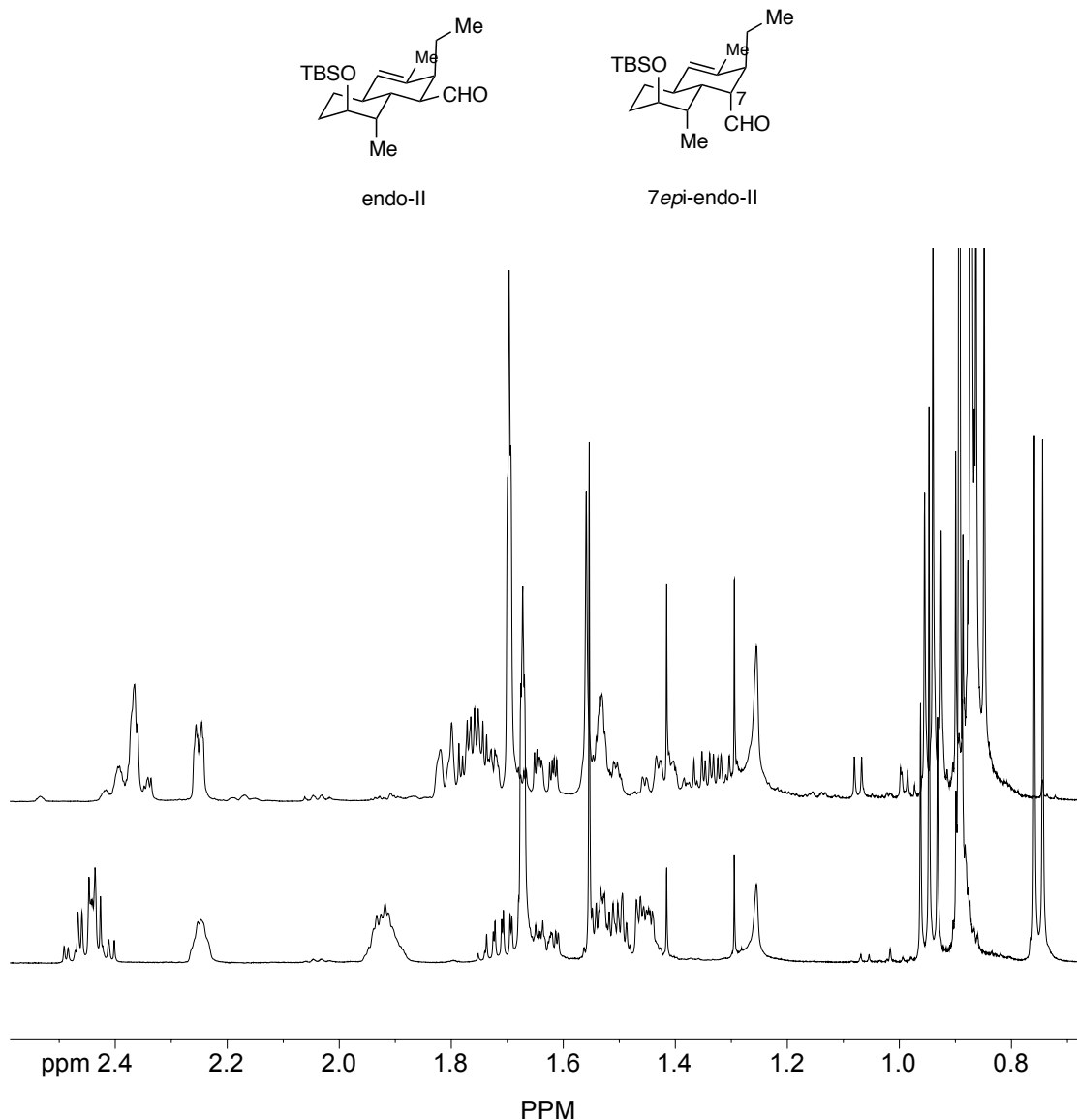


Epimerization for the minor isomer was helpful in several ways. First, the qualitative observation that it was more difficult for this transformation means that the epimer is less stable (higher energy) than the starting material. This is consistent with the aldehyde occupying an axial position that is situated 3 carbons away from the axial methyl group. 1,7-interactions are likely setting up a high energetic barrier for both CHO and C9(Me) to be axial (see rightmost 3-D representation, Scheme I-110).

A comparison NMR is provided for this discussion. (Figure I-25, bottom is the starting material, top is the epimerized product). The resonances outside this expanded region shifted very little (CHO δ 9.80 to 9.84, H14 δ 5.21 to 5.28, and H10 δ 3.72 to 3.70 ppm). More notably, the methyl doublet shifts >0.1 ppm downfield, consistent with the aldehyde being axial and able to deshield this group through space. Remarkably, the axial H13 shifts downfield almost 0.5 ppm! This is also consistent with greater through-space deshielding interaction with the carbonyl. H7 is now a ddd with small J s (5, 2, and 2 Hz), in *endo*-II, it was a ddd with a clear diaxial coupling ($J = 10, 6, \text{ and } 5$ Hz), suggesting that

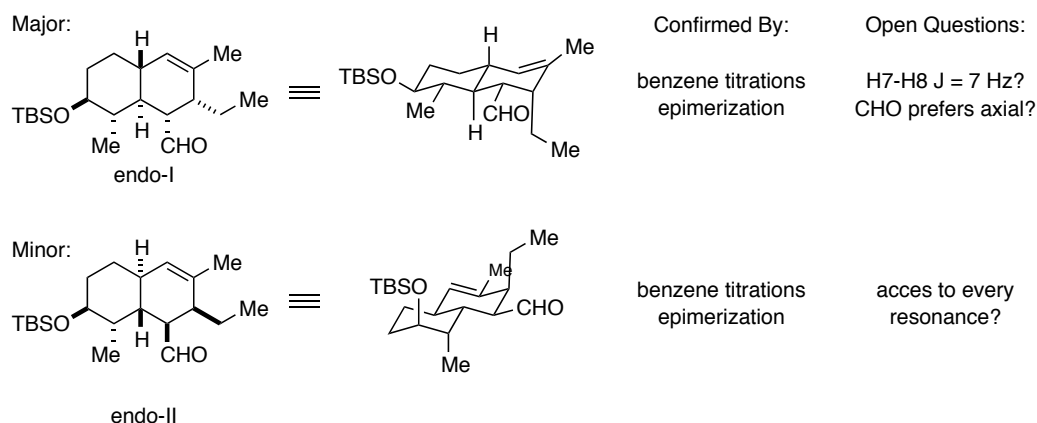
it is seated equatorially in *7epi-endo-II*. These data support the tentative assignment given earlier (c.f. Figure I-103).

Figure I-25. Stacked ^1H NMR of *endo-II* (bottom) and *7epi-endo-II* (top) in CDCl_3 .



The epimerized octalins were thoroughly analyzed by additional NMR experiments, including the use of different solvents, co-solvents, and additives. These and the data presented above all supported the assignment of the major and minor isomers (Figure I-26)

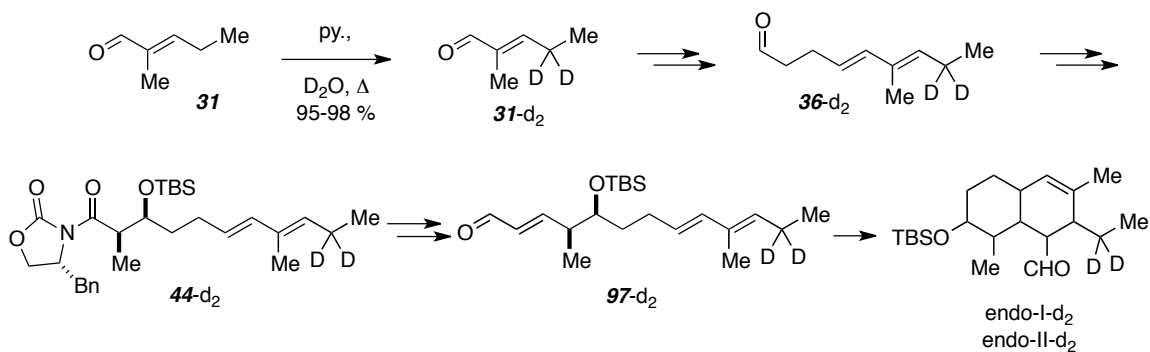
Figure I-26. Summary of Structural Assignments IMDA Products of **97**.



III.B.4. The D₂ Strategy

The benzene titrations and epimerization reactions provided a good picture of the stereoisomers, and I became more and more confident in the assignment. One final experiment was performed to prepare a substrate even more amenable to NMR analysis. Upon inspection of the NMR of the various thermal and epimerized thermal stereoisomers, it was clear that the primary interferences were coming from the methylene pair at carbon 17 (H17a/b). These resonances offered no relevant information to the stereochemistry of the octalin and only served to make the spectra more complex. Strategic incorporation of deuterium would alleviate some of these complexities but structural assignment would not be compromised. The best place in the synthetic route to install the deuterium was prior to any synthetic efforts. To this end, 2-methyl-2-pentenal **31** was heated in D₂O in the presence of pyridine⁹⁰ for 48 hours, and approximately 96% deuterium incorporation was realized (Scheme I-111). The remainder of the synthesis was enacted as previous; key d₂ intermediates are shown. Note that the numbering of these compounds based on the parent.

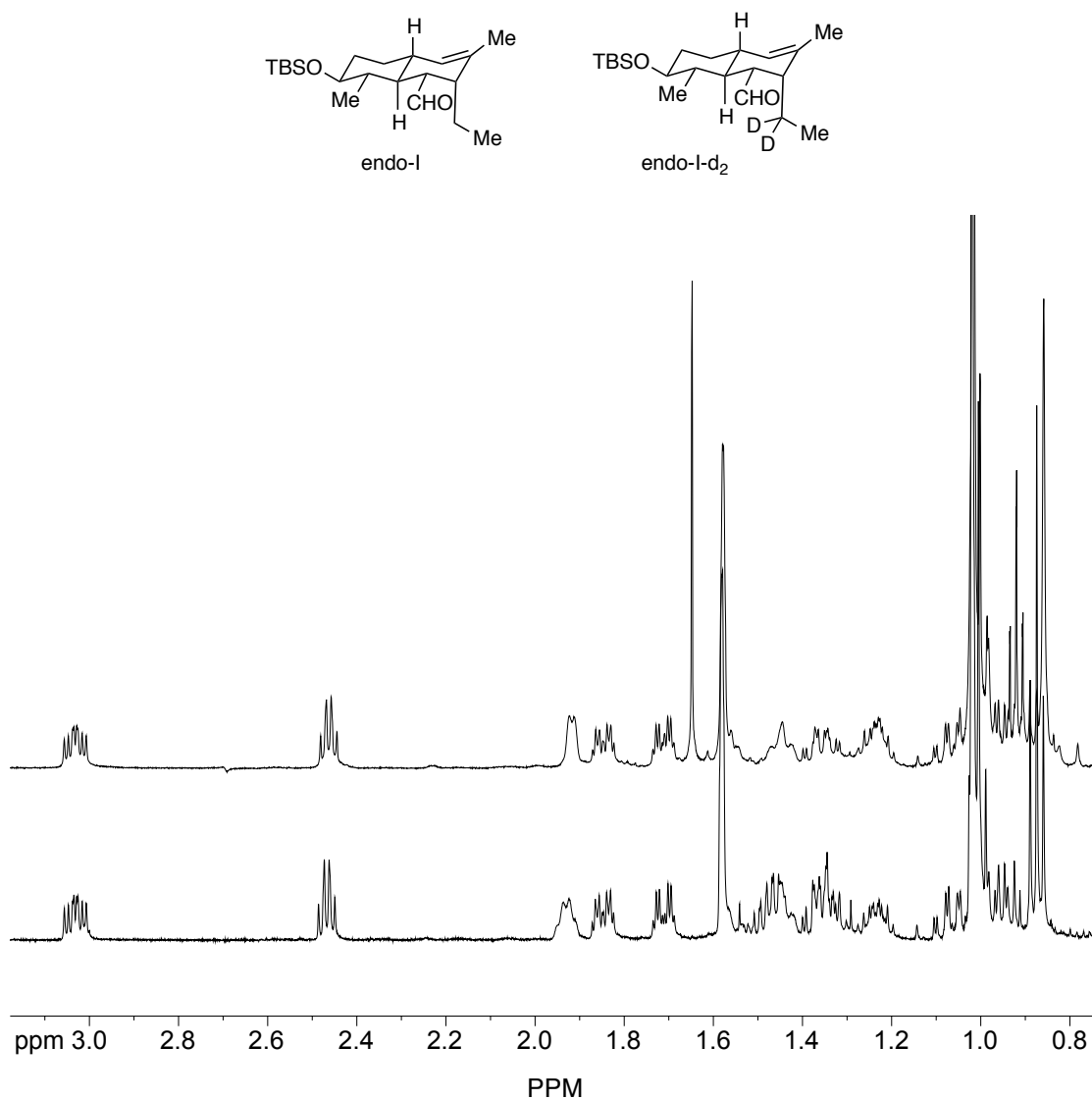
Scheme I-111. D₂ Incorporation of Octalins *endo*-I and *endo*-II from **31**.



Naturally, the **97-d₂** substrate underwent Diels-Alder reaction in the same fashion as the parent molecule, and the major and minor isomers *endo*-I and *endo*-II could be separated and characterized.

Sure enough, ¹H NMR spectrum (Figure I-27, bottom is the control and top is the d₂ analogue) was simplified and more easily interpreted. I gained access to every resonance that was critical to the identification of the stereochemistry of the octalin. Interestingly, the spectra taken in benzene-d₆ were the most informative.

Figure I-27. Stacked ^1H NMR of *endo*-I (bottom) and *endo*-I- d_2 (top) in Benzene.

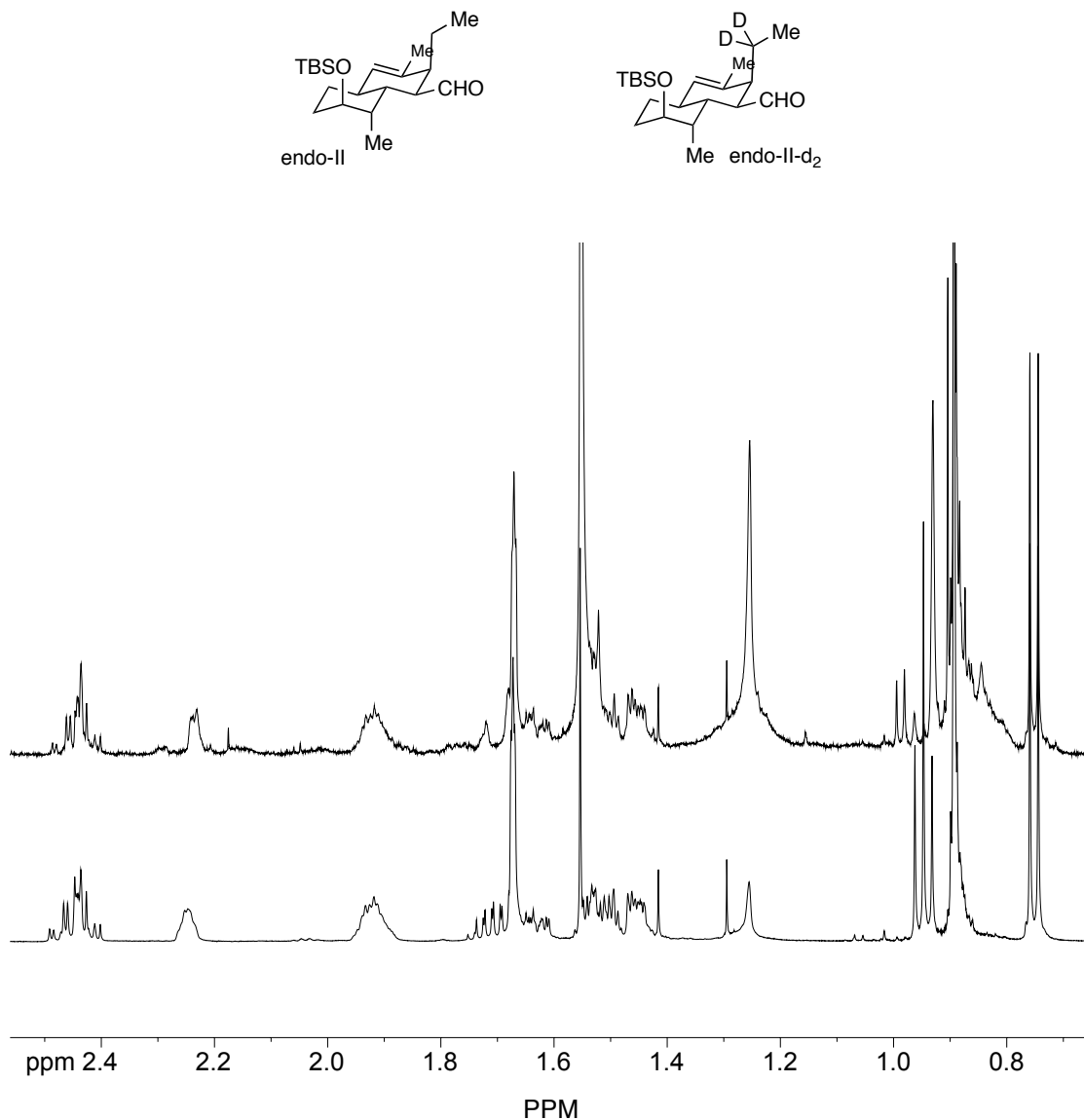


Most importantly, H13 was resolved it was convincingly assigned as an axial proton. Also, here in the d_2 case, H9 was re-analyzed for its shape and it was far easier to see that it shared two axial vicinal partners in addition to the methyl group. To my delight, every resonance could be resolved and analyzed for its shape. The full assignment is presented in Table form following the experimentals.

Admittedly, less analysis was completed on the minor isomer *endo*-II- d_2 . This isomer had been more amenable to prior characterization than the former. Nevertheless, the d_2 experiment served to support the prior assignment. In particular, the region near 1.5 ppm

(CDCl₃) was simplified (Figure I-28), enabling verification of assignments in that area. Previously, there were 4 protons in that region that were very close together.

Figure I-28. Stacked ¹H NMR of *endo*-II (bottom) and *endo*-II-d₂ (top) in CDCl₃.



Although not critical to the assignment of ring fusion (see above discussion on the most critical of peak identification), this simplification allowed for each and every resonance to be accounted for and lent much support to the tentative assignment.

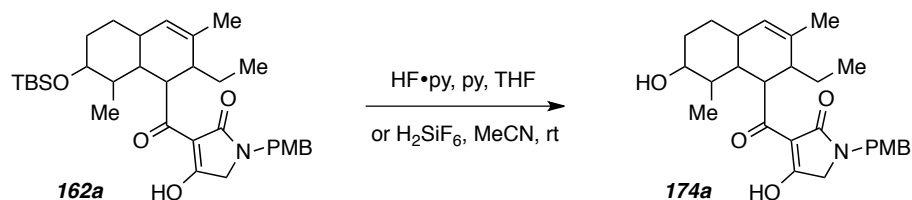
Analogous epimerization experiments were not attempted with the d₂ material. These could further support the conclusions drawn in this section for the structure and

stereochemistry of the two major Diels-Alder adducts of the system. The assignments now stand as presented in Scheme I-103, *endo*-I and *endo*-II.

III.C. Post IMDA: Additional Reactions Toward Model 26

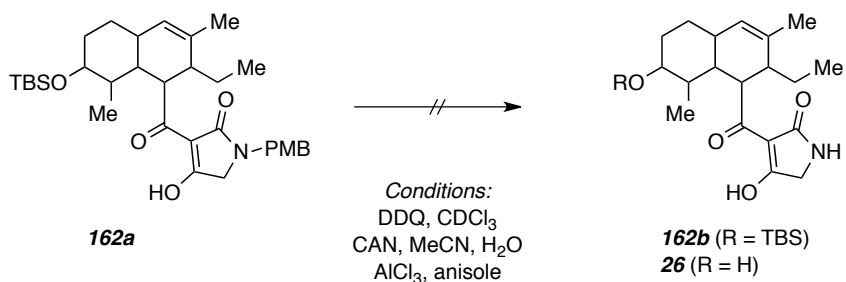
After the work in characterization of the Diels-Alder adducts, and knowing that similar activation would likely result in similar stereochemical outcomes, I made a push to acquire some of model compound **26** for analysis and potential comparison to the natural product. Some of these reactions were briefly presented at the end of Chapter II, but are discussed in more detail here. I went forward with removing the protecting groups (Scheme I-112) on the already-cyclized material **162a**. General TBS cleavage conditions were applied and this transformation was clean, but sluggish and additional fluoride reagent had to be added over the course of the reaction.

Scheme I-112. TBS Removal from Octalin **162a**.



Removal of the PMB group⁵² was far more difficult. Rather than try on alcohol **174a** (of which I had milligram quantities), I went back to the IMDA adduct **162a** (Scheme I-113). I had no success with any of the standard oxidative cleavage methods (CAN, DDQ). I tried several times and also attempted the Lewis acid AlCl_3 but the amide protecting group remained through all these efforts.

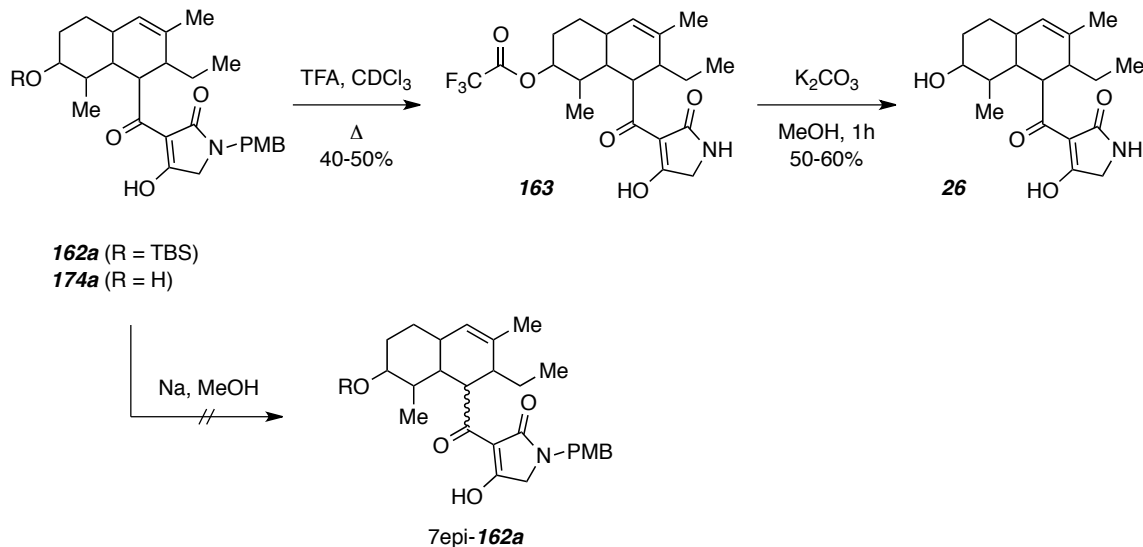
Scheme I-113. Attempted PMB Removal of Octalin **162a**.



To my relief, I found that acidic removal of the PMB group was possible in refluxing $\text{TFA}/\text{CH}_2\text{Cl}_2$ (Scheme I-114). Under these conditions, the TBS group also fell off, but the

recovery was poor and transesterification to the TFA ester **163** occurred. Methanolic K_2CO_3 smoothly gave the free alcohol **26**, but this step was also low yielding due to poor recovery. At this stage I was handling sub-milligram quantities of material, so characterization data is scarce on this compound.

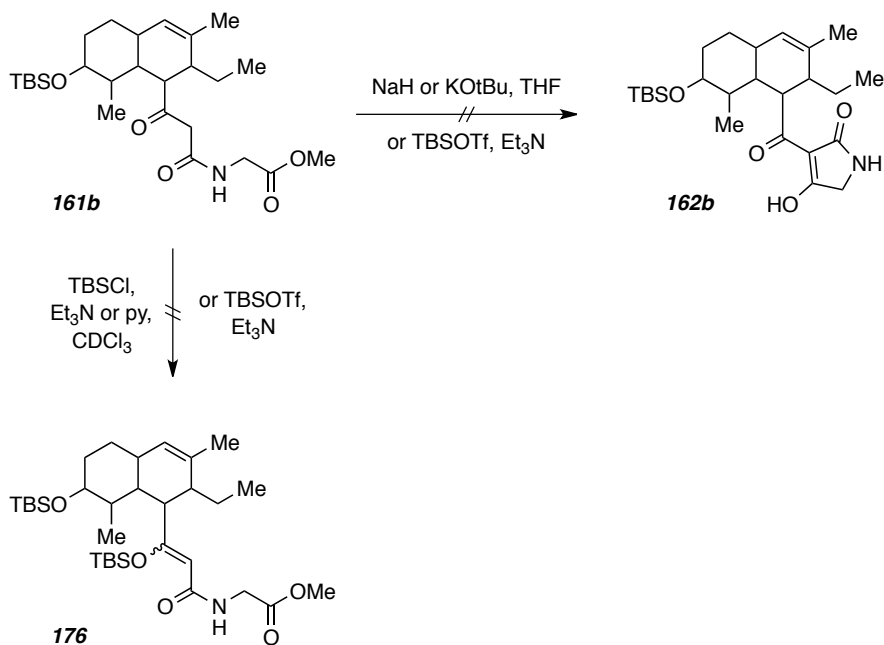
Scheme I-114. Removal of PGs.



I also attempted the epimerization under the conditions employed in the previous section (Scheme I-114, bottom arrows), but no change in the 1H NMR resulted from these conditions.

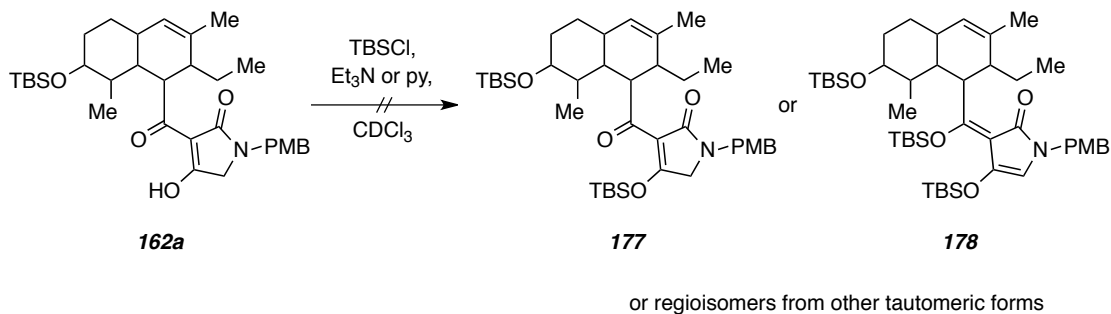
With the Diels-Alder reaction already completed to give octalin **161b**, and knowing the difficulty in removing the PMB group, **161b** was pursued as an intermediate into **162b** (Scheme I-115). Several bases were used to try to encourage the heterocycle to close to **162b**, but these failed. Likewise, silylative Dieckmann conditions did not provide access to the heterocycle. The Dieckmann reactions of primary amines are more stubborn. Even the standard silylation experiment failed; I did not observe the formation of any silyl enol ether **176**, or it was too labile to be isolated. This compound might have been worthwhile to study, to see how the tricarbonyl **161b** compared to **176** behaved (tautomeric forms, etc.).¹³

Scheme I-115. Attempted Dieckmann of **161b**.



In a similar way, I tried to understand the tetramic acid **162a** by silylating one or more of the carbonyls after the successful Dieckmann reaction (Scheme I-116). I saw no silyl incorporation at any site under these conditions. A more aggressive reagent may be necessary.

Scheme I-116. Attempted Silylation of **162a**.



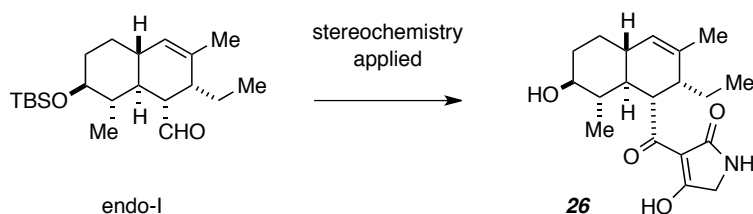
III.D. Comparison to Natural Product, Conclusions, and State of the Project

There still remains a vigorous analysis and comparison to the natural product. Admittedly, only a model compound has been prepared, (**26**, with limited spectral data) but the protons of interest have been named and noted, and should be sufficient when

returning to data given for the natural product. Without performing an exhaustive comparison, there are still conclusions that can be made.

The main conclusion is this. The aldehyde **97** was established to cyclize spontaneously into two *endo*-adducts I and II. By analogy, assuming the tetramic acid imparts similar activation, the stereochemical outcome would be the same. Thus, I would assign the structure of my synthetic intermediate **26** from what I learned from **97** (Scheme I-117).

Scheme I-117. Assumption of Identical Stereochemistry of **26**.



Then, the (limited) data for **26** must be compared to the data for **1a**.¹³ If there is a sufficient match, we have acquired data that suggests that structure of the natural product is incorrect.

Finally, a triene was prepared that mimics a growing polyketide chain in the proposed biosynthesis of integramycin. This triene underwent spontaneous Diels-Alder chemistry in the laboratory to selectively produce a mixture of *endo*-type (and no significant contribution from the *exo*-type) IMDA adducts. Although not under physiological conditions, this was still a spontaneous reaction that establishes a benchmark for the substrate in other settings.

Intuition and literature searches can be performed to develop a hypothesis for Diels-Alder under these other setting (e.g. biologically relevant conditions). My prediction is that the reaction will occur faster in aqueous medium³¹ and generate adducts with the same stereochemistry as I assigned to my products. There is already selectivity in this Diels-Alder reaction. The question of 100% selectivity (e.g. *endo*-I over *endo*-II, however, will be more difficult to face.³² Whether or not an aqueous medium will promote only *endo*, and only *one endo* product is an open question. Our hope is that the reaction will be so rapid, only one stereoisomer will be observed, and (coupled with the

expected similarity between spectral data for **26** and **2**), our hypothesis of a spontaneous biosynthetic Diels-Alder reaction will be supported.

References

- (1) Clardy, J.; Walsh, C. Lessons from natural molecules. *Nature* **2004**, *432*, 829-837.
- (2) Danishefsky, S. On the potential of natural products in the discovery of pharma leads: A case for reassessment. *Nat. Prod. Rep.* **2010**, *27*, 1114-1116.
- (3) Mickel, S. J.; Sedelmeier, G. H.; Niederer, D.; Daeffler, R.; Osmani, A.; Schreiner, K.; Seeger-Weibel, M.; B rod, B.; Schaer, K.; Gamboni, R.; Chen, S.; Chen, W.; Jagoe, C. T.; Kinder, F. R.; Loo, M.; Prasad, K.; Repic , O.; Shieh, W.; Wang, R.; Waykole, L.; Xu, D. D.; Xue, S. Large-Scale Synthesis of the Anti-Cancer Marine Natural Product (+)-Discodermolide. Part 1: Synthetic Strategy and Preparation of a Common Precursor. *Org. Proc. Res. Dev.* **2004**, *8*, 92-100.
- (4) Dalby, S. M.; Paterson, I. Synthesis of polyketide natural products and analogs as promising anticancer agents. *Curr. Opin. Drug Disc.* **2010**, *13*, 777-794.
- (5) Strohl, W. R. The role of natural products in a modern drug discovery program. *Drug Discovery Today* **2000**, *5*, 39-41.
- (6) U.S. Department of Health and Human Services The HIV Life Cycle. www.aidsinfo.nih.gov/contentfiles/HIVLifeCycle_FS_en.pdf (accessed 07/24, 2012).
- (7) Fischer, J. HIV-I Integrase Inhibitors: A Formal Total Synthesis of Lithospermic Acid and Synthetic Studies Towards Integramycin, School of Chemistry, University of Sydney, 2007.
- (8) Hazuda, D.; Blau, C. U.; Felock, P.; Hastings, J.; Pramanik, B.; Wolfe, A.; Bushman, F.; Farnet, C.; Goetz, M.; Williams, M.; Silverman, K.; Lingham, R.; Singh, S. Isolation and characterization of novel human immunodeficiency virus integrase inhibitors from fungal metabolites. *Antivir. Chem. Chemoth.* **1999**, *10*, 63-70.

- (9) Pommier, Y.; Johnson, A. A.; Marchand, C. Integrase inhibitors to treat HIV/Aids. *Nat. Rev. Drug Discov.* **2005**, *4*, 236-248.
- (10) Savarino, A. A historical sketch of the discovery and development of HIV-1 integrase inhibitors. *Expert Opin. Investig. Drugs* **2006**, *15*, 1507-1522.
- (11) Singh, S. B.; Zink, D. L.; Goetz, M. A.; Dombrowski, A. W.; Polishook, J. D.; Hazuda, D. J. Equisetin and a novel opposite stereochemical homolog phomasetin, two fungal metabolites as inhibitors of HIV-1 integrase. *Tetrahedron Lett.* **1998**, *39*, 2243-2246.
- (12) Vesonder, R. F.; Tjarks, L. W.; Rohwedder, W. K.; Burmeister, H. R.; Laugal, J.A. Equisetin, an antibiotic from *Fusarium equiseti* NRRL 5537, identified as a derivative of N-methyl-2,4-pyrrolidone. *J. Antibiot.* **1979**, *32*, 759-761.
- (13) Singh, S. B.; Zink, D. L.; Heimbach, B.; Genilloud, O.; Teran, A.; Silverman, K. C.; Lingham, R. B.; Felock, P.; Hazuda, D. J. Structure, Stereochemistry, and Biological Activity of Integramycin, a Novel Hexacyclic Natural Product Produced by *Actinoplanes* sp. that Inhibits HIV-1 Integrase. *Org. Lett.* **2002**, *4*, 1123-1126.
- (14) Wang, L.; Floreancig, P., E. Synthesis of the C16-C35 fragment of integrumycin using olefin hydroesterification as a linchpin reaction. *Org. Lett.* **2004**, *6*, 569-572.
- (15) Sun, H.; Abbott, J. R.; Roush, W. R. Stereoselective Synthesis of a Model C(18)–C(35) Spiroketal Fragment of Integramycin. *Org. Lett.* **2011**, *13*, 2734-2737.
- (16) Dineen, T. A.; Roush, W. R. Stereoselective Synthesis of the Octahydronaphthalene Unit of Integramycin via an Intramolecular Diels-Alder Reaction. *Org. Lett.* **2005**, *7*, 1355-1358.

- (17) Wang, L. Carbon-Carbon Bond Construction Using Electron Transfer Initiation Cyclization Reactions. RutheniumCatalyzed Hydroesterification and its Application Towards the Synthesis of Integramycin. University of Pittsburgh, 2005.
- (18) Roush, W. R.; Essenfeld, A. P.; Warmus, J. S. Effect of dienophile activating group on the stereoselectivity of the intramolecular diels-alder reaction. *Tetrahedron Lett.* **1987**, *28*, 2447-2450.
- (19) Dineen, T. A. Studies on the intramolecular Diels-Alder reaction : total synthesis of cochleamycin A and efforts toward the total synthesis of integramycin. 2005.
- (20) Coe, J. W.; Roush, W. R. Studies of an intramolecular Diels-Alder approach to the nargenicins: involvement of boatlike transition states in the cyclizations of substituted 1,7,9-decatrien-3-ones. *J. Org. Chem.* **1989**, *54*, 915-930.
- (21) Khuong, K. S.; Beaudry, C. M.; Trauner, D.; Houk, K. N. Dienophile twisting and substituent effects influence reaction rates of intramolecular Diels-Alder cycloadditions: a DFT study. *J. Am. Chem. Soc.* **2005**, *127*, 3688-3689.
- (22) Gras, J.; Bertrand, M. cis- Δ^5 -octahydro-1-naphthalenones and cis- Δ^5 -decahydro-1-naphthalenes (cis-1-decalones) by stereoselective intramolecular diels-alder reaction. *Tetrahedron Lett.* **1979**, *20*, 4549-4552.
- (23) Taber, D. F.; Gunn, B. P. Control elements in the intramolecular Diels-Alder reaction. Synthesis of (+-)-torreyol. *J. Am. Chem. Soc.* **1979**, *101*, 3992-3993.
- (24) Sorensen, E. J. Architectural Self-Construction in Nature and Chemical Synthesis. *Bioorg. Med. Chem.* **2003**, *11*, 3228-3228.
- (25) Oikawa, H.; Tokiwano, T. Enzymatic catalysis of the Diels-Alder reaction in the biosynthesis of natural products. *Nat. Prod. Rep.* **2004**, 321-352.

- (26) Kim, H. J.; Ruszczycky, M. W.; Choi, S.; Liu, Y.; Liu, H. Enzyme-catalysed cycloaddition is a key step in the biosynthesis of spinosyn A. *Nature* **2011**, *473*, 109-112.
- (27) Katayama, K.; Kobayashi, T.; Oikawa, H.; Honma, M.; Ichihara, A. Enzymatic activity and partial purification of solanapyrone synthase: first enzyme catalyzing Diels-Alder reaction. *Biochim Biophys Acta* **1998**, *1384*, 387-395.
- (28) Oikawa, H.; Katayama, K.; Suzuki, Y.; Ichihara, A. Enzymatic activity catalysing exo-selective Diels-Alder reaction in solanapyrone biosynthesis. *J. Chem. Soc., Chem. Commun.* **1995**, 1321-1322.
- (29) Auclair, K.; Sutherland, A.; Kennedy, J.; Witter, D. J.; Van, d. H.; Hutchinson, C. R.; Vederas, J. C. Lovastatin Nonaketide Synthase Catalyzes an Intramolecular Diels-Alder Reaction of a Substrate Analogue. *J. Am. Chem. Soc.* **2000**, *122*, 11519-11520.
- (30) Grieco, P. A. Organic Chemistry in Unconventional Solvents. *Aldrichimica Acta* **1991**, *24*, 59-66.
- (31) Breslow, R. Hydrophobic effects on simple organic reactions in water. *Acc. Chem. Res.* **1991**, *24*, 159-164.
- (32) Hoye, T. R.; Dvornikovs, V. Comparative Diels-Alder Reactivities within a Family of Valence Bond Isomers: A Biomimetic Total Synthesis of (+/-)-UCS1025A. *J. Am. Chem. Soc.* **2006**, *128*, 2550-2551.
- (33) Sizova, E. P. Second General Synthesis of UCS1025A. Synthetic Efforts Toward Total Syntheses of CJ-16,264 and Phomopsicalasin, University of Minnesota, .
- (34) Hoye, T. R. Synthesis and Structure of Antitumor Agents. *ROI CA076497-09* **2007**.

- (35) Toda, S.; Yamamoto, S.; Tenmyo, O.; Tsuno, T.; Hasegawa, T.; Rosser, M.; Oka, M.; Sawada, Y. F.; Konishi, M.; Oki, T. A new neuritogenetic compound BU-4514N produced by *Microtetraspora* sp. *J. Antibiot.* **1993**, *46*, 875-883.
- (36) Ueno, M.; Amemiya, M.; Iijima, M.; Osono, M.; Masuda, T.; Kinoshita, N.; Ikeda, T.; Iinuma, H.; Hamada, M.; Ishizuka, M. Delaminomycins, novel nonpeptide extracellular matrix receptor antagonist and a new class of potent immunomodulator. I. Taxonomy, fermentation, isolation and biological activity. *J. Antibiot.* **1993**, *46*, 719-727.
- (37) Crimmins, M. T.; King, B. W.; Tabet, E. A.; Chaudhary, K. Asymmetric aldol additions: use of titanium tetrachloride and (-)-sparteine for the soft enolization of N-acyl oxazolidinones, oxazolidinethiones, and thiazolidinethiones. *J. Org. Chem.* **2001**, *66*, 894-892.
- (38) Lacey, R. N. Derivatives of acetoacetic acid. Part VII. [α]-Acetyltetramic acids. *J. Chem. Soc.* **1954**, 850-854.
- (39) Watanabe, W. H.; Conlon, L. E. Homogeneous Metal Salt Catalysis in Organic Reactions. I. The Preparation of Vinyl Ethers by Vinyl Transesterification. *J. Am. Chem. Soc.* **1957**, *79*, 2828-2833.
- (40) Parker, K. A.; Farmar, J. G. Regioselectivity in the Claisen rearrangement of bis-allylic alcohols: Electronic and steric effects of C-4 substituents. *Tetrahedron Lett.* **1985**, *26*, 3655-3658.
- (41) Burrows, C.; Carpenter, B. K. Substituent effects on the aliphatic Claisen rearrangements. 2. Theoretical analysis. *J. Am. Chem. Soc.* **1981**, *103*, 6984-6986.
- (42) Curran, D. P.; Suh, Y. G. Substituent effects on the Claisen rearrangement. The accelerating effect of a 6-donor substituent. *J. Am. Chem. Soc.* **1984**, *106*, 5002-5004.

- (43) Hiersemann, M.; Abraham, L. Catalysis of the Claisen Rearrangement of Aliphatic Allyl Vinyl Ethers. *Euro. J. Org. Chem.* **2002**, *2002*, 1461-1471.
- (44) Lutz, R. P. Catalysis of the Cope and Claisen rearrangements. *Chem. Rev.* **1984**, *84*, 205-247.
- (45) Overman, L. E. Mercury(II)- and Palladium(II)-Catalyzed [3,3]-Sigmatropic Rearrangements [New Synthetic Methods (46)]. *Angew. Chem. Int. Ed.* **1984**, *23*, 579-586.
- (46) Booker-Milburn, K.; Baker, J. R.; Bruce, I. Rapid Access to Azepine-Fused Oxetanols from Alkoxy-Substituted Maleimides. *Org. Lett.* **2004**, *6*, 1481-1484.
- (47) Bellur, E.; Gorus, H.; Langer, P. Synthesis of 2-alkylidenepyrrolidines, pyrroles, and indoles by condensation of silyl enol ethers and 1,3-bis-silyl enol ethers with 1-azido-2,2-dimethoxyethane and subsequent reductive cyclization. *J. Org. Chem.* **2005**, *70*, 4751-4761.
- (48) Gage, J. R.; Evans, D. A. Diastereoselective Aldol Condensation Using a Chiral Oxazolidinone Auxiliary: (2S*, 3S*)-3-Hydroxy-3-Phenyl-2-Methylpropanoic Acid. *Org. Synth.* **1993**, *68*, 83-86.
- (49) Evans, D. A.; Nelson, J. V.; Vogel, E.; Taber, T. R. Stereoselective aldol condensations via boron enolates. *J. Am. Chem. Soc.* **1981**, *103*, 3099-3111.
- (50) Nahm, S.; Weinreb, S. M. N-methoxy-n-methylamides as effective acylating agents. *Tetrahedron Lett.* **1981**, *22*, 3815-3818.
- (51) Issa, F.; Fischer, J.; Turner, P.; Coster, M. J. Regioselective Reduction of 3-Methoxymaleimides: An Efficient Method for the Synthesis of Methyl 5-Hydroxytetramates. *J. Org. Chem.* **2006**, *71*, 4703-4705.

- (52) Green, T. W.; Wuts, P. G. M., Eds.; In *Protecting Groups in Organic Synthesis*; John Wiley and Sons, Inc.: New York, 1999; .
- (53) Schwartz, A. L.; Lerner, L. M. Preparation of N-substituted maleimides by direct coupling of alkyl or aralkyl halides with heavy metal salts of maleimide. *J. Org. Chem.* **1974**, *39*, 21-23.
- (54) Abdel-Magid, A.; Carson, K. G.; Harris, B. D.; Maryanoff, C. A.; Shah, R. D. Reductive Amination of Aldehydes and Ketones with Sodium Triacetoxyborohydride. Studies on Direct and Indirect Reductive Amination Procedures. *J. Org. Chem.* **1996**, *61*, 3849-3862.
- (55) Painter, F. F.; Allmendinger, L.; Bauschke, G. A General Method for the Highly Regioselective Introduction of Substituents into the 3-position of 5-unsubstituted 4-O-alkyl Tetronates. *Synlett* **2005**, *18*, 2735-2738.
- (56) Kowalski, C. J.; Weber, A. E.; Fields, K. W. .alpha.-Keto dianion precursors via conjugate additions to cyclic .alpha.-bromo enones. *J. Org. Chem.* **1982**, *47*, 5088-5093.
- (57) Schlessinger, R. H.; Beberitz, G. R.; Lin, P.; Poss, A. J. Total synthesis of (-)-tirandamycin A. *J. Am. Chem. Soc.* **1985**, *107*, 1777-1778.
- (58) Boeckman, R. K.; Perni, R. B.; MacDonald, J. E.; Thomas, A. J. 6-Diethylphosphonomethyl-2,2-Dimethyl-1,3-Dioxene-4-one. *Org. Synth.* **1993**, *8*, 192-196.
- (59) Boeckman, R. K.; Thomas, A. J. Methodology for the synthesis of phosphorus-activated tetramic acids: applications to the synthesis of unsaturated 3-acyltetramic acids. *J. Org. Chem.* **1982**, *47*, 2823-2824.
- (60) Böhme, R.; Jung, G.; Breitmaier, E. Synthesis of the Antibiotic (R)-Reutericyclin via Dieckmann Condensation. *Helv. Chim. Acta* **2005**, *88*, 2837-2841.

- (61) Ley, S. V.; Smith, S. C.; Woodward, P. R. Further reactions of t-butyl 3-oxobutanethioate and t-butyl 4-diethyl-phosphono-3-oxobutanethioate : Carbonyl coupling reactions, amination, use in the preparation of 3-acyltetramic acids and application to the total synthesis of fuligorubin A. *Tetrahedron* **1992**, *48*, 1145-1174.
- (62) Crimmins, M. T.; Washburn, D. G.; Zawacki, F. J. The Synthesis of 2-alkyl-4-pyrones from Meldrum's Acid. *Org. Synth.* **2004**, *10*, 355.
- (63) Ley, S. V.; Smith, S. C.; Woodward, P. R. Use of t-butyl 4-diethylphosphono-3-oxobutanethioate for tetramic acid synthesis: Total synthesis of the plasmodial pigment fuligorubin A. *Tetrahedron Lett.* **1988**, *29*, 5829-5832.
- (64) Ley, S. V.; Woodward, P. R. Preparation of t-butyl 4-diethylphosphono-3-oxobutanethioate and use in the synthesis of (E)-4-alkenyl-3-oxoesters and macrolides. *Tetrahedron Lett.* **1987**, *28*, 345-346.
- (65) Pronin, S. V.; Kozmin, S. A. Synthesis of Streptolydigin, a Potent Bacterial RNA Polymerase Inhibitor. *J. Am. Chem. Soc.* **2010**, *132*, 14394-14396.
- (66) Ley, S. V.; Woodward, P. R. The use of β -ketothioesters for the exceptionally mild preparation of β -ketoamides. *Tetrahedron Lett.* **1987**, *28*, 3019-3020.
- (67) Prousis, K. C.; Athanasellis, G.; Stefanou, V.; Matiadis, D.; Kokalari, E.; Igglessi-Markopoulou, O.; McKee, V.; Markopoulos, J. Synthesis and Crystal Structure Characterization of Zinc (II) Tetric Acid Complexes. *Bioinorg. Chem. Appl.* **2010**, *2010*.
- (68) Bodurow, C.; Carr, M. A.; Moore, L. L. 2,2-DIMETHYL-6-[(Triphenylphosphoranylidene)methyl]-4H-1,3-Dioxin-4-one. A Four-Carbon Homologating Agent Requiring No Activation. *Org. Prep. Proc. Int.* **1990**, *22*, 109-111.

- (69) Royles, B. J. L. Naturally Occurring Tetramic Acids: Structure, Isolation, and Synthesis. *Chem. Rev.* **1995**, *95*, 1981-2001.
- (70) Jones, R. C. F.; Peterson, G. E. Directed metallation of tetramic acids: a new synthesis of 3-acyl tetramic acids. *Tetrahedron Lett.* **1983**, *24*, 4751-4754.
- (71) Jones, R. C. F.; Sumaria, S. A synthesis of 3-acyl-5-alkyl tetramic acids. *Tetrahedron Lett.* **1978**, *19*, 3173-3176.
- (72) Hori, K.; Hikage, N.; Inagaki, A.; Mori, S.; Nomura, K.; Yoshii, E. Total synthesis of tetronomycin. *J. Org. Chem.* **1992**, *57*, 2888-2902.
- (73) Dener, J. M.; Hart, D. J.; Ramesh, S. α -Acylamino radical cyclizations: application to the synthesis of (-)-swainsonine. *J. Org. Chem.* **1988**, *53*, 6022-6030.
- (74) Ireland, R. E.; Thompson, W. J. An approach to the total synthesis of chlorothricolide: the synthesis of the top half. *J. Org. Chem.* **1979**, *44*, 3041-3052.
- (75) Kumar, S.; Ramachandran, U. An Improved Procedure For the Etherification Of Hydroxy Acid Derivatives. *Org. Prep. Proc. Int.* **2004**, *36*, 380-383.
- (76) Louwrier, S.; Ostendorf, M.; Boom, A.; Hiemstra, H.; Nico Speckamp, W. Studies towards the synthesis of (+)-ptilomycalin A; Stereoselective N-acyliminium ion coupling reactions to enantiopure C-2 substituted lactams. *Tetrahedron* **1996**, *52*, 2603-2628.
- (77) de Figueiredo, R. M.; Voith, M.; Fröhlich, R.; Christmann, M. Synthesis of a Malimide Analogue of the Telomerase Inhibitor UCS1025A Using a Dianionic Aldol Strategy. *Synlett* **2007**, *2007*, 0391-0394.
- (78) Klaver, W. J.; Henk, H.; Speckamp, W. N. Synthesis and absolute configuration of the Aristotelia alkaloid peduncularine. *J. Am. Chem. Soc.* **1989**, *111*, 2588-2595.

- (79) Asahi, K.; Nishino, H. Manganese(III)-based dioxapropellane synthesis using tricarbonyl compounds. *Tetrahedron* **2008**, *64*, 1620-1634.
- (80) Paquette, L. A.; Ezquerra, J.; He, W. Suitability of the Claisen ring expansion protocol for crenulide diterpene construction. *J. Org. Chem.* **1995**, *60*, 1435-1447.
- (81) Oare, D. A.; Henderson, M. A.; Sanner, M. A.; Heathcock, C. H. Acyclic stereoselection. 46. Stereochemistry of the Michael addition of N,N-disubstituted amide and thioamide enolates to α,β -unsaturated ketones. *J. Org. Chem.* **1990**, *55*, 132-157.
- (82) Shirokawa, S.; Kamiyama, M.; Nakamura, T.; Okada, M.; Nakazaki, A.; Hosokawa, S.; Kobayashi, S. Remote Asymmetric Induction with Vinylketene Silyl N,O-Acetal. *J. Am. Chem. Soc.* **2004**, *126*, 13604-13605.
- (83) Evans, D. A.; Kaldor, S. W.; Jones, T. K.; Clardy, J.; Stout, T. J. Total synthesis of the macrolide antibiotic cytovaricin. *J. Am. Chem. Soc.* **1990**, *112*, 7001-7031.
- (84) Zhang, Q.; Rivkin, A.; Curran, D. P. Quasiracemic Synthesis: \approx Concepts and Implementation with a Fluorous Tagging Strategy to Make Both Enantiomers of Pyridovericin and Mappicine. *J. Am. Chem. Soc.* **2002**, *124*, 5774-5781.
- (85) Kinoshita, K.; G Williard, Paul; Khosla, C.; Cane, D. E. Precursor-Directed Biosynthesis of 16-Membered Macrolides by the Erythromycin Polyketide Synthase. *J. Am. Chem. Soc.* **2001**, *123*, 2495-2502.
- (86) Boger, D. L. In *Key Bond Forming Reactions: Diels Alder Reaction*; Baraccio, R. M., Ed.; Lecture Notes. Modern Organic Synthesis. TSRI Press: La Jolla, CA, 1999; pp 213-273.
- (87) Hepperle, S. S.; Li, Q.; East, A. L. L. Mechanism of cis/trans equilibration of alkenes via iodine catalysis. *J. Phys. Chem. A* **2005**, *109*, 10975-10981.

- (88) Birnbaum, G. I.; Cygler, M.; Ekiel, I.; Shugar, D. Structure and conformation of 8-bromo-9- β -D-xylofuranosyladenine in the solid state and in solution. *J. Am. Chem. Soc.* **1982**, *104*, 3957-3964.
- (89) Schulte-Elte, K.; Giersch, W.; Winter, B.; Pamingle, H.; Ohloff, G. Diastereoselektivität der Geruchswahrnehmung von Alkoholen der Iononreihe. *Helv. Chim. Acta* **1985**, *68*, 1961-1985.
- (90) Hirose, T.; Sunazuka, T.; Yamamoto, D.; Kojima, N.; Shirahata, T.; Harigaya, Y.; Kuwajima, I.; Ōmura, S. Determination of the absolute stereochemistry and asymmetric total synthesis of madindolines A and B: a practical improvement to a second-generation approach from the first-generation. *Tetrahedron* **2005**, *61*, 6015-6039.

Part One Experimental Section

General Methods:

Reactions requiring anhydrous conditions were performed under an atmosphere of nitrogen or argon in flame-dried glassware cooled under a stream of nitrogen. Dry diisopropylethylamine and triethylamine were distilled from CaH₂; dried dimethylformamide and pyridine were stored over 3 Å MS. Anhydrous THF, diethyl ether, toluene, and methylene chloride were dried by being passed through a column of activated alumina

ⁿBuLi, was titrated with 1,4-cyclooctadiene by No-D NMR spectroscopy.

MPLC refers to medium pressure liquid chromatography (25-60 psi) using hand-packed columns of E. Merck silica gel (18-32 μm, 60 Å), a Waters HPLC pump, and Waters R403 differential refractive index detector.

Analytical TLC was performed using TLC plastic sheets with F₂₅₄ indicator and detection was performed by UV-light or potassium permanganate, *p*-anisaldehyde, or cerium ammonium nitrate/ethanol staining.

The ¹H and ¹³C NMR spectra were acquired on a Varian VI-500 (500 MHz ¹H, 125.7 MHz ¹³C), VI-300 (300 MHz ¹H, 75.4 MHz ¹³C), or VXR-300 (300 MHz ¹H, 75.4 MHz ¹³C) spectrometers. ¹H NMR chemical shifts in CDCl₃ are referenced to Me₄Si (0.00 ppm), or to CHCl₃ (7.26 ppm) where specified, in DMSO to CD₂HS(O)CD₃ peak (2.50 ppm), in CD₃CN to CD₂H₂CN peak (1.94 ppm), D₂O to HOD (4.80 ppm), CD₃OD to CD₂HOD peak (3.31 ppm), C₆D₆ to C₆D₅H peak (7.16 ppm). ¹³C NMR chemical shifts in CDCl₃ are referenced to ¹³CDCl₃ peak (77.23 ppm). ¹³C NMR chemical shifts in C₆D₆ are referenced to ¹³C₆D₆ peak (128.39 ppm). The following format was used to report ¹H NMR data: chemical shift in ppm [multiplicity, coupling constant(s) in Hz, integral]. The following abbreviations are used to describe multiplicities: s (singlet), d (doublet), t

(triplet), q (quartet), pent (pentet), m (multiplet), nform (non-first order multiplet), and br (broad). ¹H NMR assignments are indicated by number or letter (*e.g.*, H-3a), where given, and complex structures are numbered in their structures in order to simplify proton assignment numbering and naming.

Infrared (IR) spectra were recorded on a Midac Corporation Prospect 4000 FT-IR spectrometer (only the most intense and/or diagnostic peaks are reported) using a NaCl plate (thin film) or flat plate with ZnSe crystal. Absorptions are reported in cm⁻¹.

High-resolution mass spectra were recorded on a Bruker Biotof II (ESI-TOF) instrument using PEG or PPG as an internal calibrant.

Tandem gas chromatography/low resolution mass spectroscopy (GC/MS) using electron impact ionization (EI) was performed at 70 eV on an Agilent Technologies 6890N series gas chromatograph equipped with an Agilent Technologies 5975 inert XL mass selective detector. The methods are given in () and in the order : start temp-final temp-time of run.

Tandem liquid chromatography/low resolution mass spectroscopy (LC/MS) using multimode ESI- APCI ionization mode was performed on an Agilent Technologies 1100 series liquid chromatograph equipped with an Agilent Technologies G1956B LC/MSD SL mass selective detector. The Methods are labeled as follows:

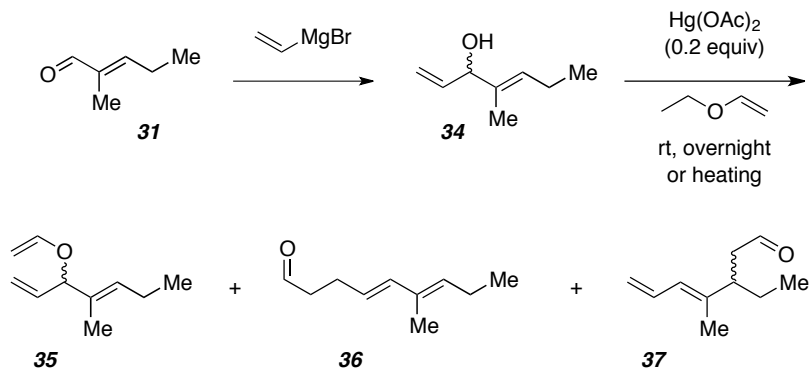
- A: 'col5, 0-100, 22, sm, ES/APC'
- B: 'col5, 50-100, sm, fr70, ES/AP, -/+'
- C: 'Pat-col1, 50-100, +/-all'

Some compounds included in the experimental section are known in the literature.

Tables mentioned but not included in the text are located at the end of this experimental.

¹H NMR file names are included. They are located at the end of the ¹H NMR data and are contained follow the general form [se(notebook number)pg(page number)...]

Experiments (Chapter II.A.)



Preparation of *E*-4-methyl-1,4-heptadien-3-ol (**34**):

To an oven-dried round bottom flask equipped with a stir bar was added *E*-2-methyl-2-pentenal **31** (104 mg, 1.06 mmol, 1 equiv). Dry THF (5 mL) was added and the reaction flask cooled to 0 °C. Vinyl magnesium bromide (solution in THF ~0.89 M, 1.5 mL, 1.3 mmol, 1.2 equiv) was added via syringe, and the internal temperature was maintained under 5 °C. The reaction was stirred for 30 minutes at 0 °C and then allowed to warm to room temperature. After one hour, the reaction was quenched with saturated NH_4Cl solution, extracted with Et_2O , dried over MgSO_4 , and concentrated to give the bis-allylic alcohol **34** (120 mg, 90%) as a pale yellow oil in >98% purity by GC-MS.

$^1\text{H NMR}$ (500 MHz, CDCl_3): δ 5.9 (ddd, 1H, $J = 17.2, 10.4, 5.6$, $\text{CH}_2=\text{CH}$), 5.5 (ddd, 1H, $J = 1.1, 7.1$, $\text{H}-\text{C}=\text{C}$), 5.3 (ddd, 1H, $J = 1.5, 1.5, 17.2$, $\text{CH}_2=\text{C}$), 5.1 (ddd, 1H, $J = 1.5, 1.5, 10.4$, $\text{CH}_2=\text{C}$), 4.5 (bd, 1H, $J = 5.6$, HCOH), 2.1 (dp, 1H, $J = 1.5, 7.5$, CH_2CH_3), 1.6 (s, 3H, CH_3), and 1.0 (t, 3H, $J = 7.5$, CH_3).

$^{13}\text{C NMR}$ (125 MHz, CDCl_3): δ 139.3, 135.2, 128.8, 114.7, 78.4, 20.9, 14.0, and 11.7.

IR: 3403, 2965, 2934, 2874, 1456, 1379, 991, and 921 cm^{-1} .

GC-MS: M^+ = 126; R_t = 4.9 min (50 °C \rightarrow 250 °C, ramp 20 °C/min, hold 250 °C 5 min).

General preparation of (*E*)-4-methyl-3-(vinyloxy)hepta-1,4-diene (**35**): (seIpg81f1)

Bis-allylic alcohol **34** was weighed into a screw-capped culture tube. An appropriate amount of $\text{Hg}(\text{OAc})_2$ (generally 20 mol %) was then added followed by ethyl vinyl ether (generally 1 ml/mmol). The culture tube was capped and left to stir overnight (even

longer times were required for full conversion) at room temperature, after which time the reaction mixture was diluted with diethyl ether. Water and brine were used to wash the inorganics, and following the final wash, the organic layer was dried over Na₂SO₄ and concentrated to give the vinylallyl ether product **35** (yields typically 85-95%) which could be chromatographed (20:1 Hexanes:EtOAc) or used crude in subsequent reactions. NMR (500 MHz, CDCl₃): δ 6.33 (dd, *J* = 16, 6.5 Hz, 1H), 5.82 (ddd, *J* = 16.1, 10.5, 5.5 Hz 1H), 5.47 (br t, *J* = 7.2 Hz 1H), 5.28 (ddd, *J* = 17.3, 1.5, 1.5 Hz 1H), 5.20 (ddd, *J* = 10.5, 1.4, 1.4 Hz, 1H), 4.52 (br d, *J* = 5.5 Hz, 1H), 4.35 (dd, *J* = 14.1, 1.4 Hz, 1H), 4.02 (dd, *J* = 6.6, 1.4 Hz, 1H), 2.05 (pent, *J* = 7.6 Hz, 2H), 1.57 (s, 3H), and 0.88 (t, *J* = 7.5 Hz, 3H)

Claisen Product (4*E*,6*E*)-6-methylnona-4,6-dienal (36):

Alternatively the procedure for allyl vinyl ether **35** could be modified so that the reaction was heated in an excess of ethyl vinyl ether overnight, where conversion to the Claisen products **36** and **37** was observed. The same workup applied, and chromatography or distillation gave a mixture of **36** and **37** in approximately 3:1 ratio. Fractionation of chromatographic fractions was commonly used to increase this ratio.

¹H NMR (500 MHz, CDCl₃): δ 9.79 (t, *J* = 1.6 Hz, 1H), 6.09 (d, *J* = 15.6 Hz, 1H), 5.53 (ddd, *J* = 15.5, 6.8, 6.8 Hz, 1H), 5.40 (t, *J* = 7.2 Hz, 1H), 2.55 (dt, *J* = 7.1, 1.4 Hz, 2H), 2.44 (q, *J* = 7.0 Hz, 2H), 2.12 (pent, *J* = 7.5 Hz, 2H), 1.71 (s, 3H), and 0.98 (t, *J* = 7.5 Hz, 3H)

¹³C NMR (125 MHz, CDCl₃): δ 202.2, 136.2, 133.5, 127.6, 124.6, 43.7, 26.2, 25.5, 21.5, and 14.2. [seVlpg76aldmixC13]

GCMS (5025015): R_t = 7.07 min, 152(M⁺, 40), 137(30), 93(100), 81(100), and 67(60)

TLC (12:1 Hex:EtOAc): R_f = 0.4

Claisen Product (E)-3-ethyl-4-methylhepta-4,6-dienal (37):

¹H NMR (500 MHz, CDCl₃): δ 9.67 (t, *J* = 2.4 Hz, 1H), 6.56 (ddd, *J* = 16.8, 10.5, 10.5 Hz, 1H), 5.92 (d, *J* = 10.8 Hz, 1H), 5.04 (dd, *J* = 16.8, 2.1 Hz, 1H), 5.04 (dd, *J* = 10.1,

2.0 Hz, 1H), 2.56 (pent, $J = 7.3$ Hz, 2H), 2.46 (dd, $J = 7.6, 2.7$ Hz, 1H), 2.44 (dd, $J = 6.7, 2.4$ Hz, 1H), 1.45 (pent, $J = 7.4$ Hz, 3H) and 0.85 (t, $J = 7.4$ Hz, 3H)

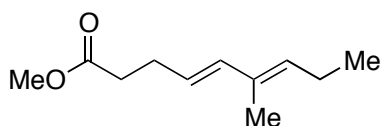
^{13}C NMR (125 MHz, CDCl_3): δ 202.4, 139.0, 132.8, 132.6, 116.1, 47.4, 45.0, 13.1, 12.3, and 11.9. [seVIpg76aldmixC13]

GCMS (5025015): $R_t = 6.35$ min, 152(M^+ , 15), 119(20), 95(80), 81(80), and 67(100).

ESI-MS: Exact Mass calc. for mixture of the aldehydes $[\text{C}_{10}\text{H}_{16}\text{OK}]^+$, 191.0833, found 191.0983.

TLC (12:1 Hex:EtOAc): $R_f = 0.4$

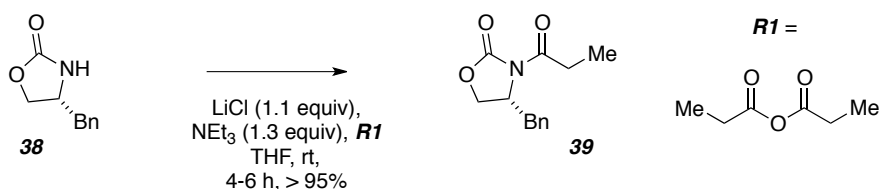
Johnson-Claisen Products:



(4E,6E)-methyl 6-methylnona-4,6-dienoate (Methyl Ester of 36)

^1H NMR (500 MHz, CDCl_3): δ 6.98 (d, $J = 15.5$ Hz, 1H), 5.52 (dt, $J = 15.4, 7.1$ Hz, 1H), 5.39 (t, $J = 7.3$ Hz, 1H), 3.67 (s, 3H), 2.49-2.31 (m, 4H), 2.12 (pent, $J = 7.5$ Hz, 2H), 1.70 (s, 3H), and 0.97 (t, $J = 7.5$ Hz, 3H). (referenced to CDCl_3) [seIpg95f2]

The intermediate and minor isomer were not characterized due to complications in the NMR. These could not be separated and individually analyzed.



(R)-3-(1-Oxopropyl)-4-(phenylmethyl)-2-oxazolidinone (39):⁵⁰

Preparation:

A flame-dried round bottom flask equipped with a stir bar was cooled under N_2 . To the flask was added (R)-4-(phenylmethyl)-2-oxazolidinone **38** (8 g, 45.2 mmol, 1.0 equiv, LiCl (2.113 g, 42.5 mmol, 1.1 equiv), Et_3N (5.94 g, 54.2 mmol, 1.3 equiv), and THF (150 mL). The reaction mixture was cooled to -20 °C at which time propionic anhydride (7.05 g, 54.2 mmol, 1.3 equiv) was added. Following stirring at room temperature for 6 hours,

the THF was removed under reduced pressure and the residue was taken up in EtOAc. HCl (0.2 N) was added, and the organic layer was separated and washed sequentially with brine, 1 M sodium bicarbonate, and brine. The organic layer was dried over sodium sulfate, filtered, and concentrated to a viscous oil containing both the product **39** and unreacted starting material. Flash column chromatography (2:1 EtOAc: Hexanes) gave the pure acylated compound (6.5 g, 90% borsm).

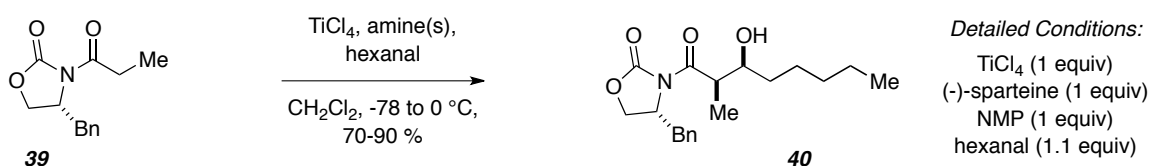
¹H NMR (500 MHz, CDCl₃): δ 7.1-7.4 (m, 5H, ArH), 4.6 (m, 1H, NCH), 4.2 (m, 2H, OCH₂CH), 3.2 (dd, 1H, *J* = 13.4, 3.3, PhCH₂), 2.9 (m, 2H, CH₂CH₃), 2.7 (dd, 1H, *J* = 13.4, 9.6, PhCH₂), and 1.2 (t, 3H, *J* = 7.4, CH₃).

¹³C NMR (125 MHz, CDCl₃): δ 174.2, 153.7, 135.5, 129.6, 129.1, 127.5, 69.2, 55.4, 38.1, 29.4, and 8.5.

IR: 2981, 2940, 1781, 1701, 1389, 1375, 1248, 1213, 1079, and 703 cm⁻¹

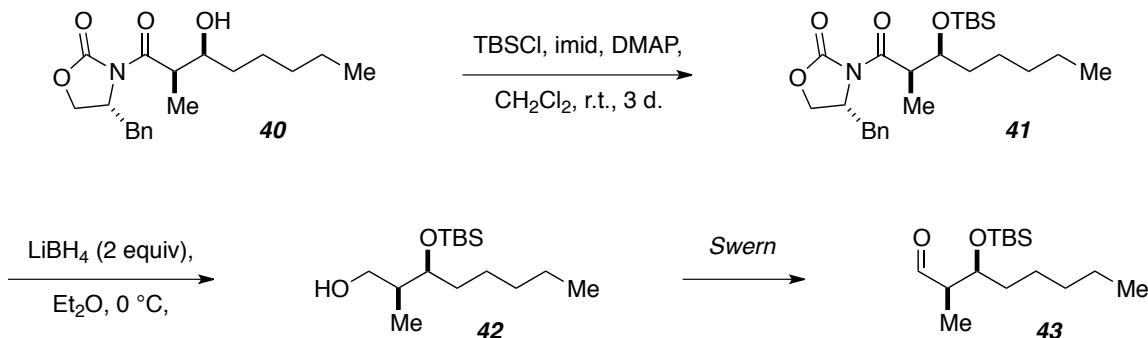
GC-MS: M⁺ = 233; R_t = 10.9 min (50 °C → 250 °C, ramp 20 °C/min, hold 250 °C 5 min).

Alternatively, the acetylated oxazolidinone could be prepared from treatment of the sm with n-BuLi followed by addition of propionyl chloride.



(R)-4-benzyl-3-((2R,3S)-3-hydroxy-2-methyloctanoyl)oxazolidin-2-one (40)

¹H NMR (500 MHz, CDCl₃): δ 7.29-7.13 (m, 5H), 4.67-4.58 (m, 1H), 4.13(dd, *J* = 10.9, 3.0 Hz, 1H), 4.11 (dd, *J* = 9.1, 3.0 Hz, 1H), 3.88 (ddd, *J* = 8.5, 4.4, 2.6 Hz, 1H), 3.69 (dq, *J* = 2.6, 7.1 Hz, 1H), 3.24 (dd, *J* = 13.5, 3.5 Hz, 1H), 2.70 (dd, *J* = 13.4, 9.9 Hz, 1H), 2.27 (app pent, *J* = 7.2 Hz, 1H), 1.30-1.21 (m, 8H), 1.19 (d, *J* = 7.1 Hz, 3), and 0.82 (t, *J* = 7.0 Hz, 3H). [senb30smwkpup]



(R)-4-benzyl-3-((2R,3S)-3-((tert-butyldimethylsilyl)oxy)-2-methyloctanoyl)oxazolidin-2-one (41)

Preparation for **40**: see the process described for unprotected **44**, next scheme in these experimentals. Preparation for **41**: A round bottom flask was charged with crude **40** (1 equiv.), imidazole (2.5 equiv.), DMAP (0 or 0.25 equiv.), and TBSCl (1.5 equiv.). This mixture of solids was dissolved in enough DMF for a concentration of 1 molar, and left to stir at room temperature overnight (up to 24 hours), where TLC (10:1 Hex:EtOAc) confirmed full consumption of the alcohol **40**. The reaction was quenched with water (same volume DMF) and extracted with ethyl acetate (3X). The organics were washed with brine, dried (Na_2SO_4), and concentrated under reduced pressure. MPLC (12:1 Hex:EtOAc) gave the protected aldol product **41** in 60-80% yield.

$^1\text{H NMR}$ (500 MHz, CDCl_3): δ 7.37-7.18 (m, 5H), 4.61 (dddd, $J = 9.8, 6.7, 3.0, 3.0$ Hz, 1H), 4.21-4.14 (m, 2H), 3.87 (dq, $J = 4.8, 6.9$ Hz 1H), 3.31 (dd, $J = 13.4, 3.3$ Hz, 1H), 2.78 (dd, $J = 13.3, 9.9$ Hz, 1H), 1.55-1.50 (m, 2H), 1.38-1.25 (m, 6H), 1.22 (d, $J = 7.0$ Hz, 3H), and 0.88 (t, $J = 7.5$ Hz, 3H). [seIpg34-3d]

(2S,3S)-3-((tert-butyldimethylsilyl)oxy)-2-methyloctan-1-ol (42)

Preparation: A solution of **41** (1 equiv.) in THF (0.5 molar) and MeOH (2 equiv) was cooled to 0 °C by an ice bath. LiBH_4 (2 M in THF, 2 equiv.) was dispensed into this solution via syringe and the resulting solution was stirred at 0 °C for one hour, followed by warming to rt and stirring an additional hour. TLC was used to confirm reduction was complete, and a saturation solution of Rochelle's salt (equal volume to reaction mixture) was added slowly and stirring continued 1 additional hour, or until 2 clear layers were observed. Extraction into Et_2O , drying over MgSO_4 , and concentration completed the

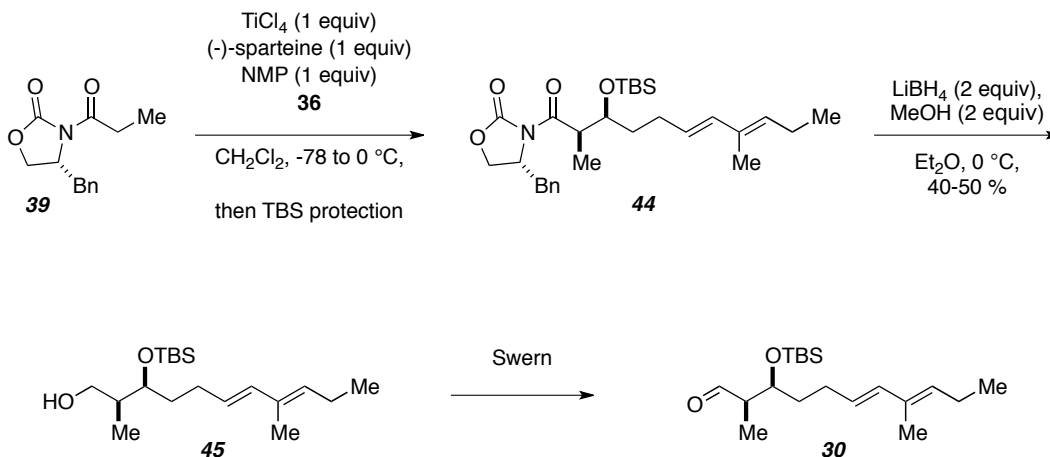
workup procedure, and the crude diol was recovered as a white solid, after which chromatography (8:1 Hex:EtOAc) gave a colorless oil. Typical yields were 40-60%, and could not be improved by additional extraction or varying the quench.

$^1\text{H NMR}$ (500 MHz, CDCl_3): δ 3.75 (ddd, $J = 8.0, 5.3, 2.9$ Hz, 1H), 3.70 (ddd, $J = 10.6, 8.6, 3.4$ Hz, 1H), 3.52 (ddd, $J = 10.4, 6.7, 5.0$ Hz, 1H), 2.67 (dd, $J = 6.8, 3.6$ Hz, 1H), 1.97 (dddq, $J = 7.9, 4.9, 3.0, 7.2$ Hz, 1H), 1.52-1.38 (m, 2H), 1.35-1.23 (m, 6H), 0.893 (s, 9H), 0.892 (t, $J = 7.5$ Hz, 3H), 0.80 (d., $J = 7.0$ Hz, 3H), 0.09 (s, 3H), and 0.07 (s, 3H). (referenced to CHCl_3) [seIpg40f2better]

(2R,3S)-3-((tert-butyldimethylsilyl)oxy)-2-methyloctanal (43)

Preparation: There were the same conditions worked out for **30** (below)

$^1\text{H NMR}$ (500 MHz, CDCl_3): δ 9.77 (s, 1H), 4.1 (ddd, $J = 6.6, 6.6, 3.5$ Hz, 1H), 2.45 (dq, $J = 3.5, 7.0$ Hz, 1H), 1.52-1.45 (m, 2H), 1.36-1.24 (m, 6H), 1.06 (d, $J = 7.0$ Hz, 3H), 0.90 (t, $J = 6.7$ Hz, 3H), 0.87 (s, 9H), 0.07 (s, 3H), and 0.04 (s, 3H). [seIpg45crd]



(R)-4-benzyl-3-((2R,3S,6E,8E)-3-hydroxy-2,8-dimethylundeca-6,8-dienoyl)oxazolidin-2-one (unprotected 44).

Preparation:

To a stirred solution of propionylated auxially **39** in CH_2Cl_2 at 0 °C was added TiCl_4 dropwise. The resulting yellow suspension was stirred for an additional 10 minutes,

followed by dropwise addition of (-)-sparteine. The resulting dark red solution was stirred for another 20 minutes, then cooled to -78 °C. NMP was added and the solution stirred for 10 minutes. Finally, a solution of aldehyde in CH₂Cl₂ was added and the reaction mixture was first stirred at -78 °C for one hour then allowed to warm to 0 °C. The amber solution was quenched with half-saturated aqueous NH₄Cl solution at 0 °C and allowed to warm to room temperature. The organic layer was separated and the aqueous later extracted twice with CH₂Cl₂. The combined organic layers were then washed with brine, dried over Na₂SO₄, and concentrated to give the crude aldol adduct as a yellow oil which was generally used without purification. Alternatively, MPLC (4:1 Hexanes:EtOAc) can be performed and yielded the purified adduct as a colorless oil.

¹H NMR (500 MHz, CDCl₃): δ 7.4-7.1 (m, 5H, ArH), 6.09 (d, *J* = 15.6 Hz, 1H), 5.54 (ddd, *J* = 15.5, 6.8, 6.8 Hz, 1H), 5.37 (t, *J* = 7.2 Hz, 1H), 4.73-4.67 (m, 1H), 4.22 (dd, *J* = 16.7, 9.0 Hz, 1H), 4.18 (dd, *J* = 9.0, 3.0 Hz, 1H), 3.97 (ddd, *J* = 8.9, 3.8, 3.8 Hz, 1H), 3.76 (dq, *J* = 7.0, 2.8 Hz, 1H), 3.24 (dd, *J* = 13.4, 3.5 Hz, 1H), 2.79 (dd, *J* = 13.4, 9.4 Hz, 1H), 2.35-2.08 (m, 4H), 1.71 (s, 3H) 1.70-1.63 (m, 1H), 1.54-1.46 (m, 1H), 1.26 (d, *J* = 7.0 Hz, 3H) and 0.97 (t, *J* = 7.2 Hz, 3H). (referenced to CHCl₃) [Ipg150c2f2]

ESI-MS: Exact mass calc. for [C₂₃H₃₁NO₄Na]⁺, 408.2145, found 408.2138.

TLC (4:1 Hex:EtOAc): R_f = 0.25

(R)-4-benzyl-3-((2R,3S,6E,8E)-3-((tert-butyldimethylsilyl)oxy)-2,8-dimethylundeca-6,8-dienoyl)oxazolidin-2-one (44)

Preparation: See 41 (above)

The crude aldol adduct was dissolved in a minimal amount of DMF (to give a 1 M solution) and imidazole (2.5 equiv), DMAP (0.25 equiv), and TBSCl (1.1 equiv) were added and the solution stirred at rt for 24 hours. Additional portions of imidazole and TBSCl (1 equiv each) were added stirring was continued for an additional 12 hours. After TLC indicated full conversion, the reaction mixture was diluted with CH₂Cl₂ and quenched with water. The organic layer was separated and washed with additional portions of water (3x), dried over Na₂SO₄, and concentrated to give the protected alcohol as a yellow oil. Flash column chromatography (or MPLC, 10:1 Hexanes:EtOAc) afforded

the desired product as a colorless oil contaminated with minor amounts of the reaction byproduct Me₃Si-O-SiMe₃.

¹H NMR (500 MHz, CDCl₃): δ 7.4-7.1 (m, 5H, ArH), 6.05 (d, *J* = 15.6 Hz, 1H), 5.53 (ddd, *J* = 15.3, 6.7, 6.7 Hz, 1H), 5.37 (t, *J* = 7.2 Hz, 1H), 4.60 (dddd, *J* = 9.9, 6.5, 3.0, 3.0 Hz, 1H), 4.18-4.11 (m, 2H), 4.02 (q, *J* = 5.5 Hz, 1H), 3.88 (dq, *J* = 6.9, 5.1 Hz, 1H), 3.29 (dd, *J* = 13.3, 3.2 Hz, 1H), 2.76 (dd, *J* = 13.4, 9.7 Hz, 1H), 2.20-2.06 (m, 4H), 1.71 (s, 3H) 1.69-1.58 (m, 2H), 1.22 (d, *J* = 6.9 Hz, 3H), 0.97 (t, *J* = 7.5 Hz, 3H), 0.89 (s, 9H), 0.05 (s, 3H), and 0.0 (s, 3H) (referenced to CHCl₃) [seIpg186f1]

¹³C NMR (125 MHz, CDCl₃): δ 175.4, 153.2, 135.5, 135.0, 133.0, 132.7, 129.6, 129.1, 127.5, 127.1, 72.9, 66.2, 55.9, 43.0, 37.8, 35.6, 28.5, 26.0, 21.5, 14.4, 14.3, 12.4, 12.1, -3.9, and -4.6. [seVIpg76aldoltbsC13]

ESI-MS: Exact mass calc. for [C₂₉H₄₅NO₄SiNa]⁺, 522.3010, found 522.3014

TLC (4:1 Hex:EtOAc): R_f = 0.8

(2S,3S,6E,8E)-3-((tert-butyldimethylsilyloxy)-2,8-dimethylundeca-6,8-dien-1-ol (45)

Preparation:

A flame-dried round bottom flask was cooled under N₂ and to it was added the protected aldol adduct, MeOH (2 equiv), Et₂O (to 0.4 M) and the ensemble cooled to 0 °C. LiBH₄ (2 M in THF, 2 equiv) was added dripwise and the reaction allowed to warm to rt and stirred for an hour. Aqueous Rochelle's salt was added to quench the reaction, and the mixture stirred for 30 minutes or under 2 clear layers were observed. The aqueous layer was extracted twice with Et₂O and dried over MgSO₄. Concentration gave the monoprotected diol as an oil, which could be carried forward in crude form or chromatographed (4:1 Hexanes:EtOAc, preferred over large scale) to yield the desired diol. Varying amounts of the cleaved auxiliary were recovered over the course of these experiments on various scales, and were responsible for a cloudy crude product.

¹H NMR (500 MHz, CDCl₃): δ 6.07 (d, *J* = 15.6 Hz, 1H), 5.54 (ddd, *J* = 15.6, 6.9, 6.9 Hz, 1H), 5.39 (t, *J* = 7.3 Hz, 1H), 3.77 (ddd, *J* = 8.0, 5.2, 3.0 Hz, 1H), 3.71 (ddd, *J* = 10.9, 8.6, 3.0 Hz, 1H), 3.52 (ddd, *J* = 10.8, 6.6, 5.1 Hz, 1H), 2.64 (dd, *J* = 6.6, 3.3 Hz, 1H), 2.26-2.18 (m, 1H), 2.13 (pent, *J* = 7.5 Hz, 2H), 2.06-1.96 (m, 1H), 1.72 (s, 3H),

1.61-1.55 (m, 2H), 0.98 (t, $J = 7.5$ Hz, 3H), 0.90 (s, 9H), and 0.81 (d, $J = 7.1$ Hz)
seIpg183f4

ESI-MS: Exact mass calc. for $[\text{C}_{19}\text{H}_{38}\text{SiO}_2\text{Na}]^+$, 349.2533, found, 349.2536.

TLC (6:1 Hex:EtOAc): $R_f = 0.4$

(2R,3S,6E,8E)-3-((tert-butyldimethylsilyloxy)-2,8-dimethylundeca-6,8-dienal (30)

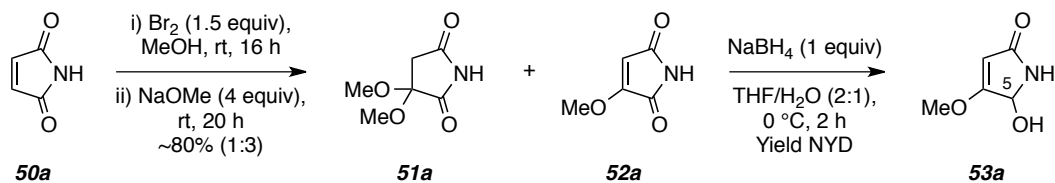
Preparation:

An oven-dried round bottom flask was cooled under a stream of N_2 and charged with DMSO (4 equiv) and CH_2Cl_2 (0.5 M). The flask and its contents were cooled to -78 °C and $(\text{ClCO})_2$ (2 equiv) was added dropwise and stirred for 10 minutes. A solution of the mono-TBS diol (1 equiv) in CH_2Cl_2 was then added slowly over 5 minutes. Stirring continued until a cloudy suspension was observed, then NEt_3 was added to the flask and the reaction mixture allowed to warm to rt. Upon completion of the reaction (monitored by TLC), saturated aqueous NH_4Cl was added and the organic layer separated, dried, and concentrated. The residue was purified by flash column chromatography (20:1 Hexanes:EtOAc) to give the aldehyde as a colorless oil (isolated yields generally 80-90%). seVpg57fc

$^1\text{H NMR}$ (500 MHz, CDCl_3): δ 9.78 (d, $J = 0.9$ Hz, 1H), δ 6.06 (d, $J = 15.6$ Hz, 1H), 5.51 (ddd, $J = 15.6, 6.8, 6.8$ Hz, 1H), 5.38 (t, $J = 7.3$ Hz, 1H), 4.12 (ddd, $J = 6.6, 6.6, 3.6$ Hz, 1H), 2.47 (ddq, $J = 7.0, 3.7, 1.0$ Hz, 1H), 2.20-2.01 (m, 4 H), 1.72 (s, 3H), 1.66-1.53 (m, 2H), 1.06 (d, $J = 7.0$ Hz, 3H), 0.98 (t, $J = 7.5$ Hz, 3H), 0.87 (s, 9H), 0.08 (s, 3H), and 0.04 (s, 3H)

LCMS (Method B): $T_R = 15.6$ min, m/z “pos” = 325.3 ($\text{M}+1$)⁺

TLC (6:1 Hex:EtOAc): $R_f = 0.6$



50a-53a were not amenable to GCMS analysis. Their NMR data were used to judge the process of most reactions and that is all that is provided here.

3,3-dimethoxypyrrolidine-2,5-dione (51a)

Preparation: A solution of **50a** (1 equiv) in MeOH (4 mL/mmol) was cooled to 0 °C (ice-salt bath) and 1.5 equiv of Br₂ were dispensed dropwise via syringe. The resulting red-brown solution was stirred at room temperature overnight or approx. 16 hrs. The reaction mixture was concentrated and fresh MeOH was applied, followed by solid NaOMe (or freshly prepared solution of Na in MeOH, 4 equiv). An exotherm was observed over this second set of events. The reaction was allowed to stir 4 hours at room temperature, when TLC indicated there was no remaining starting material. The reaction was quenched with additional MeOH and EtOAc was added. The aqueous phase was neutralized with HCl and additionally extracted into EtOAc. The combined organic layers were washed with brine, dried, and concentrated to give a mixture of **51a** and **52a**, which were separated by MPLC (1:3 Hex:EtOAc). Depending on the length of stirring, **51a** was the major product (approx. 3:1 over **52a**)

¹H NMR (500 MHz, CDCl₃): δ 3.44 (s, 6H) and 2.86 (s, 2H). [seIpg48col2f2]

3-methoxy-1H-pyrrole-2,5-dione (52a)

Preparation: Produced alongside **51a** (see preparation above). Alternatively, the ketal **51a** could be treated with catalytic TsOH (spatula tip) and heated in PhMe to reflux 1-2 hours, where conversion to **51a** was confirmed NMR.

¹H NMR (500 MHz, CDCl₃): δ 6.99 (br s, 1H), 5.44 (s, 1H), and 3.95 (s, 3H).

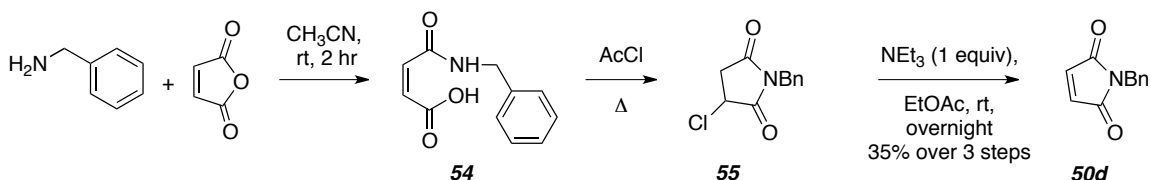
[seIpg48Af2]

5-hydroxy-4-methoxy-1H-pyrrol-2(5H)-one (53a)

Preparation: NaBH₄ (1 equiv) was added in one portion to a stirred solution of **52a** in THF/H₂O (2:1, to 0.5 molar reaction concentration) at 0 °C. The solution was kept at 0 °C for an additional two hours, then quenched with acetone. The reaction mixture was

concentrated. **53a** (and the remainder of the series **53b-d**) were typically recovered (60-70%) and used crude.

¹H NMR (500 MHz, CDCl₃): δ 5.87 (br s, 1H), 5.42 (d, *J* = 1.7Hz, 1H), 5.01 (d, *J* = 1.4 Hz, 1H), and 3.86 (s, 3H) [seIpg63crd]



(Z)-4-(benzylamino)-4-oxobut-2-enoic acid (**54**)

Preparation: Benzylamine (1 equiv) was added via syringe to a solution of maleic anhydride (1 equiv) in CH₃CN at room temperature. Within 5 minutes, a ppt was formed, and the mixture stirred another hour, when it was concentrated. The amic acid was recovered off the rotary evaporator as solid (recoveries/yields 95% to quantitative), and used as such.

¹H NMR (500 MHz, CDCl₃): δ 7.39-7.28 (m, 5H), 7.06 (br s, 1H), 6.33 (d, *J* = 12.8 Hz, 1H), 6.22 (d, *J* = 12.8 Hz, 1H), and 4.54 (d, *J* = 5.8 Hz, 2H). [seIpg67_red_1hr]

1-benzyl-3-chloropyrrolidine-2,5-dione (**55**)

Preparation: The amid acid **54** was dissolved in AcCl (1-2 equiv) and stirred for one hour at room temperature. At this point, **55** was typically observed and could be isolated by quenching with saturated NaHCO₃, dilution into water and extraction into EtOAc. Alternatively, TEA (1 equiv) could be added directly to the reaction pot, and stirred for an additional hour. Water and EtOAc were added. The organic layer was separated, dried, and concentrated to **50d**, which was recovered in sufficient purity to be used crude.

¹H NMR (500 MHz, CDCl₃): δ 7.40-7.30 (m, 5H), 4.73 (d, *J* = 14.1 Hz, 1H), 4.68 (d, *J* = 14.1 Hz, 1H), 4.62 (dd, *J* = 8.6, 3.9 Hz), 3.30 (dd, *J* = 18.8, 8.6 Hz, 1H), and 2.91 (dd, *J* = 18.8, 3.9 Hz, 1H). [seIpg195accladdn]

1-benzyl-1H-pyrrole-2,5-dione (**50d**)

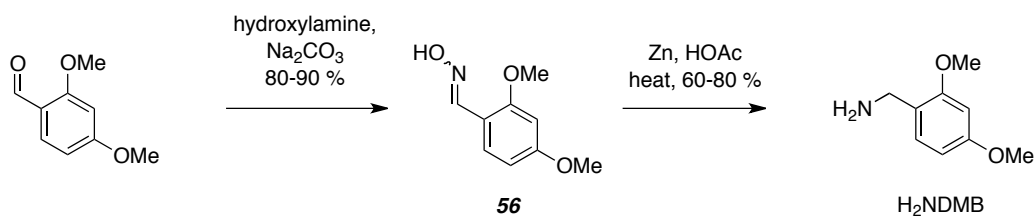
Preparation: See procedure for **55** above, where TEA is added to a solution of **55**.

¹H NMR (500 MHz, CDCl₃): δ 7.35-7.27 (m, 5H), 6.71 (s, 2H), and 4.68 (s, 2H).

[seIpg195_teaaddn]

GCMS (5027016): R_t = 9.05 min, 187(M⁺, 100), 169(10), 159(15), 130(35), 106(4), and 91(20).

TLC (1:1 Hex:EtOAc): R_f = 0.1



2,4-dimethoxybenzaldehyde oxime (**56**)

¹H NMR (500 MHz, CDCl₃): δ 8.42 (s, 1H), 7.21 (br s, 1H), 7.64 (d, *J* = 8.6 Hz, 1H), 6.51 (dd, *J* = 8.6, 2.5 Hz, 1H), 6.45 (d, *J* = 2.3 Hz, 1H), 3.840 (s, 3H), and 3.835 (s, 3H).

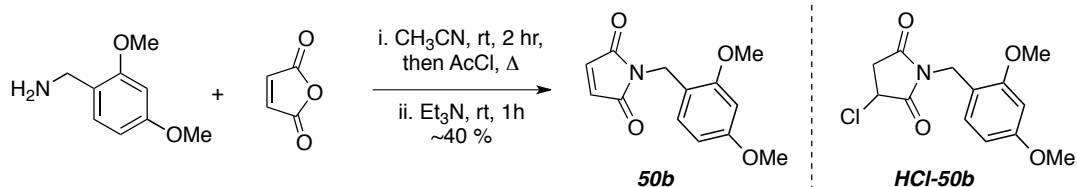
[seIpg113cry]

GCMS (5025015): R_t = 9.14 min, 181(M⁺, not observed), 163(100), 134(40), 120(30), and 77(20).

(2,4-dimethoxyphenyl)methanamine (**H₂NDBM**)

¹H NMR (500 MHz, CDCl₃): δ 7.04 (d, *J* = 8.1 Hz, 1H), 6.39 (d, *J* = 2.3 Hz, 1H), 6.36 (dd, *J* = 8.1, 2.4 Hz, 1H), 3.76 (s, 3H), 3.73 (s, 3H), and 3.68 (s, 2H) [seIpg154seccr]

GCMS (502921H): R_t = 8.66 min, 167(M⁺, not observed), 166(100), 151(50), 136(20), 121(30), and 108(10).



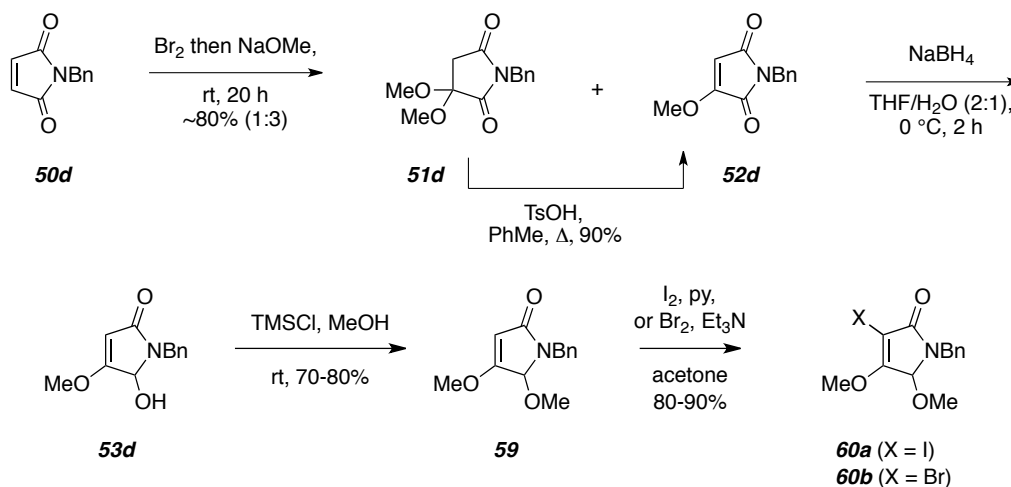
3-chloro-1-(2,4-dimethoxybenzyl)pyrrolidine-2,5-dione (**HCl-50b**)

$^1\text{H NMR}$ (500 MHz, CDCl_3): δ 7.17 (d, $J = 8.4$ Hz, 1H), 6.44-6.42 (m, 2H), 4.72 (d, $J = 14.4$ Hz, 1H), 4.66 (d, $J = 14.5$ Hz, 1H), 4.62 (dd, $J = 8.6, 3.8$ Hz, 1H), 3.793 (s, 3H), 3.788 (s, 3H), 3.29 (dd, $J = 18.7, 8.6$ Hz, 1H), and 2.90 (dd, $J = 18.7, 3.8$ Hz, 1H) [seIpg172accl]

1-(2,4-dimethoxybenzyl)-1H-pyrrole-2,5-dione (50b)

Preparation: See **50d** above.

$^1\text{H NMR}$ (500 MHz, CDCl_3): δ 7.09 (d, $J = 8.9$ Hz, 1H), 6.69 (s, 2H), 6.42-6.40 (m, 2H), 4.66 (s, 2H), 3.79 (s, 3H), and 3.78 (s, 3H). [seIpg156f2] referenced to CHCl_3 !



1-benzyl-3,3-dimethoxypyrrolidine-2,5-dione (51d)

Preparation: See **51a** and **52a** above.

$^1\text{H NMR}$ (500 MHz, CDCl_3): δ 7.36-7.28 (m, 5H), 4.68 (s, 2H), 3.42 (s, 6H), and 2.82 (s, 2H) [seIpg201af3]

1-benzyl-3-methoxy-1H-pyrrole-2,5-dione (52d)

Preparation: See **51a** and **52a** above.

$^1\text{H NMR}$ (500 MHz, CDCl_3): δ 7.36-7.28 (m, 5H), 5.41 (s, 1H), 4.66 (s, 2H), and 3.92 (s, 3H). [seIpg209f4]

GCMS (5027016): $R_t = 10.7$ min, 217(100, M^+), 189(15), 174(30), 106(60), and 69(40).

TLC (1:4 Hex:EtOAc): $R_f = 0.6$

1-benzyl-5-hydroxy-4-methoxy-1H-pyrrol-2(5H)-one (53d)

Preparation: See **53a** above.

^1H NMR (500 MHz, CDCl_3): δ 7.34-7.26 (m, 5H), 5.06 (d, $J = 9.2$ Hz, 1H), 5.03 (s, 1H), 4.95 (d, $J = 15.0$ Hz, 1H), 4.18 (d, $J = 15.2$ Hz, 1H), 3.80 (s, 3H), and 2.78 (br d, $J = 10.2$ Hz, 1H). [seIpg241cr] referenced to CHCl_3 !

GCMS (5027016): $R_t = 11.5$ min, 219(10, M^+), 106(100), and 91(25).

TLC (1:8 Hex:EtOAc): $R_f = 0.1$

1-benzyl-4,5-dimethoxy-1H-pyrrol-2(5H)-one (59)

Preparation: The carbinolamide **53d** was dissolved in MeOH (10 mL/mmol, dissolution was slow at colder temperatures) and cooled to 0 °C. TMSCl (3 equiv) was added via syringe and the reaction was allowed to warm to rt, and stirred an additional 12 hours (although it was typically complete prior to that time). The reaction was quenched with water and extracted into EtOAc (3x). The organic layers were washed with brine, dried, and concentrated. The crude product was recovered as a whitish oil, which was loaded onto the MPLC (1:1.5 Hex:EtOAc) to give the purified **59** as a white solid (yields 30-50%).

^1H NMR (500 MHz, CDCl_3): δ 7.35-7.25 (m, 5H), 5.13 (s, 3H), 5.05 (s, 1H, C(OMe)HN-), 4.97 (d, $J = 15.0$ Hz, 1H), 4.01 (d, $J = 15.0$ Hz, 1H), 3.81 (s, 3H), 3.11 (s, 3H) [seIpg2423]

^{13}C NMR (125 MHz, CDCl_3): δ 171.6, 170.3, 137.3, 128.8, 128.5, 127.6, 95.4, 85.1, 58.5, 50.6, and 42.3.

GCMS (5029021): $R_t = 11.0$ min, 233 (70, M^+), 202(20), 128(40), 113(30), 91(100).

TLC (1:2 Hex:EtOAc): $R_f = 0.5$

1-benzyl-3-iodo-4,5-dimethoxy-1H-pyrrol-2(5H)-one (60a)

Preparation: To a solution of **59** (1 equiv) in DMF (2 mL/mmol up to 1 molar) was added pyridine (1 equiv) and I_2 (4 equiv). The reaction was stirred at rt for 4-12 hours and

concentrated for direct loading onto the MPLC (1:2 Hex:EtOAc). The product iodide was isolated in 40-80% yield. Alternatively, the reaction could be worked up by addition of saturated NaHCO₃ (gas evolution) and then Na₂S₂O₃ and extraction into DCM. This procedure led to higher yields (>60%) and greater purity.

¹H NMR (500 MHz, CDCl₃): δ 7.35-7.28 (m, 5H), 5.24 (s, 1H), 5.03 (d, *J* = 14.8 Hz, 1H), 4.13 (s, 3H), 4.05 (d, *J* = 14.8 Hz, 1H), and 3.10 (s, 3H). [seIpg267f2]

GCMS (5027016): R_t = 12.6 min, 359(65, M⁺), 344(10), 328(25), 200(15), 91(100).

TLC (1:4 Hex:EtOAc): R_f = 0.3

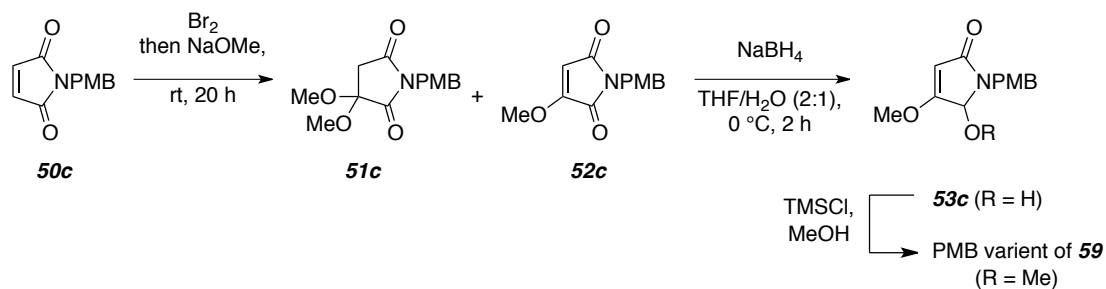
1-benzyl-3-bromo-4,5-dimethoxy-1H-pyrrol-2(5H)-one (60b)

Preparation: 59 (1equiv) was taken up in DCM (1 mL/mmol) followed by addition of TEA (1.5 equiv) and Br₂ (1 equiv). Simple concentration was not effective. A full aqueous workup was preferred. HCl (10% in water) was added to quench the reaction, DCM was the extraction solvent. After acid wash, 0.1 M NaHCO₃ was added, followed by brine. The recovered organic phase was dried (MgSO₄) and concentrated. Recoveries were >80%. The alkyl bromide was typically of sufficient purity to be used in further reactions.

¹H NMR (500 MHz, CDCl₃): δ 7.37-7.28 (m, 5H), 5.14 (s, 1H), 5.01 (d, *J*-14.8 Hz, 1H), 4.16 (s, 3H), 4.05 (d, *J* = 14.8 Hz, 1H), and 3.12 (s, 3H). [seIpg277isoMPLC2]

GCMS (5027016): R_t = 12.1 min, 313(40, M⁺), 311(40, M⁺), 281(30), 206(10), and 91(100).

TLC (1:4 Hex:EtOAc): R_f = 0.3



1-(4-methoxybenzyl)-1H-pyrrole-2,5-dione (50c)

Preparation: See 50d above using PMBNH₂ and maleic anhydride.

¹H NMR (500 MHz, CDCl₃): δ 7.29 (d, *J* = 8.6 Hz, 2H), 6.84 (d, *J* = 8.7 Hz, 2H), 6.69 (s, 2H), 4.61 (s, 2H), and 3.78 (s, 3H). [seIIpg132_accl]

GCMS (5029021): *R*_t = 10.35 min, 217(100, M⁺), 174(40), 136(35), 121(20).

3,3-dimethoxy-1-(4-methoxybenzyl)pyrrolidine-2,5-dione (51c)

Preparation: See **51a** and **52a** above.

¹H NMR (500 MHz, CDCl₃): δ 7.29 (d, *J* = 8.7 Hz, 2H), 6.82 (d, *J* = 8.5 Hz, 2H), 4.61 (s, 2H), 3.78 (s, 3H), 3.41 (s, 6H), and 2.79 (s, 2H). [some of seIIpg38f1]

GCMS (5027016): *R*_t = 11.75 min, 279(40, M⁺), 247(50), 158(20), 121(100), and 88(50).

3-methoxy-1-(4-methoxybenzyl)-1H-pyrrole-2,5-dione (52c)

Preparation: See **51a** and **52a** above.

¹H NMR (500 MHz, CDCl₃): δ 7.29 (d, *J* = 8.7 Hz, 2H), 6.82 (d, *J* = 8.7 Hz, 2H), 5.38 (s, 1H), 4.59 (s, 2H), 3.90 (s, 3H), and 3.77 (s, 3H). [seIIpg41f3] referenced to chloroform here

GCMS (5027016): *R*_t = 11.97 min, 247(100, M⁺), 232(10), 204(20), 136(50).

5-hydroxy-4-methoxy-1-(4-methoxybenzyl)-1H-pyrrol-2(5H)-one (53c)

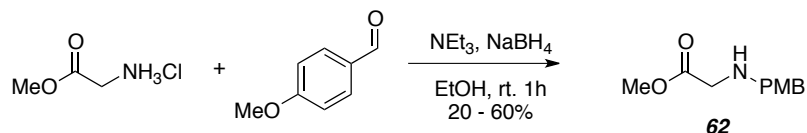
Preparation: See **53a** above.

¹H NMR (500 MHz, CDCl₃): δ 7.22 (d, *J* = 8.7 Hz, 2H), 6.85 (d, *J* = 8.7 Hz, 2H), 5.05 (d, *J* = 9.5 Hz, 1H), 5.03 (s, 1H), 4.89 (d, *J* = 14.9 Hz, 1H), 4.14 (d, *J* = 14.9 Hz, 1H), 3.81 (s, 3H), and 3.79 (s, 3H). [seIIpg47cr]

4,5-dimethoxy-1-(4-methoxybenzyl)-1H-pyrrol-2(5H)-one (PMB variant of 59)

Preparation: See preparation of **59**.

¹H NMR (500 MHz, CDCl₃): δ 7.21 (d, *J* = 8.6 Hz, 2H), 6.84 (d, *J* = 8.7 Hz, 2H), 5.12 (s, 1H), 5.03 (s, 1H), 4.90 (d, *J* = 14.8 Hz, 1H), 3.95 (d, *J* = 14.8 Hz, 1H), 3.80 (s, 3H), 3.78 (s, 3H), and 3.11 (s, 3H). [seIIpg48f3] referenced to chloroform here!

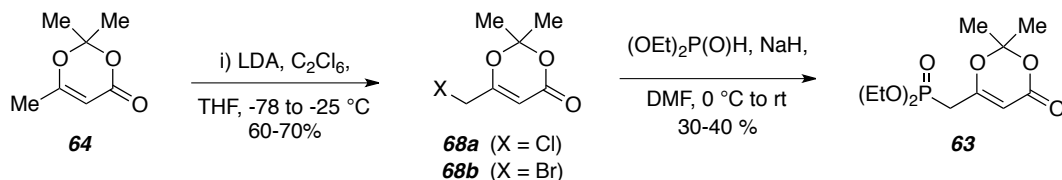


methyl 2-((4-methoxybenzyl)amino)acetate (**62**)

Preparation: A solution of glycine methyl ester (HCl salt, 1 equiv) and p-anisaldehyde (1.05 equiv) in MeOH (or EtOH, 1 molar) was stirred for 30 minutes and treated with NaBH₄ (3 equiv). The reaction was typically complete in a few hours, when it was concentrated and taken up in EtOAc. After filtration through a pad of SiO₂, it was concentrated to a liquid (occasionally a solid was observed upon storage) and used crude for further reactions. TEA was sometimes added at upon first mixing the amine and aldehyde. Yields 80-90%.

¹H NMR (500 MHz, CDCl₃): δ 7.25 (d, *J* = 8.6 Hz, 2H), 6.87 (d, *J* = 8.8 Hz, 2H), 3.80 (s, 3H), 3.74 (s, 2H), 3.73 (s, 3H), and 3.41 (s, 2H). [seVpg41 fil2]

ESI-MS: Exact mass calc. for [C₁₁H₁₅NO₃Na]⁺, 232.0944, found 232.0957.



6-(chloromethyl)-2,2-dimethyl-4H-1,3-dioxin-4-one (**68a**)

Preparation: **68a** was synthesized according to an Org. Synth. Preparation [Organic Syntheses, Coll. Vol. 8, p.192 (1993); Vol. 66, p.194 (1988)]. Both **68a** and **63** had NMR and mass data that were consistent with the reported values.

¹H NMR (500 MHz, CDCl₃): δ 5.57 (s, 1H), 4.03 (s, 2H), and 1.73 (s, 9H).

[seIIIpg183_fc1]

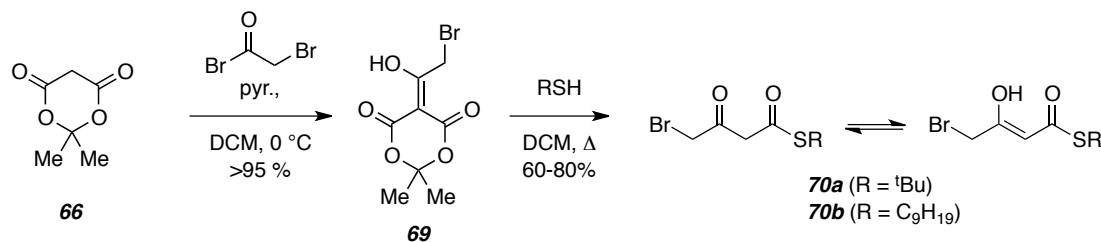
diethyl ((2,2-dimethyl-4-oxo-4H-1,3-dioxin-6-yl)methyl)phosphonate (**63**)

Preparation: See note for **68a**. It could be washed free of excess phosphite by brief exposure to water in the form of a water/EtOAc partition.

$^1\text{H NMR}$ (500 MHz, CDCl_3): δ 5.40 (d, $J = 3.7$ Hz, 1H), 4.17 (q, $J = 7.0$ Hz, 2H), 4.15 (q, $J = 7.0$ Hz, 2H), 2.80 (d, $J = 22.1$ Hz, 2H), 1.72 (s, 6H), and 1.35 (t, $J = 7.1$ Hz, 6H).
[seIII193_bat2pc3]

LCMS (Method B): $T_R = 7.51$ min, m/z "pos" = 296.0 ($M+18$) $^+$

TLC (100% EtOAc): $R_f = 0.1$



5-(2-bromo-1-hydroxyethylidene)-2,2-dimethyl-1,3-dioxane-4,6-dione (**69**)

Preparation: Meldrum's Acid (1 equiv) was weighed directly into a round bottom flask and DCM (to 1M) was added. The solution was cooled to 0 °C, and pyridine (2 equiv) was added, followed by stirring for another 10-15 minutes. Bromoacetyl bromide (1.1 equiv) was added via dropping funnel over the course of 30-40 minutes. Various levels of precipitation were observed in these reactions. The orange-brown reaction suspension was stirred for an additional 1 hour at rt, followed by quenching and concentration to a bright orange-brown solid that was used without purification. Yields >95% for this reaction.

$^1\text{H NMR}$ (500 MHz, CDCl_3) δ : 4.68 (s, 2H, $-\text{CH}_2-$) and 1.77 (s, 6, $-\text{CH}_3$) [seIVpg165cr]

IR (neat): 2983 cm^{-1}

S-tert-butyl 4-bromo-3-oxobutanethioate (**70a**)

Preparation: The acetylation Meldrum's acid (**69**) was weighed into a culture tube. $^t\text{BuSH}$ (1, but more commonly 0.90 equiv) was dispensed via syringe under the protection of a hood. The reaction mixture was dissolved in a minimal amount of DCM (or benzene, typically 1 mL/gram **69**) and the culture tube was sealed and heated with an oil bath. After one hour, the mixture had turned black and the reaction was removed from heat and cooled to rt. At this point, all thiol had had been consumed, as measured by

LCMS (Method B): $T_R = 14.0$ min, m/z "pos" = 311.0.0 (M+1)⁺

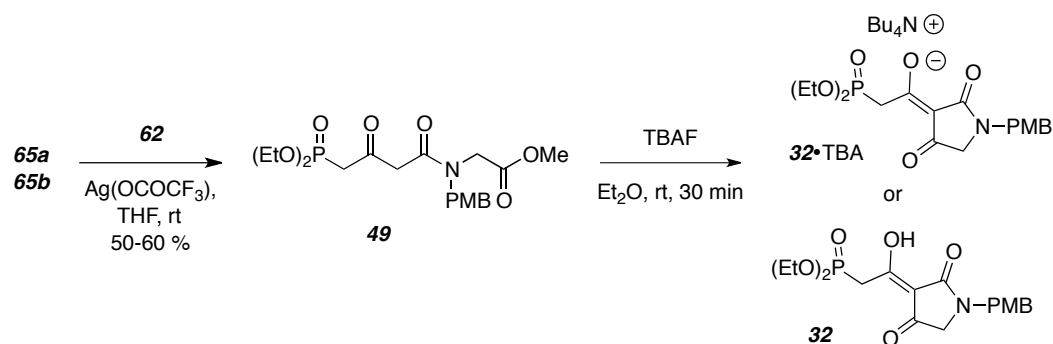
TLC (100% EtOAc): $R_f = 0.1$

S-(2-methyloctan-2-yl) 4-(diethoxyphosphoryl)-3-oxobutanethioate (65b)

¹H NMR (500 MHz, CDCl₃) δ : 12.95 (br s, enol), 5.51-5.46 (m, enol), 4.17 (dq, $J = 7.1$, 1.0 Hz, 4H), 3.81 (s, 2H), 3.25 (d, $J = 22.2$ Hz, 2H), 3.24 (d, $J = 22.3$ Hz, 2H, other form), 2.71 (d, $J = 22.3$ Hz, 2H), 1.94-1.07 (m, nonyl), 1.35 (t, $J = 7.1$ Hz, 6H), 1.34 (t, $J = 7.1$ Hz, 6H, other form), and 0.98-0.78 (m, nonyl). [seVpg176test1]

ESI-MS: Exact mass calc. for [C₁₇H₃₃O₅PSNa]⁺, 403.1679, found 403.1659.

TLC (1:2 Hex:EtOAc): $R_f = 0.1$



methyl 2-(4-(diethoxyphosphoryl)-N-(4-methoxybenzyl)-3-oxobutanamido)acetate (49)

NOTE: ¹H NMR spectrum is complicated by the interconverting rotamers for this amide. Moreover, there are various keto and enol forms. ¹H NMR data will be given in ranges wherever possible. And it appears that the ratio of either of these (keto/enol or two different rotamers) is ~3:1.

¹H NMR (500 MHz, CDCl₃): δ 7.19-7.12 (m, 2H), 6.91-6.85 (m, 2H), 5.46 (d, $J = 3.2$ Hz, 1H), 5.16 (d, $J = 3.1$ Hz, 1), 5.11-5.01 (range for enol form alkenes), 4.62-4.52 (collection of singlets for benzylic protons), 4.17-4.09 (m, 4H), 4.06-3.70 (collection of methylene pairs of various forms and methyl ether singlets), 3.32 (d, $J = 22.6$ Hz, 2H), 2.79 (d, $J = 22.2$ Hz, 2H), and 1.36-1.29 (overlapping triplets from phosphonate).

[seVlpg28cr]

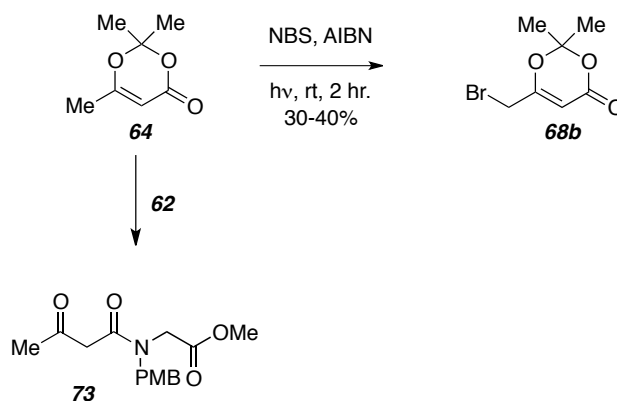
LCMS (Method B): $T_R = 12.4$ min, m/z "pos" = 430.0 (M+1)⁺, m/z "neg" = 428.0 (M-1)⁻
TLC (100% EtOAc): $R_f = 0.15$

(Z)-diethyl (2-hydroxy-2-(1-(4-methoxybenzyl)-2,4-dioxopyrrolidin-3-ylidene)ethyl)phosphonate (32)

¹H NMR (500 MHz, CDCl₃): δ 7.18 (d, $J = 8.6$ Hz, 2H), 6.87 (d, $J = 8.5$ Hz, 2H), 4.54 (s, 2H), 4.18 (app pent, $J = 7.2$ Hz, 4H), 3.80 (s, 3H), 3.61 (s, 2H), and 1.33 (app t, $J = 7.1$ Hz, 6H). [seVIpg29ppt]

LCMS (Method B): $T_R = 8.9$ min, m/z "pos" = 398.0 (M+1)⁺, m/z "neg" = 396.0 (M-1)⁻.

TLC (98:2 EtOAc:MeOH): $R_f = 0.15$



6-(bromomethyl)-2,2-dimethyl-4H-1,3-dioxin-4-one (68b)

¹H NMR (500 MHz, CDCl₃): δ 5.54 (s, 1H), 3.89 (s, 2H), and 1.73 (s, 9H). [seIIIpg67f3]

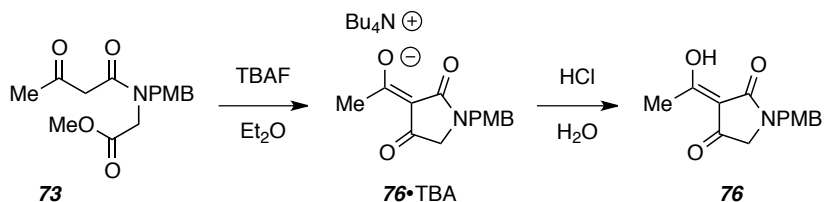
methyl 2-(N-(4-methoxybenzyl)-3-oxobutanamido)acetate (73)

¹H NMR (500 MHz, CDCl₃): δ 7.17 (d, 8.7 Hz, 1H), 7.12 (d, $J = 8.7$ Hz, 2H), 6.89 (d, $J = 8.7$ Hz, 2H), 6.85 (d, $J = 8.7$ Hz, 1H), 5.26 (s, 0.3H), 4.96 (s, 0.10H), 4.63 (s, 0.25 H), 4.60 (s, 0.8 H), 4.52 (s, 2.3 H), 4.05 (s, 0.66 H), 4.03 (s, 1.6 H), 3.92 (s, 0.8 H), 3.88 (s, 0.3 H), 3.81 (s, 3.25 H), 3.80 (s, 1.5H), 3.73 (s, 1.3H), 3.72 (s, 2.2 H), 3.70 (s, 1.2 H), 3.64 (s, 1.4 H), 3.55 (s, 0.8 H), 2.323 (s, 1.9 H), 2.315 (s, 1.1 H), 1.96 (s, 0.3 H), and 1.95 (s, 0.9 H). [seIVpg53_fc]

(also complicated by keto/enol and rotamers here. there is a bigger contribution from the enol form in this molecule. reported the two major keto forms, and just reported all the peaks here)

LCMS: Method B, $R_t = 7.0$ min, $m/z = 294$ ($M+1$)⁺

TLC (1:2 Hex/EtOAc): $R_f = 0.2$



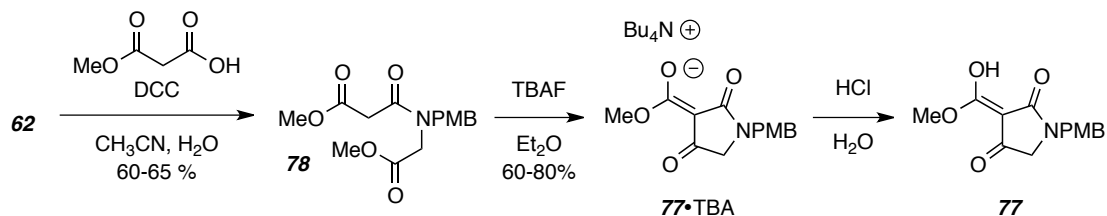
(Z)-3-(1-hydroxyethylidene)-1-(4-methoxybenzyl)pyrrolidine-2,4-dione TBA salt (76•TBA)

¹H NMR (500 MHz, CDCl₃): δ 7.7.16 (d, $J = 8.7$ Hz, 2H), 6.80 (d, $J = 8.6$ Hz, 2H), 4.48 (s, 2H), 3.78 (s, 3H), 3.37 (s, 2H), 2.42 (s, 3H) [seIVpg54_settled] NBu₄ peaks at 3.28, 1.64, 1.43, 0.99.

(Z)-3-(1-hydroxyethylidene)-1-(4-methoxybenzyl)pyrrolidine-2,4-dione (76)

¹H NMR (500 MHz, CDCl₃): δ 7.18 (d, $J = 8.7$ Hz, 2H), 6.88 (d, $J = 8.6$ Hz, 2H), 4.54 (s, 2H), 3.80 (s, 3H), and 2.45 (s, 2H). [seIVpg86_ac]

GCMS/LCMS: NA (76 does not behave on either of these instruments).



methyl 3-((2-methoxy-2-oxoethyl)(4-methoxybenzyl)amino)-3-oxopropanoate (78)

¹H NMR (500 MHz, CDCl₃): δ (major rotomer) 7.14 (d, $J = 8.7$ Hz, 2H), 6.90 (d, $J = 8.7$ Hz, 2H), 4.57 (s, 2H), 4.04 (s, 2H), 3.8 (s, 3H), 3.75 (s, 3H), 3.71 (s, 3H), and 3.60 (s,

2H). δ (minor rotomer) 7.18 (d, $J = 8.6$ Hz, 2H), 6.85 (d, $J = 8.7$ Hz, 2H), 4.61 (s, 2H), 3.95 (s, 3H), 3.80 (s, 3H), 3.76 (s, 3H), 3.71 (s, 2H), and 3.48 (s, 2H). [seIVpg42fcc]
about 2:1 ratio of rotomers here

LCMS: Method B, $R_t = 6.9$ min, $m/z = 310$ ($M+1$)⁺ [IVpg33ov]

TLC (1:2 Hex/EtOAc): $R_f = 0.2$

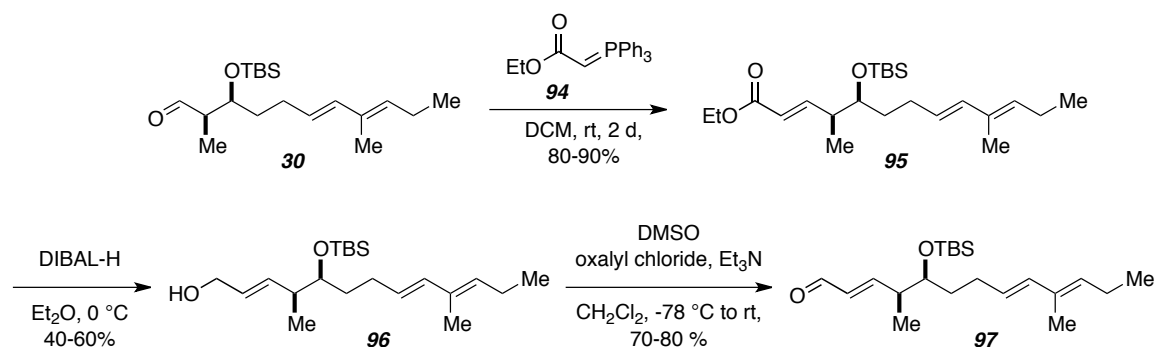
(E)-3-(hydroxy(methoxy)methylene)-1-(4-methoxybenzyl)pyrrolidine-2,4-dione-TBA salt (77•TBA)

¹H NMR (500 MHz, CDCl₃): δ 7.16 (d, $J = 8.5$ Hz, 2H), 6.79 (d, $J = 8.5$ Hz, 2H), 4.46 (s, 2H), 3.77 (s, 3H), 3.68 (s, 3H), and 3.38 (s, 2H), [seIVpg35_II] NBu₄ peaks at 3.30, 1.64, 1.44, 1.0.

(E)-3-(hydroxy(methoxy)methylene)-1-(4-methoxybenzyl)pyrrolidine-2,4-dione (77)

¹H NMR (500 MHz, CDCl₃): δ 7.17 (d, $J = 8.7$ Hz, 2H), 6.86 (d, $J = 8.7$ Hz, 2H), 4.53 (s, 2H), 3.93 (s, 3H), 3.83 (s, 2H), and 3.79 (s, 3H). [seIVpg51_accol]

Experiments (Chapter II.B.)



(2E,4S,5S,8E,10E)-ethyl 5-((tert-butyldimethylsilyl)oxy)-4,10-dimethyltrideca-2,8,10-trienoate (95)

¹H NMR (500 MHz, CDCl₃): δ 7.02 (dd, $J = 15.8, 7.2$ Hz, 1H), 6.05 (d, $J = 15.6$ Hz, 1H), 5.80 (dd, $J = 15.8, 1.3$ Hz, 1H), 5.51 (ddd, $J = 15.7, 6.9, 6.9$ Hz, 1H), 5.37 (t, $J = 6.9$ Hz, 1H), 4.19 (dq, $J = 2.3, 7.1$ Hz, 4H), 3.64 (ddd, $J = 6.8, 4.7, 4.7$ Hz, 1H), 2.48

(ddq, $J = 3.6, 2.0, 6.7$ Hz, 1H), 2.12 (app pent, $J = 7.8$ Hz, 2H), 2.19-2.00 (m, 2H), 1.71 (s, 3H), 1.54-1.43 (m, 2H), 1.29 (t, $J = 7.1$ Hz, 6H), 1.03 (d, $J = 6.8$ Hz, 3H), 0.98 (t, $J = 7.5$ Hz, 3H), 0.90 (s, 9H), 0.05 (s, 3H), and 0.04 (s, 3H). [seIIIpg151_fl1]

LCMS: Method B, $R_t = 19.7$ min, m/z “pos” = 395 (M+1)⁺, 412 (M+18)⁺.

TLC (4:1 Hex:EtOAc): $R_f = 0.6$

(2E,4S,5S,8E,10E)-5-((tert-butyldimethylsilyloxy)-4,10-dimethyltrideca-2,8,10-trien-1-ol (96)

¹H NMR (500 MHz, CDCl₃): δ 6.05 (d, $J = 15.3$ Hz, 1H), 5.75 (dddd, $J = 15.6, 6.9, 1.4, 1.4$ Hz, 1H), 5.62 (dddd, $J = 15.5, 5.7, 5.7, 1.3$), 5.53 (ddd, $J = 15.6, 7.0, 7.0$, 1H), 5.37 (br t, $J = 7.0$ Hz, 1H), 4.13-4.10 (m, 2H), 3.55 (ddd, $J = 6.8, 4.8, 4.8$ Hz, 1H), 2.34 (dd, $J = 7.0, 5.0$ Hz), 2.12 (app pent, $J = 7.4$ Hz, 2H), 2.21-2.06 (m, 2H), 1.72 (s, 3H), 1.52-1.42 (m, 2H), 0.98 (t, $J = 7.5$ Hz, 3H), 0.97 (d, $J = 7.0$ Hz, 3H), 0.90 (s, 9H), 0.05 (s, 3H), and 0.04 (s, 3H). [seIIIpg176_fc2]

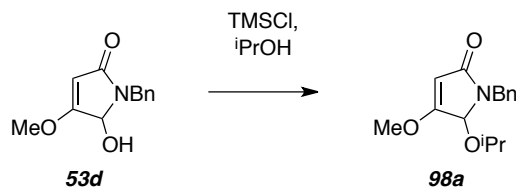
TLC (4:1 Hex:EtOAc): $R_f = 0.2$

(2E,4S,5S,8E,10E)-5-((tert-butyldimethylsilyloxy)-4,10-dimethyltrideca-2,8,10-trienal (97)

¹H NMR (500 MHz, CDCl₃): δ 9.53 (d, $J = 7.9$ Hz, 1H), 6.96 (dd, $J = 15.8, 6.5$ Hz, 1H), 6.11 (ddd, $J = 15.8, 7.9, 1.3$ Hz, 1H), 6.05 (d, $J = 15.5$ Hz, 1H), 5.50 (ddd, $J = 15.6, 7.0, 7.0$ Hz, 1H), 5.38 (t, $J = 7.0$ Hz, 1H), 3.70 (ddd, $J = 7.5, 4.5, 4.5$ Hz, 1H), 2.64 (ddq, $J = 4.3, 1.4, 6.7$ Hz, 1H), 2.22-2.16 (m, 1H), 2.12 (app pent, $J = 7.4$ Hz, 2H), 2.08-2.00 (m, 1H), 1.71 (s, 3H), 1.57-1.50 (m, 1H), 1.43 (dddd, $J = 13.3, 10.3, 7.5, 5.4$ Hz, 1H), 1.07 (d, $J = 6.9$ Hz, 3H), 0.98 (t, $J = 7.5$ Hz, 3H), 0.90 (s, 9H), 0.08 (s, 3H), and 0.05 (s, 3H). [seIIIpg22f2]

LCMS: Method A, $R_t = 18.5$ min, m/z “pos” = 351.3 (M+1)⁺.

TLC (10:1 Hex:EtOAc): $R_f = 0.2$



1-benzyl-5-isopropoxy-4-methoxy-1H-pyrrol-2(5H)-one (98a)

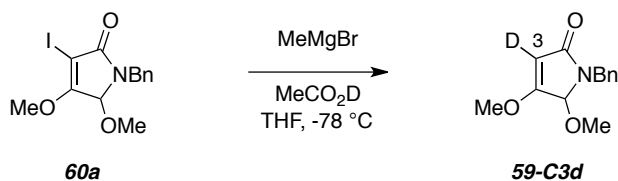
Preparation: A solution of **53d** (1 equiv) was dissolved in isopropanol (for 1 molar reaction) and treated with TMSCl (3 equiv) via syringe. The reaction was quenched with MeOH or water and the product extracted into EtOAc. MPLC (1:4 Hex:EtOAc) was performed to purify **98a**. Starting material I(10-30%) was also recovered .

¹H NMR (500 MHz, CDCl₃): δ 7.34-7.23 (m, 5H), 5.07 (s, 1H), 5.03 (d, *J* = 15.5 Hz, 1H), 4.96 (s, 1H), 4.01 (d, *J* = 15.3 Hz, 1H), 3.79 (s, 3H), 3.74 (q, *J* = 6.1 Hz, 1H), 1.17 (d, *J* = 6.2 Hz, 3H), and 1.12 (d, *J* = 6.1 Hz, 3H). [selpg250f3]

referenced to CDCl₃

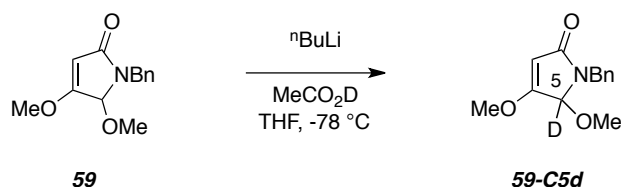
GCMS (5027016): R_t = 11.6 min, 261 (35, M⁺), 218(40), 203(50), 106(50), and 91(100).

TLC (1:2.5 Hex:EtOAc): R_f = 0.2



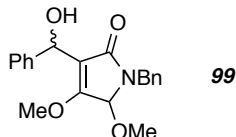
1-benzyl-4,5-dimethoxy-1H-pyrrol-2(5H)-one-C3d (59-C3d)

¹H NMR (500 MHz, CDCl₃): δ 7.34-7.28 (m, 5H), 5.05 (s, 1H), 4.95 (d, *J* = 15.2 Hz, 1H), 4.09 (d, *J* = 15.0 Hz, 1H), 3.89 (s, 3H), and 3.15 (s, 3H) [selpg281_concn]



1-benzyl-4,5-dimethoxy-1H-pyrrol-2(5H)-one-C5d (59-C5d)

¹H NMR (500 MHz, CDCl₃): δ 7.33-7.27 (m, 5H), 5.18 (s, 1H), 4.97 (d, *J* = 15.0 Hz), 4.03 (d, *J* = 15.0 Hz, 1H), 3.82 (s, 3H), and 3.11 (s, 3H). [seIpg249cr]



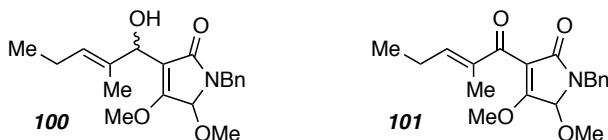
1-benzyl-3-(hydroxy(phenyl)methyl)-4,5-dimethoxy-1H-pyrrol-2(5H)-one (99)

Probably a mixture of two isomers here:

¹H NMR (500 MHz, CDCl₃): δ 7.46-7.24 (m, 20H), 5.75 (br s, 1H), 5.72 (br s, 1H), 5.22 (s, 2H), 4.97 (d, *J* = 14.9 Hz, 1H), 4.94 (d, *J* = 14.8 Hz, 1H), 4.91 (br d, *J* = 11 Hz, 1H), 4.58 (br d, *J* = 9.6 Hz, 1H), 4.02 (d, *J* = 15.4 Hz, 2H), 3.96 (s, 3H), 3.93 (s, 3H), 3.23 (s, 3H), and 3.03 (s, 3H). [seIpg284f3]

LCMS (isomer unknown): Method A, *R*_t = 17.6 min, *m/z* “pos” = 340.0 (M+1)⁺, 362.0 (M+23)⁺.

TLC (1:2 Hex:EtOAc): *R*_f = 0.2



(E)-1-benzyl-3-(1-hydroxy-2-methylpent-2-en-1-yl)-4,5-dimethoxy-1H-pyrrol-2(5H)-one (100)

One isomer:

¹H NMR (500 MHz, CDCl₃): δ 7.35-7.27 (m, 5H), 5.47 (ddpent, *J* = 7.1, 7.1, 1.5 Hz, 1H), 5.18 (s, 1H), 4.99 (br, d, *J* = 9.0 Hz, 1H), 4.97 (d, *J* = 14.9 Hz, 1H), 4.72 (d, *J* = 9.6 Hz, 1H), 3.99 (d, *J* = 14.9 Hz, 1H), 3.93 (s, 3H), 3.10 (s, 3H), 2.05 (app pent, *J* = 7.2 Hz, 2H), 1.68 (d, *J* = 1.1 Hz, 3H), and 0.96 (t, *J* = 7.5 Hz, 3H). [seIpg293f2]

Other isomer isolated:

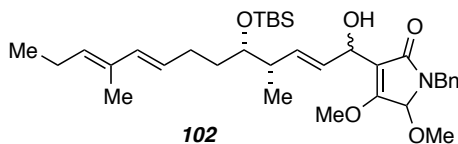
¹H NMR (500 MHz, CDCl₃): δ 7.35-7.27 (m, 5H), 5.42 (ddpent, *J* = 7.1, 7.1, 1.3 Hz, 1H), 5.20 (s, 1H), 5.02 (br d, *J* = 8.3 Hz, 1H), 4.98 (d, *J* = 14.9 Hz, 1H), 4.32 (br d, *J* = 9.5 Hz, 1H), 3.98 (d, *J* = 14.9 Hz, 1H), 3.94 (s, 3H), 3.11 (s, 3H), 2.05 (app pent, *J* = 7.5 Hz, 2H), 1.67 (d, *J* = 1.0 Hz, 3H), and 0.97 (t, *J* = 7.5 Hz, 3H). [selpg293f3]

LCMS (Both isomers): Method A, *R*_t = 15.9 min, *m/z* “pos” = 314.3 (M-17)⁺.

TLC (Both isomers, 1:1 Hex:EtOAc): *R*_f = 0.2

(E)-1-benzyl-4,5-dimethoxy-3-(2-methylpent-2-enoyl)-1H-pyrrol-2(5H)-one (101)

¹H NMR (500 MHz, CDCl₃): δ 7.34-7.27 (m, 5H), 6.54 (ddq, *J* = 7.2, 7.2, 1.4 Hz, 1H), 5.06 (s, 1H), 4.97 (d, *J* = 14.8 Hz, 1H), 4.02 (d, *J* = 14.8 Hz, 1H), 3.82 (s, 3H), 3.2 (s, 3H), 2.33 (app pent, *J* = 7.5 Hz, 2H), 1.89 (d, *J* = 1.1 Hz, 3H), and 1.08 (t, *J* = 7.5 Hz, 3H). [selpg295mplc]



1-benzyl-3-((2E,4S,5S,8E,10E)-5-((tert-butyldimethylsilyloxy)-1-hydroxy-4,10-dimethyltrideca-2,8,10-trien-1-yl)-4,5-dimethoxy-1H-pyrrol-2(5H)-one (102)

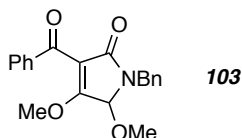
¹H NMR (500 MHz, CDCl₃): δ 7.34-7.25 (m, 5H), 6.02 (d, *J* = 15.6 Hz, 1H), 5.77-5.75 (m, 1H, overlaps with an impurity), 5.49 (ddd, *J* = 15.4, 6.9, 6.9 Hz, 1H), 5.36 (t, *J* = 7.5 Hz, 1H), 5.16-5.11 (m, 1H), 5.14 (s, 1H), 4.96 (d, *J* = 14.8 Hz, 1H), 4.27-4.19 (m, 1H), 3.98 (d, *J* = 14.9 Hz, 1H), 3.94 (s, 3H), 3.54 (ddd, *J* = 6.8, 4.6, 4.6 Hz, 1H), 3.06 (s, 3H), 2.40-2.35 (m, 1H), 2.19-2.08 (m, 1H), 2.12 (app pent, *J* = 7.4 Hz, 2H), 2.07-1.97 (m, 1H), 1.70 (s, 3H), 1.63-1.55 (m, 1H), 1.45-1.39 (m, 1H), 0.97 (t, *J* = 7.5 Hz, 3H), 0.95 (d, *J* = 6.8 Hz, 3H), 0.88 (s, 9H), and 0.04 (s, ~6H). [selpg65f4] was one isomer.

LCMS: Method B, *R*_t = 12.5 min, *m/z* “pos” = 566.3 (M-17)⁺, 606.3 (M+23)⁺.

TLC (2.5:1 Hex:EtOAc): *R*_f = 0.1

The minor stereoisomer could not be obtained in pure form. f5 has the other stereoisomer. Several isomers are observed by LCMS with the molecular ions detailed above.

[This structure is also supported by LCMS data on the corresponding ketone (oxidation product): Method B, $R_t = 12.7$ min, m/z “pos” = 582.3 (M+1)⁺, 604.3 (M+23)⁺; m/z “neg” = 580.3 (M-1)⁻].



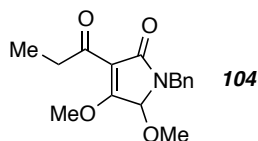
3-benzoyl-1-benzyl-4,5-dimethoxy-1H-pyrrol-2(5H)-one (103)

¹H NMR (500 MHz, CDCl₃): δ 7.92-7.88 (m, 2H), 7.52 (dddd, $J = 8.8, 6.8, 1.3, 1.3$ Hz, 1H), 7.36 (app t, $J = 7.8$ Hz, 3H), 7.25 (d, $J = 1.9$ Hz, 1H), 7.19 (d, $J = 2.0$ Hz, 1H), 7.17 (d, $J = 2.0$ Hz, 2H?), 5.32 (s, 1H), 4.61 (d, $J = 15.1$ Hz, 1H), 4.15 (d, $J = 15.1$ Hz, 1H), 3.80 (s, 3H), and 3.00 (s, 3H). [seIpg278f4] [seIpg262f2] also works

¹³C NMR (125 MHz, CDCl₃): δ 193.5, 171.1, 171.0, 137.3, 135.7, 133.3, 130.2, 129.3, 128.4, 128.1, 127.4, 96.7, 58.9, 51.0, and 43.4. (consider 97.8 also!, Ipg278f4C)

LCMS: Method A, $R_t = 15.5$ min, m/z “pos” = 338.0 (M+1)⁺, 360.0 (M+23)⁺; m/z “neg” = 336.0 (M-1)⁻.

TLC (1:2 Hex:EtOAc): $R_f = 0.3$

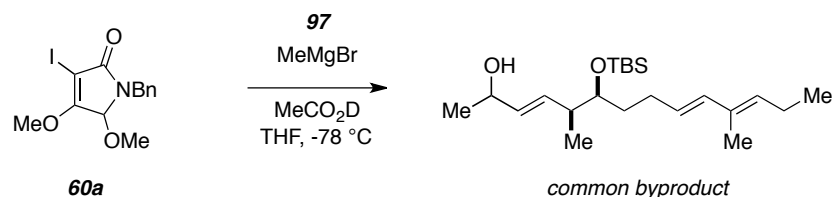


1-benzyl-4,5-dimethoxy-3-propionyl-1H-pyrrol-2(5H)-one (104)

¹H NMR (500 MHz, CDCl₃): δ 7.36-7.27 (m, 5H), 5.20 (s, 1H), 5.02 (d, $J = 14.8$ Hz, 1H), 4.08 (s, 3H), 4.00 (d, $J = 14.8$ Hz, 1H), 3.11 (s, 3H), 3.01 (dq, $J = 10.8, 7.2$ Hz, 1H), 2.95 (dq, $J = 10.9, 7.2$ Hz, 1H), and 1.11 (t, $J = 7.2$ Hz, 3H). [seIpg273f3]

LCMS: Method A, $R_t = 14.2$ min, m/z “pos” = 288.0 (M+1)⁺, m/z “neg” = 290.3.0 (M-1)⁻.

TLC (1:1 Hex:EtOAc): $R_f = 0.1$



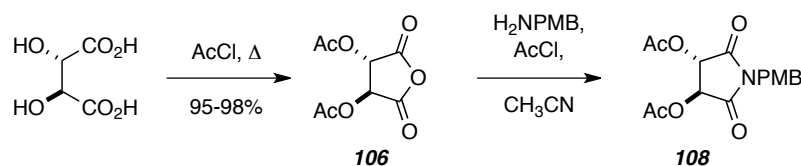
(3E,5S,6S,9E,11E)-6-((tert-butyldimethylsilyloxy)-5,11-dimethyltetradeca-3,9,11-trien-2-ol (common byproduct)

¹H NMR (500 MHz, CDCl₃): δ 6.04 (d, $J = 15.6$ Hz, 1H), 5.68 (dd, $J = 15.6, 7.0$ Hz, 1H), 5.65 (dd, $J = 15.6, 7.3$ Hz, 1H), 5.55-5.47 (m, 2H), 5.37 (t, $J = 7.2$ Hz, 1H), 4.28 (app pent, $J = 6.5$ Hz, 1H), 3.54 (ddd, $J = 6.6, 5.0, 5.0, 5.0$ Hz, 1H), 2.30 (app pent, $J = 6.8$, 1H), 2.20-1.99 (m, 3H), 2.12 (app pent, $J = 7.5$ Hz, 2H), 1.72 (s, 3H), 1.52-1.42 (m, 2H), 1.28 (d, $J = 6.3$ Hz, 3H), 0.98 (t, $J = 7.5$ Hz, 3H), 0.96 (d, $J = 6.8$ Hz, 3H), 0.90 (s, 9H), 0.05 (s, 3H), and 0.04 (s, 3H). [seIpg53f3]

LCMS: Method A, $R_t = 18.7$ min, m/z “pos” = 367.3 (M+1)⁺, 384.3 (M+18)⁺.

TLC (4:1 Hex:EtOAc): $R_f = 0.3$

[This structure is also supported by LCMS on the corresponding methyl ketone Method A, $R_t = 18.8$ min, m/z “pos” = 365.3 (M+1)⁺ (see **145**)]

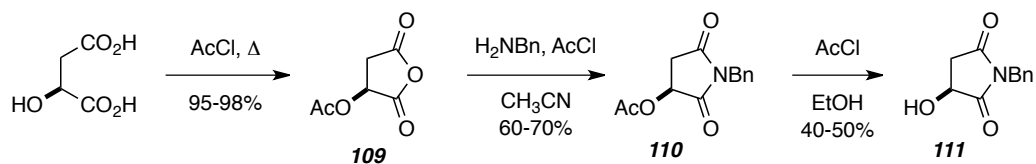


(3S,4S)-1-(4-methoxybenzyl)-2,5-dioxopyrrolidine-3,4-diyl diacetate (108)

¹H NMR (500 MHz, CDCl₃): δ 7.32 (d, $J = 8.6$ Hz, 2H), 6.85 (d, $J = 8.7$ Hz, 2H), 5.53 (s, 2H), 4.70 (d, $J = 14.1$ Hz, 1H), 4.65 (d, $J = 14.2$ Hz, 1H), 3.79 (s, 3H), and 2.19 (s, 6H). [seIpg89f4]

GCMS (5027016): $R_t = 12.8$ min, 335 (5, M⁺), 275 (10), 216(100), 121(20).

TLC (1:1 Hex:EtOAc): $R_f = 0.1$



(S)-2,5-dioxotetrahydrofuran-3-yl acetate (109)

¹H NMR (500 MHz, CDCl₃): δ 5.54 (dd, *J* = 9.6, 6.5 Hz, 1H), 3.39 (dd, *J* = 18.9, 9.6 Hz, 1H), 3.04 (dd, *J* = 18.9, 6.5 Hz, 1H), and 2.23 (s, 3H). [seIpg152cr]

(S)-1-benzyl-2,5-dioxopyrrolidin-3-yl acetate (110)

¹H NMR (500 MHz, CDCl₃): δ 7.40-7.38 (m, 2H), 7.35-7.30 (m, 3H), 5.45 (dd, *J* = 8.7, 4.8 Hz, 1H), 4.72 (d, *J* = 14.1 Hz, 1H), 4.68 (d, *J* = 14.1 Hz, 1H), 3.17 (dd, *J* = 18.3, 8.7 Hz, 1H), 2.67 (dd, *J* = 18.4, 4.8 Hz, 1H), and 2.16 (s, 3H). [seIpg153mplc]

GCMS (5027016): *R*_t = 10.9 min, 247 (1, M⁺), 187 (100), 132 (80), 91 (30).

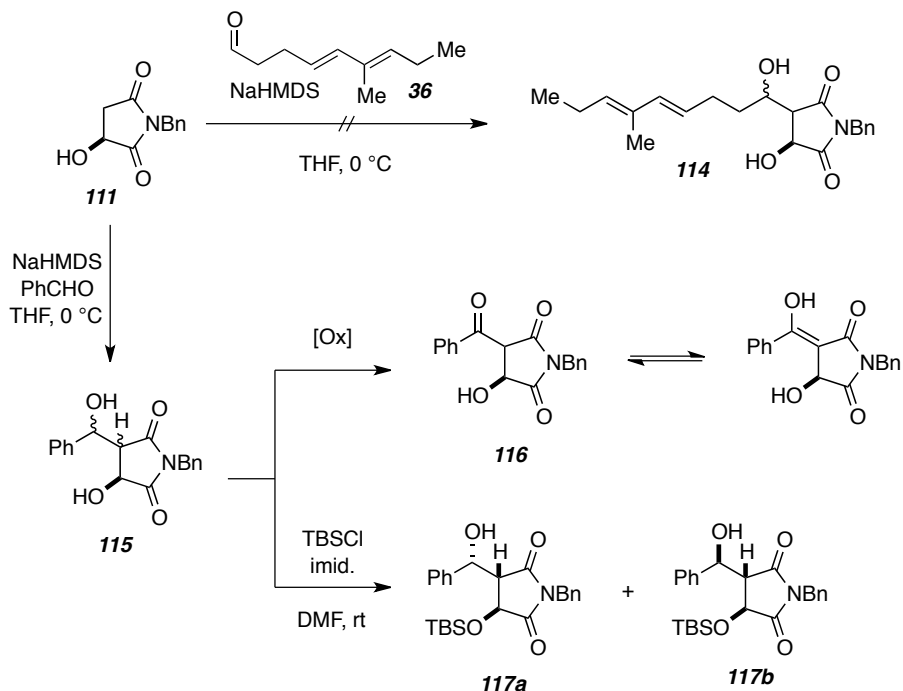
TLC (1:1 Hex:EtOAc): *R*_f = 0.1

(S)-1-benzyl-3-hydroxypyrrolidine-2,5-dione (111)

¹H NMR (500 MHz, CDCl₃): δ 7.40-7.28 (m, 5H), 4.67 (br s, 1H), 4.63 (ddd, *J* = 8.3, 5.1, 2.2 Hz, 1H), 3.08 (dd, *J* = 18.2, 8.4 Hz, 1H), 2.934 (d, *J* = 2.3 Hz, 1H), and 2.69 (dd, *J* = 18.2, 4.8 Hz, 1H). [seIpg154mplc]

GCMS (5027016): *R*_t = 10.2 min, 205 (M⁺, 100), 187(15), 148(20), 106(35), and 91(100).

TLC (1:4 Hex:EtOAc): *R*_f = 0.6



(3S)-1-benzyl-3-hydroxy-4-((4E,6E)-1-hydroxy-6-methylnona-4,6-dien-1-yl)pyrrolidine-2,5-dione (114)

¹H NMR (500 MHz, CDCl₃): δ 7.39-7.27 (m, 5H), 6.11 (d, *J* = 15.4 Hz, 1H), 5.54 (ddd, *J* = 15.2, 6.9, 6.9 Hz, 1H), 5.38 (t, *J* = 7.1 Hz, 1H), 4.74 (ddd, *J* = 3.4, 3.4, 2.3 Hz, 1H), 4.67 (overlapping singlets, 2H), 4.44-4.38 (m, 1H), 2.71 (dd, *J* = 5.2, 2.5 Hz, 1H), 2.31-2.02 (m, 2H), 2.12 (app pent, *J* = 7.4 Hz, 2H), 1.71 (d, *J* = 0.9 Hz, 3H), 1.47-1.34 (m, 2H), and 0.98 (t, *J* = 7.5 Hz, 3H). [seIpg181f2]

LCMS: Method B. Four peaks were observed in the “neg” because a mixture of 36 and 37 was used in this reaction. *R*_t = 11.3 min, 11.5 min, 11.9 min, 12.2 min *m/z* “neg” = 416 (M+59)⁻ in all cases. These structures were supported by the mono-TBS derivatives (as in 117) which ran slower (15.1 min) and *m/z* “neg” = 530 (M+59)⁻

TLC (2:1 Hex:EtOAc): *R*_f = 0.15

(3S,4S)-1-benzyl-3-hydroxy-4-((R)-hydroxy(phenyl)methyl)pyrrolidine-2,5-dione (115a, corresponds to 117a)

¹H NMR (500 MHz, CDCl₃): δ 7.41-7.28 (m, 10H), 5.57 (d *J* = 2.8 Hz, 1H), 4.78 (d, *J* = 4.9 Hz, 1H), 4.73 (d, *J* = 14.4 Hz, 1H), 4.68 (d, *J* = 14.4 Hz, 1H), 3.08 (dd, *J* = 4.9, 2.9 Hz, 1H), and 2.43 (br s, 1H). [seIpg175f2]

TLC (2:1 Hex:EtOAc): $R_f = 0.4$

(3S,4S)-1-benzyl-3-hydroxy-4-((S)-hydroxy(phenyl)methyl)pyrrolidine-2,5-dione (115b, corresponds to 117b)

$^1\text{H NMR}$ (500 MHz, CDCl_3): δ 7.39-7.27 (m, 10H), 5.14 (d, $J = 7.3$ Hz, 1H), 4.65 (d, $J = 14.3$ Hz, 1H), 4.61 (d, $J = 14.2$ Hz, 1H), 4.37 (d, $J = 5.4$ Hz, 1H), 3.19 (dd, $J = 7.2, 5.4$ Hz, 1H) and 2.61 (br s, 1H). [seIpg171c2_fl]

LCMS: Method B, one diastereomer: $R_t = 7.8$ min, m/z “neg” = 370 ($\text{M}+59$) $^-$, other diastereomer: $R_t = 8.9$ min, m/z “neg” = 356 ($\text{M}+\text{Cl}$) $^-$, 370 ($\text{M}+59$) $^-$.

TLC (2:1 Hex:EtOAc): $R_f = 0.4$

(3S,4S)-1-benzyl-3-((tert-butyldimethylsilyl)oxy)-4-((R)-hydroxy(phenyl)methyl)pyrrolidine-2,5-dione (117a)

$^1\text{H NMR}$ (500 MHz, CDCl_3): δ 7.40-7.27 (m, 10H), 5.51 (dd, $J = 4.6, 2.9$ Hz, 1H), 4.76 (d, $J = 14.4$ Hz, 1H), 4.67 (d, $J = 14.4$ Hz, 1H), 4.57 (d, $J = 3.3$ Hz, 1H), 3.04 (br t, $J = 3.2$ Hz, 1H), 2.23 (dd, $J = 4.6, 1.0$ Hz, 1H), 0.62 (s, 9H), 0.01 (s, 3H), and -0.28 (s, 3H). [seIpg176f2]

LCMS: Method B, $R_t = 14.25$ min, m/z “pos” = 426 ($\text{M}+1$) $^+$, “neg” = 484 ($\text{M}+59$) $^-$ for

TLC (8:1 Hex:EtOAc): $R_f = 0.2$

(3S,4S)-1-benzyl-3-((tert-butyldimethylsilyl)oxy)-4-((S)-hydroxy(phenyl)methyl)pyrrolidine-2,5-dione (117b)

$^1\text{H NMR}$ (500 MHz, CDCl_3): δ 7.39-7.17 (m, 10H), 5.02 (dd, $J = 7.2, 2.0$ Hz, 1H), 4.67 (d, $J = 14.1$ Hz, 1H), 4.59 (d, $J = 14.1$ Hz, 1H), 4.33 (d, $J = 4.0$ Hz, 1H), 3.15 (dd, $J = 7.1, 4.0$ Hz, 1H), 0.78 (s, 9H), 0.09 (s, 3H), and -0.13 (s, 3H). [seIpg177f2]

LCMS: Method B, $R_t = 14.28$ min, m/z “neg” = 484.0 ($\text{M}+59$) $^-$

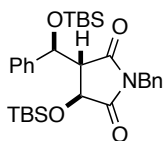
TLC (8:1 Hex:EtOAc): $R_f = 0.3$

(4S)-3-benzoyl-1-benzyl-4-hydroxypyrrolidine-2,5-dione (116)

¹H NMR (500 MHz, CDCl₃): δ 8.065 (d, *J* = 8.2 Hz, 1H), 8.062 (d, *J* = 8.6 Hz, 1H), 7.66 (ddt, *J* = 8.7, 6.9, 1.3, 1.3 Hz, 1H), 7.54 (d, *J* = 8.3 Hz, 1H), 7.53 (d, *J* = 8.2 Hz, 1H), 7.38-7.27 (m, 5H), 5.18 (d, *J* = 4.8 Hz, 1H), 4.70 (d, *J* = 14.0 Hz, 1H), 4.69 (d, *J* = 4.8 Hz, 1H), 4.64 (d, *J* = 14.1 Hz, 1H), 0.85 (s, 9H), 0.16 (s, 3H), and 0.05 (s, 3H).

[seIpg179cr]

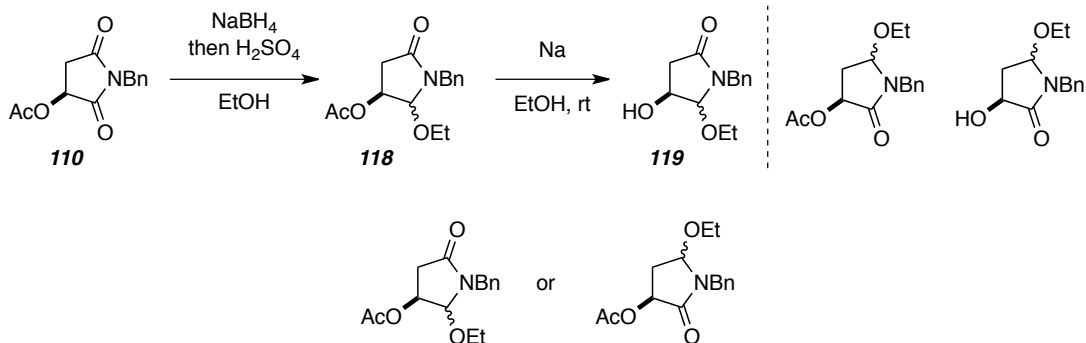
GCMS (5029021): *R*_t = 14.45 min, 309 (0, M⁺), 291(100), 158(10), 130(100), 102(60).



(3S)-1-benzyl-3-((tert-butyldimethylsilyloxy)(phenyl)methyl)pyrrolidine-2,5-dione (bis protected 115)

¹H NMR (500 MHz, CDCl₃): δ 7.39-7.17 (m, 10H), 5.34 (d, *J* = 3.5 Hz, 1H), 4.54 (d, *J* = 14.3 Hz, 1H), 4.48 (d, *J* = 14.1 Hz, 1H), 4.40 (d, *J* = 3.2 Hz, 1H), 3.08 (t, *J* = 3.3 Hz, 1H), 0.91 (s, 9H), 0.85 (s, 9H), 0.19 (s, 3H), 0.17 (s, 3H), 0.01 (s, 3H), and -0.05 (s, 3H).

[seIpg177f2]



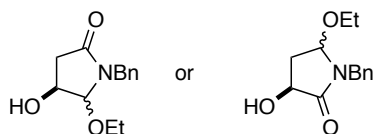
(3S)-1-benzyl-2-ethoxy-5-oxopyrrolidin-3-yl acetate (118)

¹H NMR (500 MHz, CDCl₃): δ 7.35-7.24 (m, 5H), 5.07 (d, *J* = 6.3 Hz, 1H), 5.00 (d, *J* = 15.1 Hz, 1H), 4.47 (s, 1H), 4.04 (d, *J* = 15.0 Hz, 1H), 3.65 (dq, *J* = 9.4, 7.0 Hz, 1H), 3.46 (dq, *J* = 9.3, 7.0 Hz, 1H), 2.96 (dd, *J* = 17.9, 6.4, 0.9 Hz, 1H), 2.41 (d, *J* = 17.9 Hz, 1H), 2.01 (s, 3H), and 1.18 (t, *J* = 7.0 Hz, 3H). [seIpg170f2]

GCMS (5027016): *R*_t = 11.16 min, 277 (10, M⁺), 232(10), 217(8), 189(10), 91(100),

There are two diastereomers by **GCMS** for **118**.

TLC (1:2 Hex:EtOAc): $R_f = 0.1$

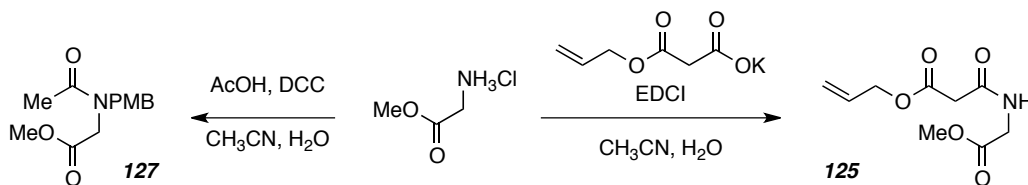


(4S)-1-benzyl-5-ethoxy-4-hydroxypyrrolidin-2-one (119)

$^1\text{H NMR}$ (500 MHz, CDCl_3): δ 7.35-7.23 (m, 5H), 4.98 (d, $J = 15.0$ Hz, 1H), 4.50 (s, 1H), 4.25 (br d, $J = 6.1$ Hz, 1H), 4.07 (d, $J = 15.1$ Hz, 1H), 3.53 (dq, $J = 9.2, 7.1$ Hz, 1H), 3.44 (dq, $J = 9.2, 7.0$ Hz, 1H), 2.90 (ddd, $J = 17.6, 6.3, 0.9$ Hz, 1H), 2.34 (dd, $J = 17.6, 1.4$ Hz, 1H), and 1.18 (t, $J = 7.0$ Hz, 3H). [seIIpg165mplc] see also IIpg174mplc very good lots of sample

GCMS (5027016): $R_t = 11.16$ min, 235 (15, M^+), 191(10), 118(10), 91 (100).

TLC (1:4 Hex:EtOAc): $R_f = 0.2$



allyl 3-((2-methoxy-2-oxoethyl)amino)-3-oxopropanoate (125)

$^1\text{H NMR}$ (500 MHz, CDCl_3): δ 7.60 (br s, 1H), 5.92 (dddd, $J = 16.4, 10.4, 5.9, 5.9$ Hz, 1H), 5.36 (dq, $J = 17.2, 1.6$ Hz, 1H), 5.28 (dq, $J = 10.4, 1.3$ Hz, 1H), 4.86 (dt, $J = 5.9, 1.4$ Hz, 2H), 4.09 (d, $J = 5.3$ Hz, 2H), 3.77 (s, 3H), and 3.4 (s, 2H). [seIIpg131cr]

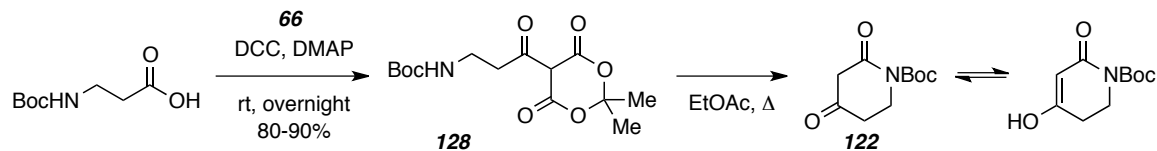
LCMS: Method A, $R_t = 11.5$ min., $m/z = 216$ ($\text{M}+1$) $^+$

methyl 2-(N-(4-methoxybenzyl)acetamido)acetate (127)

$^1\text{H NMR}$ (500 MHz, CDCl_3): δ (major rotamer) 7.12 (d, $J = 8.8$ Hz, 2H), 6.89 (d, $J = 8.7$ Hz, 2H), 4.56 (s, 2H), 4.03 (s, 2H), 3.81 (s, 3H), 3.71 (s, 3H), and 2.24 (s, 3H). δ (minor rotamer) 7.17 (d, $J = 8.7$ Hz, 2H), 6.85 (d, $J = 8.7$ Hz, 2H), 4.58 (s, 2H), 3.91 (s, 2H), 3.79 (s, 3H), 3.71 (s, 3H), and 2.11 (s, 3H). [seIVpg55_testfc18] about a 2:1 or 2.5:1 ratio of rotamers here.

LCMS (Method B): $T_R = 6.8$ min, m/z “pos” = 252 ($M+1$)⁺

TLC (1:4 Hex:EtOAc): $R_f = 0.25$



tert-butyl (3-(2,2-dimethyl-4,6-dioxo-1,3-dioxan-5-yl)-3-oxopropyl)carbamate (128)

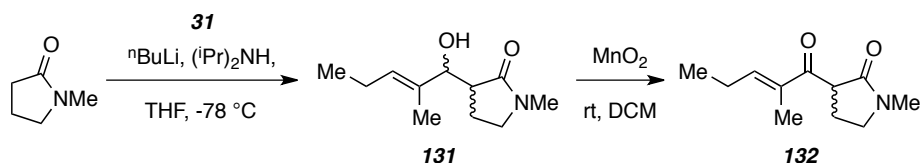
¹H NMR (500 MHz, CDCl₃): δ 5.12 (br s, 1H), 3.52 (br q, $J = 6.3$ Hz, 2H), 3.22 (t, $J = 6.3$ Hz, 2H), 1.71 (s, 6H), and 1.42 (br s, 9H). [seIIIpg137_ch1_14_10]

tert-butyl 4-hydroxy-2-oxo-5,6-dihydropyridine-1(2H)-carboxylate (122)

¹H NMR (500 MHz, DMSO-d₆): δ 4.94 (br s, 1H), 3.69 (t, $J = 6.5$ Hz, 2H), 2.42 (t, $J = 6.4$ Hz, 2H), and 1.42 (s, 9H). [seIIIpg136_crRECR]

LCMS: Method B, $R_t = 2.1$ min “neg” $m/z = 212$ ($M-1$)⁻; “pos” = 157 ($M-^t\text{Bu}$)⁺

[IIIpg168_TRP6]



(E)-3-(1-hydroxy-2-methylpent-2-en-1-yl)-1-methylpyrrolidin-2-one (131)

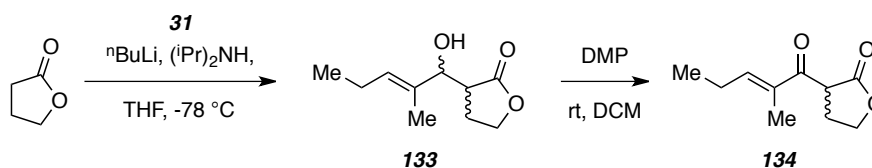
¹H NMR (500 MHz, CDCl₃): δ 5.42 (tq, $J = 7.1, 1.5$ Hz, 1H), 5.27 (s, 1H), 3.98 (d, $J = 10.1$ Hz, 1H), 3.32 (ddd, $J = 9.7, 9.7, 7.3$ Hz, 1H), 3.28 (ddd, $J = 9.7, 9.7, 2.4$ Hz, 1H), 2.87 (s, 3H), 2.58 (q, $J = 9.8$ Hz, 1H), 2.07 (pent, $J = 7.6$ Hz, 1H), 2.03 (pent, $J = 7.6$ Hz, 1H), 1.91 (dddd, $J = 13.3, 9.5, 7.3, 2.4$ Hz, 1H), 1.64 (s, 3H), 1.59 (dddd, $J = 13.2, 9.4, 9.4, 9.4$ Hz, 1H), and 0.96 (t, $J = 7.5$ Hz, 3H). [seIIIpg70f2]

LCMS: Method A, $R_t = 16.9$ min “pos” $m/z = 180.3$ ($M-17$)⁺, 198.3 ($M+1$)⁺.

TLC (1:1 Hex:EtOAc): $R_f = 0.1$

(E)-1-methyl-3-(2-methylpent-2-enoyl)pyrrolidin-2-one (132, keto form)

$^1\text{H NMR}$ (500 MHz, CDCl_3): δ 6.89 (tq, $J = 7.2, 1.0$ Hz, 1H), 4.25 (dd, $J = 9.3, 4.8$ Hz, 1H), 3.56 (ddd, $J = 8.9, 8.9, 6.3$ Hz, 1H), 3.34 (ddd, $J = 9.0, 9.0, 4.3$ Hz, 1H), 2.85 (s, 3H), 2.44 (ddd, $J = 13.0, 8.8, 4.6, 4.6$ Hz, 1H), 2.34 (pent, $J = 7.5$ Hz, 1H), 2.33 (pent, $J = 7.6$ Hz, 1H), 2.16 (dddd, $J = 12.8, 9.1, 9.1, 6.3$ Hz, 1H), 1.81 (s, 3H), and 1.12 (t, $J = 7.6$ Hz, 3H). [seIIIpg73cr]



(E)-3-(1-hydroxy-2-methylpent-2-en-1-yl)dihydrofuran-2(3H)-one (133)

One diastereomer:

$^1\text{H NMR}$ (500 MHz, CDCl_3): δ 5.47 (tq, $J = 7.1, 1.6$ Hz, 1H), 4.39 (ddd, $J = 9.0, 9.0, 2.1$ Hz, 1H), 4.22 (ddd, $J = 10.5, 9.1, 6.6$ Hz, 1H), 4.12 (d, $J = 1.1$ Hz, 1H), 4.09 (d, $J = 9.7$ Hz, 1H), 2.76 (ddd, $J = 11.3, 11.3, 9.3$ Hz, 1H), 2.12 (dddd, $J = 13.1, 8.9, 6.6, 2.1$ Hz, 1H), 2.07 (pent, $J = 7.3$ Hz, 1H), 2.05 (pent, $J = 7.2$ Hz, 1H), 1.90 (dddd, $J = 13.2, 10.9, 10.9, 8.8$ Hz, 1H), 1.66 (d, $J = 1.0$ Hz, 3H), and 0.97 (t, $J = 7.2$ Hz, 3H), [seIIIpg71f2]

LCMS (Method B): $T_R = 7.28$ min, m/z "pos" = 167.3 (M-17) $^+$ and 202.3 (M+18) $^+$.

TLC (3:1 Hex:EtOAc): $R_f = 0.15$

Another diastereomer:

$^1\text{H NMR}$ (500 MHz, CDCl_3): δ 5.57 (tpent, $J = 7.2, 1.4$ Hz, 1H), 4.58 (br s, 1H), 4.37 (ddd, $J = 8.8, 8.8, 4.0$ Hz, 1H), 4.23 (ddd, $J = 8.6, 8.6, 8.6$ Hz, 1H), 4.12 (br s, 1H), 4.10 (d, $J = 9.6$ Hz, 1H), 2.81 (ddd, $J = 9.3, 9.3, 2.9$ Hz, 1H), 2.33 (dq, $J = 12.9, 8.8$ Hz, 1H), (taken from above):) 2.12 (dddd $J = 13.1, 8.9, 6.6, 2.1$ Hz, 1H), 2.07 (pent, $J = 7.3$ Hz, 1H), 2.05 (pent, $J = 7.2$ Hz, 1H), 1.96 (br d, $J = 3.9$ Hz, 1H), 1.90 (dddd, $J = 13.2, 10.9, 10.9, 8.8$ Hz, 1H), 1.61 (br s, 3H), and 0.98 (t, $J = 7.5$ Hz, 3H). [seIIIpg71f4]

LCMS (Method B): $T_R = 7.72$ min, m/z "pos" = 167.3 (M-17) $^+$ and 202.3 (M+18) $^+$

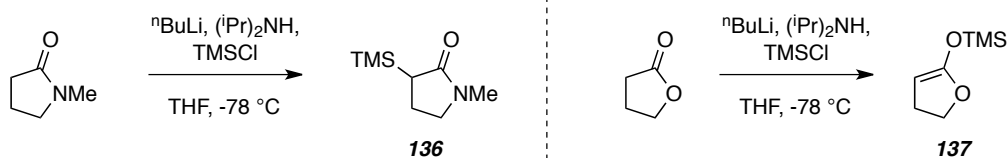
(could be reversed with its diastereomer)

TLC (3:1 Hex:EtOAc): $R_f = 0.15$

(E)-3-(2-methylpent-2-enoyl)dihydrofuran-2(3H)-one (134)

$^1\text{H NMR}$ (500 MHz, CDCl_3): δ 6.86 (tq, $J = 7.2, 1.4$ Hz, 1H), 4.47 (ddd, $J = 8.7, 7.3, 7.3$ Hz, 1H), 4.37 (ddd, $J = 8.4, 8.4, 5.3$ Hz, 1H), 4.33 (dd, $J = 9.3, 5.5$ Hz, 1H), 2.71 (dddd, $J = 13.1, 7.8, 5.4, 5.4$ Hz, 1H), 2.40 (dddd, $J = 12.9, 9.2, 8.3, 7.1$ Hz, 1H), 2.36 (pent, $J = 7.6$ Hz, 1H), 2.35 (pent, $J = 7.6$ Hz, 1H), 1.83 (d, $J = 1.1$ Hz, 3H), and 1.13 (t, $J = 7.6$ Hz, 3H). [seIIIpg75cr] also looks to be in the enol form here from 5 H's on ring.

TLC (1:1 Hex:EtOAc): $R_f = 0.5$



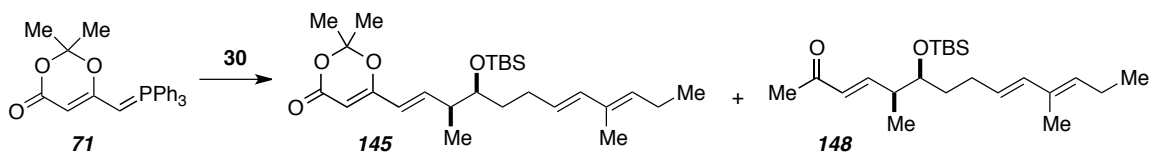
1-methyl-3-(trimethylsilyl)pyrrolidin-2-one (136)

$^1\text{H NMR}$ (500 MHz, CDCl_3): δ 3.34 (ddd, $J = 9.4, 9.4, 4.3$ Hz, 1H), 3.30 (dd, $J = 8.2, 7.2$ Hz, 1H), 2.81 (d, $J = 0.7$ Hz, 3H), 2.21 (ddd, $J = 12.2, 9.9, 5.0$ Hz, 1H), 1.96 (br dd, $J = 10.2, 4.8$ Hz, 1H), 1.91 (ddd, $J = 12.5, 8.4, 4.0$ Hz, 1H), and 0.11 (s, 9H). [seIIIpg88cr]

((4,5-dihydrofuran-2-yl)oxy)trimethylsilane (137)

$^1\text{H NMR}$ (500 MHz, CDCl_3): δ 4.29 (dd, $J = 9, 8$ Hz, 2H), 3.68 (t, $J = 2.2$ Hz, 1H), 2.63 (dt, $J = 2.2, 9.0$ Hz, 2H) and 0.27 (s, 9H). (referenced to CHCl_3) [seIIIpg95d3]

Experiments (Chapter II.C.)



6-((1E,3S,4S,7E,9E)-4-((tert-butyldimethylsilyl)oxy)-3,9-dimethyldodeca-1,7,9-trien-1-yl)-2,2-dimethyl-4H-1,3-dioxin-4-one (145)

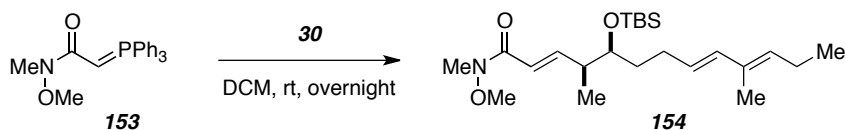
¹H NMR (500 MHz, CDCl₃): δ 6.63 (dd, *J* = 15.7, 7.4 Hz, 1H), 6.05 (d, *J* = 15.6 Hz, 1H), 5.88 (dd, *J* = 15.7, 1.2 Hz, 1H), 5.51 (ddd, *J* = 15.6, 6.9, 6.9 Hz, 1H), 5.38 (t, *J* = 7.5 Hz, 1H), 5.25 (s, 1H), 3.67-3.61 (m, 1H), 2.50-2.43 (m, 1H), 2.18-2.00 (m, 2H), 2.13 (app pent, *J* = 7.5 Hz, 2H), 1.72 (s, 3H), 1.71 (s, 3H), 1.70 (s, 3H), 1.65-1.54 (m, 2H), 1.06 (d, *J* = 6.9 Hz, 3H), 0.98 (t, *J* = 7.5 Hz, 3H), 0.89 (s, 9H), 0.05 (s, 3H), and 0.04 (s, 3H). [seIVpg106recre]

(3E,5S,6S,9E,11E)-6-((tert-butyldimethylsilyl)oxy)-5,11-dimethyltetradeca-3,9,11-trien-2-one (148)

¹H NMR (500 MHz, CDCl₃): δ 6.88 (dd, *J* = 16.2, 6.9 Hz, 1H), 6.05 (app dd, *J* = 16.2, 1.2 Hz, 2H), 5.51 (ddd, *J* = 15.6, 6.9, 6.9 Hz, 1H), 5.38 (t, *J* = 7.4 Hz, 1H), 3.67 (ddd, *J* = 7.1, 4.7, 4.7 Hz, 1H), 2.51 (ddq, *J* = 4.5, 1.6, 6.8 Hz, 1H), 2.26 (s, 3H), 2.24-2.01 (m, 2H), 2.12 (app pent, *J* = 7.5 Hz, 2H), 1.71 (d, *J* = 0.9 Hz, 3H), 1.56-1.50 (m, 1H), 1.43 (dddd, *J* = 13.0, 10.3, 7.3, 5.6 Hz, 1H), 1.04 (d, *J* = 6.9 Hz, 3H), 0.98 (t, *J* = 7.5 Hz, 3H), 0.90 (s, 9H), 0.07 (s, 3H), and 0.05 (s, 3H). [seIIpg54cr]

LCMS (Method A): T_R = 18.6 min, m/z “pos” = 365.3 (M+1)⁺

TLC (4:1 Hex:EtOAc): R_f = 0.2



(2E,4S,5S,8E,10E)-5-((tert-butyldimethylsilyl)oxy)-N-methoxy-N,4,10-trimethyltrideca-2,8,10-trienamide (154)

¹H NMR (500 MHz, CDCl₃): δ 7.00 (dd, *J* = 15.6, 7.6 Hz, 1H), 6.39 (dd, *J* = 15.8, 1.4 Hz, 1H), 6.04 (dq, *J* = 15.6, 1.5 Hz, 1H), 5.51 (ddd, *J* = 15.7, 6.9, 6.9 Hz, 1H), 5.36 (t, *J* = 7.2 Hz), 3.69 (s, 3H), 3.64 (ddd, *J* = 6.5, 4.9, 4.9 Hz, 1H), 3.24 (s, 3H), 2.52 (br sextet, *J* = 6.7 Hz, 1H), 2.12 (pent, *J* = 7.3 Hz, 2H), 2.20-2.01 (m, 2H), 1.71 (s, 3H), 1.56-1.47

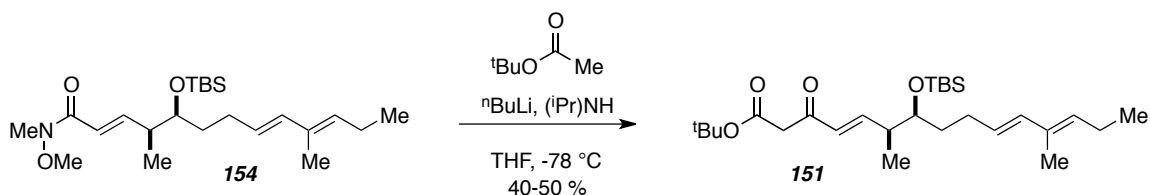
(m, 2H), 1.05 (d, $J = 6.8$ Hz, 3H), 0.98 (t, $J = 7.5$ Hz, 3H), 0.90 (s, 9H), and 0.05 (s, 6H).

[seIIIpg113mplc1]

^{13}C NMR (125 MHz, CDCl_3): δ 167.1, 150.4, 135.1, 133.0, 132.6, 127.1, 118.4, 75.3, 61.8, 42.2, 34.2, 28.8, 26.2, 26.0, 21.5, 18.3, 15.0, 14.4, 12.4, -4.1, and -4.2.

LCMS: Method B, $R_t = 15.1$ min, $m/z = 410$ ($M + 1$)⁺ [IIIpg169_cr]

TLC (4:1 Hex:EtOAc): $R_f = 0.2$



(4E,6S,7S,10E,12E)-tert-butyl 7-((tert-butyldimethylsilyl)oxy)-6,12-dimethyl-3-oxopentadeca-4,10,12-trienoate (151)

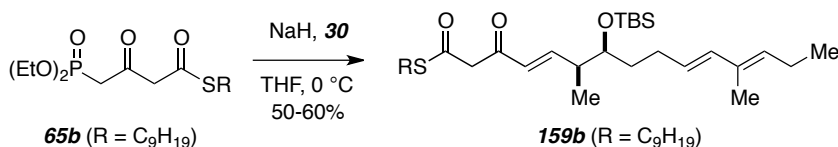
Probably the enol?

^1H NMR (500 MHz, CDCl_3): δ 6.63 (dd, $J = 15.7, 7.6$ Hz, 1H), 6.04 (d, $J = 15.5$ Hz, 1H), 5.73 (ddd, $J = 15.6, 1.5, 1.5$ Hz, 1H), 5.58-5.46 (m, 2H), 5.37 (t, $J = 7.2$ Hz, 1H), 4.90 (s, 1H), 3.65 (ddd, $J = 7.1, 4.7, 4.7$ Hz, 1H), 2.55-2.37 (m, 1H), 2.19-1.99 (m, 2H), 2.12 (app pent, $J = 7.5$ Hz, 2H), 1.71 (s, 3H), 1.49-1.42 (m, 2H), 1.04 (d, $J = 6.9$ Hz, 3H), 0.98 (t, $J = 7.5$ Hz, 3H), 0.902 (s, 9H), 0.895 (s, 9H), 0.06 (s, 3H), and 0.04 (s, 3H).

[seIVpg89_mplcchk]

LCMS (Method B): $T_R = 17.5$ min, m/z "pos" = 496.3($M+1$)⁺, m/z "neg" = 463.3($M-1$)⁻,

TLC (10:1 Hex:EtOAc): $R_f = 0.4$



(4E,6S,7S,10E,12E)-S-(2-methyloctan-2-yl) 7-((tert-butyldimethylsilyl)oxy)-6,12-dimethyl-3-oxopentadeca-4,10,12-trienethioate (159b)

Preparation:

NaH (12 equiv, 60% dispersion in mineral oil) was measured into an oven-dried round bottom flask and placed under an atmosphere of N₂. THF was added via syringe and the suspension cooled to 0 °C. A solution of the phosphonate thioester (6 equiv) in THF was then added and stirred for 60 minutes, when a solution of the aldehyde (1 equiv) was added and the flask allowed to warm to rt. When TLC indication complete consumption of the aldehyde, the reaction was worked up as follows. Saturated NH₄Cl was added, the layers separated, and the aqueous extracted with two portions of Et₂O. The combined organic layers were dried over Na₂SO₄ and concentrated to give the crude product as a pale yellow oil. MPLC (2x, 1:2 Hexanes:EtOAc then 20:1 Hexanes:EtOAc) separated the unreacted phosphonate and triene product. Typical yield were 60-70%.

¹H NMR (500 MHz, CDCl₃): δ 12.61-12.51 (m, various enol protons), 6.75-6.69 (m, 1H), 6.04 (d, *J* = 15.6 Hz, 1H), 5.66 (d, *J* = 15.6 Hz, 1H), 5.51 (ddd, *J* = 15.5, 6.9, 6.9 Hz, 1H), 5.37 (t, *J* = 7.2 Hz, 1H), 5.34, 5.32 (various enol form d, *J* = 1.7 Hz), 3.71 (s, 2H), 3.61 (appq, *J* = 5.2 Hz, 1H), 2.44 (sextet, *J* = 6.4, 1H), 2.18-2.00 (m, 4H), 1.71 (s, 3H), 1.53-1.41 (m, 4H), 1.38-1.17 (m, 8H), 1.01 (d, *J* = 6.8 Hz, 3H), 0.98 (t, *J* = 7.5 Hz, 3H), 0.94 (t, *J* = 6.8 Hz, 3H), 0.89 (s, 9H), 0.87 (s, 6H), 0.05 (s, 3H), and 0.03 (s, 3H)
seVpg153redol1f2 or seVpg177mplcf2

ESI-MS: Exact Mass calc. for [C₃₂H₅₈O₃SSiNa]⁺, 573.3768, found 573.3781.

(4E,6S,7S,10E,12E)-S-tert-butyl 7-((tert-butyldimethylsilyloxy)-6,12-dimethyl-3-oxopentadeca-4,10,12-trienethioate (157a, R = C₉H₁₉)

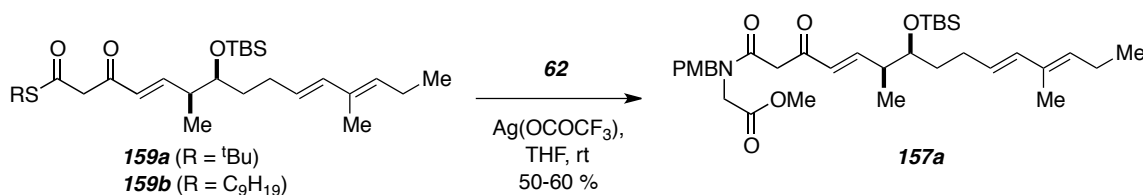
¹H NMR (500 MHz, CDCl₃): δ 12.59 (d, *J* = 1.4 Hz, 1H), 6.73 (dd, *J* = 15.6, 7.5 Hz, 1H), 6.04 (d, *J* = 15.6 Hz, 1H), 5.66 (ddd, *J* = 15.7, 1.5, 1.5 Hz, 1H), 5.51 (ddd, *J* = 15.5, 6.8, 6.8 Hz, 1H), 5.37 (br t, *J* = 7.2 Hz, 1H), 5.32 (s, 1H), 3.61 (ddd, *J* = 6.4, 6.4, 4.8 Hz, 1H), 2.45 (br sextet, *J* = 6.7 Hz, 1H), 2.12 (pent, *J* = 7.5 Hz, 2H), 2.21-1.99 (m, 2H), 1.71 (s, 3H), 1.54-1.47 (m, 1H), 1.52 (s, 9H), 1.32-1.25 (m, 1H), 1.01 (d, *J* = 6.8 Hz, 3H), 0.98 (t, *J* = 7.5 Hz, 3H), 0.89 (s, 9H), 0.05 (s, 3H), and 0.03 (s, 3H). (reported for the main tautomeric form, seVpg64mplc).

^{13}C NMR (125 MHz, CDCl_3): δ (mixture of tautomers) 196.5, 166.9, 152.9, 145.2, 135.4, 135.2, 133.03, 133.0, 132.9, 132.7, 129.4, 127.1, 126.8, 123.9, 100.6, 75.4, 75.1, 56.1, 48.4, 42.4, 42.3, 34.3, 34.0, 30.44, 30.38, 29.9, 29.84, 29.79, 29.1, 29.0, 26.1, 26.03, 25.98, 21.6, 18.3, 14.7, 14.38, 14.36, 14.35, 12.49, 12.47, -4.09, -4.13, and -4.19.

[seVIpg74_Vpg64C]

LCMS: Method B, $R_t = 19.6$ min, “pos” $m/z = 481.2 (M + 1)^+$, $503.0 (M+23)^+$, “neg” = $479.3 (M-1)^-$.

TLC (20:1 Hex:EtOAc): $R_f = 0.2$



Methyl 2-((4E,6S,7S,10E,12E)-7-((tert-butyldimethylsilyloxy)-N-(4-methoxybenzyl)-6,12-dimethyl-3-oxopentadeca-4,10,12-trienamido)acetate (157a**)**

Preparation:

An oven dried culture tube was cooled under N_2 and to it was added the thioester triene (1 equiv), amine (1.3 equiv), and THF to a concentration of typically 0.2 M. Crushed molecular sieves were added and the mixture was rapidly stirred. Meanwhile, a solution of $\text{Ag}(\text{OCOCF}_3)$ was prepared by measuring the solid salt into a test tube and adding approximately 1 mL dry THF. This solution was added dropwise to the reaction mixture. Within 5 minutes, the mixture turned a dark orange color and TLC indicated the reaction was completed. The entire mixture was passed through a pipette of Celite and diluted with Et_2O , washed with saturated NaHCO_3 , dried and concentrated. The residue was purified by MPLC (8:1 Hexanes:EtOAc), yielding the amide as an orange oil (typically 50-60%).

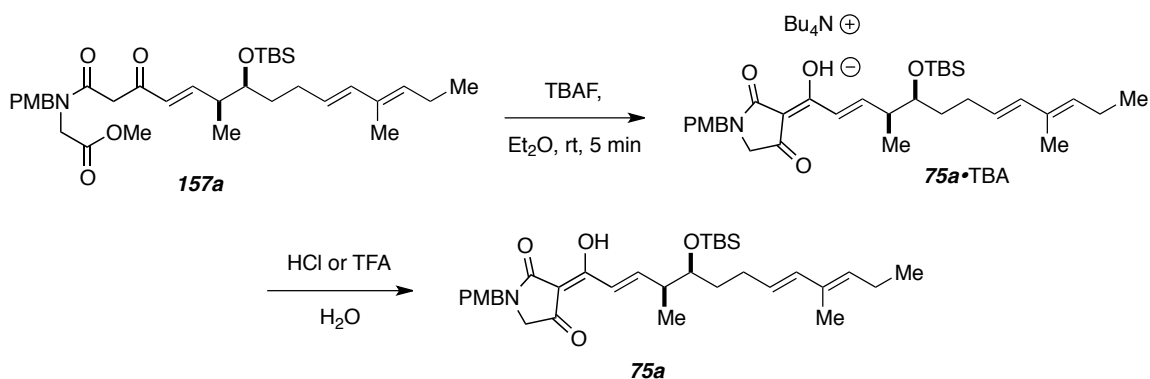
^1H NMR (500 MHz, CDCl_3): δ 14.03 (s, enolic H), 7.14 (d, $H=8.6$ Hz, 2H), 6.89 (d, $J = 8.6$ Hz, 2H), 6.04 (d, $J = 15.6$ Hz, 1H), 5.75 (d, $J = 15.6$ Hz, 1H), 5.51 (ddd, $J = 14.4$, 7.0, 7.0 Hz, 1H), 5.37 (t, $J = 7.2$ Hz, 1H), 5.26 (s, enol H, 1H), 4.58-4.50 (m, 2H), 4.10 (d, $J = 17.2$ Hz, 1H), 4.04 (d, $J = 17.2$ Hz, 1H), 3.81 (s, 3H), 3.80 (appq, $J = 5.4$ Hz, 1H),

3.73 (s, 3H), 3.70 (d, $J = 10.2$ Hz, 1H), 3.69 (d, $J = 10.2$ Hz, 1H), 3.61 (appq, $J = 5.4$ Hz, 1H), 2.43 (sextet, $J = 5.9$ Hz, 1H), 2.16-2.08 (m, 1H), 2.11 (pent, $J = 7.4$ Hz, 2H), 2.08-2.01 (m, 1H), 1.71 (s, 3H), 1.53-1.47 (m, 2H), 1.01, (d, $J = 6.9$ Hz, 3H), 0.98 (t, $J = 7.5$ Hz, 3H), 0.88 (s, 9H), 0.04 (s, 3H), and 0.03 (s, 3H). seVpg155pc4 or seVIpg36f3dp

ESI-MS: Exact Mass calc. for $[C_{34}H_{53}NO_6SiNa]^+$, 622.3534, found 622.3558.

LCMS: Method C, $R_t = 6.7$ min, m/z "pos" = 582.3 $(M-17)^+$, 600.3 $(M+1)^+$, m/z "neg" = 634.3 $(M+35)^-$, 658.3 $(M+59)^-$.

TLC (4:1 Hex:EtOAc): $R_f = 0.2$



(Z)-3-((2E,4S,5S,8E,10E)-5-((tert-butyldimethylsilyl)oxy)-1-hydroxy-4,10-dimethyltrideca-2,8,10-trien-1-ylidene)-1-(4-methoxybenzyl)pyrrolidine-2,4-dione (75a•TBA)

In a typical experiment, the amide was taken up in THF (for about 0.2 M) and a solution of TBAF (1M in THF, 2 equiv.) was added dropwise. A precipitate (or in most cases, a ring of an orange oil was formed on the stir bar and sides of the culture tube) was observed within a few minutes (but often was stirred as long as overnight) and the reaction mixture was then concentrated under reduced pressure to give the tetramate-ammonium salt as a viscous orange oil.

1H NMR (500 MHz, $CDCl_3$): δ 7.74 (d, $J = 15.6$ Hz, 1H), 7.16 (d, $J = 8.6$ Hz, 2H), 6.80 (d, $J = 8.6$ Hz, 2H), 6.74 (dd, $J = 15.5, 7.4$ Hz, 1H), 6.02 (d, $J = 15.6$ Hz, 1H), 5.51 (ddd, $J = 14.2, 6.9$ Hz, 1H), 5.35 (t, $J = 7.0$, 1H), 4.51 (app d, $J = 14.8$ Hz, 1H), 4.47 (app d, $J = 14.8$ Hz, 1H), 3.77 (s, 3H), 3.71 (appq, $J = 8.4$ Hz, 1H), 3.35 (s, 2H), 2.53-2.49 (m,

1H), 2.20-2.03, m, 4H), 1.70 (s, 3H), 1.52-1.48 (m, 1H), 1.32-1.26 (m, 1H), 1.05 (d, $J = 6.8$ Hz, 3H), 0.97 (t, $J = 7.5$ Hz, 3H), 0.90 (s, 9H), 0.06 (s, 3H), and 0.04 (s, 3H).

Various TBAF peaks were found to complicate the analysis of this compound (3.29, 1.63, 1.43, 0.99) and of the ion pair. [seVIpg37ov]

(Z)-3-((2E,4S,5S,8E,10E)-5-((tert-butyl dimethylsilyl)oxy)-1-hydroxy-4,10-dimethyltrideca-2,8,10-trien-1-ylidene)-1-(4-methoxybenzyl)pyrrolidine-2,4-dione (75a)

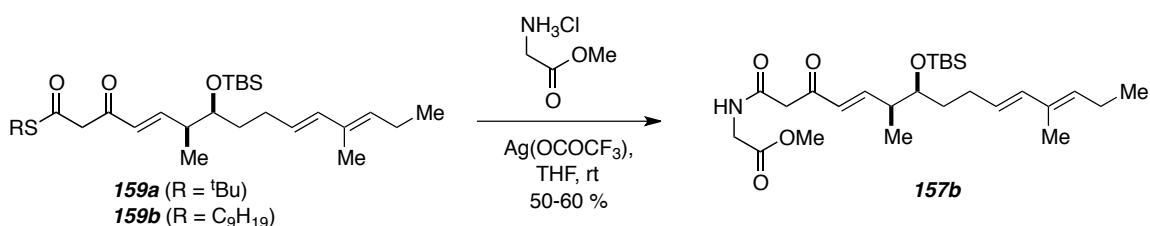
The crude orange oil was dissolved in deionized water and the solution acidified with dropwise addition of HCl (TFA was also used for this protonation reaction) until the pH of the water was ~ 2 . At this point a brown precipitate was usually observed. The water was drawn off with a pipette, leaving the precipitate as the crude product. Additional product could be obtained by extraction of the aqueous phase with ethyl acetate, drying the organic layer over Na_2SO_4 and concentrated to give an oil with the same spectroscopic data as that observed for the originally acquired solid.

$^1\text{H NMR}$ (500 MHz, CDCl_3): δ 7.25 (dd, $J = 15.9, 7.4$ Hz, 1H), 7.10 (dd, $J = 15.9, 1.3$ Hz, 1H), 6.05 (d, $J = 15.8$ Hz, 1H), 5.51 (ddd, $J = 15.6, 7.2, 7.2$ Hz, 1H), 5.37 (t, $J = 6.3$ Hz, 1H), 4.58 (d, $J = 12.1$ Hz, 1H), 4.54 (d, $J = 12.1$ Hz, 1H), 3.80 (s, 3H), 3.70-3.66 (m, 1 Hz), 3.59 (s, 2H), 2.60 (app sextet, $J = 6.7$ Hz, 1H), 2.21-2.00 (m, 4H), 1.71 (s, 3H), 1.59-1.43 (m, 2H), 1.08 (d, $J = 6.8$ Hz, 3H), 0.97 (t, $J = 7.5$ Hz, 3H), 0.90 (s, 9H), 0.06 (s, 3H), and 0.05 (s, 3H).

seVIpg42ppt? and also VIpg42pptH series (VIpg42pptH1, VIpg42pptH6 (think I took the same tube, twice to NMR)

LCMS (Method C): $T_R = 6.1$ min, m/z "pos" = 568 ($M+1$)⁺, m/z "neg" = 566 ($M-1$)⁻,

TLC (4:1 Hex:EtOAc): $R_f = 0.1$



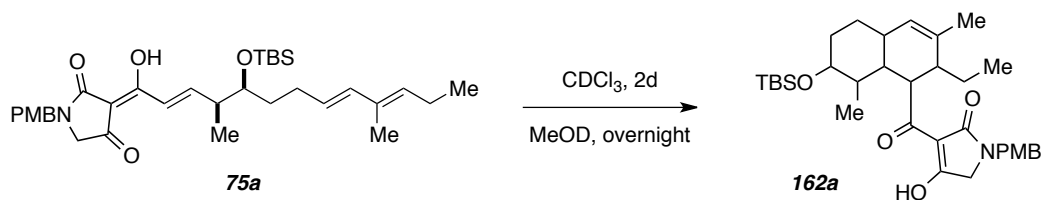
methyl 2-((4E,6S,7S,10E,12E)-7-((tert-butyldimethylsilyl)oxy)-6,12-dimethyl-3-oxopentadeca-4,10,12-trienamido)acetate (157b)

$^1\text{H NMR}$ (500 MHz, CDCl_3): δ 7.73 (bs, 1H), 7.05 (dd, $J = 16.1, 6.9$ Hz, 1H), 6.13 (dd, $J = 16.1, 1.3$ Hz, 1H), 6.05 (d, $J = 15.5$ Hz, 1H), 5.50 (ddd, $J = 15.5, 6.9, 6.9$ Hz, 1H), 5.38 (t, $J = 6.9$ Hz, 1H), 4.08 (d, $J = 5.4$ Hz, 2H), 3.96 (s, 3H), 3.76 (s, 2H), 3.67 (ddd, $J = 9.1, 4.6, 4.6$ Hz, 1H), 2.54 (dq, $J = 4.4, 1.3$ Hz, 1H), 2.12 (quint, $J = 7.6$ Hz, 1H), 2.19-2.00 (m, 2H), 1.71 (s, 3H), 1.56-1.49 (m, 1H), 1.45-1.38 (m, 1H), 1.05 (d, $J = 6.8$ Hz, 3H), 0.99 (t, $J = 8.5$ Hz, 3H), 0.90 (s, 9H), 0.06 (s, 3H), and 0.04 (s, 3H). seVpg111 (stuff)

LCMS (of ocatlin pdt of IMDA): Method C: $T_R = 5.9$ min, m/z "pos" = 480 ($M+1$) $^+$, m/z "neg" = 478 ($M-1$) $^-$

Structure additionally supported by **LCMS** (Method C): $T_R = 5.8$ min, m/z "pos" = 366 ($M+1$) $^+$, m/z "neg" = 364 ($M-1$) $^-$ of the deprotected variant.

TLC (1:2 Hex:EtOAc): $R_f = 0.4$



3-(7-((tert-butyldimethylsilyl)oxy)-2-ethyl-3,8-dimethyl-1,2,4a,5,6,7,8,8a-octahydronaphthalene-1-carbonyl)-4-hydroxy-1-(4-methoxybenzyl)-1H-pyrrol-2(5H)-one (162a).

Octalin **162a** was commonly observed upon storage of **75a** under ambient conditions. Quantities were also gathered from NMR samples of **75a** in various solvents (CDCl_3 , or MeOH-d_4 , or C_6D_6). These were typically concentrated under reduced pressure and loaded onto the MPLC (4:1 Hex:EtOAc) for separation of the major isomer (tentatively assigned the configuration of *endo*-I) and the minor (assigned the relative configuration of *endo*-II)

$^1\text{H NMR}$ (500 MHz, CDCl_3): δ 7.19 (d, $J = 8.7$ Hz, 2H, aromatic), 6.88 (d, $J = 8.7$ Hz, 2H, aromatic), 5.49 (br sextet, $J = 1.4$ Hz, H14), 4.55 (d, $J = 14.6$ Hz, benzylic), 4.51 (d, $J = 14.7$ Hz, benzylic), 3.82 (t, $J = 6.7$ Hz, H7), 3.81 (s, 3H, -OMe), 3.60 (d, $J = 17.4$ Hz,

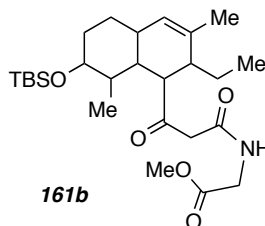
H2a), 3.56 (d, $J = 17.4$ Hz, H2b), 3.12 (ddd, $J = 10.6, 9.2, 4.4$ Hz, H10), 2.25 (br q, $J = 6.4$ Hz, H16), 1.95 (dq, $J = 12.9, 3.3$ Hz, H12eq), 1.89 (dq, $J = 12.3, 3$ Hz, H11eq), 1.76 (s, 3H, Me36), 1.71 (br t, $J = 10$ Hz, H13), 1.51 (app pent, $J = 7.2$ Hz, H17a), 1.47-1.22 (m, 5H, H8, H9, H11ax, H12ax, H17b), 0.93 (t, $J = 7.4$ Hz, Me18), 0.90 (d, $J = 6.4$ Hz, 3H, Me37), 0.87 (s, 9H, ^tBu), 0.03 (s, 3H, SiMe), and 0.01 (s, 3H, SiMe).

[seVIpg60IImain] Note also that within the multiplet δ 1.47-1.22 ppm, COSY analysis indicated that the order of those resonances is something like: H9/H11ax, H17b, H12ax, H8.

¹³C NMR (125 MHz, CDCl₃): δ 192.0, 191.4, 173.7, 159.7, 138.2, 130.0, 129.9, 127.4, 114.6, 102.6, (77.1), 55.5, 55.1, 49.5, 46.7, 46.2, 45.2, 43.7, 39.7, 35.8, 30.1, 26.1, 21.8, 19.6, 18.3, 16.1, 13.9, -3.7, -4.5. [seVIpg60commajC]

LCMS: Method C, $R_t = 7.4$ min, m/z "pos" = 568.3 (M+1)⁺, m/z "neg" = 566.3 (M-1)⁻.

TLC (4:1 Hex:EtOAc): $R_f = 0.1$



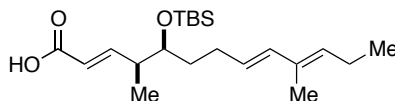
methyl 2-(3-(7-((tert-butyldimethylsilyl)oxy)-2-ethyl-3,8-dimethyl-1,2,4a,5,6,7,8,8a-octahydronaphthalen-1-yl)-3-oxopropanamido)acetate (161b)

¹H NMR (500 MHz, CDCl₃): δ 13.37 (d, $J = 1.3$ Hz, enolic), 7.69 (br t, $J = 5.0$ Hz, NH), 5.53 (br q, $J = 2$ Hz, H14), 4.05 (dd, $J = 5.5, 1.7$ Hz, H4), 3.75 (s, 3H, OMe), 3.42 (d, $J = 17.1$ Hz, H2a), 3.31 (d, $J = 17.2$ Hz, H2b), 3.14 (ddd, $J = 10.4, 9.3, 4.4$ Hz, H10), 2.85 (t, $J = 7.0$ Hz, H7), 2.19 (br q, $J = 6.7$ Hz, H16), 1.96 (dq, $J = 12.7, 3$ Hz, H12eq), 1.93-1.89 (m, 1H, H11eq), 1.78 (q, $J = 1.7$ Hz, Me36), 1.72-1.54 (m, H13, H17a), 1.43-1.21 (H9, H11ax, H12ax, H17b), 1.06 (ddd, $J = 10.6, 10.6, 6.7$ Hz, H8), 0.98 (t, $J = 7.3$ Hz, 3H, Me18), 0.878 (d, $J = 6.8$ Hz, 3H, Me37), 0.877 (s, 9H, ^tBu), 0.04 (s, 3H, SiMe), and 0.03 (s, 3H, SiMe).

LCMS: Method C, $R_t = 6.0$ min, m/z "pos" = 480.3 (M+1)⁺, m/z "neg" = 478.3 (M-1)⁻, 514.3 (M+35)⁻.

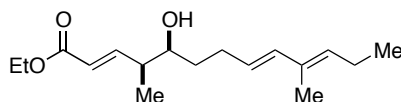
TLC (4:1 Hex:EtOAc): $R_f = 0.1$

Auxiliary Compounds:



(2E,4S,5S,8E,10E)-5-((tert-butyldimethylsilyl)oxy)-4,10-dimethyltrideca-2,8,10-trienoic acid

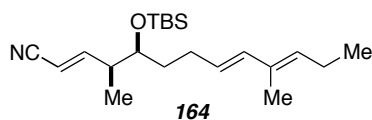
$^1\text{H NMR}$ (500 MHz, CDCl_3): δ 6.98 (dd, $J = 16.0, 7.1$ Hz, 1H), 6.04 (d, $J = 15.4$ Hz, 1H), 5.81 (d, $J = 16.0$ Hz, 1H), 5.51 (ddd, $J = 15.2, 7.1, 7.1$ Hz, 1H), 5.37 (t, $J = 7.1$ Hz, 1H), 3.66 (ddd, $J = 6.7, 5.0, 5.0$ Hz, 1H), 2.48 (app sextet, $J = 7$ Hz, 1H), 2.12 (pent, $J = 7.5$ Hz, 2H), 2.19-2.00 (m, 2H), 1.71 (s, 3H), 1.56-1.41 (m, 2H), 1.03 (d, $J = 6.8$ Hz, 3H), 0.98 (t, $J = 7.5$ Hz, 3H), 0.89 (s, 9H), 0.05 (s, 3H), and 0.04 (s, 3H). [seIIIpg148rpt7]



(2E,4S,5S,8E,10E)-ethyl 5-hydroxy-4,10-dimethyltrideca-2,8,10-trienoate

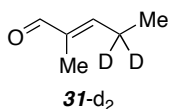
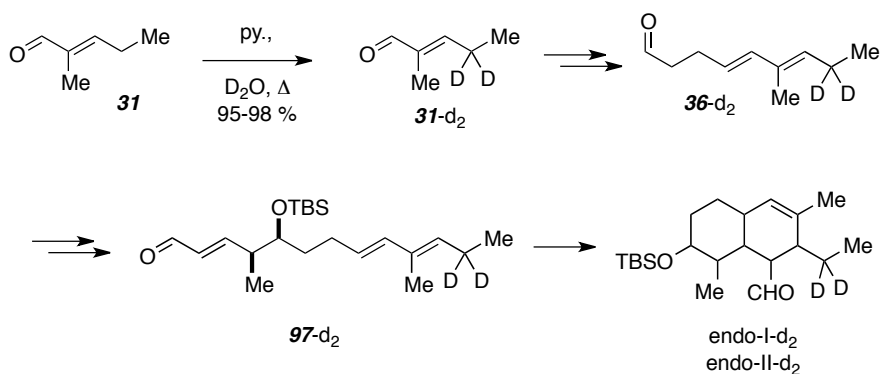
$^1\text{H NMR}$ (500 MHz, CDCl_3): δ 6.94 (dd, $J = 15.7, 7.8$ Hz, 1H), 6.09 (d, $J = 15.3$ Hz, 1H), 5.86 (dd, $J = 15.8, 1.4$ Hz, 1H), 5.53 (ddd, $J = 15.5, 7.0, 7.0$, 1H), 5.39 (t, $J = 7.3$ Hz, 1H), 4.19 (q, $J = 7.1$ Hz, 2H), 3.60 (ddd, $J = 8.9, 5.2, 3.2$ Hz, 1H), 2.43 (dddq, $J = 7.2, 5.2, 1.4, 6.8$ Hz, 1H), 2.29, (app sextet, $J = 7$ Hz, 1H), 2.18 (app pent, $J = 7$ Hz, 1H), 2.12 (app pent, $J = 7.4$ Hz, 2H), 1.72 (s, 3H), 1.59 (dddd, $J = 13.9, 8.6, 6.8, 3.1$ Hz, 1H), 1.49 (dddd, $J = 14.0, 9.4, 8.5, 5.9$ Hz, 1H), 1.30 (t, $J = 7.1$ Hz, 3H), 1.09 (d, $J = 6.8$ Hz, 3H), and 0.98 (t, $J = 7.5$ Hz, 3H). [seIIpg44f2]

Experiments (Chapter III)



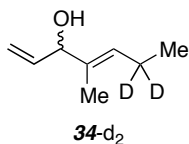
(2E,4S,5S,8E,10E)-5-((tert-butyltrimethylsilyloxy)-4,10-dimethyltrideca-2,8,10-trienenitrile (154)

$^1\text{H NMR}$ (500 MHz, CDCl_3): δ 6.82 (dd, $J = 16.6, 6.6$ Hz, 1H), 6.05 (d, $J = 15.4$ Hz, 1H), 5.52 (ddd, $J = 15.5, 6.9, 6.9$ Hz, 1H), 5.38 (t, $J = 7.2$ Hz, 1H), 5.30 (dd, $J = 16.5, 1.7$ Hz, 1H), 3.634 (ddd, $J = 7.2, 4.4, 4.4$ Hz, 1H), 2.50 (ddq, $J = 4.3, 1.7, 6.8$ Hz, 1H), 2.13 (app pent, $J = 7.4$ Hz, 2H), 2.19-1.98 (m, 2H), 1.72 (s, 3H), 1.69-1.57 (m, 1H), 1.53-1.46 (m, 1H), 1.02 (d, $J = 6.9$ Hz, 3H), 0.98 (t, $J = 7.6$ Hz, 3H), 0.90 (s, 9H), 0.054 (s, 3H), and 0.048 (s, 3H). [seeIIpg117mplc1, seems to be contaminated with some of the – HOTBS elimination product]



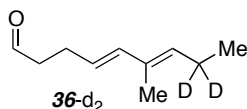
(E)-2-methylpent-2-enal (31-d₂)

$^1\text{H NMR}$ (500 MHz, CDCl_3): δ 9.40 (s, 1H), 6.47 (s, 1H), 1.73 (d, $J = 1.3$ Hz, 3H), and 1.09 (s, 3H). [seeIIpg35or 44_3d]



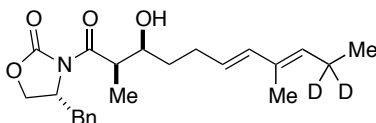
E-4-methyl-1,4-heptadien-3-ol (34-d₂)

$^1\text{H NMR}$ (500 MHz, CDCl_3): δ 5.87 (ddd, $J = 17.2, 10.5, 5.6$, 1H), 5.47 (s, 1H), 5.28 (ddd, $J = 17.3, 1.5, 1.5$ Hz, 1H), 5.15 (ddd, $J = 10.4, 1.3, 1.3$ Hz, 1H), 4.51 (br s, 1H), 1.60 (s, 3H), and 0.96 (s, 3H). [seIIIpg43c]



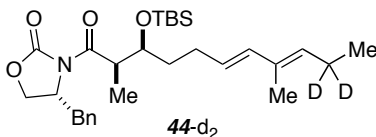
(4E,6E)-6-methylnona-4,6-dienal (36-d₂):

$^1\text{H NMR}$ (500 MHz, CDCl_3): δ 9.78 (t, $J = 1.5$ Hz, 1H), 6.09 (d, $J = 15.6$ Hz, 1H), 5.52 (ddd, $J = 15.7, 6.8, 6.8$ Hz, 1H), 5.39 (br s, 1H), 2.55 (dddd, $J = 8.6, 6.8, 1.2, 1.2$, 1H), 1.70 (d, $J = 1.2$ Hz, 3H), and 0.96 (s, 3H) [seIIIpg43f4]



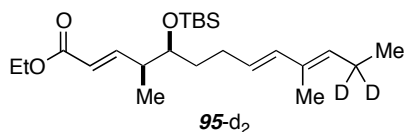
(R)-4-benzyl-3-((2R,3S,6E,8E)-3-hydroxy-2,8-dimethylundeca-6,8-dienoyl)oxazolidin-2-one (noTBS-44-d₂)

$^1\text{H NMR}$ (500 MHz, CDCl_3): δ 7.36-7.18 (m, 5H), 6.09 (d, $J = 15.6$ Hz, 1H), 5.54 (ddd, $J = 15.5, 7.0, 7.0$ Hz, 1H), 5.36 (br s, 3H), 4.74-4.63 (m, 1H), 4.27-4.10 (m, 2H), 3.97 (ddd, $J = 9.0, 4.1, 2.7$ Hz, 1H), 3.75 (dq, $J = 2.8, 7.0$ Hz, 1H), 3.24 (dd, $J = 13.4, 3.4$ Hz, 1H), 2.78 (dd, $J = 13.4, 9.4$ Hz, 1H), 2.40-1.96 (m, 4H), 1.71 (d, $J = 1.3$ Hz, 1H), 1.69-1.60 (m, 1H), 1.55-1.43 (m, 1H), 1.26 (d, $J = 7.1$ Hz, 3H), and 0.95 (s, 3H). [seIIIpg49_chk1.5h]



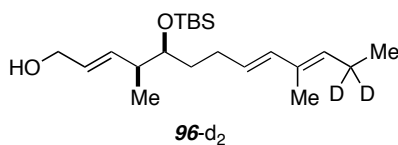
(R)-4-benzyl-3-((2R,3S,6E,8E)-3-((tert-butyldimethylsilyloxy)-2,8-dimethylundeca-6,8-dienoyl)oxazolidin-2-one (44-d₂)

¹H NMR (500 MHz, CDCl₃): δ 7.35-7.20 (m, 5H), 6.05 (dq, *J* = 15.6, 1.5 Hz, 1H), 5.53 (ddd, *J* = 15.6, 6.8, 6.8 Hz, 1H), 5.36 (s, 1H), 4.60 (dddd, *J* = 12.7, 6.8, 3.0, 3.0, 1H), 4.16 (ddd, *J* = 9.1, 9.1, 2.7 Hz, 1H), 4.02 (app q, *J* = 5.6 Hz, 1H), 3.88 (dq, *J* = 5.1, 6.9 Hz, 1H), 3.29 (dd, *J* = 13.3, 2.3 Hz, 1H), 2.76 (dd, *J* = 14.6, 9.7 Hz, 1H), 2.20-2.07 (m, 2H), 1.71 (d, *J* = 1.3 Hz, 3H), 1.69-1.58 (m, 2H), 1.22 (d, *J* = 6.9 Hz, 3H), 0.95 (br s, 3H), 0.89 (s, 9H), 0.05 (s, 3H), and 0.01 (s, 3H). [seIIIpg50f1]



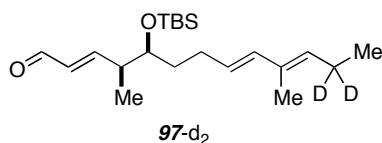
(2E,4S,5S,8E,10E)-ethyl 5-((tert-butyldimethylsilyl)oxy)-4,10-dimethyltrideca-2,8,10-trienoate (95-d₂)

¹H NMR (500 MHz, CDCl₃): δ 7.02 (dd, *J* = 15.8, 7.2 Hz, 1H), 6.04 (dq, *J* = 15.5, 1.4 Hz, 1H), 5.79 (dd, *J* = 15.8, 1.4 Hz, 1H), 5.50 (ddd, *J* = 15.6, 7.1, 7.1 Hz, 1H), 5.36 (br s, 1H), 4.18 (dq, *J* = 1.1, 7.1 Hz, 1H), 3.63 (ddd, *J* = 6.6, 4.8, 4.8 Hz, 1H), 2.47 (ddq, *J* = 4.8, 1.4, 6.7 Hz, 1H), 2.21-1.97 (m, 2H), 1.71 (d, *J* = 1.3 Hz, 3H), 1.64-1.41 (m, 2H), 1.29 (t, *J* = 7.1 Hz, 3H), 1.02 (d, *J* = 6.8 Hz, 3H), 0.96 (br s, 3H), 0.89 (s, 9H), 0.05 (s, 3H), and 0.04 (s, 3H). [seIIIpg52mplc] referenced to CHCl₃ here



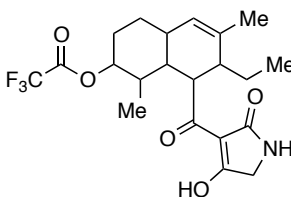
(2E,4S,5S,8E,10E)-5-((tert-butyldimethylsilyl)oxy)-4,10-dimethyltrideca-2,8,10-trien-1-ol (96-d₂)

¹H NMR (500 MHz, CDCl₃): δ 6.05 (dq, *J* = 15.5, 1.4 Hz, 1H), 5.73 (ddd, 15.5, 7.0, 1.3, 1.3 Hz, 1H), 5.62 (ddd, *J* = 15.6, 5.8, 5.8, 1.1 Hz, 1H), 5.53 (ddd, *J* = 15.7, 6.9, 6.9 Hz, 1H), 5.36 (br s, 1H), 4.14-4.08 (m, 2H), 3.55 (ddd, *J* = 6.8, 4.8, 4.8 Hz, 1H), 2.34 (app sextet, *J* = 7 Hz, 1H), 2.20-2.13 (m, 1H), 2.08-2.00 (m, 1H), 1.71 (d, *J* = 1.3 Hz, 3H), 1.53-1.42 (m, 2H), 0.97 (d, *J* = 6.9 Hz, 3H), 0.96 (br s, 3H), 0.90 (s, 9H), 0.05 (s, 3H), and 0.04 (s, 3H). [seIIIpg59extraf]



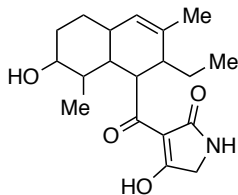
(2E,4S,5S,8E,10E)-5-((tert-butyldimethylsilyloxy)-4,10-dimethyltrideca-2,8,10-trienal (97-d₂)

¹H NMR (500 MHz, CDCl₃): δ 9.52 (d, *J* = 7.9 Hz, 1H), 6.96 (dd, *J* = 15.9, 6.5 Hz, 1H), 6.11 (ddd, *J* = 15.9, 9.1, 1.2 Hz, 1H), 6.05 (d, *J* = 15.6 Hz, 1H), 5.50 (ddd, *J* = 15.6, 6.9, 6.9 Hz, 1H), 5.37 (br s, 1H), 3.70 (ddd, *J* = 7.6, 4.5, 4.5 Hz, 1H), 2.64 (ddq, *J* = 1.7, 4.9, 6.7 Hz, 1H), 2.22-2.14 (m, 1H), 2.08-2.00 (m, 1H), 1.71 (d, *J* = 1.3 Hz, 3H), 1.56-1.50 (m, 1H), 1.46-1.39 (m, 1H), 1.07 (d, *J* = 6.9 Hz, 3H), 0.96 (br s, 3H), 0.90 (s, 9H), 0.07 (s, 3H), and 0.05 (s, 3H). (referenced to CHCl₃) [seIIIpg54f3]



7-ethyl-8-(4-hydroxy-2-oxo-2,5-dihydro-1H-pyrrole-3-carbonyl)-1,6-dimethyl-1,2,3,4,4a,7,8,8a-octahydronaphthalen-2-yl 2,2,2-trifluoroacetate (163)

ESI-MS: Exact mass calc. for [C₂₁H₂₆F₃NO₅Na]⁺, 452.1655, found 452.1636.



3-(2-ethyl-7-hydroxy-3,8-dimethyl-1,2,4a,5,6,7,8,8a-octahydronaphthalene-1-carbonyl)-4-hydroxy-1H-pyrrol-2(5H)-one (26)

ESI-MS: Exact mass calc. for [C₁₉H₂₇NO₄Na]⁺, 356.1832, found 356.1848.

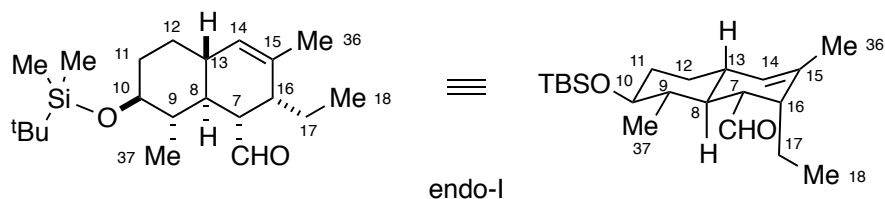


Table I-4: ^{13}C and ^1H NMR Data for *endo-I* (CDCl_3 , 125 and 500 MHz).

Atom Number ^a	Carbon	Proton		
	δ_c	δ_H	mult	J (Hz)
CHO	205.4	9.47	d	5.4
7	56.1	2.58	ddd	6.7, 6.7, 5.4
8	44.7	1.13	ddd	10.6, 10.6, 7.0
9	45.3	1.47-1.34	m	
10	77	3.17	ddd	10.7, 9.1, 4.2
11ax	35.8	1.47-1.34	m	
11eq	35.8	1.95-1.89	m	
12ax	30.2	1.31-1.22	m	
12eq	30.2	1.95-1.89	m	
13	39.7	1.75-1.65	m	
14	129.6	5.42	br s	
15	137.3	NA		
16	42	2.19	br q	6.8
17a	22	1.75-1.65	m	
17b	22	1.52	app sextet	7.4
18	13.2	1.00	t	7.4
Me36	19.9	1.73	q	1.6
Me37	16.8	0.93	d	6.4
Si-Me	-3.7	0.05	s	
Si-Me	-4.5	0.04	s	
4° of ^t Bu	21	NA		
^t Bu methyl groups	26.1	0.88	s	

^a numbering as in integramycin (**1a**). Me36 is allylic. Me37 is the substituent at C9.

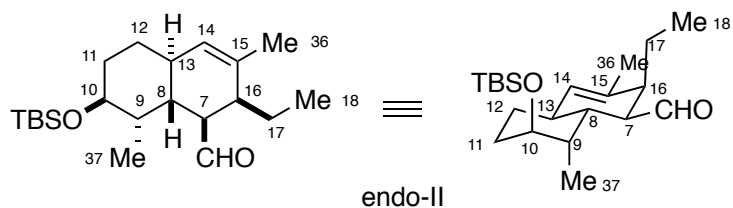


Table I-5: ^{13}C and ^1H NMR Data for *endo*-II (CDCl_3 , 125 and 500 MHz).

Atom Number ^a	Proton		
	δ_{H}	mult	J (Hz)
CHO	9.8	d	4.5
7	2.49-2.4	m	(10.1, 5.7, 4.7)
8	1.56-1.42	m	
9	1.96-1.88	m	
10	3.71	app q, ddd	2.8
11ax	1.56-1.42	m	
11eq	1.62	nform	(12.2, 5.6, 2.0)
12ax	2.49-2.4	m	(12.3, 10.3, 3.7)
12eq	1.56-1.42	m	
13	1.96-1.88	m	
14	5.21	br s	
15	NA		
16	2.25	nform	
17a	1.71	app pent	7.5
17b	1.56-1.42	m	
18	0.95	t	7.6
36	1.67	t	1.8
37	0.754	d	7.3
Si-Me	0.04	s	
Si-Me	0.03	s	
4° of ^t Bu	NA		
^t Bu methyl groups	0.89	s	

^a numbering as in integramycin (**1a**). Me36 is allylic. Me37 is the substituent at C9.

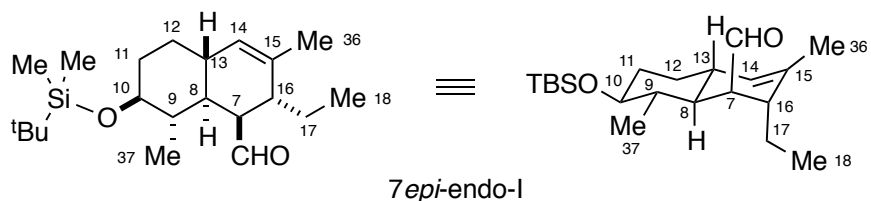


Table I-6: ^{13}C and ^1H NMR Data for 7-*epi*-endo-I (CDCl_3 , 125 and 500 MHz).

Atom Number ^a	Carbon		Proton	
	δ_{C}	δ_{H}	mult	J (Hz)
CHO	205.2	9.73	d	1.7
7	48.4	2.69	ddd	3.4, 1.4, 1.4
8	41.5 ^b	1.14	ddd	11.2, 11.2, 3.3
9	41.6 ^b	1.68	ddq	11.0, 9.3, 6.4
10	77.4	3.16	ddd	10.9, 9.3, 4.6
11ax	35.9	1.42	dddd	13.2, 13.2, 10.8, 4.3
11eq	35.9	1.92	dddd	10.9, 4, 4, 4
12ax	25.1	1.01	ddd	13.1, 12.2, 12.2, 3.5
12eq	25.1	1.2	dddd	11.3, 4.3, 4.3, 4.3
13	38.1	1.87	br dd	11.2, 11.2
14	126.8	5.18	q	1.4
15	135.6	NA		
16	41.1 ^b	2.18	m	very br d, 9 or 10 Hz
17a	31.6	1.79-1.70	m	
17b	31.6	1.79-1.70	m	
18	12.9	0.94	t	7.4
36	22.2	1.72	t	1.6
37	15.2	1.07	d	6.5
Si-Me	-3.7 ^c	0.07	s	
Si-Me	-4.4 ^c	0.06	s	
4° of ^t Bu	18.3	NA		
^t Bu methyl groups	26.1	0.9	s	

^a numbering as in integramycin (**1a**). Me36 is allylic. Me37 is the substituent at C9.

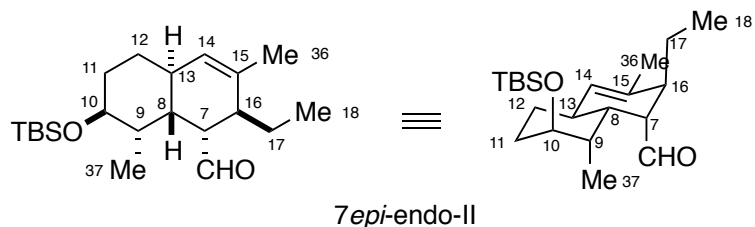


Table I-7: ^{13}C and ^1H NMR Data for *7-epi-endo-II* (CDCl_3 , 125 and 500 MHz)

Atom Number	Proton		
	δ_{H}	mult	J (Hz)
CHO	9.84	d	5.1
7	2.25	ddd	5.1, 1.7, 1.7
8	1.57-1.50		
9	1.83-1.71		
10	3.7	app q	2.8
11ax	1.65	dddd	4.3, 14.3, 4.5, 2.1
11eq	1.57-1.50		
12ax	1.46-1.40		
12eq	2.35	ddd	11.8, 3.7, 2.5
13	2.39	dd sextets	11.9, 11.8, 1.8
14	5.28	ddq	1.4, 1.4, 0.7
15	NA		
16	1.83-1.71		
17a	1.83-1.71		
17b	1.34	ddd	14.0, 10.1, 7.1
18	0.94	t	7.4
36	1.7	t	1.7
37	0.86	d	7.4
Si-Me	0.022	s	
Si-Me	0.018	s	
4° of ^tBu	NA		
^tBu methyl group	0.87	s	

^a numbering as in integramycin (**1a**). Me36 is allylic. Me37 is the substituent at C9.

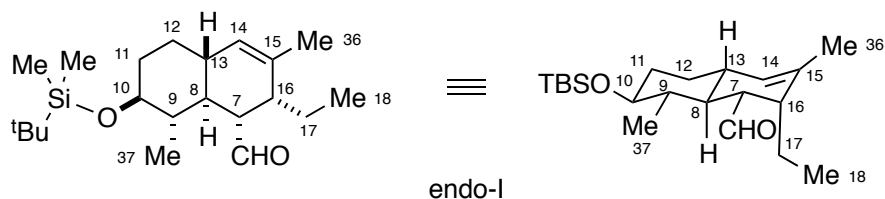


Table I-8: ^{13}C and ^1H NMR Data for Endo-I (C_6D_6 , 125 and 500 MHz)

Atom Number ^a	Proton		
	δ H	mult	J (Hz)
CHO	9.39	d	5.2
7	2.47	ddd	6.6, 6.6, 5.1
8	0.95	ddd	13.9, 13.9, 6.3, 6.3
9	1.24	ddq	10.8, 9.0, 6.4
10	3.03	ddd	10.8, 9.1, 4.6
11ax	1.40-1.30	m	
11eq	1.85	dq	12.6, 3.4 (or 4.4!)
12ax	1.08	ddd	13.1, 13.1, 3.4
12eq	1.71	dq	13.1, 3.5
13	1.54-1.42	m	
14	5.29	ddq	3.4, 1.7, 1.7
15	NA		
16	1.93	br q, app q	7
17a	1.54-1.42	m	
17b	1.40-1.30	m	
18	0.87	t	7.4
36	1.58	ddd	2.5, 1.5, 1.5
37	1.01	d	6.3
Si-Me	0.07	s	
Si-Me	0.06	s	
4° of ^t Bu	NA		
^t Bu methyl groups	1.02	s	

^a numbering as in integramycin (**1a**). Me36 is allylic. Me37 is the substituent at C9.

PART TWO: Isolation of Natural Products

Chapter IV. Alkaloids from Amazonian Plants

IV.A. Introduction and Background

Drug discovery and development is a costly and time-consuming process. There are many different approaches, but all require an understanding of both the target disease and the chemistry of small molecules. The process must involve scientists and medical specialists with a wealth of specialty training and a defined goal.

IV.A.1. Ethnopharmacology and Schizophrenia

One of the many approaches for drug discovery is investigation of natural products (NPs), many of which are known to have biological activity. The ability to harness this activity in a safe and effective way for the treatment of a wide variety of diseases would have a monumental effect in health care today. Of course, there must be a strategy in-hand before conducting research. The number and type of living organisms capable of providing natural products is overwhelming.

In the specific case of botanical natural products, there is a wealth of information available. Many times, this knowledge comes from traditional medicine and folklore around these plants, guiding Western research aimed at the discovery of new therapeutic agents. After all, it must be that when these plants have a known effect on humans, there are chemical components responsible for those effects. Ethnopharmacology – the interdisciplinary investigation of biologically active substances used by indigenous cultures – is commonly used to describe this approach to drug discovery.⁹¹ Ethnopharmacology has been discussed at-length in the literature and there is much journal space and many volumes dedicated to the topic (e.g. *J. of Ethnopharmacology*). As such an established method, it is an attractive place to begin.

Richard Evans Schultes is commonly considered the Father of Ethnobotany. This field focuses not only on the medical arena, but also the areas of food coloring, fiber, poison, fertilizers, ornamentals, and oils. Schultes spent his career developing and illustrating the utility of ethnobotany. One of his most relevant contributions for

ethnopharmacologists was a series of publications reviewing Amazonian plants, particularly those of the Apocynaceae family (see Section **IV.C.2.a**).^{92,93} This large and diverse collection of plants is reputedly the most abundant in alkaloids. Though taxonomically very difficult to understand, it is worth the challenge. There are number of species with known medicinal properties to probe, and the identification of their alkaloidal components is a necessary step in the development of treatments derived from them.

Dennis J. McKenna, an ethnopharmacologist and our collaborator in pharmacy, recognized that the plants profiled by Schultes were specifically used for their psychoactive properties. Prof. McKenna also had a long-standing interest in developing treatments for diseases of the central nervous system, namely, schizophrenia. Professor McKenna noted the connection between Schultes' psychoactive plants and schizophrenia. He felt that launching a project, which took advantage of Schultes' guidance, would be worthwhile.⁹⁴ There are treatments available for schizophrenia but there is room for improvement. For example, there has been an imbalance in treatment of the positive (overt, like hallucinations, disorganized speech, catatonic behavior) versus negative (neurocognitive deficits, like in attention, long-term memory, and verbal ability) symptoms of this disease. Because schizophrenia has not yet been addressed from the perspective of natural product treatments, there was great potential in using the information gathered by Schultes. The goal was to gain an even better understanding of what it is that makes these plants psychoactive and to leverage those small molecules in disease therapy today.

IV.A.2. The Approach (Scheme II-1)

The process proposed by McKenna begins with the collection of Amazonian plants.⁹⁵ Once obtained, he aimed to (i) discern which plants contain biologically active components (ii) isolate and perform structure elucidation of the chemical components present in these plants (iii) perform additional biological testing on pure natural products^{96,97} and (iv) develop these natural products into potential treatments. The first step requires that the plant components be extracted and tested for biological activity. The

extracts proven to be most active (by radioligand binding assays, discussed later) would be probed for their phytochemical components (step ii). The hope was that the natural products would have novel structures. Following this, a more in-depth biological activity profile could be generated from testing the isolated molecule rather than the crude extract (step iii). Finally, the natural product could be chemically modified or a library be built to examine how changes in the structure affect the biological activity of the natural product (step iv); this information would be used to guide the development of a possibly more potent molecule with the desired characteristics for a drug.

The guidance provided by Schultes was very useful, but due to the botanical diversity he presented and the wealth of plants that Prof. McKenna and his partners collected, we needed a way to further prioritize the plants for study. The method had to quickly and easily determine which species were most likely to be psychoactive. Professor McKenna proposed that radioligand binding methodologies be employed.⁹⁸ Various targets were sought, including serotonin, adrenergic, dopamine, opiate, muscarinic acetylcholine, and cholinergic receptors.⁹⁵ Radioligand binding is commonly used in the drug discovery process. It is rapid, cost-effective, and widely applicable for a number of receptors (those listed above, especially serotonin, muscarinic acetylcholine, and cholinergic). This last feature is why radioligand binding is so well suited for the neurosciences.⁹⁹⁻¹⁰¹ In fact, it has already been demonstrated to be useful in other research endeavors.¹⁰² With all these details of the project planned, Professor McKenna was successful in acquiring the funds and launched a research project.

IV.A.3. Final Consideration/Motivation

We recognize that we are not undertaking a brand new program for drug discovery. We simply note that previous findings for active plant components have been more of the serendipitous type, where alleviation of symptoms was observed for various ethnomedicines.¹⁰³ Prof. McKenna designed a more formal approach and aimed to identify the particular chemical components responsible for these effects. This will lead to a better understanding of the mode of action (particularly in reversing the neurocognitive deficit symptoms by its sufferers). Such a systematic research endeavor

should result in the identification of particular natural products and their corresponding biological activity. We also recognize that regardless of our success in NP isolation, drug discovery is far longer-term goal. It would be beneficial if we could simply arrive at a structural scaffold from which other bioactive agents might be envisioned.^{102,104}

Lastly, it is worth emphasizing the critical nature of proper structural determination. The literature is replete with many instances where new natural product structures have been incorrectly assigned.¹⁰⁵ Professor Hoye has extensive expertise in both the development and use of NMR analysis techniques for determination of complex molecular structures—a skill set that will also be very valuable to me. In order to understand how a molecule behaves toward its biological target (for example, a CNS receptor), structure is of utmost importance. As already mentioned, it is not uncommon for other investigators (for example, medicinal chemists involved in drug discovery) to use the discoveries of natural products chemists as a launching pad for the development of new drug leads. This opportunity is severely compromised when a new compound is incorrectly assigned. As a synthetic organic chemist, I am familiar with the power and limitations of the various methods for determining structure, and these I kept in mind when conducting isolation and structure elucidation work.

IV.B. Previous Work

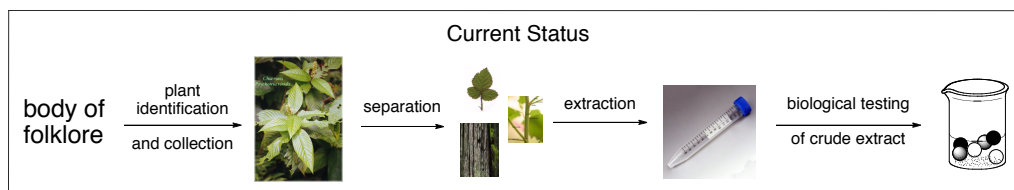
Previous work was performed both abroad and locally. The process began with a literature survey and field expeditions. Various Amazonian plants were extracted and tested for biological activity. Several plants were advanced into a study of their phytochemistry.

IV.B.1. McKenna and Roth⁹⁵

As described in section **IV.A.2**, the work began with an identification and pre-selection of targeted species. Professor McKenna enlisted the help of collaborators at the Universidad Nacional de la Amazonia Peruana and Gracia Ethnobotanicals (both located in Iquitos, Peru). This entailed an exhausting literature survey, (including many of the published works by Schultes^{92,93}), NAPRALERT surveys, herbarium surveys, and

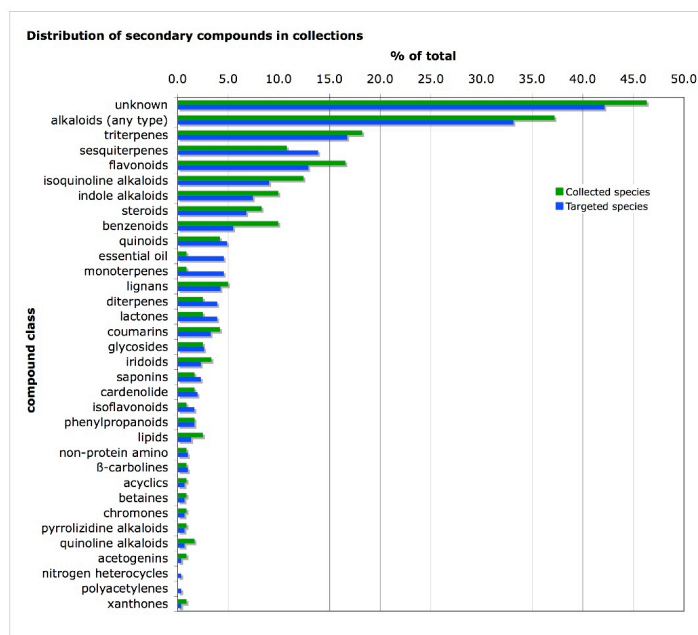
interviews with local informants. (Scheme II-1, “body of folklore”). From this, a list of targeted species was generated and priorities were assigned. The next step was specimen collection. Over the course of approximately 20 months, several expeditions were conducted in the Loreto province of Peru.

Scheme II-1. Steps in McKenna’s Ethnopharmacological Approach



Following documentation (vouchers and collection numbers were assigned) and export authorizations, the collected species were analyzed and arranged according to their folk uses and phytochemical distribution (information gathered from the literature). Chart II-1 shows that alkaloids, aside from those labeled unclassified, are among the most represented. Thus, these are the types of compounds expected to be present and isolable in the plant samples. This information was important for me, a chemist, to envision the ways in which expected chemical constituents were to be handled.

Chart II-1. Phytochemical Distribution of McKenna’s Collection⁹⁵

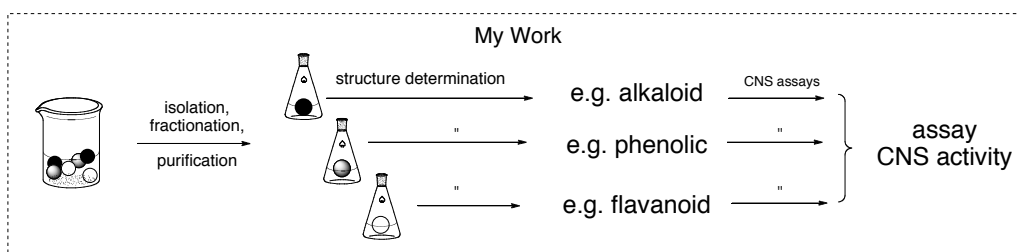


After the various ethnobotanical characteristics were summarized, the plants were prepared for the biological testing phase of this project. Professor McKenna enlisted the help of the Hoye laboratory. Extracts were performed as prescribed (and are detailed in a later section). For most plant material, crude extracts were used in the biological testing, but in some cases, partially fractionated extracts were also tested. Bryan Roth's NIMH Psychoactive Drug Screening Program at the University of North Carolina – Chapel Hill performed both receptor binding and, on a subset of extracts, functional assays. The former assay assigned "hits," or those samples that displayed inhibition of the radioactive ligand. The latter determined if any samples had agonist or antagonist activity. The receptors under study were subtypes of the general type serotonin, alpha adrenergic, dopamine, histamine, muscarinic acetylcholine, and several reuptake inhibitors.⁹⁵ The *Tabernaemontana* family¹⁰⁶ gave promising results in both of these assays, and were noted as high priority in the isolation work. This was somewhat expected after reading through Schultes' commentary on the family.

IV.B.2. Ziyad and Laura

This was the status of the project for a number of months until a graduate researcher initiated research into the alkaloidal content of the most promising fractions. The next steps required further understanding the exact chemical components (Scheme II-2).

Scheme II-2. Remaining Steps in McKenna's Ethnopharmacological Approach



Ziyad Al-Rashid completed a thorough screen of the most promising biological extracts. He narrowed the number to the most promising samples with respect to alkaloid content, again, these were the most likely constituents present in the plant samples. By TLC, then ¹H NMR analysis of crude extracts, Al-Rashid identified the most deserving species of study to be (* denotes where species yielded pure alkaloids in tractable quantities)

Ambolania occidentales A*

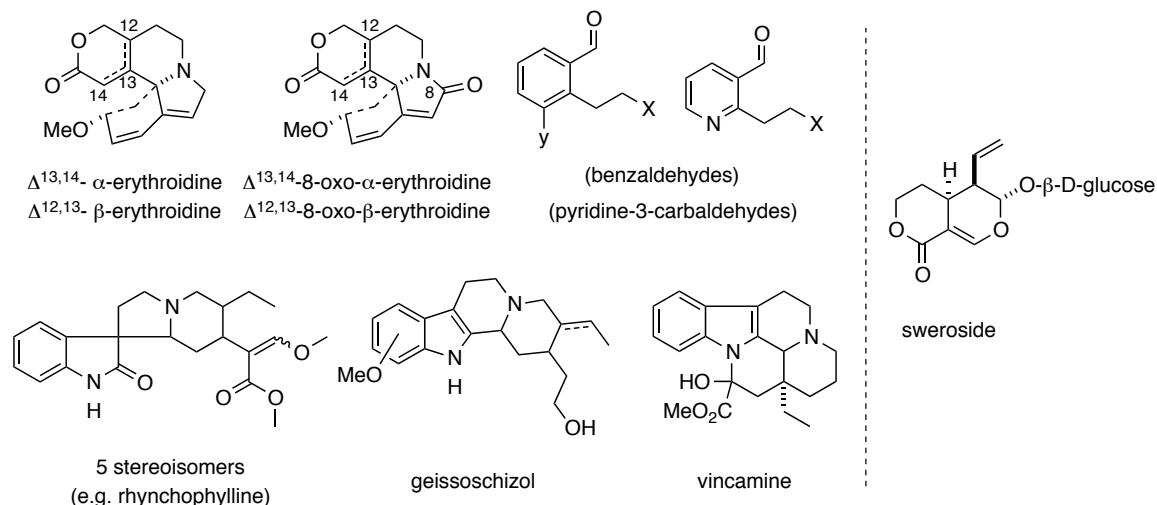
Aspidosperma excelsum A*

Erythrina ulei harm*
 Hamelia patens*
 Tabernaemontana heterophylla

Eucharis ulei
 Potalia resinifera*
 Yohimbine bark

The alkaloids isolated from this study are shown in Figure II-1 (left panel). These were already known in the literature,¹⁰⁷⁻¹⁰⁹ but demonstrated that our lab was capable of this type of research.

Figure II-1. Compounds Isolated in Previous Studies.



Another previous group member was able to successfully identify an alkaloidal component out of *Potalia resinifera*. Laura Kwong, an undergraduate researcher, performed the same extraction protocol on this species (out of the family Gentianaceae), and using MPLC techniques (CMA mobile phase) and isolated sweroside¹¹⁰ (Figure II-1, right panel). The assignment was based on the comparison of ¹H NMR chemical shifts and *J*-couplings with the literature. Although successful in this investigation, Laura was unable to isolate and identify the chemical components of the other species she studied: *Remijia peruviana* (rubiaceae), *Tabernaemontana heterophylla* (apocynaceae), *Rinora racemosa* (violaceae), *Hamelia patens* (rubiaceae), and *Mansoa alliacea* (bignoniaceae).

IV.C. My Contributions to This Project

When I entered the project, a list of plants of interest had already been generated, and several had been studied for their phytochemical content. With advances in our

laboratory in reverse phase application of our MPLC instrumentation, there was interest in developing and applying this technique to the remaining plants species of interest.

IV.C.1. Reverse-Phase Medium Pressure Liquid Chromatography (RPLC) as the Primary Technique

The first step was development of the proper technique for isolation. Ideally, this would also be useful in preliminary analysis.

IV.C.1.a. Motivation for Reverse Phase Liquid Chromatography

Alkaloids like those in Figure II-1 are typically isolated by column chromatography on standard reverse-phase conditions and preparative TLC. In situations where dimers are present, there is a Size Exclusion Chromatography (SEC) step to separate the components. In addition to these commonly used techniques, others were employed by both Ziyad and Laura, and I wanted to consider those as well. For TLC study of our selected plant species, Sonnenschein's reagent had already been used and was chosen. There are a variety of stains available that are useful in testing for alkaloidal-like molecules, but based on experimentation with brucine and cinchona alkaloid (see Figure II-2), this was the most robust. Sonnenschein's stain is a solution of phosphomolybdic acid in aqueous nitric acid (HNO₃).

From the previous work, I had some ideas (beyond TLC) for the best methods for analysis and isolation. Moreover, knowing the preponderance of dimers that might be present, I was unsure that GC (as used by previous workers) would be the proper analytical technique. Our LCMS instrument is a very powerful tool, and I had experience with it, so I chose that as my primary analytical tool. Learning LCMS instrumentation, data analysis, and design of experiments would be crucial to the identification of the components in our plants of choice.

Along with LCMS for analysis, I needed a method for isolation. Despite the tendency for using reverse-phase techniques (mentioned above), Ziyad and Laura had used normal phase and preparative TLC. I sought techniques that were more robust and applicable to the very polar compounds I was expecting. Higher throughput of material was a primary

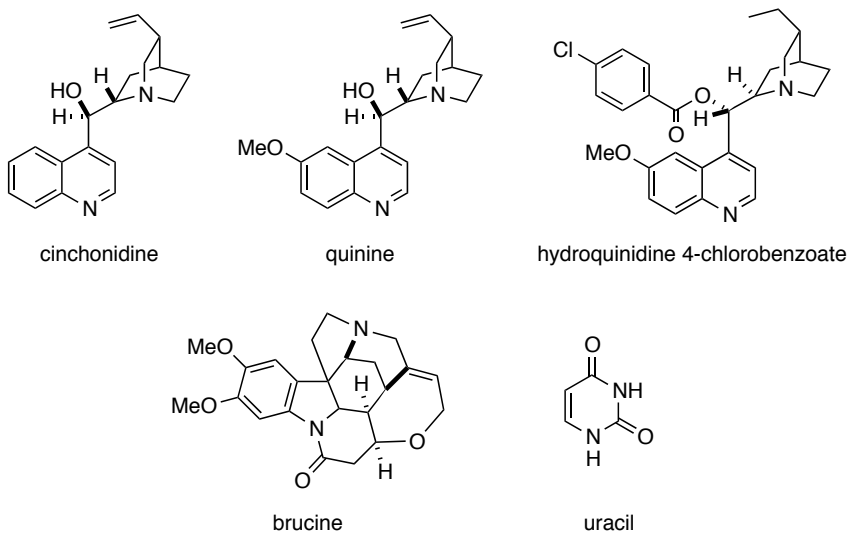
goal. Moreover, we knew that we would be attempting to analyze the most minor components, and I desired a way (beyond LCMS) to detect these. I settled on Reverse Phase Liquid Chromatography (RPLC). It could be correlated with LCMS data and it was an opportunity to use my skills from MPLC and develop this technique.

There were some concerns. Even with my comfort with the MPLC (generally normal phase, which I had already decided might not be suitable for this study), I did not have the experience working with very basic and polar nitrogenous compounds. Further, it had to be established that the detection method (RI) was effective.

IV.C.1.b. RPLC Development

A test set of alkaloids was selected to develop a proper chromatographic method^{111,112} (see Figure II-2). These were chosen based on availability and similarity to natural products expected from our plant sources. A few more alkaloids came online as the project progressed, courtesy of Prof. McKenna, and these were incorporated into the experiments.

Figure II-2. Model Alkaloids for RPLC Development.

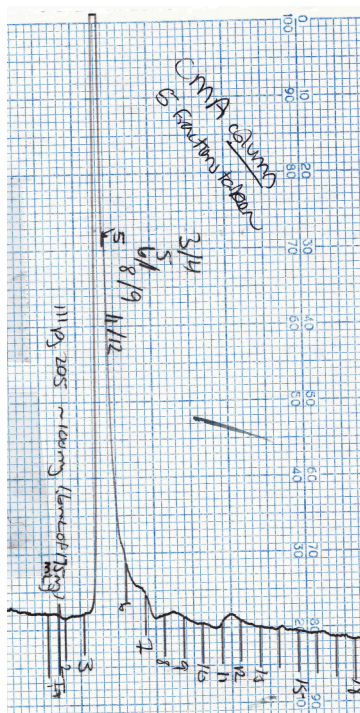


My experience in MPLC was limited to normal phase separations using standard mobile phases and packing materials. I began with these types of systems, knowing that I would be working out more exotic conditions and branching into reverse-phase quickly.

Previous group members had worked on both of these fronts (Ziyad had primarily used preparative TLC, where Laura used MPLC and CMA-type mobile phases)

With normal phase, it was clear that while solvent mixtures such as 1:1 hexanes:ethyl acetate could be used to move a number of components in crude extracts, a more powerful system was CMA (chloroform:methanol:ammonium hydroxide).¹¹³ CMA was therefore selected for initial MPLC runs [standard packing materials, MPLC grade silica gel (32-60 angstrom)]. The typical composition in CMA was 80:18:2. Although Laura found these types of systems useful, I soon discovered these to be too polar, and application of these chromatographic conditions to the crude extracts showed all components eluting with the solvent front. (see example, Picture II-1). A number of other systems were screened, containing varying ratios of chloroform, methanol, and ammonium acetate (95:5:0 to 98:1:1).¹¹⁴ In the end, although useful for TLC analysis, in my hands, none of these were highly successful in separation technology.

Picture II-1. Normal Phase Chromatogram of *T. heterophylla* (CMA mobile phase)



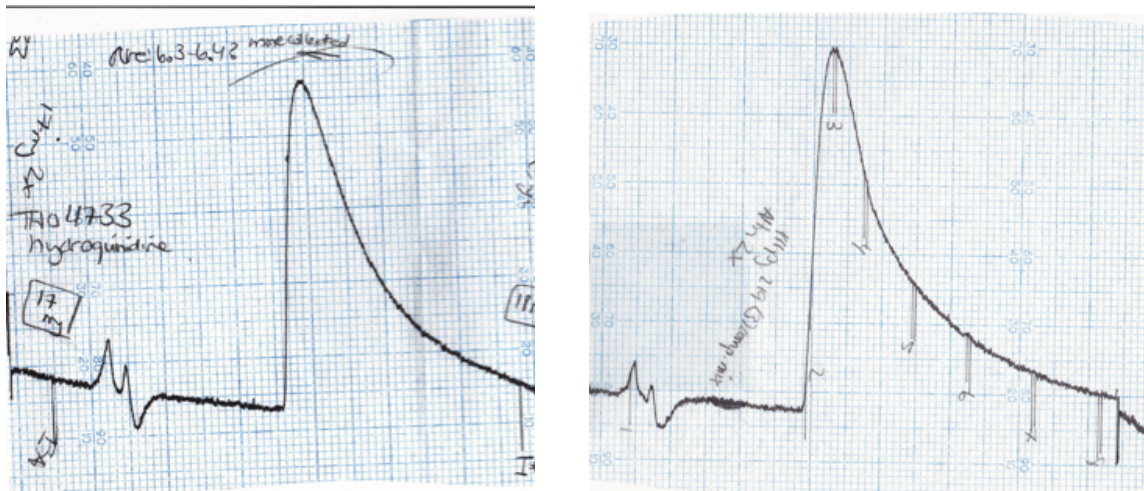
In reverse-phase systems, there are several considerations. The main is whether our current techniques would be applicable. Our pumps had to be able to withstand the increased backpressure expected from aqueous phases. We had to learn to pack our

columns with different materials. As mentioned, there is the ability to separate based on size, and we had to decide if that was an important feature for us. There was an open question of loading capabilities. We had to consider our RI detectors (sensitivity and detection) and look to add another method of detection (UV).

Based on work by previous group members (M.J. Richards), our pumps were demonstrated to be suitable for the new solvent systems. Ms. Richards also found column packing was best performed by a slurry method. Her previous studies indicated that at least a 7:3 MeOH:H₂O could be used at a flow rate of 5 ml/min. I found that increasing the water content did not bring significant issues. Moreover, a flow rate of 6 mL/min was effective for all samples, and that I did not have a problem loading up to 100 mg onto the column (standard loop injection as in normal phase).

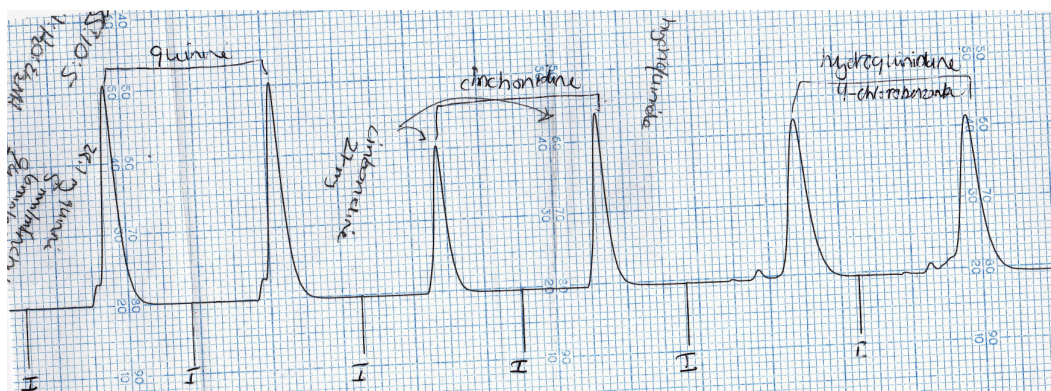
The biggest problem that I encountered with initial RPLC experiments was peak shape. No matter the composition (polarity) of the solvent system or the flow rate, peak tailing was observed. Even the different types of molecules studied (brucine, closely associated with strychnos alkaloids, versus cinchona alkaloid, see Figure II-2) showed similar behavior. Some examples are given at throughout this section. One particularly disappointing experiment is where I combined three commercial samples (quinine, hydroquinidine 4-Clbenzoate, and the cinchonidine alkaloid). LCMS indicated these to be separable and I had observed them to be differentially retained on the column. These components co-eluted and the peak looked no different than as if one chemical were present (compare Pictures II-2 and II-3). Thus, although I was able to move components off the column, the similar retention and tailing was surely going to hinder separation attempts

Picture II-2. Hydroquinidine 4-Cl-benzoate (Alone) and **Picture II-3.** Mixture of 3 Test Alkaloids (Quinine, Hydroquinidine 4-Cl-benzoate, and the Cinchonidine alkaloid)



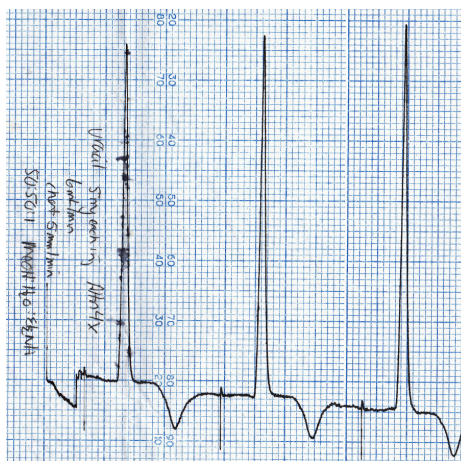
Tailing is a common concern in reverse phase chromatography. There are many additives that can be used to adjust the mobile phase properties and improve peak shape. Although differing the composition of the MeOH/H₂O system did not work, I thought additives were promising. DMF is commonly added¹¹⁵ but I did not see an improvement when I attempted to follow quinine elution under 80:10:10 MeOH:H₂O:DMF conditions. I then tried both an acid (TFA)¹¹⁴ and base (diethylamine)¹¹⁶ and both immediately improved peak shape and elution behavior for all compounds in the test series. For the latter, I began by using 80:10:10 MeOH:H₂O:Et₂NH, but through experimentation, I found that scaling back to 80:19:1 had the same beneficial effect. Loadings as low as 0.5 % Et₂NH were attempted, but tailing was found to become observable in these cases. Thus, I settled on Et₂NH as an additive, and depending on the polarity, the ratio of MeOH to H₂O would be varied. This was tested and proven effective on all the alkaloids in the test set (Picture II-4).

Picture II-4. Quinine, Cinchonidine, and Hydroquinidine Alkaloids (New Conditions).



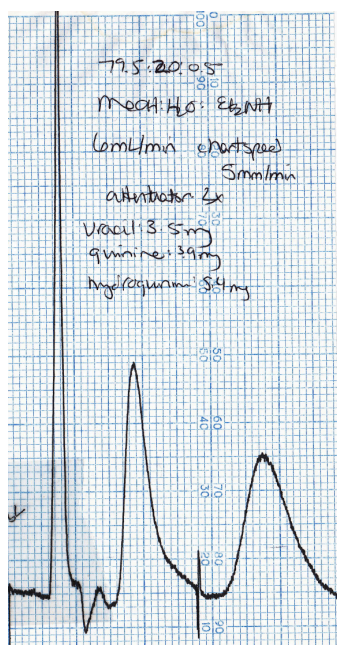
Before applying to the real system, I also confirmed that my system would be effective for another test molecule. Uracil is often used as a standard in reverse-phase HPLC, and it was important that it behaved well under the chromatographic conditions I designed. Moreover, it was important that I be convinced that changing the solvent system could vary the retention of uracil. Uracil¹¹⁷ is so polar that it seemed to elute with the solvent front (Picture II-5) regardless of how I varied the mobile phase, even to contain mostly MeOH. I could not even successfully load the sample of uracil in anything containing more than 50% MeOH. However, I was satisfied that I actually saw this very sticky molecule move effectively down a preparative reverse phase column (albeit at the solvent front), and I moved forward. I also reasoned that uracil would not interfere with separation of the other less polar compounds since it could always be assumed to elute quickly off the column, leaving the rest of components to elute, subject to increasing or decreasing polarity as I pleased.

Picture II-5. Uracil Behavior (and Replications).



I began with another proof of principle experiment for my chosen mobile phase with Et₂NH additive. I mixed a selection of my test compounds, as previously attempted, for separation (Picture II-6). With the new solvent system, I was delighted to see baseline separation of the three alkaloids I chose. I also noticed as I was working with these that they had different RI responses. That is, uracil seemed to elicit the most dramatic response with the same mass loading of sample. That became a factor to consider when moving onto more complicated samples, as well as a reason for including a UV detector in line for additional analytical power.

Picture II-6. Improved Separation of a Mixture of Test Alkaloids (Uracil, Quinine, Hydroquinidine 4-chlorobenzoate).



NMR spectroscopy and, more commonly, LCMS evaluated the success of these types of experiments. This provided a way to judge not only the purity of the eluting compounds but also test if materials were stable to conditions. It gave yet another measure of the polarity of the expected alkaloids and an opportunity to tune the methods of the instrument to work best for the expected compounds.

Finally, the stage was set for the purification of crude extracts. The only remaining concern is that RPLC solvents are higher boiling (compared to hexanes, ethyl acetate used in corresponding normal phase) and that column fractions might be difficult to concentrate. Moreover, there always seemed to be remaining Et₂NH (although it being

the lowest boiling of the mobile phase constituents). Or rather, it was retained in my fractions by some other form (protonation or otherwise). Later, in some cases I found this impurity could be removed by running the sample through plug of silica gel.

IV.C.2. Application of RPLC to Collected Amazonian Plants

With the chromatographic conditions developed and proven to be robust, I moved onto more challenging samples. The typical process was to test the crude extracts and some of the roughly partitioned extracts. Because of the wide variety and varying levels of polarity in the components of a plant, these rough partitions were beneficial in roughly separating less polar components by way of hexane/ACN partition. With these less polar species, normal phase chromatography could also be considered. In fact, it was expected that iterative use of the appropriate chromatographies (normal phase, reverse phase, or a series which used both) would be required to supply our alkaloids in pure form.

As the project advanced, we hoped to identify the actual chemical structures that are responsible for the biological activity. At the very least, we would make an original contribution to the field by reporting the novel natural products we isolate. Success at the outset was very likely - we had already discovered that there are biologically active components contained in these plants and we have the tools (now I could confidently use RPLC) to isolate and identify them.

We identified which species were most promising through the biological testing. We were also looking to select species that met the following qualifications:

sufficient plant material in stock

relatively understudied – chances to novel structures would be higher

IV.C.2.a. History of *T. heterophylla*, *T. siphilita*, and *T. sananho*

The first species, *Tabernaemontana heterophylla* (Picture **II-6**¹¹⁸) is most commonly referred to by the *heterophylla* identifier but has several synonyms: *T. tenuiflora*, *Peschiera heterophylla*, *P. diversifolia*, *P. senuifolia*, and *Stenosolen heterophyllus*. It was identified by Vahl,¹¹⁹ and has been called into question, but is unquestionably a member of Apocynaceae. It has a number of folk uses in Amazonian ethnomedicine,⁹³ including

Peru and Brazil, where it is used in tea for “old people who are slow and forgetful.” Its ethnopharmacology is relatively well studied and it is known to contain indole alkaloids.^{120,121} Some examples are provided in Figure II-3. Laura Kwong performed some preliminary work on this species, but there was still promise of identifying the chemical components. In fact, since this species is so well understood, it seemed an appropriate way to begin my endeavors in natural product isolation. As a novice, I would be working with extracts known to contain tractable quantities of alkaloids and practice my techniques before moving on to more challenging systems.

Picture II-7. *Tabernaemontana heterophylla*.

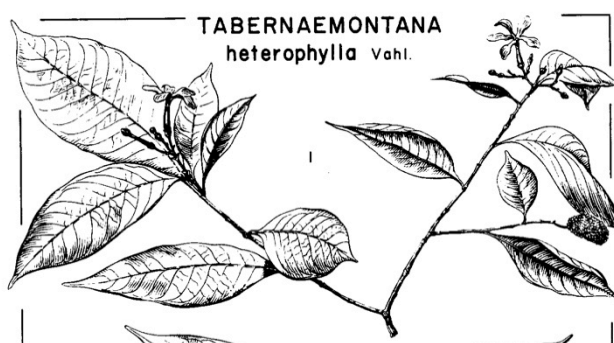
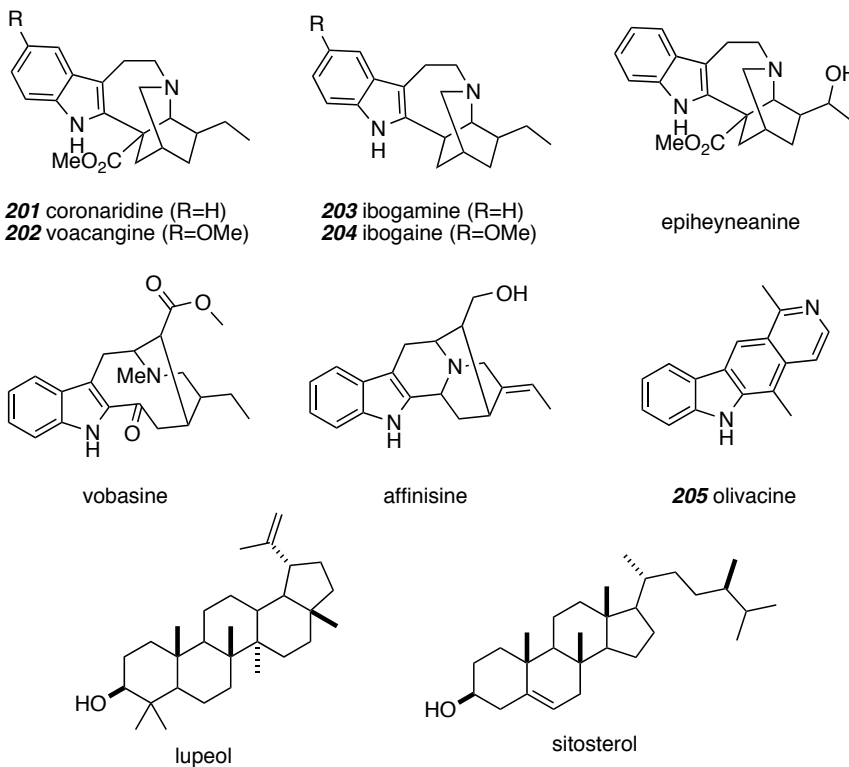
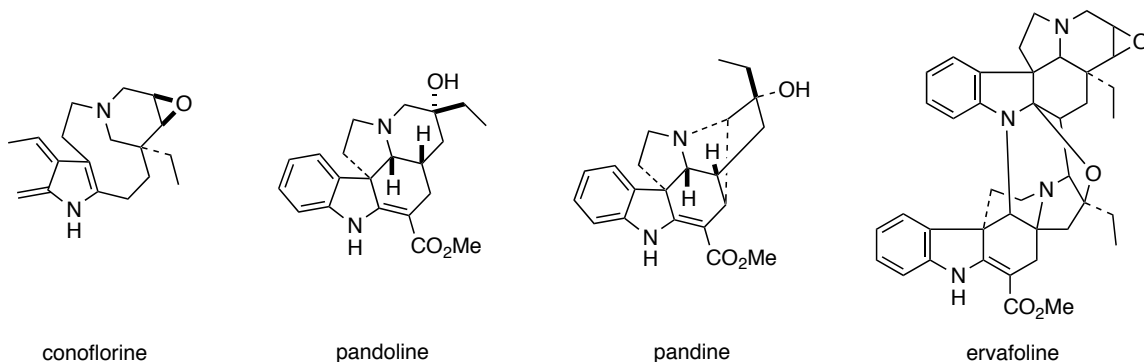


Figure II-3. Selected Alkaloids from *T. heterophylla*.



From another source, dimers^{121,122} have been found in the extracts (Figure II-4), as well as some other indole alkaloids of interest.

Figure II-4. Alkaloids from *T. heterophylla*, Representing a More Diverse Family.



It was with this information that I approached the species (see Section IV.C.2.b.)

T. siphilita (Picture II-8¹¹⁸) was also selected for study. This species is widely distributed in South America and has a large part of its history in Columbia and Ecuador. Its folk uses include treating eyes with drops of its latex to prevent sleep and taking the root in water for rheumatism.

Picture II-8. *Tabernaemontana siphilitica*.

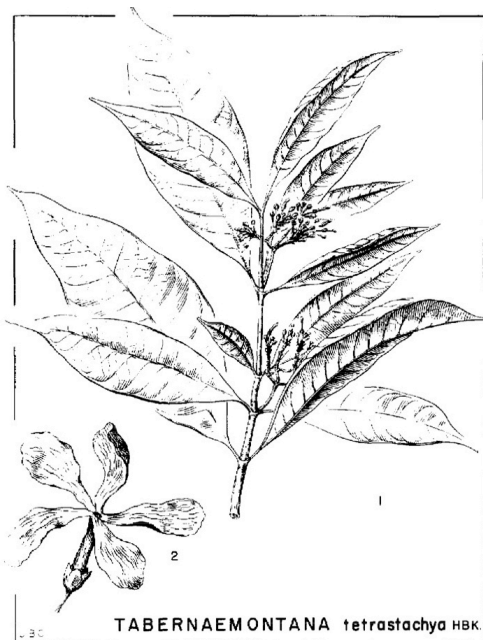
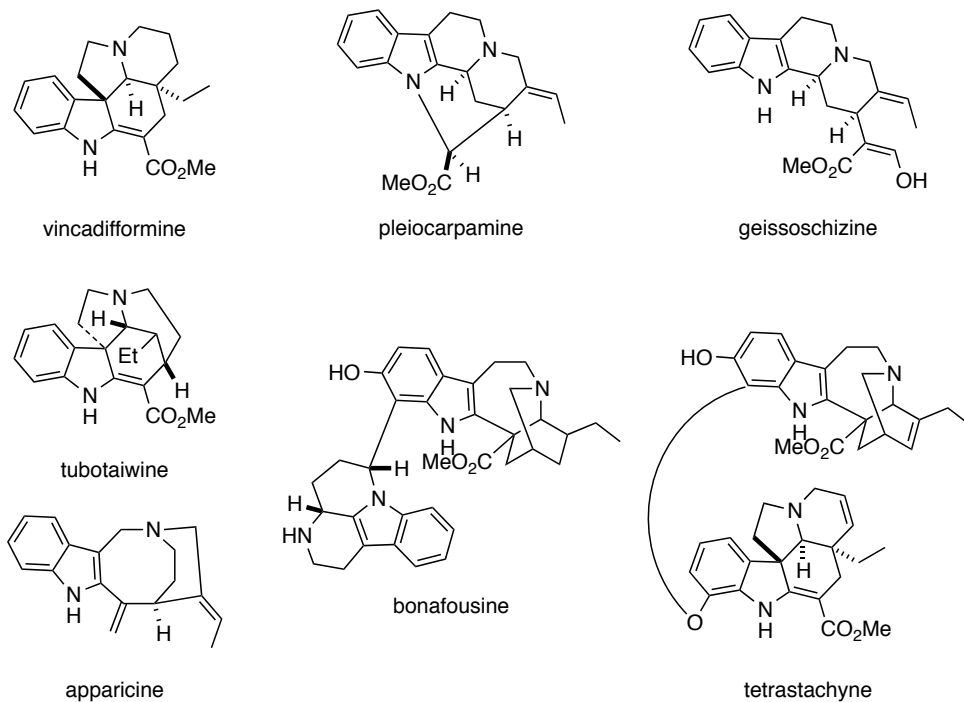


Fig. 12. *Tabernaemontana tetrastachya* Humboldt, Bonpland et Kunth: 1, habit with buds (x 3/4); 2, flower (x 2). (Drawn by J. B. Clark.)

The photochemistry of *T. siphilitica* is also fairly diverse, and it is known to contain several types of indole alkaloids and dimers (representative are shown in Figure II-

5)^{122,123}. It is probably the second best known of the three *Tabernaemontana* species discussed in this chapter.

Figure II-5. Selected Alkaloids from *T. siphitiica*.



What is evident from this sampling is that the *T. siphitiica* (*tetrastachya*¹²⁴) species contains a number of different skeletal systems. These have been discussed in numerous sources. Moreover, the set of dimers are fundamentally different than *T. heterophylla*.

*T. Sananho*¹²⁵ (Picture II-9) was the final species chosen for study. It is most widely distributed in the uppermost Amazon and has the most and best-documented folk uses of all the plants chosen for this study. It is best described as an all-purpose medicinal plant.¹¹⁸ Its many uses include fever reduction, emesis, diuresis, and calmative therapy. The plant can be used orally (the root in water) or topically (wash wounds with ground bark and leaves).

Picture II-9. *Tabernaemontana sananho*.

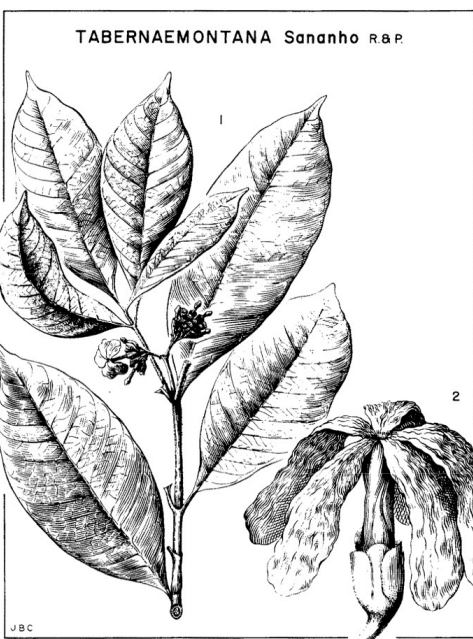
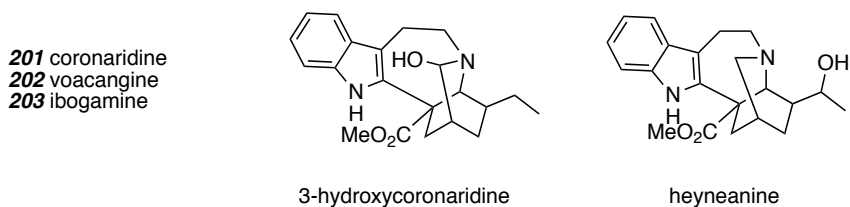


Fig. 11. *Tabernaemontana Sananho* Ruzé et Pavón: 1, habit with flower and buds ($\times \frac{2}{3}$); 2, flower ($\times 2 \frac{2}{3}$). (Drawn by J. B. Clark.)

T. sananho is understudied compared to *T. heterophylla*. Schultes strongly encouraged a thorough phytochemical and pharmacological investigation. In fact, it has only been reported to contain a few alkaloids¹²⁶ (notably, esters **201** and **202**) that were mentioned in the previous text and figures.

Figure II-6. Selected Alkaloids from *T. sananho*.



We had various parts of the plants on hand, and the typical extraction process was used.

IV.C.2.b. Alkaloids of *T. heterophylla*, *T. siphilita*, and *T. sananho*

The extraction process was performed exactly how prescribed. The details of the process are summarized in Table II-1. In general, the parts of the plants were extracted as they came, and in this series, they were divided by part. Between 9 and 25 g of plant material were extracted into 1:1 MeOH:CH₂Cl₂ for 6 days. In some cases, the extraction

solvent was decanted one or more times during this process and fresh solvent was supplied for further extraction. Crude mass recovery was typically 3-9 % of dried plant weight. Further extraction (beyond 6 days) was attempted in some cases, but never greatly contributed to the mass recovery.

Table II-1. Extraction Details for Plant Samples.

Species	Identifier	NB page	mass material	extraction recovery	partition	insoluble	hexane layer	acetonitrile layer
heterophylla	87RTS	IIIpg203	25 g	870 mg	Hex/MeCN (IIIpg227)	215 mg	25 mg	45 mg
	87BK	IIIpg205	25 g	750 mg	Hex/MeCN (IIIpg228)	285 mg	26 mg	38 mg
siphiitica	42WP	IIIpg234	15 g	720 mg	no			
sananho	97LVS	IIIpg235	9 g	790 mg	no			
	97RTS	IIIpg236	20 g	1.01 g	no			

As the table indicates, recoveries around 1g were realized for all extractions, regardless of the starting mass of plant material. If partitioning was attempted, the recoveries suffered even more. For example, in the first entry, 2/3 of the extract was lost, and it seemed like very little of the crude extract was contained in either the hexane or acetonitrile layers. Most was insoluble. This was also observed in the second entry, where over half the extract was lost upon fractionation. For future endeavors here, a better partition process must be adopted.

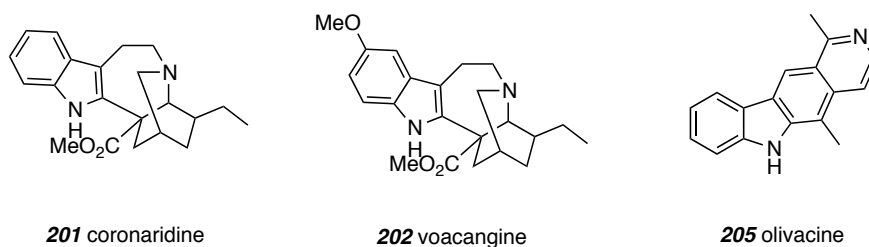
After the crude material was submitted to LC/MS, I analyzed the data. I was looking for general features such as a measure of the rough number, polarity, and mass of the components. Based on the literature, I could hypothesize the identity of various components, but verification by other means (typically ¹H NMR spectroscopy) was necessary.

T. HETEROPHYLLA

In the case of T. heterophylla, I partitioned the recovered crude material (approx. 0.9 g) but most of the mass remained insoluble when treated with 1:1 Hexanes:MeCN solvent pair; only 70 mg total were obtained from concentration of the hexane or acetonitrile layer). This insoluble material was further examined when the soluble

material was spent. Because the partition did not yield material with dramatically different LC/MS chromatograms, this process was not applied to the crude extracts of *T. siphilitica* or *T. sananho*. At this stage, extracts in various forms were taken onto MPLC separation under the conditions developed in the first part. Three compounds were identified with confidence, with the iboga alkaloids (**201**, **202**) the more abundant.

Figure II-7. Alkaloids found from *T. heterophylla*



The iboga type alkaloids **201** and **202** were expected, the first indication that they were present came for LCMS analysis of the acetonitrile layer from the secondary partition. Though seemingly easily separable, they were more difficult in practice, but using my optimized conditions and fractionation of MPLC peaks, I was able to separate these two alkaloids. Their identity is based on LCMS ionization behavior and congruence with the reported ^1H NMR data.^{127,128} Likewise, olivacine (**205**) gave appropriate mass and spectral data to confirm its identity by comparison to literature.¹²⁹⁻¹³¹

T. SIPHILITICA

For *T. siphilitica*, a partition was not performed, but crude extracts were loaded directly (or after Celite filtration, see experimental) onto the RPLC. Pictures II-10 and II-11 show that iterative chromatographies were required for separation of the compounds of interest. The first RPLC collected the iboga-type alkaloids **201** and **202**, and the second was needed to separate these from one another.

Picture II-10. RPLC of Crude *T. siphitica* Extracts and **Picture II-11** RPLC to separate **201** and **202**.

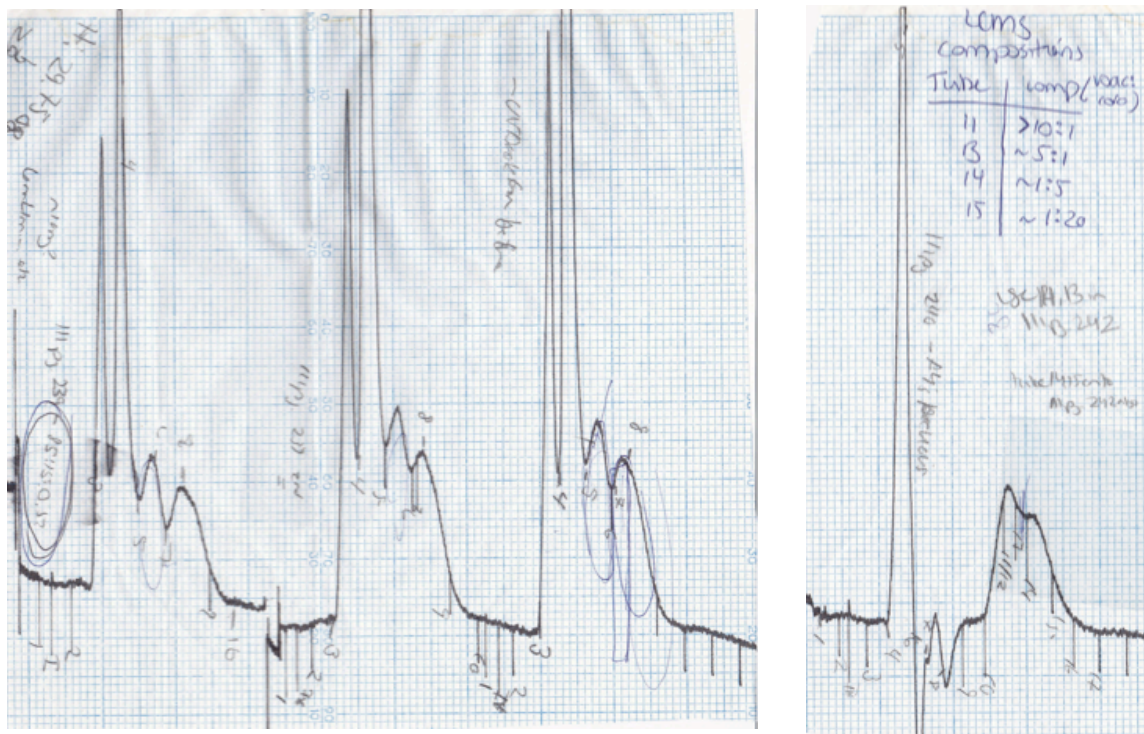
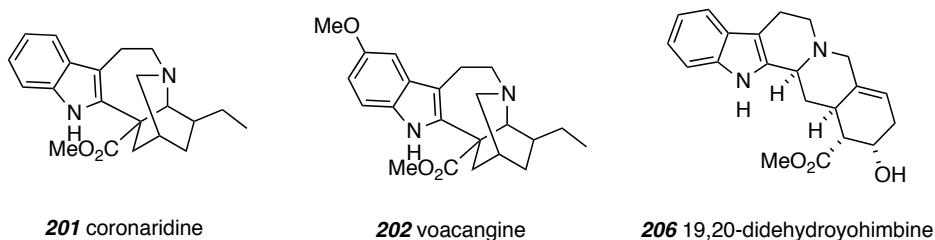


Figure II-8. Alkaloids found from *T. siphitica*

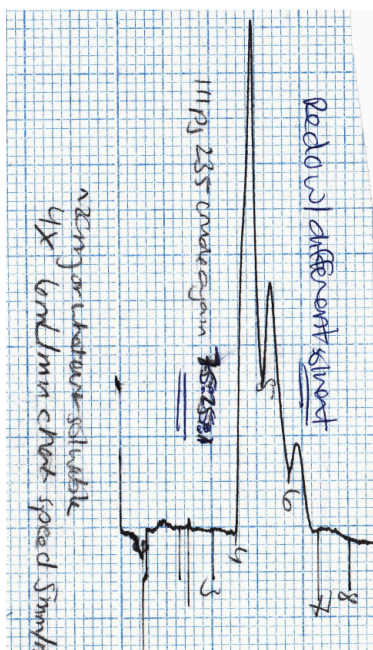


In the *T. siphitica* case, coronaridine (**201**) was identified as the main component based on the LCMS trace of a crude extract. A number of other components were present with varying polarities, and these masses were consistent with the known alkaloids already presented in Figure II-5, but these were never definitely identified. Discussion on **206** (a yohimbine derivative) is deferred to the following section, because it remained unassigned until it was also acquired from *Tabernaemontana sananho*.

T. SANANHO

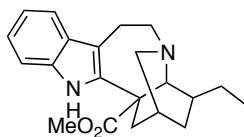
For T. sananho. again the crude extracts were subjected to RPLC without prior fractionation. A typical trace is given in Picture II-12 and shows that partial purification is necessary, but components were never directly isolated from the first RPLC run since baseline separation was not realized under these conditions.

Picture II-12. RPLC of crude T. sananho extracts.

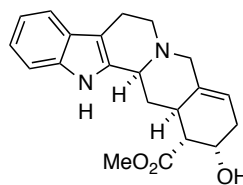


The experience allowed from investigation into T. heterophylla and T. siphitica was a valuable leading into study of T. sananho. This species was unlike the previously studied in two ways. First, the alkaloidal content seemed to vary based on the part of the plant under study. Further, T. sananho gave LCMS data that suggested that corynanthe-, not the expected (and previously observed) iboga-type alkaloids were the most prevalent

Figure II-9. Alkaloids found from T. sananho



201 coronaridine



206 19,20-didehydroyohimbine

For example, the main component ionized in the positive to give an adduct with m/z 353 and in the negative m/z 411 (LCMS). As more data was collected and a literature search

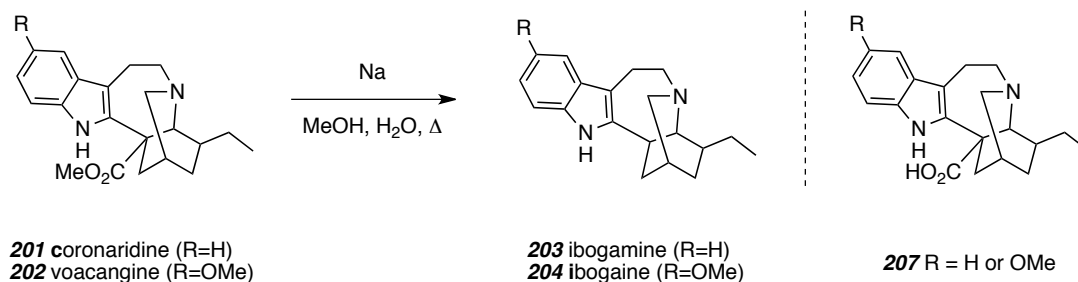
was undertaken,¹³²⁻¹³⁵ this was assigned as 19,20-didehydroyohimbine.^{136,137} LCMS analysis of the bark of this plant suggested a much smaller contribution of this alkaloid, where the iboga type (e.g. **201**) was more represented.

IV.C.3. Alkaloids Prepared

As further verification of structure and demonstration of functionality, alkaloids **201** and **202** were used in further reactions.¹³⁸ Besides these goals, there was an added opportunity to acquire data on the reaction products, which were also known natural products (Scheme II-3, alkaloids **203** and **204**). In this way, specific reactions were chosen to lead to these chemicals, and verification of my assignment of **201** and **202** was completed. These reactions were monitored by LCMS and the products analyzed by LCMS and ¹H NMR data.

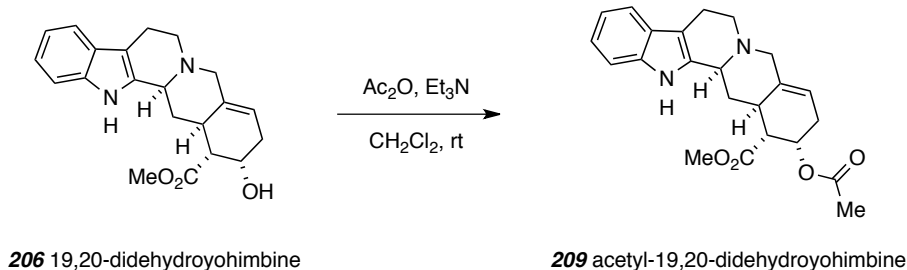
In the event, the base was prepared by dissolution of sodium metal in methanol (Scheme II-3). A small quantity of water was added, followed by a solution of either **201** or **202** in methanol. Surprisingly, supposed intermediate acid **207** was not observed, even when the reaction was attempted at room temperature. Upon heating, the mass corresponding to either ibogamine or ibogaine was observed by LCMS, and heating was discontinued when LCMS indicated full conversion of the esters. RPLC provided ibogamine (**203**) and ibogaine (**204**) with satisfactory ¹H NMR spectra, enabling verification of both these desired decarboxylated products and further evidence for the presence of coronaridine (**201**) and voacangine (**202**) in the plant samples studied.

Scheme II-3. Decarboxylation of **201** and **202**.¹³⁸



One of the goals at the outset of this project was to design a way to incorporate different functionality for the ultimate goal of library construction. This remains to be done on the alkaloids of Scheme II-3. I only had the opportunity to attempt a couple

Scheme II-5. Acetylation of **206**.¹³⁹



IV.D. Concluding remarks and Future Directions

Over the course of 10 months, I succeeded in using RPLC for the isolation and identification of the major components of three plant species. This was only a small advance in the overall goal of the project. Gratifyingly, this project did empower me as an organic chemist. I added the skills of a natural products chemistry and now have a more diverse, alternative perspective on how to identify and approach new opportunities in the field of ethnopharmacology.

Ultimately, the goal was to identify a novel structure and developing it into a potential therapeutic. I was not able to advance to the medicinal chemistry component of the project.

IV.D.1. Known Biological Activity of Alkaloids in *Tabernaemontana* Series.

The successful isolation and preliminary manipulations of these indole alkaloids shows them to be robust to handling and storage, but can undergo reaction. Along with our preliminary screening that identified them as biologically active, this makes them ideal candidates for future study. A number of reports on the activity of these compounds have appeared over the years, but study of analogues could yield promising results in the area of diseases of the central nervous system. These reported findings will not be discussed at length, but the references given provide a more detailed discussion.

The isolated alkaloids all had been shown to have some level of biological activity. Voacangine (**202**) has been tested in pharmacological screening and found to have a slight central stimulating effect. However, it appeared to have no effect on the heart and

was inactive in P388 and KB cell cultures. Coronaridine (**201**) had autonomic and CNS activity and exhibited estrogenicity. Interestingly, it was active against P388 cell cultures. **206** has not been studied for its biological activity. However, yohimbine has been extensively studied and is best known to have an effect in erectile dysfunction. It also has an effect on memory and could be used in treating Alzheimer's. Olivacine (**205**) was researched in different ways, but found to inhibit the growth of Protozoa. It also displayed KB and L-1210 activities.

The alkaloids I prepared also appear in the literature for their activity. Ibogaine (**204**) is probably the most studied of the alkaloids that I observed.¹⁴⁰ It has extensive central-stimulating properties and a transient hypotensive effect. It is labeled as a true hallucinogenic agent.¹⁴¹ It is not surprising, then, that ibogamine (**203**) has central-stimulating properties. Disappointingly, it is inactive in both the P-388 and KB systems in cell cultures studies. It has also been thoroughly evaluated for its CNS activity, but research into it as a therapeutic agent has ceased due to high cytotoxicity. *O*-Ac 19,20-didehydroyohimbine (**209**) was isolated as a natural product, but no biological testing has been performed to date.

IV.D.2. Future directions

This project holds a lot of promise. Methodology (RPLC) was developed for handling the various components present in extracts of Amazonian plants. Alkaloids from these extracts were successfully isolated and characterized. The next step would be continue study on these alkaloids for different ways that their known (or unknown) biological activity could be exploited. New alkaloids are also likely to be discovered by further investigation into the plant species. In the future, not only should the more minor components be targeted, but also lesser-known plants should be investigated by the same method. For this exercise, a lot was learned and a methodology developed, but the brightest future is in what is not known and is yet to be discovered about these Amazonian plants.

Certainly, in the long-term, a research program with this focus has the potential to impact modern medicine. Using clues from traditional medicine, new drug candidates could be discovered and new therapies could be developed.

Finally, this study was only enabled by a healthy working relationship between Prof. McKenna and all the required partners. These number many, and include traditional healers, faculty at the Universidad Nacional Amazonia Peruana in Iquitos, government officials both in the United States and abroad, Dr. Bryan Roth and scientists at the NIMH Psychoactive Drug Screening Program, and faculty at the University of Minnesota. At this stage, the project is best described as an exercise in ethnopharmacology, but as it advances, it becomes part a much more complex process of mass bioprospecting.¹⁴² Mass bioprospecting, or biodiversity prospecting encompasses the steps taken to convert indigenous or traditional medicine knowledge to commercial product. It is a much larger-scale operation and requires an agreement on issues such as genetic access, prior informed consent, intellectual property, and sharing of benefits. It is these requirements, as well as the necessity for highly trained botanists to live with and gain the trust of indigenous community, and competition from other technologies such as combinatorial chemistry and natural product libraries that limit the expansion of our studies.

IV.E. Selected Experimentals and ¹H NMR data

Various RPLC traces are provided in the text of this section. Additional information relevant to the handling and chemistry of the alkaloids (where applicable) is given below. This includes processes starting with plant extraction, sample preparation, and further chemistries performed on the natural products. For example, experimental details of reactions in Scheme II-2, II-3, and II-5 are described.

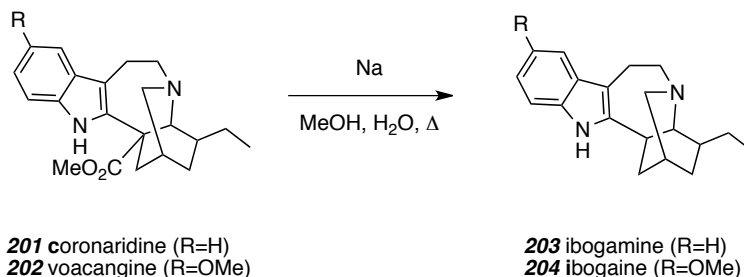
The acquired ¹H NMR spectra for all the known alkaloids are provided in this section. The reader is directed to the references for the known data on compounds **201-206** and **209**.

*General Extraction Process:*⁹⁵

Plants were extracted as they came: dried, ground, and sorted by plant part. Between 9 and 25 g of plant material were extracted into 1:1 MeOH:CH₂Cl₂ (approximately 100 mL for 25 g material) for 6 days. Gravity filtration and concentration resulted in the crude extract, which was submitted to LC/MS for analysis. Typical mass recovery was 3-9 % of dried plant weight. If further fractionation was desired, the crude extract was partitioned between hexanes and acetonitrile (40 mL total per gram crude extract). These fractions, and any remaining insoluble material were analyzed in the same way as the crude extracts.

Crude or partitioned extracts could be loaded directly onto a flash or pipette column and eluted with the chosen mobile phase, typically solutions comprised of chlorinated solvents (DCM or chloroform), methanol, and NH₄OH. Further preparation was required for the RPLC process. Methanol was added to the sample, the suspension was vigorously mixed and then filtered through a pipette of Celite. The resulting solution was concentrated under reduced pressure, then diluted by a minimal amount of solvent (0.5 mL for a 50 mg RPLC sample). The mobile phase was individually chosen for each RPLC run, and was always the chosen proportion of methanol and water. RPLC instrument loading was performed in the standard way. Elution of components was detected by differential RI and UV absorbance. Concentration was followed by LCMS and collection of the ¹H NMR spectrum for analysis of purity, and the process repeated if further purification was necessary.

Saponification of **201** to **203** and **202** to **204**



201 coronaridine¹⁴³ to **203** ibogamine:

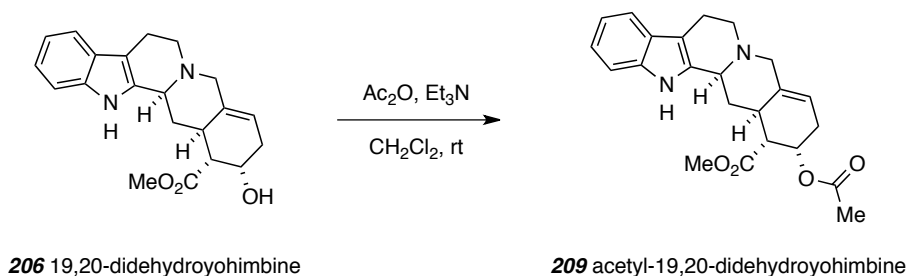
The residue from column chromatography (**201**, 10 mg, 0.027 mmol, 1 equiv) was dissolved in a solution of NaOH (0.5 M, 0.2 mL, 0.1 mmol, 4 equiv) followed by addition

of 0.2 mL of water. The solution was stirred at room temperature for 1 hour, at which point the volatiles were removed by rotary evaporation. The residue was dissolved in water (0.2 mL) and treated with concentrated HCl (approx. 5 μ L, pH of resulting solution \sim 1) and heated to 100 $^{\circ}$ C for 5 minutes. The solution was neutralized with NaHCO₃ and subjected to LCMS analysis. The major peak gave the mass of the desired decarboxylated product II-3. The crude ibogamine (**203**) could be purified by pipette column (1:1 Hexanes:Ethyl Acetate) and the resulting ¹H NMR data was consistent with that reported for the natural product.¹⁴³

202 voacangine to **204** ibogaine:

15 mg of voacangine¹⁴³ (**202**, 0.044 mmol, 1 equiv) was dissolved in a solution of NaOH (0.5 M, 0.4 mL, 0.2 mmol, ca. 4 equiv). Following addition of water (0.4 mL), the solution was stirred at rt for one hour then concentrated by rotary evaporator. The resulting residue was dissolved in water (0.5 mL) and acidified to pH \sim 1 by addition of HCl. This solution was heated to 100 $^{\circ}$ C for 5 minutes, followed by cooling and neutralization by dropwise addition of a saturated solution of NaHCO₃. The crude product was analyzed by LCMS, which indicated that **204** was the major product. The crude ibogaine (**204**) was purified by RPLC (80:20:1 MeOH:H₂O:Et₂NH) and gave ¹H NMR data that matched that reported for the natural product. The spectrum is provided below.

Acetylation of **206** to **209**:



19,20-didehydroyohimbine^{136,137} (5 mg, 0.014 mmol) was dissolved in DCM (50 μ L) and treated with 10 μ L each Ac₂O and Et₃N. The mixture was stirred at room temperature for 12 hours, at which time LCMS indicated that the starting material had completely

undergone reaction to the bis-ester **209**. The reaction was concentrated under reduced pressure and loaded directly onto a pipette column (eluting with 94:4:2 CHCl₃:MeOH:NH₄OH), providing acetylated derivative **209** (1 mg, 20%) whose spectral data was consistent with that known for **209**.¹³⁹ Both the starting material and product ¹H NMR spectra are provided.

References

- (91) Heinrich, M.; Gibbons, S. Ethnopharmacology in drug discovery: an analysis of its role and potential contribution. *J. Pharm. Pharmacol.* **2001**, *53*, 425-432.
- (92) Schultes, R. E. Plants in treating senile dementia in the northwest Amazon. *J. of Ethnopharmacol.* **1993**, *38*, 129-135.
- (93) Schultes, R. E. In *Phytochemical Gaps in our Knowledge of Hallucinogens*; Reingold, L., Harbourne, J. B. and Swain, T., Eds.; Progress in Phytochemistry; Pergamon Press: Oxford, UK, 1981; pp 301-331.
- (94) McKenna, D. J. Application of Ethnopharmacology and Receptor Screening Technologies to the Identification of Novel Natural Products for the Treatment of Cognitive Deficits in Schizophrenia. **2004**.
- (95) McKenna, D. J.; Ruiz, J. M.; Hoye, T. R.; Roth, B. L.; Shoemaker, A. T. Receptor screening technologies in the evaluation of Amazonian ethnomedicines with potential applications to cognitive deficits. *J. of Ethnopharmacol.* **2011**, *134*, 475-492.
- (96) Schotte, A.; Janssen, P. F.; Gommeren, W.; Luyten, W. H.; Van Gompel, P.; Lesage, A. S.; De Loore, K.; Leysen, J.E. Risperidone compared with new and reference antipsychotic drugs: in vitro and in vivo receptor binding. *Psychopharmacology* **1996**, *124*, 57-73.
- (97) Roth, B. L.; Lopez, E.; Patel, S.; Kroeze, W. K. The Multiplicity of Serotonin Receptors: Uselessly Diverse Molecules or an Embarrassment of Riches? *The Neuroscientist* **2000**, *6*, 252-262.
- (98) Phillipson, J. D. Radioligand-receptor binding assays in the search for bioactive principles from plants. *J. Pham. Pharmacol.* **1999**, *51*, 493-503.

- (99) Roth, B. L.; Sheffler, D. J.; Kroeze, W. K. Magic shotguns versus magic bullets: selectively non-selective drugs for mood disorders and schizophrenia. *Nat Rev Drug Discov* **2004**, *3*, 353-359.
- (100) Gray, J. A.; Roth, B. L. The pipeline and future of drug development in schizophrenia. *Molecular Psychiatry* **2007**, *12*, 904-922.
- (101) Gray, J. A.; Roth, B. L. Molecular Targets for Treating Cognitive Dysfunction in Schizophrenia. *Schizophr. Bull.* **2007**, *33*, 1100-1119.
- (102) Harvey, A. L. Natural products in drug discovery. *Drug Discovery Today* **2008**, *13*, 894-901.
- (103) Sullivan, R. J.; Allen, J. S.; Otto, C.; Tiobech, J.; Nero, K. Effects of chewing betel nut (*Areca catechu*) on the symptoms of people with schizophrenia in Palau, Micronesia. *The British journal of psychiatry : the journal of mental science* **2000**, *177*, 174-178.
- (104) Newman, D. J.; Cragg, G. M. Natural products as sources of new drugs over the last 25 years. *J. of Nat. Prod.* **2007**, *70*, 461-477.
- (105) Nicolaou, K. C.; Snyder, S. A. Chasing Molecules That Were Never There: Misassigned Natural Products and the Role of Chemical Synthesis in Modern Structure Elucidation. *Angew. Chem. Int. Ed.* **2005**, *44*, 2050-2050.
- (106) Van Beek, T. A.; Verpoorte, R.; Svendsen, A. B.; Leeuwenberg, A. J. M.; Bisset, N. G. *Tabernaemontana* L. (Apocynaceae): A review of its taxonomy, phytochemistry, ethnobotany and pharmacology. *J. Ethnopharmacol.* **1984**, *10*, 1-156.
- (107) Boekelheide, V.; Grundon, M. F. A Characterization of $\hat{1}\pm$ -Erythroidine. *J. Am. Chem. Soc.* **1953**, *75*, 2563-2566.

- (108) TrojÁnek, J.; Åtrouf, O.; Holubek, J.; ÅEekan, Z. Structure of Vincamine. *Tetrahedron Lett.* **1961**, *2*, 702-706.
- (109) Lounasmaa, M.; Jokela, R.; Anttila, U.; Hanhinen, P.; Laine, C. Short synthetic route to (T₁)-geissoschizine. *Tetrahedron* **1996**, *52*, 6803-6810.
- (110) Inouye, H.; Ueda, S.; Nakamura, Y. Struktur des swerosids, eines neuen glucosides aus swertia japonica makino. *Tetrahedron Lett.* **1966**, *7*, 5229-5234.
- (111) Stimson, M. M.; Reuter, M. A. The Spectrophotometric Estimation of Methoxy-cinchona Alkaloids1. *J. Am. Chem. Soc.* **1946**, *68*, 1192-1196.
- (112) McCalley, D. Analysis of the cinchona alkaloids by liquid chromatography. Reversed-phase chromatography on octadecylsilyl columns. *Chromatographia* **1983**, *17*, 264-266.
- (113) Kingston, D. G. I.; Li, B. T. Preliminary investigation of the use of high-pressure liquid chromatography for the separation of indole alkaloids. *J. Chromatogr. A* **1975**, *104*, 431-437.
- (114) Perera, P.; Van Beek, T. A.; Verpoorte, R. High-performance liquid chromatography of some Tabernaemontana alkaloids. *J. Chromatogr. A* **1984**, *285*, 214-220.
- (115) Ryba, M. Dimethylformamide as a mobile phase component in reversed-phase liquid column chromatography on octadecylsilica. *Chromatographia* **1982**, *15*, 227-230.
- (116) Wehrli, A.; Hildenbrand, J. C.; Keller, H. P.; Stampfli, R.; Frei, R. W. Influence of organic bases on the stability and separation properties of reversed-phase chemically bonded silica gels. *J. Chromatogr. A* **1978**, *149*, 199-210.

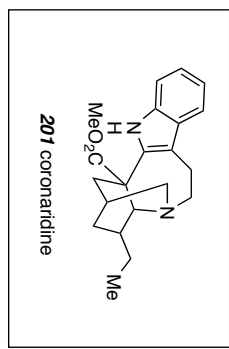
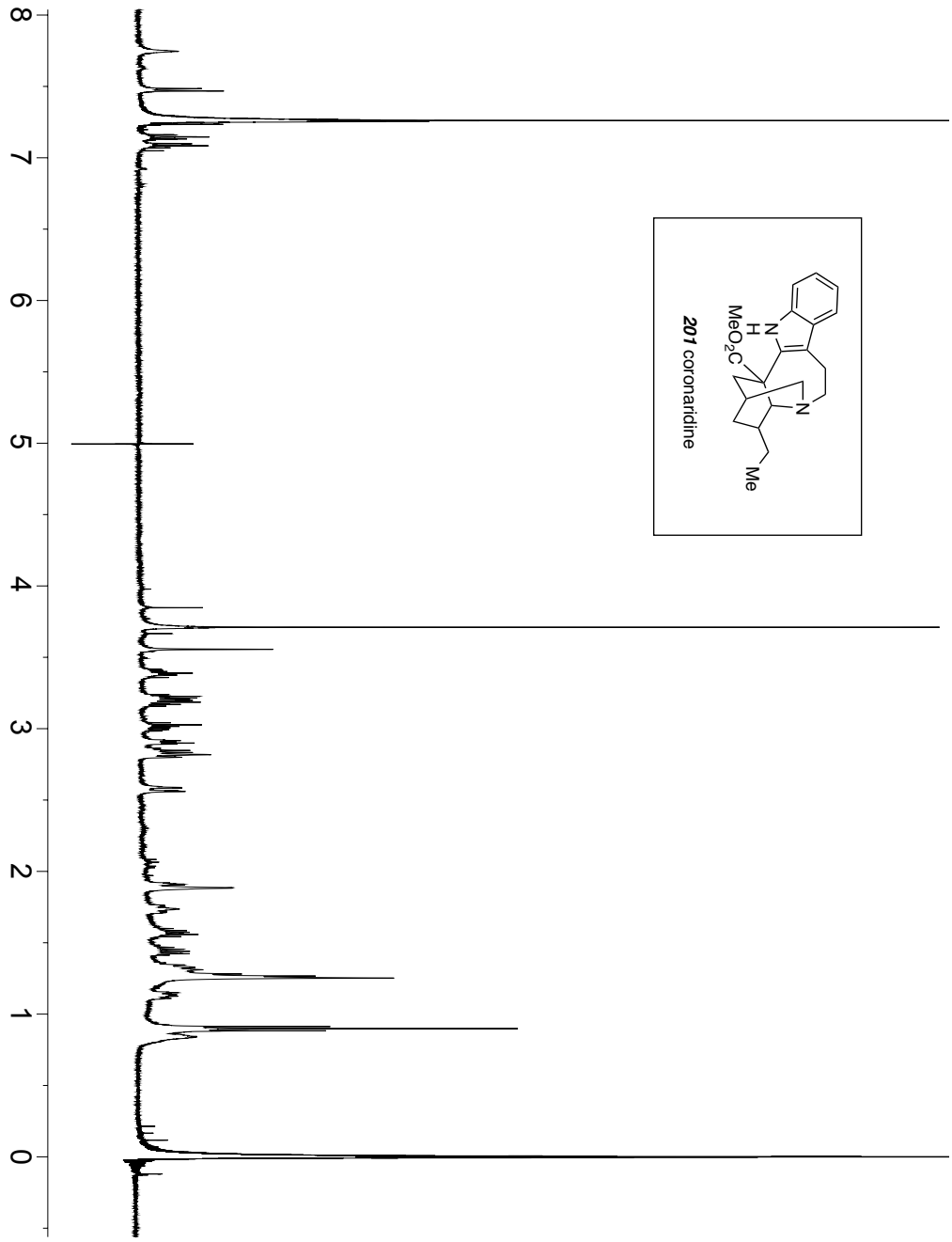
- (117) Gustavsson, T.; Sarkar, N.; Bányász, Á; Markovitsi, D.; Improta, R. Solvent Effects on the Steady-state Absorption and Fluorescence Spectra of Uracil, Thymine and 5-Fluorouracil? *Photochem. Photobiol.* **2007**, *83*, 595-599.
- (118) Evans Schultes, R. De plantis toxicariis e mundo novo tropicale commentationes. XIX. Biodynamic apocynaceous plants of the northwest amazon. *J. Ethnopharmacol.* **1979**, *1*, 165-192.
- (119) Vahl, M. In *Eclogae Americanae*; 1796.
- (120) Wolter Filho, W.; Pinheiro, M. L. B.; Imbiriba de Rocha, A. Alkaloids of *Tabernaemontana heterophylla* Vahl. (Apocynaceae). *Acta Amazonica* **1983**, *13*, 409-412.
- (121) Henriques, A.; Kan, C.; Chiaroni, A.; Riche, C.; Husson, H. P.; Kan, S. K.; Lounasmaa, M. New dimeric indole alkaloids from *Stenosolen heterophyllus*: structure determinations and synthetic approach. *J. Org. Chem.* **1982**, *47*, 803-811.
- (122) Abaul, J.; Philog, P.; Bourgeois, P.; Ahond, A.; Poupat, C.; Potier, P. Study on American *Tabernaemontanas*. VI. Alkaloids from the Leaves of *Tabernaemontana citrifolia*. *J. Nat. Prod.* **1989**, *52*, 1279-1283.
- (123) Leeuwenberg, A. J. M. In *A Chemotaxonomic Investigation of the Plant Families of Apocnaceae, Loganiaceae, and Rubaceae by Their Indole Alkaloid Content*; Pelletier, S. W., Ed.; Alkaloids: Chemical and Biological Perspectives; New York, Chichester, Brisbane, Toronto, and Singapore, 1983; pp 211-376.
- (124) Bonpland, A.; Humboldt, A. v.; Kunth, K. S. In *Nova genera et species plantarum : Lutetiae Parisiorum : sumtibus Librariae Graeco-Latino-Germanico*: 1818; Vol. v. 3, pp 641.
- (125) Ruiz, H.; Pavón, J.; Pavón, J. In *Flora Peruviana, et Chilensis, sive, Descriptiones et icones plantarum Peruvianarum, et Chilensium, secundum systema*

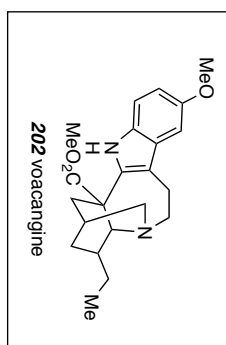
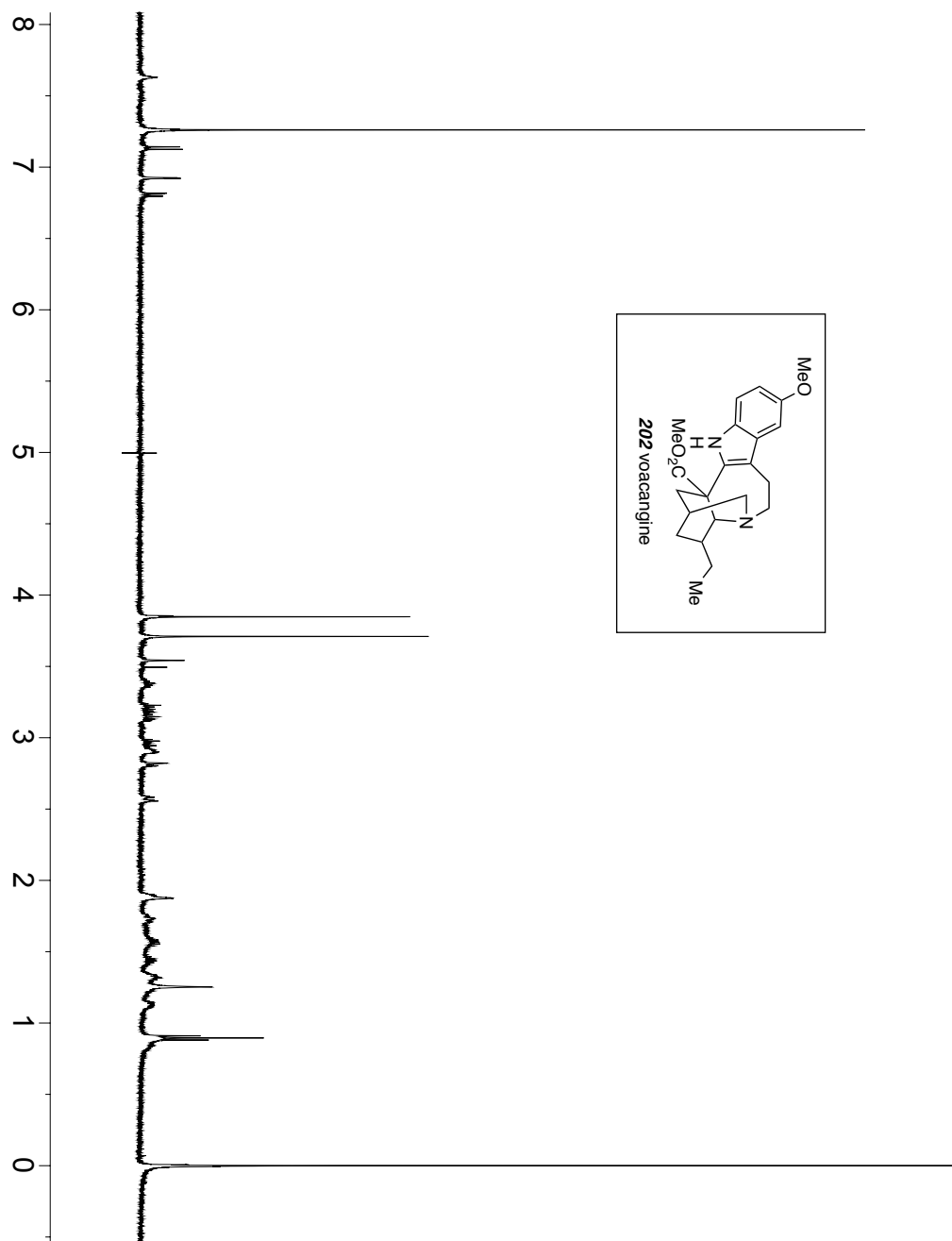
Linnaeanum digestae, cum characteribus plurium generum evulgatorum reformatis;
Madrid :Typis Gabrielis de Sancha: 1799; Vol. v. 2, pp 79.

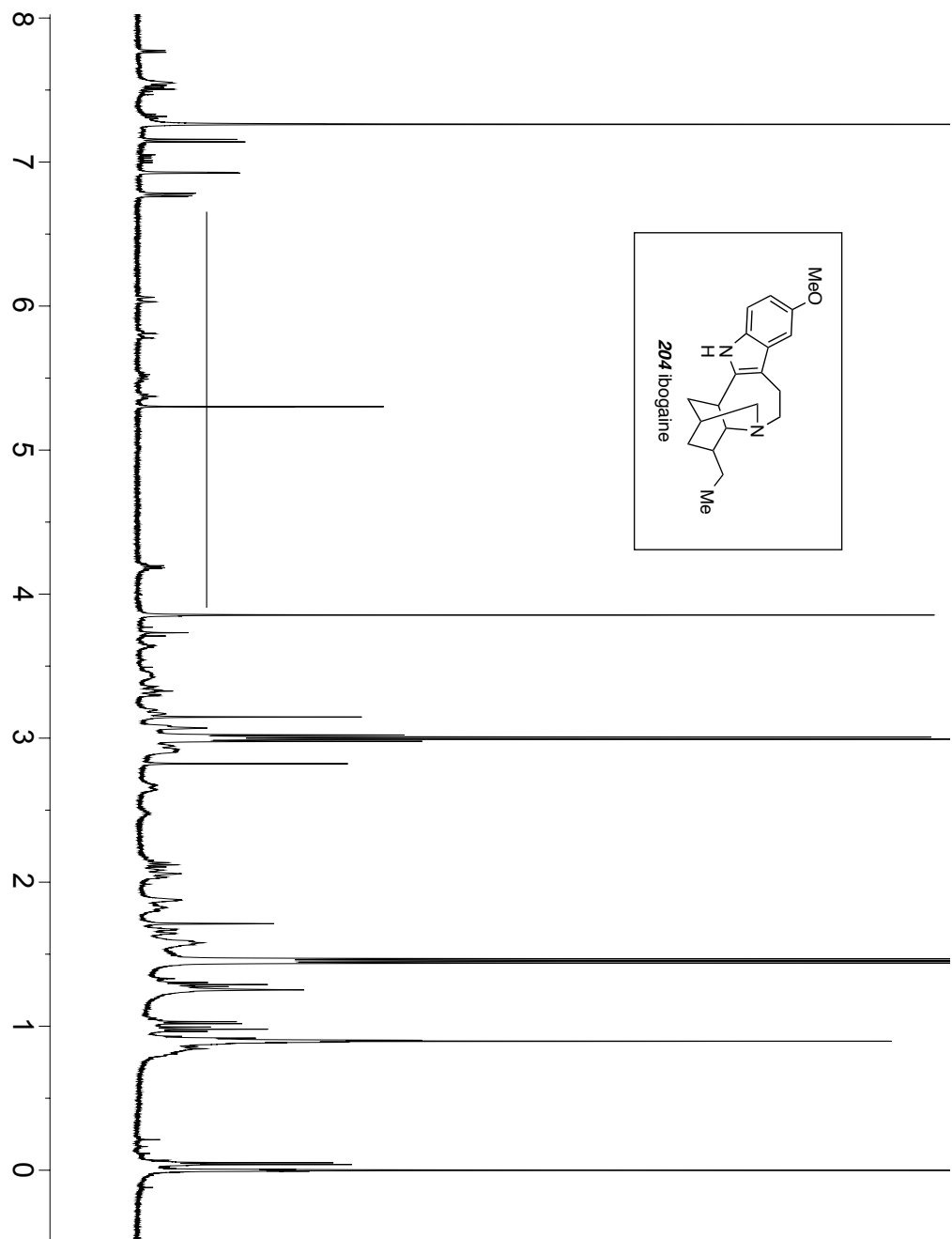
- (126) Delle-Monache, G.; Montenegro de Matta, S.; Delle-Monache, F.; Marini-Bettolo, G. B. Alkaloids of *Tabernaemontana sananho* R & P. *Atti della Accademia Nazionale dei Lincei* **1977**, *62*, 221-226.
- (127) Zocoler, M. A.; Oliveira, Arildo J. B. de; Sarragiotto, M. H.; Grzesiuk, V. L.; Vidotti, G. J. Qualitative determination of indole alkaloids of *Tabernaemontana fuchsiaefolia* (Apocynaceae). *J. Brazil. Chem. Soc.* **2005**, *16*, 1372-1377.
- (128) Jokela, R.; Lounasmaa, M. ¹H- and ¹³C-NMR Spectral Data of Five Sarpagine-Type Alkaloids. *Heterocycles* **1996**, *43*, 1015-1020.
- (129) Azoug, M.; Loukaci, A.; Richard, B.; Nuzillard, J.; Moreti, C.; Zeches-Hanrot, M.; Le Men-Olivier, L. Alkaloids from stem bark and leaves of *Peschiera buchtieni*. *Phytochemistry* **1995**, *39*, 1223-1228.
- (130) Sha, C.; Yang, J. Total syntheses of ellipticine alkaloids and their amino analogues. *Tetrahedron* **1992**, *48*, 10645-10654.
- (131) Ishikura, M.; Hino, A.; Yaginuma, T.; Agata, I.; Katagiri, N. A Novel Entry to Pyrido[4,3-b]carbazoles: An Efficient Synthesis of Ellipticine. *Tetrahedron* **2000**, *56*, 193-207.
- (132) Ghedira, K.; Zeches-Hanrot, M.; Richard, B.; Massiot, G.; Le Men-Olivier, L.; Sevenet, T.; Goh, S. H. Alkaloids of *Alstonia angustifolia*. *Phytochemistry* **1988**, *27*, 3955-3962.
- (133) Clivio, P.; Richard, B.; Deverre, J.; Sevenet, T.; Zeches, M.; Le Men-Olivier, L. Alkaloids from leaves and root bark of *Ervatamia hirta*. *Phytochemistry* **1991**, *30*, 3785-3792.

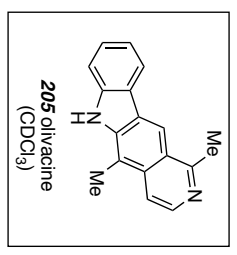
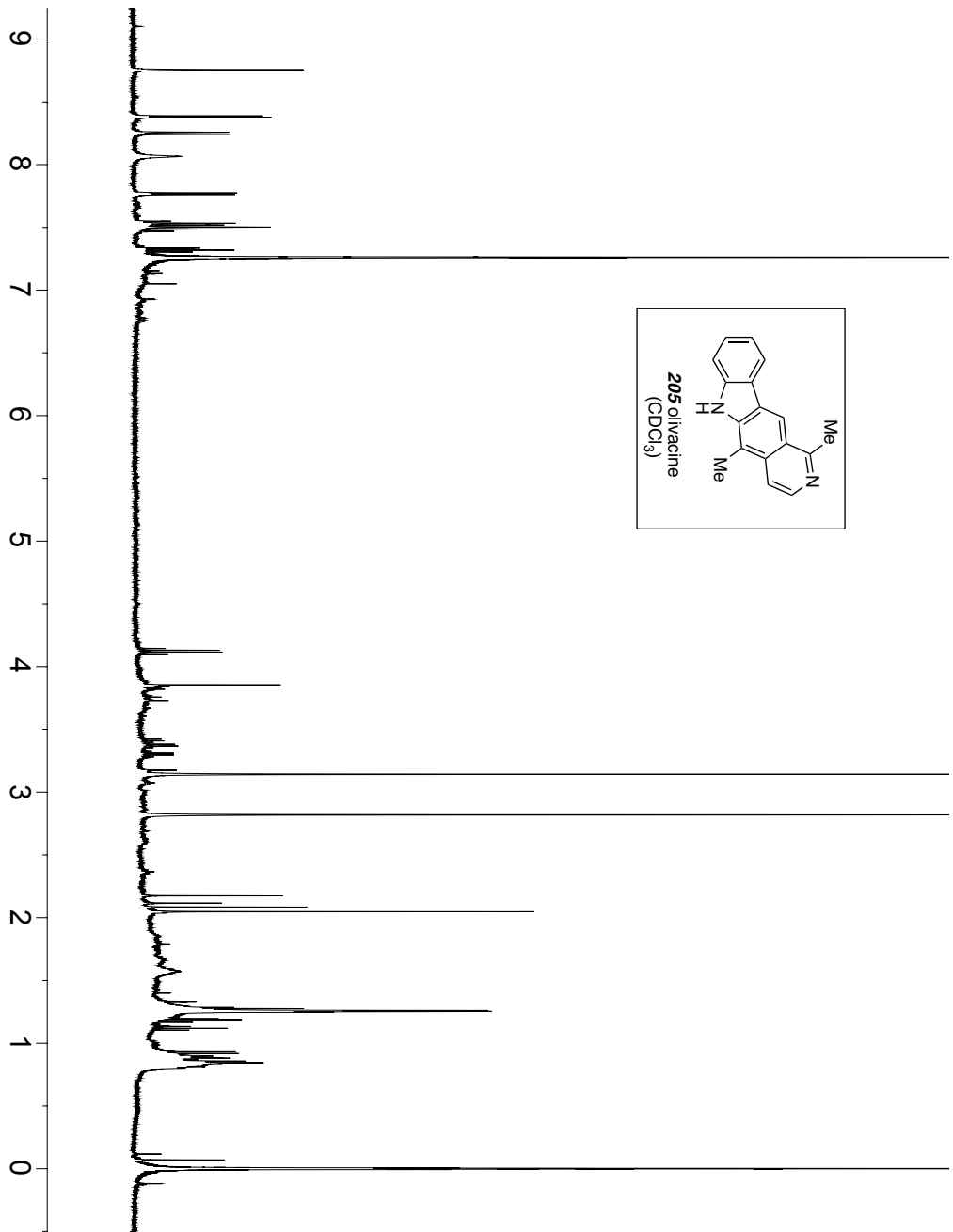
- (134) Timmins, P.; Court, W. E. Stem alkaloids of *Rauwolfia obscura*. *Phytochemistry* **1976**, *15*, 733-735.
- (135) Bennasar, M. -.; Vidal, B.; Bosch, J. Biomimetic Total Synthesis of Ervitsine and Indole Alkaloids of the Ervatamine Group via 1,4-Dihydropyridines. *J. Org. Chem.* **1997**, *62*, 3597-3609.
- (136) Naito, T.; Hirata, Y.; Miyata, O.; Ninomiya, I. Photocyclisation of enamides. Part 27. Total syntheses of (+/-)-yohimbine, (+/-)-alloyohimbine, and (+/-)-19,20-didehydroyohimbines. *J. Chem. Soc., Perkin Trans. 1* **1988**, 2219-2225.
- (137) Miyata, O.; Hirata, Y.; Naito, T.; Ninomiya, I. Total Synthesis of (+/-)-19,20-didehydroyohimbines. *Heterocycles* **1984**, *22*, 2719-2722.
- (138) Janot, M.; Goutarel, R. United States Patent, 1957.
- (139) Brown, R. T.; Pratt, S. B. Stereoselective synthesis of yohimbine alkaloids from secologanin. *J. Chem. Soc., Chem. Commun.* **1980**, 165-167.
- (140) Maciulaitis, R.; Kontrimaviciute, V.; Bressolle, F. F. M.; Briedis, V. Ibogaine, an anti-addictive drug: pharmacology and time to go further in development. A narrative review. *Human & experimental toxicology* **2008**, *27*, 181-194.
- (141) Bowen, W. D. In *Sigma Receptors and Iboga Alkaloids*; Cordell, G. A., Ed.; The Alkaloids: Chemistry and Biology; Academic Press: San Diego, 2001; pp 173-191.
- (142) Soejarto, D. D.; Fong, H. H. S.; Tan, G. T.; Zhang, H. J.; Ma, C. Y.; Franzblau, S. G.; Gyllenhaal, C.; Riley, M. C.; Kadushin, M. R.; Pezzuto, J. M.; Xuan, L. T.; Hiep, N. T.; Hung, N. V.; Vu, B. M.; Loc, P. K.; Dac, L. X.; Binh, L. T.; Chien, N. Q.; Hai, N. V.; Bich, T. Q.; Cuong, N. M.; Southavong, B.; Sydara, K.; Bouamanivong, S.; Ly, H. M.; Thuy, T. V.; Rose, W. C.; Dietzman, G. R.
Ethnobotany/ethnopharmacology and mass bioprospecting: Issues on intellectual property and benefit-sharing. *J. Ethnopharmacol.* **2005**, *100*, 15-22.

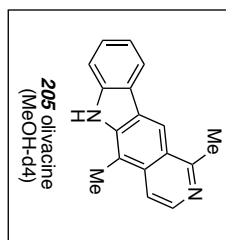
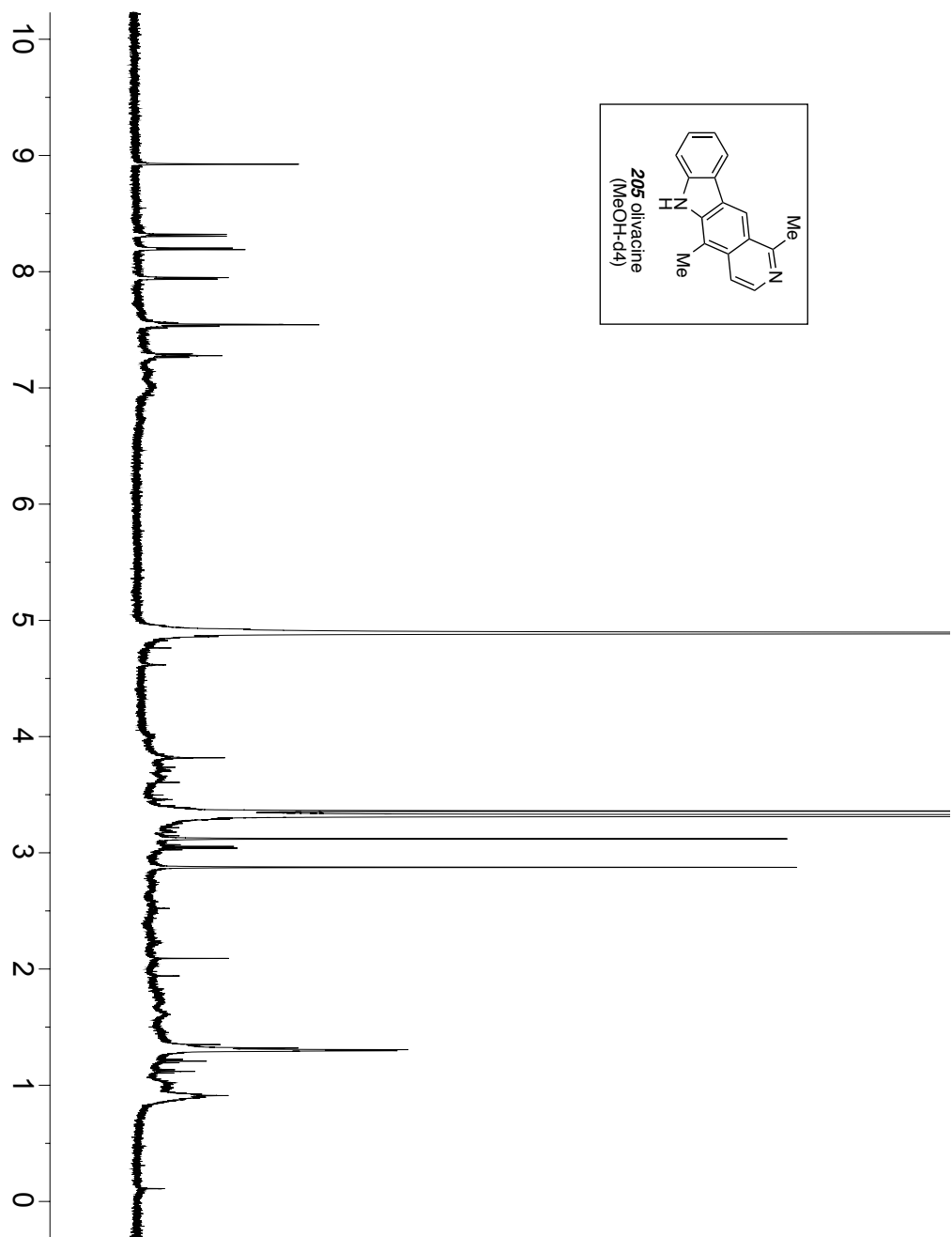
- (143) Pereira, P. S.; França, S. d. C.; Oliveira, Paulo Vinicius Anderson de; Breves, Camila Moniz de Souza; Pereira, S. I. V.; Sampaio, S. V.; Nomizo, A.; Dias, D. A. Chemical constituents from *Tabernaemontana catharinensis* root bark: a brief NMR review of indole alkaloids and in vitro cytotoxicity. *Química Nova* **2008**, *31*, 20-24.

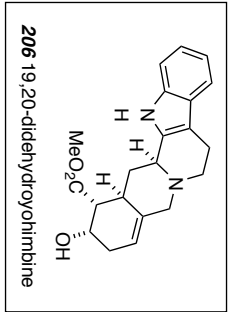
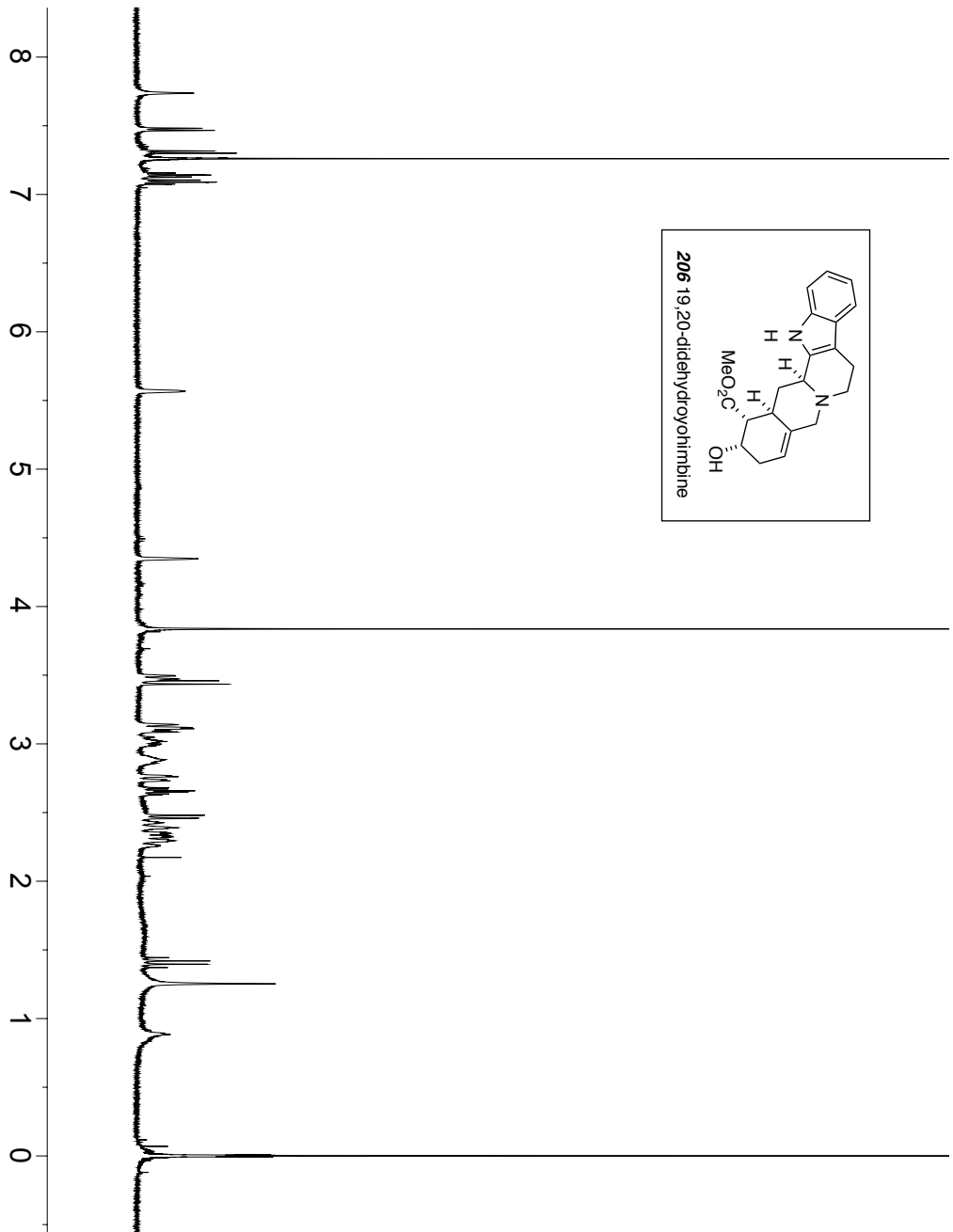


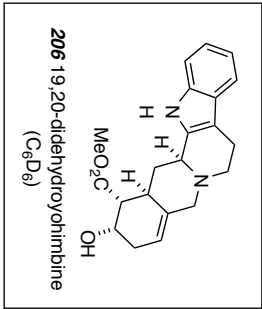
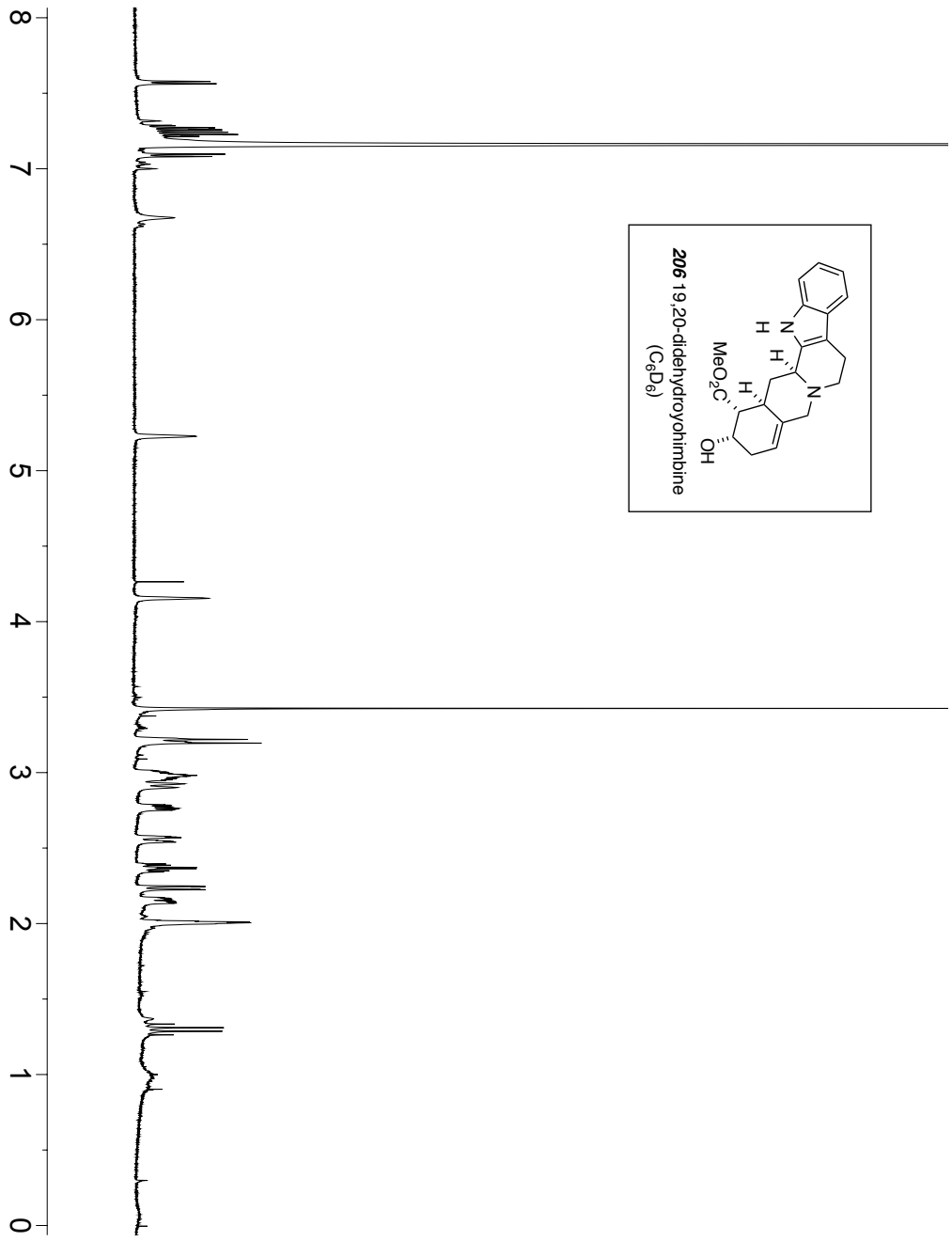


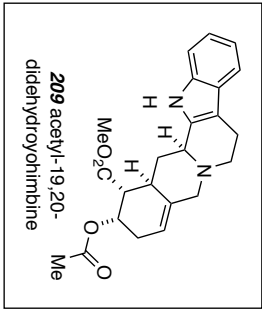
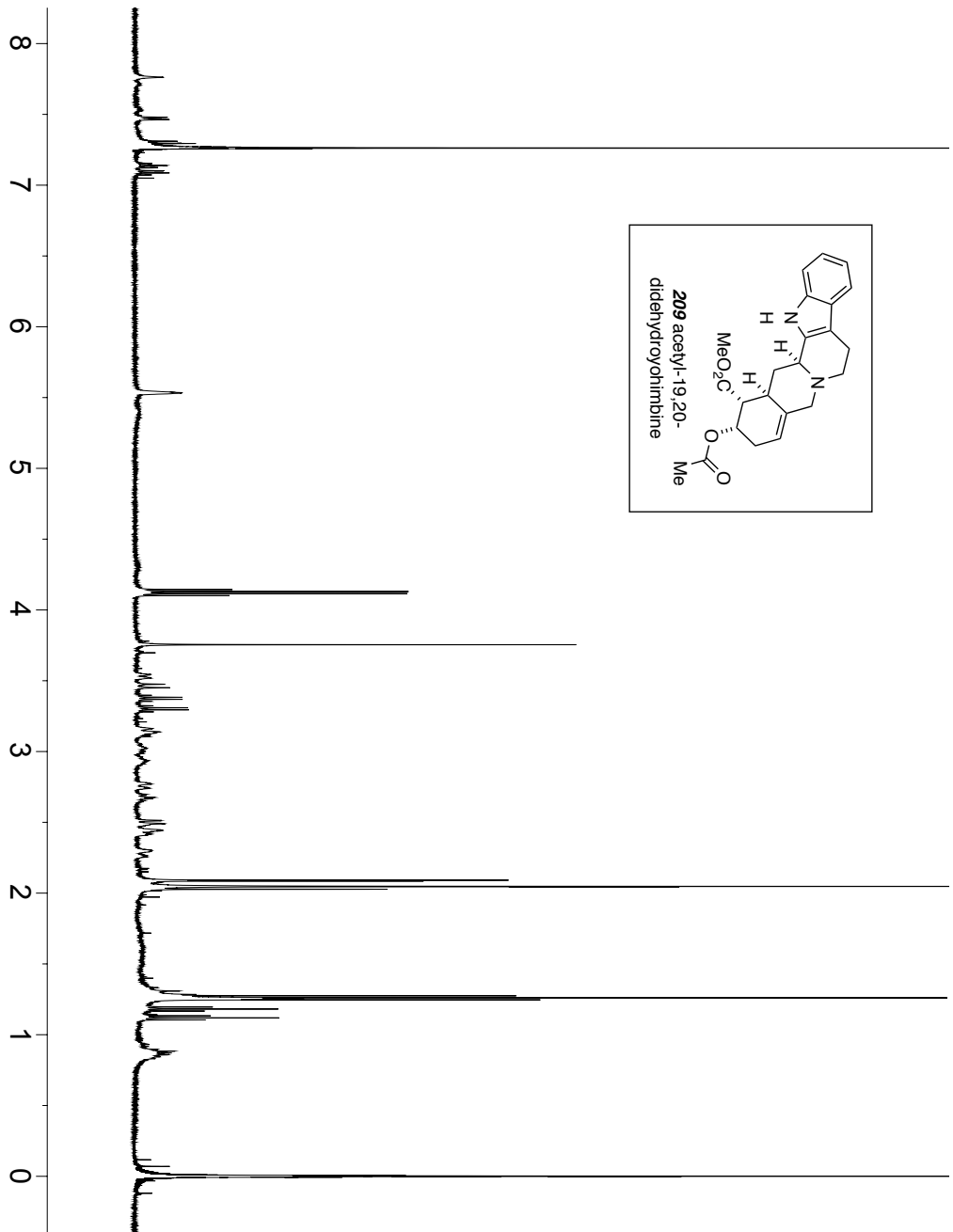










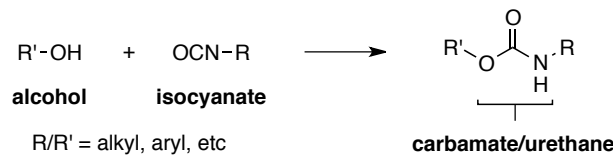


PART THREE – Polyols From Renewable Resources

General Introduction and background

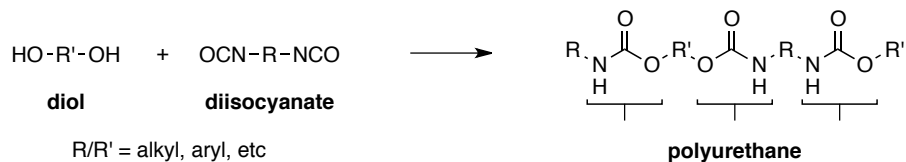
Polymers, or plastics, are materials that humanity cannot live without. There are many different types and applications, but a common feature of all is that they are built from much smaller units, monomers. For one particular type of polymer, a polyurethane (PU), the starting materials are an alcohol and an isocyanate (Scheme III-1). The reaction results in a carbamate, or urethane linkage that is denoted by the bracket.

Scheme III-1. General Reaction to a Carbamate.



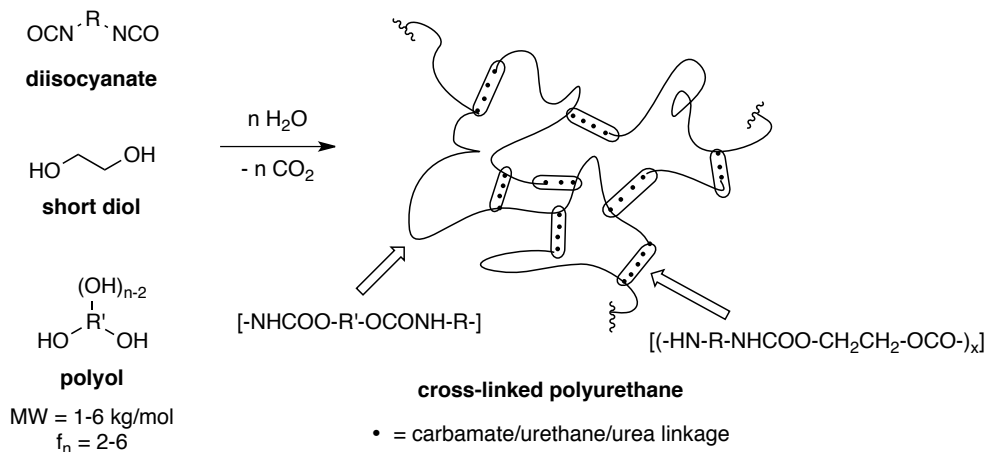
For polymerization leading to a polyurethane, these components must be difunctional so that more than two units can be chemically linked (Scheme III-2). Now there are multiple carbamates (brackets), all connected by whatever is contained in R and R'.

Scheme III-2. General Reaction to a Polyurethane.



For many applications, one of these starting materials should be at least trifunctional. In this way, different polymer chains can be connected together (i.e. cross-linked, see network of PU, Scheme III-3). In a real formulation, there are many additives. A short chain diol is commonly added for the construction of a polyurethane. This results in a series of carbamate linkages that are closely spaced. This creates hard segments amidst what might otherwise be soft, longer carbon chains (depending on the identity of R and R'). The number and ratio and use of even more additives depend on the application of the final PU.

Scheme III-3. Construction of a Cross-linked PU.



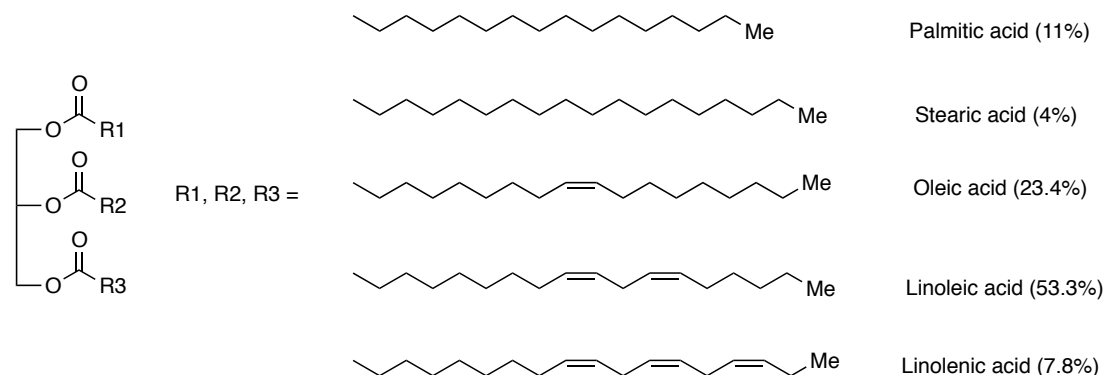
Because of the volume of PU-plastics and the increasing demand for them, coupled with decreasing supply of the starting materials (typically petroleum based), there is a need for renewable materials to contribute to the final product. The biggest way to make an impact is the polyols component of the final PU. If we can synthesize a polyol that is made from renewable, rather than petroleum-based resources, we could make a difference in the PU industry, and plastics in general. We chose soybean oil as the first renewable pre-monomer¹⁴⁴ (Chapter V) and later studied terpenoids (Chapter VI) for this purpose.

Chapter V. Polyols from Soybean Oil

V.A. Introduction and Previous Work

Soyoil is a triglyceride with an array of side chain fatty acids (Figure III-1).^{145,146} In nature, one discrete soyoil triglyceride contains any three of several fatty acid side chains. These side chains are named based on their length (16 or 18 carbons) and their lipid number (number of double bonds/unsaturation). Possible side chains for a soy triglyceride include (# carbons:lipid #): palmitic (16:0), stearic (18:0), oleic (18:1), linoleic (18:2), or linolenic (18:3). The prevalence of these side chains varies but follows roughly the percentages listed alongside the various chains in Figure III-1.

Figure III-1. A Soyoil Triglyceride.



The use of soybean oil as a monomer in polymer synthesis has been the subject of study for a long time. The plastics industry already developed and commercialized a vegetable oil-based polyol BiOH®.¹⁴⁷ This product arises from a two-step sequence where the alkenes of vegetable oils are epoxidized, then opened by action a nucleophile like methanol. This generates a secondary alcohol from what used to be an alkene. Thus, diols or triols are obtained if this sequence is performed on the linoleic or linolenic components of the triglyceride. This polyol has seen most of its application in flexible PU foams. The other main industry contribution is Renuva technology,¹⁴⁸ which converts soyoil to a polyol. Polyols generated under the Renuva technology are used in more varied PU applications (beyond flexible foams for Cargill's BiOH®). In academia, there are a number of ways vegetable oil alkenes have been functionalized. One of the most promising is hydroformylation of the alkene, followed by reduction to a primary alcohol.

We targeted a polyol of MW 2-6 kg/mol and containing anywhere from 2-6 hydroxyl groups. We first considered that we would have to oligomerize soyoil. One clear way is through the alkene functionality. A leader in the field of vegetable oil oligomerization is Richard Larock. His research group has investigated soyoil as well as other oils for their metathesis behavior.¹⁴⁹⁻¹⁵¹ Likewise, other groups have polymerized soyoil through alternative (i.e. non metathesis) methods. We hope to make use of this known oligomerization chemistry but add an additional alkene functionalization step to prepare suitable polyols for our targeted PUs.

V.B. My Studies on Soybean Oil (SBO)

The first step in working with a new molecule is gaining an understanding of its fundamental properties. After that, working on a particular part or functional group becomes more intuitive.

V.B.1 General Characteristics and Handling of Soybean Oil

My first question was whether or not soyoil could be chromatographed (Scheme III-4). Under standard MPLC conditions, I found that the commercial soybean oil could be chromatographed, and contained (as expected) an array of triglycerides. The fastest moving molecules were the most saturated, while those at the tail of the peak had greater levels of unsaturation (as indicated by more linolenic methyl groups in the NMR spectrum).

Scheme III-4. Chromatography of Soyoil.

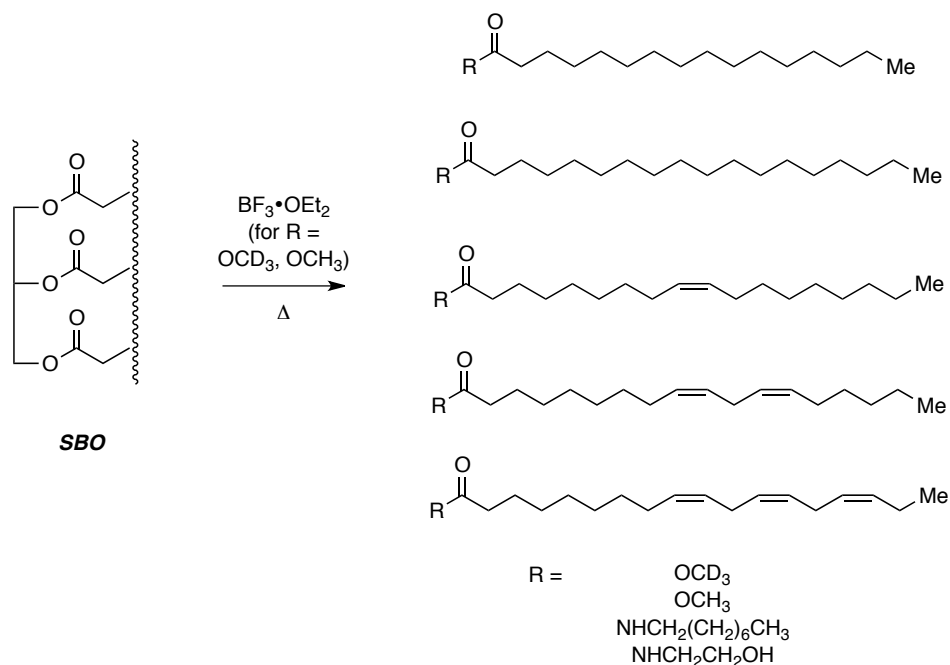


There was also an additional, more polar component. By LCMS, this was an array of species with added mass compared to the main peak. These are likely products of autoxidation (a way to add mass to molecules that occurs just upon storage). This is discussed in later section.

V.B.1.a Cleavage to Methyl Esters or Di- and Mono- Glycerides

Soyoil can be cleaved to the fatty acids (or esters or amides) that comprise it. This can be performed under a variety of conditions, and the resulting esters or amides are easily analyzed by GCMS and LCMS (Scheme III-5). The first experiment revealed (as expected) that the resulting fatty acid chains exist in varying degrees of unsaturation. Complete cleavage to the methyl esters was induced by heating in methanol with $\text{BF}_3 \cdot \text{OEt}_2$. This reaction released the entire glycerol backbone and afforded only methyl esters. Amines were also used to cleave the side chains. If amides were desired, the reaction proceeded without the catalyst, but still required heating (approximately 2 hours for full conversion).

Scheme III-5. Cleavage of Soyoil Into Component Fatty Acid Esters/Amides.



The resulting esters and amides were not separable by MPLC, but they were all discrete, observable peaks on GCMS and our high-performance LCMS. The elution order changed depending on the functional group. For the esters, this order was observed by GCMS [ester (boiling point at 760 mm Hg)]: methyl palmitate (335), methyl linoleic (369), methyl oleate (354), methyl linolenate (364), and methyl stearate (355-56). This does not follow a molecular weight or boiling point trend. Presumably there are

variations in the contribution from polarity and boiling point that make this order more random.

The same experiment and analysis by LCMS displayed the following elution order: methyl palmitate, methyl linolenate, methyl linoleate, and methyl oleate. Methyl stearate was not observed under the same method. This trend indicates that the more unsaturated fatty acids are more polar. This behavior profile matches what was observed by preliminary MPLC experiments with soyoil triglycerides themselves.

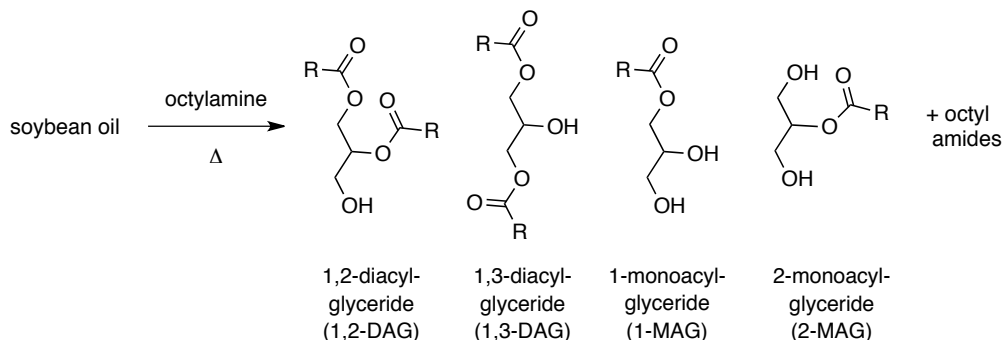
The presence of octyl and 2-hydroxyl propyl amides (from SBO cleavage with octyl amine and ethanol amine, Scheme III-5) were also easily confirmed by LCMS. The octyl amides were retained longer than the esters, but displayed the same trend in elution: octyl linolenamide, octyl linoleamide, octyl palmamide, octyl oleamide, and octyl stearamide. The same general trend is confirmed, where the singly, doubly, and triply unsaturated compounds are increasingly polar. The saturated hydrocarbon chains did not fit into this trend. When cleavage occurred by heating with ethanolamine, most polar component was the amide corresponding to the linolenate side chain, followed by linoleate, oleate, and stearate. The amide derived from palmitate seemed to elute slightly after the linolenic amide. This collected of experiments gave behavior profiles for not only the individual fatty acids, but an idea for how soyoil might be handled in future experiments.

The use of $\text{BF}_3 \cdot \text{OEt}_2$ in these reactions gave interesting results. For example, there were often several peaks in the crude reaction LCMS trace with the same nominal masses. It was soon revealed that this catalyst is used for cationic polymerization of alkenes.^{152,153} In promoting such a union, isomerization into conjugation or isomerization to *trans* alkenes may occur (an example on individual fatty acids is given in Scheme III-10). Unfortunately, ^1H NMR analysis did not support this prediction. Studies on the action of $\text{BF}_3 \cdot \text{OEt}_2$ on alkenes will be discussed in **V.B.1.c**. Here, it just noted that during the cleavage of soyoil, the $\text{BF}_3 \cdot \text{OEt}_2$ conditions carried with it the possibility of *cis/trans* isomerization, positional isomerization, and even crosslinking of chains.

Another useful experiment was the partial cleavage of the triglyceride to mono and di-glycerides (Scheme III-6).¹⁵⁴ The rate of the first cleavage had to be studied and compared to the second and third. There were other questions to be answered. Can it be

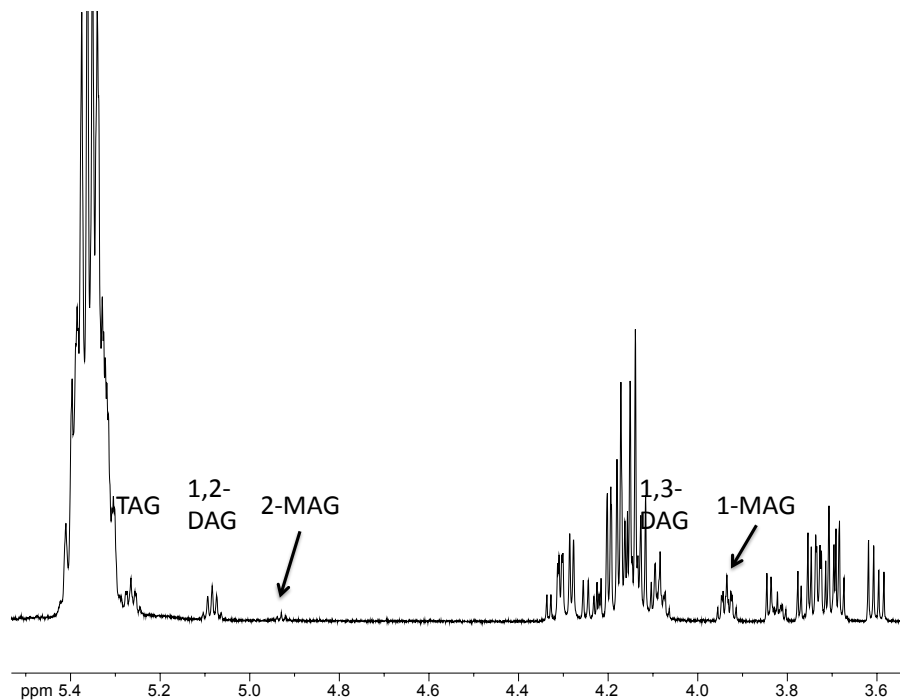
performed under controlled conditions to get only one product? Which is preferred, the 1,2- or the 1,3-diglyceride?

Scheme III-6. Partial Cleavage of Soyoil.



In the event, the soyoil was heated neat with one equivalent of octylamine. I isolated each of the diacylglycerides (DAGs, Scheme III-5), where the 1,3- variety predominated in the crude reaction mixture. Although both monoacylglycerides (MAGs) were observed as the reaction was monitored (see Figure III-2), I was unable to isolate them; presumably the chromatographic conditions were not suitable for the high polarity of these diols. Future work could include pre-treating the columns with a suitable reagent (typically triethylamine) to reduce the acidity, enabling the elution of these diols.

Figure III-2. NMR spectrum of Cleavage with Octyl Amine at Low Conversion.

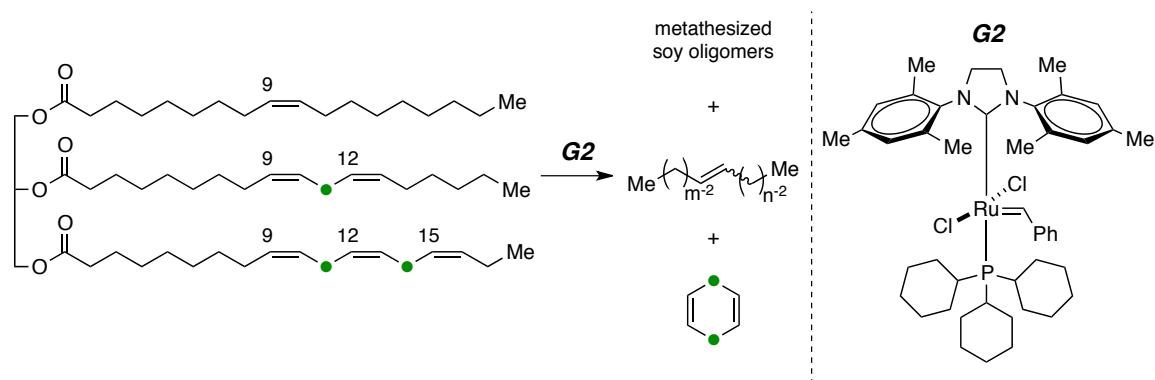


As Figure III-2 indicates, all expected species (Scheme III-6) were observed as the reaction proceeded. The DAGs were most amenable to chromatography and could be further studied. The 1,3-DAG and 1,2-DAG were independently dissolved in toluene and heated. They gave identical product ratios, 1,3-DAG to 1,2-DAG of 4:1. This confirmed what the crude soyoil cleavage reaction had indicated, that under these conditions, DAGs are likely in the form of the 1,3-isomer. Though the mechanism is still under debate, it is clear that the acyl shift from the secondary to the primary hydroxyl group is favored.¹⁵⁵ Lastly, I considered that the partial cleavage to a MAG or DAG resulted in available hydroxyl groups for further reaction. This strategy could be developed to furnish our target polyol itself, provided we can work off the remaining side chain.

V.B.1.b Metathesis of Soybean Oil

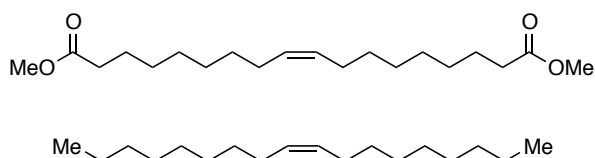
Now with an understanding of how soyoil could be handled and some ways to analyze it, it was time to test out metathesis as a way to grow molecular weight of the polymer. The general reaction is shown in Scheme III-7. We are not the first to study this type of oligomerization methodology.^{149,150,156} In the presence of a metathesis catalyst like G2 (right panel, Scheme III-7), any alkene of the triglyceride is prone to insertion to form a metal carbene. This species can react with any available remaining alkene. When that alkene is on another soyoil molecule, a cross linking event occurs and a hydrocarbon is released. Dihydrobenzene is formed in this reaction when the metal inserts into the terminal end of a linolenic side chain, then reacts further down the chain¹⁵⁷.

Scheme III-7. Metathesis of Soybean Oil.



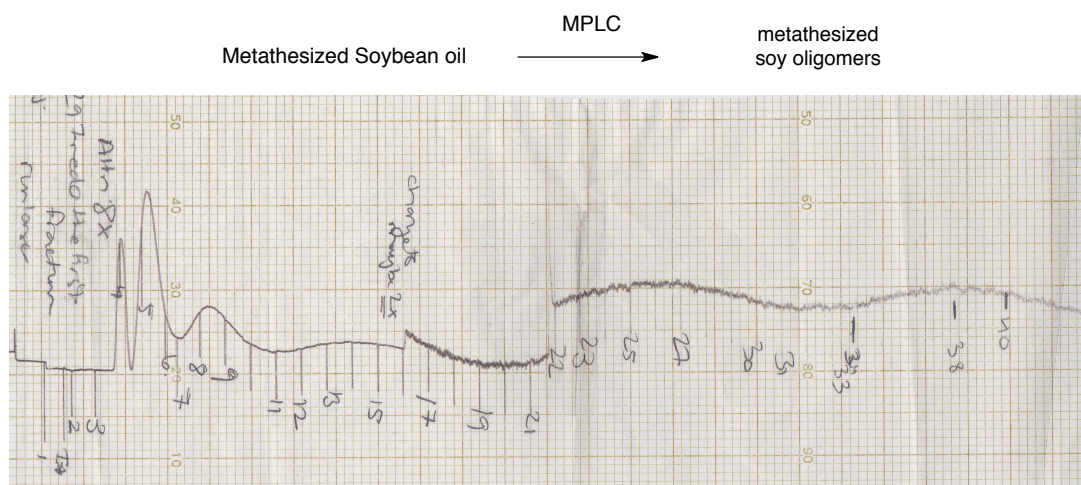
The formal study of this chemistry was charged to a post-doc working on the project, Senthil A. Gurusamy-Thalavelu. He performed the reaction and routinely provided crude samples to me for additional studies. The first of these was methanolic cleavage of the crude reaction product. The GCMS showed evidence for the bisester and hydrocarbon product in Figure III-3. These could only arise after a successful metathesis event.

Figure III-3. Cleavage Products of MSBO.



Second, I submitted the crude product to MPLC and found that separation of the soyoil oligomers was possible (Scheme III-8 and picture of MPLC trace).

Scheme III-8. MPLC of Crude MSBO.^a



^a the sensitivity of the RI detector was adjusted at the middle of this run to observe the slowest eluting components. Mass data for each component cannot be gathered from just looking at this trace.

As expected, the slower eluting peaks become broader, and represented a decreasing percentage of the total composition (by concentration of MPLC fractions). The later fractions had a lower ratio of vinyl protons to those corresponding to the triglyceride backbone. This indicated (as expected) that there was further oligomerization in these samples. At the limit of infinite retention times, it appeared that there had to be at least 1.5 double bonds for each backbone unit. This information has implications for the limit of oligomerization by metathesis chemistry.

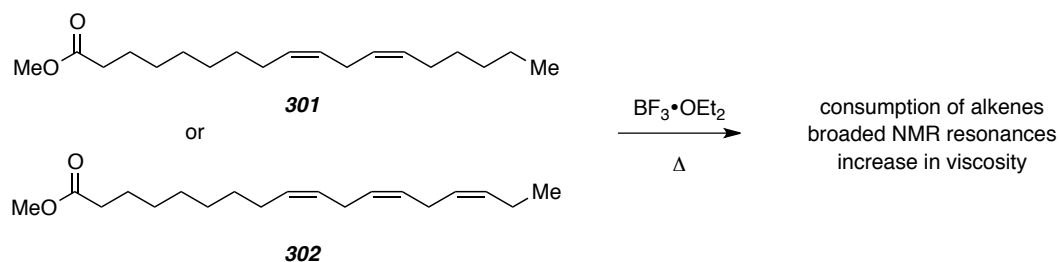
The mass recovery for the column was approximately 95%. This was true for solvent systems ranging from 1:1 to 12:1 (Hexanes:Ethyl Acetate). Thus, there were likely very few (or no) further oligomers present prior to MPLC. Understanding this result was critical for the success of the methodology. If the greatest level of oligomerization is that which was indicated by the MALDI data (7 or 8), there will be a practical limit to the molecular weight of the polyol.

V.B.1.c. Oligomerization of Soybean Oil by Other Methods

There are many additional ways to polymerize alkenes.¹⁵⁸⁻¹⁶¹ Even over the course of my studies, I discovered what appeared to be oligomerization of alkenes under the $\text{BF}_3 \cdot \text{OEt}_2$ cleavage conditions (discussed in section **V.B.1.a**, Scheme III-5). After the reaction was judged complete, the crude mixture was loaded onto the MPLC. While there was evidence for the methyl esters from triglyceride cleavage, all fractions still contained the glycerol backbone by ^1H NMR analysis. This means that a reaction was occurring, but it was not only the cleavage. Moreover, these spectra for these gave poor peak shape and resolution, indicating that oligomerization had occurred. A search of the literature revealed that BF_3 does, in fact, promote oligomerization of alkenes.^{152,153} Thus, a short study of alkene polymerization under such conditions was conducted.

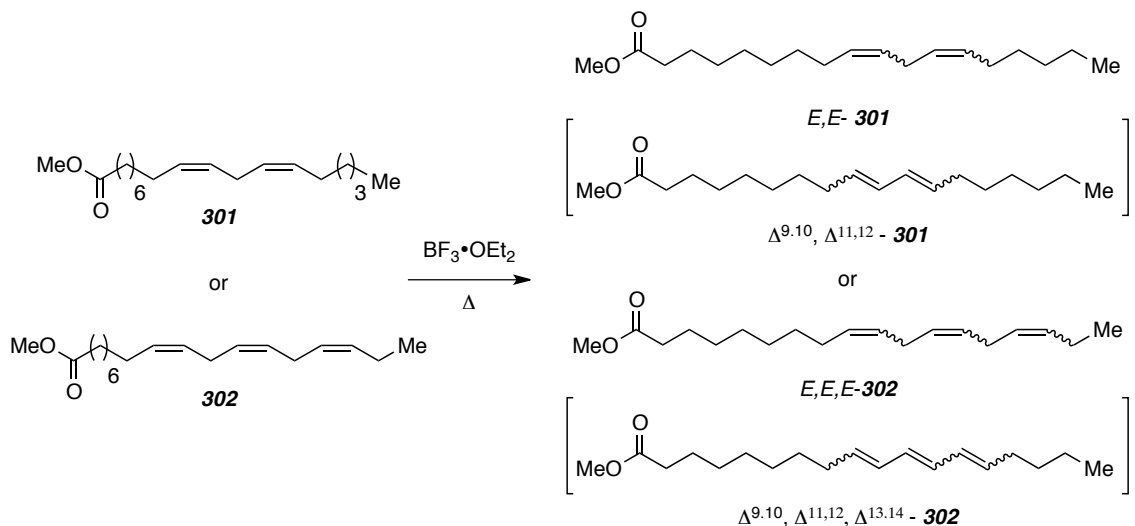
By NMR analysis, disappearance of alkene functionality was noted upon heating methyl linoleate (**301**) or methyl linolenate (**302**) with $\text{BF}_3 \cdot \text{OEt}_2$ (Scheme III-9). Both the vinyl resonances and those assigned to allylic protons disappeared. Additionally, the ^1H NMR spectrum had broadened resonances, characteristic of oligomerization and ^{13}C NMR data did not indicate the presence of any olefins in the reaction mixture. Beyond the use of NMR spectroscopy, however, studies on the linking of fatty acid esters were complicated. Unfortunately, the nonpolar nature and higher molecular weight of the substrates limited the available methods for their analysis. Neither LCMS (too greasy) nor GCMS (too high molecular weight) would be able to accurately convey the chemistry.

Scheme III-9. Observed Oligomerization of **301** and **302**.



I also attempted to intercept this reaction before all of the olefins were consumed (Scheme III-10).¹⁶² The goal was to observe any changes in the alkene region such as isomerization¹⁶³ from *cis* to *trans* (e.g. *E,E*-**301** or *E,E,E*-**302**) or from skipped into conjugated (e.g. $\Delta^{9,10}$, $\Delta^{11,12}$ -**301** or $\Delta^{9,10}$, $\Delta^{11,12}$, $\Delta^{13,14}$ -**302**) olefins. Although identification of various species could not be confirmed by NMR data, after only 15 minutes of heating **301** or **302**, the GCMS showed the appearance of several more peaks bearing the same molecular weight.

Scheme III-10. Alkene Isomerization of **301** and **302** Under $\text{BF}_3 \cdot \text{OEt}_2$.

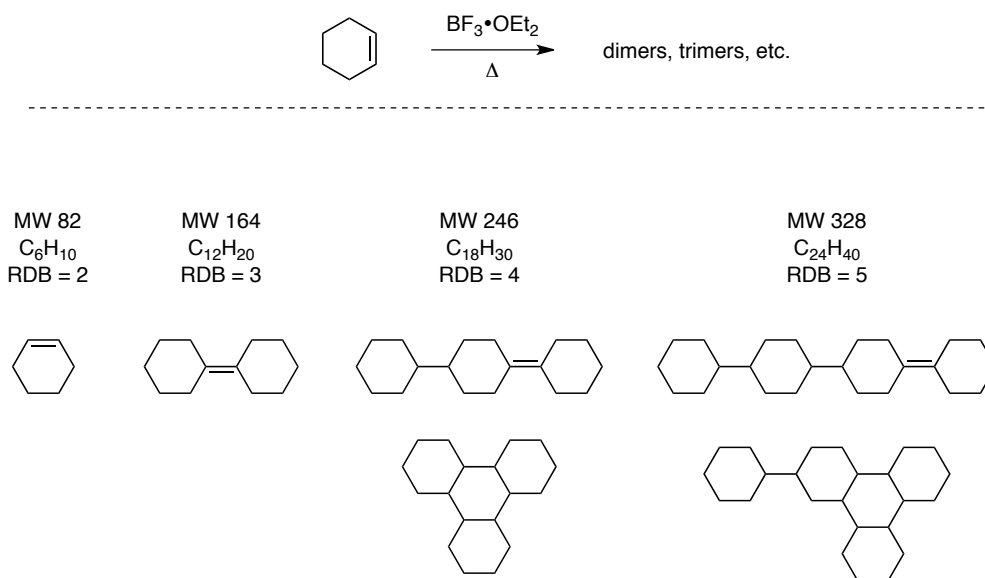


The fragmentation pattern was not used to draw conclusions as to which isomers were present, but the presence of isomers was indicated. Likely these were a combination of *cis/trans* isomers but not alkene positional isomers, since the NMR spectrum did not contain any resonances for conjugated dienes or trienes. In the future, more attention could be given to this study and investigation into the products of this reaction could be performed

A more tractable reaction to probe the $\text{BF}_3 \cdot \text{OEt}_2$ reaction was with a lower molecular weight starting material, where the products could be isolated and chromatographed. In this study, I also planned to investigate the difference between using stoichiometric versus catalytic $\text{BF}_3 \cdot \text{OEt}_2$.

Linear hydrocarbons were too volatile, but cyclohexene worked well. In the study, the alkene was heated in the presence of the catalyst (Figure III-4, reaction arrow) and the reaction monitored by GCMS. For a stoichiometric charging of catalyst, GCMS clearly showed dimers, trimers, tetramers, and in one case, the mass corresponding to a pentamer. The molecular formulas consistent with these masses give UN (unsaturation) or RDB (ring double bond) values of 3, 4, and 5 for these oligomers, respectively. This is expected for the union of alkenes. Unfortunately, the various oligomers could not be separated and were analyzed together. ^1H NMR analysis indicated that few (if any) vinyl protons remaining after the reaction. Examples of structures that account for the observed masses and that are consistent with the NMR data are given in Figure III-4.

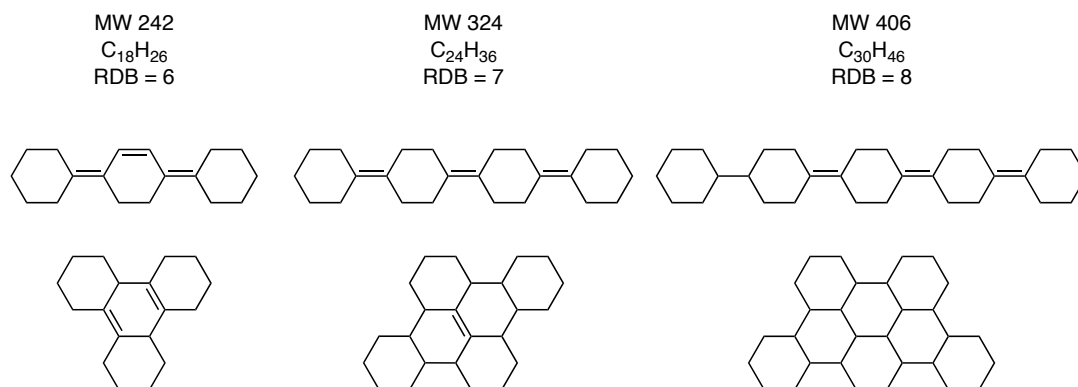
Figure III-4. Potential Products of Cyclohexene Oligomerization.



When the reaction was conducted with only catalytic $\text{BF}_3 \cdot \text{OEt}_2$, the GCMS told a different story (Figure III-5). Oligomers were formed, but they were often oxidized relative to those structures reported above.¹⁶⁴ For example the trimer in this case was observed to have a MW of 242 (vs. 246) and the tetramer weighed 324 (vs. 328).

Additionally, the GC suggested a pentamer, but one that was further oxidized than what would be expected. Potential structures for these oxidized oligomerization products are given in the Figure III-5, along with their UNs.

Figure III-5. Potential Products of Oxidative Oligomerization of Cyclohexene.



This study clearly illustrated the capability of alkenes to oligomerize by heating with BF₃•OEt₂, and it was useful to learn and think about how spectra and GCMS behavior might change when this occurs. While those details of soybean oil polymerization were being sorted by Senthil, it was necessary to move on to the next step in the construction of the polyol: olefin functionalization.

V.B.1.d. Oxidation Studies of Soybean Oil and Fatty Acid Methyl Esters

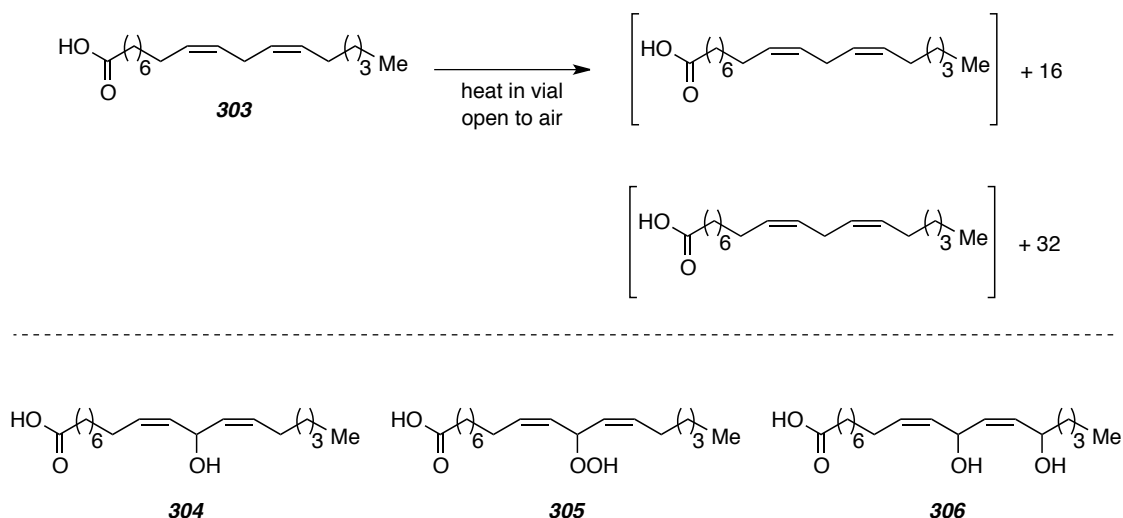
One last consideration before moving forward was the general reactivity of the skipped dienes and trienes present in the triglyceride. From the MPLC of soyoil (section V.B.1, Scheme III-4) we already had a concern about oxidation of these molecules. What is the stability of these skipped dienes and trienes?

Commercial soyoil is slightly yellow color; this indicates that a reaction has occurred.¹⁶⁵ Under normal phase chromatography conditions, the collected sections of one broad peak gave slightly varied ¹H NMR data. More polar cuts of the peak had higher levels of unsaturation. This was established by the study in Scheme III-4. The most noteworthy observation from these studies is that there was a much slower eluting peak representing 5-10% of the mass balance of each soyoil sample. Although the LCMS is sometimes difficult to interpret due to fragmentation of samples, it was clear that this

more polar peak has substantial mass increase, far more than possible for a soy triglyceride. Somehow, upon storage, incorporation of mass had occurred. Based on the general array, it appeared that 34 mass units were added to each triglyceride. A possible explanation is addition of H₂O₂. Other than these observations, however, there are few firm conclusions to make.

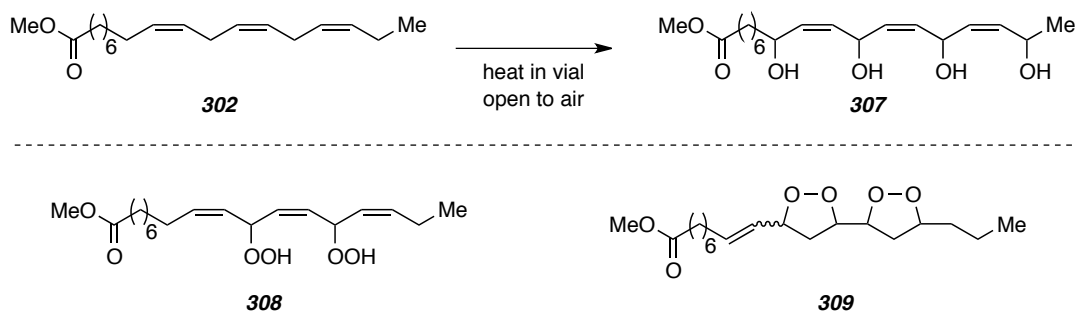
I tried to gather evidence for autoxidation by moving to a simpler system. Linoleic acid (**303**) was exposed to air at either room temperature or heating to high temperatures (>200 °C, Scheme III-11). By LCMS, it appeared that 16 and (upon further heating) 32 mass units were added to the acid. There are a lot of possible explanations, but structures like bis-allylic alcohol **304**, peroxide **305**, and diol **306** would account for those masses.¹⁶⁶ I did not gather any evidence with a peroxide test. The ¹H NMR spectrum displayed resonances in the region expected for the new functionality that is exemplified in Scheme III-11 (**304**, **305**, and **306**).

Scheme III-11. Observed Autoxidation of Linoleic Acid (**303**).



In a similar experiment performed on methyl linolenate (**302**, Scheme III-12), more rapid conversion of the starting material was noted. The most abundant of the molecular ions indicated the products added 64 mass units to their starting molecular weights. There was evidence that was as few as 48 to as many as 96 mass units added to the methyl linolenate.

Scheme III-12. Observed Autoxidation of **302**.



There are many ways to account for this extra mass (64 units). The first shown is the result of tetra-allylic oxidation (**307**). Bishydrogenperoxide **308** would also give rise to that mass. The ^1H NMR spectrum showed a reduction the number of alkenes, so the bisdioxane **309** should be considered. Of those alkenes remaining, a number have moved into conjugation with one another; now resonances between 6.3-6.6 ppm were present. Further analysis was not performed. The present study supports the prediction of autoxidation chemistry, but there is an opportunity for further investigation (such as exposure of **302** or **303** to sunlight). These studies taught us that autoxidation should be considered, but it is not a big concern. After all, harsh conditions were required for these decomposition pathways.

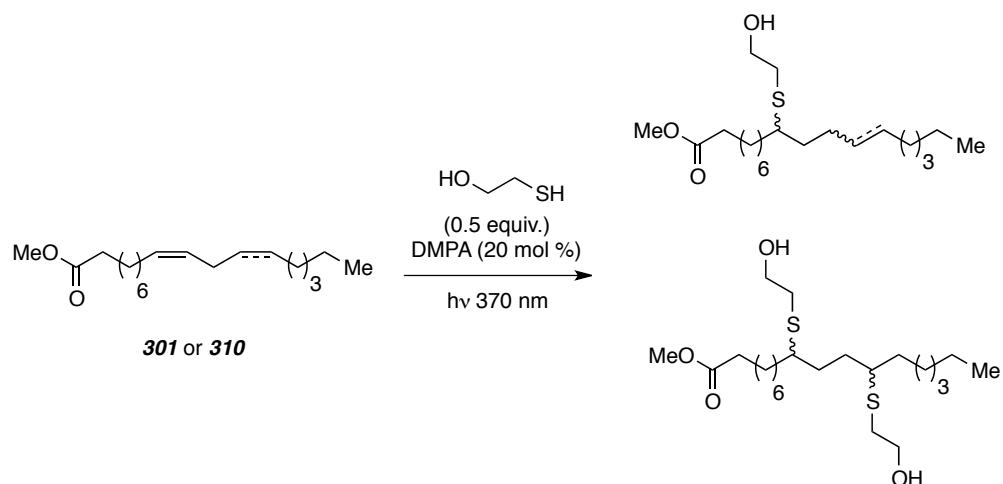
V.B.2 Studies on Olefin Functionalization

The oligomerization of soyoil now safely in Senthil's hands, it was time to move onto the incorporation of alcohol functionality on the soy molecule. A number of model studies were designed; some were based on a previous group member's work in this area.

V.B.2.a. Brief Background and Mandy Schmit's Studies

Mandy worked on modifying the alkene into the desired hydroxyl functionality.^{167,168} She used mercaptoethanol (**332**, Scheme III-13) to effectively click the unit onto methyl oleate (**310**) and linoleate (**301**).¹⁶⁹ The thiol-ene reaction can occur at either end of the alkene, and for the remainder of this chapter, the products shown will be named by the carbon number that the C-S bond forms (starting from the terminus of the fatty acids).

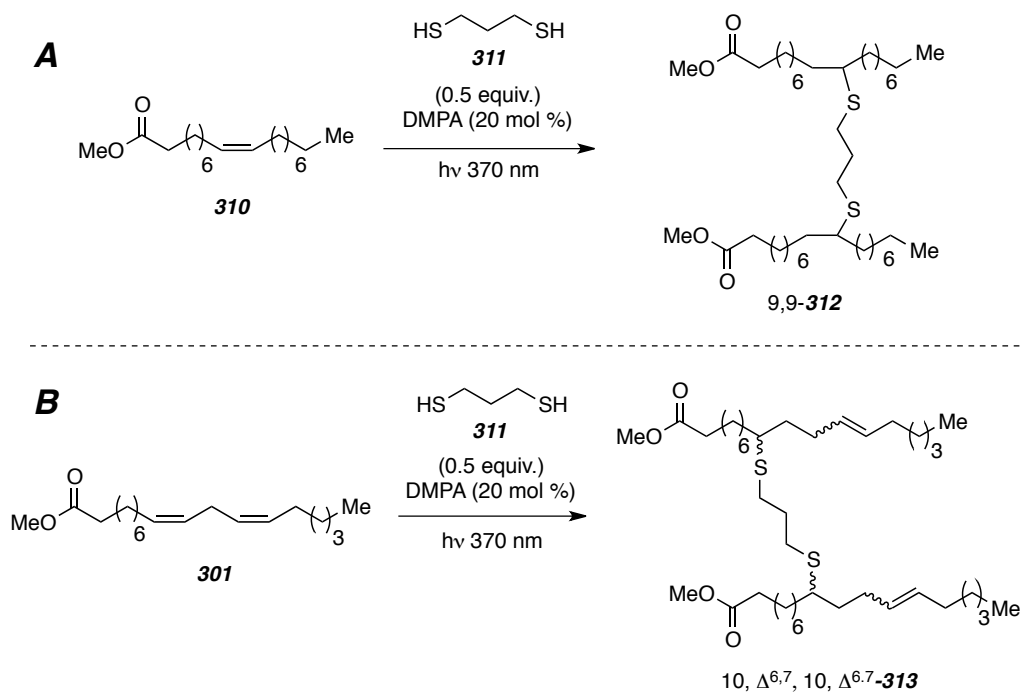
Scheme III-13. Mandy's Thiol-ene on Methyl Oleate (**310**) and **301**.



The chemistry was easily evaluated on the individual fatty acids but there was an added complication using this methodology on soybean oil. The molecular weight is too high for many analytical methods we were accustomed to using. Nevertheless, Mandy found evidence for mercaptoethanol incorporation onto the fatty acid side chain under radical conditions. This was the first important result. She also saw isomerization of remaining alkenes under the reaction conditions.

Mandy's most relevant observation was the cross-linking reaction of oleate **310** with a difunctional thiol (1,3-propane dithiol, **311**, Scheme III-14A). This reaction was powerful in that it combined a cross-linking (method to grow molecular weight) event with an olefin functionalization (hydroxyl incorporation) event.¹⁷⁰

Scheme III-14. Mandy's Bis Thiol-ene on **310** and **301** with 1,3-propanedithiol (**311**).



Mandy also did the reaction on linoleate-type dienes (**301**, Scheme III-14B). She saw conversion to the net bis-ene product **313**, which is still capable of further ene reactions and greater cross linking for molecular weight growth. Additionally, every added chain contributes an ester group. These esters can be converted to alcohols through the appropriate chemical modification.

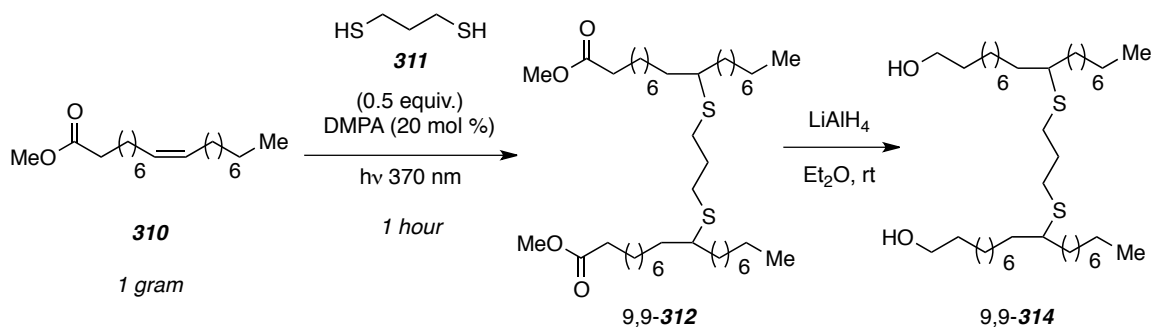
Mandy's studies proved that thiol-ene reactions are effective in joining alkenes of fatty acids together. Her research culminated in the successful cross-linking of soybean oil itself. She reacted soybean oil with enough dithiol for one half of the double bonds to be affected. Though the analysis of this reaction was difficult, there were several conclusions. Mainly, the viscosity increased dramatically, the dithiol appeared to fully react under the conditions, and that C-C bond formation was likely occurring alongside the thiol-ene chemistry. It is difficult to account for the variations in soybean oil and analysis methods are very limited, but there is promise for this methodology.

V.B.2.b. My Contributions to the Use of Thiol-Ene Chemistry Soybean Oil

The first experiment that I did was reproducing Mandy's result and evaluating the cross-linking reaction. If the bis thiol-ene reaction was going to be useful, it needed to be

performed on a bigger scale. Fortunately, this reaction proved robust and worked nicely on one gram of material (Scheme III-15); it was complete in one hour, and it was easily purified by MPLC. The bis-ester **312** was smoothly reduced by treatment with LiAlH₄. The product diol **314** was also amenable to chromatography.

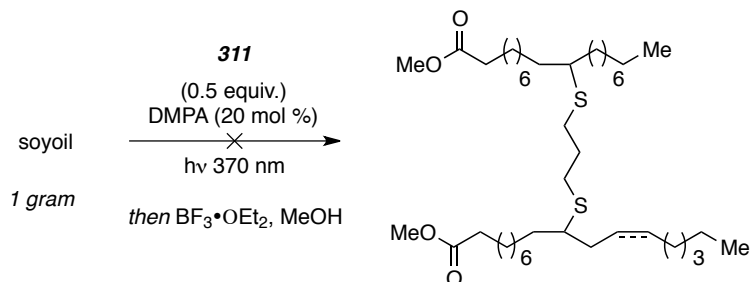
Scheme III-15. Scale-up of Thiol-ene of **310** and Reduction to Diol.



This chemistry was only used to prepare the diol **314**, but further crosslinking/reduction sequences on more unsaturated systems (see Scheme III-14B with **301**) has the potential to generate polyols of higher molecular weights and variable functionalities.

I also wanted to repeat and understand more about the click reaction on soybean oil. (Scheme III-16). I found similar issues surrounding the viscosity and solubility of the resulting crude material. In fact, solubility issues (with the dithiol **311** and the DMPA) were the main issue and made research difficult. I attempted to take the crude reaction product and cleave the triglyceride backbone, leaving only the functionalized (and linked) alkenes. I saw none of the expected products from this sequence (and examples is shown in Scheme III-16). This was another situation where we were limited in our choice of analytical tools. Further research in this area requires methods that are adept for much higher molecular weight materials.

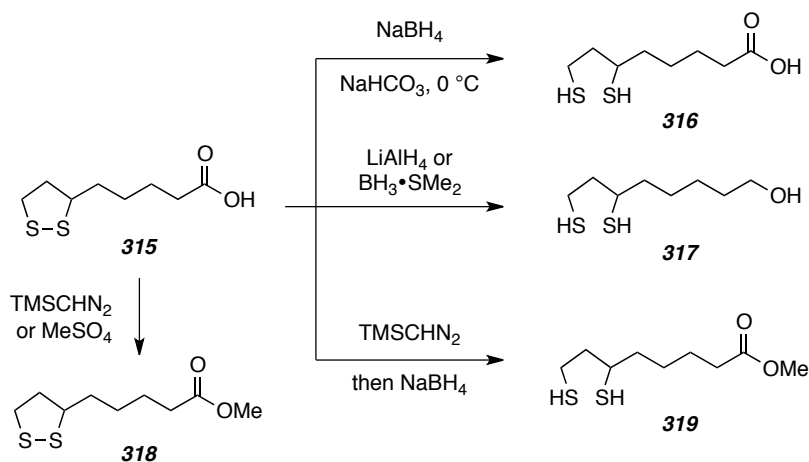
Scheme III-16. Thiol-ene Reaction on Soyoil.



As an extension of Mandy's work, and with the goal of using the thiol-ene not only as a cross-linking tool, but a way to add another reactive group, I elected to use thiol-ene with a new difunctional thiol. This one was designed to bring in an alcohol concurrently with the cross-linking event.

Lipoic acid (LA, or **315**, Scheme III-17) is a natural product that arises from action on octanoic acid. I performed functional group manipulations¹⁷¹ to test an array of LA derivatives (Scheme III-17) and determine which would be best suited for the proposed click chemistry. In all cases the disulfide bond was reduced and various chemistry was performed on the side chain to generate the acid, alcohol, and ester dithiols (**316**, **317**, and **319**, respectively).

Scheme III-17. Transformations of LA.

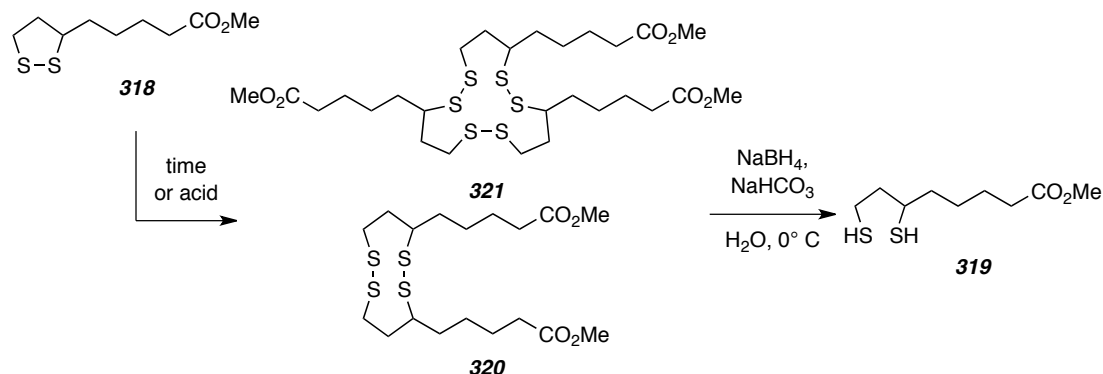


The reduction reaction was straightforward, complete in less than one hour, and the product dithiol acid **316** was very clean, but could be chromatographed if desired. The LiAlH_4 (or borane) reduction gave full conversion to the dithiol alcohol **317**, but mass recovery was a big problem and only small quantities of this material were ever available after the reaction.¹⁷² The formation of dithiol ester **319** was also difficult. I had already started to notice that acid **315** and ester **318** (from reaction of **315** and diazomethane) had a tendency to undergo a different reaction under various conditions, so I had limited success in accessing **319**, which requires the same esterification step.

This is a known difficulty of working with LA and disulfides in general. It is the polymerization of disulfides¹⁷³⁻¹⁷⁶ (Scheme III-18) that reduces the utility of any reaction on LA. The mass of both the dimerized (**320**) and trimerized (**321**) LA was observed by

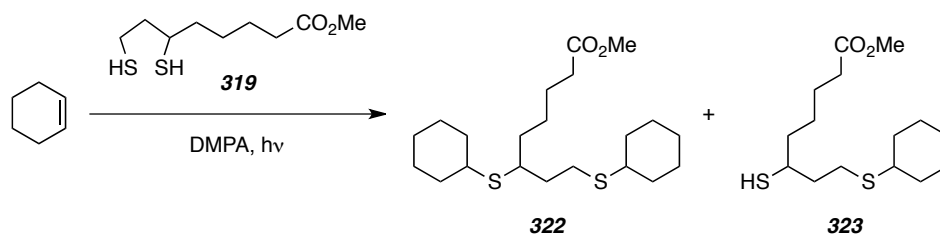
LCMS under many of the methylation conditions that I used (Scheme III-18). I realized, however, that the products are disulfide bonds themselves, and these I knew how to reduce (as in Scheme III-17). This strategy would provide access to a useful dithiol (e.g. **319**) after decomposition of the disulfide bonds.

Scheme III-18. Observed Oligomerization of **318** and Route to Potential Recovery.



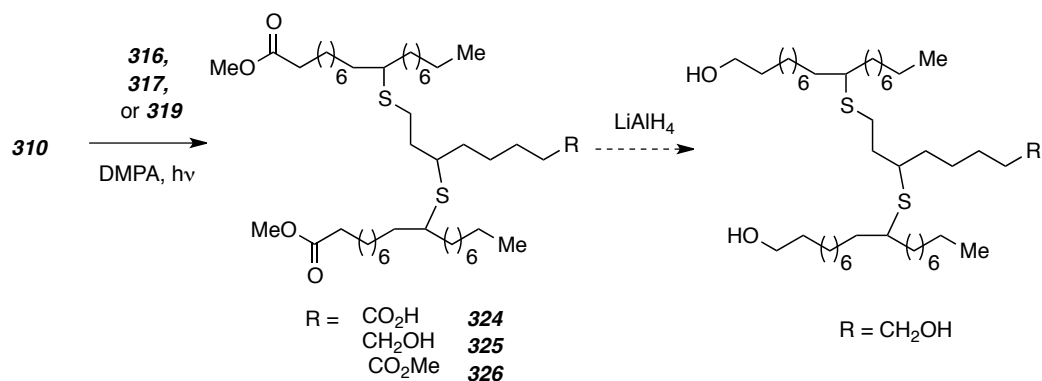
Despite these difficulties, I still had small quantities of dithiol ester **319** in hand, and wanted to test the thiol-ene reaction. I chose cyclohexene as a model system (Scheme III-19). This reaction immediately worked to afford the linked cyclohexane **322**, but there was a small amount of mono-ene product **323** that had to be removed by chromatography.

Scheme III-19. Bis Thiol-ene of LA Dithiol (**319**) With Cyclohexene.



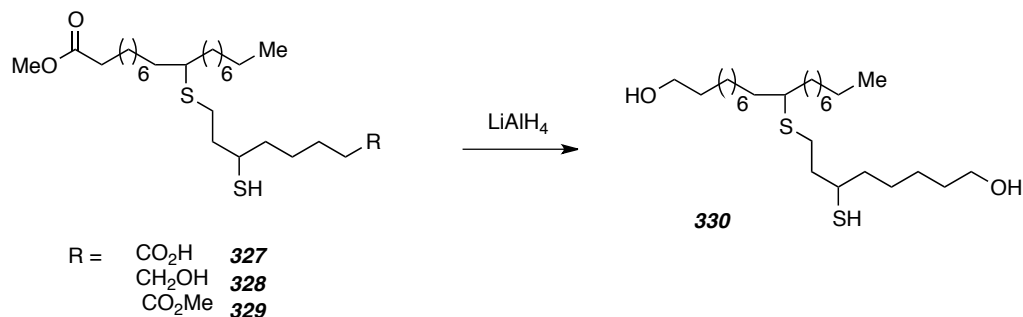
With this result, I returned to the fatty acids to see if long chain alkenes could be linked in the same way. I tried this reaction on all variants of the dithiol (**316**, **317**, and **319**) from Scheme III-17. Using the same conditions that worked for thiol-ene **311**, oleate **310** was subjected to the thiol-ene linking reaction, Scheme III-20.

Scheme III-20. Attempted Cross-linking of **310** With Dithiols **316**, **317**, and **319**.



The reaction with acid **316** (Scheme III-20, R = CO₂H) was monitored by LCMS and within an hour, several reaction intermediates appeared. The mono-ene product (**327**, Scheme III-21) was produced cleanly but conversion was low. Upon reacting for several more hours, and following chromatography, small quantities of the desired product **324** were obtained with the rest of the mass balance from the starting methyl oleate (**310**, now isomerized to a 4:1 ratio *trans*:*cis* alkene). For further support of this structure, the linked monomer **324** was subjected to LiAlH₄ treatment. Sadly, this is not reveal any of the expected mass. Similarly, I tried to gather evidence for the mono-ene product **327** (Scheme III-21). Though there appeared to be some present in the crude reaction mixture but no masses corresponding to diol **330** were observed after attempted reduction of **327**.

Scheme III-21. Attempted Reduction of Mono-ene Products **327-329**.



These reactions were also analyzed to see if any C-C bond formation had occurred. By mass, I saw no direct dimerization of the starting material (**310**), but carbon radicals are generated in this process, and this side reaction might be a factor in the efficiency of the thiol-ene chemistry.

In the reaction with lipoic acid alcohol (**317**, Scheme III-20) the first ene reaction also occurred quickly (Scheme III-21, **328**) with the product **325** appearing by LCMS within one hour. After two hours, the olefin looked to be mostly consumed, along with the dithiol starting material. Like the previous experiment, I successfully isolated the geometrically-isomerized starting material (*trans*-**310**, confirmed by the shift of the vinyl resonances in the NMR spectrum). I was, however, unable to find any desired product (**325**) alongside it. I did not attempt to reduce the expected product to the triol.

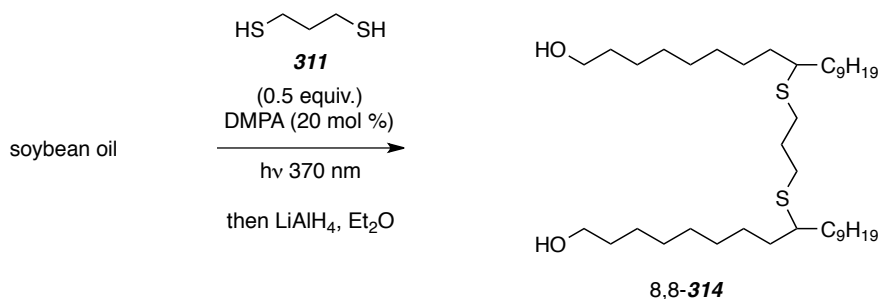
Having only modest success with the bis-thiol ene click reaction, I did not spend any time optimizing, but I tried one last time with the methyl ester of lipoic acid (**319**, Scheme III-20). The result was similar to the previous trials. In one hour, LCMS showed conversion to the product of mono-ene reaction **329**, but no further linking to bis-ene product **326** was observed. To promote this second ene reaction, another portion of DMPA was added. Although analysis was complicated by the abundant DMPA byproducts,^{177,178} the mass of the desired linked monomers appeared by LCMS. Unfortunately, I was unable to isolate the desired bisester **326** for further characterization and reduction was also forgone.

The general trend with these thiol-ene reactions, is that the first click reaction is fairly rapid, but the secondary thiol does not undergo addition at a comparable rate. Only with more initiator does the second ene event occur (and even then, the conversion is modest). Although not thoroughly examined due to lack of material, these reactions would be extremely useful since LiAlH₄ reduction would give produce a triol (as shown in Scheme III-20). Molecular weight could be grown using the more oxidized fatty acids (e.g. linoleate, linolenate), where additional linking is possible.

Similar reactions were attempted on soyoil (Scheme III-22) and a few observations were made. The most relevant are that the click reactions will occur without direct light treatment in the Rayonet. When the reaction is performed on soyoil, DCM is required to solubilize the DMPA. Lastly, the dimers and further oligomers obtained from reaction on soyoil are difficult to analyze. ¹H NMR spectroscopy gives an idea for consumption of alkene functionality, but the degree of molecular weight growth was not investigated. A destructive way to approach this is LiAlH₄ reduction of the crude reaction mixture. When

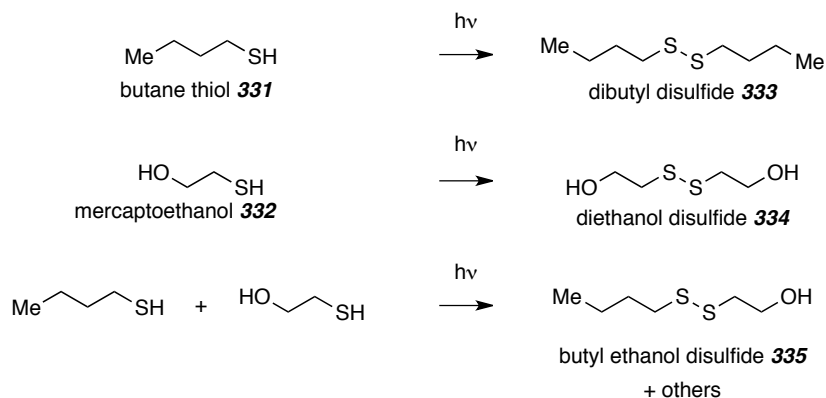
this was attempted, the main peak of the LCMS gave the mass appropriate for linked oleol alcohol (e.g. 8,8-**314**). Interestingly, no other nominal mass was observed in this experiment. Perhaps the more highly cross-linked products were not visible by LCMS. By NMR analysis, it would be difficult to tell the difference between **314** and further oligomers.

Scheme III-22. Attempted Cross-linking of Soyoil by **311**.



Mandy had seen the thiol-ene reaction (Scheme III-22) occur without an initiator. She (and subsequently, I) tested the reaction using the disulfide as the thiol radical generator. The reaction could also be reversed, where thiols become thiol radicals. I ran a control reaction (Scheme III-23) to see if dimerization (**331** to **333**, **332** to **334**) was occurring under these conditions.

Scheme III-23. Radical Chemistry of Thiols.



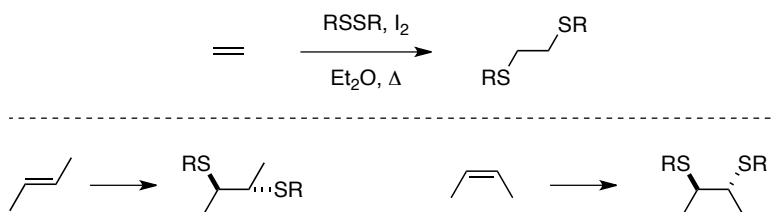
I observed very little disulfide formation for any thiols I tried, but if the disulfide enters back into radical chemistry, there should be little change in the reaction. This remains for future work; if thiol-ene chemistry can be enacted under ambient light with no special initiator that holds even more power.

V.B.2.c. Disulfide Addition to the Alkenes in Soybean Oil

Among the many more ways there are to append a group to one or both carbons of an alkene is disulfide chemistry.^{179,180} One advantage to this chemistry is that disulfides are less odorous than thiols. Additionally, the reaction introduces functionality at both carbon atoms, thus expanding our ability to design and synthesize polyols with a range of molecular weights and functional numbers. Moreover, the products may be slightly easier to analyze by NMR spectroscopy since the expected resonances are more spread out. Unlike the thiol-ene, however, there are not as many cross-linking opportunities.

The general reaction is shown in Scheme III-24. The main features are bis-functionalization of the alkene, two new C-S bonds, and anti addition of the disulfide. The bottom panel illustrates this last point. Anti addition to a *trans* alkene gives the erythro product, whereas the theryo product arises from anti addition to a *cis* alkene. The latter is expected for the alkenes in this study.

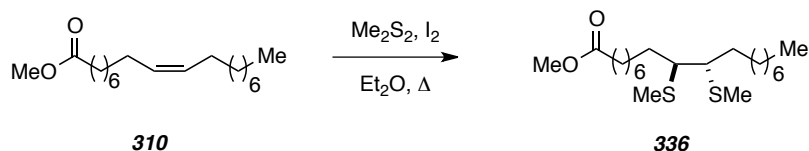
Scheme III-24. General Disulfide Addition Across an Alkene.



Historically, this reaction was performed as a means of analysis of double bonds, both their stereochemistry and their position on long alkyl chains. Because it is reportedly high-yielding and capable of adding to both ends of an alkene, it was worthwhile to investigate on our systems. I set out to examine how well it worked on individual fatty acids, as well as explore the substrate scope of the disulfide. For example, can R (Scheme III-24) somehow carry in the desired OH functionality to the alkene?

I chose dimethyl disulfide as a starting point. The expected products would have suitable masses for analysis and informative NMR properties. It was a basic starting point before more complex case. I found this reaction worked well right away (Scheme III-25); it required heating but only catalytic I_2 , with typical isolated yields up to 80% of addition product **336**. Only one of the two possible threo stereoisomers is drawn. Bis-sulfide **336** was easily purified and analyzed.

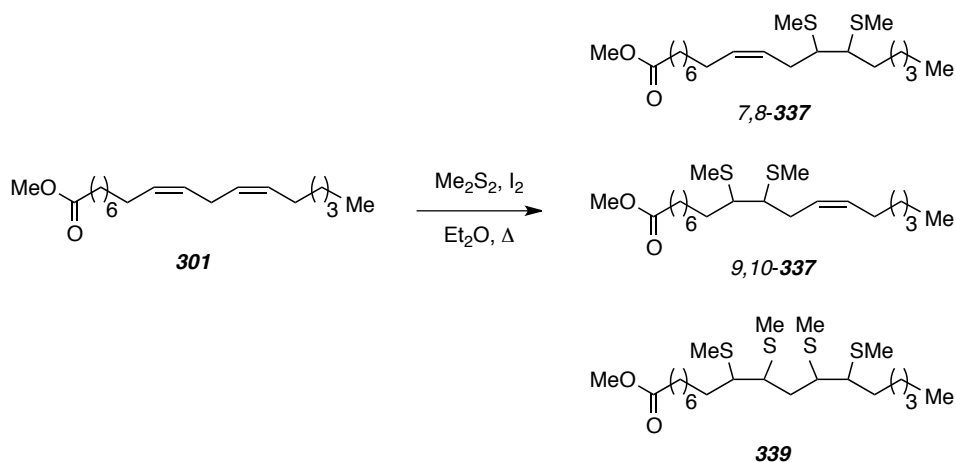
Scheme III-25. Disulfide Reaction under I₂ conditions: DMDS and **310**.



The only problem with this reaction was conversion. I had to use two-fold excess of the disulfide for acceptable conversion (approximately 90%). I did not systematically optimize this reaction, so this is an area for improvement. The workup was also relatively involved, but could be managed.

Although our methodology for polyol synthesis required only chemistry on isolated olefins (those likely to arise after metathesis of soyoil), I also attempted this reaction on the linoleate (Scheme III-26) and linolenate (Scheme III-27) methyl esters.¹⁸¹ This was an opportunity to investigate the conversion problem¹⁸² and see how much functionality could be installed. Using an excess of DMDS, reaction on methyl linoleate gave a mixture of products, those corresponding to one disulfide addition (i.e. **337s**).¹⁸³ Based on the MPLC recovery, it seems that one isomer is favored 2:1 (7,8-**337** : 9,10-**337**). These seemed to be partially separable, but were characterized as a mixture.

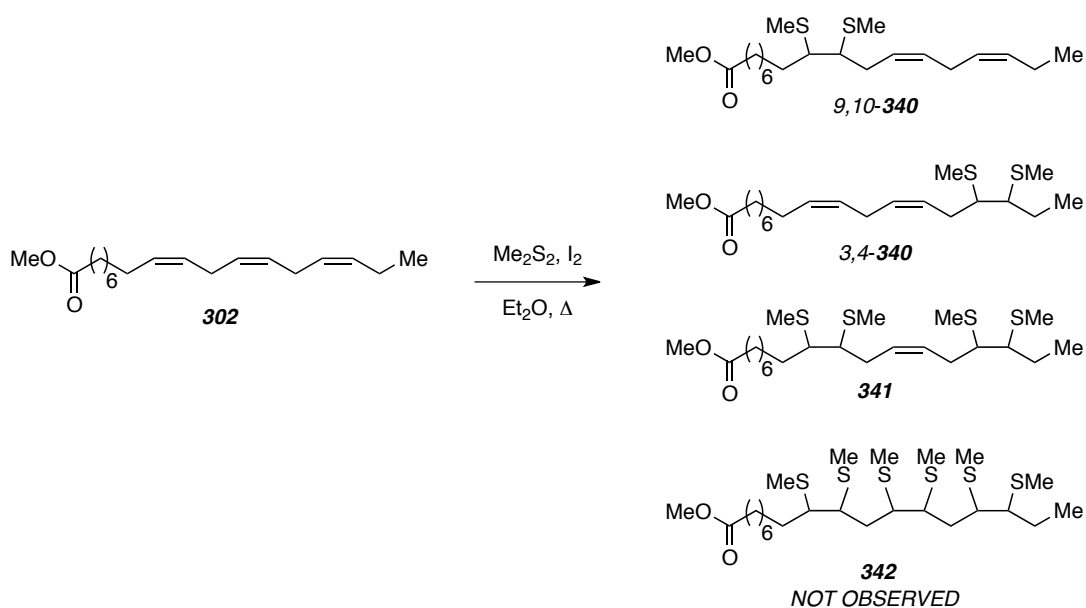
Scheme III-26. Disulfide Reaction Under I₂ Conditions on **301**.



The rate of the reaction was approximately the same as in the oleate case (c.f. Scheme III-25). Sadly, the fully reacted **339** was not observed to a large extent, even with a huge excess disulfide and extended reaction times. This suggests that it would be hard to install >2 hydroxyls on each chain, if so desired on our real substrate.

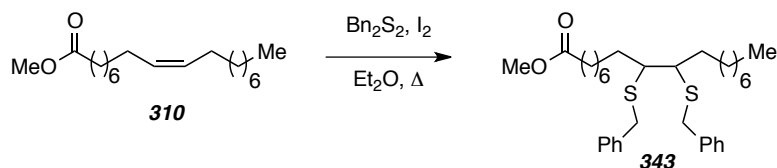
In the reaction of linolenate (Scheme III-27), the mono- and bis-reacted (e.g. **340** and **341**, respectively) substrate could be isolated and characterized. Three regioisomers are available for the former, but based on the diagnostic linolenate methyl resonance, reaction at the Ω -3 lipid surely occurred (i.e. **3,4-340**) and the GCMS indicated the other major mono-reacted product was where the Ω -9 lipid had been engaged (i.e. **9,10-340**). Only the flanking alkenes reacted to form the bis-product **341**. The perfunctionalized **342** was not observed, even with a huge excess DMDS. These last two observations were indicated by the low conversion to **339** in Scheme III-26.

Scheme III-27. Disulfide Reaction Under I_2 Conditions on **302**.



I did not optimize this reaction for each fatty acid variant. If the chemistry was clean enough on a more useful disulfide, attention had to there. I did, however, perform one more practice reaction before moving on to installing hydroxyls. Scheme III-28 shows dibenzyl disulfide reacting with methyl oleate under I_2 catalysis. The reaction is clean to vicinal sulfides **343**, but the conversion was never as high as required. This reaction served to demonstrate that the disulfides can carry other functional groups, and these can be reasonably large. The reaction was not attempted with the linoleate or linolenate variants.

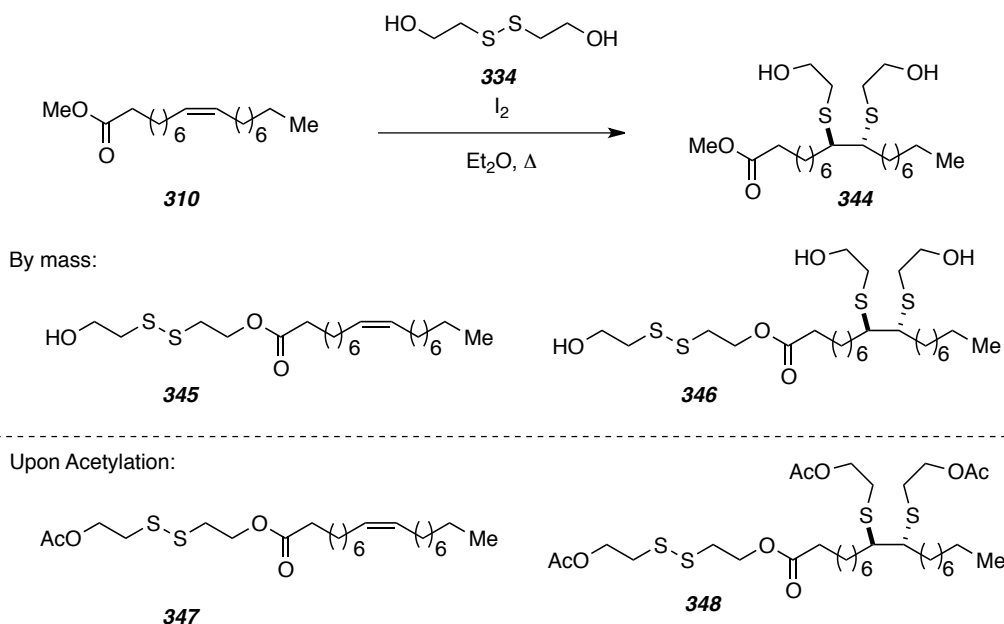
Scheme III-28. Disulfide Reaction of Dibenzyl disulfide under I₂ conditions on **310**.



I discovered limitations in this reaction, similar to those I had already encountered over the course of soyoil studies. For higher molecular weight disulfide reactions, such as the one shown in Scheme III-28, the GCMS cannot be used for analysis. This reaction also introduced some complexity due to diastereotopic groups and made NMR analysis difficult. These issues were understood as best as I could and I was confident that the reaction with a more useful disulfide (diethanol disulfide, **334**) would be tractable.

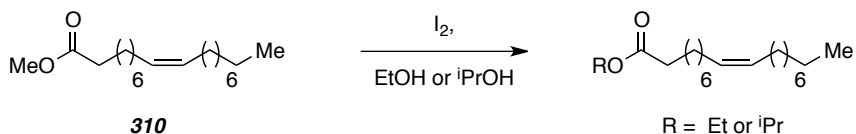
The conditions that worked best for DMDS were used for the reaction of diethanol disulfide (**334**) and methyl oleate (**310**, Scheme III-29). The result was satisfactory. The reaction proceeded more slowly than the previous studies and conversion to the diol **344** was modest. The reason for this seemed to be transesterification of both the starting material (giving rise to **345**) and the bis-sulfide product (giving rise to **346**). These proposed structures were supported by acetylation studies (lower panel), which gave the expected masses for products **347** and **348**.

Scheme III-29. Disulfide Reaction of **334** and **310** under I₂ conditions.



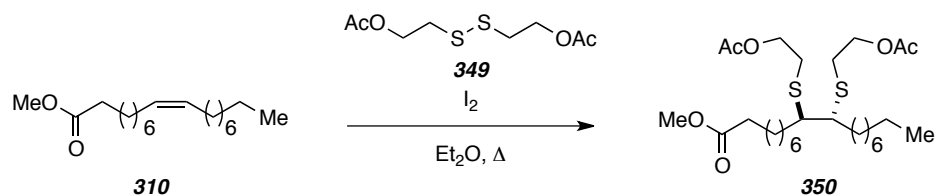
Transesterification under I₂ conditions was confirmed by a model study (Scheme III-30) where methyl oleate (**310**) was treated with I₂ and stirred in either EtOH or ⁿPrOH. The ethyl and propyl esters of oleate appeared at room temperature after only a few hours.

Scheme III-30. Observed Transesterification of **310** promoted by I₂.



In the real system, where extended reaction times (and heating) was necessary, transesterification would continue to be a problem. It would certainly lead to lower conversions and yields. With the protected form of the disulfide (**349**, Scheme III-31), the reaction was much improved. There were still issues with modest conversion, and the unreacted disulfide was difficult to remove from the crude mixture, but the desired functionalized alkene product **350** was isolated. I tried higher temperatures as a way to approach the conversion issues. Under these conditions, the reaction was more efficient with less byproduct (likely a reaction intermediate) formation. As encouraging as this modification, the burden of having to unveil the diol limited the utility of **349**. However, if the deprotection could be performed efficiently or in a controlled way to release only certain amounts of hydroxyls, it might still be useful. This would be yet another way to tailor our polyol to fit into the desired specifications (functional numbers).

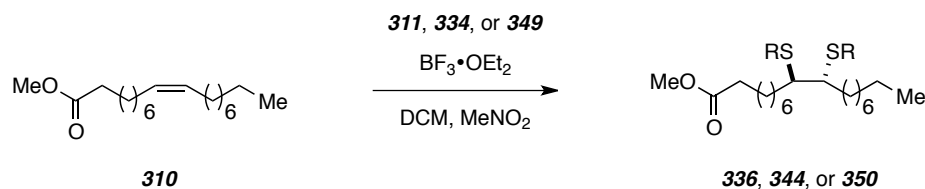
Scheme III-31. Attempted disulfide reaction of **349** with **310** under I₂ conditions.



Although the I₂ reaction was worthwhile on a fairly large range of substrates, BF₃•OEt₂ was found to be a superior catalyst.¹⁸⁴ The yield immediately improved in the reaction of methyl oleate (**310**) and dimethyl disulfide (Scheme III-32). These conditions were far more mild and efficient; the reaction occurred at room temperature and only required a slight excess of the disulfide for full conversion. The only problem was the use of MeNO₂ and DCM as a solvent, but it was quickly discovered that the reaction worked

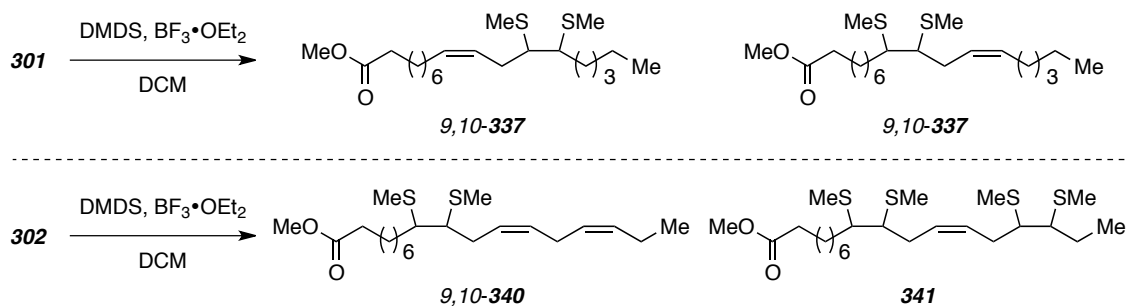
wells in DCM alone. The reaction with the diethanol disulfide (**334**), however, was sluggish unless a stoichiometric amount of $\text{BF}_3 \cdot \text{OEt}_2$ was used. With the protected diol **349**, the reaction furnished desired product **350** cleanly, but again, required stoichiometric catalyst for reasonable rates.

Scheme III-32. Disulfide Reaction of **310** Under $\text{BF}_3 \cdot \text{OEt}_2$ Conditions.



Although not completely optimized, these new conditions were applied to the DMDS reaction with doubly and triply unsaturated fatty acid esters (**301** and **302**, Scheme III-33). The mono addition products (**337** and **338**) were cleanly generated, but as a mixture. Even with a large excess of the disulfide and extended reaction times, the bis-addition product (**339**, Scheme III-26) was not observed by LCMS or NMR analysis. The reaction of triply unsaturated methyl linolenate (**302**, Scheme III-33, lower panel) was then studied. In this case, the reaction was again rapid to produce the mono addition product **9,10-340**, but further additions were slower and reaction at the third and final alkene seemed impossible. The mono- (**340**) and bis- addition (**341**) products were easily separable and could be characterized. The former was produced as a mixture of regioisomers (with **3,4-340**, see Scheme III-27). With more effort, these might be separable from one another. The tetra functionalized, **341**, again seemed to be produced as one regioisomer. That is, the reaction always proceeded to give functionalization at the flanking alkenes. This mimics the results presented in Scheme III-27.

Scheme III-33. Disulfide Reaction of **301** and **302** under $\text{BF}_3 \cdot \text{OEt}_2$ Conditions.

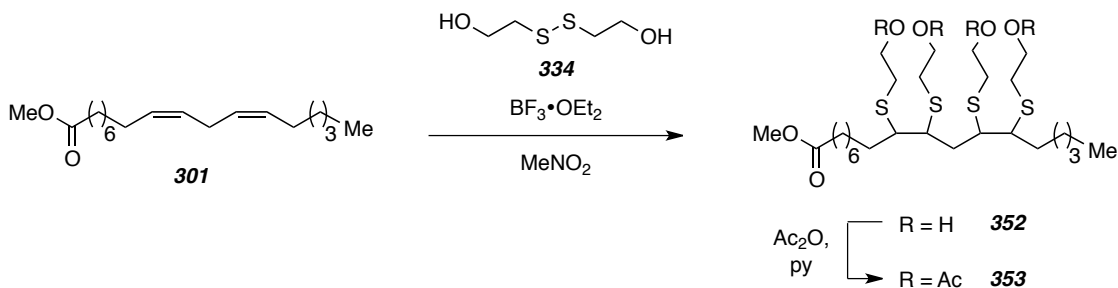


In general, the $\text{BF}_3 \cdot \text{OEt}_2$ made the reaction more efficient, scalable, and reproducible. Complete consumption of alkene and methods of analysis continued to be a problem. It might be that the fatty acid chain cannot support per-functionalization of its alkenes (e.g. **302**, where 6 new bonds have to form). The conversion, of course, is not an issue if the reaction can be performed in a controlled way. Leftover alkene is not likely to be a problem in the formulation of a PU.

The LCMS (the preferred method of analysis for this reaction) problem was more serious. The data from this instrument was often misleading. The molecular ion was not always observed; some of these sulfides occasionally lost (SMe) upon ionization. This problem was somewhat mitigated by use of the negative ionization mode, if the analyte was capable of this adduction.

Following these studies with DMDS (and the lessons learned from using the LCMS as a tool in this reaction), the new conditions were applied to more complex starting materials and diethanol disulfide. Although the double addition product was not observed with DMDS, it was worth trying to push that reaction with **301** and diol **334** (Scheme III-34), since it directly installs the required alcohols for PUs. In the event, it was possible to set up this reaction to consume all alkenes, but it required a large excess of disulfide (>10 equiv) and purification of **352** was tedious and usually unsuccessful.

Scheme III-34. Disulfide reaction of **334** and 310 Under $\text{BF}_3 \cdot \text{OEt}_2$ Conditions.

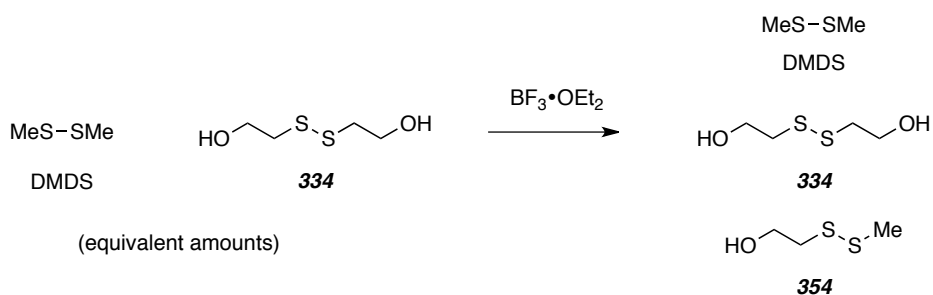


The unreacted diol **334** interfered with product isolation. Acetylation (to **353**) did help, but purification was still troublesome. I also tried reduction of the remaining disulfide to its components mercapoethanol (**332**). This reduction did work, but the new contaminant was the TPPO that was difficult to remove. So under I_2 versus the BF_3 conditions, the addition of disulfide **334** was superior with the latter because the threat of

transesterification (c.f. Scheme III-30) was eliminated, making more starting diol available for alkenes.

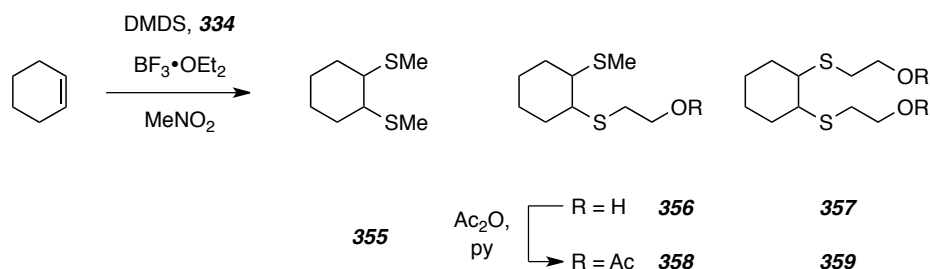
Along the course of these studies, the chemistry was working well enough that it seemed reasonable to move forward with various unsymmetrical disulfides. The advantage was that we could start to control how many hydroxyl groups were incorporated. We could adjust to only one, or in the case of a diol, perhaps we would be able to spread them a little farther apart (spacing of the OH functionality has implications for the properties of the PU). Disulfide exchange in the presence of BF_3 and other catalysts^{185,186} is well-known and occurs readily to give a statistical mixture of products (Scheme III-35). In my system, two main disulfides (i.e. DMDS and **334**) were available.

Scheme III-35. Disulfide Exchange Reaction of DMDS and **334**.



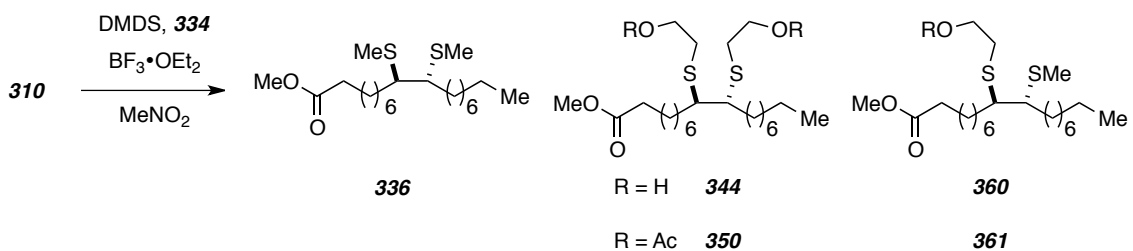
A mixture of DMDS, **334**, and **354** was observed from this reaction.¹⁸⁷ The mixture was used as such in the subsequent reaction with an alkene. To begin with, I attempted it on the more manageable cyclohexene (Scheme III-36). There were minor difficulties in the analysis (cleavage of the C-S bond upon chemical ionization of the LCMS), but the expected products (symmetrical **355** and **357** and crossed product **356**) were separated with modest success. They were taken on to acetylation for more structural support. The separation of the acetylated derivatives **358** and **359** was not trivial, but they could be identified with confidence in the ^1H NMR spectrum from a rough separation. Mass balance was not taken to confirm that a statistical mixture was in fact, realized. Alternatively, the disulfides DMDS and **334** could be added directly to the reaction pot with the alkene without premixing. In this case, the reaction profile was identical. This confirms the exchange reaction is rapid and reaches equilibrium complete prior to addition to alkenes.

Scheme III-36. Mixed Disulfide Reaction of DMDS and **334** on Cyclohexene.



This reaction was then applied to our methyl oleate system (Scheme III-37). It was monitored by LCMS and after only a few hours, there were peaks corresponding to the expected three products **336**, **344**, and **360**. Once again, molecular ions were difficult to discern. Acetylation and separation gave the adducts of both symmetrical disulfides (**350**) and the mixed one (**361**). Key NMR features gave confidence to the assigned structures.

Scheme III-37. Mixed Disulfide Reaction of DMDS and **334** on **310**.



The key feature of this reaction is that diethanol disulfide (**334**) reacts far slower than either the DMDS or the mixed disulfide. Further study would provide more information for the best way to vary the starting ratio to optimize both the exchange and addition reaction. That is, the alcohol or diol products **360** and **344** could be obtained at will, depending on which was desired for PU formation.

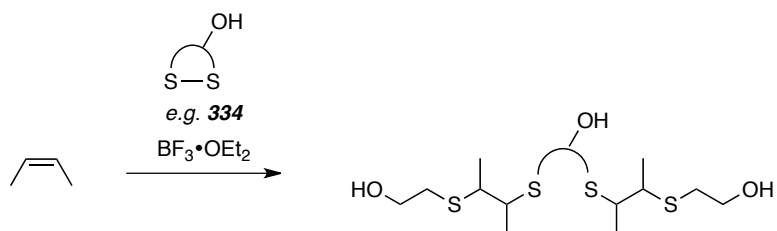
Lipoic acid can also undergo disulfide exchange under the same conditions (Scheme III-38). The newly formed disulfides (although existing as a mixture with the starting materials) could be used in this same reaction. This strategy was promising in a similar way to section **V.B.2.b**, where lipoic acid dithiol addition to two fatty acids does the job of cross-linking chains and installing hydroxyl groups simultaneously (c.f. Scheme III-20). The proposed disulfide exchange is illustrated in Scheme III-38.

Scheme III-38. Disulfide Exchange reaction of **318** and DMDS or **334**.



The general reaction preparation is shown in Scheme III-39. In the end, two alkenes react at both of their carbon centers to furnish 4 new bonds and afford a triol.

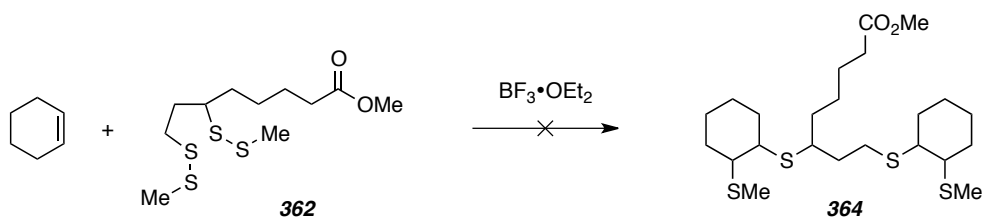
Scheme III-39. General Strategy for Simultaneous Cross-linking/Functionalization of Alkenes.



The exchange reactions (Scheme III-38) were somewhat easy to monitor. The DMDS-exchanged **318** (=362) can be observed by GCMS (although the molecular ion was very weak), but the diethanol disulfide-exchanged **334** (to give the analogous structure to **362**) was more difficult. I tried with lipoic acid (**315**) and the diol **334**, but this reaction was difficult to analyze as well.

Despite the uncertainty surrounding the extent of exchange, the disulfide addition reaction was attempted on cyclohexene (Scheme III-40). The problem was probably the small scale. The product **364** should have been, but was not, easily observed by LCMS. Besides scale, perhaps additional Lewis acid treatment of the fragile bis-disulfide **362** enabled re-exchange and damaged the reagent before it could engage in the reaction.

Scheme III-40. Attempted Cross-linking / Functionalization of Cyclohexene.



This was the last of the studies performed with the intent of functionalizing the alkene with a sulfide group. By the time I would have been able to go through and scale up for this (already) unreliable chemistry, the project had advanced.

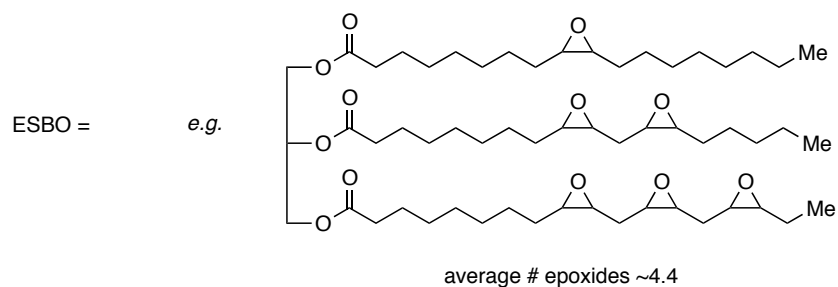
V.C. Studies on Epoxidized Soybean Oil

Epoxidized soybean oil (ESBO) is readily available and cheap. It provided an alternative to soybean oil and a whole new set of functionality (epoxides) to learn how to react. As with soybean oil itself, I looked to understand ESBO before I went ahead and performed chemistry to transform it.

V.C.1. General Studies With Methyl Epoxy Soyates

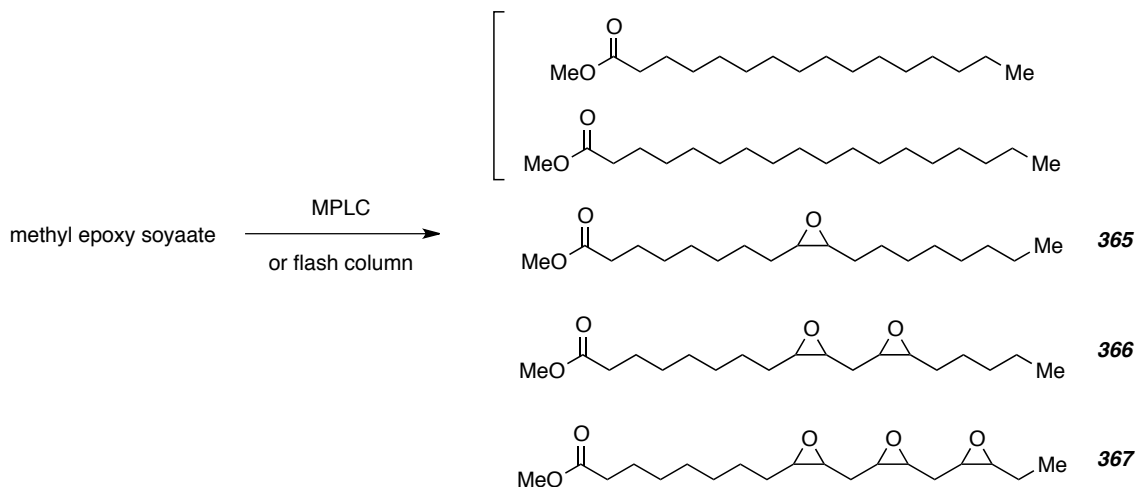
Epoxidized soybean oil (Figure III-6) is where all the alkenes of the triglyceride have undergone conversion to epoxides. Just as there are an average of 4.4 double bonds per soyoil triglyceride, there is an average of 4.4 epoxides for each ESBO molecule.

Figure III-6. Epoxidized Soy Triglyceride with 6 Epoxides.



Epoxy methyl soyate can be purchased as a mixture of methyl esters where each chain has 0, 1, 2, or 3 epoxides, arising from stearate, oleate, linoleate, and linolenete esters, respectively.

Scheme III-41. MPLC Separation of Methyl Epoxy Soyates.



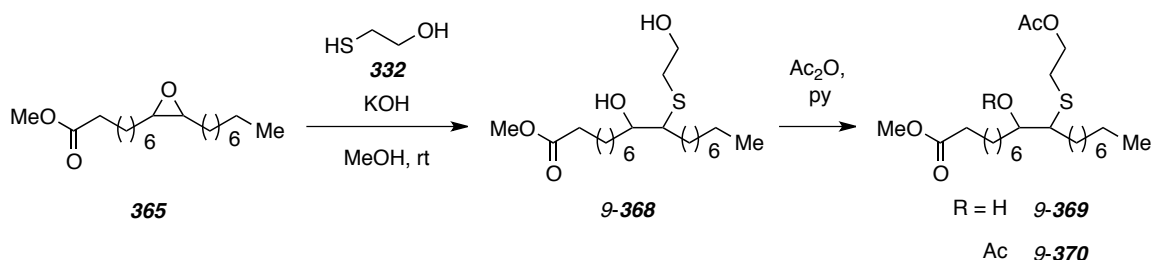
All of these esters were GCMS and LCMS compatible. By GC, there appeared to be two diastereomers of the bis epoxide **366**, and three of the tris epoxide **367** (Scheme III-41). The diastereomers could not be resolved by LCMS technology. All of the components of methyl epoxy soyate were amenable to MPLC or flash chromatography. Currently, it is unknown whether the diastereomers are separable; chromatographic conditions were not optimized for that application.

V.C.2. Thiolate Opening of Methyl Epoxy Soyates

Epoxides can be opened in a wealth of ways.¹⁸⁸ The method chosen for these epoxides was thiolate opening. We already had the raw materials and it was well known that using a variety of bases, thiolates were capable of doing the job.¹⁸⁹ We started with a monofunctional thiol but hoped to progress to a dithiol for a simultaneous ring-opening/chain-linking event.

The first reaction was conducted on methyl epoxy oleate (**365**). In the event, the alkene was treated with mercaptoethanol (**332**) and a catalytic amount of KOH (Scheme III-42). There is likely no regiochemical preference for this nucleophilic attack; only the result of ring opening at carbon 9 is shown (**9-368**). Indeed, the diol appeared to be isolated as a mixture of regioisomers (with *10-368*, not shown). For the remainder of this discussion, where there is potential for regioisomers, the ring-opened products are distinguished by the carbon number where thiolate attack occurred.

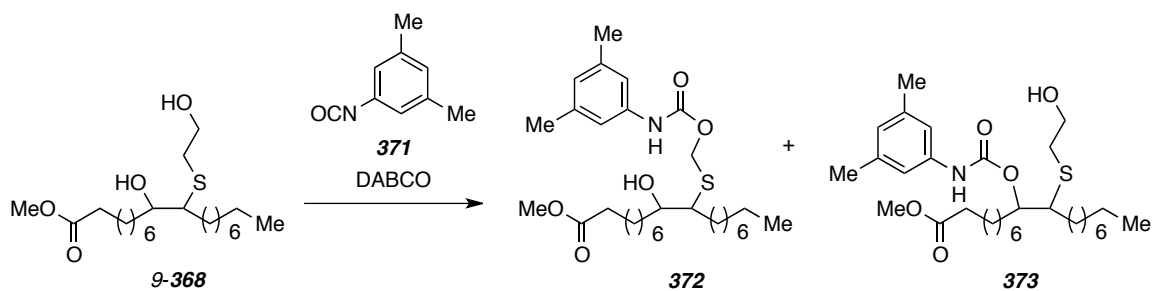
Scheme III-42. 365 opening by 332.



The reaction was easy to monitor and conversions were typically good. Both Na metal and KOH were found to be effective, but the latter was chosen because of ease of handling. The product diol **368** can be further modified to confirm both the structure and NMR features. Acetylation with one or two equivalents of Ac₂O furnished the mono-protected **9-369** or bis-protected **9-370**.

The diol **368** was also used in a model experiment to test a carbamate linkage reaction (with an isocyanate, Scheme III-43). The reactivity difference between a primary and secondary hydroxyl is important to understand when we are designing and crafting polyols for our renewable PUs. Surprisingly, the secondary alcohol was somewhat competitive with the primary, and the result of this reaction was a mixture of mono-carbamates **372** and **373**. The bis-reacted product (not shown) was not observed. This reaction was only performed once, however, and little was discovered about ratios at lower conversions and whether a second carbamate is even possible on this diol.

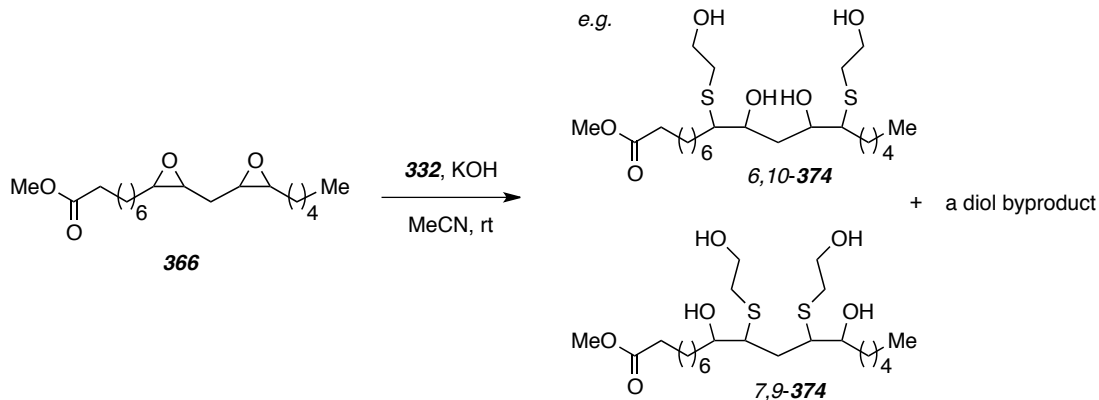
Scheme III-43. Reaction of 368 with Isocyanate 371.



Although the yields were modest in the ring-opening reaction, the results were encouraging enough to move onto the bis-epoxide (**366**, Scheme III-44). Action of thiol **332** on this substrate gave the desired tetraol products **374**. Again, they are named based on which site the sulfide bond forms. Only two examples are shown, I did not investigate the regiochemistry of these reactions. The high level of hydroxyl functionality was

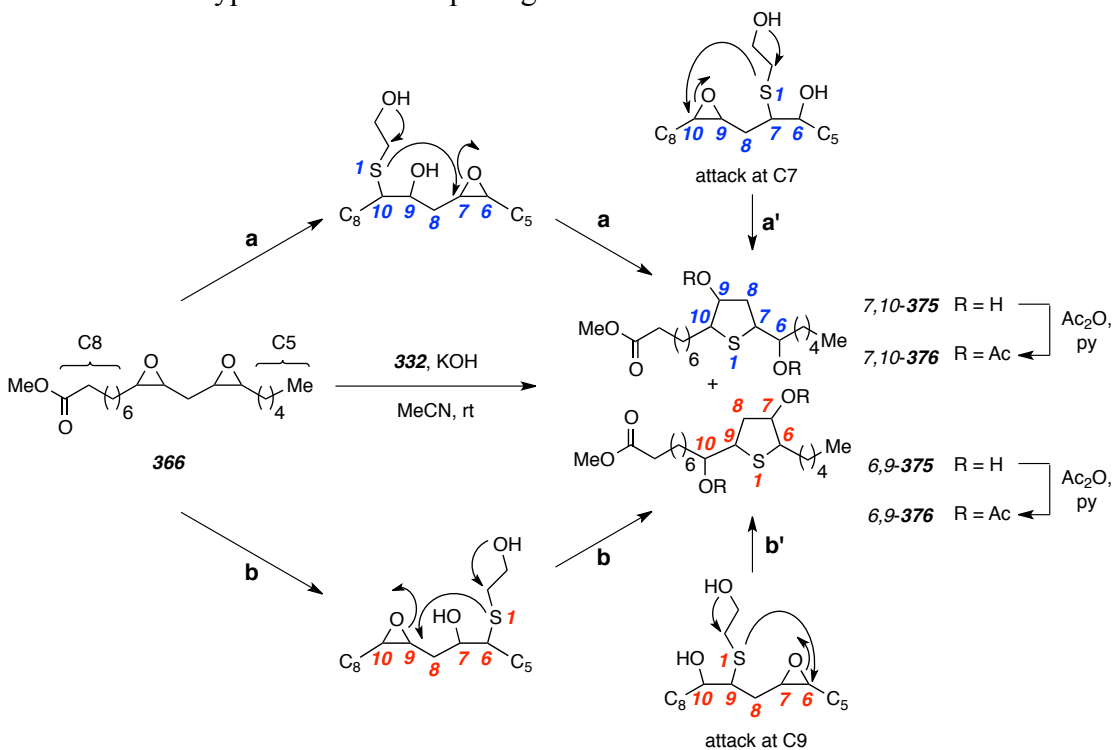
confirmed by NMR integrations and preparation of the per-acetylated derivatives of **374**. Unfortunately, the yields of the epoxide opening were low with the formation of one other major product.^{190,191}

Scheme III-44. Epoxy Methyl Linoleate (366) Opening by 332.



The byproduct appeared to be a diol based on the number of acetyl groups added onto the molecule from the acetylation experiment. After a number of methods to characterize this byproduct, the data is consistent with the structure of tetrahydrothiophene **375** (Scheme III-45). COSY data and comparison to known compounds¹⁹² guided this structural assignment.

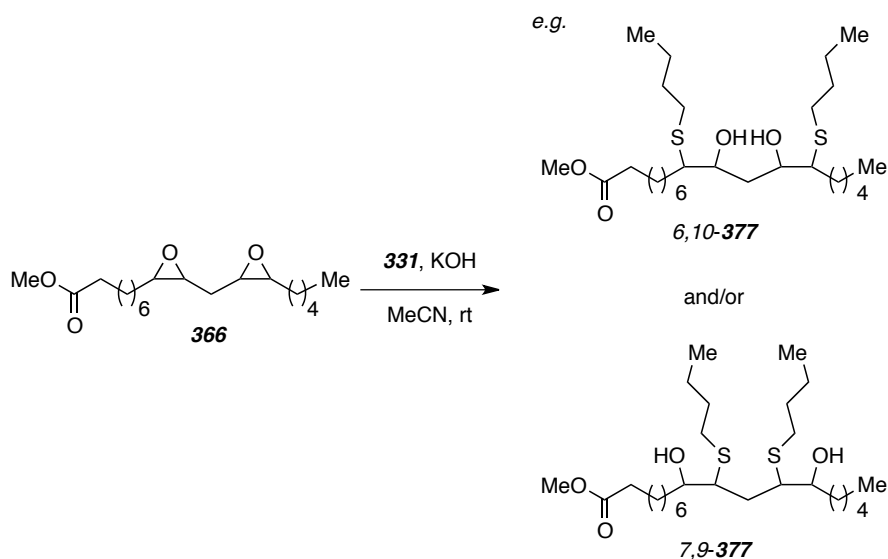
Scheme III-45. Byproduct of 332 Opening of 366.



When **366** is attacked by a thiol nucleophile at one of the termini of the bis-epoxide system [numbering as in fatty acid chain, either C10 (path a) or C6 (path b)],^{193,194} the sulfur is situated 5 atoms away from the proximal end of the remaining epoxide. In path a, it can open the other epoxide at C7, 5 atoms away, to give the tetrahydrothiophene. In path b, the sulfur (now at C6) opens the second epoxide at C9. At some point the pendant alcohol must release the thiol (or thionium) for product formation.¹⁹⁵ Assuming no regiochemical preference exists, both thiophenes **375** are produced and have very similar NMR properties. Attack at one of the internal carbons (C7 in path a' and C9 in path b') results in a sulfide that is still situated for attack at the remaining epoxide (C10 in path a' and C6 in path b'). These processes are essentially the reverse order of the first, so they afford the same isomers *7,10-375* and *6,9-375* that were already accounted for. The NMR data is consistent with structures **375**, and comparison to similar compounds in the literature support this assignment. The expected shifts occurred upon acetylation to **376**.

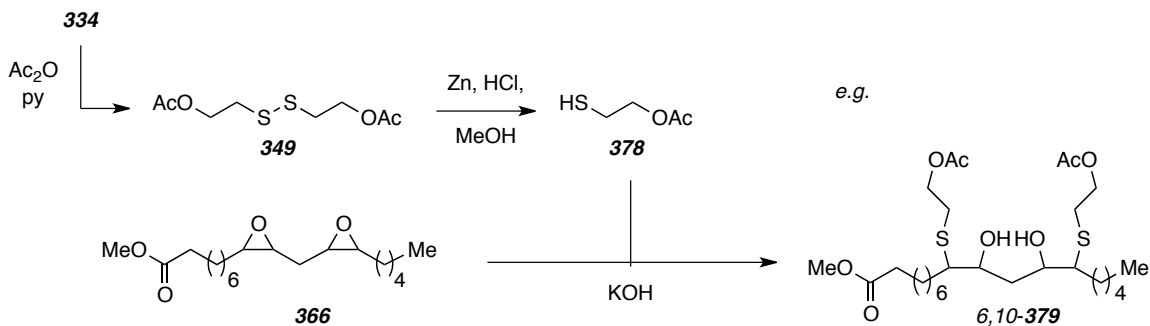
If in play, the mechanism for the formation of the **375** requires the presence of the pendant hydroxyl group. This byproduct would not be observed for other thiolate nucleophiles. To test this, the analogous reaction was performed with butane thiol (**331**) on the bis epoxide **366** (Scheme III-46). When 2 equivalents of the thiolate were added to the bisepoxide, the mass of the desired double addition product [**377**, two examples of regiochemical attacks (6,10- and 7,9-) are provided] appeared in the LCMS, along with some of a presumed minor regioisomer, the starting material, and a little saponification product. When the reaction was performed with only one equivalent, there was still a majority of the bis addition product **377**, followed by unreacted **366**, and a few minor peaks. One of these minor components gave the mass of the compound that arises from attack at one epoxide, with one intact. This experiment was run a few times, and although the results were not always identical, the thiophane product mass was never observed. Instead, the problem was poor conversion and difficulty in separating the components of the reaction mixture.

Scheme III-46. 366 Opening by Butanethiol (331).



Since the formation of the byproduct appears to rely on the pendant hydroxyl group, I considered the reaction of a protected variant (**378**). The best way to access the starting material was the two step sequence from diethanol disulfide (**334** to **349**, Scheme III-47, first arrow). The acetylated mercaptoethanol **378** was then used in the ring opening reaction under the previously established conditions.

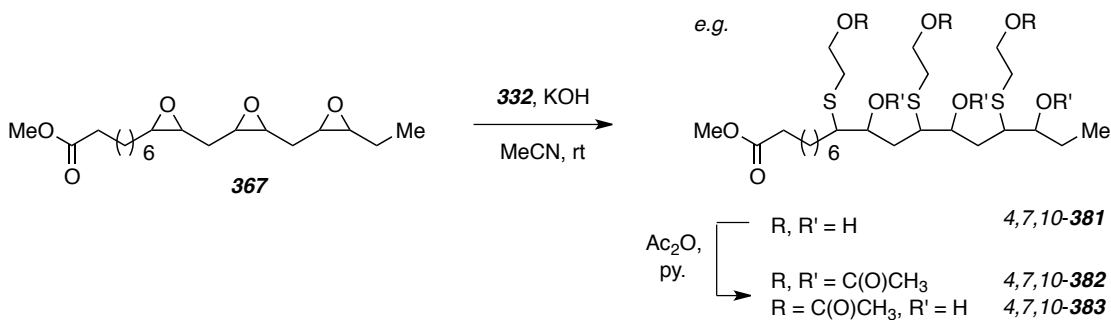
Scheme III-47. Opening of 366 by Mono-protected Mercaptoethanol (378).



Sadly, this reaction did not work as well. It was too complicated to be useful, and the mass of the desired product (example 6,10-**379** is provided) was not observed. The free alcohol variant was far superior.

Despite the byproduct of the reaction of **366** with **332**, these studies clearly show that reaction at both epoxides is possible. Further experimentation is required to determine if reaction at one and only one epoxide center can be accomplished. Preliminary work

Scheme III-49. Opening of **367** opening by **332**.



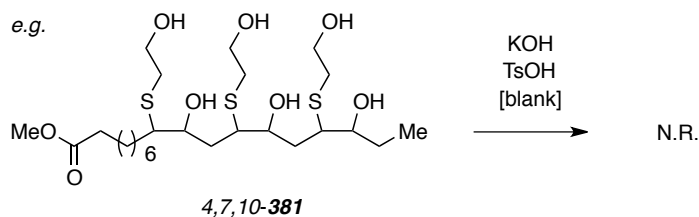
Although the reaction seemingly proceeded very cleanly (by LCMS, the desired was the main product), purification of the highly polar **381** was problematic. Normal phase chromatography under a variety of mobile phases was unsuccessful, with excess **332** contaminating all samples. However, these preliminary studies show that since the reaction was so efficient, perhaps a huge excess of thiol **332** was not required. If so, the purification step would be rendered unnecessary. Another consideration is that the hexaols are so densely functionalized, they might not be useful in PU formation. Acetylation did well to mitigate the polarity (last arrow, Scheme III-49). The per-acetylated species (**4,7,10-382**) appeared by LCMS, and the purification gave a satisfactory sample. The 1H NMR spectrum, however, is complicated by what has to be a number of diastereomers (three different for the starting material). I could not resolve them by LCMS, but more work could be done with the method to see if that is possible.

Acetylation was also performed with an undercharging of the reagents (Scheme III-49, last arrow). If selective capping of the primary alcohols was possible, this was another way to control exactly how many hydroxyls were free to react in the polyurethane-forming reaction. When the hexaol was treated with slightly over 3 equivalents of acetic anhydride, within two hours, the mass of the tris-reacted hexaol **383** was observed by LCMS, along with various amounts of the product of one or two acetyl additions, alongside starting material. When the reaction was allowed to continue, these ratios did not change. After stirring overnight, the products were approximately half tris-reacted hexaol **383** and half have tetra-reacted (not shown). Other species were present, even quantities of the hexa-reacted **382** were observed by LCMS. Unfortunately, it was not straightforward to separate all the various esters, and full characterization of each was

not completed. It is clear, however, that acetylation must be optimized for control over how many free hydroxyls are desired in the product.

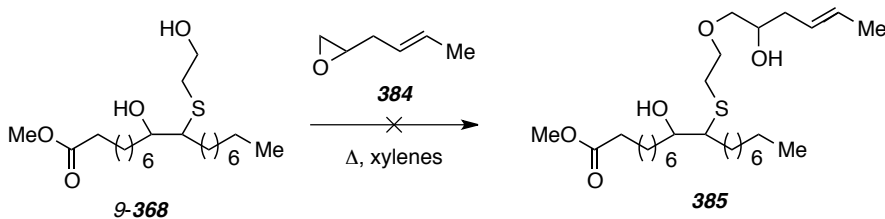
I had enough crude material (**381**) for a few more experiments to contribute to our understanding of the hexaol. First, I was suspicious that no tetrahydrothiophene was observed with the tris epoxide reaction. I took the hexaol and heated it further in basic, neutral, and acidic media to see if displacement by the sulfide and loss of ethylene oxide was possible (Scheme III-50). This would also give some idea of the mechanism if cyclization occurred. Surprisingly, the hexaol was robust to all these conditions. In the future, doing the ring-opening with an undercharging of thiol would be worthwhile in case we desired a few epoxides to remain intact (and provided the byproduct pathway can be rendered inoperative).

Scheme III-50. Stability of Hexaol **381** Under Various Conditions.



Hydroxyls can also be nucleophiles for these types of epoxide opening reactions. I attempted to react **368** (c.f. Scheme III-42) with epoxide **384** to see if any union would occur. Unfortunately, this was not a promising experiment (I observed no reaction), but it is important to consider that the hydroxyls obtained from these thiolate reactions. The reactivity of these alcohols is of utmost importance because they are the key players in PU synthesis.

Scheme III-51. Attempted Opening of Epoxide with **368**.



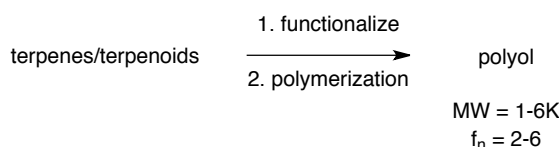
V.D. Summary and Outlook

The thiol-ene reaction, disulfide addition to alkenes, and epoxide opening were all moderately successful. The first was a novel way to cross link alkene chains while also installing required alcohol functionality. Disulfide addition was complicated by low conversion and transesterification. This would likely be a problem on soyoil. The last method, epoxide opening, must be optimized if the byproduct formation continues. Based on the understanding gained by the experiments surrounding that reaction, it would be a problem wherever any linoleic fatty acid chains were present.

Chapter VI. Polyols from Terpenoids

Terpenes and terpenoids are renewable small molecules. They have natural, sustainable sources (commonly plants). They can be converted to suitable substrates for polymerization (Scheme III-52). One way is oxidation of the cyclic ketone to a lactone, which is known to undergo ring-opening polymerization (ROP, discussed in section VI.B). Besides their use in generation of a polyol, these small molecules display interesting NMR behavior that warranted further study (discussed in section VI.C.)

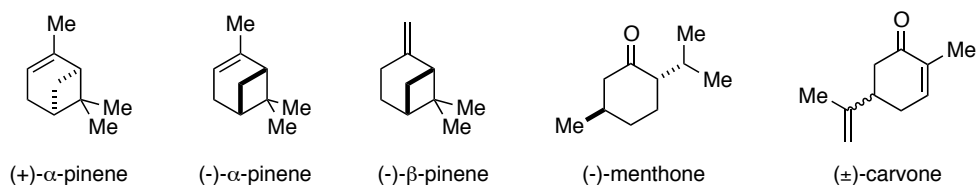
Scheme III-52. General Strategy for Converting Terpenes to Polyols



VI.A. Background and Previous Work

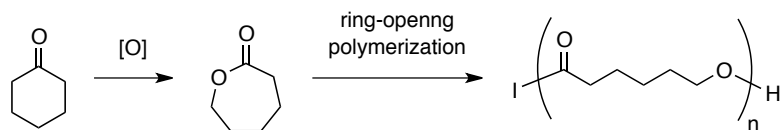
Terpenes and terpenoids are diverse and abundant in nature. Some examples are shown in Figure III-7. Many make up a large proportion of oil extracted from various plant sources. Examples of terpenes are α - and β -pinene, whereas menthone and carvone are terpenoids. These latter compounds are labeled as such because they contain oxygen.

Figure III-7. Terpenes and Terpenoids.



Currently, the most common methodology for conversion of these small molecules into a polymer is to incorporate the desired functionality into the monomer (Scheme III-53, first arrow). The example is cyclohexanone oxidation ϵ -caprolactone, a more suitable substrate for polymerization. The lactone can undergo ROP to the targeted polyol (second arrow). For our soyoil studies (Chapter V), we desired a polyol with 2-6 hydroxyl groups and a molecular weight of 2-6 kg/mol and these too were the ranges we sought with the terpenoid methodology.

Scheme III-53. Polymerization of Cyclohexanone.



From reading previous work of other groups, we know that both the oxidation and ROP reactions work on a wide variety of substrates.¹⁹⁶ We were building off specific research from the Hillmyer group, which demonstrated that this sequence was possible starting from menthone and carvone (Figure III-7).¹⁹⁷ We hoped to take their methodology one step further and use the polyol in a polyurethane reaction.

The sequence began with Baeyer-Villiger methodology¹⁹⁸ as a convenient and well-established way to achieve oxidation to the lactone. For the lactones we anticipated, the ROP would likely be run under metal catalysis, although a number of other catalysts were known and available. Finally, a partnership with the Macaskco group would enable us to learn the art of polyurethane formulation for the construction of a PU film. Senthil (his work was discussed in Chapter V) was the main polymer chemist in this collaborative effort, and I performed a number of supporting experiments that are discussed in the next section.

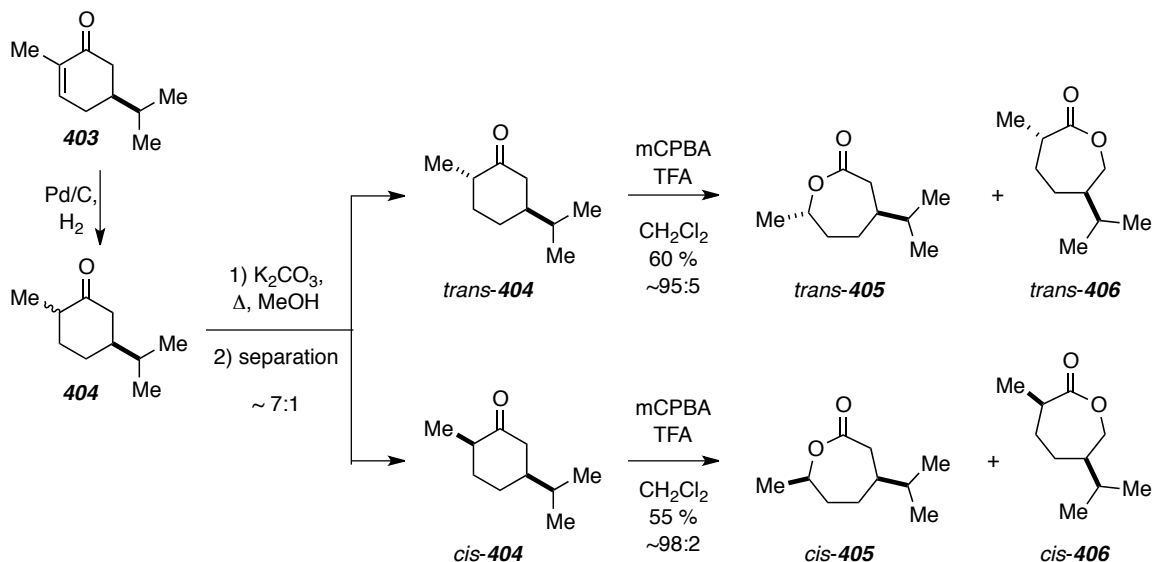
VI.B. Menthone and Carvomenthone

As mentioned, menthone and carvomenthone were chosen as the renewable terpenoids. This study first requires an understanding of the Baeyer-Villiger reaction, then model studies could be performed on the ring opening of the resulting lactones. Lastly, reaction with an isocyanate as a further model for the polyurethane formation was conducted on the ring-opened lactones.

VI.B.1. The Baeyer-Villiger (BV) Reaction

The Baeyer-Villiger reaction was first performed on menthone (*trans*-**400**, Scheme III-54).¹⁹⁹ The oxidation was effected by mixing the cyclic ketone with a stoichiometric quantity of TFA followed by portion-wise addition of mCPBA. A smooth conversion to

Scheme III-55. Synthesis of *trans* and *cis* Carvomenthide (**405**).

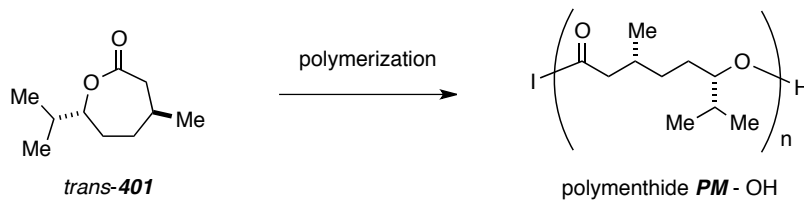


In practice, carvomenthide (Scheme III-55) was used as a mixture of *trans* and *cis* isomers (approx. 6:1) for the polymerization. However, for later studies (particularly the NMR properties of these small molecules, see section VI.C.), the regioisomers and diastereomers needed to be pure form. At the time, however, the BV chemistry was most useful in generating material for the synthesis of a series of model compounds from which we could understand the results of Senthil's ROP reactions.

VI.B.2. Ring-Opening of Menthlide and Carvomenthide

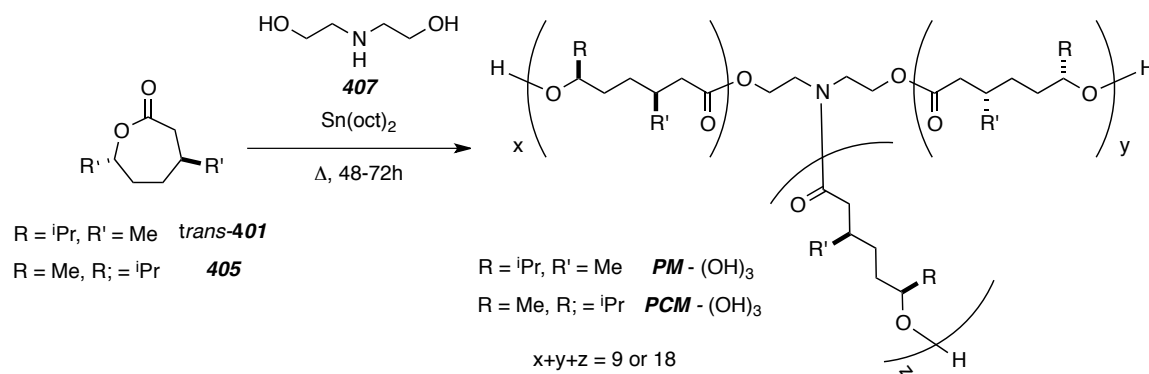
In the previous section, material was obtained for the model study of ring opening polymerization, shown generally in Scheme III-56. A high-yielding and straightforward polymerization reaction was required toward the successful preparation of a polyurethane film.

Scheme III-56. General ROP of Menthlide.



If this reaction were performed as indicated in the scheme, the resulting polymer would contain only one hydroxyl group and could not be used as an effective crosslinking agent (see Part Three Introduction). The trifunctional initiator diethanolamine (**407**) was chosen due to its resemblance to ethylene glycol (previously used effectively in polyol synthesis) and good solubility properties. The general scheme is then represented in Scheme III-57.

Scheme III-57. General ROP of Lactones *trans*-**401** and **405** With Initiator **407**.



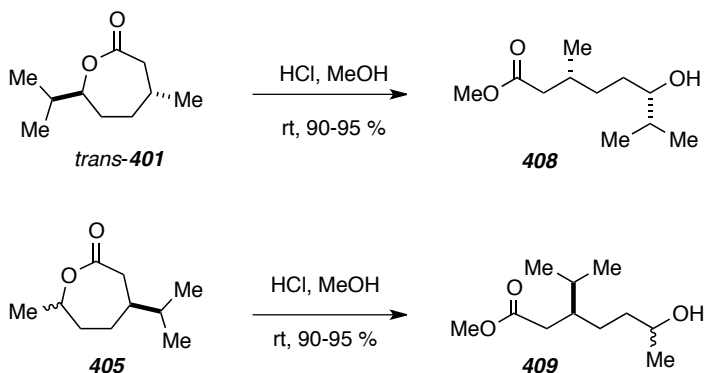
Also shown are the conditions and catalyst [Sn(oct)₂]. The result is a triol (denoted (OH)₃, either **PM** or **PCM**). The target molecular weight of either polyol was 1-3K for this study, so for each initiator molecule, 9 or 18 equivalents of *trans*-**401** or **405** were used. The reaction was performed essentially neat, and the crude polymer was subject to a short workup to remove unreacted lactone.

Senthil's work on the synthesis of polyols from menthone-derived lactones revealed some interesting features of this reaction. The key observations were i) the amine reacted first to open the lactone ii) both a 9:1 or 18:1 loading of monomer to initiator could be used iii) menthide and carvomenthide behaved drastically different in the ring opening and iv) there was complexity in the ¹H NMR spectrum. To aid the analysis (especially point iv), I was charged with the preparation of a series of model compounds.

First, I used general ring opening conditions to prepare set of methyl ester alcohols that would serve as a starting point (Scheme III-58). These would be especially useful in understanding the differences between the constitutional isomers menthide and carvomenthide, but also help to understand the differences between *cis* and *trans* diastereomers. The methyl esters **408** and **409** were easily obtained by acidic ring

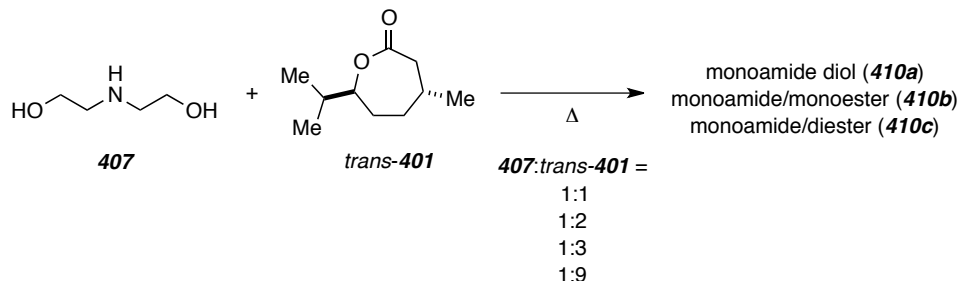
opening of the precursor lactones (*trans*-**401** and **405**). The reaction occurred quickly at room temperature and gives a high yield of the lactones for future study. Note that the carvomenthide isomers were used as mixture.

Scheme III-58. Ring Opening to Methyl Esters **408** and **409**.



With a firm understanding of the NMR properties of these alcohol esters, it was time to prepare the model compounds relevant to Senthil's polymers. Menthide was found to ring open by action of diethanolamine (**407**) under thermal conditions (Scheme III-59). Depending the load of lactone *trans*-**401**, temperature, and reaction time, various ratios of monoamide diol, monoamide/monoester, and monoamide/diester (compounds **410a-c**) were obtained. Up to 9 equivalents of the lactone were charged in this reaction. This encouraged greater conversion and a higher proportion of the monoamide **410a** was converted to the monoamide/monoester **410b**. Interestingly, this higher loading did not dramatically increase the proportion of triol **410c**. This was the first indication that initiation of the third arm of trifunctional **407** posed some difficulty.

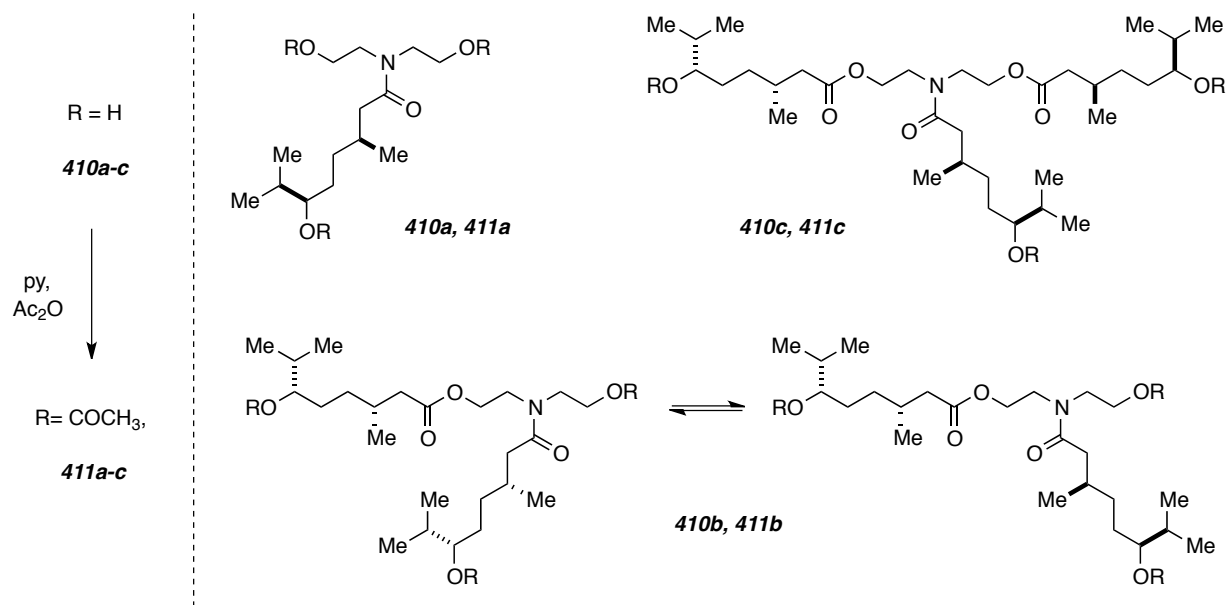
Scheme III-59. Ring-opening of Menthide Under Different Monomer Loadings.



Analysis of these molecules was much more complex than the esters in Scheme III-58. First, the presence of a stereogenic center, which was not a problem in esters **408** and **409**, led to many unique resonances for each of the diastereotopic protons in **410a-c**

(Figure III-8). Additionally, there are two unique rotamers for monoamide/monoester **410b** model. These rotamers are unequally populated and give rise to different resonances in different ratios in the NMR spectrum. This added to the difficulty in the analysis of both my model compounds and the polyols prepared by Senthil.

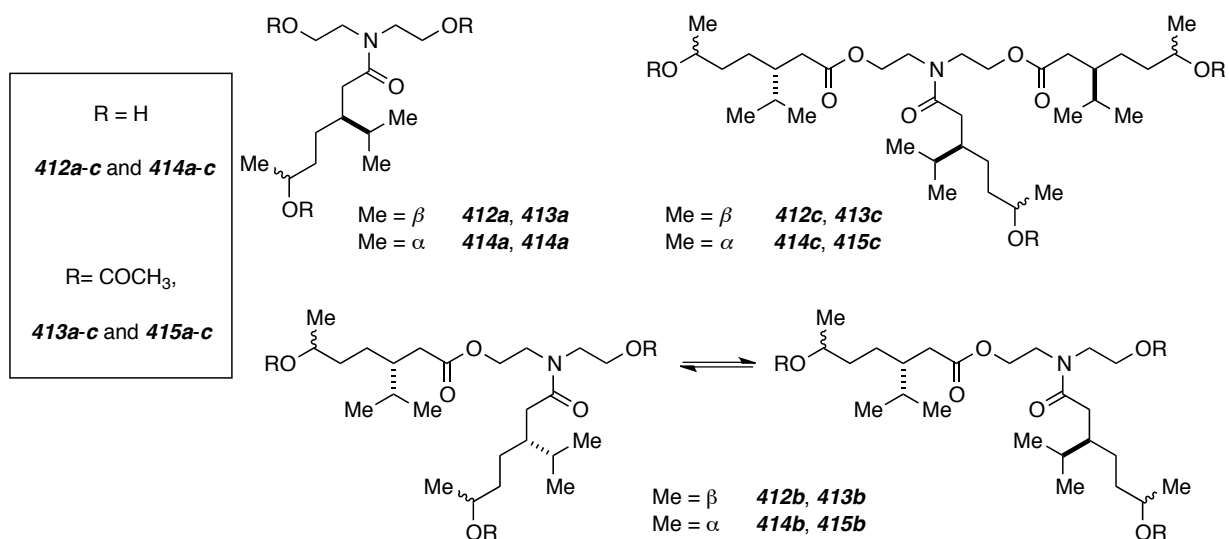
Figure III-8. Model Compounds Derived from Menthide and **407**.



All the resulting menthanoyl-reacted initiator molecules (**410a-c**) were acetylated to further mimic the environment they might experience in the polyol (reaction, left panel of Figure III-8, products are the acetylated compounds **411a-c**). All of these were useful in understanding the complex NMR behavior of Senthil's polyol **PM**. Much of the complexity comes from the region of the spectrum where the initiator protons reside. Depending on the rotamer, and the exact distance from the stereogenic center, diastereotopic protons were identical or had their own unique chemical shift and peak shape. Understanding all these details of the NMR spectroscopic data was a massive undertaking, but the experimental section illustrates the attention given.

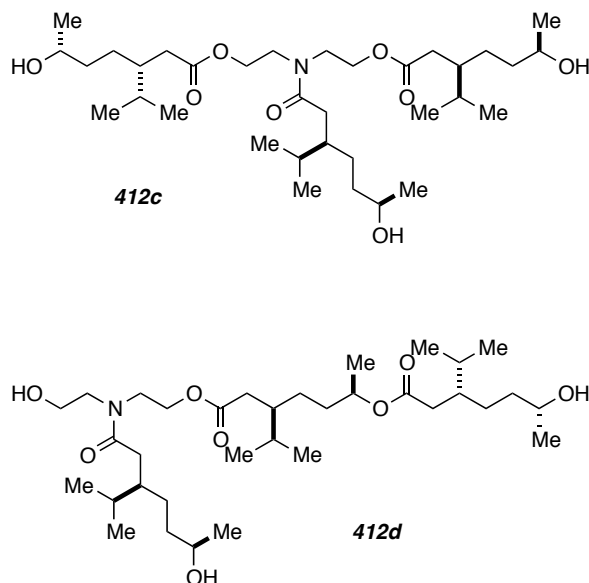
In the case of carvomenthide, each diastereomer (*trans*-**405** and *cis*-**405**) was subject to the same conditions (Figure III-8). These reactions afforded compounds **412a-c** and **414a-c** (derived from *trans*-**405** and *cis*-**405**, respectively). The acetylation reaction was again conducted, furnishing **413a-c** and **415a-c** in high yields. In this way, 12 analogous model compounds were obtained.

Figure III-9. Model Compounds Derived From *trans* and *cis* Carvomenthide (**405**).



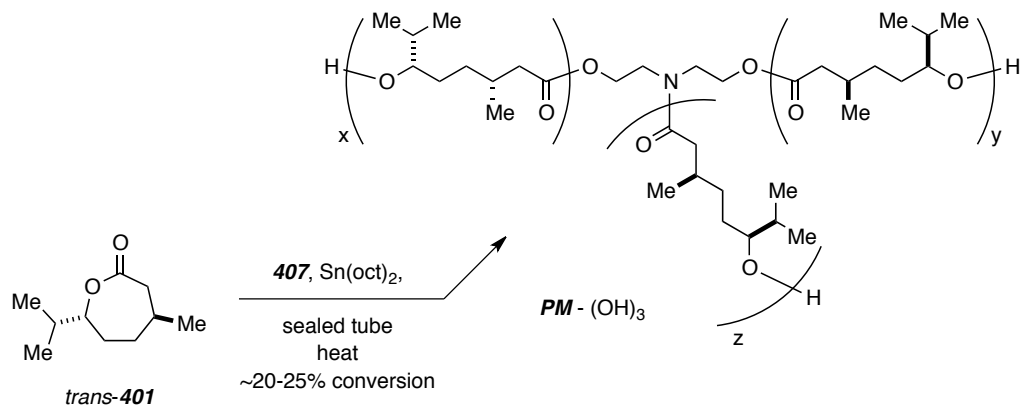
There were only subtle differences in the ring opening of the carvomenthides compared to the menthine series. The former were slightly more complicated by the fact that the secondary alcohol obtained after ring opening became competitive with the primary alcohols of the initiator. When the secondary alcohol was particularly aggressive, various quantities of 1,2,2 monoamide/bisester (e.g. **412d**, Figure III-10) were observed alongside the desired 1,2,3 monoamide/bisester **412c**. This seemed to be a bigger problem for *trans*-**405**.

Figure III-10. Different Ways to Attach Three Monomers to **407**.



experiments, I tested polymerization using reagents out of the bottle and took no special care to protect them from air and moisture (Scheme III-60).

Scheme III-60. Ring-opening Polymerization Study.



I found that employing all the other experimental conditions but using reagents as received, the ring opening reaction occurred. However, the conversion was poor; about 25% of the monomer reacted and no further conversion was noted upon heating for an extended time. Thus, there are practical limitations to this reaction and some care has to be taken in the handling of reagents. It is not as robust as might be desired.

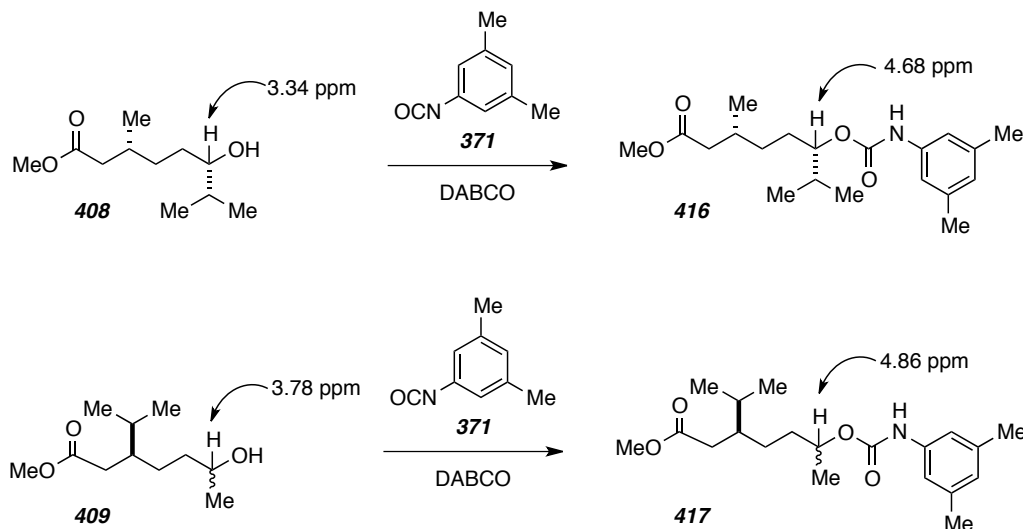
VI.B.3. Trial Carbamate Linkage Reactions

The next step in the construction of polyurethanes (either films or foams, for any application) is reacting the polyol in a formulation that typically consists of varying amounts of a diisocyanate, short chain diol, a catalyst, and a number of other additives for various reasons (see the General Introduction for Part Three). The key reaction, of course, is the urethane bond-forming event. This type of reaction occurs readily between any alcohol and an isocyanate, according to the sterics and electronics of the alcohol and isocyanate.

The goal of my next short study was to use my previously prepared compounds (Scheme III-58) to determine if our polyols would participate in the reaction. If so, I was interested in the main differences between the alcohols. As shown earlier, the alcohols **408** and **409** are similar but different. They are both secondary, but **408** (derived from menthicide) contains a greater degree of branching at its adjacent carbons compared to **409** (from carvomenthicide). We predicted this would slow its reaction with isocyanate. In the

study, the methyl ester alcohols were first reacted separately to understand the products and their diagnostic GCMS, LCMS, and ^1H NMR characteristics. The relevant reaction details and NMR resonances in both the starting materials and products (**416** and **417**) are shown in Scheme III-61.

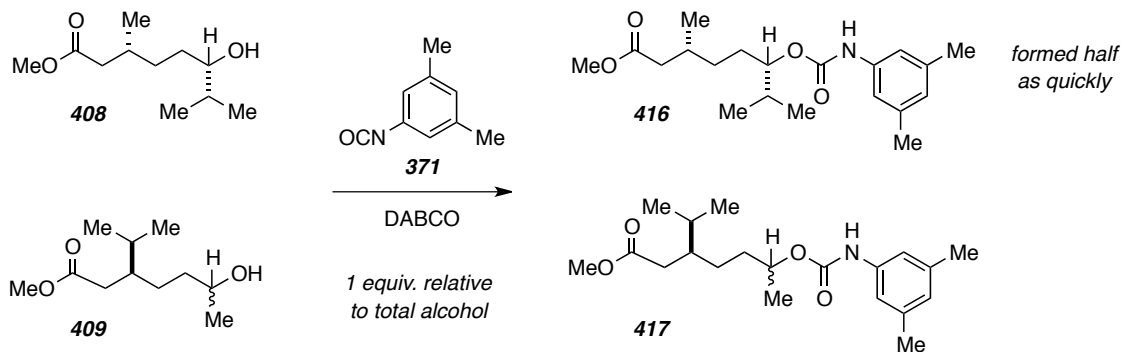
Scheme III-61. Carbamate Reaction Diagnostic NMR Resonances.



These reactions occurred quickly at room temperature and the carbamates were easily chromatographed. Importantly, all four of the carbinol resonances were unique in the ^1H NMR spectrum, meaning these reactions could be confidently followed by this method.

With the products understood from Scheme III-61 studies, the lactones were then mixed in a competition experiment (Scheme III-62). The reaction with isocyanate **371** was performed at room temperature and monitored by ^1H NMR analysis. At the first time point, it appeared that there was twice as much of the carbamate was formed from carvomenthine (i.e. **417**) versus menthine (i.e. **416**).

Scheme III-62. Competition Experiment for Carbamate Formation.



In conclusion, some supporting studies were performed for the ring opening polymerization project headed by Senthil. I found that the Baeyer-Villiger worked especially well on menthone (*trans*-**400**), but generated small quantities of abnormal carvomenthides (**406**). The thermal ring opening of the lactones *trans*-**401** and **405** by diethanolamine (**407**) occurred to give varying ratios of mono-, bis-, and tris-derivatized initiator. The carvomenthide suffered from competitive chain elongation versus initiation. The ring opening polymerization reaction was investigated to see if how robust it was. The alcohols resulting from ring opening of menthine (*trans*-**401**) and carvomenthide (**405**) were tested in carbamate-forming reactions where the secondary alcohol derived from carvomenthide was shown to be about twice as reactive towards isocyanates.

VI.C. NMR studies and Comparison to Computational Studies

VI.C.1. Motivation

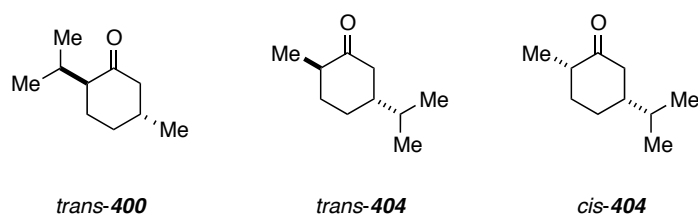
The goal of the Center for Sustainable Polymers project was the synthesis of a renewable polyol to use in the construction of a polyurethane. As small molecule chemists, we were happy to learn the polymerization reactions. However, we had interest in the details of the small monomers we were using. We wanted to understand some of their complex NMR behavior. Literature searches revealed that detailed analysis of both the ketones and lactones had not been performed (or reported). We were particularly suited to complement the existing literature knowledge with our expertise in NMR analysis. We looked to contribute to both the experimental and computational data on these substrates. In particular, we wanted to challenge our computational methods²⁰² as they apply to stereoisomers. Since I had acquired all the necessary data on a number of *cis/trans* isomers, this was a natural progression. In the following sections, the ketones will be under study first, followed by the lactones. Special care is taken to discuss conformation of these ring systems, and key features of the NMR data will be noted. Tables III-1-10 were constructed to display the data, and these are located at the end of the experimental for Part Three.

Mr. Josh Marell is the computational expert. He took over every feature of these small molecules that can be studied with a computer. His data will be mentioned along the way as it relates to each molecule. His modeling experiments on conformation are usually mentioned for each molecule at the outset. An in-depth comparison of the computed and experimental data (^{13}C and ^1H chemical shifts) will not be presented. This document only contains a short discussion on highlights of that study.

VI.C.2. Collection of Experimental Data Set on Menthones and Carvomenthone

The ketones we faced were those terpenoids we used for conversion to lactones (Figure III-7, see also section VI.B.1). We had access to several renewable ketones (Figure III-12).

Figure III-12. Renewable Ketones From Previous Studies.



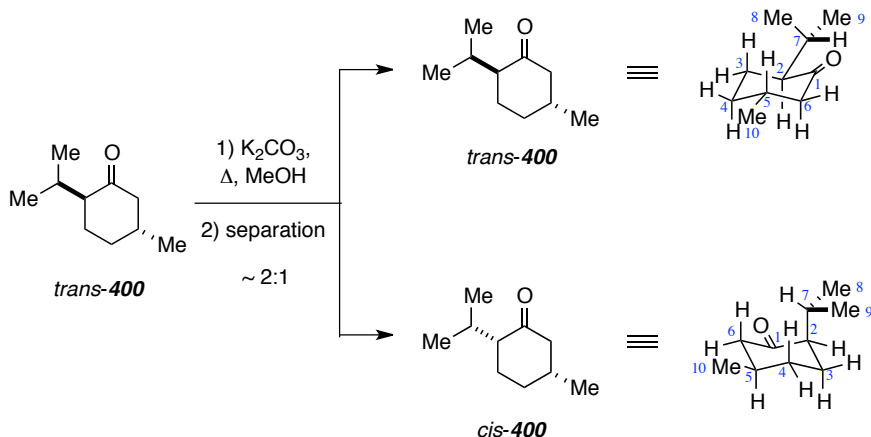
A battery of experiments was conducted on each of these ketones. Besides the standard ^1H and ^{13}C NMR methods, these included various solvent ^1H , DEPT, ^1H - ^1H COSY, and ^1H - ^{13}C HMQC. The computational information (^{13}C and ^1H) was easily obtained and analysis was commenced on *trans* and *cis* menthone (**400**) and *trans* and *cis* carvomenthone (**404**). Each stereoisomer had its own set of data. Key features of the data set collected for each molecule will be discussed in the text with references to Tables III-1-10, located at the end of the experimental for Part Three, for more information.

VI.C.2.a. Experimental Data for Methone and Isomenthone

Menthone (*trans-400*) is isolated in enantiopure form, so much less is known about isomenthone, the *cis*-variant (*cis-400*). Moreover, oftentimes *trans* and *cis* carvomenthone are used together, so their individual spectroscopic behavior remains to be studied. These ketones were first set of molecules to undergo the joint experimental and computational study.

To furnish a complete set of data, menthone was epimerized to a mixture of menthone and isomenthone by heating a methanolic solution in the presence of K_2CO_3 (*trans*- and *cis*-**400**, Scheme III-63). This resulted in a 2:1 mixture of stereoisomers that were separated by MPLC. The major conformers based on computational methods are depicted in this scheme. These served as a starting point for peak shape and patterns in NMR data.

Scheme III-63. Epimerization of Menthone (**400**).

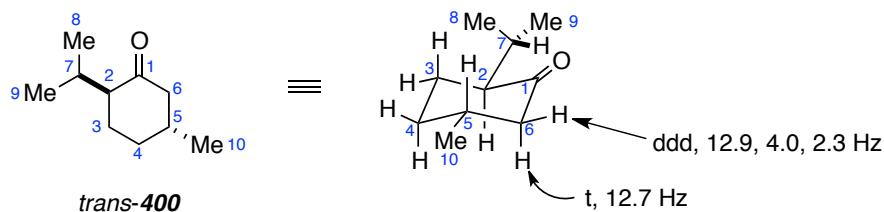


Conformation has a direct effect on NMR peak shape. Before analyzing such data, general features of these conformers are noteworthy. Both isomers have major conformers where the 6-membered ring is in the expected chair conformation. The minor contributors to the conformational make-up of these cyclohexanones are chair-flipped versions and rotational isomers about the isopropyl group.²⁰³

MENTHONE (Table III-1)

The major conformation of menthone (*trans*-**400**, Figure III-13) is where the chair form seats the isopropyl substituent axially. Minor conformations are different rotamers about the isopropyl group and, to a far lesser extent, the chair-flipped conformer where the isopropyl becomes axial.

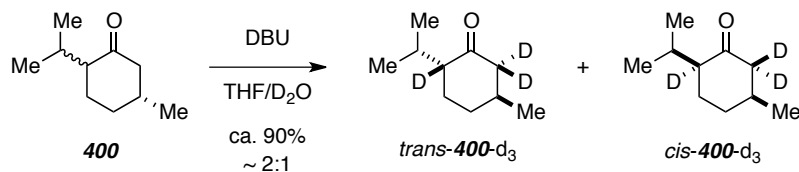
Figure III-13. Major Conformation of Menthone (**400**).



With this background, analysis of the NMR properties of this molecule commenced. Unfortunately, many of the resonances were overlapping and peak shape data could not be reliably obtained. Benzene titrations were not effective in this case, and few other solvents were attempted (the computational methods were best where chloroform was the designated solvent). Gratifyingly, both H6s were resolved, and their peak shape (especially H6 β having two large coupling constants) confirmed that Me10 is equatorial. Unfortunately, the relationship to the ⁱPr group could not be confirmed by coupling constant data, so besides literature precedent, we do not know this to be *trans* based only on ¹H NMR data.

Deuterium incorporation (Scheme III-64) was attempted to gain access into a few more details of the overlapping multiplets (or at least to simplify some regions of the spectrum). The reaction set up was extremely straightforward. A mixture of *cis* and *trans* menthone (**400**, approximately 1:1) was treated with DBU and heated in THF/D₂O for a few hours, when analysis by ¹H NMR indicated that approximately 90% of the starting material had been thrice deuterated. As expected, the starting material was also isomerized to give a greater proportion of *trans* isomer.

Scheme III-64. Deuterium Incorporation of **400**.



Unfortunately, deuterium incorporation only served to remove NMR resonances that were already easy to interpret. The simplification of other peaks was not as dramatic as I desired, so this experiment was not particularly effective in understanding ketones *trans*

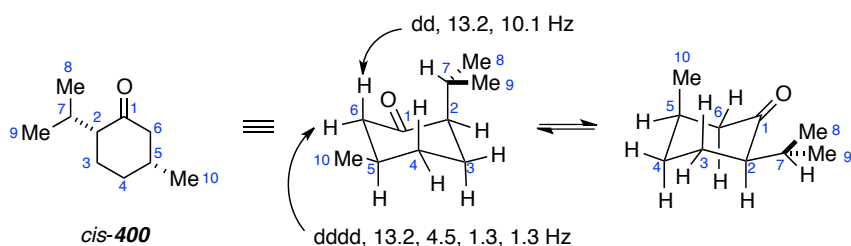
and *cis*-**400**. It guided the placement of some resonances within the multiplets, however, so better chemical shift information could be provided for computational comparison.

Despite these limitations, NMR (including COSY and HMQC) information was obtained for *trans*-**400** in this section. The data is provided in Table III-1. Where overlapping multiplets were a problem, an appropriate range of ppm's was used to compare to the computational results. HMQC was used to assign the ^{13}C spectrum. This data was then sent to Josh for comparison with the computed data.

ISOMENTHONE (Table III-2)

In the case of isomenthone (*cis*-**400**), the major conformer was predicted to be as shown in Scheme III-63 and Figure III-14. This conformer is far less intuitive; from molecular mechanics, the preferred chair form has the isopropyl situated axially. The second major conformer is the chair-flipped version followed by rotational conformers of the isopropyl substituent. A similar experimental data set was obtained for this molecule.

Figure III-14. Major Conformers of Isomenthone (*cis*-**400**).

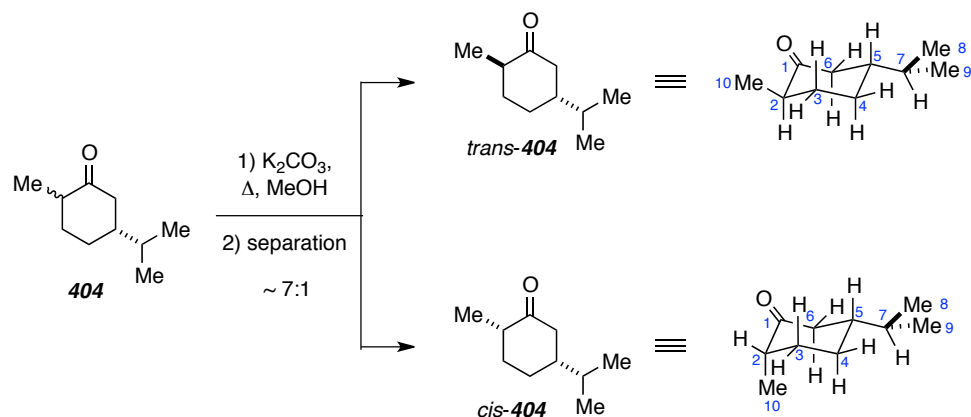


The NMR spectrum for *cis*-**400** was also complicated by overlapping multiplets (especially H3 α / β). Importantly, both of the H6 protons could be resolved and coupling constant information was obtained. The axial H6 β had two large couplings, so the adjacent H5 had to be axial. H6 α (only one large J , geminal) and H4 β (three large J s) also supported a conformation where Me10 is equatorial. Comparison to *cis*-**400**-d₃ (Scheme III-64) did not strengthen any additional assignments. For *cis*-**400**, like *trans*-**400**, where overlapping multiplets were observed, a suitable range or average chemical shift was assigned to the proton. Carbon assignments were made through the help of HMQC. This experimental information for comparison to menthone (*trans*-**400**) was sent to Josh for further analysis.

VI.C.2.b. Experimental Data for *Trans*- and *Cis*- Carvomenthone

Cis and *trans* carvomenthone (**404**) were obtained by a similar epimerization experiment (Scheme III-55, redrawn in Scheme III-65). This could only be driven to a 7:1 ratio of isomers, and they proved more difficult to separate than the corresponding menthones. Through careful MPLC, I obtained diastereomerically pure samples of *trans*-**404** and the *cis*-**404**. The major conformers are shown alongside the reaction scheme.

Scheme III-65. Epimerization of Carvomenthone (**404**).

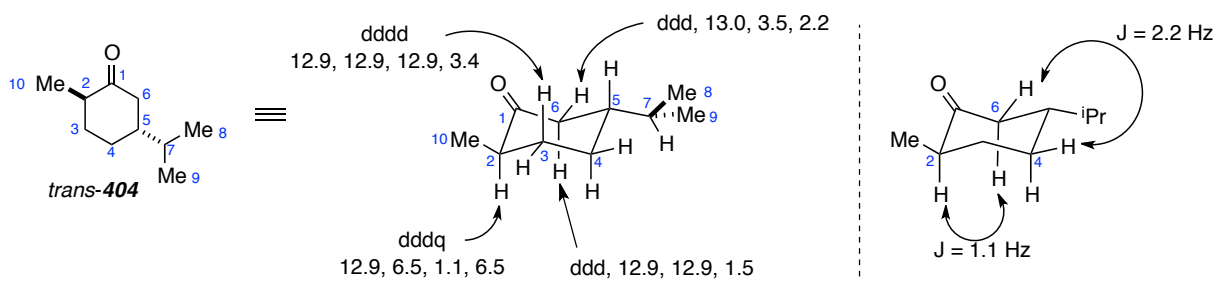


These constitutional isomers were better behaved than the menthone series. Their NMR spectra contained fewer overlapped regions.

TRANS CARVOMENTHONE (Table III-3)

General conformational analysis suggested that isomer *trans*-**404** adopted a conformation where both substituents occupy equatorial sites on the chair cyclohexanone (Figure III-15). The 1H data was remarkable. All but two protons (or methyl groups) could be analyzed reliably. The data for H6 β (2 large J s for germinal and *trans* diaxial) as well as H2 (one large J) was consistent with the major conformer being chair-like with two equatorial substituents and supported the *trans* stereochemical assignment.

Figure III-15. Conformational Preference of *trans* Carvomenthone (*trans*-**404**).

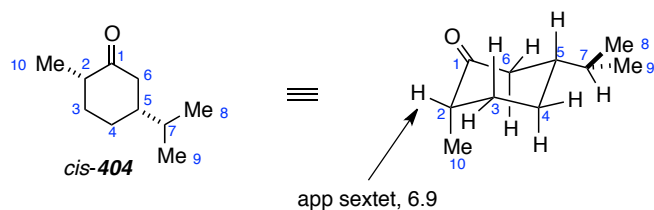


Even more exciting was the ability to see a few of the more obscure couplings (Figure III-15, right panel) such as $^4J_{\text{HH}}$ between H2-H6 β (diaxial) and $^4J_{\text{HH}}$ 4 α -6 α (W). Both the chemical shift (^1H and ^{13}C , assigned from HMQC) and coupling constant data was sent to Josh for comparisons to the computational data.

CIS CARVOMENTHONE (Table III-4)

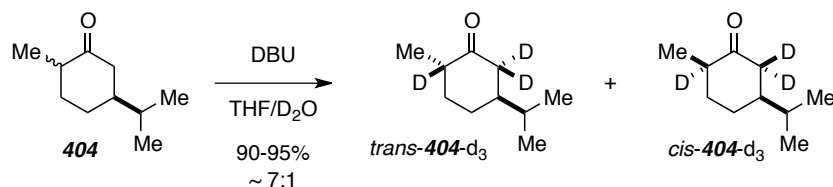
The story was slightly different for *cis* carvomenthone (*cis*-**404**, Figure III-16). Here, overlapping resonances made stereochemical assignment difficult and conformational preferences were not so easily judged. At least H2 was observed to be an apparent sextet. This indicated that H2 is equatorial and the methyl substituent at that site is axial, thus the molecule adopts a chair conformation where the isopropyl group is equatorial, although there are no other experimental peak shape details to support this. Sadly, this meant that the ^{13}C data was not as easily assigned.

Figure III-16. Major Conformer of *cis* Carvomenthone (*cis*-**404**).



An analogous set (to menthone) of deuterated compounds were also prepared (Scheme III-66). These served to support the already completed proton assignments (or in the case of *cis*-**404**, aid additional assignments). The conditions used were identical to those for menthone (c.f. Scheme III-64), and deuterium incorporation reached about the same level. Epimerization also occurred under these conditions to give the (now) expected ratio 7:1 diastereomers of carvomenthone (*trans*-**404**-d₃ and *cis*-**404**-d₃)

Scheme III-66. Deuterium Incorporation of **404**.



VI.C.2.c. Comparison to Computed Data

With these data analyzed as best it could be, these data were sent to Josh. Armed with the full set of constitutional and stereochemical isomers, the computational method was put to the test. Josh found that his computations successfully predicted both the stereoisomeric pairs for menthone and carvomenthone. Importantly, the computations gave warnings of the danger in using the expected conformational preferences (e.g. *cis* carvomenthone with an axial ¹Pr instead of Me group) and the experimental data supported this prediction. Besides conformational predictions, Josh's data matched well with ¹H and ¹³C chemical shift data.

VI.C.3. Collection of Experimental Data Set on Menthides and Carvomenthides

A similar motivation and reasoning exists for our study of the lactones. However, there is an added factor in these studies. A greater understanding of these molecules could directly impact their use in ring-opening polymerization reactions.²⁰⁴ In general, the same experimental and computational methods were used in the study of the lactones. With a ring size of 7, a chair-like conformation is still expected, and these types of representations will continue to be used, as well as the terminology axial and equatorial as it applies to ring protons or the substituents.

VI.C.3.a. Experimental Data for Menthide and Isomenthide

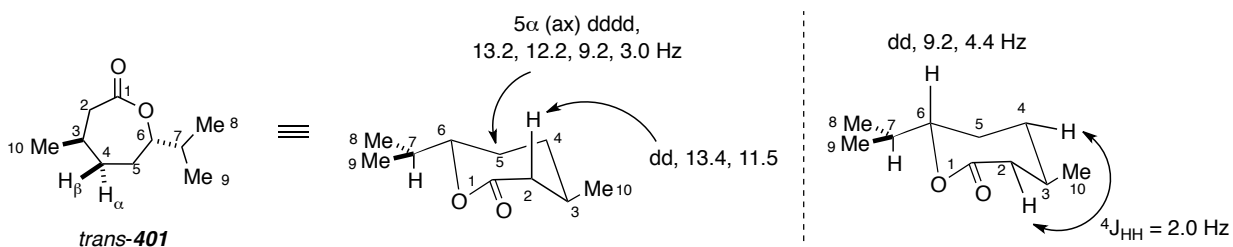
Trans and *cis* menthide (**401**, section VI.B.1. Scheme III-54) was obtained as in a previous section by BV oxidation of menthone. This reaction gave no abnormal menthide (*trans*-**402**). *Cis* menthide (*cis*-**401**) was prepared in an analogous fashion (not shown) from isomenthone acquired from experiments in Scheme III-63. Lactones **401** were taken forward to the full set of NMR experiments. Gratifyingly, the data were more amenable

to full scale analysis for these lactones compared to the corresponding ketones (see previous section).

MENTHIDE (Table III-5)

By molecular mechanics, the major conformer resembles the chair-like cyclohexanone, and in isomer *trans*-**401**, both substituents occupy equatorial positions on the ring (Figure III-17, most ring protons omitted for clarity). This NMR data for this lactone was good. All but three resonances could be independently and confidently assigned. All but two of the ^{13}C NMR shifts were assigned with ease. H2 β (2 large $^3J_{\text{HH}}$) and H5 α (3 large $^3J_{\text{HH}}$) confirm the equatorial orientation of their neighbor Me10 and ^iPr groups, respectively.

Figure III-17. Conformational Preference of *trans*-**401**.



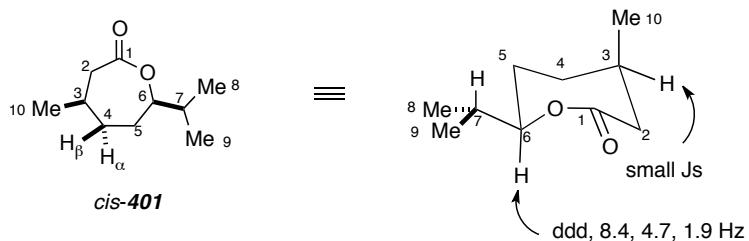
There were some additional interesting features of this molecule. The splitting pattern for H6 is interesting. A dd is far simpler than expected for a proton with 3 different neighbors. However, a value of 9.2 indicated that the proton is axial, so the conformer drawn in Figure III-17 is supported despite the fact that H3 is buried in a 3-proton multiplet. Lastly, even with the 7-membered ring, $^4J_{\text{HH}}$ H2 α to H4 α (W coupling) was observed.

ISOMENTHIDE (Table III-6)

In the case of *cis* menthide (*cis*-**401**, Figure III-18), the conformer predicted by molecular mechanics is again chair-like with the isopropyl equatorial. Although H4 α / β and H5 α / β were inaccessible, H3 was found to have a number of small coupling constants (likely equatorial) and H6 had two small and one larger couplings, so it is likely

axial. Difficulty in resolving any of the other resonances prohibited more complete analysis for this isomer.

Figure III-18. Conformational Preference of *cis*-**401**.



The same approach was taken for the multiplets as in the ketone case (section VI.C.2.), where protons part of a multiplet were given the average value, or placed in the multiplet based on resolved COSY data. The ^{13}C data for *cis*-**401** were assigned with almost 100% certainty and the compiled experimental data for lactones **401** was given to Josh for further study.

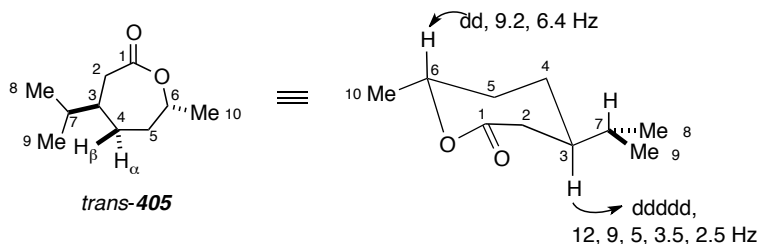
VI.C.3.b. Experimental Data for *Trans* and *Cis* Normal Carvomenthide

Trans and *cis* carvomenthide (**405**) were approached next. These had been scaled up for a previous study with a different focus (Section VI.B.1, Scheme III-55), and engaged in the full set of NMR experiments. Again, we were looking to verify conformational preferences and acquire trustworthy chemical shift data to marry the computational data.

TRANS NORMAL CARVOMENTHIDE (Table III-7)

Trans carvomenthide (*trans*-**405**, Figure III-19), although prepared and reported previously, had not been analyzed to our satisfaction. Gratifyingly, the NMR behavior of *trans*-**405** was suitable for our extensive study. Every single proton except two could be assigned and a large volume of coupling constant data was collected. Importantly, both H6 and H3 were accessible, and their coupling constant data clearly illustrated that both Me10 and the ^iPr group are situated equatorially around the lactone in a chair form.

Figure III-19. Conformational Preference of *trans*-405.

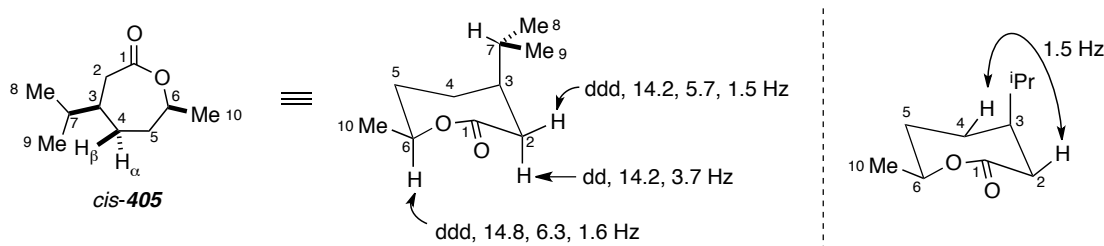


Carbon assignment was completed without difficulty, and this isomer fit very well into our study because of the availability of the proton data and the level of detail with which it could be studied.

CIS NORMAL CARVOMENTHIDE (Table III-8)

Cis carvomenthide was also studied, and we hoped for a similar outcome for the NMR data and full understanding of all the details of structure available from it. At the outset, computational methods suggested that the lactone was slightly unique in that the major conformer was one with an axial isopropyl and equatorial methyl substituent (Figure III-20). This is analogous to *cis* carvomenthone (*cis*-404, section VI.C.2.b.).

Figure III-20. Conformational Preference of *cis*-405.



In this isomer, unfortunately, H3, although having a unique chemical shift, was a complex non-first-order multiplet. Its coupling constant data could not confirm that it was equatorial. However, both H2_α and H2_β were resolved, and their shape (both with only one large *J*, for their geminal relationship) supported the equatorial placement of H3. Unfortunately, most of the remaining resonances had to be assigned as multiplets. Interestingly, the ⁴J_{HH} between H2_β and H4_β long range interaction was present in the NMR data (Figure III-20, right panel). The carbon data was surprisingly robust, and assignments were straightforward. The multiplets were interpreted as best as they could

be, and the data for *cis*-**405** was ready for comparison to that for the isomer *trans*-**405** and to the computed data for both.

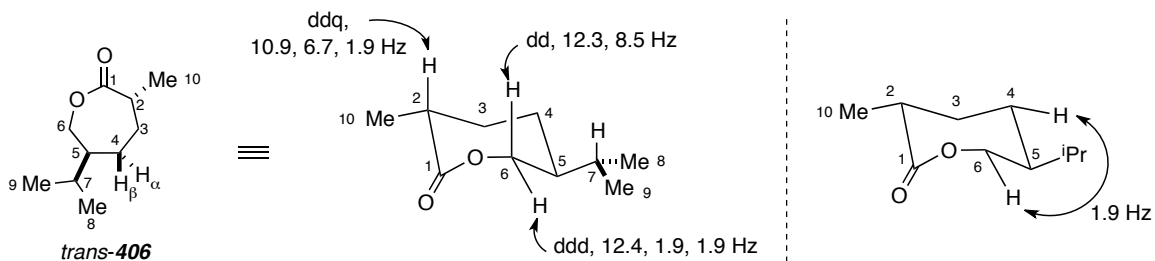
VI.C.3.c. Experimental Data for *Trans* and *Cis* Abnormal Carvomenthide

As the Baeyer-Villiger reaction was under study in section VI.B.1, the application to the carvomenthone **404** was observed to produce the abnormal BV product in small quantities (c.f Scheme III-55, lactones **406**). This provided another opportunity for a set of experimental NMR data to be collected and yet other opportunity for our computational methods to be tested. This set of stereoisomers would likely not be difficult to distinguish from the normal series (**405**), but *trans*-**406** and *cis*-**406** against one another could be a challenge for our methods.

TRANS ABNORMAL CARVOMENTHIDE (Table III-9)

Josh found the abnormal *trans* carvomenthide *trans*-**406** to adopt a chair-like conformation with both substituents situated equatorially (Figure III-21). It was difficult to confirm this with experimental NMR data. There were several overlapping multiplets. However, H2 was resolved and had a unique shift, and with a large (i.e. 10.9 Hz) coupling constant, it was concluded to be axial (meaning the methyl group is equatorial). There was support from H6 β (two large *J*s) and H6 α (one large value, for $^2J_{\text{HH}}$) for the isopropyl group to be equatorial.

Figure III-21. Conformational Preference of Abnormal *trans*-carvomenthide (*trans*-**406**).

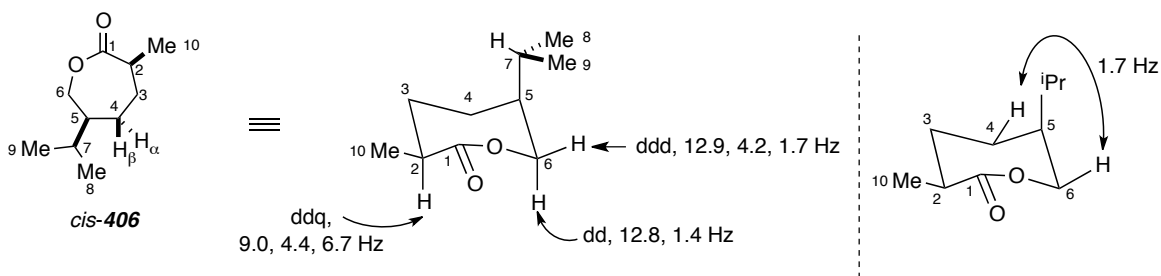


Here, I also observed $^4J_{\text{HH}}$ for the equatorial protons H4 α and H6 α (Figure III-21, right panel). The remainder of the chemical shift data was collected and the ^{13}C spectrum was assigned with only minor reservations prior to comparison to the computed data.

CIS ABNORMAL CARVOMENTHIDE (Table III-10)

For the abnormal *cis* carvomenthide (*cis*-**406**), the major conformer had similar non-intuitive characteristics as the *cis* carvomenthone (*cis*-**404**) and *cis* carvomenthide (*cis*-**405**). This isomer was found to enjoy a low energy conformation where the isopropyl group is axial rather than the methyl group (Figure III-22).

Figure III-22. Conformational Preference of Abnormal *cis* carvomenthide (*cis*-**406**).



Peak shape analysis of the ^1H NMR spectrum supported this prediction. Although there was severe overlapping in one particular region of the spectrum, H2 and both H6 α and H6 β were accessible. H2 had a large coupling constant, so it must be axial, and with the pair H6 α / β , each only contained one large J , representing a germinal interaction. Thus, despite the overlap, there was a high level of confidence in the data. The ^{13}C data was similarly assigned. This analysis completed the pair of abnormal isomers relevant to the study of our computational methods.

VI.C.3.d. Comparison to Computed Data

For the lactones, the match between the experimental data and computed data was even better than for the ketones (section VI.C.2.) In every case, Josh was able to distinguish between stereoisomers. That is, the match was far better for the correct stereoisomer. The model test set was the *cis* and *trans* carvomenthides (**405**). The best experimental data was obtained for these molecules, so fewer tactics had to be employed for choosing in the midst of overlapping multiplets.

In conclusion, there are few directions for this type of study to go. Here, I already knew the stereochemical identity for each substrate. The next step is to collect a set of experimental data for a small molecule with similar features for which the stereochemistry is unknown. Then, the computed data for all possible stereoisomers

would be generated and the best match to the computed data would be the predicted isomer.

VI.D. Concluding Remarks

Terpenes and terpenoids are interesting natural products that can be studied in a number of ways. In this chapter, their use as precursors to ROP monomers was investigated. First, menthone and carvomenthone were *transformed* into lactones, then thermal ring-opening was used to synthesize various oligomers. Lastly, the alcohols were studied for their potential use in carbamate formation with isocyanates.

Additionally, terpenoids can be studied for their own interesting properties. Our computational methods for NMR data were developed and tested using the small molecule ketones and lactones. For 10 discrete cyclic species, a full battery of NMR experiments was completed and the data presented in Tables III-1-10. Likewise, a wealth of computational data was obtained and direct comparisons between the two. The computer modeling was able to successfully predict the stereochemistry of these ketones and lactones.

References

- (144) Lligadas, G.; Ronda, J. C.; Galiañ, M.; Caló, V. Plant Oils as Platform Chemicals for Polyurethane Synthesis: Current State-of-the-Art. *Biomacromolecules* **2010**, *11*, 2825-2835.
- (145) Lay, J. O.; Liyanage, R.; Durham, B.; Brooks, J. Rapid characterization of edible oils by direct matrix-assisted laser desorption/ionization time-of-flight mass spectrometry analysis using triacylglycerols. *Rapid Commun. Mass Spectrom.* **2006**, *20*, 952-958.
- (146) Gidden, J.; Liyanage, R.; Durham, B.; Lay, J. O. Reducing fragmentation observed in the matrix-assisted laser desorption/ionization time-of-flight mass spectrometric analysis of triacylglycerols in vegetable oils. *Rapid Commun. Mass Spectrom.* **2007**, *21*, 1951-1957.
- (147) The BiOH Experience. <http://www.experiencebioh.com/> (accessed 6/20, 2012).
- (148) Cleaner, Greener, Performance Polyols. *Renuva, Renewable Resource Technology* **2008**.
- (149) Li, F.; Hanson, M. V.; Larock, R. C. Soybean oil-divinylbenzene thermosetting polymers: synthesis, structure, properties and their relationships. *Polymer* **2001**, *42*, 1567-1579.
- (150) Tian, Q.; Larock, R. Model studies and the ADMET polymerization of soybean oil. *J. Am. Oil Chem. Soc.* **2002**, *79*, 479-488.
- (151) Yongshang, L.; Larock, R. C. In *Novel Biobased Plastics, Rubbers, Composites, Coatings and Adhesives from Agricultural Oils and By-Products*; Cheng, H. N., Gross, R. A., Eds.; Green Polymer Chemistry: Biocatalysis and Biomaterials; American Chemical Society: 2010; Vol. 1043, pp 87-102.

- (152) Lachance, P.; Eastham, A. M. Olefin oligomerization by boron fluoride. *J. Polym. Sci. Pol. Sym.* **1976**, *56*, 203-210.
- (153) Croston, C.; Tubb, I.; Cowan, J.; Teeter, H. Polymerization of drying oils. VI. Catalytic polymerization of fatty acids and esters with boron trifluoride and hydrogen fluoride. *J. Am. Oil Chem. Soc.* **1952**, *29*, 331-333.
- (154) Laszlo, J.; Compton, D.; Vermillion, K. Acyl Migration Kinetics of Vegetable Oil 1,2-Diacylglycerols. *J. Am. Oil Chem. Soc.* **2008**, *85*, 307-312.
- (155) Kodali, D. R.; Tercyak, A.; Fahey, D. A.; Small, D. M. Acyl migration in 1,2-dipalmitoyl-sn-glycerol. *Chem. Phys. Lipids* **1990**, *52*, 163-170.
- (156) Rybak, A.; Fokou, P. A.; Meier, M. A. R. Metathesis as a versatile tool in oleochemistry. *Eur. J. Lipid Sci. Technol.* **2008**, *110*, 797-804.
- (157) Schrodi, Y.; Ung, T.; Vargas, A.; Mkrtumyan, G.; Lee, C. W.; Champagne, T. M.; Pederson, R. L.; Hong, S. H. Ruthenium Olefin Metathesis Catalysts for the Ethenolysis of Renewable Feedstocks. *Clean Soil Air Water* **2008**, *36*, 669-673.
- (158) Leitao, E. M.; Eide, E. F. v. d.; Romero, P. E.; Piers, W., E.; McDonald, R. Kinetic and Thermodynamic Analysis of Processes Relevant to Initiation of Olefin Metathesis by Ruthenium Phosphonium Alkylidene Catalysts. *J. Am. Chem. Soc.* **2010**, *132*, 2784-2794.
- (159) Forman, G. S.; Bellabarba, R. M.; Tooze, R. P.; Slawin, A. M. Z.; Karch, R.; Winde, R. Metathesis of renewable unsaturated fatty acid esters catalysed by a phoban-indenylidene ruthenium catalyst. *J. Organomet. Chem.* **2006**, *691*, 5513-5516.
- (160) Biswas, A.; Sharma, B. K.; Willett, J. L.; Erhan, S. Z.; Cheng, H. N. Room-temperature self-curing ene reactions involving soybean oil. *Green Chem.* **2008**, *10*, 290-295.

- (161) Liu, Z.; Sharma, B. K.; Erhan, S. Z. From oligomers to molecular giants of soybean oil in supercritical carbon dioxide medium: 1. Preparation of polymers with lower molecular weight from soybean oil. *Biomacromolecules* **2007**, *8*, 233-239.
- (162) Onopchenko, A.; Cupples, B. L.; Kresge, A. N. Boron fluoride-catalyzed oligomerization of alkenes: structures, mechanisms, and properties. *Ind. Eng. Chem. Prod. Res. Dev.* **1983**, *22*, 182-191.
- (163) Fokou, P. A.; Meier, M. A. R. Studying and Suppressing Olefin Isomerization Side Reactions During ADMET Polymerizations. *Macromol. Rapid Comm.* **2010**, *31*, 368-373.
- (164) Deno, N. C.; Peterson, H. J.; Saines, G. S. The Hydride-Transfer Reaction. *Chem. Rev.* **1960**, *60*, 7-14.
- (165) Porter, N.; Caldwell, S.; Mills, K. Mechanisms of free radical oxidation of unsaturated lipids. *Lipids* **1995**, *30*, 277-290.
- (166) Frankel, E. N. Lipid oxidation. *Prog. Lipid Res.* **1980**, *19*, 1-22.
- (167) Kade, M. J.; Burke, D. J.; Hawker, C. J. The power of thiol-ene chemistry. *J. Polym. Sci. Pol. Chem.* **2010**, *48*, 743-750.
- (168) Bantchev, G. B.; Kenar, J. A.; Biresaw, G.; Han, M. G. Free Radical Addition of Butanethiol to Vegetable Oil Double Bonds. *J. Agric. Food Chem.* **2009**, *57*, 1282-1290.
- (169) Desroches, M.; Caillol, S.; Lapinte, V.; Auvergne, R.; Boutevin, B. Synthesis of Biobased Polyols by Thiol-Ene Coupling from Vegetable Oils. *Macromolecules* **2011**, *44*, 2489-2500.
- (170) Turunc, O.; Meier, M. A. R. Thiol-ene vs. ADMET: a complementary approach to fatty acid-based biodegradable polymers. *Green Chem.* **2011**, *13*, 314-320.

- (171) Schmidt, U.; Grafen, P.; Goedde, H. W. Chemistry and Biochemistry of \pm -Lipoic Acid. *Angew. Chem. Int. Ed Engl.* **1965**, *4*, 846-856.
- (172) Howard, S.,C.; McCormick, D.,B. High-performance liquid chromatography of lipoic acid and analogues. *J. Chromatogr. A* **1981**, *208*, 129-131.
- (173) Kisanuki, A.; Kimpara, Y.; Oikado, Y.; Kado, N.; Matsumoto, M.; Endo, K. Ring-opening polymerization of lipoic acid and characterization of the polymer. *J. Polym. Sci. A Polym. Chem.* **2010**, *48*, 5247-5253.
- (174) Endo, K.; Shiroy, T.; Murata, N.; Kojima, G.; Yamanaka, T. Synthesis and Characterization of Poly(1,2-dithiane). *Macromolecules* **2004**, *37*, 3143-3150.
- (175) Arakawa, R.; Watanabe, T.; Fukuo, T.; Endo, K. Determination of cyclic structure for polydithiane using electrospray ionization mass spectrometry. *J. Polym. Sci. A Polym. Chem.* **2000**, *38*, 4403-4406.
- (176) Ishida, H.; Kisanuki, A.; Endo, K. Ring-Opening Polymerization of Aromatic 6-Membered Cyclic Disulfide and Characterization of the Polymer. *Polym. J.* **2008**, *41*, 110-117.
- (177) Sandner, M. R.; Osborn, C. L. Photochemistry of 2,2-dimethoxy-2-phenylacetophenone-triplet detection via "spin memory". *Tetrahedron Lett.* **1974**, *15*, 415-418.
- (178) Baxter, J. E.; Davidson, R. S.; Hageman, H. J.; Hakvoort, G. T. M.; Overeem, T. A study of the photodecomposition products of an acylphosphine oxide and 2,2-dimethoxy-2-phenylacetophenone. *Polymer* **1988**, *29*, 1575-1580.
- (179) Vincent, M.; Guglielmetti, G.; Cassani, G.; Tonini, C. Determination of double-bond position in diunsaturated compounds by mass spectrometry of dimethyl disulfide derivatives. *Anal. Chem.* **1987**, *59*, 694-699.

- (180) Buser, H. R.; Arn, H.; Guerin, P.; Rauscher, S. Determination of double bond position in mono-unsaturated acetates by mass spectrometry of dimethyl disulfide adducts. *Anal. Chem.* **1983**, *55*, 818-822.
- (181) Yamamoto, K.; Shibahara, A.; Nakayama, T.; Kajimoto, G. Determination of double-bond positions in methylene-interrupted dienoic fatty acids by GC-MS as their dimethyl disulfide adducts. *Chem. Phys. Lipids* **1991**, *60*, 39-50.
- (182) Carballeira, N. M.; Shalabi, F.; Cruz, C. Thietane, tetrahydrothiophene and tetrahydrothiopyran formation in reaction of methylene-interrupted dienoates with dimethyl disulfide. *Tetrahedron Lett.* **1994**, *35*, 5575-5578.
- (183) Schwartzbeck, J. L.; Jung, S.; Abbott, A. G.; Mosley, E.; Lewis, S.; Pries, G. L.; Powell, G. L. Endoplasmic oleoyl-PC desaturase references the second double bond. *Phytochemistry* **2001**, *57*, 643-652.
- (184) Caserio, M. C.; Fisher, C. L.; Kim, J. K. Boron trifluoride catalyzed addition of disulfides to alkenes. *J. Org. Chem.* **1985**, *50*, 4390-4393.
- (185) Caraballo, R.; Rahm, M.; Vongvilai, P.; Brinck, T.; Ramstrom, O. Phosphine-catalyzed disulfide metathesis. *Chem. Commun.* **2008**, 6603-6605.
- (186) Caraballo, R.; Sakulsombat, M.; Ramstrom, O. Phosphine-mediated disulfide metathesis in aqueous media. *Chem. Commun.* **2010**, *46*, 8469-8471.
- (187) Lees, W. J.; Whitesides, G. M. Equilibrium constants for thiol-disulfide interchange reactions: a coherent, corrected set. *J. Org. Chem.* **1993**, *58*, 642-647.
- (188) Dai, H.; Yang, L.; Lin, B.; Wang, C.; Shi, G. Synthesis and Characterization of the Different Soy-Based Polyols by Ring Opening of Epoxidized Soybean Oil with Methanol, 1,2-Ethenediol and 1,2-Propanediol. *J. Am. Oil Chem. Soc.* **2009**, *86*, 261-267.

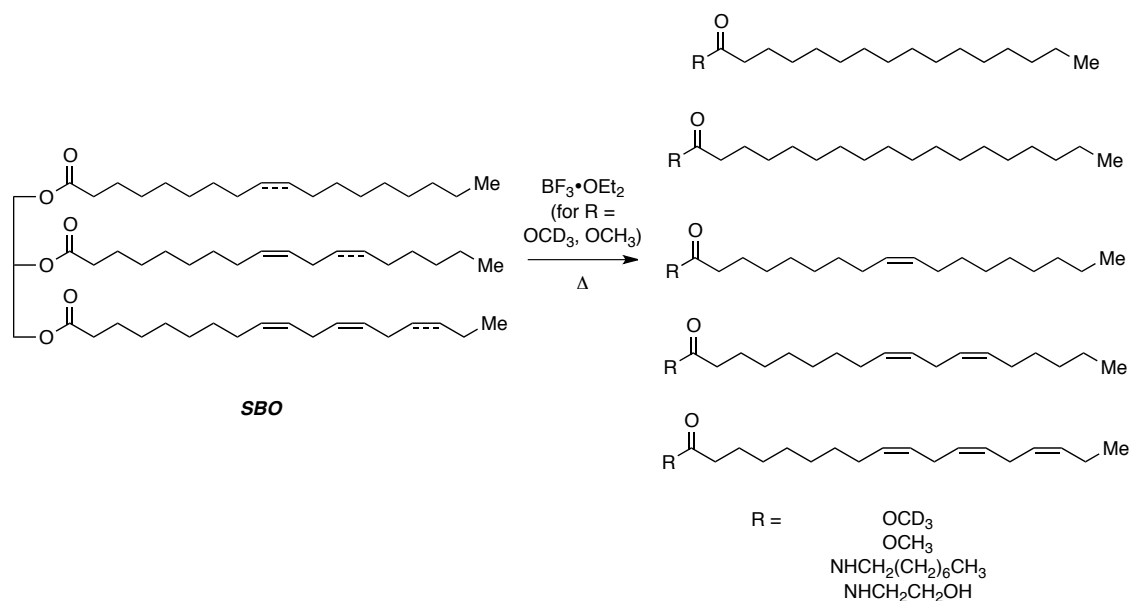
- (189) Forristal, I.; Lawson, K. R.; Rayner, C. M. Optically active 2,3-epoxy sulfides as precursors to 3-hydroxy-1,2-dithioethers and 3-hydroxy-1-alkenylthioethers. *Tetrahedron Lett.* **1999**, *40*, 7015-7018.
- (190) Naghipur, A.; Lown, J. W.; Jain, D. C.; Sapse, A. Ab initio studies on 1,2-oxathietane, Z and E 3,4-dimethyl-1,2-oxathietane, and their products of formal cycloreversion. *Can. J. Chem.* **1988**, *66*, 1890-1894.
- (191) Lown, J. W.; Koganty, R. R. Formation of novel 1,2-oxathietanes from 2-chloroethyl sulfoxide precursors and their reactions in solution, including formal cycloreversions and rearrangements. *J. Am. Chem. Soc.* **1986**, *108*, 3811-3818.
- (192) Giannella, M.; Pignini, M.; Rãedi, P.; Eugster, C. H. The Four Diastereomeric Thio-Analogues of (±)-Muscarine. *Helv. Chim. Acta* **1979**, *62*, 2329-2337.
- (193) Capon, R. J.; Barrow, R. A. Acid-Mediated Conversion of Methylene-Interrupted Bisepoxides to Tetrahydrofurans: A Biomimetic Transformation. *J. Org. Chem.* **1998**, *63*, 75-83.
- (194) Glueck, S. M.; Fabian, W. M. F.; Faber, K.; Mayer, S. F. Biocatalytic Asymmetric Rearrangement of a Methylene-Interrupted Bis-epoxide: Simultaneous Control of Four Asymmetric Centers Through a Biomimetic Reaction Cascade. *Chem. Eur. J.* **2004**, *10*, 3467-3478.
- (195) Malievskii, A. Exchange reaction of oxiranes with β -hydroxyalkyl sulfides, selenides, -amines, and-phosphines. *Russ. Chem. Bull.* **2000**, *49*, 579-587.
- (196) Jãrme, C.; Lecomte, P. Recent advances in the synthesis of aliphatic polyesters by ring-opening polymerization. *Adv. Drug Deliv. Rev.* **2008**, *60*, 1056-1076.

- (197) Lowe, J. R.; Martello, M. T.; Tolman, W. B.; Hillmyer, M. A. Functional biorenewable polyesters from carvone-derived lactones. *Polym. Chem.* **2011**, *2*, 702-708.
- (198) Baeyer, A.; Villiger, V. Einwirkung des Caro'schen Reagens auf Ketone. *Ber. Dtsch. Chem. Ges.* **1899**, *32*, 3625-3633.
- (199) Shin, J.; Martello, M. T.; Shrestha, M.; Wissinger, J. E.; Tolman, W. B.; Hillmyer, M. A. Pressure-Sensitive Adhesives from Renewable Triblock Copolymers. *Macromolecules* **2011**, *44*, 87-94.
- (200) Qian, H.; Wohl, A. R.; Crow, J. T.; Macosko, C. W.; Hoye, T. R. A Strategy for Control of α -Random Copolymerization of Lactide and Glycolide: Application to Synthesis of PEG-b-PLGA Block Polymers Having Narrow Dispersity. *Macromolecules* **2011**, *44*, 7132-7140.
- (201) Lohmeijer, B. G. G.; Pratt, R. C.; Leibfarth, F.; Logan, J. W.; Long, D. A.; Dove, A. P.; Nederberg, F.; Choi, J.; Wade, C.; Waymouth, R. M.; Hedrick, J. L. Guanidine and Amidine Organocatalysts for Ring-Opening Polymerization of Cyclic Esters. *Macromolecules* **2006**, *39*, 8574-8583.
- (202) Wiitala, K. W.; Cramer, C. J.; Hoye, T. R. Comparison of various density functional methods for distinguishing stereoisomers based on computed ^1H or ^{13}C NMR chemical shifts using diastereomeric penam $\hat{\text{I}}^2$ -lactams as a test set. *Magn. Reson. Chem.* **2007**, *45*, 819-829.
- (203) Smith, W. B.; Amezcua, C. NMR versus molecular modelling: menthone and isomenthone. *Magn. Reson. Chem.* **1998**, *36*, S3-S10.
- (204) Saiyasombat, W.; Molloy, R.; Nicholson, T. M.; Johnson, A. F.; Ward, I. M.; Poshychinda, S. Ring strain and polymerizability of cyclic esters. *Polymer* **1998**, *39*, 5581-5585

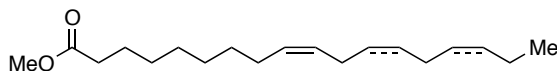
Part Three Experimental

General Methods: See Part One Experimental and note about the included file names

Experiments (Chapter V)



Cleavage to Methyl Esters of General Structure:



A sample (1 g, 1.15 mmol) of soyoil was weighed into a culture tube. 10 mL MeOH, followed by $\text{BF}_3 \cdot \text{OEt}_2$ (180 ul, 1.15 mmol). The tube was sealed and heated to reflux for 1 hour. The esters were purified by MPLC (20:1 Hex:EtOAc) to a mixture methyl esters. $^1\text{H NMR}$ (500 MHz, CDCl_3): δ 5.42-5.29 (m, 3H), 3.67 (s, 3H), 2.81/2.77 (br t, $J = 6$ Hz, t, $J = 6.8$ Hz, 2H), 2.30 (t, $J = 7.5$ Hz, 2H), 2.10-1.99 (m, 4H), 1.62 (app pent, $J = 7.2$ Hz, 2H), 1.39-1.23 (m, 18H), 0.98/0.89/0.88 (t, $J = 7.5$ Hz, t, $J = 6.9$ Hz, and t, $J = 7.0$ Hz, 3H). [seIVpg222_mteset]

LCMS (Method B):

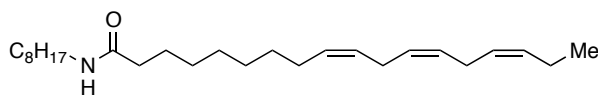
(palmitate) $T_R = 14.6$ min, m/z "pos" = 293.35 ($M+23$)⁺, 309.3 ($M+39$)⁺.

(linolenate) $T_R = 16.1$ min, m/z "pos" = 293.3 ($M+1$)⁺, 310.3 ($M+18$)⁺.

(linoleate) $T_R = 16.7$ min, m/z "pos" = 295.3 ($M+1$)⁺, 312.3 ($M+18$)⁺.

(oleate) $T_R = 17.4$ min, m/z “pos” = 314.3.5 (M+18)⁺.

Cleavage to Octyl Amides of General Structure:



These were recovered from the partial cleavage of soyoil triglycerides. (see next scheme)

¹H NMR (500 MHz, CDCl₃): δ 5.43-5.28 (m, ~4.5 H), 3.24 (ddd, $J = 7.1, 7.1, 5.9$ Hz, 2H), 2.77 (t, $J = 5.9$ Hz, 2H), 2.15 (t, $J = 7.5$ Hz, 2H), 2.09-1.97 (m, 4H), 1.68-1.57 (m, 2H), 1.55-1.43 (m, 2H), 1.40-1.20 (m, 28H), and 0.98/0.89/0.88 (t, $J = 7.5$ Hz, t, $J = 6.9$ Hz, and t, $J = 6.9$ Hz, 6H). [seIVpg302m1f4] seIVpg247_mplc also works.

LCMS (Method B):

(linolenate) $T_R = 16.9$ min, m/z “pos” = 390.5 (M+1)⁺, 412.3 (M+23)⁺, m/z “neg” = 448.3 (M+59)⁻

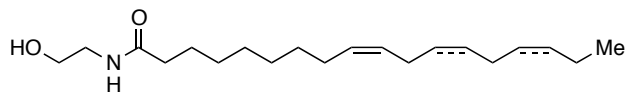
(linoleate) $T_R = 17.5$ min, m/z “pos” = 392.5.3 (M+1)⁺, 414.5 (M+23)⁺, m/z “neg” = 450.5 (M+59)⁻

(palmitate) $T_R = 18.0$ min, m/z “pos” = 368.5 (M+1)⁺, 390.3 (M+23)⁺.

(oleate) $T_R = 18.3$ min, m/z “pos” = 394.5 (M+1)⁺, 416.5 (M+23)⁺, m/z “neg” = 452.5 (M+59)⁻

(stearate) $T_R = 19.2$ min, m/z “pos” = 396.5 (M+1)⁺, 418.3 (M+23)⁺.

Cleavage to Ethanol Amides of General Structure:



Soyoil (100 mg, approx. 0.115 mmol) was mixed with ethanolamine (150 uL, 2.5 mmol) were mixed together in a screw capped vial. The vessel was sealed and heated to 100 °C for one hour, where full consumption the triglyceride was noted by NMR. The mixture ethanol amides were purified by MPLC (1:14 Hex:EtOAc). About 100 mg of the amides were isolated (60% yield). The discrete fatty acid chains were observable by LCMS, but were characterized as a mixture.

¹H NMR (500 MHz, CDCl₃): δ 6.00 (br s, 1H), 5.44-5.28 (m, 3H), 3.73 (t, $J = 4.9$ Hz, 2H), 3.43 (app br q, $J = 5.2$ Hz, 2H), 2.77 (t, $J = 5.9$ Hz, 2H), 2.21 (t, $J = 7.6$ Hz, 2H),

2.10-1.97 (m, 4H), 1.63 (app pent, $J = 7.3$ Hz, 2H), 1.38-1.25 (m, 16H), 0.98/0.89/0.88 (t, $J = 7.5$ Hz, t, $J = 6.8$ Hz, and t, $J = 6.8$ Hz, 3H). [seIVpg248_mplc]

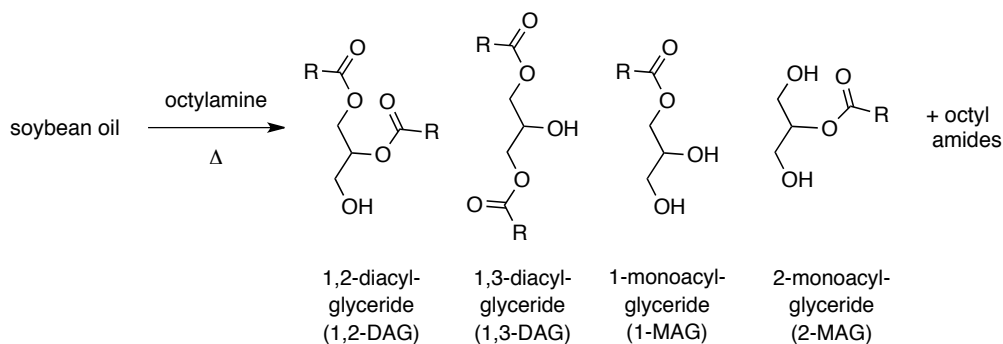
LCMS (Method B):

(linolenate) $T_R = 14.9$ min, m/z "pos" = 322.3 (M+1)⁺, m/z "neg" = 380.3 (M+59)⁻

(linoleate) $T_R = 15.3$ min, m/z "pos" = 324.3 (M+1)⁺, m/z "neg" = 382.3 (M+59)⁻

(oleate) $T_R = 15.3$ min, m/z "pos" = 326.3 (M+1)⁺, m/z "neg" = 384.3 (M+59)⁻

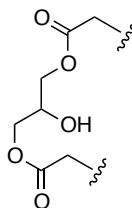
(stearate) $T_R = 16.2$ min, m/z "pos" = 328.3 (M+1)⁺, m/z "neg" = 386.3 (M+59)⁻



Triglyceride Cleavage to 1,2-DAG and 1,3-DAGs:

Soyoil (1 g, approx. 1.15 mmol) was mixed with octylamine (150 mg, 1.15 mmol) were mixed together in a screw capped vial. The vessel was sealed and heated to 100 °C overnight, where most (>90 %) of the amine had been converted to the amide(s). The mixture of 1,3-DAG and 1,2-DAGs were separated by MPLC (4:1 Hex:EtOAc), usually resulting in a ratio of 2:1 ratio of these constitutional isomers.

General 1,3-DAG

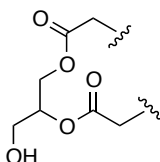


¹H NMR (500 MHz, CDCl₃): δ 5.41-5.30 (m, 4.7H), 4.19 (dd, $J = 11.4, 4.3$ Hz, 2H), 4.13 (dd, $J = 11.2, 5.8$ Hz, 2H), 4.11-4.06 (m, 1H), 2.811/2.806/2.77 (t, $J = 5.5$ Hz, t, $J = 5.5$

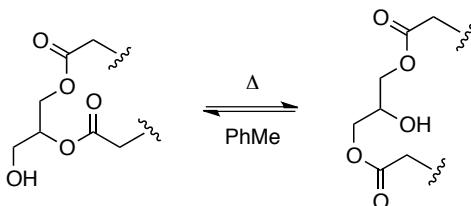
Hz, and t, $J = 6.5$ Hz, 2.3H), 2.35 (t, $J = 7.6$ Hz, 2H), 2.10-1.99 (m, 6H), 1.63 (app br pent, $J = 7.3$ Hz, 4H), 1.40-1.21 (m, 36H), and 0.98/0.89/0.88 (t, $J = 7.6$ Hz, t, $J = 7.0$ Hz, and t, $J = 6.9$ Hz, 6H). [seIVpg302f2]

seIVpg302f2 appears to be 1,3 isomer. seIVpg304f1s also give good spectra for this 1,3-isomer.

General 1,2-DAG



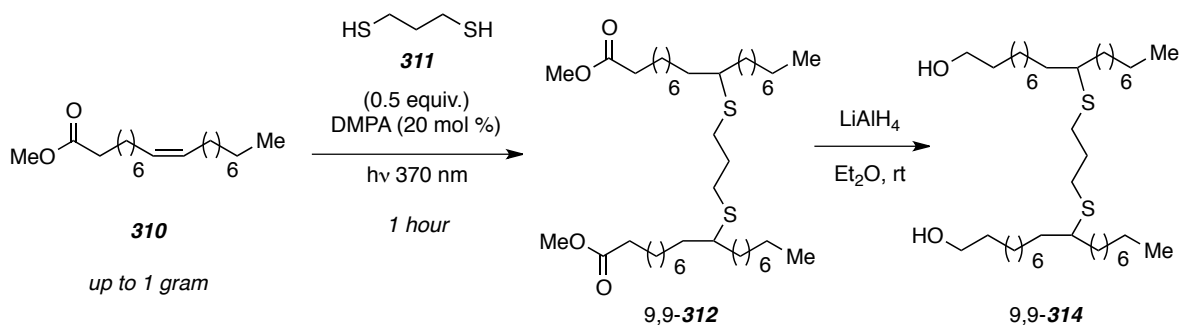
$^1\text{H NMR}$ (500 MHz, CDCl_3): δ 5.42-5.30 (m, 6.2H), 5.08 (pent, $J = 5.0$ Hz, 1H), 4.32 (dd, $J = 11.9, 4.6$ Hz, 1H), 4.24 (dd, $J = 11.9, 5.6$ Hz, 1H), 3.734 (dd, $J = 6.4, 4.7$ Hz, 1H), 3.731 (dd, $J = 6.6, 5.1$ Hz, 1H), 2.810/2.806/2.77 (t, $J = 5.3$ Hz, t, $J = 5.5$ Hz, and t, $J = 6.6$ Hz, 3H), 2.34/2.33 (t, $J = 7.5$ Hz, t, $J = 7.5$ Hz, 4H), 2.10-1.99 (m, 8H), 1.63/1.62 (pent, $J = 7.1$ Hz, pent, $J = 7.2$ Hz, 5H), 1.41-1.24 (m, 40H), 0.98/0.89/0.88 (t, $J = 7.5$ Hz, t, $J = 6.9$ Hz, and t, $J = 7.0$ Hz, 6H). [seIVpg304_2_f2, where seIVpg302f3 is the 1,2-isomer, which eluted slower]



Procedure for equilibration of 1,2-DAGs of 1,3-DAGs.

Pure samples (15 mg) of either 1,2-DAG or 1,3-DAG were independently subjected to high heat to force acyl migration. Either species was recovered from triglyceride cleavage and transferred to a culture tube via PhMe washings (0.5 mL total for this process). They were then placed in an oil bath and heated (>100 °C) for 6-8 hours at which point NMR indicated that both had converted to an approximate ratio of 4:1 (1,3-DAG to 1,2-DAG). Further heating did not change this ratio, and the reaction vessels were cooled before concentration. The equilibrated samples could be chromatographed in the same fashion as described for the TAG cleavage.

Ratio: 1,3;DAG favored over 1,2-DAG by 4:1. See above for spectral data.



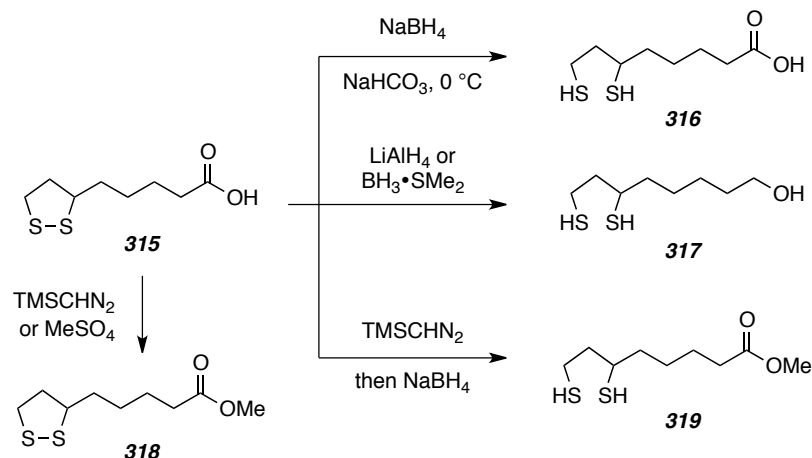
dimethyl 9,9'-(propane-1,3-diylbis(sulfanediyl))dioctadecanoate (9,9-312).

Technical grade methyl oleate (0.5 g, 1.7 mmol), 1,3-propane dithiol (85 μ l, 0.9 mmol), and DMPA (85 mg, 0.7 mmol) were combined in a screw capped culture tube. 100 μ l DCM was added, and the reaction vessel was placed in the Rayonet reactor for one hour. At this stage, LCMS indicated almost quantitative conversion of the alkene. The volatiles were removed by vacuum pump and the product purified by MPLC (20:1 Hex:EtOAc), providing **312** in 80% yield.

¹H NMR (500 MHz, CDCl₃): δ 3.67 (s, 6H), 2.56 (t, J = 7.2 Hz, 4H), 2.55 (app pent, J = 6.5 Hz, 2H), 2.30 (t, J = 7.5 Hz, 4H), 1.82 (pent, J = 7.2 Hz, 2H), 1.62 (br pent, J = 7.4 Hz, 4H), 1.57-1.46 (m, 8H), 1.45-1.345 (m, 8H), 1.33-1.24 (m, 36H), and 0.88 (t, J = 7.0 Hz, 6H). [seVpg243m1major]

9,9'-(propane-1,3-diylbis(sulfanediyl))bis(octadecan-1-ol) (9,9-314). A sample of **312** (80 mg, approx. 0.1 mmol) was dissolved in THF (0.5 mL) and LiAlH₄ (22 mg, 0.6 mmol) was added in one portion. The reaction stirred for one hour, and was concentrated *in vacuo* before subjecting to MPLC (2:1 Hex:EtOAc), which returned 60 mg of diol.

¹H NMR (500 MHz, CDCl₃): δ 3.64 (t, J = 6.6 Hz, 4H), 2.58 (t, J = 7.2 Hz, 4H), 2.56 (app pent, J = 6.5 Hz, 2H), 1.82 (pent, J = 7.2 Hz, 2H), 1.61-1.47 (m, 14H), 1.45-1.23 (m, 48H), and 0.88 (t, J = 6.6 Hz, 6H). [seVpg240mplc]



5-(1,2-dithiolan-3-yl)pentanoic acid (Lipoic Acid, 315). Used as Received

¹H NMR (500 MHz, CDCl₃): δ 10.39 (br s, 1H), 3.58 (dq, *J* = 8.5, 6.4 Hz, 1H), 3.19 (ddd, *J* = 11.0, 7.1, 5.3 Hz, 1H), 3.12 (dt, *J* = 11.1, 6.9 Hz, 1H), 2.47 (dddd, *J* = 13.0, 6.6, 6.6, 5.3 Hz, 1H), 2.38 (t, *J* = 7.4 Hz, 2H), 1.92 (dq, *J* = 12.6, 6.9 Hz, 1H), 1.76-1.62 (m, 4H), and 1.57-1.43 (m, 2H). [seVpg281sm]

¹³C NMR (125 MHz, CDCl₃): δ 209.5 (or 180.0?), 56.5, 40.4, 38.7, 34.8, 34.0, 28.9, and 24.6. [seVpg265sm]

GCMS (5027016): R_t = 8.69 min, 206(M⁺,100), 155(20), 123(50), 95(45), and 81(40).

methyl 5-(1,2-dithiolan-3-yl)pentanoate (318). To a weighed sample of lipoic acid (315, 100 mg, 0.49 mmol) in a screw capped vial was added DMF-dimethyl acetal (130 ul, 0.97 mmol). The resulting solution was stirred overnight added and the residue was loaded directly onto an MPLC (4:1 Hex:EtOAc). The product methyl ester (20 mg, 20%) was isolated as a colorless oil. I found that not all of the crude sample could be dissolved in the MPLC mobile phase. There was a gelish solid in a lot of these reactions that could be explained by LA polymerization.

¹H NMR (500 MHz, CDCl₃): δ 3.68 (s, 3H), 3.58 (dq, *J* = 8.2, 6.5 Hz, 1H), 3.19 (ddd, *J* = 11.0, 7.1, 5.4 Hz, 1H), 3.12 (dt, *J* = 11.5, 6.8 Hz, 1H), 2.47 (dddd, *J* = 12.9, 6.6, 6.6, 5.4 Hz, 1H), 2.33 (t, *J* = 7.3 Hz, 2H), 1.91 (dq, *J* = 12.6, 7.0 Hz, 1H), 1.74-1.61 (m, 4H), and 1.53-1.40 (m, 2H). [seVpg275_fcc]

GCMS (5027016): R_t = 8.70 min, 220(M⁺,100), 155(30), 123(55), 95(40), and 81(35).

6,8-dimercaptooctanoic acid (316). Lipoic acid (315, 200 mg, 1 mmol) was dissolved in an aqueous solution of NaHCO₃ (1 mL, 0.5 M) and cooled at 0 °C. Portions of NaBH₄ (total 150 mg, 4 mmol) were added and the reaction was allowed to stir at room temperature for 2 hours, at which time NMR indicated the reduction was complete. The reaction mixture was acidified to pH ~ 2, extracted with CH₂Cl₂, dried over Na₂SO₄, filtered, and concentrated ca. 250 mg of crude material. Purification by MPLC (1:1 Hex:EtOAc) returned 190 mg dithiol (90%) as a colorless oil. Alternatively the crude reaction product can be flushed through a pipette of SiO₂, rinsed with EtOAc, concentrated as used as recovered.

¹H NMR (500 MHz, CDCl₃): δ 2.93 (dddd, *J* = 9.3, 7.8, 7.8, 4.6, 4.6 Hz, 1H), 2.75 (dddd, *J* = 13.1, 8.0, 8.0, 5.1 Hz, 1H), 2.67 (ddd, *J* = 13.2, 7.8, 7.8 Hz, 1H), 2.39 (t, *J* = 7.3 Hz, 1H), 1.91 (dddd, *J* = 14.1, 7.9, 7.9, 4.4 Hz, 1H), 1.75 (dddd, *J* = 14.4, 9.5, 7.8, 5.1 Hz, 1H), 1.71-1.43 (m, 6H), 1.36 (t, *J* = 8.0 Hz, 1H), and 1.30 (d, *J* = 7.7 Hz, 1H).

[seVpg149cr] or [seVpg231fl1]

¹³C NMR (125 MHz, CDCl₃): δ 180.2, 42.9, 39.5, 38.9, 34.1, 26.6, 24.5, and 22.5.

[seVpg265_C13]

GCMS (5027016): R_t = 8.55 min, 208(M⁺, 100), 156(50), 125(45), 95(70), and 81(75).

TLC (1:1 Hex:EtOAcv): R_f = 0.1

6,8-dimercaptooctan-1-ol (317). A solution of LiAlH₄ (68 mg, 1.8 mmol) in Et₂O (2 mL) was prepared at room temperature. To it was added a solution of lipoic acid (100 mg, 0.49 mmol) in THF (2 mL) and the reaction stirred at rt for 1 hour, when the reaction was judged to be complete by NMR. Water (4 mL) was added to the reaction mixture, the layers were separated, and the aqueous layer was acidified to pH = 1-2. CH₂Cl₂ was used to extract the crude product (2x 5 mL), and the combined organic layers were dried over Na₂SO₄ and concentrated to the crude alcohol. 317 underwent purification by MPLC (1:1 Hex:EtOAc), producing 20 mg (20%) of the alcohol dithiol as a whitish residue.

Alternatively, a non aqueous workup can be performed, affording 44 mg (31%) of the alcohol **317**.

The reduction can also be performed with $\text{BH}_3 \cdot \text{SMe}_2$. The LA (50 mg, 0.25 mmol) was prepared as a solution in THF (200 ul) and the reagent $\text{BH}_3 \cdot \text{SMe}_2$ (100 ul, 3 equiv) was added via syringe. The reaction was quenched by addition of MeOH and concentrated under reduced pressure to recover approx. 50 mg crude 317. MPLC (1:1 Hex:EtOAc) was performed to yield 317 as a white residue in 10%.

$^1\text{H NMR}$ (500 MHz, CDCl_3): δ 3.66 (t, $J = 6.5$ Hz, 2H), 2.93 (dddd, $J = 9.3, 7.6, 7.6, 4.6, 4.6$ Hz, 1H), 2.75 (dddd, $J = 13.2, 8.0, 8.0, 5.3$ Hz, 1H), 2.66 (ddd, $J = 13.2, 7.8, 7.8$ Hz, 1H), 1.92 (dddd, $J = 14.0, 7.8, 7.8, 4.5$ Hz, 1H), 1.75 (dddd, $J = 14.3, 9.3, 7.7, 5.3$ Hz, 1H), 1.73-1.24 (m, 8H), 1.36 (t, $J = 8.0$ Hz, 1H), and 1.31 (d, $J = 7.6$ Hz, 1H).

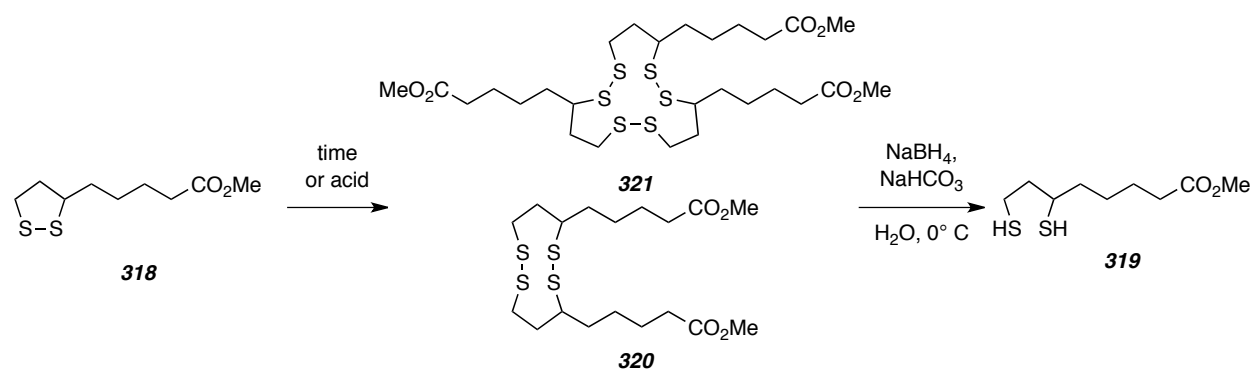
[seVpg264f1]

$^{13}\text{C NMR}$ (125 MHz, CDCl_3): δ 62.9, 42.9, 39.6, 39.2, 32.7, 26.9, 25.6, 22.5.

[seVpg264redo_cr]

LCMS (Method B): $T_R = 4.9$ min, m/z "neg" = 193.0.3 ($\text{M}-1$)⁻

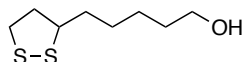
TLC (1:1 Hex:EtOAc): $R_f = 0.1$



methyl 6,8-dimercaptooctanoate (319). 319 was actually isolated from the reaction mixture of 318 after treatment with NaBH_4 . Reactions of LA with DMF-dimethyl acetal typically gave measurable quantities of material that was insoluble in most solvents. MeOH and water, and sometimes THF were added to dissolve the polymeric LA and NaBH_4 was added. After a suitable times (typically 1 hour), the reaction mixture was extracted into DCM and the crude esterdithiol was subjected to purification by MPLC (4:1 Hex:EtOAc). For every 100 mg of the gelish material from reaction to 318, 10-20 mg of the esterdithiol could be recovered by this process.

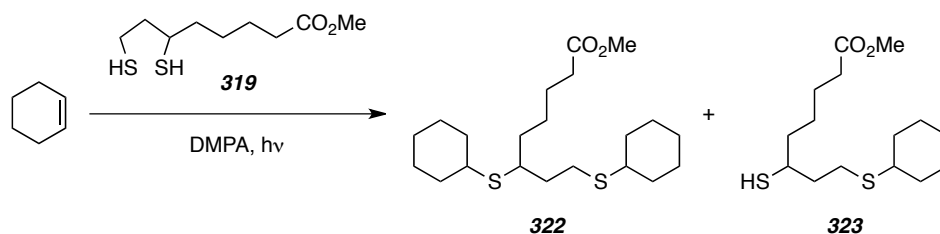
¹H NMR (500 MHz, CDCl₃): δ 3.68 (s, 3H), 2.93 (dddd, *J* = 9.5, 7.8, 7.8, 4.8, 4.8 Hz, 1H), 2.74 (dddd, *J* = 13.1, 7.9, 7.9, 5.0 Hz, 1H), 2.67 (ddd, *J* = 13.2, 7.8, 7.8 Hz, 1H), 2.33 (t, *J* = 7.4 Hz, 2H), 1.91 (dddd, *J* = 14.0, 7.9, 7.9, 4.4 Hz, 1H), 1.75 (dddd, *J* = 14.3, 9.5, 7.9, 5.1 Hz, 1H), 1.71-1.40 (m, 6H), 1.35 (t, *J* = 7.9 Hz, 1H), and 1.30 (d, *J* = 7.6 Hz, 1H). [seVpg247f1]

Alcohol **S1** was also prepared for potential reaction in disulfide chemistry:



5-(1,2-dithiolan-3-yl)pentan-1-ol (S1). To a solution of lipoic acid (100 mg, 0.49 mmol) in THF (0.5 mL) was added catecholborane (100 ul, 0.97 mmol) via syringe. The reaction was monitored by NMR of aliquots, and after 4-6 hours, water was added to quench the reaction. The mixture was extracted by Et₂O, dried, concentrated, and subjected to chromatography (MPLC, 3:1 Hex:EtOAc). The catechol eluded first, followed by the desired product over the course of a broad peak, which was collected and concentrated to a residue of approx. 10 mg.

¹H NMR (500 MHz, CDCl₃): δ 3.66 (t, *J* = 6.6 Hz, 2H), 3.58 (dq, *J* = 8.6, 6.5 Hz, 1H), 3.19 (ddd, *J* = 11.0, 7.2, 5.3 Hz, 1H), 3.12 (ddd, *J* = 11.0, 6.9, 6.9 Hz, 1H), 2.47 (dddd, *J* = 13.0, 6.6, 6.6, 5.3 Hz, 1H), 1.92 (dddd, *J* = 12.6, 7.0, 7.0, 7.0 Hz, 1H), 1.76-1.65 (m, 2H), 1.59 (app pent, *J* = 7.0 Hz, 2H), and 1.53-1.36 (m, 4H). [seVpg270f2]



methyl 6,8-bis(cyclohexylthio)octanoate (322) and methyl 8-(cyclohexylthio)-6-mercaptocaptoate (323).

Cyclohexene (10 uL, 0.1 mmol), dithiol 319 (10 mg, 0.05 mmol), and DMPA (a small crystal) were combined in a screw capped vial. The sides of the vial were washed with 50

uL CDCl₃, and placed in the Rayonet. Monitoring by NMR, the reaction was judged complete in 3 hours. The reaction mixture was concentrated under reduced pressure and the products were separated by MPLC (8:1 Hex:EtOAc) to afford the **322** (4 mg) and **323** (3 mg) products, which were characterized by LCMS and ¹H NMR.

Data for 322

¹H NMR (500 MHz, CDCl₃): δ 3.67 (s, 3H), 2.78 (dddd, *J* = 7.3, 7.3, 5.6, 5.6 Hz, 1H), 2.67 (ddd, *J* = 8.4, 7.2, 2.1 Hz, 2H), ~2.68-2.60 (m, 2H), 2.33 (t, *J* = 7.4 Hz, 2H), 2.00-1.92 (m, 4H), 1.84-1.70 (m, 6H), 1.66-1.40 (m, 8H), and 1.36-1.19 (m, 10H).

[seVpg245f1]

LCMS (Method C): R_t = 8.8 min, m/z “pos” = 387.3. (M+1)⁺, m/z “neg” = 385.0 (M-1)⁻.

TLC (8:1 Hex:EtOAc): R_f = 0.4

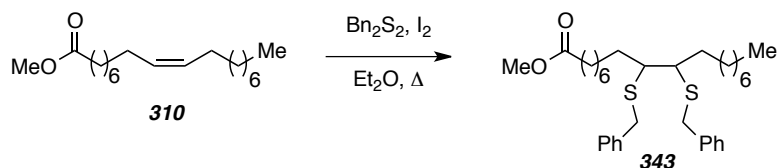
Data for 323

¹H NMR (500 MHz, CDCl₃): δ 3.67 (s, 3H), 2.90 (dddd, *J* = 12.4, 9.3, 7.6, 4.8 Hz, 1H), 2.74 (ddd, *J* = 13.9, 8.7, 4.2 Hz, 1H), 2.71-2.62 (m, 1H), 2.64 (ddd, *J* = 12.6, 8.7, 7.1 Hz, 1H), 2.33 (t, *J* = 7.4 Hz, 2H), 2.01-1.92 (m, 2H), 1.90 (dddd, *J* = 13.6, 8.7, 7.1, 4.5 Hz), 1.81-1.57 (m, 7H), 1.56-1.40 (m, 3H), 1.35 (d, *J* = 7.4 Hz, 1H), and 1.36-1.20 (m, 5H).

[seVpg245f2]

LCMS (Method C): R_t = 6.4 min, m/z “pos” = 305.2 (M+1)⁺,

TLC (8:1 Hex:EtOAc): R_f = 0.2



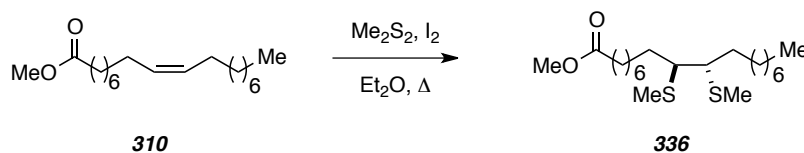
methyl 9,10-bis(benzylthio)octadecanoate (343). Methyl oleate (100 mg, 0.34 mmol), was measured into a screw capped culture tube followed by addition of the benzyl disulfide (400 mg, 1.6 mmol) and lastly, I₂ (43 mg, 0.16 mmol). A minimal amount of Et₂O (approx. 100 ul) was added to confer homogeneity, the tube was capped and heated to 40 °C for 2 hours, at which time, NMR revealed that almost all olefinic resonances had

disappeared. The reaction vessel was allowed to cool to room temperature and the reaction mixture was diluted with 4-6 mL Et₂O before addition of Na₂S₂O₃ (2 mL saturated aqueous solution). This mixture was stirred until the reaction became colorless or nearly colorless. The organic layer was separated, and the aqueous layer was extracted twice with additional Et₂O. The organic layers were combined, dried over Na₂SO₄, filtered, and concentrated. Purification by MPLC (30:1 Hex:EtOAc) afforded the bis-sulfide **343** in 50-60% yield with varying amounts of unreacted methyl oleate. See text for discussion on catalyst loadings and conversions.

¹H NMR (500 MHz, CDCl₃): δ 7.31-7.20 (m, 10H), 3.68 (s, 3H), 3.61 (dd, *J* = 13.5, 3.9 Hz, 2H), 3.57 (dd, *J* = 13.5, 1.5 Hz, 2H), 2.62-2.58 (m, 2H), 2.31 (t, *J* = 7.5 Hz, 2H), 1.78-1.68 (m, 2H), 1.61 (app pent, *J* = 7.2 Hz, 2H), 1.43-1.35 (m, 2H), 1.33-1.03 (m, 20H), and 0.89 (t, *J* = 7.0 Hz, 3H). [seIVpg213f2]

LCMS (Method B): T_R = 18.7 min, m/z “pos” = 419.3.0.3 (M-123)⁺

TLC (30:1 Hex:EtOAc): R_f = 0.4

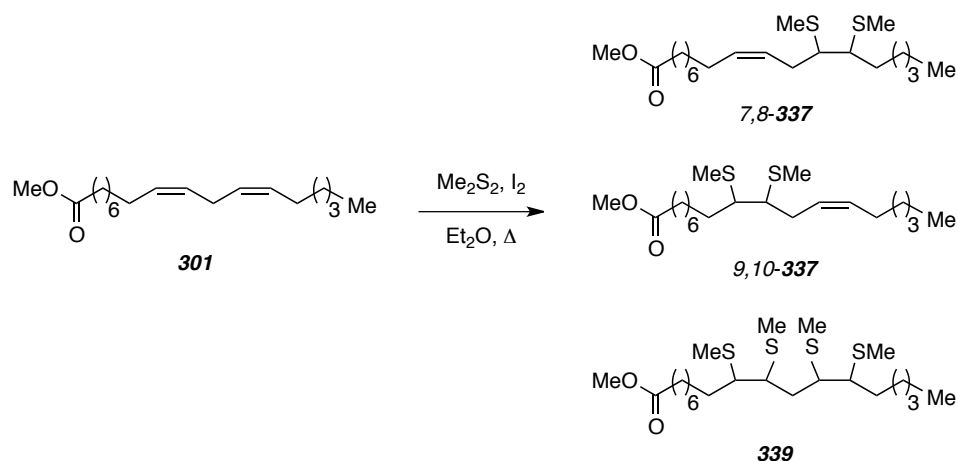


(9S,10S)-methyl 9,10-bis(methylthio)octadecanoate (336). An analogous procedure was utilized for the reaction of methyl oleate with DMDS. Full conversions could be reached in less than one hour with fewer equivalents (usually 2) of the DMDS and 20 mol % I₂. Yields 60% or better in all cases.

¹H NMR (500 MHz, CDCl₃): δ 3.67 (s, 3H), 2.70-2.67 (nfom, 2H), 2.31 (t, *J* = 7.5 Hz, 2H), 2.10 (s, 6H), 1.88-1.81 (m, 2H), 1.65-1.55 (m, 4H), 1.40-1.21 (m, 20H), 0.88 (t, *J* = 6.9 Hz, 3H). [seIVpg216_f1]

LCMS (Method C): T_R = 19.1 min, m/z “pos” = 343.3 (M-47)⁺.

TLC (16:1 Hex:EtOAc): R_f = 0.8



(Z)-methyl 12,13-bis(methylthio)octadec-9-enoate and (Z)-methyl 9,10-bis(methylthio)octadec-12-enoate (7,8-337 and 9,10-337). Methyl linoleate (**301**, 100 mg, 0.34 mmol), DMDS (150 μL , 1.3 mmol), were combined in a 1:1 mixture of DCM and MeNO_2 (total of 1 mL) and cooled to 0 $^\circ\text{C}$. $\text{BF}_3 \cdot \text{OEt}_2$ (20 μL , 0.15 mmol, .2 equiv/db) was added and the resulting solution allowed to warm to rt. The reaction was typically done in < 2 hours, but was occasionally stirred at room temperature overnight. The reactions were monitored by GCMS and TLC, which indicated that even with extended reaction times, no further reaction to the tetralkylated linoleate was observed. The reaction was diluted with additional DCM, and a NaHCO_3 (saturated aqueous) solution was added. and stirred for 5-10 minutes. The organic layer was separated, dried over Na_2SO_4 , and concentrated to a mixture of regioisomers. These could be partially separated with MPLC (15:1 Hex:EtOAc, combined yield 40-50%).

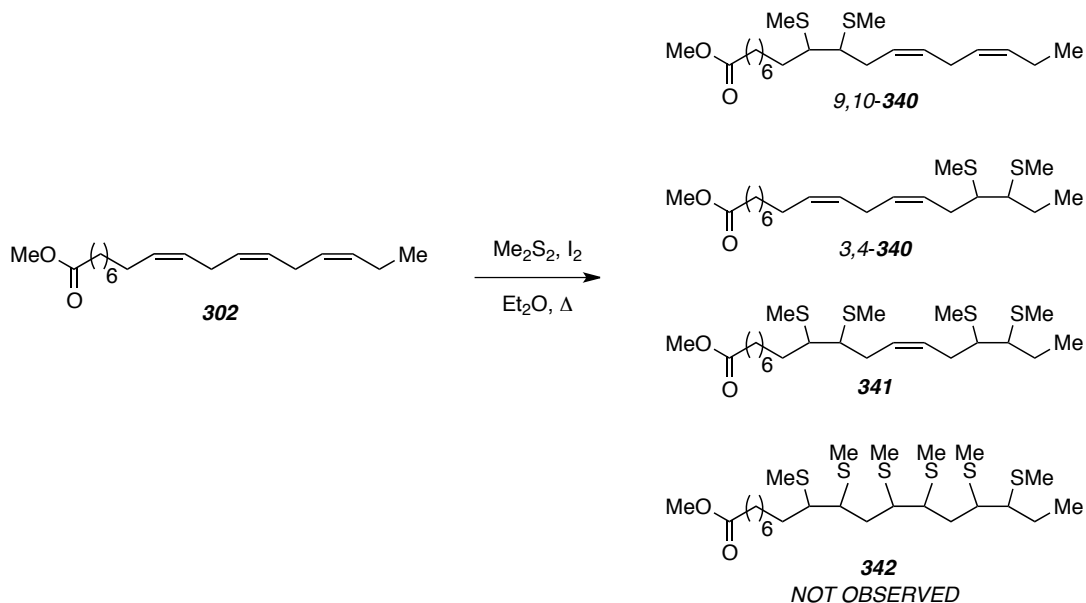
The ratio of regioisomers was typically between 1:1 and 2:1 (when lowering loading), depending on the loading of DMDS.

Data for Mixture of 7,8-337 and 9,10-337).

$^1\text{H NMR}$ (500 MHz, CDCl_3): δ 5.51-5.42 (m, 2H), 3.670 and 3.667 (singlets, 3H), 2.78-2.65 (m, 3H), 2.31 and 2.30 (ts, $J = 7.5$ Hz, add to 2H), 2.16-2.04 (m, 4H), 2.116, 2.108, 2.106 (s, add to 6 H), 1.91-1.82 (m, 1H), 1.66-1.53 (m, 4H), 1.43-1.25 (m, 13H), and 0.90 and 0.89 (t, $J = 6.6$ Hz, add to 3H). [seIVpg270m2f2]

LCMS (Method B): $T_R = 17.3$ min, m/z “pos” = 341.0 (M-47)⁺. Another same nominal mass $T_R = 16.9$ min, m/z “pos” = 341.0 (M-47)⁺.

TLC (16:1:Hex:EtOAc): $R_f = 0.4$.



Preparation of 9,10- and 3,4-340 and 341.

Methyl linolenate (**302**, 50 mg, 0.17 mmol) was mixed with DMDS (94 mg, 90 μL , 2 equiv/db) in DCM and cooled to 0 °C. $\text{BF}_3 \cdot \text{OEt}_2$ (approx 10 μL , 0.05 mmol) was dispensed via wiretrol into the loosely closed culture reaction tube. The reaction was allowed to stir at rt for 24 hours, when it was quenched with a saturated solution of NaHCO_3 . The organic layer was separated, dried, and concentrated. Crude LCMS analysis suggested approx. 80% conversion to (generally) a 3:1 ratio of mono- and bis-addition products (reacting at 1 or 2 alkenes, respectively). These were separated by MPLC (15:1 Hex:EtOAc) and analyzed by GCMS for their proposed regiochemistries. Data for:

(12Z,15Z)-methyl 9,10-bis(methylthio)octadeca-12,15-dienoate (9,10-340) and (9Z,12Z)-methyl 15,16-bis(methylthio)octadeca-9,12-dienoate (3,4-340).

$^1\text{H NMR}$ (500 MHz, CDCl_3): δ 5.53-5.30 (m, 4H), 3.675 and 3.673 (s, 3H), 2.90-2.68 (m, 4H), 2.65 (ddd, $J = 9.6, 4.2, 3.0$ Hz, 1H), 2.32 and 2.31 (t, $J = 7.6$ Hz, 2H), 2.27-2.04

(m, 4H), 2.13/2.12/2.11 (s, 6H), 2.00-1.84 (m, 1H), 1.66-1.59 (m, 2H), 1.48-1.28 (m, 9H), and 1.02/0.99/0.98 (t, $J = 7.5$ Hz, 3H). [seIVpg273f2]

LCMS (Method B): $T_R = 17.6$ min, m/z “pos” = 339.0 (M-47)⁺.

TLC (16:1 Hex:EtOAc): $R_f = 0.2$

Data for:

(Z)-methyl 9,10,15,16-tetrakis(methylthio)octadec-12-enoate (341).

¹H NMR (500 MHz, CDCl₃): δ 5.63-5.57 (nfom, 2H), 3.67 (s, 3H), 2.82 (ddd, $J = 9.5$, 4.4, 3.0 Hz, 1H), 2.80-2.67 (m, 4H), 2.65 (ddd, $J = 9.4$, 4, 4 Hz, 1H), 2.31 (t, $J = 7.5$ Hz, 2H), 2.27-2.08 (m, 2H), 2.130/2.127/2.119/2.111 (s, 12H), 1.99-1.82 (m, 2H), 1.66-1.54 (m, 2H), 1.49-1.26 (m, 12H), and 1.069/1.067 (t, $J = 7.3$ Hz, 3H). [seIVpg273f3]

GCMS (5029021): $R_t = 17.44$ min, 480 (M⁺, not observed), 465(M-15,1), 433(40), 385(45), 217(30), and 89(100).

LCMS (Method B): $T_R = 17.2$ min, m/z “pos” = 433.0 (M-47)⁺, 481.0 (M+1)⁺.

TLC (16:1 Hex:EtOAc): $R_f = 0.15$



(9S,10S)-methyl 9,10-bis(methylthio)octadecanoate (336). Described above.

(10S)-methyl 9,10-bis((2-hydroxyethyl)thio)octadecanoate 344. Methyl oleate (**310**, 100 mg, 0.34 mmol) and diethanoldisulfide (**334**, 105 mg, 0.68 mmol) were combined in 1 mL Et₂O in a screw capped culture tube. I₂ (43 mg, 0.17 mmol) was added, the vessel was sealed and heated for 1.5 hours, when NMR confirmed >95% conversion of starting material. The reaction was allowed to cool to room temperature. It was diluted with Et₂O, stirred with Na₂S₂O₃ (concentrated aqueous solution) until the color diminished. The aqueous phase was extracted with Et₂O, and the combined organic layers were dried, filtered, and concentrated. Crude recovery was typically very good in these reactions.

MPLC (1:4 Hex:EtOAc) afforded the purified diol in 26% yield. The pure material which could be adequately analyzed by LCMS (GCMS was not useful for this compound) and NMR.

¹H NMR (500 MHz, CDCl₃): δ 3.73 (t, *J* = 5.9 Hz, 4H), 3.67 (s, 3H), 2.82-2.75 (m, 2H), 2.734 (br t, *J* = 5.8 Hz, 2H), 2.727 (t, *J* = 6.0 Hz, 2H), 2.31 (t, *J* = 7.5 Hz, 2H), 1.90-1.83 (m, 2H), 1.65-1.56 (m, 4H), 1.39-1.23 (m, 20H), and 0.88 (t, *J* = 7.0 Hz, 3H).

[seIVpg259f2] could use also seIVpg226_mplc]

LCMS (Method C): T_R = 16.4 min, m/z “pos” = 373.03 (M-77)⁺, m/z “neg” = 509.0 (M+59)⁻

TLC (16:1nHex:EtOAc): R_f = 0.1

(((10S)-1-methoxy-1-oxooctadecane-9,10-diyl)bis(sulfanediyl))bis(ethane-2,1-diyl) diacetate (350). **350** can be prepared by the above method (disulfide addition chemistry with **349**) or alternatively, by modification of **334** (acetylation with an excess (e.g. 10 equivalents each) acetic anhydride and pyridine). Purification by MPLC (4:1 Hex:EtOAc) provided **350** in 80% yield.

Data for **350**:

¹H NMR (500 MHz, CDCl₃): δ 4.20 (dddd, *J* = 11.1, 7.1, 7.1 Hz, 4H), 3.67 (s, 3H), 2.82-2.67 (m, 6H), 2.31 (t, *J* = 7.5 Hz, 2H), 2.07 (s, 6H), 1.88-1.79 (m, 2H), 1.67-1.55 (m, 4H), 1.39-1.19 (m, 20H), and 0.88 (t, *J* = 6.8 Hz, 3H). [seIVpg232_mredo]

LCMS (Method B): T_R = 16.8 min, m/z “pos” = 552.0 (M+18)⁺.

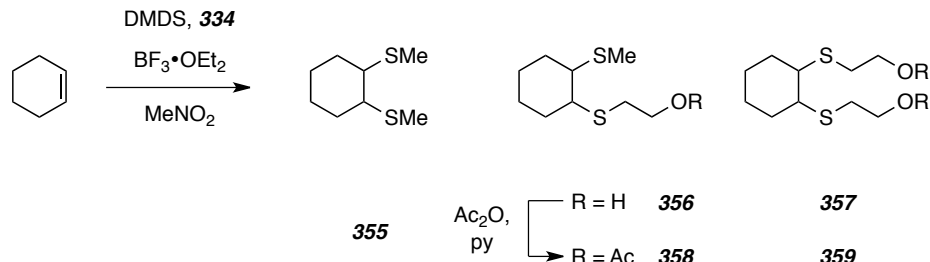
TLC (5:1:Hex:EtOAc): R_f = 0.3

Starting material 349 disulfanediylbis(ethane-2,1-diyl) diacetate. **334** was acetylated under the standard conditions (acetic anhydride, pyridine) and used without purification.

¹H NMR (500 MHz, CDCl₃): δ 4.33 (t, *J* = 6.6 Hz, 4H), 2.93 (t, *J* = 6.6 Hz, 4H), and 2.09 (s, 6H). [seIVpg264_wp1]

LCMS (Method B): T_R = 11.5 min, m/z “pos” = 256.00 (M+18)⁺.

TLC (1:8 Hex:EtOAc): R_f = 0.1



DMDS (110 uL, 1.22 mmol) and **334** (188 mg, 1.22 mmol) were mixed together in the solvent pair DCM and MeNO₂ (1:1, 2mL total) at room temperature and BF₃•OEt₂ (30 uL, 0.24 mmol) was added and the solution stirred for 30 minutes. Cyclohexene (100 mg, 123 uL, 1.22 mmol) was then added and stirred for 16 hours at room temperature. The reaction was monitored by GCMS. Workup proceeded as described above, and iterative MPLC (2:1 to 1:8 Hex:EtOAc) was required to separate the dimethylsulfide, mixed, and dimercaptoethanol adducts.

1,2-bis(methylthio)cyclohexane (**355**)

¹H NMR (500 MHz, CDCl₃): δ 2.67-2.62 (m, 2H), 2.21-2.16 (m, 2H), 2.13 (s, 6H), 1.78-1.68 (m, 2H), 1.56-1.46 (m, 2H), and 1.40-1.30 (m, 2H). [seVIpg279o_f1]

GCMS (5029021): R_t = 6.99 min, 176 (M⁺, 90), 129(85), and 81(100).

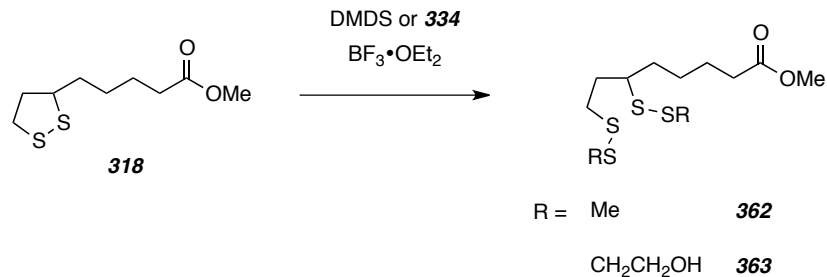
TLC (4:1 Hex:EtOAc): R_f = 0.9

2-((2-(methylthio)cyclohexyl)thio)ethanol (**356**)

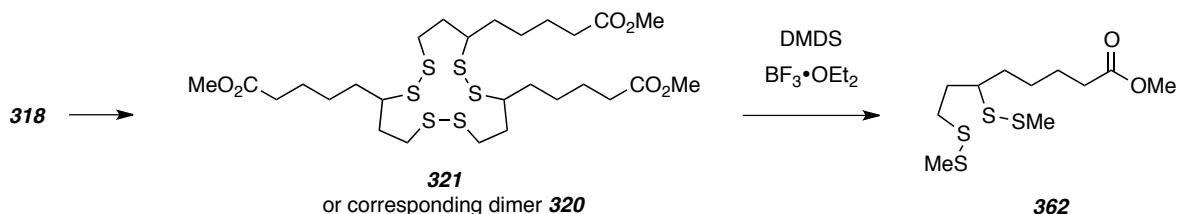
¹H NMR (500 MHz, CDCl₃): δ 3.74 (br t, *J* = 5.7 Hz, 2H), 2.810 (t, *J* = 5.8 Hz, 1H), 2.807 (t, *J* = 5.9 Hz, 1H), 2.70 (ddd, *J* = 9.1, 9.1, 3.9 Hz, 1H), 2.61 (ddd, *J* = 9.2, 9.2, 3.8 Hz, 1H), 2.22-2.17 (m, 2H), 2.15 (s, 3H), 1.77-1.70 (m, 2H), 1.56-1.46 (m, 2H), and 1.38-1.29 (m, 2H). [seIVpg278f2_tt16]

GCMS (5029021): R_t = 8.90 min, 206 (M⁺, 10), 188(10), 129(40), and 81(100).

TLC (4:1 Hex:EtOAc): R_f = 0.4



methyl 6,8-bis(methyldisulfany)octanoate (362). The disulfide-exchanged product could be prepared as a mixture with **318** as presented above, but it was commonly obtained by cleaving the presumed polymeric lipoic acid (or associated dimers **320** and trimers **321**) that resulted from the esterification reaction to **318**.



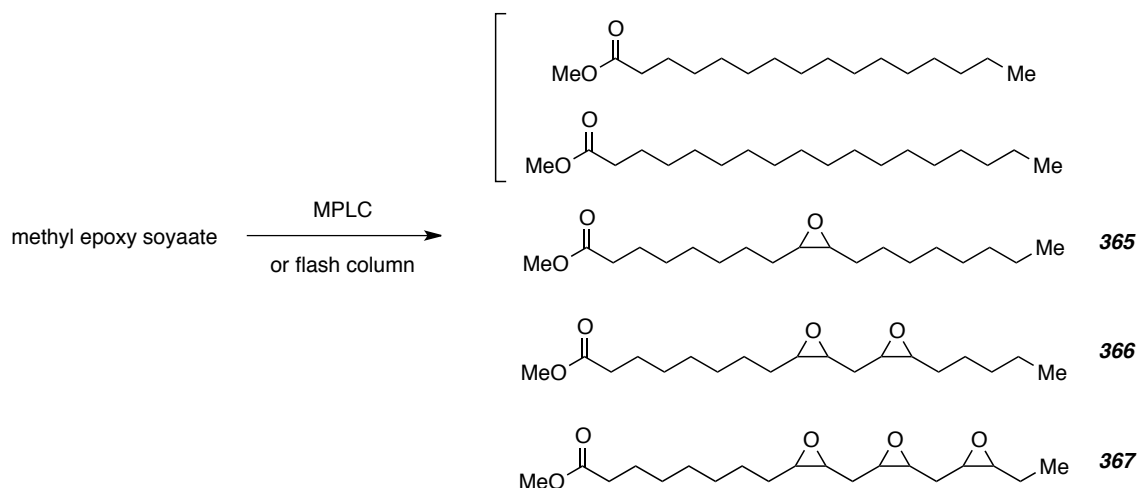
A portion of this gelish solid (50 mg) was dissolved in DCM (approx. 100 μL). To it, $\text{BF}_3 \cdot \text{OEt}_2$ (15 μL) and DMDS (80 μL) were added and the reaction stirred for two days at room temperature. Additional DMDS (50 μL) was added after one day (reaction monitored by LCMS). The reaction mixture was concentrated in vacuo and the crude exchanged product was loaded directly onto the MPLC (6:1 Hex:EtOAc). Collection and concentration afforded **362** as a residue, which amounted to approximately 10 mg.

$^1\text{H NMR}$ (500 MHz, CDCl_3): δ 3.68 (s, 3H), 2.87 (app pent, $J = 6.8$ Hz, 1H), 2.811 (ddd, $J = 13.4, 6.8, 6.8$ Hz, 1H), 2.807 (ddd, $J = 13.2, 7.6, 7.6$ Hz, 1H), 2.41 (s, 3H), 2.40 (s, 3H), 2.34 (t, $J = 7.4$ Hz, 2H), 2.02 (app q, $J = 7.1$ Hz, 2H), and 1.76-1.37 (m, 6H).

[seVpg259f2]---[seVpg259f1redo] about the same

LCMS (for the corresponding *acid*, Method C): $T_R = 5.0$ min, m/z "neg" = 299.0 (M-1).

TLC (6:1:Hex:EtOAc): $R_f = 0.6$



methyl 8-(3-octyloxiran-2-yl)octanoate (365).

$^1\text{H NMR}$ (500 MHz, CDCl_3): δ 3.67 (s, 3H), 2.92-2.88 (m, 2H), 2.31 (t, $J = 7.5$ Hz, 2H), 1.67-1.59 (m, 2H), 1.55-1.20 (m, 24H), and 0.88 (br t, $J = 6.7$ Hz, 3H). [seVpg226f2]

GCMS (5029021H): $R_t = 11.0$ min, 312(M^+ , 1), 281(3), 199(20), 155(100), 97(30), and 55(60).

LCMS (Method C): $T_R = 5.7$ min, m/z "pos" = 313.3 ($M+1$) $^+$, 330.3 ($M+18$) $^+$, 362.3 ($M+60$) $^+$.

TLC (6:1 Hex:EtOAc): $R_f = 0.9$

methyl 8-(3-((3-pentyloxiran-2-yl)methyl)oxiran-2-yl)octanoate (366)

$^1\text{H NMR}$ (500 MHz, CDCl_3): δ 3.67 (s, 3H), 3.12 (ddd, 6.0, 6.0, 4.2 Hz, 1H), 3.08 (ddd, $J = 6.4, 6.4, 4.2$ Hz, 1H), 3.02-3.2.94 (m, 2H), 2.31 (t, $J = 7.5$ Hz, 2H), 1.86-1.71 (overlapping t, $J = 6.4$ Hz, 2H), 1.65-1.58 (m, 2H), 1.57-1.25 (m, 18H), and 0.90 (t, $J = 6.8$ Hz, 3H). [seVpg226f3]

GCMS (5029021H): One diastereomer: $R_t = 11.6$ min, 326(M^+ , 2), 295(5), 187(5), 155(100), 109(30), and 55(70). Other diastereomer: $R_t = 11.7$ min, 326(M^+ , 2), 308(5), 277(5), 187(10), 155(100), 109(30), and 55(60).

LCMS (Method C): $T_R = 4.6$ min, m/z "pos" = 344.3 ($M+18$) $^+$.

TLC (6:1 Hex:EtOAc): $R_f = 0.2$

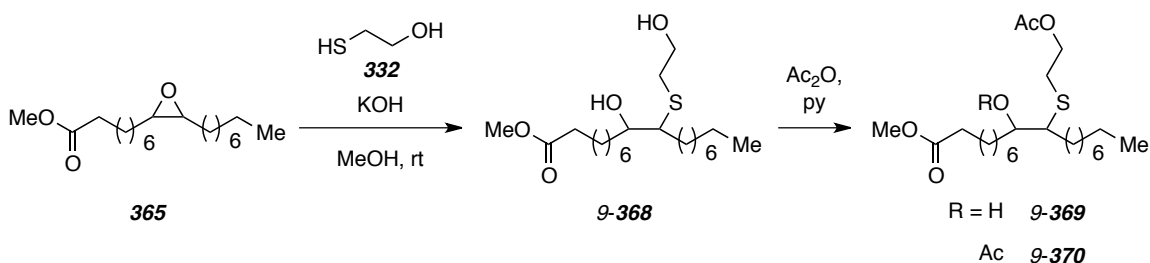
methyl 8-(3-((3-((3-ethyloxiran-2-yl)methyl)oxiran-2-yl)methyl)oxiran-2-yl)octanoate (367)

¹H NMR (500 MHz, CDCl₃): δ 3.67 (s, 3H), 3.21-3.08 (m, 4H), 3.01-2.94 (m, 2H), 2.31 (t, *J* = 7.4 Hz, 2H), 1.86-1.67 (m, 4H), 1.65-1.41 (m, 7H), 1.39-1.29 (m, 7H), and 1.09-1.05 (overlapping t, *J* = 7.5 Hz, 3H). [seVpg226m2tt9]

GCMS (5029021H): One diastereomer: *R*_t = 12.2 min, 340(*M*⁺,2), 322(5), 221(10), 155(80), 81(75), and 55(100). Other diastereomer: *R*_t = 12.3 min, 340(*M*⁺,2), 221(5), 187(5), 155(80), 109(55), 81(90), and 55(100). Other diastereomer: *R*_t = 12.35 min, 340(*M*⁺,2), 322(5), 221(10), 155(100), 109(60), 81(95), and 67(100).

LCMS (Method C): *T*_R = 3.9 min, *m/z* “pos” = 341.3 (*M*+1)⁺, 358.3 (*M*+18)⁺.

TLC (1:1 Hex:EtOAc): *R*_f = 0.2



Procedure: A culture tube was charged with 100 ul of a stock solution of KOH in MeOH [(25 mg in 1 mL), amounted to 2.5 mg, 0.045 mmol]. Mercaptoethanol (16 uL, 0.23 mmol) was added via wiretrol, and the solution stirred briefly before a solution of methyl epoxy oleate (70 mg, 0.23 mmol) in MeOH (0.8 mL) was added. The reaction was monitored by LCMS, and the mass of the desired product appeared within an hour. The crude diol was recovered by rotatly evaporation of the reaction solution, and MPLC (3:1 Hex:EtOAc) afforded the pure diol as a colorless oil in 40% yield. Alternatively, this reaction can be performed neat or in ACN.

methyl 9-hydroxy-10-((2-hydroxyethyl)thio)octadecanoate (9-368) or methyl 10-hydroxy-9-((2-hydroxyethyl)thio)octadecanoate (10-368, not shown)).

¹H NMR (500 MHz, CDCl₃): δ 3.79-3.72 (overlapping t, *J* = 5.8 Hz, 2H), 3.671 and 3.668 (s, add to 3H), 3.52-3.47 (m, 2H), 2.81-2.71 (m, 2H), 2.54 (ddd, *J* = 9.0, 6.5, 4.1

Hz, 1H), 2.310 and 2.306 (t, $J = 7.5$ Hz, adds to 2H), 1.71-1.22 (m, 28H), and 0.884 and 0.881 (t, $J = 7.1$ Hz, adds to 3H). [seVpg224mplc]

LCMS (Method C): $T_R = 5.6$ min, m/z “pos” = 373.0.3 (M-17)⁺, m/z “neg” = 449.0 (M+59)⁻.

TLC (3:1 Hex:EtOAc): $R_f = 0.1$

methyl 10-((2-acetoxyethyl)thio)-9-hydroxyoctadecanoate (9-369) or methyl 9-((2-acetoxyethyl)thio)-10-hydroxyoctadecanoate (10-369), not shown). A crude sample of diol **368** (50 mg, 0.13 mmol) in $CDCl_3$ was measured into a culture tube and treated with acetic anhydride (12 μ l, 0.13 mmol) and pyridine (11 μ l, 0.13 mmol). After 12 hours at rt, the volatiles were removed by vacuum, and the residue subjected to MPLC (5:1 Hex:EtOAc) to provide the mono-acetylated diol as a pure residue for characterization by LCMS and ¹H NMR.

¹H NMR (500 MHz, $CDCl_3$): δ 4.20 (t, $J = 6.9$ Hz, 2H), 3.67 (s, 3H), 3.50-3.45 (m, 1H), 2.82-2.72 (overlapping t, $J = 6.8$ Hz, adds to 2H), 2.53 (ddd, $J = 9.2, 6.3, 4.3$ Hz, 1H), 2.47 (br dd, $J = 12.1, 3.8$ Hz, 1H), 2.33-2.28 (overlapping t, $J = 7.5$ Hz, 2H), 2.08 (s, 3H), 1.70-1.23 (m, 26H), and 0.883 and 0.881 (t, $J = 7.0$ Hz, adds to 3H). [seVpg219_e]

LCMS (Method C): $T_R = 5.3$ min, m/z “pos” = 414.3 (M-17)⁺, 450.3 (M+18)⁺, m/z “neg” = 491.3 (M+59)⁻.

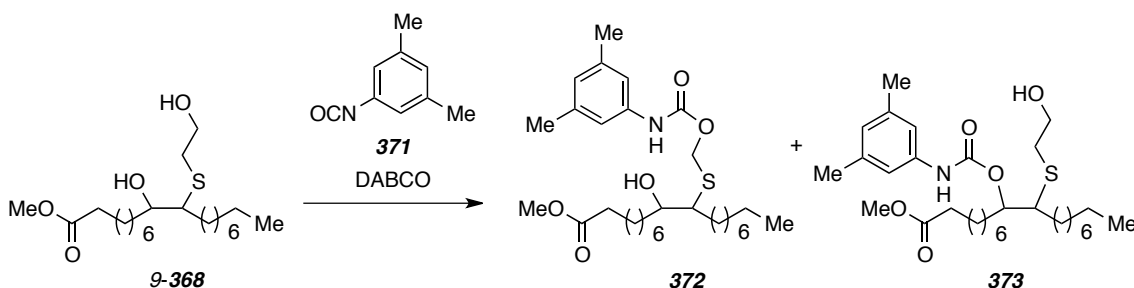
TLC (5:1 Hex:EtOAc): $R_f = 0.1$

methyl 9-acetoxy-10-((2-acetoxyethyl)thio)octadecanoate (9-370) or methyl 10-acetoxy-9-((2-acetoxyethyl)thio)octadecanoate (10-370). Alternatively, the **368** can be treated with two equivalents of acetic anhydride and pyridine and purified by MPLC (same conditions) for access to the bis-acetylated diols **370**.

¹H NMR (500 MHz, $CDCl_3$): δ 4.96 (br ddd, $J = 9.2, 3.5, 3.5$ Hz, 1H), 4.26-4.16 (overlapping ddds, 2H), 3.67 (s, 3H), 2.85 (ddd, $J = 2.69$ (br q, $J = 4$ Hz, 1H), 2.90-2.72 (overlapping ddds, 2H), 2.31 (t, $J = 7.5$ Hz, 2H), 2.07 (s, 6H), 1.79-1.50 (m, 6H), 1.39-1.25 (m, 20H) and 0.88 (t, $J = 6.8$ Hz, 3H). [seVpg219_2f1]

LCMS (Method C): $T_R = 6.0$ min, m/z “pos” = 492.3 (M+18)⁺.

TLC (5:1 Hex:EtOAc): $R_f = 0.3$



methyl 10-((2-(((3,5-dimethylphenyl)carbamoyl)oxy)ethyl)thio)-9-

hydroxyoctadecanoate or methyl 9-((2-(((3,5-

dimethylphenyl)carbamoyl)oxy)ethyl)thio)-10-hydroxyoctadecanoate (372). A round bottom flask contained approximately 10 mg (0.026 mmol) of the diol **368** was rinsed with 0.5 mL CDCl_3 and this was added to an NMR tube. Approximately 3 mg DABCO was pulled into a wiretrol, and this was administered to the wall of the NMR tube. The isocyanate was transferred the same way (approx. 4 mg, 0.03 mmol, 1 equiv) and the tube was shaken to incorporate all the elements. The reaction was monitored by NMR and LCMS, and following concentration and purification by MPLC (2:1 Hex:EtOAc), ca. 2 mg of the mono-carbamate **372** was obtained for analysis

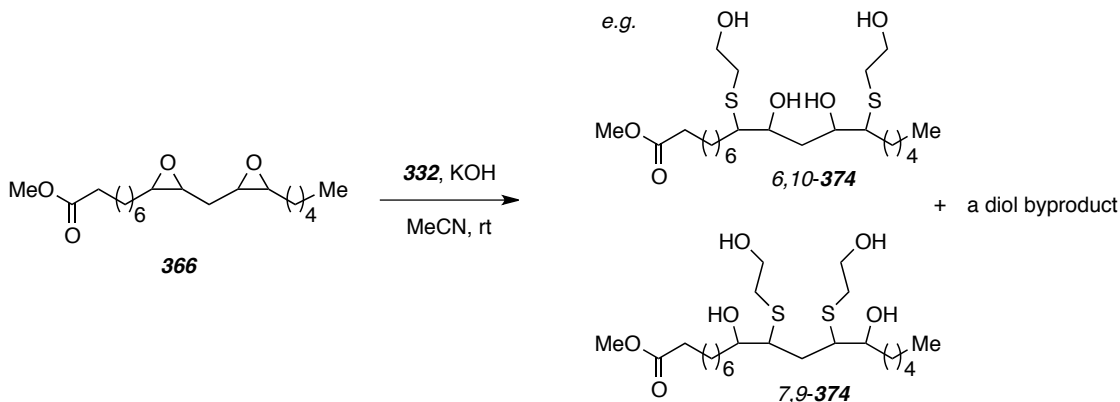
Spectral Data for **372**.

$^1\text{H NMR}$ (500 MHz, CDCl_3): δ 7.01 (s, 2H), 6.72 (s, 1H), 4.29 (t, $J = 6.7$ Hz, 2H), 3.67 (s, 3H), 3.49 (br t, $J = 6.8$ Hz, 1H), 2.89-2.74 (overlapping t, $J = 6.7$ Hz, 2H), 2.58-2.50 (m, 1H), 2.29 (s, 6H), 1.71-1.24 (m, 26H), and 0.88 (t, $J = 6.8$ Hz, 3H).

[seVpg220_2mplc] only had one carbamate there.

LCMS (Method C): $T_R = 5.8$ min, m/z "pos" = 520.3 ($\text{M}-17$) $^+$, 555.3 ($\text{M}+18$) $^+$, m/z "neg" = 536.3 ($\text{M}-1$) $^-$, 596.3 ($\text{M}+59$) $^-$.

TLC (2:1 Hex:EtOAc): $R_f = 0.2$



Procedure: Ground KOH pellets (10 mg, 0.18 mmol) were added to a round bottom flask and MeOH (4 mL) was added to dissolve the solid before mercaptoethanol (130 μL , 1.84 mmol) was added. This solution was stirred as a solution of methyl epoxy linoleate (300 mg, 0.92 mmol) in MeOH (1 mL) was prepared. After addition of the epoxide, the reaction mixture was allowed to stir for 8 hours (monitoring by LMCS). The crude tetraol was obtained by rotary evaporation, and the product was separated from byproduct by MPLC (1:4 Hex:EtOAc). Typically, a 1:1 mixture of the tetraol and byproduct were produced by this procedure.

Data for mixture of **374**:

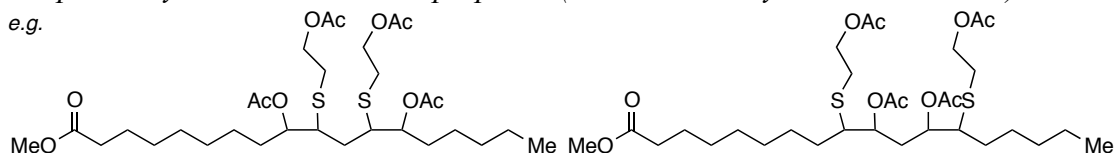
methyl 10,12-dihydroxy-9,13-bis((2-hydroxyethyl)thio)octadecanoate (6,10-374) or methyl 9,13-dihydroxy-10,12-bis((2-hydroxyethyl)thio)octadecanoate (7,9-374) are examples.

$^1\text{H NMR}$ (500 MHz, CDCl_3): δ 3.84-3.74 (m, 6H), 3.67 (s, 3H), 2.85-2.69 (m, 6H), 2.31 (t, $J = 7.3$ Hz, 2H), 1.83-1.28 (m, 24H), and 0.90 (t, $J = 6.9$ Hz, 3H). [seVpg214_3f2]

LCMS (Method C): $T_R = 5.0$ min, m/z "pos" = 465.3 ($\text{M}-17$)⁺, m/z "neg" = 527.3 ($\text{M}+35$)⁻, 541.3 ($\text{M}+59$)⁻.

TLC (1:4 Hex:EtOAc): $R_f = 0.1$

The per-acetylated variants were prepared (no number, only mentioned in text)



7,9-bis((2-acetoxyethyl)thio)-18-methoxy-18-oxooctadecane-6,10-diyl diacetate (first isomer shown) or **((7,9-diacetoxy-18-methoxy-18-oxooctadecane-6,10-diyl)bis(sulfanediyl))bis(ethane-2,1-diyl) diacetate** (second isomer). The crude tetraol (80 mg, 0.17 mmol) was treated with acetic anhydride and pyridine (8 equiv each). The reaction was monitored by LCMS. Full conversion of the starting material occurred within 4 hours, and the product was purified by MPLC (7:1 Hex:EtOAc) to a pair of isomers which were analyzed by ^1H and ^1H - ^1H correlation NMR.

One isomer:

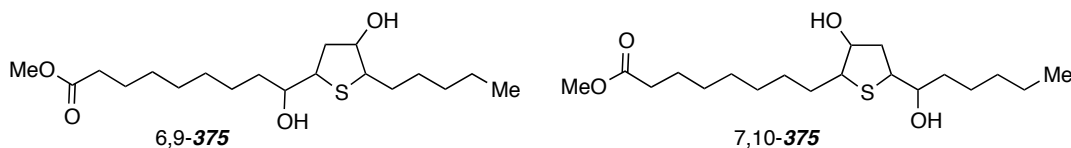
^1H NMR (500 MHz, CDCl_3): δ 4.93 (ddd, $J = 7.9, 4.1, 2.7$ Hz, 1H), 4.92 (ddd, $J = 8.3, 4.4, 2.8$ Hz, 1H), 4.23 (t, $J = 6.9$ Hz, 4H), 3.67 (s, 3H), 3.14 (app ddd, $J = 8.8, 5.6, 3.7$ Hz, 2.90 (ddd, $J = 13.4, 6.6, 1.9$ Hz, 1H), 2.88 (ddd, $J = 13.5, 6.8, 1.9$ Hz, 1H), 2.80 (ddd, $J = 14.0, 7.1, 1.5$ Hz, 1H), 2.78 (ddd, $J = 13.3, 6.9, 1.5$ Hz, 1H), 2.31 (t, $J = 7.5$ Hz, 2H), 2.07 (br s, 12 H), 1.80-1.75 (m, 2H), 1.62 (app br pent, $J = 7.2$ Hz, 2H), 1.51-1.45 (m, 2H), 1.40-1.22 (m, 16H), and 0.89 (t, $J = 6.9$ Hz, 3H). [seVpg213_8f2cleans1]

Other isomer:

^1H NMR (500 MHz, CDCl_3): δ 5.20 (ddd, $J = 8.8, 3.6, 3.6$ Hz, 1H), 5.01 (dddd, $J = 9.4, 7.0, 3.6, 3.6$ Hz, 1H), 4.27-4.18 (overlapping t, $J = 6.9$ Hz, 4H), 3.67 (s, 3H), 2.92-2.72 (m, 6H), 2.31 (t, $J = 7.5$ Hz, 2H), 2.18 (ddd, $J = 14.7, 7.7, 3.8$ Hz, 1H), 2.07 (s, 12H), 1.82-1.46 (m, 4H), 1.78 (ddd, $J = 15.1, 8.8, 6.8$ Hz, 1H), 1.39-1.23 (m, 16H), and 0.89 (t, $J = 6.9$ Hz, 3H). [seVpg213_8f2cleans2]

LCMS (both isomers, Method C): $T_R = 4.9$ min, m/z “pos” = 668.3 (M+18) $^+$, m/z “neg” = 709.0 (M+59) $^-$. Another peak with the same nominal mass at $T_R = 5.1$ min.

TLC (2:1 Hex:EtOAc): $R_f = 0.2$



One isomer:

¹H NMR (500 MHz, CDCl₃): δ 4.15 (br q, *J* = 4 Hz, 1H), 3.67 (s, 3H), 3.67-3.62 (m, 2H), 3.38 (nform, 1H), 2.35 (ddd, *J* = 14.2, 9.9, 4.3 Hz, 1H), 2.30 (t, *J* = 7.4 Hz, 2H), 1.87-1.80 (m, 1H), 1.70-1.58 (m, 4H), 1.43-1.26 (m, 18H), and 0.89 (t, *J* = 6.8 Hz, 3H). [seVpg216redofl_slice1]

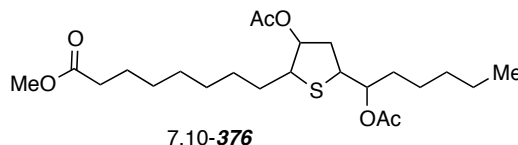
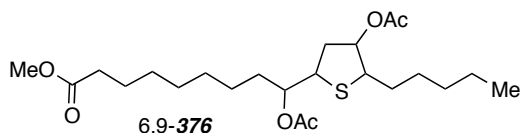
Other isomer:

¹H NMR (500 MHz, CDCl₃): 4.32 (br s, 1H), 3.75 (ddd, *J* = 10.2, 6, 3 Hz, 1H), 3.67 (s, 3H), 3.50 (m, 1H), 3.39 (nform, 1H), 2.30 (t, *J* = 7.5 Hz, 2H), 2.18 (ddd, *J* = 13.3, 6.7, 1.6 Hz, 1H), 2.12-2.06 (m, 1H), 1.96 (dddd, *J* = 13.0, 10.2, 2.6, 2.6 Hz, 1H), 1.88 (br s, 1H), 1.75 (dddd, *J* = 13.5, 9.8, 6.3, 6.3 Hz, 1H), 1.66-1.57 (m, 4H), 1.47-1.25 (m, 15H), 0.90-0.87 (overlapping t, *J* = 6.8 Hz, 3H). [seVpg216test_tt16]

LCMS (Method C): One isomer: T_R = 4.1 min, m/z “pos” = 343.3 (M-17)⁺, 361.3 (M+1)⁺, 378.3 (M+18)⁺; m/z “neg” = 405.3 (M+35)⁻, 419.3 (M+59)⁻.

Other isomer: (Method C): T_R = 4.5 min, m/z “pos” = 343.3 (M-17)⁺, 361.30(M+1)⁺; m/z “neg” = 405.3 (M+35)⁻, 419.3 (M+59)⁻.

TLC (both isomers, 1:4 Hex:EtOAc): R_f = 0.4



One isomer:

¹H NMR (500 MHz, CDCl₃): δ 5.46 (app pent, *J* = 2.8 Hz, 1H), 5.00 (dddd, *J* = 8.0, 6.5, 4.3, 3.6 Hz, 1H), 3.79 (dddd, *J* = 10.6, 6.4, 6.4, 2.6 Hz, 1H), 3.67 (s, 3H), 3.54 (br dddd, *J* = 9.2, 4.6, 4.6, 4.6 Hz, 1H), 2.30 (t, *J* = 7.5 Hz, 2H), 2.20 (ddd, *J* = 13.6, 6.2, 2.4 Hz, 1H), 2.11 (s, 3H), 2.09 (s, 3H), 1.78 (dddd, *J* = 13.9, 10.6, 3.6, 1.4 Hz, 1H), 1.70-1.45 (m, 5H), 1.34-1.23 (m, 15H), and 0.87 (br t, *J* = 6.5 Hz, 3H). [seVpg212sw]

Other isomer:

¹H NMR (500 MHz, CDCl₃): δ 5.26 (ddd, *J* = 7.9, 7.9, 5.4 Hz, 1H), 4.95 (m, 1H), 3.67 (s, 3H), 3.50 (ddd, *J* = 7.4, 7.4, 1.3 Hz, 1H), 3.37 (ddd, *J* = 9.9, 6.9, 2.3 Hz, 1H), 2.29 (dt, *J* = 1.6, 7.4 Hz, 2H), 2.15 (nform, 1H), 2.10 (s, 3H), 2.09 (s, 3H), 1.89 (ddd, *J* = 13.1,

7.6, 7.6 Hz, 1H), 1.67-1.55 (m, 5H), 1.34-1.21 (m, 15H), and 0.90-0.85 (overlapping t, J = 6.9 Hz, 3H). [seVpg212_f12minor]

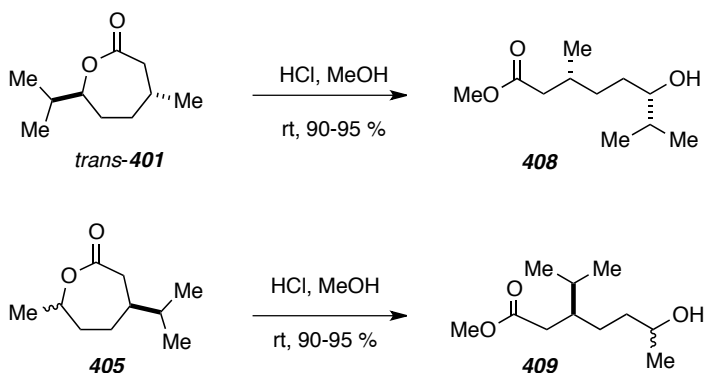
LCMS (Method C): One isomer: T_R = 5.7 min, m/z "pos" = 385.0 (M-59)⁺, 462.0 (M+18)⁺.

Other isomer: (Method C): T_R = 6.2 min, m/z "pos" = 385.0 (M-59)⁺, 462.0 (M+18)⁺.

TLC (both isomers, 7:1 Hex:EtOAc): R_f = 0.15

Experiments (Chapter VI)

Note: the preparation of **401** and **405** (and other compounds discussed at the beginning of Chapter VI) is deferred to the end of this experimental so that all Tables and Figures relevant to **400**, **404**, **401**, and **405** are located together.



methyl 6-hydroxy-3,7-dimethyloctanoate (menthide methyl ester, 408). To a stirred solution of menthide (**401**) in MeOH was added HCl and the solution stirred for 5 minutes, after which the solvent was removed under reduced pressure and the crude alcohol was purified by MPLC. Typical yields were 80-90% and the alcohol were colorless oils.

¹H NMR (500 MHz, CDCl₃): δ 3.67 (s, 3H), 3.34 (br s, 1H), 2.34 (dd, *J* = 14.8, 6.0 Hz, 1H), 2.14 (dd, *J* = 14.8, 8.1 Hz, 1H), 1.97 (oct, *J* = 6.5 Hz, 1H), 1.66 (dsept, *J* = 4.9, 6.8 Hz, 1H), 1.56-1.47 (m, 2H), 1.38-1.31 (m, 2H), 1.24-1.18 (m, 1H), 0.96 (d, *J* = 6.7 Hz, 3H), 0.92 (d, *J* = 6.8 Hz, 3H), and 0.91 (d, *J* = 6.7 Hz, 3H). [seVpg207mnmplc]

LCMS (Method C): *T_R* = 3.6 min, *m/z* “pos” = 203.3 (M+1)⁺, 220.3 (M+18)⁺.

TLC (3:1 Hex:EtOAc): *R_f* = 0.15

methyl 6-hydroxy-3-isopropylheptanoate (carvomenthide methyl ester, 409). **409**

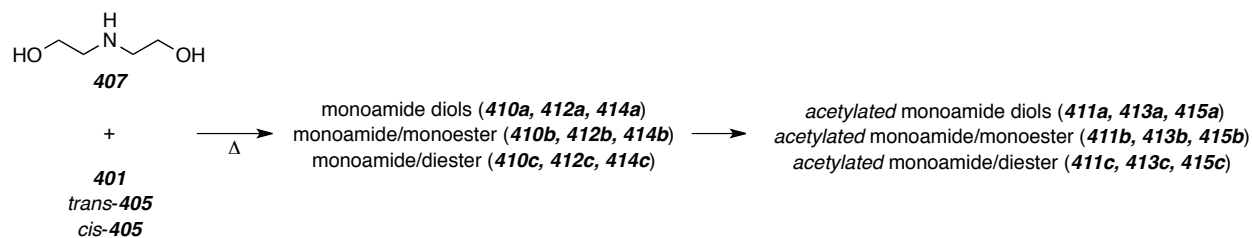
was prepared from **405** in an analogous fashion as **408** and was purified by MPLC (10:1 Hex:EtOAc). Yields > 80% for all attempts.

¹H NMR (500 MHz, CDCl₃): δ 3.78 (sextet, *J* = 6.2 Hz, 1H), 3.67 (s, 3H), 2.31 (dd, *J* = 15.2, 5.8 Hz), 2.15 (dd, *J* = 15.2, 6.3 Hz, 1H), 1.82-1.75 (m, 1H), 1.73 (dsept, *J* = 4.2, 6.8

Hz, 1H), 1.51-1.29 (m, 4H), 1.19 (d, $J = 6.2$ Hz, 3H), 0.88 (d, $J = 6.8$ Hz, 3H), and 0.85 (d, $J = 6.8$ Hz, 3H). [seVpg207cmmplc]-only major isomer here

LCMS (Method C): $T_R = 3.5$ min, m/z “pos” = 203.3 (M+1)⁺, 220.3 (M+18)⁺.

TLC (3:1 Hex:EtOAc): $R_f = 0.1$



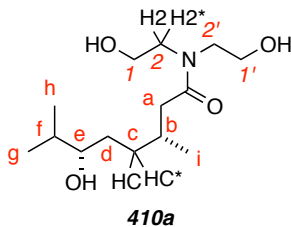
See Figure III-8 and III-9 in the text.

Preparation of 410a-c, 412a-c, 414a-c

In a typical experiment, the appropriate quantities of diethanolamine (1 equiv) and lactone (3 equiv) were weighed directly into a culture tube. The vessel was then sealed and heated for 2-4 hours (conversion was monitored by LC/MS). The crude reaction mixture was loaded directly onto an MPLC column and eluted with ethyl acetate containing 1% methanol. The compounds eluted in the following order and had the indicated composition: unreacted lactone (~30-45%), the monoamide diester (~5-10%), the monoamide monoester (~20-25%), and the monoamide diol (~20-25%).

Note for 410a-c, 411a-c, 412a-c, 413a-c, 414a-c, 415a-c: * protons are diastereotopic to their (unstarred) partners. *e.g.* see 410a and the remaining 410-415 compounds follow this convention.

Spectral data for monoamide 410a



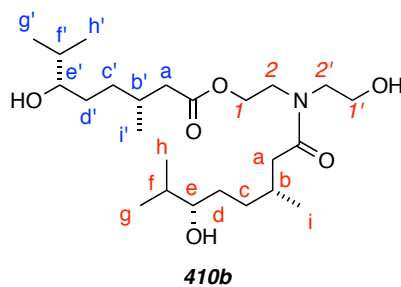
¹H NMR (500 MHz, CDCl₃) δ 3.81 (ddd, *J* = 11.0, 6.8, 3.7 Hz, 1H, H₁), 3.77 (ddd, *J* = 11.6, 5.9, 3.9 Hz, 1H, H₁*), 3.74 (br t, *J* = 5.1 Hz, 2H, H₁'), 3.56 (ddd, *J* = 14.2, 5.7, 3.7 Hz, 1H, H₂), 3.54 (ddd, *J* = 15.2, 5.2, 5.2 Hz, 1H, H₂*), 3.48 (ddd, *J* = 14.2, 6.8, 3.9 Hz, 1H, H₂'), 3.43 (ddd, *J* = 15.1, 5.2, 5.2 Hz, 1H, H₂'*), 3.27 (ddd, *J* = 7.9, 5.2, 2.6 Hz, 1H, H_e), 2.36 (dd, *J* = 15.0, 7.6 Hz, 1H, H_a), 2.26 (dd, *J* = 15.0, 6.5 Hz, 1H, H_a*), 2.08-1.99 (m, 1H, H_b), 1.63 (dq, *J* = 6.8, 6.8, 6.8 Hz, 1H, H_f), 1.56-1.52 (m, 2H, H_c/H_d), 1.33-1.24 (m, 1H, H_c*), 1.15-1.08 (m, 1H, H_d*), 0.94 (d, *J* = 6.8 Hz, 3H, H_i), 0.89 (d, *J* = 6.8 Hz, 3H, H_h), and 0.88 (d, *J* = 6.8 Hz, 3H, H_g).

¹³C NMR (125 MHz, CDCl₃) δ 175.0, 77.2, 60.9, 60.7, 52.4, 50.5, 41.1, 33.9, 33.5, 31.8, 31.0, 20.4, 19.0, and 17.5.

IR (neat): 3550-3250, 2956, 2874, 1617, 1465, 1421, and 1054.

HRMS (ESI) (m/z): [M+Na]⁺ calculated for [C₁₄H₂₉NO₄Na]⁺ 298.1989, found 298.1959.

Spectral data for monoester 410b



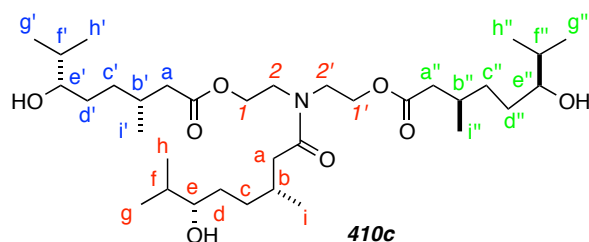
¹H NMR (500 MHz, CDCl₃) δ 4.25 (ddd, *J* = 11.1, 5.6, 5.6 Hz, 1H, H₁), 4.21 (ddd, *J* = 11.1, 5.9, 5.9 Hz, 1H, H₁*), 3.77+ (ddd, *J* = 12.1, 5.6, 5.6 Hz, 1H, H₁'), 3.77- (ddd, *J* = 12.1, 5.8, 5.8 Hz, 1H, H₁'*), 3.70-3.46 (m, 4H, H₂/H₂*/H₂'/H₂'*), 3.32+ (ddd, *J* = 8.6, 5.2, 2.6 Hz, 1H, H_e'), 3.32- (ddd, *J* = 8.6, 5.2, 2.7 Hz, 1H, H_e), 2.39 (dd, *J* = 15.1, 6.7 Hz, 1H, H_a), 2.30 (dd, *J* = 14.9, 6.7 Hz, 1H, H_a'), 2.26 (dd, *J* = 15.5, 7.5 Hz, 1H, H_a*), 2.20 (dd, *J* = 15.8, 7.3 Hz, 1H, H_a*), 2.10-2.02 (m, 1H, H_b), 1.99-1.91 (m, 1H, H_b'), 1.68-1.61 (m, 2H, H_f/H_f'), 1.60-1.49 (m, 4H, H_c/H_d/H_c'/H_d'), 1.38-1.25 (m, 2H, H_c*/H_c'*), 1.23-1.12 (m, 2H, H_d*/H_d'*), 0.98 (d, *J* = 6.6 Hz, 3H, H_f'), 0.96 (d, *J* = 6.7 Hz, 3H, H_i), 0.92 (d, *J* = 6.8, 6H, H_g, H_g'), and 0.91 (d, *J* = 6.9 Hz, 6H, H_h/H_h')

^{13}C NMR (125 MHz, CDCl_3) δ 174.5, 173.7, 173.2, 173.0, 77.0, 76.8, 76.7, 62.3, 61.6, 61.2, 60.2, 51.0, 49.5, 47.9, 45.8, 41.82, 41.76, 40.5, 40.4, 33.64, 33.61, 33.6, 33.4, 33.1, 31.7, 31.64, 31.60, 31.55, 30.9, 30.69, 30.67, 30.62, 20.3, 20.2, 19.99, 19.94, 18.97, 18.94, 17.35, 17.29, and 17.24.

IR (neat) 3600-3200 (OH), 2957, 2873 (NH), 1734 (ester CO), 1623 (amide CO), 1461, 1419, 1383 (OH), 1201, 1201, 1163, 1058, and 999 cm^{-1} .

HRMS (ESI) (m/z): $[\text{M}+\text{Na}]^+$ calculated for $[\text{C}_{14}\text{H}_{47}\text{NO}_6\text{Na}]^+$ 468.3295, found 468.3345.

Spectral data for diester 410c



^1H NMR (500 MHz, CDCl_3) δ 4.22 (t, $J=5.6$ Hz, 2H, H_1/H_1^*), 4.21 (dd, $J=11.6, 5.8$ Hz, 1H, H_1'), 4.18 (dd, $J=11.7, 5.9$ Hz, 1H, $\text{H}_1'^*$), 3.61 (t, $J=5.6$ Hz, 4H, $\text{H}_2/\text{H}_2'/\text{H}_2^*/\text{H}_2'^*$), 3.36-3.28 (m, 3H, $\text{H}_c/\text{H}_c'/\text{H}_c''$), 2.39 (dd, $J=15.1, 6.7$ Hz, 1H, H_a), 2.34 (dd, $J=14.9, 6.7$ Hz, 1H, H_a'/H_a''), 2.24 (dd, $J=15.5, 7.5$ Hz, 1H, H_a^*), 2.21 (dd, $J=15.8, 7.3$ Hz, 1H, $\text{H}_a'^*$), 2.18 (dd, $J=15.8, 7.3$ Hz, 1H, H_a^*), 2.10-2.02 (m, 1H, H_b), 1.98-1.89 (m, 2H, H_b'/H_b''), 1.68-1.62 (m, 3H, $\text{H}_f/\text{H}_f'/\text{H}_f''$), 1.59-1.48 (m, 6H, $\text{H}_c/\text{H}_d/\text{H}_c'/\text{H}_d'/\text{H}_c''/\text{H}_d''$), 1.38-1.27 (m, 3H, $\text{H}_c^*/\text{H}_c'^*/\text{H}_c''^*$), 1.22-1.12 (m, 3H, $\text{H}_d^*/\text{H}_d'^*/\text{H}_d''^*$), 0.96 (d, $J=6.6$ Hz, 3H, H_i'), 0.95 (d, $J=6.7$ Hz, 3H, H_i), 0.92 (d, $J=6.8$, 9H, $\text{H}_g, \text{H}_g', \text{H}_g''$), and 0.91 (d, $J=6.9$ Hz, 9H, $\text{H}_h, \text{H}_h', \text{H}_h''$).

^{13}C NMR (125 MHz, CDCl_3) δ 173.3, 173.1, 173.0, 77.2, 76.93, 76.88, 62.1, 61.6, 47.3, 45.4, 41.8, 41.7, 40.5, 33.7, 33.66, 33.63, 33.23, 33.21, 31.8, 31.7, 31.6, 30.75, 30.71, 31.66, 20.3, 20.1, 20.0, 19.1, 19.0, 17.34, 17.30, and 17.27.

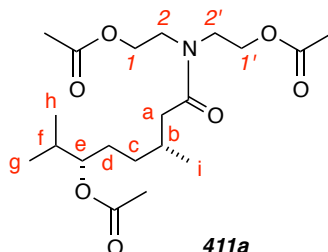
HRMS (ESI) (m/z): $[\text{M}+\text{Na}]^+$ calculated for $[\text{C}_{34}\text{H}_{65}\text{NO}_8\text{Na}]^+$ 638.4602, found 638.4630.

Acetylation of amide alcohols.

In a typical experiment the isolated model triol (~50 mg) was dissolved in pyridine and acetic anhydride (1:1, 0.5 mL). The reaction mixture was stirred at rt for 30 minutes and

then partitioned between water and ethyl acetate. The organic layer was dried over Na_2SO_4 , filtered, concentrated, and purified by MPLC (ca. 1:1 Hexanes:EtOAc) to give the acetylated derivatives (yields ca. 80%).

Spectral data for monoamide triacetate 411a



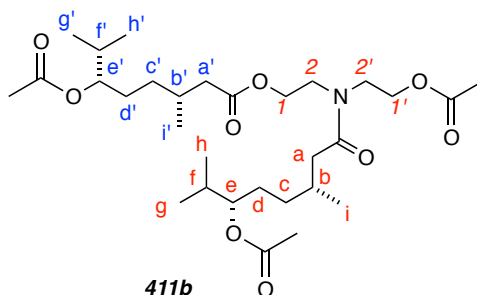
$^1\text{H NMR}$ (500 MHz, CDCl_3) δ 4.71 (dddd, $J = 13.8, 11.7, 4.7, 4.7$ Hz, 1H, H_e), 4.21+ (dt, $J = 11.3, 5.7$ Hz, 1H, H_1), 4.21- (dt, $J = 11.3, 5.6$ Hz, 1H, H_1'), 4.18+ (dt, $J = 11.6, 6.1$ Hz, 1H, H_1^*), 4.18- (dt, $J = 11.6, 5.9$ Hz, 1H, $\text{H}_1'^*$), 3.61 (brt, $J = 5.5$ Hz, 2H, H_2/H_2^*), 3.60 (brt, $J = 6$ Hz, 2H, $\text{H}_2'/\text{H}_2'^*$), 2.31 (dd, $J = 15.1, 5.5$ Hz, 1H, H_a), 2.18 (dd, $J = 15.1, 8.2$ Hz, 1H, H_a^*), 2.08 (s, 3H, $-\text{O}_2\text{CCH}_3$), 2.06 (s, 3H, $-\text{O}_2\text{CCH}_3$), 2.05 (s, 3H, $-\text{O}_2\text{CCH}_3$), 2.04-1.98 (m, 1H, H_b), 1.81 (dsept, $J = 6.6$ Hz, 1H, H_f), 1.59 (dddd, $J = 13.8, 11.7, 4.7, 4.7$ Hz, 1H, H_d), 1.49 (dddd, $J = 13.6, 11.4, 8.5, 4.7$ Hz, 1H, H_d^*), 1.35 (dddd, $J = 13.3, 11.8, 5.0, 5.0$ Hz, 1H, H_c), 1.14 (dddd, $J = 13.0, 11.4, 7.9, 4.9$ Hz, 1H, H_c^*), 0.94 (d, $J = 6.6$ Hz, 3H, H_i), 0.89 (d, $J = 6.8$ Hz, 3H, H_g), and 0.885 (d, $J = 6.8$ Hz, 3H, H_h).

$^{13}\text{C NMR}$ (125 MHz, CDCl_3) δ 172.9, 171.3, 171.0, 170.8, 78.8, 62.5, 62.0, 47.5, 45.7, 40.4, 33.1, 31.5, 30.6, 29.0, 21.4, 21.1, 21.0, 20.1, 18.8, and 17.7.

IR (neat) 2960, 1738, 1646, 1460, 1421, 1371, 1236, 1047, and 1027 cm^{-1} .

HRMS (ESI) (m/z): $[\text{M}+\text{Na}]^+$ calculated for $[\text{C}_{20}\text{H}_{35}\text{NO}_7\text{Na}]^+$ 424.2305, found 424.2311.

Spectral data for monoester triacetate 411b



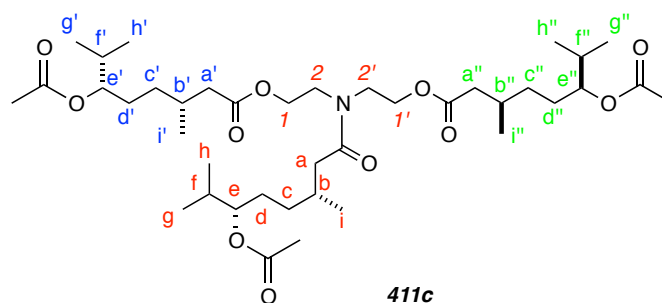
¹H NMR (500 MHz, CDCl₃) δ 4.74-4.68 (m, 2H, H_e/H_{e'}), 4.21 (ddd, *J* = 5.7, 5.7, 2.2, 2H, H₁/H₁*), 4.18 (ddd, *J* = 6.3, 6.3, 2.8, 2H, H₁'/H₁'*), 3.66-3.54 (m, 4H, H₂/H₂*/H₂'/H₂'*), 2.32 (dd, *J* = 15.0, 5.7 Hz, 1H, H_a), 2.31 (dd, *J* = 15.1, 5.7 Hz, 1H, H_a'), 2.18 (dd, *J* = 15.0, 8.4 Hz, 1H, H_a*), 2.12 (dd, *J* = 15.1, 8.4 Hz, 1H, H_a'*), 2.05 (2, 9H, -CO₂CH₃), 2.04-1.98 (m, 1H, H_b), 1.95-1.88 (m, 1H, H_b'), 1.85-1.77 (m, 2H, H_f/H_f'), 1.63-1.53 (m, 2H, H_d/H_d'), 1.52-1.44 (m, 2H, H_d*/H_d'*), 1.40-1.25 (m, 2H, H_c/H_c'), 1.22-1.11 (m, 2H, H_c*/H_c'*), 0.94 (d, *J* = 6.6 Hz, 3H, H_i), 0.93 (d, *J* = 6.6 Hz, 3H, H_i'), 0.89 (d, *J* = 6.8 Hz, 6H, H_g/H_g'), and 0.88 (d, *J* = 6.8 Hz, 6H, H_h/H_h'*)

¹³C NMR (125 MHz, CDCl₃) δ 172.92, 172.87, 172.8, 171.2, 171.14, 171.13, 170.9, 170.7, 78.7, 78.6, 78.5, 62.4, 62.2, 61.9, 61.7, 47.42, 47.40, 45.70, 45.65, 41.6, 41.5, 40.31, 40.27, 33.0, 32.99, 32.6, 31.4, 31.3, 30.6, 30.5, 30.43, 30.41, 28.92, 28.91, 28.6, 21.2, 21.0, 20.9, 19.98, 19.97, 19.8, 18.75, 18.72, and 17.6.

IR (neat) 2960, 2876, 1733, 1649, 1460, 1419, 1372, 1240, 1048, and 1022 cm⁻¹.

HRMS (ESI) (*m/z*): [M+Na]⁺ calculated for [C₃₀H₅₃NO₉Na]⁺ 594.3612, found 594.3645.

Spectral data for diester triacetate 411c



¹H NMR (500 MHz, CDCl₃) δ 4.74-4.68 (m, 3H, H_e/H_e'/H_e''), 4.20 (app q, *J* = 5.8 Hz, 2H, H₁/H₁*), 4.18 (app q, *J* = 6 Hz, 2H, H₁'/H₁'*), 3.61 (t, *J* = 5.8 Hz, 2H, H₂/H₂*), 3.60 (app q, *J* = 6.1 Hz, 2H, H₂'/H₂'*), 2.32 (dd, *J* = 15.1, 5.6 Hz, 1H, H_a), 2.306 (dd, *J* = 15.1, 5.5 Hz, 1H, H_a'), 2.301 (dd, *J* = 15.1, 5.5 Hz, 1H, H_a''), 2.18 (dd, *J* = 15.1, 8.4 Hz, 1H, H_a*), 2.10 (dd, *J* = 15.1, 8.5 Hz, 1H, H_a'*), 2.09 (dd, *J* = 15.0, 8.5 Hz, 1H, H_a''), 2.05 (s, 9H, -O₂CCH₃), 2.04-1.97 (m, 1H, H_b), 1.96-1.88 (m, 2H, H_b'/H_b''), 1.86-1.77 (m, 3H, H_f/H_f'/H_f''), 1.63-1.53 (m, 3H, H_d/H_d'/H_d''), 1.52-1.43 (m, 3H, H_d*/H_d'*/H_d''), 1.40-1.27 (m, 3H, H_c/H_c'/H_c''), 1.22-1.11 (m, 3H, H_c*/H_c'*/H_c''), 0.94 (d, *J* = 6.6 Hz, 3H, H_i), 0.93 (d, *J* =

6.6 Hz, 6H, H_i/H_i'), 0.890 (d, $J = 6.8$ Hz, 9H, $H_g, H_g'/H_g''$), and 0.887 (d, $J = 6.8$ Hz, 9H, $H_h/H_h'/H_h''$).

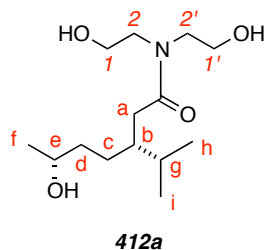
^{13}C NMR (125 MHz, CDCl_3) δ 172.9, 172.84, 172.81, 171.22, 171.18, 171.64, 78.8, 78.62, 78.59, 62.2, 61.8, 47.4, 45.7, 41.6, 41.5, 40.4, 33.1, 32.6, 31.43, 31.40, 30.6, 30.50, 30.47, 29.0, 28.7, 21.34, 21.33, 20.0, 19.9, 18.82, 18.79, and 17.6.

IR (neat) 2961, 2875, 1733, 1650, 1461, 1373, 1243, 1167, and 1021 cm^{-1} .

HRMS (ESI) (m/z): $[M+\text{Na}]^+$ calculated for $[\text{C}_{40}\text{H}_{71}\text{NO}_{11}\text{Na}]^+$ 764.4919, found 764.4949.

Preparation of model amide esters S3a-c derived from diethanolamine (7) *trans*-carvomenthide (*trans*-405).

Spectral data for 412a (monoamide derived from *trans*-carvomenthide)



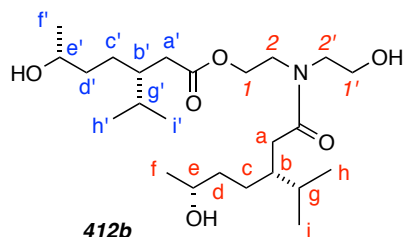
^1H NMR (500 MHz, CDCl_3) δ 3.91 (ddd, $J = 11.3, 7.3, 3.3$ Hz, 1H, H_1), 3.82 (ddd, $J = 11.3, 6.1, 3.4$ Hz, 1H, H_1^*), 3.80 (app t, $J = 5.1$ Hz, 2H, $H_1'/H_1''^*$), 3.77-3.70 (m, 1H, H_e), 3.67 (ddd, $J = 14.2, 5.9, 3.2$ Hz, 1H, H_2), 3.61 (ddd, $J = 15.1, 5.0, 5.0$ Hz, 1H, H_2'), 3.48 (ddd, $J = 14.2, 7.2, 3.4$ Hz, 1H, H_2^*), 3.45 (ddd, $J = 15.0, 5.1, 5.1$ Hz, 1H, $H_2'^*$), 2.34 (dd, $J = 15.1, 4.4$ Hz, 1H, H_a), 2.25 (dd, $J = 15.1, 9.3$ Hz, 1H, H_a^*), 1.94 (nfom, 1H, H_b), 1.74 (dsxtet, $J = 4.2, 6.8$ Hz, 1H, H_g), 1.51-1.44 (m, 1H, H_d), 1.43-1.29 (m, 3H, $H_c/H_c^*/H_d^*$), 1.17 (d, $J = 6.2$ Hz, 3H, H_f), 0.90 (d, $J = 6.8$ Hz, 3H, H_h), and 0.85 (d, $J = 6.8$ Hz, 3H, H_i).

^{13}C NMR (125 MHz, CDCl_3) δ 175.7, 68.7, 60.9, 60.8, 52.5, 50.7, 41.0, 37.4, 34.9, 30.2, 27.9, 23.7, 20.0, and 18.5.

IR (neat): 3550-3200, 2959, 2873, 1617, 1464, 1420, and 1054 cm^{-1} .

HRMS (ESI) (m/z): mass calc. for $[\text{C}_{14}\text{H}_{29}\text{NO}_4\text{Na}]^+$, 298.1989, found 298.1988.

Spectral data for 412b (monoamide monoester derived from *trans* carvomenthide)



$^1\text{H NMR}$ (500 MHz, CDCl_3) δ 4.33-4.2 (m, 1H, H₁), 4.2-4.10 (m, 1H, H₁*), 3.89-3.39 (m, 8H, H₁'/H₁'*/H₂/H₂*/H₂'/H₂'*/H_e/H_e'), 2.36 (dd, $J = 15.3, 4.8$ Hz, 1H, H_a), 2.34 (dd, $J = 15.4, 5.1$ Hz, 1H, H_a'), 2.24 (dd, $J = 15.2, 8.9$ Hz, 1H, H_a*), 2.12 (dd, $J = 15.3, 8.4$ Hz, 1H, H_a*), 1.95-1.88 (m, 1H, H_b), 1.80-1.69 (m, 3H, H_b'/H_g/H_g'), 1.51-1.3 (m, 4H, H_c/H_d/H_c'/H_d'), 1.19 (d, $J = 6.0$ Hz, 3H, H_f or f'/minor), 1.182 (d, $J = 6.2$ Hz, 3H, H_f or f'/major), 1.176 (d, $J = 6.2$ Hz, H_f or f'/major), 1.17 (d, $J = 6.1$ Hz, H_f or f'/minor), 0.92-0.82 (overlapping ds, 12H, H_h'/H_h/H_i'/H_i).

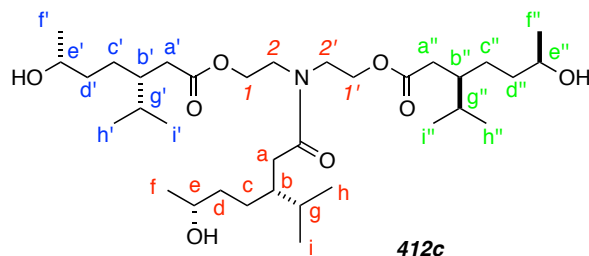
$^{13}\text{C NMR}$ the spectral data for this mixture of two (inequivalently populated) rotamers is sufficiently complex that it was difficult to determine with confidence the appropriate set of resonances; these values were reported as observed.

(125 MHz, CDCl_3) δ 175.6, 174.4, 174.2, 174.0, 68.74, 68.67, 68.4, 68.3, 62.6, 61.7, 61.5, 60.5, 51.2, 49.9, 48.2, 46.2, 41.10, 41.08, 40.6, 37.5, 37.2, 36.1, 36.0, 34.64, 34.57, 30.1, 30.0, 29.9, 29.8, 27.84, 27.75, 23.74, 23.71, 20.0, 19.9, 19.8, 18.7, 18.5, 18.3, and 18.2.

IR (neat): 3500-3300, 2960, 2874, 1734, 1623, 1462, 1370, 1275, 1162, 1113, and 1066 cm^{-1} .

HRMS (ESI) calc. for $[\text{C}_{14}\text{H}_{47}\text{NO}_6\text{Na}]^+$, 468.3296, found 468.3315.

Spectral data for 412c (monoamide bisester derived from *trans* carvomenthide)



$^1\text{H NMR}$ (500 MHz, CDCl_3) δ 4.29 (ddd, $J = 11.6, 6.8, 5.5$ Hz, 1H, H₁), 4.22 (t, $J = 5.6$ Hz, 2H, H₁'/H₁'*), 4.13 (ddd, $J = 11.6, 5.7, 5.7$ Hz, 1H, H₁*), 3.8-3.7 (m, 3H, H_e/H_e'/H_e'), 3.66-3.58 (m, 4H, H₂/H₂*/H₂'/H₂'), 2.35 (dd, $J = 15.7, 5.0$ Hz, 1H, H_a),

2.33 (dd, $J = 15.4, 5.1$ Hz, 1H, H_{a'}), 2.31 (dd, $J = 15.4, 5.4$ Hz, 1H, H_{a''}), 2.18 (dd, $J = 15.7, 8.3$ Hz, 1H, H_{a*}), 2.133 (dd, $J = 15.4, 7.8$ Hz, 1H, H_{a'*}), 2.129 (dd, $J = 15.4, 8.3$ Hz, 1H, H_{a''*}), 1.93-1.88 (m, 1H, H_b), 1.80-1.69 (m, 5H, H_{b'}/H_{b''}/H_g/H_{g'}/H_{g''}), 1.49-1.29 (m, 12H, H_c/H_{c*}/H_d/H_{d*}/H_{c'}/H_{c'*}/H_{d'}/H_{d'*}/H_{c''}/H_{c''*}/H_{d''}/H_{d''*}), 1.183 (d, $J = 6.2$ Hz, 3H, H_f), 1.181 (d, $J = 6.2$ Hz, 3H, H_{f'}), 1.17 (d, $J = 6.2$ Hz, 3H, H_f), 0.90 (d, $J = 6.8$ Hz, 3H, H_h), 0.881 (d, $J = 6.7$ Hz, 3H, H_{h'}), 0.878 (d, $J = 6.7$ Hz, 3H, H_{h''}), 0.86 (d, $J = 6.8$ Hz, 3H, H_i), 0.84 (d, $J = 6.6$ Hz, 3H, H_{i'}), and 0.83 (d, $J = 6.7$ Hz, 3H, H_{i''}).

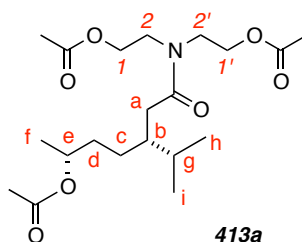
¹³C NMR (125 MHz, CDCl₃) δ 174.1, 173.99, 173.97, 68.7, 68.4, 68.3, 62.2, 61.6, 47.3, 45.6, 41.0, 40.5, 37.3, 36.1, 35.9, 34.5, 30.0, 29.9, 29.8, 27.81, 27.76, 27.6, 23.79, 23.77, 23.75, 23.7, 19.92, 19.86, 19.8, 18.7, 18.6, and 18.3.

IR (neat): 3550-3250, 2960, 2874, 1734, 1630, 1461, 1370, 1274, 1160, and 1115 cm⁻¹.

HRMS (ESI) mass calc. for [C₃₄H₆₅NO₈Na]⁺, 638.4602, found 638.4649.

Preparation of acetate derivatives S4a-c of model amide/esters S3a-c from *trans*-carvomenthide.

Spectral data for 413a (acetylated 412a)



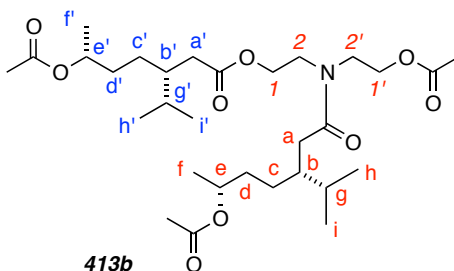
¹H NMR (500 MHz, CDCl₃) δ 4.85 (sextet, *J* = 6.3 Hz, 1H, H_e), 4.21 (t, *J* = 5.6 Hz, 2H, H1/H1*), 4.20 (t, *J* = 5.9 Hz, 2H, H1'/H1'*), 3.63 (t, *J* = 6.6 Hz, 2H, H2'/H2'*), 3.61, (t, *J* = 5.9 Hz, 2H, H2/H2*), 2.33 (dd, *J* = 15.6, 5.6 Hz, 1H, H_a), 2.14 (dd, *J* = 15.6, 7.5 Hz, 1H, H_a*), 2.08 (s, 3H, -C1O₂CCH₃), 2.06 (s, 3H, -C1'O₂CCH₃), 2.02 [s, 3H, -R₂C(H)O₂CCH₃], 1.95-1.88 (m, 1H, H_b), 1.75 (dsept, *J* = 6.9, 4 Hz, 1H, H_g), 1.57 (dddd, *J* = 13.4, 11.0, 7.2, 5.3 Hz, 1H, H_d), 1.49 (dddd, *J* = 13.4, 10.9, 5.4, 5.4 Hz, 1H, H_d*), 1.34-1.2 (m, 2H, H_c/H_c*), 1.20 (d, *J* = 6.2 Hz, 3H, H_f), 0.87 (d, *J* = 6.9 Hz, 3H, H_h), and 0.85 (d, *J* = 6.9 Hz, 3H, H_i).

¹³C NMR (125 MHz, CDCl₃) δ 173.5, 170.99, 170.98, 170.9, 71.4, 62.4, 62.1, 47.5, 45.9, 40.2, 34.3, 33.9, 29.8, 27.0, 21.6, 21.1, 21.0, 20.1, 19.6, and 18.8.

IR (neat): 2958, 2873, 1734, 1622, 1461, 1419, 1251, 1163, 1058, and 1029 cm⁻¹.

HRMS (ESI) mass calc. for [C₂₀H₃₅NO₇Na]⁺, 424.2306, found 424.2260.

Spectral data for 413b (acetylated 412b)



¹H NMR (500 MHz, CDCl₃) δ 4.858 (app sextet, *J* = 6.2 Hz, 1H, H_e or H_e'), 4.856 (app sextet, *J* = 6.2 Hz, 1H, H_e or H_e'), 4.22-4.17 (m, 4H, H1/H1*/H1'/H1'*), 3.66-3.56 (m, 4H, H2/H2*/H2'/H2'*), 2.33 (dd, *J* = 15.4, 5.5 Hz, 0.5H, H_a), 2.32 (dd, *J* = 15.4, 5 Hz, 0.5H, H_a), 2.31 (dd, *J* = 15.6, 6.1 Hz, 0.5H, H_a'), 2.29 (dd, *J* = 15.4, 6.1 Hz, 0.5H, H_a'),

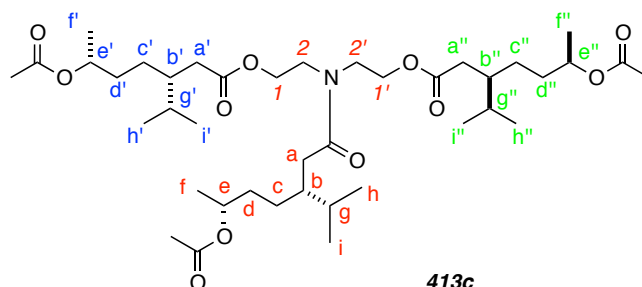
2.15 (two dds, $J = 15.7, 7.1$ Hz, 1H, H_{a^*}), 2.14 (dd, $J = 15.4, 7.3$ Hz, 0.5H, $H_{a'^*}$), 2.13 (dd, $J = 15.5, 7.0$ Hz, 0.5H, $H_{a''^*}$), 2.08 (s, 1.5H, $-C1'O_2CCH_3$), 2.06 (s, 1.5H, $-C1'O_2CCH_3$), 2.025 (s, 3H, $-C_e$ or e' - O_2CCH_3), 2.019 (s, 3H, $-C_e$ or e' - O_2CCH_3), 1.94-1.87 (m, 1H, H_b), 1.79-1.67 (m, 3H, $H_b'/H_g/H_g'$), 1.62-1.53 (m, 2H, H_d/H_d'), 1.53-1.43 (m, 2H, $H_d^*/H_d'^*$), 1.37-1.2 (m, 4H, $H_c/H_c^*/H_c'/H_c'^*$), 1.20 (br d, $J = 6.3$ Hz, 6H, H_f/H_f'), 0.876 (d, $J = 6.6$ Hz, 1.5H, H_i or i' of h or h'), 0.871 (d, $J = 6.9$ Hz, 1.5H, H_i or i' of h or h'), 0.865 (d, $J = 6.6$ Hz, 1.5H, H_i or i' of h or h'), 0.863 (d, $J = 6.6$ Hz, 1.5H, H_i or i' of h or h'), 0.850 (d, $J = 6.6$ Hz, 3H, H_i or i' of h or h'), and 0.833 (d, $J = 7.0$ Hz, 3H, H_i or i' of h or h').

^{13}C NMR (125 MHz, $CDCl_3$) δ 173.53, 173.46, 173.2, 170.7, 71.18, 71.16, 71.0, 70.9, 62.2, 62.1, 61.9, 61.8, 47.34, 47.31, 47.28, 47.26, 45.7, 45.6, 40.5, 40.4, 40.1, 39.9, 35.84, 35.84, 35.76, 34.24, 34.19, 33.8, 33.7, 33.48, 33.46, 29.7, 29.61, 29.58, 26.80, 26.76, 26.7, 26.6, 21.8, 21.39, 21.38, 20.9, 20.81, 20.78, 20.75, 20.3, 20.25, 19.99, 19.96, 19.94, 19.92, 19.43, 19.37, 19.32, 19.27, 19.25, 18.81, 18.78, 18.64, 18.6, 18.5, 18.44, and 18.43.

IR (neat): 2957, 2873, 1734, 1649, 1460, 1371, 1242, 1164, 1131, and 1050 cm^{-1} .

HRMS (ESI) mass calc. for $[C_{30}H_{53}NO_9Na]^+$, 594.3613, found 594.3639.

Spectral data for 413c (acetylated 412c)



1H NMR (500 MHz, $CDCl_3$) δ 4.86 (sextet, $J = 6.2$ Hz, 3H, $H_e/H_e'/H_e''$), 4.24-4.15 (m, 4H, $H1/H1^*/H1'/H1'^*$), 3.67-3.57 (m, 4H, $H2/H2^*/H2'/H2'^*$), 2.34 (dd, $J = 15.5, 5.7$ Hz, 1H, H_a), 2.31 (dd, $J = 15.3, 5.9$ Hz, 1H, $H_{a'}$), 2.28 (dd, $J = 15.4, 6.1$ Hz, 1H, $H_{a''}$), 2.15 (dd, $J = 15.4, 6.9$ Hz, 1H, H_{a^*}), 2.14 (dd, $J = 15.5, 7.4$ Hz, 1H, $H_{a'^*}$), 2.13 (dd, $J = 15.5, 7.2$ Hz, 1H, $H_{a''^*}$), 2.025 (s, 3H, $-O_2CCH_3$), 2.024 (s, 3H, $-O_2CCH_3$), 2.02 (s, 3H, $-O_2CCH_3$), 1.94-1.87 (nfom, 1H, H_b), 1.80-1.66 (m, 5H, $H_g/H_b'/H_b''/H_g'/H_g''$), 1.62-1.53 (m, 3H, $H_d/H_d'/H_d''$), 1.52-1.43 (m, 3H, $H_d^*/H_d'^*/H_d''^*$), 1.37-1.20 (m, 6H, $H_c/H_c'/H_c''/H_c^*/H_c'^*/H_c''^*$), 1.206 (d, $J = 6.3$ Hz, 6H, H_f/H_f'), 1.204 (d, $J = 6.3$ Hz, 3H,

H_f), 0.874 (d, $J = 6.7$ Hz, 3H, H_g), 0.863 (d, $J = 6.4$ Hz, 3H, H_{g'}), 0.862 (d, $J = 6.3$ Hz, 3H, H_{g''}), 0.850 (d, $J = 6.7$ Hz, 3H, H_h), 0.833 (d, $J = 6.7$ Hz, 3H, H_{h'}), and 0.832 (d, $J = 6.7$ Hz, 3H, H_{h''}).

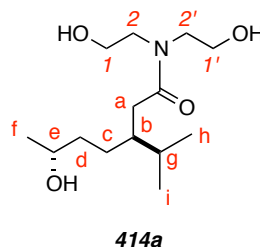
¹³C NMR (125 MHz, CDCl₃) δ 173.7, 173.6, 173.4, 170.94, 170.91, 71.4, 71.2, 71.1, 62.3, 62.0, 47.5, 45.8, 40.7, 40.6, 40.2, 36.0, 35.9, 34.4, 33.9, 33.7, 33.6, 30.0, 29.9, 29.8, 26.94, 26.87, 26.83, 21.60, 21.58, 20.2, 20.1, 19.7, 19.6, 19.5, 18.8, 18.7, and 18.66.

IR (neat): 2958, 2874, 1734, 1650, 1461, 1371, 1244, 1163, 1132, and 1021 cm⁻¹.

HRMS (ESI) mass calc. for [C₄₀H₇₁NO₁₁Na]⁺, 764.4919, found 764.4958.

Preparation of model amide esters 414a-c derived from diethanolamine (7) and *cis*-carvomenthide (*cis*-405).

Spectral data for 414a (monoamide derived from *cis* carvomenthide)



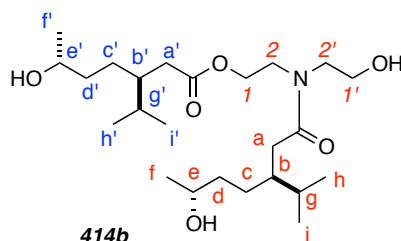
¹H NMR (500 MHz, CDCl₃) δ 3.92 (ddd, *J* = 11.0, 7.3, 3.3 Hz, 1H, H₁), 3.89-3.84 (m, 1H, H_e), 3.81 (ddd, *J* = 11.0, 6.0, 3.5 Hz, 1H, H₁*), 3.79 (t, *J* = 5.1 Hz, 2H, H₁'/H₁'*), 3.67 (ddd, *J* = 14.4, 6.1, 3.3 Hz, 1H, H₂), 3.62 (ddd, *J* = 15.1, 5.2, 5.2 Hz, 1H, H₂'), 3.46 (ddd, *J* = 14.2, 7.3, 3.4 Hz, 1H, H₂*), 3.42 (ddd, *J* = 15.1, 5.0, 5.0 Hz, 1H, H₂'*), 2.35 (dd, *J* = 15.5, 3.8 Hz, 1H, H_a), 2.26 (dd, *J* = 15.5, 9.9 Hz, 1H, H_a*), 1.99-1.93 (m, 1H, H_b), 1.72 (dsept, *J* = 4.3, 6.8 Hz, 1H, H_g), 1.50-1.34 (m, 4H, H_c/H_c*/H_d/H_d*), 1.17 (d, *J* = 7.3 Hz, 3H, H_f), 0.91 (d, *J* = 6.9 Hz, 3H, H_h), and 0.85 (d, *J* = 6.8 Hz, 3H, H_i).

¹³C NMR (125 MHz, CDCl₃) δ 175.7, 66.9, 60.8, 60.7, 52.4, 50.6, 39.2, 36.0, 34.5, 29.6, 26.9, 23.2, 20.5, and 18.4.

IR (neat): 3530-3100, 2959, 1617, 1464, 1421, 1368, 1128, and 1055 cm⁻¹.

HRMS (ESI) mass calc. for [C₁₄H₂₉NO₄Na]⁺ 298.1989, found 298.1996.

Spectral data for 414b (monoamide monoester derived from *cis*-carvomenthide)



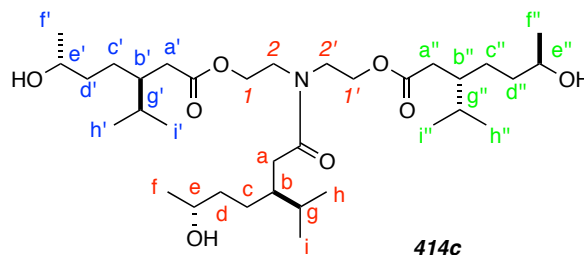
¹H NMR (500 MHz, CDCl₃) δ 4.34-4.10 (m, 2H, H₁/H₁*), 3.91-3.84 (m, 1H, H₂), 3.82-3.43 (m, 7H, H₁'/H₁'*/H₂*/H₂'*/H₂'*/H₂'*/H_c/H_c'), 2.37 (dd, *J* = 15.5, 4.0 Hz, 1H, H_a), 2.35 (dd, *J* = 15.5, 4.9 Hz, 1H, H_a'), 2.22 (dd, *J* = 15.5, 9.6 Hz, 1H, H_a*), 2.12 (dd, *J* = 15.3, 9.1 Hz, 1H, H_a*'), 1.97-1.91 (m, 1H, H_b), 1.81-1.68 (m, 3H, H_b/H_g/H_g'), 1.49-1.21 (m, 8H, H_c/H_c*/H_d/H_d*/H_c'/H_c'*/H_d'/H_d'*), 1.178 (d, *J* = 6.2 Hz, 3H, H_f or H_f'), 1.176 (d, *J* = 6.2

Hz, 3H, H_f or H_{f'}), 0.888 (d, $J = 6.8$ Hz, 3H, H_h or H_{h'}), 0.886 (d, $J = 6.9$ Hz, 3H, H_h or H_{h'}), 0.86 (d, $J = 6.9$ Hz, 3H, H_i or H_{i'}), and 0.83 (d, $J = 6.8$ Hz, 3H, H_i or H_{i'}).

IR (neat): 3580-3200, 2960, 1734, 1623, 1462, 1370, 1161, 1111, and 1066 cm⁻¹.

HRMS (ESI) mass calc. for [C₁₄H₁₇NO₆Na]⁺ 468.3296, found 468.3294.

Spectral data for 414c (monoamide bisester derived from *cis*-carvomenthide)



¹H NMR (500 MHz, CDCl₃) δ 4.32-4.10 (m 4H, H₁/H₁*/H₁'/H₁'*), 3.91-3.84 (m, 1H, H_e), 3.82-3.49 (m, 6H, H₂/H₂*/H₂'/H₂'*/H_e*/H_e''), 2.343 (dd, $J = 15.3, 5.1$ Hz, 1H, H_a), 2.338 (dd, $J = 15.5, 4.6$ Hz, 1H, H_a'), 2.31 (dd, $J = 15.1, 5.1$ Hz, 1H, H_a''), 2.16 (dd, $J = 15.9, 8.4$ Hz, 1H, H_a*), 2.13 (dd, $J = 15.5, 8.4$ Hz, 1H, H_a*), 2.10 (dd, $J = 15.2, 8.4$ Hz, 1H, H_a''), 1.95 (dddd, $J = 8.4, 8.4, 4.2, 4.2, 4.2$ Hz, 1H, H_b), 1.80-1.69 (m, 5H, H_b*/H_b'*/H_g*/H_g'*/H_g''), 1.49-1.22 (m, 12H, H_c*/H_c'*/H_d*/H_d'*/H_c'*/H_c'*/H_d'*/H_d'*/H_c'*/H_c'*/H_d'*/H_d'*), 1.182 (d, $J = 6.2$ Hz, 6H, two of H_f*/H_f'*/H_f''), 1.176 (d, $J = 6.2$ Hz, 3H, one of H_f*/H_f'*/H_f''), 0.92 (d, $J = 6.8$ Hz, 3H, H_h) 0.885 (d, $J = 6.7$ Hz, 3H, H_h'), 0.881 (d, $J = 6.8$ Hz, 3H, H_h''), 0.85 (d, $J = 6.8$ Hz, 3H, H_i, H_i' or H_i''), 0.84 (d, $J = 6.5$ Hz, 3H, H_i, H_i' or H_i''), and 0.82 (d, $J = 6.2$ Hz, 3H, H_i, H_i' or H_i'').

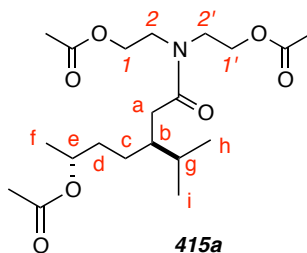
IR (neat): 3600-3300, 2960, 1735, 1631, 1461, 1370, 1275, 1159, 1113, and 1070 cm⁻¹.

HRMS (ESI) mass calc. for [C₃₄H₆₅NO₈Na]⁺ 638.4602, found 638.4648.

Acetate derivatives S2a-c of model amide esters S1a-c from *cis*-carvomenthide.

These tris-acetate derivatives were prepared in analogous manner to the acetates **11a-c**, as described directly above.

Spectral data for **415a** (acetylated **414a**)



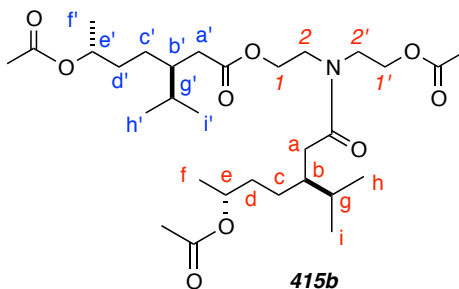
$^1\text{H NMR}$ (500 MHz, CDCl_3) δ 4.84 (sextet, $J = 6.3$ Hz, 1H, H_e), 4.22 (t, $J = 5.6$ Hz, 2H, H_1/H_1^*), 4.20 (t, $J = 5.9$ Hz, 2H, $\text{H}_1'/\text{H}_1'^*$), 3.65-3.55 (4 overlapping dts, 4H, $\text{H}_2/\text{H}_2^*/\text{H}_2'/\text{H}_2'^*$), 2.32 (dd, $J = 15.6, 5.5$ Hz, 1H, H_a), 2.15 (dd, $J = 15.6, 7.7$ Hz, 1H, H_a^*), 2.08 (s, 3H, $-\text{O}_2\text{CCH}_3$), 2.06 (s, 3H, $-\text{O}_2\text{CCH}_3$), 2.02 (s, 3H, $-\text{O}_2\text{CCH}_3$), 1.91 (dddd, $J = 6.8, 6.8, 6.8, 5.5, 3.8$ Hz, 1H, H_b), 1.76 (dq, $J = 4.0, 6.8, 6.8$ Hz, 1H, H_g), 1.60 (dddd, $J = 13.5, 11.8, 7.3, 4.8$, 1H, H_d), 1.48 (dddd, $J = 13.7, 11.0, 5.3, 5.3$ Hz, 1H, H_d^*), 1.34 (dddd, $J = 13.4, 11.1, 6.4, 4.7$ Hz 1H, H_c), 1.20 (dddd, $J = 13.4, 11.7, 6.5, 5.1$ Hz, 1H, H_c^*), 1.20 (d, $J = 6.3$ Hz, 3H, H_f), 0.88 (d, $J = 6.9$ Hz, 3H, H_h), and 0.85 (d, $J = 6.8$ Hz, 3H, H_i).

$^{13}\text{C NMR}$ (125 MHz, CDCl_3) δ 173.4, 170.99, 170.98, 170.8, 71.5, 62.5, 62.1, 47.5, 45.1, 40.3, 34.3, 34.0, 29.6, 27.2, 21.6, 21.1, 21.0, 20.2, 19.6, and 18.7.

IR (neat): 2957, 1738, 1648, 1371, 1236, and 1047 cm^{-1} .

HRMS (ESI) mass calc. for $[\text{C}_{20}\text{H}_{35}\text{NO}_7\text{Na}]^+$ 424.2306, found 424.2308.

Spectral data for **415b** (acetylated **414b**)



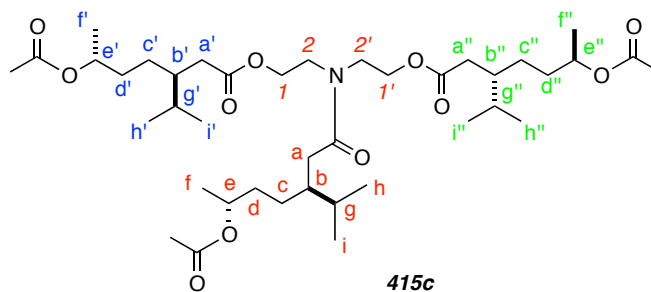
¹H NMR (500 MHz, CDCl₃) δ 4.85 (sextet, *J* = 6.1 Hz, 1H, H_e), 4.84 (sextet, *J* = 6.2 Hz, 1H, H_{e'}), 4.14-4.21 (m, 4H, H1/H1*/H1'/H1'*), 3.68-3.53 (m, 4H, H2/H2*/H2'/H2'*), 2.31 (dd, *J* = 15.2, 5.8 Hz, 1H, H_a), 2.29 (dd, *J* = 15.6, 6.2 Hz, 1H, H_{a'}), 2.16 (dd, *J* = 15.0, 7.7 Hz, 1H, H_{a*}), 2.15 (dd, *J* = 15.3, 7.8 Hz, 1H, H_{a''*}), 2.09 (s, 3H, -O₂CCH₃), 2.03 (s, 3H, -O₂CCH₃), 2.02 (s, 3H, -O₂CCH₃), 1.95-1.87 (m, 1H, H_b), 1.65-1.53 (m, 2H, H_d/H_{d'}), 1.52-1.43 (m, 2H, H_{d*}/H_{d''*}), 1.40-1.31 (m, 2H, H_c/H_{c'}), 1.25-1.15 (m, 2H, H_{c*}/H_{c''*}), 1.204 (d, *J* = 6.2 Hz, 3H, H_f), 1.20 (d, *J* = 6.2 Hz, 3H, H_{f'}), 0.87 (d, *J* = 6.8 Hz, 3H, H_h), 0.86 (d, *J* = 6.6 Hz, 3H, H_{h'}), 0.85 (d, *J* = 6.8 Hz, 3H, H_i), and 0.83 (d, *J* = 6.7 Hz, 3H, H_{i'}).

¹³C NMR (125 MHz, CDCl₃) δ 173.74, 173.65, 173.5, 173.4, 171.0, 170.98, 170.96, 170.8, 71.48, 71.46, 71.3, 71.2, 62.4, 62.3, 62.1, 62.0, 47.51, 47.50, 45.9, 45.8, 40.72, 40.70, 40.4, 40.3, 35.9, 35.8, 34.33, 34.27, 34.0, 33.8, 33.7, 29.7, 29.63, 29.60, 27.13, 27.08, 26.98, 26.97, 26.90, 21.58, 21.57, 21.1, 21.0, 20.8, 20.1, 19.73, 19.70, 19.64, 19.60, 19.58, 18.7, 18.6, and 18.5.

IR (neat): 2958, 1734, 1649, 1371, 1243, 1050, and 753 cm⁻¹.

HRMS (ESI) mass calc. for [C₃₀H₅₃NO₉Na]⁺ 594.3613, found 594.3626.

Spectral data for 415c (acetylated 414c)

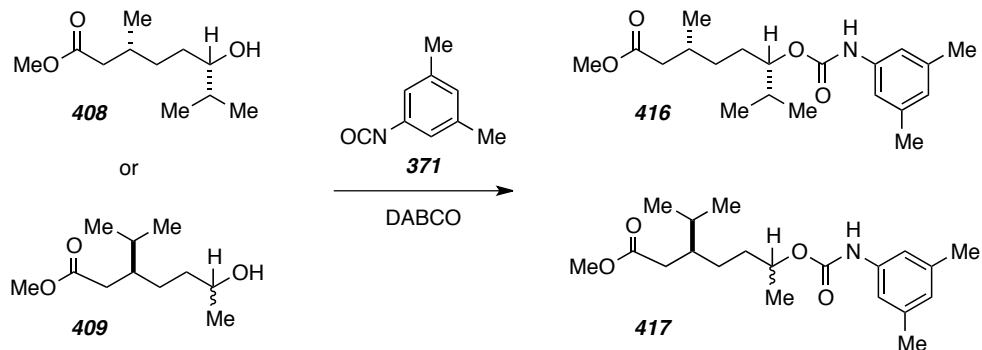


¹H NMR (500 MHz, CDCl₃) δ 4.85 [sextets, *J* = 6.0 Hz, 3H, H_e/H_{e'}/H_{e''}], 4.23-4.15 (m, 4H, H1/H1*/H1'/H1'*), 3.68-3.57 (m, 4H, H2/H2*/H2'/H2'*), 2.36-2.26 (3H, H_a/H_{a'}/H_{a''}), 2.17-2.1 (3H, H_{a*}/H_{a''*}/H_{a'''*}), 2.03 (s, 6H, -COCH₃), 2.02 (s, 3H, -COCH₃), 1.93-1.87 (m, 1H, H_b), 1.78-1.68 (m, 5H, H_b'/H_b''/H_g/H_g'/H_g''), 1.63-1.54 (m, 3H, H_d/H_d'/H_d''), 1.51-1.43 (m, 3H, H_{d*}/H_d'*/H_d''*), 1.41-1.31 (m, 3H, H_c/H_c'/H_c''), 1.29-1.14 (m, 3H, H_{c*}/H_c'*/H_c''*), 1.204 (d, *J* = 6.3 Hz, 6H, H_f/H_f''), 1.20 (d, *J* = 6.3 Hz, 3H, H_f'),

0.88 (d, $J = 6.8$ Hz, 3H, H_h), 0.86 (d, $J = 6.6$ Hz, 6H, H_{h'}/H_{h''}), 0.85 (d, $J = 6.7$ Hz, 3H, H_i), 0.833 (d, $J = 6.7$ Hz, 3H, H_{i'}), and 0.831 (d, $J = 6.7$ Hz, 3H, H_{i''}).

IR (neat): 2958, 1734, 1651, 1461, 1371, 1244, 1164, and 1022 cm⁻¹.

HRMS (ESI) mass calc. for [C₄₀H₇₁NO₁₁Na]⁺ 764.4919, found 764.4951.



(3R,6S)-methyl 6-(((3,5-dimethylphenyl)carbamoyl)oxy)-3,7-dimethyloctanoate (416). Alcohol **408** (30 mg, 0.15 mmol) was dissolved in CDCl_3 (0.6 mL). A wiretrol contained approx. 2 mg DABCO was applied to the side wall of the culture tube, followed by the isocyanate (**371**, 11 mg, 0.075 mmol), dispensed through wiretrol. The reaction stirred at rt for 1 hour and was monitored by NMR and TLC. Concentration by rotary evaporation and application to MPLC (4:1 Hex:EtOAc) afforded the carbamate **416** in 50% yield.

$^1\text{H NMR}$ (500 MHz, CDCl_3): δ 7.04 (s, 2H), 6.70 (s, 1H), 6.53 (br s, 1H), 4.68 (ddd, $J = 8.0, 5.4, 4.2$ Hz, 1H), 3.65 (s, 3H), 2.32 (dd, $J = 14.7, 5.8$ Hz, 1H), 2.29 (s, 6H), 2.11 (dd, $J = 14.7, 8.2$ Hz, 1H), 2.02-1.81 (m, 2H), 1.66-1.34 (m, 3H), 1.30-1.15 (m, 1H), 0.95 (d, $J = 6.6$ Hz, 3H), 0.933 (d, $J = 6.8$ Hz, 3H), and 0.929 (d, $J = 6.8$ Hz, 3H).

[seVpg206mnf2]

LCMS (Method C): $T_R = 4.5$ min, m/z "pos" = 350.0 ($M+1$)⁺, 367.3 ($M+18$)⁺, m/z "neg" = 348.3 ($M-1$)⁻.

TLC (4:1 Hex:EtOAc): $R_f = 0.2$

(3S)-methyl 6-(((3,5-dimethylphenyl)carbamoyl)oxy)-3-isopropylheptanoate (417).

Identical conditions were applied for the preparation of the carbamate **417**. The same purification method was used, and the yield was improved to ca. 60-70 % in this case.

$^1\text{H NMR}$ (500 MHz, CDCl_3): δ 7.00 (s, 2H), 6.70 (s, 1H), 6.54 (br s, 1H), 4.86 (sextet, $J = 6.2$ Hz, 1H), 3.66 (s, 3H), 2.31 (dd, $J = 15.1, 6.1$ Hz, 1H), 2.29 (s, 6H), 2.15 (dd, $J =$

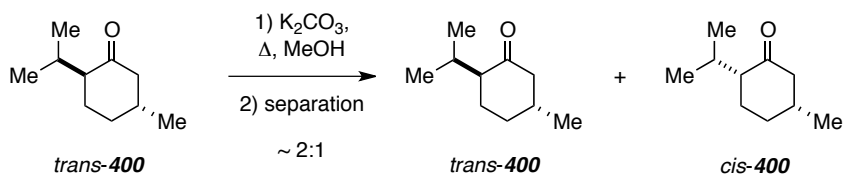
15.1, 7.4 Hz, 1H), 1.86-1.23 (m, 6H), 1.27 (d, $J = 6.3$ Hz, 3H), 0.87 (d, $J = 6.7$ Hz, 1H), and 0.84 (d, $J = 6.7$ Hz, 3H). [seVpg206cmf1]

LCMS (Method C): $T_R = 4.6$ min, m/z "pos" = 350.3 ($M+1$)⁺, 367.3 ($M+18$)⁺, m/z "neg" = 348.3 ($M-1$)⁻, 408.0 ($M+59$)⁻.

TLC (4:1 Hex:EtOAc): $R_f = 0.2$

Chapter VI.B. covers the extensive characterization efforts for both isomers of menthones **400**, carvomenthones **404**, menthides **401**, carvomenthides **405**, and abnormal carvomenthides **406**.

Characterization data for menthone is contained first, followed by carvomenthone.



***trans*-400 and *cis*-400.**

A commercial sample of menthone (10g) was weighed into a culture tube, followed by 1 g of K_2CO_3 . The suspension was homogenized by addition of 20 mL MeOH. The tube was sealed and heated to reflux for 4 hours, at which time NMR indicated a 2:1 ratio *trans*:*cis*-400. The reaction mixture was cooled to room temperature, and concentrated to a slurry of salt and ketone products. This mixture was washed with hexanes and the filtered through a pad of silica gel. The hexane washes were concentrated under reduced pressure to the crude ketones, which could be separated by MPLC (20:1 Hex:EtOAc) to afford 6 grams *trans*-400 and 2 grams *cis*-400. Mixed fractions were resubjected to the chromatography conditions for higher recovery of each isomer.

***trans*-400**

¹H NMR (500 MHz, $CDCl_3$) and ¹³C NMR (125 MHz, $CDCl_3$) data are contained in Table III-1.

IR (neat): 2955, 2871, 1710, 1456, and 1202 cm^{-1} .

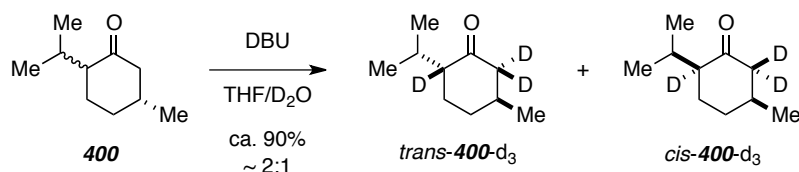
HRMS (ESI) mass calc. for $[\text{C}_{10}\text{H}_{18}\text{ONa}]^+$, 177.1250, found 177.1253.

***cis*-400**

^1H NMR (500 MHz, CDCl_3) and ^{13}C NMR (125 MHz, CDCl_3) data are contained in Table III-2.

IR (neat): 2957, 2871, 1708, 1457, and 1274 cm^{-1} .

HRMS (ESI) mass calc. for $[\text{C}_{10}\text{H}_{18}\text{ONa}]^+$, 177.1250, found 177.1265.



***trans*-400-d₃ and *cis*-400-d₃**

A mixture of *cis* and *trans* menthone (**400**, approximately 1:1) was treated with DBU and heated in THF/ D_2O for a few hours, when NMR indicated that approximately 90% of the starting material had been thrice deuterated and isomerized to a 2:1 ratio of *trans* to *cis*-**400-d₃**. These were separated by MPLC as described for the parent *trans* and *cis*-**400**.

Mass measurements were taken independently to confirm the presence of three D in each ketone:

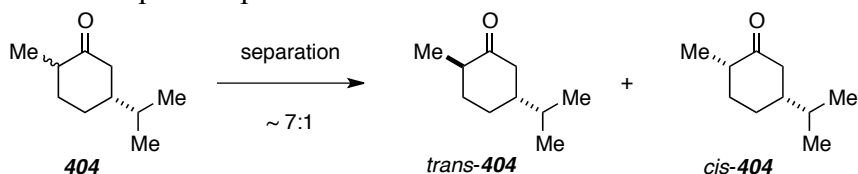
***trans*-400-d₃**

Exact mass calc. for $[\text{C}_{10}\text{H}_{15}\text{D}_3\text{ONa}]^+$, 180.1438, found 180.1451.

***cis*-400-d₃**

Exact mass calc. for $[\text{C}_{10}\text{H}_{15}\text{D}_3\text{ONa}]^+$, 180.1438, found 180.1439.

Carvomenthone was used as received from Senthil (from reduction of **403**) but the stereoisomers were separated prior to characterization and deuterium studies.



Separation of *trans* and *cis*-**404** was performed in the same way as **400** but required selective collection of peaks and iterative chromatographies of mixed samples.

***trans*-404**

$^1\text{H NMR}$ (500 MHz, CDCl_3) and $^{13}\text{C NMR}$ (125 MHz, CDCl_3) data are contained in Table III-3.

IR (neat): 2961, 2872, 1711, 1455, 1370, and 1221 cm^{-1} .

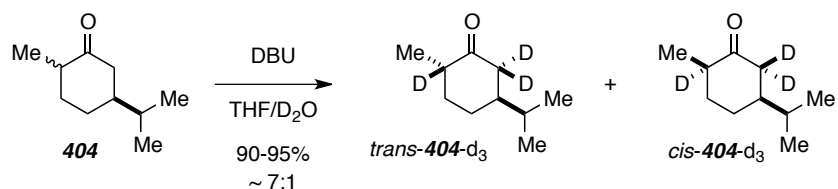
HRMS (ESI) mass calc. for $[\text{C}_{10}\text{H}_{18}\text{ONa}]^+$, 177.1250, found 177.1254.

***cis*-404**

$^1\text{H NMR}$ (500 MHz, CDCl_3) and $^{13}\text{C NMR}$ (125 MHz, CDCl_3) data are contained in Table III-4.

IR (neat): 2962, 2871, 1710, 1456, and 1218 cm^{-1} .

HRMS (ESI) mass calc. for $[\text{C}_{10}\text{H}_{18}\text{ONa}]^+$, 177.1250, found 177.1231.



***trans*-404-d₃ and *cis*-404-d₃**

A mixture of *trans* and *cis*-**404** (approximately 10:1) was deuterated in an analogous way as **400**. Again, ca. 90% D incorporation of the starting material was observed and isomerized to a 7:1 ratio of *trans* to *cis*-**400-d₃**. These were separated by MPLC as described for the parent *trans* and *cis*-**404**.

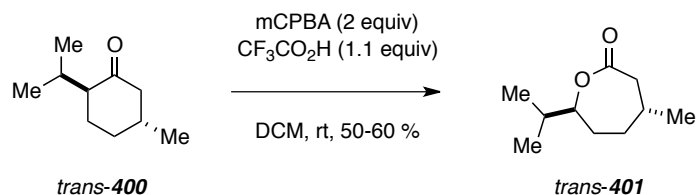
Mass measurements were taken independently to confirm the presence of three deuterium in each ketone:

***trans*-404-d₃**

Exact mass calc. for $[\text{C}_{10}\text{H}_{15}\text{D}_3\text{ONa}]^+$, 180.1438, found 180.1452.

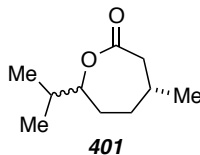
***cis*-404-d₃**

Exact mass calc. for $[\text{C}_{10}\text{H}_{15}\text{D}_3\text{ONa}]^+$, 180.1438, found 180.1452.



Trans and *cis*-**401** and *trans* and *cis*-**405** were all prepared in the same fashion as described (for *trans*-**401**) below.

To a stirred solution of (–)-menthone (*trans*-**400**, 1 equiv) and TFA (1 equiv) in CH_2Cl_2 (for reaction 0.2 M) was added 3-chloroperoxybenzoic acid (77% wt %, 2 equiv) at rt in small portions over a period of 10 min. After the addition, the reaction mixture was stirred for 1 h. The progress of the reaction was monitored by TLC. The slurry was filtered and the filtrate cooled to 0 °C to give an additional amount of precipitate, which were removed via a second filtration. The resulting filtrate was washed with aqueous sodium bisulfite (saturated), saturated sodium bicarbonate, and saturated sodium chloride solution. The combined organic layers were dried over sodium sulfate and the solvent was removed via rotary evaporation. The resulting crude compound was purified by MPLC (12:1 Hex:EtOAc) to afford (–)-menthide (and corresponding lactones *cis*-**401**, **405**, and **406**). Isolated yields 50-80% (77%) as a colorless oil. *Cis*-**401** was prepared in an identical fashion.



Data for *trans*-**401**

$^1\text{H NMR}$ (500 MHz, CDCl_3) and $^{13}\text{C NMR}$ (125 MHz, CDCl_3) data are contained in Table III-5.

IR (neat): 2961, 2930, 1726, 1279, 1226, 1106, 1049, and 1019 cm^{-1} .

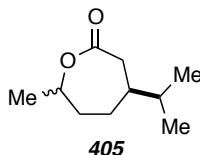
HRMS (ESI) mass calc. for $[\text{C}_{10}\text{H}_{18}\text{O}_2\text{Na}]^+$ 193.1199, found 193.1197.

Data for *cis*-**401**

$^1\text{H NMR}$ (500 MHz, CDCl_3) and $^{13}\text{C NMR}$ (125 MHz, CDCl_3) data are contained in Table III-6.

IR (neat): 2963, 2934, 1728, 1267, 1166, and 1031 cm^{-1} .

HRMS (ESI) mass calc. for $[\text{C}_{10}\text{H}_{18}\text{O}_2\text{Na}]^+$ 193.1199, found 193.1201.



Data for *trans*-**405**

$^1\text{H NMR}$ (500 MHz, CDCl_3) and $^{13}\text{C NMR}$ (125 MHz, CDCl_3) data are contained in Table III-7.

IR (neat): 2960, 2934, 1727, 1279, 1251, 1170, 1044 cm^{-1} .

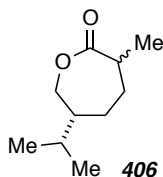
HRMS (ESI) mass calc. for $[\text{C}_{10}\text{H}_{18}\text{O}_2\text{Na}]^+$ 193.1199, found 193.1198

Data for *cis*-**406**

$^1\text{H NMR}$ (500 MHz, CDCl_3) and $^{13}\text{C NMR}$ (125 MHz, CDCl_3) data are contained in Table III-8

IR (neat): 2957, 2934, 1726, 1279, 1253, 1182, and 1047 cm^{-1} .

HRMS (ESI) mass calc. for $[\text{C}_{10}\text{H}_{18}\text{O}_2\text{Na}]^+$ 193.1199, found 193.1201.



Trans and *cis*-**406** were byproducts from the preparation of **405**. They were obtained as 3-5% of the total recovered lactone and separated from **405**, by careful chromatography (16:1 Hex:EtOAc) and analyzed separately.

Data for *trans*-**406**

¹H NMR (500 MHz, CDCl₃) and **¹³C NMR** (125 MHz, CDCl₃) data are contained in Table III-9

IR (neat): 2961, 2934, 1730, 1274, 1182, 1092, and 1028 cm⁻¹.

HRMS (ESI) mass calc. for [C₁₀H₁₈O₂Na]⁺ 193.1199, found 193.1196.

Data for *cis*-**406**

¹H NMR (500 MHz, CDCl₃) and **¹³C NMR** (125 MHz, CDCl₃) data are contained in Table III-10.

IR (neat): 2951, 2921, 1725, 1461, 1272, 1254, and 1175 cm⁻¹.

HRMS (ESI) mass calc. for [C₁₀H₁₈O₂Na]⁺ 193.1199, found 193.1209.

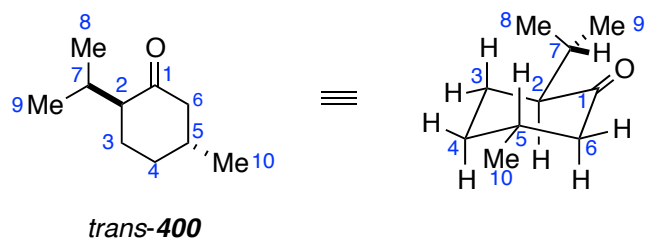


Table III-1: ^{13}C and ^1H NMR Data for Menthone (*trans-400*) (CDCl_3 , 125 and 500 MHz).

Atom number ¹	Carbon		Proton		COSY (to $^1\text{H}\#$) ²
	δ_{C}	δ_{H}	mult	J [Hz]	
1	212.2				
2	56.0	2.09-2.01 m			H3 α , H3 β , H7
3 β	28.0	2.09-2.01 m			H3 α , H4 β , H2, H4 α
3 α	28.0	1.43-1.31 m			H3 β , H2, H4 β , H4 α
4 β	34.1	1.43-1.31 m			H4 α , H3 α , H3 β , H5
4 α	34.1	1.92-1.88 nform ³			H4 β , H5, H3 α , H3 β , H3 α , H6 α
5	35.6	1.91-1.80 nform ³			H6 α (weak), H6 β , Me10, H4 β , H4 α
6 β	51.0	1.99 t		12.7	H6 α , H5
6 α	51.0	2.35 ddd		12.9, 4.0, 2.3	H6 β , H5, H4 α
7	26.1	2.14 dsept		6.8, 5.2	Me8, Me9, H2
Me8	21.3	0.91 d		6.8	H7
Me9	18.8	0.85 d		6.8	H7
Me10	22.3	1.01 d		6.4	H5

¹ α (= *trans*), β (= *cis*) are given relative to the Me10 group

² correlations into multiplets are given to the expected proton.

³ non first-order multiplet.

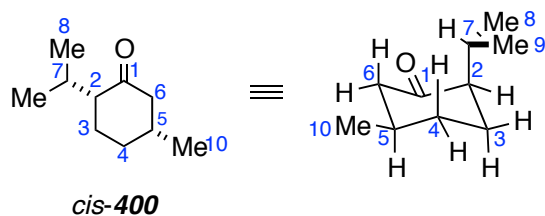


Table III-2: ^{13}C and ^1H NMR Data for Isomenthone (*cis-400*) (CDCl_3 , 125 and 500 MHz).

Atom number ¹	Carbon		Proton		COSY (to $^1\text{H}\#$) ²
	δ_{C}	δ_{H}	mult	J [Hz]	
1	214.4				
2	57.3	2.07-1.91 m			H7, H6 α , H3 β , H3 α
3 β	26.9	2.07-1.91 m			H3 α , H4 α , H4 β , H2
3 α	26.9	1.77-1.66 m			H3 β , 4H α , H4 β , H2
4 β	29.6	1.48	dddd	14.0, 11.2, 9.3, 4.2 ³	H4 α , H5, H3 β , H3 α
4 α	29.6	1.77-1.66 m			H3 α , H3 β , H5, H4 β
5	34.4	2.07-1.91 m			H6 β , H6 α , Me10, H4 β , H4 α
6 β	48.2	2.11	dd	13.2, 10.1 ³	H6 α , H5
6 α	48.2	2.30	dddd	13.2, 4.5 1.3, 1.3	H6 β , H5, H2
7	27.0	2.07-1.91m			H2, Me8, Me9
Me8	21.0	0.94	d	6.5	H7
Me9	20.0	0.85	d	6.6	H7
Me10	21.5	0.99	d	6.6	H5

¹ α (= *trans*), β (= *cis*) are given relative to the Me10 group

² correlations into multiplets are given to the expected proton.

³ Me10 is equatorial in the major conformer, so H4 β is axial and has two large $^3J_{\text{HH}}$ values in addition to its $^2J_{\text{HH}}$. Similarly, H6 β is axial and has a large $^3J_{\text{HH}}$ value in addition to its $^2J_{\text{HH}}$.

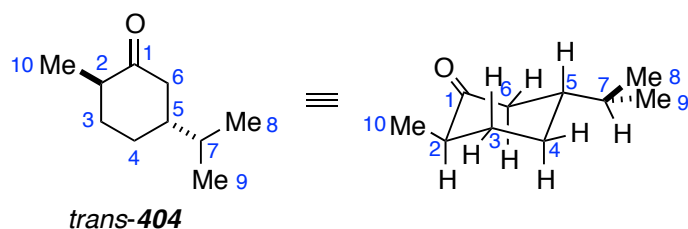


Table III-3: ^{13}C and ^1H NMR for Trans Carvomenthone (*trans-404*) (CDCl_3 , 125; 500 MHz).

Atom number ¹	Carbon		Proton		COSY (to ^1H #) ²
	δ_{C}	δ_{H}	mult	J [Hz]	
1	213.7				
2	45.0	2.33	dddq	12.9, 6.5, 1.1 ³ , 6.5	Me10, H3 α , H3 β , H6 β
3 β	35.2	2.10	dddd	12.6, 6.1, 3.1, 3.0	H3 α , H4 β , H4 α , H2
3 α	35.2	1.30	dddd	12.9, 12.9, 12.9, 3.4	H2, H3 β , H4 α , H4 β
4 β	29.0	1.44	dddd	12.9, 12.9, 12.9, 3.5	H3 α , H3 β , H5, H4 α
4 α	29.0	1.86	dddddd	12.9, 3, 3, 3, 3 ³	H3 α , H3 β , H4 β , H5, H6 α
5	46.7	1.51 – 1.61	m		H7, H4 α , H4 β , H6 α , H6 β
6 β	45.5	2.06	ddd	12.9, 12.9, 1.5 ³	H6 α , H5, H2
6 α	45.5	2.40	ddd	13.0, 3.5, 2.2 ³	H6 β , H5, H4 α
7	32.9	1.51 – 1.61	m		Me8, Me9, H5
Me8	19.7	0.90	d	6.6	H7
Me9	19.4	0.89	d	6.6	H7
Me10	14.5	1.01	d	6.5	H2

¹ α (= *trans*), β (= *cis*) are given relative to the C5 ^iPr group.

² correlations into multiplets are given to the expected proton.

³ $^4J_{\text{HH}}$ correlations are observed for H2-H6 β (4-bond diaxial) and H4 α -H6 α (W coupling).

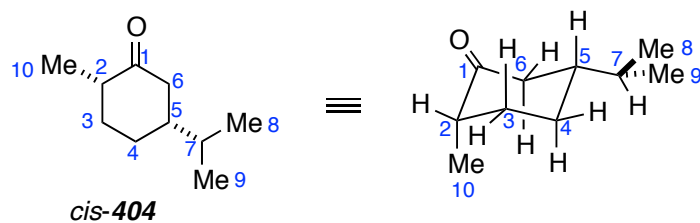


Table III-4: ^{13}C and ^1H NMR for Cis Carvomenthone (*cis-404*) (CDCl_3 , 125 and 500 MHz).

Atom number ¹	Carbon		Proton		COSY (to ^1H) ²
	δ_{C}	δ_{H}	mult	J [Hz]	
1	215.3				
2	44.4	2.45	sextet	6.9	Me10, H3 α , H3 β
3 β	31.5	1.75 – 1.60 m			H3 α , H2, H4 α , H4 β
3 α	31.5	1.87	nfom ³		H3 β , H2, H4 α , H4 β
4 β	25.0	1.75 – 1.60 m			H4 α , H3 α , H3 β , H5
4 α	25.0	1.75 – 1.60 m			H4 β , H5, H3 α , H3 β
5	44.9	1.75 – 1.60 m			H6 α , H6 β , H4 α , H4 β
6 β	43.1	2.38 – 2.28 m			H6 α , H5
6 α	43.1	2.38 – 2.28 m			H6 β , H5
7	30.7	1.49	dsept	6.9, 6.9	H5, Me8, Me9
Me8	20.14	0.91	d	6.9	H7
Me9	20.07	0.89	d	6.9	H7
Me10	16.0	1.10	d	6.9	H2

¹ α (= *trans*), β (= *cis*) are given relative to the C5 ^iPr group.

² correlations into multiplets are given to the expected proton.

³ non first-order multiplet.

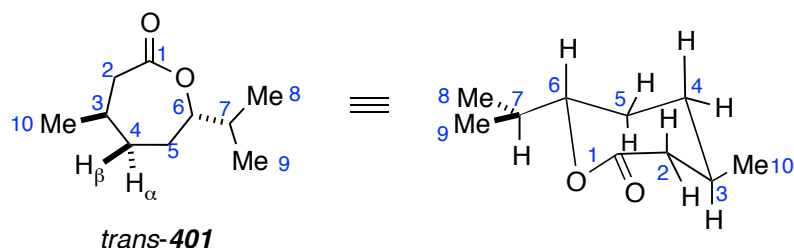


Table III-5: ^{13}C and ^1H NMR Data for Menthede (*trans-401*) (CDCl_3 , 125 and 500 MHz).

Atom number ^a	Carbon		Proton		COSY (to $^1\text{H}\#$) ^b
	δ_{C}	δ_{H}	mult	J [Hz]	
1	174.8				
2 β	42.3	2.54	dd	13.4, 11.5	2 α , 3
2 α	42.3	2.47	ddd	13.4, 1.9, 1.9 ^d	2 β , 3, 4 α^d
3	30.2 ^c	1.90-1.80 m			Me10, 2 α , 2 β , 4 β
4 β	37.2	1.29	dddd	13.5, 13.5, 11.5, 3.5	4 α , 3, 5 α , 5 β
4 α	37.2	1.95	dddd	13.5, 3.5, 3.5, 3.5, 2.0 ^d	4 β , 5 β , 2 α^d
5 β	30.7	1.90-1.80 m			4 α , 4 β , 5 α , 6
5 α	30.7	1.60	dddd	13.2, 12.2, 9.2, 3.0	4 β , 5 β
6	84.5	4.05	dd	9.2, 4.4	5 β , 5 α , 7
7	33.1 ^c	1.90-1.80 m			6, Me8, Me9
Me8	18.1	0.98	d	7.0	7
Me9	16.8	0.97	d	6.9	7
Me10	23.7	1.04	d	6.7	3

^a α (= *trans*), β (= *cis*) are relative to Me10

^b correlations into multiplets are assigned to the expected proton

^c assignments could be reversed

^d H2 α to H4 α ($^4J_{\text{HH}}$) is observed

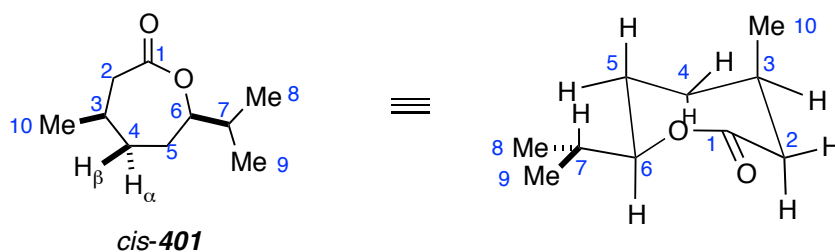


Table III-6: ^{13}C and ^1H NMR Data for Isomenthide (*cis-401*) (CDCl_3 , 125 and 500 MHz).

Atom number ^a	Carbon		Proton		COSY (to $^1\text{H}\#$) ^b
	δ_{C}	δ_{H}	mult	J [Hz]	
1	174.5				
2 β	40.8	2.89	dd	13.6, 3.4	2 α , 3
2 α	40.8	2.54	dd	13.6, 5.9	2 β , 3
3	26.70	2.18	ddddq	7.2, 5.9, 4.4, 3.7, 3.2	2 α , 2 β , Me10
4 β	34.3 ^c	1.80-1.69	m		4 α , 5 β , 5 α
4 α	34.3 ^c	1.80-1.69	m		4 β , 5 β , 5 α
5 β	26.74 ^c	1.80-1.69	m		5 β , 4 α , 4 β , 6
5 α	26.74 ^c	1.80-1.69	m		5 α , 4 α , 4 β , 6
6	84.9	4.02	ddd	8.4, 4.7, 1.9	5 α , 5 β , 7
7	33.3	1.87	dsept	6.8, 4.7	6, Me8, Me9
Me8	17.3	0.982	d	6.8	7
Me9	17.7	0.977	d	6.8	7
Me10	18.5	1.05	d	7.2	3

^a α (= *trans*), β (= *cis*) are relative to Me10

^b correlations into multiplets are assigned to the expected proton

^c assignments could be reversed

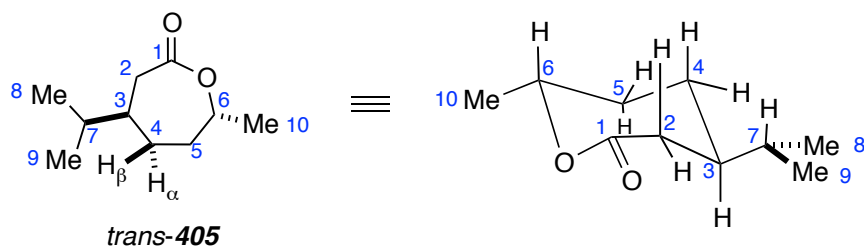


Table III-7: ^{13}C , and ^1H NMR for Trans Carvomenthide (*trans-405*) (CDCl_3 , 125, 500 MHz).

Atom number ^a	Carbon		Proton		COSY (to $^1\text{H-#}$) ^b
	δ_{C}	δ_{H}	mult	J [Hz]	
1	175.6				
2 β	38.0	2.51–2.42	m		2 α , 3, 4 α
2 α	38.0	2.51–2.42	m		2 β , 3, 4 α
3	40.2	1.57	dddd	12, 9, 5, 3.5, 2.5	2 α , 2 β , 4 β , 7
4 α	31.1	1.82	br dddd	13.5, 3.5, 3.5, 3.5	4 β , 5 α
4 β	31.1	1.47	dddd	13, 13, 13, 3.5	3, 4 α , 5 β , 5 α
5 α	35.7	1.65	dddd	15.2, 12.5, 9.0, 3.0	5 β , 4 β , 4 α , 6
5 β	35.7	1.91	ddd	15.2, 3.9, 3.9	4 β , 5 α , 6
6	76.5	4.42	dq	9.2, 6.4	Me10, 5 α , 5 β
7	33.4	1.69	dqq	6.9, 6.9, 3.9	3, Me8, Me9
Me8	18.6	0.90	d	6.9	7
Me9	18.4	0.87	d	6.8	7
Me10	22.4	1.35	d	6.4	6

^a α (=trans) and β (=cis) are given relative to C3 ^1Pr group

^b correlations into multiplets are assigned to the expected proton

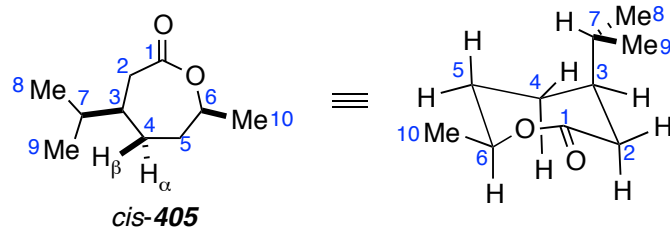


Table III-8: ^{13}C , and ^1H NMR for Cis Carvomenthide (*cis-405*) (CDCl_3 , 125 and 500 MHz).

Atom number ^a	Carbon		Proton		COSY (to $^1\text{H}\#$) ^b
	δ_{C}	δ_{H}	mult	J [Hz]	
1	174.2				
2 β	38.3	2.80	ddd	14.2, 5.7, 1.5 ^d	2 α , 3, 4 β ^d
2 α	38.3	2.76	dd	14.2, 3.7	2 β , 3
3	38.7	1.57-1.51	inform ^c		2 α , 2 β , 3
4 α	30.0	1.98	dddd	14.1, 5.0, 5.0, 5.0, 1.2	5 α , 5 β , 4 β , 3
4 β	30.0	1.65-1.58	m		4 α , 3, 2 β ^d
5 α	32.0	1.80-1.66	m		5 β , 6, 4 α
5 β	32.0	1.80-1.66	m		5 α , 6, 4 α
6	76.3	4.44	ddq	14.8, 6.3, 1.6	Me10, 5 α , 5 β
7	28.9	1.65-1.58	m		3, Me8, Me9
Me8	20.6	1.02	d	6.4	7
Me9	20.3	0.90	d	6.5	7
Me10	22.2	1.35	d	6.3	6

^a α (=trans) and β (=cis) are given relative to C3 ^iPr group

^b correlations into multiplets are assigned to the expected proton

^c non first-order multiplet

^d H4 β and H2 β experience $^4J_{\text{HH}}$ (4 bond diaxial)

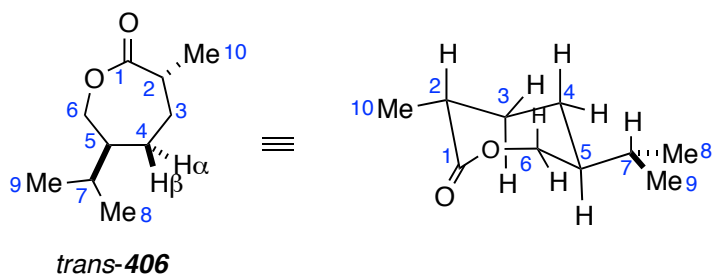


Table III-9: ^{13}C , ^1H NMR for Abnormal Trans Carvomenthide (*trans-406*) (CDCl_3 , 125, 500 MHz).

Atom number ^a	Carbon		Proton		COSY (to $^1\text{H}\#$) ^b
	δ_{C}	δ_{H}	mult	J [Hz]	
1	178.1				
2	37.1	2.72	ddq	10.9, 6.7, 1.9 ^d	Me10, 3 β , 3 α
3 β	31.9	1.78	nfom		3 α , 2
3 α	31.9	1.60-1.48	m		4 β , 3 β , 4 α
4 β	31.08 ^c	1.60-1.48	m		3 α , 5
4 α	31.08 ^c	1.88-1.84	m		3 α , 4 β , 5, 6 α ^d
5	44.6	1.60-1.48	m		6 α , 6 β , 4 β , 4 α , 7
6 β	71.6	4.07	dd	12.3, 8.5	6 α , 5
6 α	71.6	4.16	ddd	12.4, 1.9, 1.9 ^d	6 β , 5, 4 α ^d
7	31.12 ^c	1.68	dsept	6.9, 3.9	Me8, Me9, 5
Me8	19.4	0.91	d	6.9	7
Me9	19.2	0.90	d	6.9	7
Me10	18.4	1.20	d	6.7	2

^a α (= *trans*) and β (= *cis*) relative to C5 ^iPr group.

^b correlations into multiplets are assigned to the expected proton

^c assignments could be reversed

^d W coupling between 4H α and 6H α was observed (small $^4J_{\text{HH}}$).

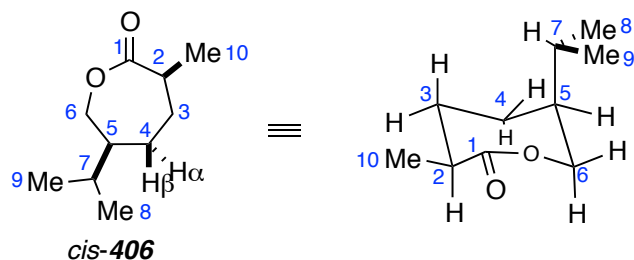


Table III-10: ^{13}C , ^1H NMR for Abnormal Cis Carvomenthide (*cis-406*) (CDCl_3 , 125, 500 MHz).

Atom number ^a	Carbon δ_{C}	Proton δ_{H}	mult	Proton J [Hz]	COSY (to $^1\text{H}\#$) ^b
1	178.1				
2	37.6	.75	ddq	9.0, 4.4, 6.7	3 α , 3 β , Me10
3 β	30.5	.01	nform		3 α , 4 α , 4 β , 2
3 α	30.5	.69-1.52	m		3 β , 4 α , 4 β , 2
4 β	28.1	.69-1.52	m		4 α , 3 α , 3 β , 5
4 α	28.1	.69-1.52	m		4 β , 3 α , 3 β , 5
5	43.6	.42	dddd	10.2, 4.3, 4.3, 4.3, 1.7	6 α , 6 β , 7, 4 α , 4 β
6 β	69.6	.36	ddd	12.9, 4.2, 1.7 ^d	6 α , 5
6 α	69.6	.30	dd	12.8, 1.4	6 β , 5
7	25.6	.73	dsept	9.9, 6.7	5, Me8, Me9
Me8	20.82 ^c	.01	d	6.5	7
Me9	20.75 ^c	0.91	d	6.7	7
Me10	18.6	1.20	d	6.7	2

^a α (= *trans*) and β (= *cis*) relative to C5 ^1Pr group.

^b correlations into multiplets are assigned to the expected proton

^c assignments could be reversed

^d small J indicates W coupling to H4 β

References

- (1) Clardy, J.; Walsh, C. Lessons from natural molecules. *Nature* **2004**, *432*, 829-837.
- (2) Danishefsky, S. On the potential of natural products in the discovery of pharma leads: A case for reassessment. *Nat. Prod. Rep.* **2010**, *27*, 1114-1116.
- (3) Mickel, S. J.; Sedelmeier, G. H.; Niederer, D.; Daeffler, R.; Osmani, A.; Schreiner, K.; Seeger-Weibel, M.; B rod, B.; Schaer, K.; Gamboni, R.; Chen, S.; Chen, W.; Jagoe, C. T.; Kinder, F. R.; Loo, M.; Prasad, K.; Repic , O.; Shieh, W.; Wang, R.; Waykole, L.; Xu, D. D.; Xue, S. Large-Scale Synthesis of the Anti-Cancer Marine Natural Product (+)-Discodermolide. Part 1: Synthetic Strategy and Preparation of a Common Precursor. *Org. Proc. Res. Dev.* **2004**, *8*, 92-100.
- (4) Dalby, S. M.; Paterson, I. Synthesis of polyketide natural products and analogs as promising anticancer agents. *Curr. Opin. Drug Disc.* **2010**, *13*, 777-794.
- (5) Strohl, W. R. The role of natural products in a modern drug discovery program. *Drug Discovery Today* **2000**, *5*, 39-41.
- (6) U.S. Department of Health and Human Services The HIV Life Cycle. www.aidsinfo.nih.gov/contentfiles/HIVLifeCycle_FS_en.pdf (accessed 07/24, 2012).
- (7) Fischer, J. HIV-I Integrase Inhibitors: A Formal Total Synthesis of Lithospermic Acid and Synthetic Studies Towards Integramycin, School of Chemistry, University of Sydney, 2007.
- (8) Hazuda, D.; Blau, C. U.; Felock, P.; Hastings, J.; Pramanik, B.; Wolfe, A.; Bushman, F.; Farnet, C.; Goetz, M.; Williams, M.; Silverman, K.; Lingham, R.; Singh, S. Isolation and characterization of novel human immunodeficiency virus integrase inhibitors from fungal metabolites. *Antivir. Chem. Chemoth.* **1999**, *10*, 63-70.

- (9) Pommier, Y.; Johnson, A. A.; Marchand, C. Integrase inhibitors to treat HIV/Aids. *Nat. Rev. Drug Discov.* **2005**, *4*, 236-248.
- (10) Savarino, A. A historical sketch of the discovery and development of HIV-1 integrase inhibitors. *Expert Opin. Investig. Drugs* **2006**, *15*, 1507-1522.
- (11) Singh, S. B.; Zink, D. L.; Goetz, M. A.; Dombrowski, A. W.; Polishook, J. D.; Hazuda, D. J. Equisetin and a novel opposite stereochemical homolog phomasetin, two fungal metabolites as inhibitors of HIV-1 integrase. *Tetrahedron Lett.* **1998**, *39*, 2243-2246.
- (12) Vesonder, R. F.; Tjarks, L. W.; Rohwedder, W. K.; Burmeister, H. R.; Laugal, J.A. Equisetin, an antibiotic from *Fusarium equiseti* NRRL 5537, identified as a derivative of N-methyl-2,4-pyrrolidone. *J. Antibiot.* **1979**, *32*, 759-761.
- (13) Singh, S. B.; Zink, D. L.; Heimbach, B.; Genilloud, O.; Teran, A.; Silverman, K. C.; Lingham, R. B.; Felock, P.; Hazuda, D. J. Structure, Stereochemistry, and Biological Activity of Integramycin, a Novel Hexacyclic Natural Product Produced by *Actinoplanes* sp. that Inhibits HIV-1 Integrase. *Org. Lett.* **2002**, *4*, 1123-1126.
- (14) Wang, L.; Floreancig, P., E. Synthesis of the C16-C35 fragment of integrumycin using olefin hydroesterification as a linchpin reaction. *Org. Lett.* **2004**, *6*, 569-572.
- (15) Sun, H.; Abbott, J. R.; Roush, W. R. Stereoselective Synthesis of a Model C(18)–C(35) Spiroketal Fragment of Integramycin. *Org. Lett.* **2011**, *13*, 2734-2737.
- (16) Dineen, T. A.; Roush, W. R. Stereoselective Synthesis of the Octahydronaphthalene Unit of Integramycin via an Intramolecular Diels-Alder Reaction. *Org. Lett.* **2005**, *7*, 1355-1358.

- (17) Wang, L. Carbon-Carbon Bond Construction Using Electron Transfer Initiation Cyclization Reactions. RutheniumCatalyzed Hydroesterification and its Application Towards the Synthesis of Integramycin. University of Pittsburgh, 2005.
- (18) Roush, W. R.; Essinfeld, A. P.; Warmus, J. S. Effect of dienophile activating group on the stereoselectivity of the intramolecular diels-alder reaction. *Tetrahedron Lett.* **1987**, *28*, 2447-2450.
- (19) Dineen, T. A. Studies on the intramolecular Diels-Alder reaction : total synthesis of cochleamycin A and efforts toward the total synthesis of integramycin. 2005.
- (20) Coe, J. W.; Roush, W. R. Studies of an intramolecular Diels-Alder approach to the nargenicins: involvement of boatlike transition states in the cyclizations of substituted 1,7,9-decatrien-3-ones. *J. Org. Chem.* **1989**, *54*, 915-930.
- (21) Khuong, K. S.; Beaudry, C. M.; Trauner, D.; Houk, K. N. Dienophile twisting and substituent effects influence reaction rates of intramolecular Diels-Alder cycloadditions: a DFT study. *J. Am. Chem. Soc.* **2005**, *127*, 3688-3689.
- (22) Gras, J.; Bertrand, M. cis- Δ^5 -octahydro-1-naphtalenones and cis- Δ^5 -decahydro-1-naphthalenes (cis-1-decalones) by stereoselective intramolecular diels-alder reaction. *Tetrahedron Lett.* **1979**, *20*, 4549-4552.
- (23) Taber, D. F.; Gunn, B. P. Control elements in the intramolecular Diels-Alder reaction. Synthesis of (+-)-torreyol. *J. Am. Chem. Soc.* **1979**, *101*, 3992-3993.
- (24) Sorensen, E. J. Architectural Self-Construction in Nature and Chemical Synthesis. *Bioorg. Med. Chem.* **2003**, *11*, 3228-3228.
- (25) Oikawa, H.; Tokiwano, T. Enzymatic catalysis of the Diels-Alder reaction in the biosynthesis of natural products. *Nat. Prod. Rep.* **2004**, 321-352.

- (26) Kim, H. J.; Ruszczycky, M. W.; Choi, S.; Liu, Y.; Liu, H. Enzyme-catalysed cycloaddition is a key step in the biosynthesis of spinosyn A. *Nature* **2011**, *473*, 109-112.
- (27) Katayama, K.; Kobayashi, T.; Oikawa, H.; Honma, M.; Ichihara, A. Enzymatic activity and partial purification of solanapyrone synthase: first enzyme catalyzing Diels-Alder reaction. *Biochim Biophys Acta* **1998**, *1384*, 387-395.
- (28) Oikawa, H.; Katayama, K.; Suzuki, Y.; Ichihara, A. Enzymatic activity catalysing exo-selective Diels-Alder reaction in solanapyrone biosynthesis. *J. Chem. Soc., Chem. Commun.* **1995**, 1321-1322.
- (29) Auclair, K.; Sutherland, A.; Kennedy, J.; Witter, D. J.; Van, d. H.; Hutchinson, C. R.; Vederas, J. C. Lovastatin Nonaketide Synthase Catalyzes an Intramolecular Diels-Alder Reaction of a Substrate Analogue. *J. Am. Chem. Soc.* **2000**, *122*, 11519-11520.
- (30) Grieco, P. A. Organic Chemistry in Unconventional Solvents. *Aldrichimica Acta* **1991**, *24*, 59-66.
- (31) Breslow, R. Hydrophobic effects on simple organic reactions in water. *Acc. Chem. Res.* **1991**, *24*, 159-164.
- (32) Hoye, T. R.; Dvornikovs, V. Comparative Diels-Alder Reactivities within a Family of Valence Bond Isomers: A Biomimetic Total Synthesis of (+/-)-UCS1025A. *J. Am. Chem. Soc.* **2006**, *128*, 2550-2551.
- (33) Sizova, E. P. Second General Synthesis of UCS1025A. Synthetic Efforts Toward Total Syntheses of CJ-16,264 and Phomopsicalasin, University of Minnesota, .
- (34) Hoye, T. R. Synthesis and Structure of Antitumor Agents. *ROI CA076497-09* **2007**.

- (35) Toda, S.; Yamamoto, S.; Tenmyo, O.; Tsuno, T.; Hasegawa, T.; Rosser, M.; Oka, M.; Sawada, Y. F.; Konishi, M.; Oki, T. A new neuritogenetic compound BU-4514N produced by *Microtetraspora* sp. *J. Antibiot.* **1993**, *46*, 875-883.
- (36) Ueno, M.; Amemiya, M.; Iijima, M.; Osono, M.; Masuda, T.; Kinoshita, N.; Ikeda, T.; Iinuma, H.; Hamada, M.; Ishizuka, M. Delaminomycins, novel nonpeptide extracellular matrix receptor antagonist and a new class of potent immunomodulator. I. Taxonomy, fermentation, isolation and biological activity. *J. Antibiot.* **1993**, *46*, 719-727.
- (37) Crimmins, M. T.; King, B. W.; Tabet, E. A.; Chaudhary, K. Asymmetric aldol additions: use of titanium tetrachloride and (-)-sparteine for the soft enolization of N-acyl oxazolidinones, oxazolidinethiones, and thiazolidinethiones. *J. Org. Chem.* **2001**, *66*, 894-892.
- (38) Lacey, R. N. Derivatives of acetoacetic acid. Part VII. [α]-Acetyltetramic acids. *J. Chem. Soc.* **1954**, 850-854.
- (39) Watanabe, W. H.; Conlon, L. E. Homogeneous Metal Salt Catalysis in Organic Reactions. I. The Preparation of Vinyl Ethers by Vinyl Transesterification. *J. Am. Chem. Soc.* **1957**, *79*, 2828-2833.
- (40) Parker, K. A.; Farmar, J. G. Regioselectivity in the Claisen rearrangement of bis-allylic alcohols: Electronic and steric effects of C-4 substituents. *Tetrahedron Lett.* **1985**, *26*, 3655-3658.
- (41) Burrows, C.; Carpenter, B. K. Substituent effects on the aliphatic Claisen rearrangements. 2. Theoretical analysis. *J. Am. Chem. Soc.* **1981**, *103*, 6984-6986.
- (42) Curran, D. P.; Suh, Y. G. Substituent effects on the Claisen rearrangement. The accelerating effect of a 6-donor substituent. *J. Am. Chem. Soc.* **1984**, *106*, 5002-5004.

- (43) Hiersemann, M.; Abraham, L. Catalysis of the Claisen Rearrangement of Aliphatic Allyl Vinyl Ethers. *Euro. J. Org. Chem.* **2002**, *2002*, 1461-1471.
- (44) Lutz, R. P. Catalysis of the Cope and Claisen rearrangements. *Chem. Rev.* **1984**, *84*, 205-247.
- (45) Overman, L. E. Mercury(II)- and Palladium(II)-Catalyzed [3,3]-Sigmatropic Rearrangements [New Synthetic Methods (46)]. *Angew. Chem. Int. Ed.* **1984**, *23*, 579-586.
- (46) Booker-Milburn, K.; Baker, J. R.; Bruce, I. Rapid Access to Azepine-Fused Oxetanols from Alkoxy-Substituted Maleimides. *Org. Lett.* **2004**, *6*, 1481-1484.
- (47) Bellur, E.; Gørls, H.; Langer, P. Synthesis of 2-alkylidenepyrrolidines, pyrroles, and indoles by condensation of silyl enol ethers and 1,3-bis-silyl enol ethers with 1-azido-2,2-dimethoxyethane and subsequent reductive cyclization. *J. Org. Chem.* **2005**, *70*, 4751-4761.
- (48) Gage, J. R.; Evans, D. A. Diastereoselective Aldol Condensation Using a Chiral Oxazolidinone Auxiliary: (2S*, 3S*)-3-Hydroxy-3-Phenyl-2-Methylpropanoic Acid. *Org. Synth.* **1993**, *68*, 83-86.
- (49) Evans, D. A.; Nelson, J. V.; Vogel, E.; Taber, T. R. Stereoselective aldol condensations via boron enolates. *J. Am. Chem. Soc.* **1981**, *103*, 3099-3111.
- (50) Nahm, S.; Weinreb, S. M. N-methoxy-n-methylamides as effective acylating agents. *Tetrahedron Lett.* **1981**, *22*, 3815-3818.
- (51) Issa, F.; Fischer, J.; Turner, P.; Coster, M. J. Regioselective Reduction of 3-Methoxymaleimides: An Efficient Method for the Synthesis of Methyl 5-Hydroxytetramates. *J. Org. Chem.* **2006**, *71*, 4703-4705.

- (52) Green, T. W.; Wuts, P. G. M., Eds.; In *Protecting Groups in Organic Synthesis*; John Wiley and Sons, Inc.: New York, 1999; .
- (53) Schwartz, A. L.; Lerner, L. M. Preparation of N-substituted maleimides by direct coupling of alkyl or aralkyl halides with heavy metal salts of maleimide. *J. Org. Chem.* **1974**, *39*, 21-23.
- (54) Abdel-Magid, A.; Carson, K. G.; Harris, B. D.; Maryanoff, C. A.; Shah, R. D. Reductive Amination of Aldehydes and Ketones with Sodium Triacetoxyborohydride. Studies on Direct and Indirect Reductive Amination Procedures. *J. Org. Chem.* **1996**, *61*, 3849-3862.
- (55) Painter, F. F.; Allmendinger, L.; Bauschke, G. A General Method for the Highly Regioselective Introduction of Substituents into the 3-position of 5-unsubstituted 4-O-alkyl Tetronates. *Synlett* **2005**, *18*, 2735-2738.
- (56) Kowalski, C. J.; Weber, A. E.; Fields, K. W. α -Keto dianion precursors via conjugate additions to cyclic α -bromo enones. *J. Org. Chem.* **1982**, *47*, 5088-5093.
- (57) Schlessinger, R. H.; Beberitz, G. R.; Lin, P.; Poss, A. J. Total synthesis of (-)-tirandamycin A. *J. Am. Chem. Soc.* **1985**, *107*, 1777-1778.
- (58) Boeckman, R. K.; Perni, R. B.; MacDonald, J. E.; Thomas, A. J. 6-Diethylphosphonomethyl-2,2-Dimethyl-1,3-Dioxene-4-one. *Org. Synth.* **1993**, *8*, 192-196.
- (59) Boeckman, R. K.; Thomas, A. J. Methodology for the synthesis of phosphorus-activated tetramic acids: applications to the synthesis of unsaturated 3-acyltetramic acids. *J. Org. Chem.* **1982**, *47*, 2823-2824.
- (60) Böhme, R.; Jung, G.; Breitmaier, E. Synthesis of the Antibiotic (R)-Reutericyclin via Dieckmann Condensation. *Helv. Chim. Acta* **2005**, *88*, 2837-2841.

- (61) Ley, S. V.; Smith, S. C.; Woodward, P. R. Further reactions of t-butyl 3-oxobutanethioate and t-butyl 4-diethyl-phosphono-3-oxobutanethioate : Carbonyl coupling reactions, amination, use in the preparation of 3-acyltetramic acids and application to the total synthesis of fuligorubin A. *Tetrahedron* **1992**, *48*, 1145-1174.
- (62) Crimmins, M. T.; Washburn, D. G.; Zawacki, F. J. The Synthesis of 2-alkyl-4-pyrones from Meldrum's Acid. *Org. Synth.* **2004**, *10*, 355.
- (63) Ley, S. V.; Smith, S. C.; Woodward, P. R. Use of t-butyl 4-diethylphosphono-3-oxobutanethioate for tetramic acid synthesis: Total synthesis of the plasmodial pigment fuligorubin A. *Tetrahedron Lett.* **1988**, *29*, 5829-5832.
- (64) Ley, S. V.; Woodward, P. R. Preparation of t-butyl 4-diethylphosphono-3-oxobutanethioate and use in the synthesis of (E)-4-alkenyl-3-oxoesters and macrolides. *Tetrahedron Lett.* **1987**, *28*, 345-346.
- (65) Pronin, S. V.; Kozmin, S. A. Synthesis of Streptolydigin, a Potent Bacterial RNA Polymerase Inhibitor. *J. Am. Chem. Soc.* **2010**, *132*, 14394-14396.
- (66) Ley, S. V.; Woodward, P. R. The use of β -ketothioesters for the exceptionally mild preparation of β -ketoamides. *Tetrahedron Lett.* **1987**, *28*, 3019-3020.
- (67) Prousis, K. C.; Athanasellis, G.; Stefanou, V.; Matiadis, D.; Kokalari, E.; Igglessi-Markopoulou, O.; McKee, V.; Markopoulos, J. Synthesis and Crystal Structure Characterization of Zinc (II) Tetric Acid Complexes. *Bioinorg. Chem. Appl.* **2010**, *2010*.
- (68) Bodurow, C.; Carr, M. A.; Moore, L. L. 2,2-DIMETHYL-6-[(Triphenylphosphoranylidene)methyl]-4H-1,3-Dioxin-4-one. A Four-Carbon Homologating Agent Requiring No Activation. *Org. Prep. Proc. Int.* **1990**, *22*, 109-111.

- (69) Royles, B. J. L. Naturally Occurring Tetramic Acids: Structure, Isolation, and Synthesis. *Chem. Rev.* **1995**, *95*, 1981-2001.
- (70) Jones, R. C. F.; Peterson, G. E. Directed metallation of tetramic acids: a new synthesis of 3-acyl tetramic acids. *Tetrahedron Lett.* **1983**, *24*, 4751-4754.
- (71) Jones, R. C. F.; Sumaria, S. A synthesis of 3-acyl-5-alkyl tetramic acids. *Tetrahedron Lett.* **1978**, *19*, 3173-3176.
- (72) Hori, K.; Hikage, N.; Inagaki, A.; Mori, S.; Nomura, K.; Yoshii, E. Total synthesis of tetronomycin. *J. Org. Chem.* **1992**, *57*, 2888-2902.
- (73) Dener, J. M.; Hart, D. J.; Ramesh, S. α -Acylamino radical cyclizations: application to the synthesis of (-)-swainsonine. *J. Org. Chem.* **1988**, *53*, 6022-6030.
- (74) Ireland, R. E.; Thompson, W. J. An approach to the total synthesis of chlorothricolide: the synthesis of the top half. *J. Org. Chem.* **1979**, *44*, 3041-3052.
- (75) Kumar, S.; Ramachandran, U. An Improved Procedure For the Etherification Of Hydroxy Acid Derivatives. *Org. Prep. Proc. Int.* **2004**, *36*, 380-383.
- (76) Louwrier, S.; Ostendorf, M.; Boom, A.; Hiemstra, H.; Nico Speckamp, W. Studies towards the synthesis of (+)-ptilomycalin A; Stereoselective N-acyliminium ion coupling reactions to enantiopure C-2 substituted lactams. *Tetrahedron* **1996**, *52*, 2603-2628.
- (77) de Figueiredo, R. M.; Voith, M.; Fröhlich, R.; Christmann, M. Synthesis of a Malimide Analogue of the Telomerase Inhibitor UCS1025A Using a Dianionic Aldol Strategy. *Synlett* **2007**, *2007*, 0391-0394.
- (78) Klaver, W. J.; Henk, H.; Speckamp, W. N. Synthesis and absolute configuration of the Aristotelia alkaloid peduncularine. *J. Am. Chem. Soc.* **1989**, *111*, 2588-2595.

- (79) Asahi, K.; Nishino, H. Manganese(III)-based dioxapropellane synthesis using tricarbonyl compounds. *Tetrahedron* **2008**, *64*, 1620-1634.
- (80) Paquette, L. A.; Ezquerra, J.; He, W. Suitability of the Claisen ring expansion protocol for crenulide diterpene construction. *J. Org. Chem.* **1995**, *60*, 1435-1447.
- (81) Oare, D. A.; Henderson, M. A.; Sanner, M. A.; Heathcock, C. H. Acyclic stereoselection. 46. Stereochemistry of the Michael addition of N,N-disubstituted amide and thioamide enolates to α,β -unsaturated ketones. *J. Org. Chem.* **1990**, *55*, 132-157.
- (82) Shirokawa, S.; Kamiyama, M.; Nakamura, T.; Okada, M.; Nakazaki, A.; Hosokawa, S.; Kobayashi, S. Remote Asymmetric Induction with Vinylketene Silyl N,O-Acetal. *J. Am. Chem. Soc.* **2004**, *126*, 13604-13605.
- (83) Evans, D. A.; Kaldor, S. W.; Jones, T. K.; Clardy, J.; Stout, T. J. Total synthesis of the macrolide antibiotic cytovaricin. *J. Am. Chem. Soc.* **1990**, *112*, 7001-7031.
- (84) Zhang, Q.; Rivkin, A.; Curran, D. P. Quasiracemic Synthesis: \approx Concepts and Implementation with a Fluorous Tagging Strategy to Make Both Enantiomers of Pyridovericin and Mappicine. *J. Am. Chem. Soc.* **2002**, *124*, 5774-5781.
- (85) Kinoshita, K.; G Williard, Paul; Khosla, C.; Cane, D. E. Precursor-Directed Biosynthesis of 16-Membered Macrolides by the Erythromycin Polyketide Synthase. *J. Am. Chem. Soc.* **2001**, *123*, 2495-2502.
- (86) Boger, D. L. In *Key Bond Forming Reactions: Diels Alder Reaction*; Baraccio, R. M., Ed.; Lecture Notes. Modern Organic Synthesis. TSRI Press: La Jolla, CA, 1999; pp 213-273.
- (87) Hepperle, S. S.; Li, Q.; East, A. L. L. Mechanism of cis/trans equilibration of alkenes via iodine catalysis. *J. Phys. Chem. A* **2005**, *109*, 10975-10981.

- (88) Birnbaum, G. I.; Cygler, M.; Ekiel, I.; Shugar, D. Structure and conformation of 8-bromo-9- β -D-xylofuranosyladenine in the solid state and in solution. *J. Am. Chem. Soc.* **1982**, *104*, 3957-3964.
- (89) Schulte-Elte, K.; Giersch, W.; Winter, B.; Pamingle, H.; Ohloff, G. Diastereoselektivität der Geruchswahrnehmung von Alkoholen der Iononreihe. *Helv. Chim. Acta* **1985**, *68*, 1961-1985.
- (90) Hirose, T.; Sunazuka, T.; Yamamoto, D.; Kojima, N.; Shirahata, T.; Harigaya, Y.; Kuwajima, I.; Ōmura, S. Determination of the absolute stereochemistry and asymmetric total synthesis of madindolines A and B: a practical improvement to a second-generation approach from the first-generation. *Tetrahedron* **2005**, *61*, 6015-6039.
- (91) Heinrich, M.; Gibbons, S. Ethnopharmacology in drug discovery: an analysis of its role and potential contribution. *J. Pharm. Pharmacol.* **2001**, *53*, 425-432.
- (92) Schultes, R. E. Plants in treating senile dementia in the northwest Amazon. *J. of Ethnopharmacol.* **1993**, *38*, 129-135.
- (93) Schultes, R. E. In *Phytochemical Gaps in our Knowledge of Hallucinogens*; Reingold, L., Harbourne, J. B. and Swain, T., Eds.; Progress in Phytochemistry; Pergamon Press: Oxford, UK, 1981; pp 301-331.
- (94) McKenna, D. J. Application of Ethnopharmacology and Receptor Screening Technologies to the Identification of Novel Natural Products for the Treatment of Cognitive Deficits in Schizophrenia. **2004**.
- (95) McKenna, D. J.; Ruiz, J. M.; Hoye, T. R.; Roth, B. L.; Shoemaker, A. T. Receptor screening technologies in the evaluation of Amazonian ethnomedicines with potential applications to cognitive deficits. *J. of Ethnopharmacol.* **2011**, *134*, 475-492.

- (96) Schotte, A.; Janssen, P. F.; Gommeren, W.; Luyten, W. H.; Van Gompel, P.; Lesage, A. S.; De Loore, K.; Leysen, J.E. Risperidone compared with new and reference antipsychotic drugs: in vitro and in vivo receptor binding. *Psychopharmacology* **1996**, *124*, 57-73.
- (97) Roth, B. L.; Lopez, E.; Patel, S.; Kroeze, W. K. The Multiplicity of Serotonin Receptors: Uselessly Diverse Molecules or an Embarrassment of Riches? *The Neuroscientist* **2000**, *6*, 252-262.
- (98) Phillipson, J. D. Radioligand-receptor binding assays in the search for bioactive principles from plants. *J. Pharm. Pharmacol.* **1999**, *51*, 493-503.
- (99) Roth, B. L.; Sheffler, D. J.; Kroeze, W. K. Magic shotguns versus magic bullets: selectively non-selective drugs for mood disorders and schizophrenia. *Nat Rev Drug Discov* **2004**, *3*, 353-359.
- (100) Gray, J. A.; Roth, B. L. The pipeline and future of drug development in schizophrenia. *Molecular Psychiatry* **2007**, *12*, 904-922.
- (101) Gray, J. A.; Roth, B. L. Molecular Targets for Treating Cognitive Dysfunction in Schizophrenia. *Schizophr. Bull.* **2007**, *33*, 1100-1119.
- (102) Harvey, A. L. Natural products in drug discovery. *Drug Discovery Today* **2008**, *13*, 894-901.
- (103) Sullivan, R. J.; Allen, J. S.; Otto, C.; Tiobech, J.; Nero, K. Effects of chewing betel nut (*Areca catechu*) on the symptoms of people with schizophrenia in Palau, Micronesia. *The British journal of psychiatry : the journal of mental science* **2000**, *177*, 174-178.
- (104) Newman, D. J.; Cragg, G. M. Natural products as sources of new drugs over the last 25 years. *J. of Nat. Prod.* **2007**, *70*, 461-477.

- (105) Nicolaou, K. C.; Snyder, S. A. Chasing Molecules That Were Never There: Misassigned Natural Products and the Role of Chemical Synthesis in Modern Structure Elucidation. *Angew. Chem. Int. Ed.* **2005**, *44*, 2050-2050.
- (106) Van Beek, T. A.; Verpoorte, R.; Svendsen, A. B.; Leeuwenberg, A. J. M.; Bisset, N. G. Tabernaemontana L. (Apocynaceae): A review of its taxonomy, phytochemistry, ethnobotany and pharmacology. *J. Ethnopharmacol.* **1984**, *10*, 1-156.
- (107) Boekelheide, V.; Grundon, M. F. A Characterization of $\hat{I}\pm$ -Erythroidine1. *J. Am. Chem. Soc.* **1953**, *75*, 2563-2566.
- (108) TrojÄnek, J.; Åtrouf, O.; Holubek, J.; ÄEekan, Z. Structure of Vincamine. *Tetrahedron Lett.* **1961**, *2*, 702-706.
- (109) Lounasmaa, M.; Jokela, R.; Anttila, U.; Hanhinen, P.; Laine, C. Short synthetic route to (T₁)-geissoschizine. *Tetrahedron* **1996**, *52*, 6803-6810.
- (110) Inouye, H.; Ueda, S.; Nakamura, Y. Struktur des swerosids, eines neuen glucosides aus swertia japonica makino. *Tetrahedron Lett.* **1966**, *7*, 5229-5234.
- (111) Stimson, M. M.; Reuter, M. A. The Spectrophotometric Estimation of Methoxy-cinchona Alkaloids1. *J. Am. Chem. Soc.* **1946**, *68*, 1192-1196.
- (112) McCalley, D. Analysis of the cinchona alkaloids by liquid chromatography. Reversed-phase chromatography on octadecylsilyl columns. *Chromatographia* **1983**, *17*, 264-266.
- (113) Kingston, D. G. I.; Li, B. T. Preliminary investigation of the use of high-pressure liquid chromatography for the separation of indole alkaloids. *J. Chromatogr. A* **1975**, *104*, 431-437.

- (114) Perera, P.; Van Beek, T. A.; Verpoorte, R. High-performance liquid chromatography of some *Tabernaemontana* alkaloids. *J. Chromatogr. A* **1984**, *285*, 214-220.
- (115) Ryba, M. Dimethylformamide as a mobile phase component in reversed-phase liquid column chromatography on octadecylsilica. *Chromatographia* **1982**, *15*, 227-230.
- (116) Wehrli, A.; Hildenbrand, J. C.; Keller, H. P.; Stampfli, R.; Frei, R. W. Influence of organic bases on the stability and separation properties of reversed-phase chemically bonded silica gels. *J. Chromatogr. A* **1978**, *149*, 199-210.
- (117) Gustavsson, T.; Sarkar, N.; Bányász, Á; Markovitsi, D.; Improta, R. Solvent Effects on the Steady-state Absorption and Fluorescence Spectra of Uracil, Thymine and 5-Fluorouracil? *Photochem. Photobiol.* **2007**, *83*, 595-599.
- (118) Evans Schultes, R. De plantis toxicariis e mundo novo tropicale commentationes. XIX. Biodynamic apocynaceous plants of the northwest amazon. *J. Ethnopharmacol.* **1979**, *1*, 165-192.
- (119) Vahl, M. In *Eclogae Americanae*; 1796; .
- (120) Wolter Filho, W.; Pinheiro, M. L. B.; Imbiriba de Rocha, A. Alkaloids of *Tabernaemontana heterophylla* Vahl. (Apocynaceae). *Acta Amazonica* **1983**, *13*, 409-412.
- (121) Henriques, A.; Kan, C.; Chiaroni, A.; Riche, C.; Husson, H. P.; Kan, S. K.; Lounasmaa, M. New dimeric indole alkaloids from *Stenosolen heterophyllus*: structure determinations and synthetic approach. *J. Org. Chem.* **1982**, *47*, 803-811.
- (122) Abaul, J.; Philoglyne, B.; Bourgeois, P.; Ahond, A.; Poupat, C.; Potier, P. Study on American *Tabernaemontanas*. VI. Alkaloids from the Leaves of *Tabernaemontana citrifolia*. *J. Nat. Prod.* **1989**, *52*, 1279-1283.

- (123) Leeuwenberg, A. J. M. In *A Chemotaxonomic Investigation of the Plant Families of Apocnaceae, Loganiaceae, and Rubaceae by Their Indole Alkaloid Content*; Pelletier, S. W., Ed.; Alkaloids: Chemical and Biological Perspectives; New York, Chichester, Brisbane, Toronto, and Singapore, 1983; pp 211-376.
- (124) Bonpland, A.; Humboldt, A. v.; Kunth, K. S. In *Nova genera et species plantarum : Lutetiae Parisiorum :sumtibus Librariae Graeco-Latino-Germanico: 1818; Vol. v. 3, pp 641.*
- (125) Ruiz, H.; Pavón, J.; Pavón, J. In *Flora Peruviana, et Chilensis, sive, Descriptiones et icones plantarum Peruvianarum, et Chilensium, secundum systema Linnaeanum digestae, cum characteribus plurium generum evulgatorum reformatis*; Madrid :Typis Gabrielis de Sancha: 1799; Vol. v. 2, pp 79.
- (126) Delle-Monache, G.; Montenegro de Matta, S.; Delle-Monache, F.; Marini-Bettolo, G. B. Alkaloids of *Tabernaemontana sananho* R & P. *Atti della Accademia Nazionale dei Lincei* **1977**, *62*, 221-226.
- (127) Zocoler, M. A.; Oliveira, Arildo J. B. de; Sarragiotto, M. H.; Grzesiuk, V. L.; Vidotti, G. J. Qualitative determination of indole alkaloids of *Tabernaemontana fuchsiaeifolia* (Apocynaceae). *J. Brazil. Chem. Soc.* **2005**, *16*, 1372-1377.
- (128) Jokela, R.; Lounasmaa, M. ¹H- and ¹³C-NMR Spectral Data of Five Sarpagine-Type Alkaloids. *Heterocycles* **1996**, *43*, 1015-1020.
- (129) Azoug, M.; Loukaci, A.; Richard, B.; Nuzillard, J.; Moreti, C.; Ziches-Hanrot, M.; Le Men-Olivier, L. Alkaloids from stem bark and leaves of *Peschiera buchtieni*. *Phytochemistry* **1995**, *39*, 1223-1228.
- (130) Sha, C.; Yang, J. Total syntheses of ellipticine alkaloids and their amino analogues. *Tetrahedron* **1992**, *48*, 10645-10654.

- (131) Ishikura, M.; Hino, A.; Yaginuma, T.; Agata, I.; Katagiri, N. A Novel Entry to Pyrido[4,3-b]carbazoles: An Efficient Synthesis of Ellipticine. *Tetrahedron* **2000**, *56*, 193-207.
- (132) Ghedira, K.; Zeches-Hanrot, M.; Richard, B.; Massiot, G.; Le Men-Olivier, L.; Sevenet, T.; Goh, S. H. Alkaloids of *Alstonia angustifolia*. *Phytochemistry* **1988**, *27*, 3955-3962.
- (133) Clivio, P.; Richard, B.; Deverre, J.; Sevenet, T.; Zeches, M.; Le Men-Olivier, L. Alkaloids from leaves and root bark of *Ervatamia hirta*. *Phytochemistry* **1991**, *30*, 3785-3792.
- (134) Timmins, P.; Court, W. E. Stem alkaloids of *Rauwolfia obscura*. *Phytochemistry* **1976**, *15*, 733-735.
- (135) Bennasar, M. -.; Vidal, B.; Bosch, J. Biomimetic Total Synthesis of Ervitsine and Indole Alkaloids of the Ervatamine Group via 1,4-Dihydropyridines. *J. Org. Chem.* **1997**, *62*, 3597-3609.
- (136) Naito, T.; Hirata, Y.; Miyata, O.; Ninomiya, I. Photocyclisation of enamides. Part 27. Total syntheses of (+/-)-yohimbine, (+/-)-alloyohimbine, and (+/-)-19,20-didehydroyohimbines. *J. Chem. Soc., Perkin Trans. 1* **1988**, 2219-2225.
- (137) Miyata, O.; Hirata, Y.; Naito, T.; Ninomiya, I. Total Synthesis of (+/-)-19,20-didehydroyohimbines. *Heterocycles* **1984**, *22*, 2719-2722.
- (138) Janot, M.; Goutarel, R. United States Patent, 1957.
- (139) Brown, R. T.; Pratt, S. B. Stereoselective synthesis of yohimbine alkaloids from secologanin. *J. Chem. Soc., Chem. Commun.* **1980**, 165-167.

- (140) Maciulaitis, R.; Kontrimaviciute, V.; Bressolle, F. F. M.; Briedis, V. Ibogaine, an anti-addictive drug: pharmacology and time to go further in development. A narrative review. *Human & experimental toxicology* **2008**, *27*, 181-194.
- (141) Bowen, W. D. In *Sigma Receptors and Iboga Alkaloids*; Cordell, G. A., Ed.; The Alkaloids: Chemistry and Biology; Academic Press: San Diego, 2001; pp 173-191.
- (142) Soejarto, D. D.; Fong, H. H. S.; Tan, G. T.; Zhang, H. J.; Ma, C. Y.; Franzblau, S. G.; Gyllenhaal, C.; Riley, M. C.; Kadushin, M. R.; Pezzuto, J. M.; Xuan, L. T.; Hiep, N. T.; Hung, N. V.; Vu, B. M.; Loc, P. K.; Dac, L. X.; Binh, L. T.; Chien, N. Q.; Hai, N. V.; Bich, T. Q.; Cuong, N. M.; Southavong, B.; Sydara, K.; Bouamanivong, S.; Ly, H. M.; Thuy, T. V.; Rose, W. C.; Dietzman, G. R. Ethnobotany/ethnopharmacology and mass bioprospecting: Issues on intellectual property and benefit-sharing. *J. Ethnopharmacol.* **2005**, *100*, 15-22.
- (143) Pereira, P. S.; França, S. d. C.; Oliveira, Paulo Vinicius Anderson de; Breves, Camila Moniz de Souza; Pereira, S. I. V.; Sampaio, S. V.; Nomizo, A.; Dias, D. A. Chemical constituents from *Tabernaemontana catharinensis* root bark: a brief NMR review of indole alkaloids and in vitro cytotoxicity. *Química Nova* **2008**, *31*, 20-24.
- (144) Lligadas, G.; Ronda, J. C.; Galiañ, M.; Calóndiz, V. Plant Oils as Platform Chemicals for Polyurethane Synthesis: Current State-of-the-Art. *Biomacromolecules* **2010**, *11*, 2825-2835.
- (145) Lay, J. O.; Liyanage, R.; Durham, B.; Brooks, J. Rapid characterization of edible oils by direct matrix-assisted laser desorption/ionization time-of-flight mass spectrometry analysis using triacylglycerols. *Rapid Commun. Mass Spectrom.* **2006**, *20*, 952-958.
- (146) Gidden, J.; Liyanage, R.; Durham, B.; Lay, J. O. Reducing fragmentation observed in the matrix-assisted laser desorption/ionization time-of-flight mass spectrometric

- analysis of triacylglycerols in vegetable oils. *Rapid Commun. Mass Spectrom.* **2007**, *21*, 1951-1957.
- (147) The BiOH Experience. <http://www.experiencebioh.com/> (accessed 6/20, 2012).
- (148) Cleaner, Greener, Performance Polyols. *Renuva, Renewable Resource Technology* **2008**.
- (149) Li, F.; Hanson, M. V.; Larock, R. C. Soybean oil-divinylbenzene thermosetting polymers: synthesis, structure, properties and their relationships. *Polymer* **2001**, *42*, 1567-1579.
- (150) Tian, Q.; Larock, R. Model studies and the ADMET polymerization of soybean oil. *J. Am. Oil Chem. Soc.* **2002**, *79*, 479-488.
- (151) Yongshang, L.; Larock, R. C. In *Novel Biobased Plastics, Rubbers, Composites, Coatings and Adhesives from Agricultural Oils and By-Products*; Cheng, H. N., Gross, R. A., Eds.; Green Polymer Chemistry: Biocatalysis and Biomaterials; American Chemical Society: 2010; Vol. 1043, pp 87-102.
- (152) Lachance, P.; Eastham, A. M. Olefin oligomerization by boron fluoride. *J. Polym. Sci. Pol. Sym.* **1976**, *56*, 203-210.
- (153) Croston, C.; Tubb, I.; Cowan, J.; Teeter, H. Polymerization of drying oils. VI. Catalytic polymerization of fatty acids and esters with boron trifluoride and hydrogen fluoride. *J. Am. Oil Chem. Soc.* **1952**, *29*, 331-333.
- (154) Laszlo, J.; Compton, D.; Vermillion, K. Acyl Migration Kinetics of Vegetable Oil 1,2-Diacylglycerols. *J. Am. Oil Chem. Soc.* **2008**, *85*, 307-312.
- (155) Kodali, D. R.; Tercyak, A.; Fahey, D. A.; Small, D. M. Acyl migration in 1,2-dipalmitoyl-sn-glycerol. *Chem. Phys. Lipids* **1990**, *52*, 163-170.

- (156) Rybak, A.; Fokou, P. A.; Meier, M. A. R. Metathesis as a versatile tool in oleochemistry. *Eur. J. Lipid Sci. Technol.* **2008**, *110*, 797-804.
- (157) Schrodi, Y.; Ung, T.; Vargas, A.; Mkrtumyan, G.; Lee, C. W.; Champagne, T. M.; Pederson, R. L.; Hong, S. H. Ruthenium Olefin Metathesis Catalysts for the Ethenolysis of Renewable Feedstocks. *Clean Soil Air Water* **2008**, *36*, 669-673.
- (158) Leitao, E. M.; Eide, E. F. v. d.; Romero, P. E.; Piers, W., E.; McDonald, R. Kinetic and Thermodynamic Analysis of Processes Relevant to Initiation of Olefin Metathesis by Ruthenium Phosphonium Alkylidene Catalysts. *J. Am. Chem. Soc.* **2010**, *132*, 2784-2794.
- (159) Forman, G. S.; Bellabarba, R. M.; Tooze, R. P.; Slawin, A. M. Z.; Karch, R.; Winde, R. Metathesis of renewable unsaturated fatty acid esters catalysed by a phoban-indenylidene ruthenium catalyst. *J. Organomet. Chem.* **2006**, *691*, 5513-5516.
- (160) Biswas, A.; Sharma, B. K.; Willett, J. L.; Erhan, S. Z.; Cheng, H. N. Room-temperature self-curing ene reactions involving soybean oil. *Green Chem.* **2008**, *10*, 290-295.
- (161) Liu, Z.; Sharma, B. K.; Erhan, S. Z. From oligomers to molecular giants of soybean oil in supercritical carbon dioxide medium: 1. Preparation of polymers with lower molecular weight from soybean oil. *Biomacromolecules* **2007**, *8*, 233-239.
- (162) Onopchenko, A.; Cupples, B. L.; Kresge, A. N. Boron fluoride-catalyzed oligomerization of alkenes: structures, mechanisms, and properties. *Ind. Eng. Chem. Prod. Res. Dev.* **1983**, *22*, 182-191.
- (163) Fokou, P. A.; Meier, M. A. R. Studying and Suppressing Olefin Isomerization Side Reactions During ADMET Polymerizations. *Macromol. Rapid Comm.* **2010**, *31*, 368-373.

- (164) Deno, N. C.; Peterson, H. J.; Saines, G. S. The Hydride-Transfer Reaction. *Chem. Rev.* **1960**, *60*, 7-14.
- (165) Porter, N.; Caldwell, S.; Mills, K. Mechanisms of free radical oxidation of unsaturated lipids. *Lipids* **1995**, *30*, 277-290.
- (166) Frankel, E. N. Lipid oxidation. *Prog. Lipid Res.* **1980**, *19*, 1-22.
- (167) Kade, M. J.; Burke, D. J.; Hawker, C. J. The power of thiol-ene chemistry. *J. Polym. Sci. Pol. Chem.* **2010**, *48*, 743-750.
- (168) Bantchev, G. B.; Kenar, J. A.; Biresaw, G.; Han, M. G. Free Radical Addition of Butanethiol to Vegetable Oil Double Bonds. *J. Agric. Food Chem.* **2009**, *57*, 1282-1290.
- (169) Desroches, M.; Caillol, S.; Lapinte, V.; Auvergne, R.; Boutevin, B. Synthesis of Biobased Polyols by Thiol-Ene Coupling from Vegetable Oils. *Macromolecules* **2011**, *44*, 2489-2500.
- (170) Turunc, O.; Meier, M. A. R. Thiol-ene vs. ADMET: a complementary approach to fatty acid-based biodegradable polymers. *Green Chem.* **2011**, *13*, 314-320.
- (171) Schmidt, U.; Grafen, P.; Goedde, H. W. Chemistry and Biochemistry of \pm -Lipoic Acid. *Angew. Chem. Int. Ed Engl.* **1965**, *4*, 846-856.
- (172) Howard, S.,C.; McCormick, D.,B. High-performance liquid chromatography of lipoic acid and analogues. *J. Chromatogr. A* **1981**, *208*, 129-131.
- (173) Kisanuki, A.; Kimpara, Y.; Oikado, Y.; Kado, N.; Matsumoto, M.; Endo, K. Ring-opening polymerization of lipoic acid and characterization of the polymer. *J. Polym. Sci. A Polym. Chem.* **2010**, *48*, 5247-5253.
- (174) Endo, K.; Shiroy, T.; Murata, N.; Kojima, G.; Yamanaka, T. Synthesis and Characterization of Poly(1,2-dithiane). *Macromolecules* **2004**, *37*, 3143-3150.

- (175) Arakawa, R.; Watanabe, T.; Fukuo, T.; Endo, K. Determination of cyclic structure for polydithiane using electrospray ionization mass spectrometry. *J. Polym. Sci. A Polym. Chem.* **2000**, *38*, 4403-4406.
- (176) Ishida, H.; Kisanuki, A.; Endo, K. Ring-Opening Polymerization of Aromatic 6-Membered Cyclic Disulfide and Characterization of the Polymer. *Polym. J.* **2008**, *41*, 110-117.
- (177) Sandner, M. R.; Osborn, C. L. Photochemistry of 2,2-dimethoxy-2-phenylacetophenone-triplet detection via "spin memory". *Tetrahedron Lett.* **1974**, *15*, 415-418.
- (178) Baxter, J. E.; Davidson, R. S.; Hageman, H. J.; Hakvoort, G. T. M.; Overeem, T. A study of the photodecomposition products of an acylphosphine oxide and 2,2-dimethoxy-2-phenylacetophenone. *Polymer* **1988**, *29*, 1575-1580.
- (179) Vincent, M.; Guglielmetti, G.; Cassani, G.; Tonini, C. Determination of double-bond position in diunsaturated compounds by mass spectrometry of dimethyl disulfide derivatives. *Anal. Chem.* **1987**, *59*, 694-699.
- (180) Buser, H. R.; Arn, H.; Guerin, P.; Rauscher, S. Determination of double bond position in mono-unsaturated acetates by mass spectrometry of dimethyl disulfide adducts. *Anal. Chem.* **1983**, *55*, 818-822.
- (181) Yamamoto, K.; Shibahara, A.; Nakayama, T.; Kajimoto, G. Determination of double-bond positions in methylene-interrupted dienoic fatty acids by GC-MS as their dimethyl disulfide adducts. *Chem. Phys. Lipids* **1991**, *60*, 39-50.
- (182) Carballeira, N. M.; Shalabi, F.; Cruz, C. Thietane, tetrahydrothiophene and tetrahydrothiopyran formation in reaction of methylene-interrupted dienoates with dimethyl disulfide. *Tetrahedron Lett.* **1994**, *35*, 5575-5578.

- (183) Schwartzbeck, J. L.; Jung, S.; Abbott, A. G.; Mosley, E.; Lewis, S.; Pries, G. L.; Powell, G. L. Endoplasmic oleoyl-PC desaturase references the second double bond. *Phytochemistry* **2001**, *57*, 643-652.
- (184) Caserio, M. C.; Fisher, C. L.; Kim, J. K. Boron trifluoride catalyzed addition of disulfides to alkenes. *J. Org. Chem.* **1985**, *50*, 4390-4393.
- (185) Caraballo, R.; Rahm, M.; Vongvilai, P.; Brinck, T.; Ramstrom, O. Phosphine-catalyzed disulfide metathesis. *Chem. Commun.* **2008**, 6603-6605.
- (186) Caraballo, R.; Sakulsombat, M.; Ramstrom, O. Phosphine-mediated disulfide metathesis in aqueous media. *Chem. Commun.* **2010**, *46*, 8469-8471.
- (187) Lees, W. J.; Whitesides, G. M. Equilibrium constants for thiol-disulfide interchange reactions: a coherent, corrected set. *J. Org. Chem.* **1993**, *58*, 642-647.
- (188) Dai, H.; Yang, L.; Lin, B.; Wang, C.; Shi, G. Synthesis and Characterization of the Different Soy-Based Polyols by Ring Opening of Epoxidized Soybean Oil with Methanol, 1,2-Ethanediol and 1,2-Propanediol. *J. Am. Oil Chem. Soc.* **2009**, *86*, 261-267.
- (189) Forristal, I.; Lawson, K. R.; Rayner, C. M. Optically active 2,3-epoxy sulfides as precursors to 3-hydroxy-1,2-dithioethers and 3-hydroxy-1-alkenylthioethers. *Tetrahedron Lett.* **1999**, *40*, 7015-7018.
- (190) Naghipur, A.; Lown, J. W.; Jain, D. C.; Sapse, A. Ab initio studies on 1,2-oxathietane, Z and E 3,4-dimethyl-1,2-oxathietane, and their products of formal cycloreversion. *Can. J. Chem.* **1988**, *66*, 1890-1894.
- (191) Lown, J. W.; Koganty, R. R. Formation of novel 1,2-oxathietanes from 2-chloroethyl sulfoxide precursors and their reactions in solution, including formal cycloreversions and rearrangements. *J. Am. Chem. Soc.* **1986**, *108*, 3811-3818.

- (192) Giannella, M.; Pignini, M.; Ruedi, P.; Eugster, C. H. The Four Diastereomeric Thio-Analogues of (\pm)-Muscarine. *Helv. Chim. Acta* **1979**, *62*, 2329-2337.
- (193) Capon, R. J.; Barrow, R. A. Acid-Mediated Conversion of Methylene-Interrupted Bisepoxides to Tetrahydrofurans: A Biomimetic Transformation. *J. Org. Chem.* **1998**, *63*, 75-83.
- (194) Glueck, S. M.; Fabian, W. M. F.; Faber, K.; Mayer, S. F. Biocatalytic Asymmetric Rearrangement of a Methylene-Interrupted Bis-epoxide: Simultaneous Control of Four Asymmetric Centers Through a Biomimetic Reaction Cascade. *Chem. Eur. J.* **2004**, *10*, 3467-3478.
- (195) Malievskii, A. Exchange reaction of oxiranes with β -hydroxyalkyl sulfides, selenides, -amines, and-phosphines. *Russ. Chem. Bull.* **2000**, *49*, 579-587.
- (196) JÄrme, C.; Lecomte, P. Recent advances in the synthesis of aliphatic polyesters by ring-opening polymerization. *Adv. Drug Deliv. Rev.* **2008**, *60*, 1056-1076.
- (197) Lowe, J. R.; Martello, M. T.; Tolman, W. B.; Hillmyer, M. A. Functional biorenewable polyesters from carvone-derived lactones. *Polym. Chem.* **2011**, *2*, 702-708.
- (198) Baeyer, A.; Villiger, V. Einwirkung des Caro'schen Reagens auf Ketone. *Ber. Dtsch. Chem. Ges.* **1899**, *32*, 3625-3633.
- (199) Shin, J.; Martello, M. T.; Shrestha, M.; Wissinger, J. E.; Tolman, W. B.; Hillmyer, M. A. Pressure-Sensitive Adhesives from Renewable Triblock Copolymers. *Macromolecules* **2011**, *44*, 87-94.
- (200) Qian, H.; Wohl, A. R.; Crow, J. T.; Macosko, C. W.; Hoye, T. R. A Strategy for Control of α -Random Copolymerization of Lactide and Glycolide:

Application to Synthesis of PEG-b-PLGA Block Polymers Having Narrow Dispersity. *Macromolecules* **2011**, *44*, 7132-7140.

- (201) Lohmeijer, B. G. G.; Pratt, R. C.; Leibfarth, F.; Logan, J. W.; Long, D. A.; Dove, A. P.; Nederberg, F.; Choi, J.; Wade, C.; Waymouth, R. M.; Hedrick, J. L. Guanidine and Amidine Organocatalysts for Ring-Opening Polymerization of Cyclic Esters. *Macromolecules* **2006**, *39*, 8574-8583.
- (202) Wiitala, K. W.; Cramer, C. J.; Hoye, T. R. Comparison of various density functional methods for distinguishing stereoisomers based on computed ¹H or ¹³C NMR chemical shifts using diastereomeric penam ¹H²-lactams as a test set. *Magn. Reson. Chem.* **2007**, *45*, 819-829.
- (203) Smith, W. B.; Amezcua, C. NMR versus molecular modelling: menthone and isomenthone. *Magn. Reson. Chem.* **1998**, *36*, S3-S10.
- (204) Saiyasombat, W.; Molloy, R.; Nicholson, T. M.; Johnson, A. F.; Ward, I. M.; Poshyachinda, S. Ring strain and polymerizability of cyclic esters. *Polymer* **1998**, *39*, 5581-5585.